THE ROLE OF LIPOPROTEINS IN VASCULAR CALCIFICATION AND PLAQUE STABILISATION

A thesis submitted by

EMMA JILL AKERS

BSc (Hons)

To

The University of Adelaide

South Australia, Australia

For the degree of

Doctor of Philosophy

THE UNIVERSITY of ADELAIDE

South Australian Health and Medical Research Institute

January 2021

Table of Contents

List of Figures

List of Tables

Declaration

I certify that this work contains no material which has been accepted for the award of any other degree or diploma in my name in any university or other tertiary institution and, to the best of my knowledge and belief, contains no material previously published or written by another person, except where due reference has been made in the text. In addition, I certify that no part of this work will, in the future, be used in a submission in my name for any other degree or diploma in any university or other tertiary institution without the prior approval of the University of Adelaide and where applicable, any partner institution responsible for the joint award of this degree. I give permission for the digital version of my thesis to be made available on the web, via the University's digital research repository, the Library Search and also through web search engines, unless permission has been granted by the University to restrict access fora period of time.

I acknowledge the support I have received for my research through the provision of an Australian Government Research Training Program Scholarship and the Lion's Medical Research Foundation.

Emma Akers

Date: 4th February 2021

Signature:

Abstract

Vascular calcification (VC) is a feature of atherosclerotic plaques and is associated with co-morbidities such as diabetes and chronic kidney disease. While its presence is used by cardiologists to identify higher risk patients, increasing data suggests that the morphology of calcification is also important to the stability of a plaque, whereby smaller growths, particularly in the fibrous cap, increase likelihood of rupture and larger sheets decrease likelihood. Although lipoproteins, namely high (HDL), low (LDL), very low (VLDL) density lipoproteins and lipoprotein (a) (Lp(a)), have been previously studied in their relationship to general plaque growth and progression, their roles in influencing plaque calcification are less understood due to experimental variations within the literature. This thesis therefore aims to study the roles of HDL, LDL, VLDL and their pro-atherogenic oxidised forms (ox) on atherosclerotic VC *in vitro*, *in vivo* and in human plasma samples *ex vivo*, and aims to assess these using standardised models. Using *in vitro* calcification assays developed in chapter 3, we observed that both oxVLDL and oxLDL increase vascular smooth muscle cell (VSMC) calcification, whereas native HDL reduces mineralisation. This effect of HDL however is not observed in reconstituted or oxidised species, showing a pro-calcification effect for oxidised lipoprotein species. PCR and western blot techniques identified raised Runx2, RANKL, RANK and lowered OPG as potential calcification molecules that may be influenced by lipoproteins in these cells, however further studies are needed to elucidate the full mechanisms and solidify these results. *In vivo*, modifying VLDL into a pro-atherogenic phenotype via apo CIII deletion on an Apo E knock out background had only minor effects on plaque characteristics when challenged with an atherogenic diet. Interestingly, triglyceride levels positively correlated with calcification markers both *in vivo* and *ex vivo*, suggesting a role for triglyceride rich lipoproteins in the

stabilisation of plaques. Furthermore, the results for triglyceride involvement in VC carried into *in vivo* studies using pro-atherogenic Apo E knockout and pro-atherogenic/pro-calcification Apo E x OPG double knock out mice fed an atherogenic diet for 40 weeks and infused with HDL during the final 4 weeks of the study. Alongside the *in vivo* results, the triglyceride level in human plasma correlated with calcification markers in *ex vivo* human studies. While we expected to see changes in correlation with Lp(a) levels, none were detected in this thesis, prompting more precise investigation in the future when examining this particle. This thesis therefore shows roles for several lipoprotein forms in vascular calcification in standardised experiments, providing a starting point for comparison and further experimentation in the future. In continuing this research, a broader spectrum of markers will need to be analysed and further mechanistic studies would provide insight into molecules which may be therapeutically targeted for late-stage and culprit plaque stabilisation.

Acknowledgements

What a journey! Over the last 4 years, not only have I faced many academic and professional challenges, but also many personal challenges. The end result was well worth it however, as through this PhD I have learnt a huge deal about resilience and have made many new lifelong friends, alongside dear colleagues and mentors. First and foremost, there are a handful of people who were instrumental to me making it through this PhD. They include my supervisors, immediate family and closest friends, who listened not only to my successes but also to my worries, and often just general complaining!

To my supervisors Steve and Belinda, thank you so much for always providing the support I needed through every stage of my PhD. Although having no internal supervisors for half of my PhD is unconventional, I always felt supported and heard. You both have supported me through difficult times, helped me grow my knowledge of science, introduced me to careers, provided me with invaluable opportunities and generously donated your time to help me make big decisions about my future. I have never heard of better supervisors and I feel extremely lucky to have done a PhD with no regrets.

To my family, even though some parts you might not have understood, you all supported me through this journey anyway, thank you. To my mum, Jennifer, your support of my education and personal life has been a blessing. You have always been there for me, whether by providing a loving home or by dropping me into SAHMRI! I'm grateful to have such a wonderful mum. To my dad, grandparents, uncles, aunts and cousins, thank you for always supporting me and providing encouragement and perspective on several aspects of the PhD Journey.

To Jocelyne, I am so lucky to have such a wonderful friend to complete this PhD with! Without you, the journey would not be anywhere near as fun and I'm sure much more

difficult. To Laura, Ben, Panashe and Zarah, the lunch breaks, coffee breaks and social outings were the best! Looking forward to many more in the years to come! To everyone in the Vascular Research Centre, Thank you for your friendship, scientific guidance and emotional support throughout the years. I hold many memories with you all very dear and can't wait to see where everyone will be in the years to come. To the core-lab guys, thank you for always lending an ear and making such a great team environment. To the Psalties and Bursill-Tans/Johans (the lab members), I will miss working in the lab with such a fun group of people! To the support staff, bioresources and admin staff, your support has made the completion of this thesis so much more efficient and your advice has been invaluable. To Peter, Chris, Jo and Johan, I have enjoyed learning from and collaborating with each of you and I am grateful to have received your advice.

To my wonderful friends Tanya, Vic, Tim, Thom, Martha, Michelle, Willa and many others, your support has been a blessing and I am lucky to have a group of friends who try to understand my project. I can't wait to celebrate with you all! Lastly, to my partner Nick, thank you for enduring this rollercoaster for the last year. Not only have you supported me by looking through overly complicated figures and sentences, but you have giving me space and encouragement to complete my PhD. I will always be grateful for your support.

Publications

1. **Emma Akers**, Stephen Nicholls, Belinda Di Bartolo. Plaque calcification: Do lipoproteins have a role? *Atherosclerosis, Thrombosis and Vascular Biology, Volume 39, Issue 10, Page 1902-1910, August 29th, 2019*
2. Stephen Nicholls, **Emma Akers**, Belinda Di Bartolo. Vascular Calcification in Response to Pharmacological Interventions. Elsevier, *Book Chapter in Coronary Calcium, Chapter 7, Page 181, January 1st, 2019*
3. Jiawen Li, Simon Thiele, Bryden Quirk, Rodney Kirk, Johan Verjans, **Emma Akers**, Christina Bursill, Stephen Nicholls, Alois M. Herkommer, Harald Giessen, Robert A. McLaughlin. Ultrathin monolithic 3D printed OCT endoscope for preclinical and clinical use. *Light: Science & Applications, Volume 9, Article Number 124, July 20th, 2020*
4. Fiona Young, John Drummond, **Emma Akers**, Louise Bartle, David Kennedy and Mohammad Asaduzzaman. Effects of ovarian disaggregation on adult murine follicle yield and viability. *Reproduction, Fertility and Development, Volume 29, Issue 12, June 1st, 2017*

Presentations

Oral Presentations

Oct 2019 Melbourne, AUS - Australian Atherosclerosis Society – Reconstituted high-density lipoproteins modulate vascular calcification: Potential implications for plaque stability

May 2019 Maastricht, Netherlands – European Atherosclerosis Society – Lipoproteins and their modified forms regulate early stage vascular smooth muscle cell calcification

Nov 2018 Adelaide, AUS - Australian Atherosclerosis Society - The role of lipoproteins in vascular calcification

Oct 2018 Adelaide, AUS - Australian Atherosclerosis Society - The role of lipoproteins in vascular calcification

Oct 2018 Adelaide, AUS - SAHMRI Annual Scientific Meeting - The role of lipoproteins in vascular calcification

Aug 2018 Adelaide, AUS - SAHMRI Heart Health Seminar Invited Speaker - The role of lipoproteins in vascular calcification

Aug 2018 Adelaide, AUS - Adelaide Uni 3 Minute Thesis Competition - Curing cardiovascular disease: Can we hijack the risk factors?

June 2018 Adelaide, AUS - Australian Society for Medical Research - The role of lipoproteins in vascular calcification

Oct 2017 Sydney, AUS - Australian Atherosclerosis Society - Lipoproteins and their modified forms regulate smooth muscle cell calcification

June 2017 Adelaide, AUS - Australian Society for Medical Research - Lipoproteins and their modified forms regulate smooth muscle cell calcification

June 2017 Adelaide, AUS - SAHMRI Heart Health Seminar Invited Speaker - Lipoproteins and their modified forms regulate smooth muscle cell calcification

Poster Presentations

Oct 2019 Melbourne, AUS - Australian Atherosclerosis Society - The impact of very low-density lipoproteins and Apo CIII in vascular calcification

Oct 2019 Melbourne, AUS - Australian Atherosclerosis Society - Reconstituted high-density lipoproteins modulate vascular calcification: Potential implications for plaque stability

May 2019, Boston, USA - Atherosclerosis, Thrombosis and Vascular Biology - Lipoproteins and their modified forms regulate early stage vascular smooth muscle cell calcification

Nov 2018 Adelaide, AUS - Heart Foundation Research Day - The role of lipoproteins in vascular calcification

Sept 2018 Adelaide, AUS - Florey Research Showcase - The role of lipoproteins in vascular calcification

May 2018 San Francisco, USA - Atherosclerosis, Thrombosis and Vascular Biology (Presented by Dr Belinda Di Bartolo) - Lipoproteins influence vascular smooth muscle cell calcification in vitro and in vivo

Oct 2017 Adelaide, AUS - SAHMRI Annual Scientific Meeting - Lipoproteins and their modified forms regulate smooth muscle cell calcification

Sept 2017 Adelaide, AUS - Florey Research Showcase - Lipoproteins and their modified forms regulate smooth muscle cell calcification

Committees and Community Engagement

2019 University of Adelaide Undergraduate Medicine Interviews - Interviewer

2019 SAHMRI Social Committee - Committee Member: Sports

2019- 20 European Atherosclerosis Society - Member

2019 Science Week Student Showcase - ASMR Demonstrator

2019 Highschool Visits to Adelaide University - Presenter for Careers in Medical Research

2018 University of Adelaide Executive Dean Student Leaders Group - HeSPA Committee Representative

2018-2020 Health Sciences Post-Graduate Association Committee (HeSPA) - Committee Member: Secretary

2018 SAHMRI REC Meeting Attendee - SAHMRI Student Association Committee Representative

2017-21 Australian Atherosclerosis Society - Member

2017-21 Australian Society for Medical Research - Member

2017- 2019 SAHMRI Student Association Committee (SSAC) - Committee Member

2017-18 Events

2018-19 Treasurer

2016-20 SAHMRI Animal User Group - Member

2015-Present St. Vincent's Hospital Student's Society - Member/Alumni

Awards and Grants

2019 Australian Atherosclerosis Society - Travel grant

2019 Australian Atherosclerosis Society - International Travel Grant

2019 Adelaide Graduate Centre - International Travel Grant

2019 Walter and Dorothy Duncan Trust - International Travel Grant

2019 European Atherosclerosis Society - Research travel fellowship

2019 University of Adelaide - 3MT Faculty Finalist

2018 University of Adelaide - 3MT Faculty Finalist

2018 IMNIS Program - Industry mentor program

2017 Lion's Medical Research Foundation - PhD top-up scholarship

2017 Research Training Program - PhD scholarship

Abbreviations

Abbreviation	Full Name
ABCA1	ATP-Binding Cassette A1
ABCG1	ATP-Binding Cassette G1
ACAT	Acetyl-CoA Acetyl-Transferase
AD	Atherogenic Diet
AGE	Advanced Glycation End Product
AKT	Also known as Protein Kinase B (PKB)
ALP	Alkaline Phosphatase
Apo	Apolipoprotein
AR	Aortic Root Leaflets
AR	Aortic Root Leaflets
ARS	Alizarin Red S
ARS	Alizarin Red S
ATP	Adenosine Tri-Phosphate
BCA	Brachiocephalic Artery
BCA	Brachiocephalic Artery
BMP	Bone Morphogenic Protein
Ca	Calcium
CAC	Coronary Artery Calcification
CAD	Coronary Artery Disease

cAMP	Cyclic Adenosine Monophosphate
$CaPO_4$	Calcium Phosphate
CE	Cholesterol Ester
CETP	Cholesteryl Ester Transfer Protein
CKD	Chronic Kidney Disease
CM	Calcification Medium
Cu	Copper
CVD	Cardiovascular Disease
EC	Endothelial Cell
ECM	Extracellular Matrix
ELISA	Enzyme-Linked Immunosorbent Assay
ER	Endoplasmic Reticulum
ERK	Extracellular-Signal Regulated Kinase
FGF23	Fibroblast Growth Factor 23
FH	Familial Hypercholesterolemia
FSH	Follicle Stimulating Hormone
GoF	Gain of Function
GWAS	Genome Wide Association Studies
H&E	Haematoxylin and Eosin
H_2O_2	Hydrogen Peroxide
HDL	High Density Lipoprotein

HMGCoAR	3-hydroxy-3-methylglutaryl-CoEnzyme A Reductase
HOCl	Hypochlorous Acid
ICAM	Intracellular Adhesion Molecule
IDL	Intermediate Density Lipoprotein
IL	Interleukin
JNK	c-Jun-N Terminal Kinase
LCAT	Lecithin:Cholesterol Acyltransferase
LDL	Low Density Lipoprotein
LDLR	LDL Receptor
Lp(a)	Lipoprotein (a)
LRP1	LDL Receptor-Related Protein
MAPK	Mitogen Activated Protein Kinase
MGP	Matrix Gla Protein
miRNA	Micro RNA
MITF	Microphthalmia-Associated Transcription Factor
MMP	Matrix Metalloproteinase
MPO	Myeloperoxidase
mRNA	Messenger RNA
mTOR	Mechanistic Target of Rapamycin
MV	Matrix Vesicles
NETs	Neutrophil Extracellular Traps

OCN	Osteocalcin
OPG	Osteoprotegerin
OPN	Osteopontin
ox	Oxidised
PBS	Phosphate Buffered Saline
PCSK9	Proprotein convertase subtilisin/kexin type 9
PECAM	Platelet Endothelial Cell Adhesion Molecule
PI3K	Phosphoinositide 3-Kinase
PLCy	Phospholipase C gamma
PLPC	1-Palmitoyl-2-linoeoyl-sn-glycero-3-phosphocholine (16:0-18:2 PC)
PO_4	Phosphate
PON1	Paraoxonase 1
PTH	Parathyroid Hormone
qRT-PCR	Quantitative Real Time Polymerase Chain Reaction
RAGE	Advanced Glycation End Product Receptor
RANK	Receptor Activator of NF-κB
RANKL	Receptor Activator of NF-κB Ligand
rHDL	Reconstituted High Density Lipoprotein
RNA	Ribonucleic Acid
ROS	Reactive Oxygen Species

Runx2	Runt-Related Transcription Factor 2
SMαActin	Smooth Muscle α Actin
SR-B1	Scavenger Receptor, Class B type 1
Src	Proto-Oncogene Tyrosine-Protein Kinase
SREBP	Sterol Regulatory Element Binding Protein
TGF	Transforming Growth Factor
TNF-α	Tumour Necrosis Factor alpha
TRAF	TNF-Receptor Associated Factor
TRAIL	TNF-Related Apoptosis-Inducing Ligand
TRL	Triglyceride Rich Lipoprotein
VC	Vascular Calcification
VCAM	Vascular Cell Adhesion Molecule
VEGF	Vascular Endothelial Growth Factor
VLDL	Very Low Density Lipoprotein
VLDLR	VLDL Receptor
VSMC	Vascular Smooth Muscle Cell
WB	Western Blot
WNT	Wingless-Related Integration Site

1 : Chapter One

Introduction

Vascular calcification (VC) is to date an untreatable phenomenon, characterised by the development of calcium phosphate ($CaPO_4$) crystals in the artery wall in a process mirroring bone formation. Although the molecular mechanisms behind VC are becoming clearer, there remains a lack of understanding surrounding the initiating factors of the disease. As lipoproteins, cholesterol transport vesicles, interact with artery walls to modulate plaque development, this thesis investigates the hypothesis that lipoproteins will have an additional role in modulating atherosclerotic VC.

This thesis aims to address this issue over 4 results chapters, whereby an *in vitro* calcification assay is developed in chapter 3 to be used in chapters 4, 5 and 6 to assess the calcification potentials of VLDL, LDL and HDL respectively, and their oxidised and/or reconstituted forms. Briefly, we discovered a progressive role for oxidised lipoproteins in vascular calcification and a potentially protective role for HDL. Furthermore, we identified potential roles for these lipoproteins in the modulation of calcification or its co-markers *in vivo* and *ex situ*. Upon reflection of this thesis, we now have numerous leads to follow to better understand the development and potential therapeutics for this disease. All diagrammatic figures in this thesis were created with BioRender.com.

1.1 Cardiovascular Disease

As the cause of ~17.9 million deaths in 2016, with 85% due to heart attack or stroke, and with a predicted death estimate of >23 million by 2030, cardiovascular disease (CVD) remains the leading cause of death worldwide [1]. Despite efforts made by cardiologists, researchers, general practitioners, dietitians, fitness professionals and a myriad of other health professionals, and although from 2000 -2015 the mortality rates from CVD declined by 7%[2], CVD remains the leading cause of mortality worldwide[3].

Although information on CVD prevention is now widely distributed and understood by the general population, CVD continues to grow. Most notably, cholesterol measurements are strongly correlated with risk of cardiovascular events[4, 5] as high plasma cholesterol affects approximately 40% of the global population[6, 7]. Common factors which also influence cardiovascular risk include hypertension, age[8], childhood obesity and hypertension[9], regular aerobic exercise[10, 11], sleep quality[12], race[13], gender[14] and cigarette smoking[15, 16], almost all of which have the potential to be controlled by lifestyle. Interestingly, psychological analysis reveals that the language used on social media was also able to predict the mortality rate, in the USA at the county level, of atherosclerotic heart disease[17].

1.2 Atherosclerosis

Atherosclerosis is fundamentally an accumulation of lipids and cells in an artery wall. This deposition of materials is often referred to as arterial plaques and causes the blockage of arteries by either growing too large or by rupturing, initiating uncontrolled blood clot formations (thrombosis). Depending on the artery affected by the plaque, a range of different clinical outcomes are possible, including myocardial infarction (heart attack), stroke and tissue ischemia (loss of oxygen from lack of blood) leading to organ failure or limb amputations (for example in peripheral arterial disease).

The initiation of atherosclerosis commences early in life, depending on lifestyle factors and genetics, and can begin as early as childhood and often in adolescence[18, 19]. These plaques continue to grow throughout life, until they become obstructive and resistant to treatment[20]. Resulting from the human predisposition to atherosclerosis development, preventative methods are often too late, or too difficult for patients to follow in western culture. It is for this reason therapeutic discoveries to target late stage plaque regression or stabilisation are in need to reduce cardiovascular morbidities and mortalities.

The complexity of atherosclerosis arises from the involvement of a large variety of cell types and molecules involved in disease progression. Plaques develop through delicate imbalances in the local biology of the artery wall, as stimulated by sheer stress, oxidative stress, injury responses, circulating blood components, the response to other local modifications or any combination of these. Understanding the vascular regulation of atherosclerosis, the involvement of other tissues in molecular regulation of blood components and the contribution of these circulating components themselves is therefore vital for the development of plaque regressing and stabilising therapeutics.

1.2.1 Vascular Structure

Endothelial cells line the luminal side of the artery walls and function to regulate vascular tone[21], maintain homeostasis[22, 23] and prevent any unnecessary migration of large molecules and cells through the vessel wall[23, 24]. Endothelial cells typically maintain a cobblestone like morphology with tight junctions, however these tight junctions between cells become leaky when exposed to environments of high sheer stress, for example at arterial branch points or when exposed to inflammatory molecules[25]. Other stressors such as inflammation[26, 27], dyslipidaemia[28] and hypertension[29], are also able to cause the endothelial cells to express molecules which encourage the migration of white blood cells (leukocytes) into the vessel wall.

The endothelial cells line the innermost layer of the artery; the tunica intima. The tunica intima is comprised of connective tissue and vascular smooth muscle cells (VSMC) which interact with lumen components. As such, the tunica intima is the site of atherosclerosis formation[30]. The following layer, the tunica media, it the thickest layer of the artery wall and comprises VSMCs embedded in a collagenous matrix, rich with elastin and proteoglycans. The VSMCs themselves are responsible for the regulation of the matrix, which can be remodelled via the secretion of matrix vesicles[31, 32]. The tunica media is contained by cell permeable elastic laminae which function to add elasticity and barriers to the artery[33]. The outermost layer of the artery wall, the adventitia, was recently characterised as a hive of atherosclerosis-inducing activity[34]. The adventitial layer contains fibroblasts, collagen, nerves, lymphatics, adipose cells and importantly blood vessels. These blood vessels, called the vasa vasorum, transport blood nutrients to the artery wall itself and as such provide a second entry portal for circulating component infiltration[35]. The adventitial milieu also supports stem cells, capable of differentiating into many of the cells required for both vessel repair and atherosclerosis[36] (figure 1.2.1).

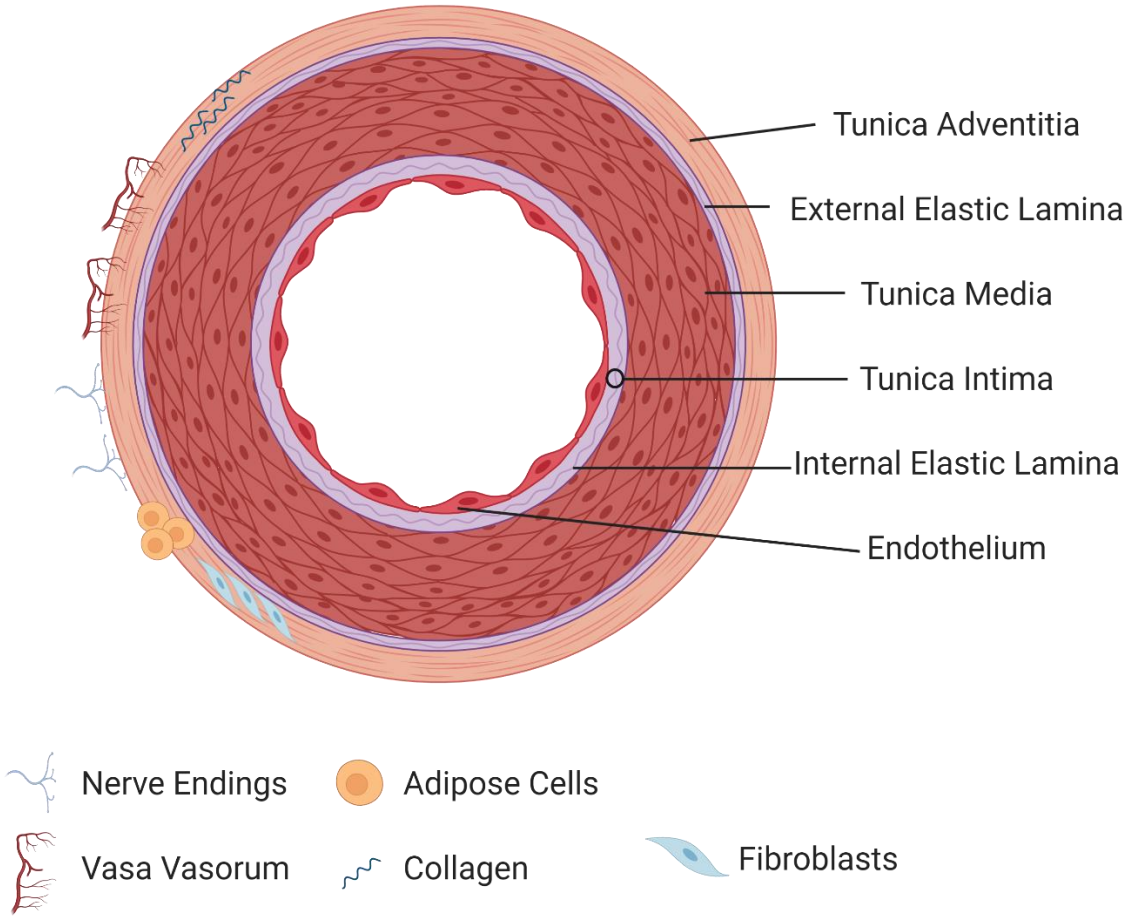

Figure 1.2.1.1 Structure of the artery wall.

1.2.2 Initial Phase of Atherosclerosis –Sheer Stress and Leukocytes

As mentioned above, shear stress or other factors initiate the process of atherosclerosis by increasing the leaky junctions on the endothelial lining. Shear stress also inflames the endothelial cells, increasing their expression of adhesion molecules such as P-selectin, vascular cell adhesion molecule (VCAM, CD106), intercellular adhesion molecule (ICAM, CD54) and platelet endothelial cell adhesion molecule (PECAM, CD31)[37]. Normally, leukocytes would circulate in the bloodstream without interaction with the endothelium, however when the inflamed endothelium expresses these adhesion molecules, leukocyte capture, and transport can occur[38] (figure 1.2.2). Physiologically, this process allows for

the effective healing of wounds[39] and removal of infectious diseases[40]. Pathologically, this process results in the capture and accumulation of lipoproteins and leukocytes into the artery wall, initiating atherosclerotic plaque development[40].

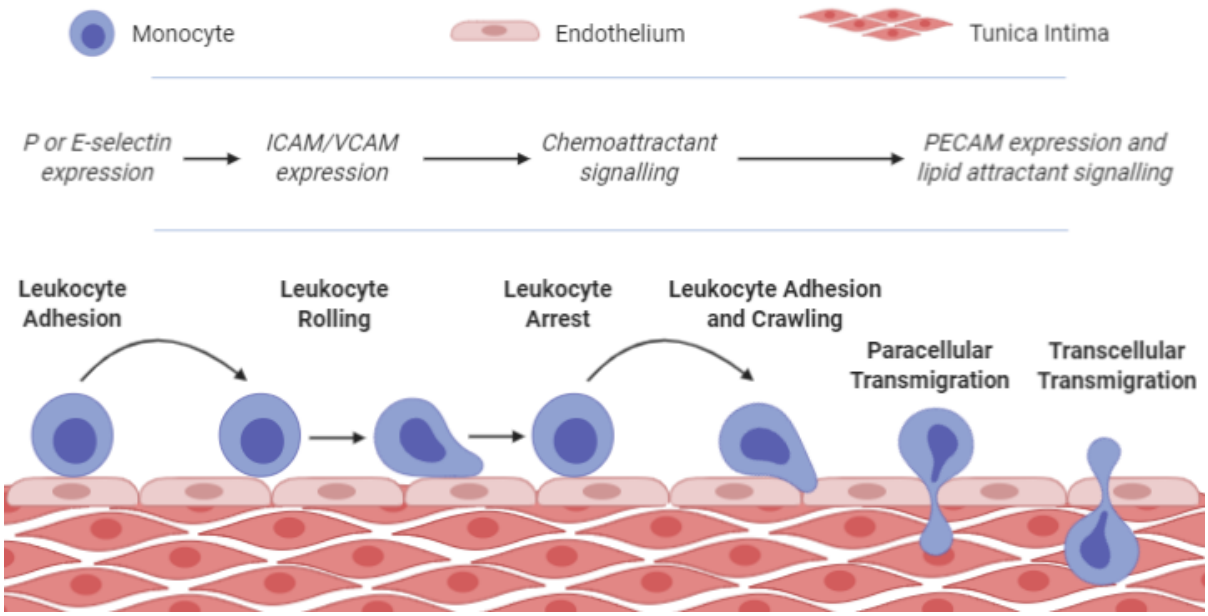

Figure 1.2.2.1 Migration of leukocytes through the endothelium into the tunica media.

In conditions of high plasma cholesterol concentration, the lipoproteins which usually use the vascular network to deliver cholesterol to tissues in need of energy are also captured by and accumulated in the vessel wall[41]. This localisation of leukocytes and cholesterol to the tunica intima increases local inflammation, causing the leukocytes to phagocytose and degrade the lipoproteins[42, 43]. However, due to an inflammatory and often oxidative milieu, this results in further inflammation and the initiation of an atherosclerotic plaque[43].

While all leukocytes have a role in the regulation of atherosclerosis, the most heavily implicated cell type is the monocyte. Once recruited and trapped within the vessel wall, the monocyte differentiates into macrophages able to absorb local cholesterol deposits[44]. The differentiation of these monocytes produces a wide variety of macrophage

classifications with a range of functions; however, we traditionally refer to only 2 subsets, macrophages skewed to either an M1 or M2 phenotype. While M2 macrophages have plaque regressing and stabilising functions, the M1 inflammatory macrophage is the preferential differentiation state in the initial stages of plaque development. These macrophages physiologically function to remove pathogens, and absorbs, degrades and removes cholesterol[45]. Due to their physical appearance under the microscope, cholesterol laden macrophages are referred to as foam cells. Foam cells are dysfunctional, inflammatory cells that accelerate atherosclerosis by encouraging further infiltration of leukocytes and cholesterol, and in the later stages transform into a necrotic core[46].

1.2.3 Mid and Late Stage Atherosclerotic Characteristics

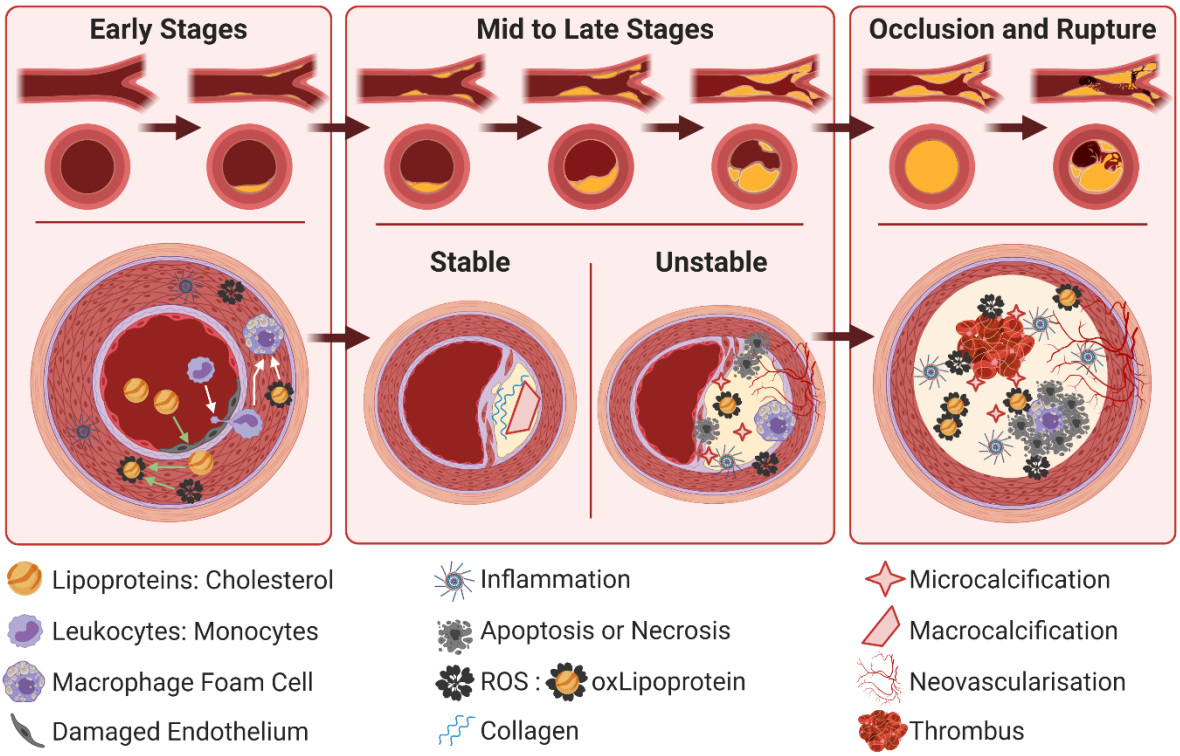

Figure 1.2.3.1 Atherosclerotic plaque progression.

The plaque continues progressing to a stage where it becomes complex with many features, including necrotic cores, vascular calcifications (VCs) and a fibrous cap to contain the plaque contents[47]. As the plaque grows, it may either occlude the vessel via rupture or erosion causing thrombus formation, or via physical size of the plaque (figure 1.2.3). Plaque rupture begins when the fibrous cap becomes compromised, releasing plaque components into the lumen of the vessel[48]. This expulsion of plaque contents actives circulating platelets in order to contain the wound to the artery wall, however from the overload of necrotic and fatty debris, uncontrolled platelet activation occurs[49]. Plaque erosion is a process that occurs with a type of plaque rich with VSMC and proteoglycans at the luminal cap with a small or absent lipid rich core and is the most common cause of thrombosis in premenopausal women. The rough definition of plaque erosion is a thrombus causing plaque without lipid core exposure to lumen. As such, there exists a large amount of heterogeneity in plaque characteristics, the causes of resulting thrombi and molecular mechanisms behind these characteristics and causes[50].

A fibrous cap lines the luminal edge of the developed plaque and functions as a structural barrier to the plaque. Fibrous cap formation occurs as a result of VSMC migration and collagen deposition. Plaques with thin fibrous caps are more likely to rupture, cause thrombus formation and cardiovascular events[51]. The composition of the plaque and cap also affects its stability. Collagenous fibres act to hold the plaque together through the fibrous cap[52, 53] and also form the structure of the arterial extracellular matrix, contributing to arterial stiffness[53]. Collagen also adds to the stability of an atherosclerotic plaque[54, 55]. Foam cells trapped in the plaque eventually undergo necrosis, or apoptosis in some cases. The resulting necrotic cores within the plaques significantly correlate to decreased plaque stability[51]. Another feature of unstable plaques are cholesterol crystals. With sharp edges,

large size and inflammatory properties, cholesterol crystals create the perfect environment for puncture of a thin fibrous cap and subsequent rupture and thrombus formation[56].

In the latest stages of plaque progression, a source of fuel is required to maintain and increase the proliferation rate of the inflammatory cells involved. To achieve this, the vasa vasorum grows capillaries into the plaque, called neovascularisation. This neo-vasculature supplies the plaque with nutrients from the plasma needed to continue growth[57].

Beginning late in the early stages of plaque development, and continuing into the latest stages, vascular calcification (VC) plays a vital role in plaque stability. Briefly, the size[58] and location[59] of the calcium crystals affects the likelihood of plaque rupture, with mineralization occurring in a process mirroring that of bone marrow formation. As the topic of this thesis focuses on VC, an extended introduction on this process is presented later in this chapter.

1.3 Lipoproteins

1.3.1 Overview of Lipoproteins

Cholesterol is transported through the body in specialised vesicles called lipoproteins. The functionality of these lipoproteins, whether they transport cholesterol to or from peripheral tissues, are dependent on their surface protein (apolipoprotein) content. The different lipoproteins are traditionally labelled by their density (<0.95 - 1.21 g/mL) or size (10 -1000 nm), however more modern techniques have allowed the classification of lipoproteins to extend beyond physical characteristics and into molecular compositions, such as protein, lipid and RNA content, allowing for an almost infinite number of lipoprotein subsets.

The lipoproteins used in this thesis are high density lipoproteins (HDLs), low density lipoproteins (LDLs), lipoprotein (a) (Lp(a)), and triglyceride rich lipoproteins (TRLs) focusing

on very low density lipoproteins (VLDLs) (figure 1.3.1). Briefly, HDL is generally regarded as anti-atherogenic due to its capacity to efflux cholesterol away from peripheral tissues, whereas LDL, Lp(a) and TRLs are considered pro-atherogenic lipoproteins as they function to deliver cholesterol and triglycerides to the peripheral tissues, including the artery wall. Lipoproteins can perform these functions because of their apolipoprotein content and in the context of atherosclerosis, these apolipoproteins bind to receptors in the artery wall.

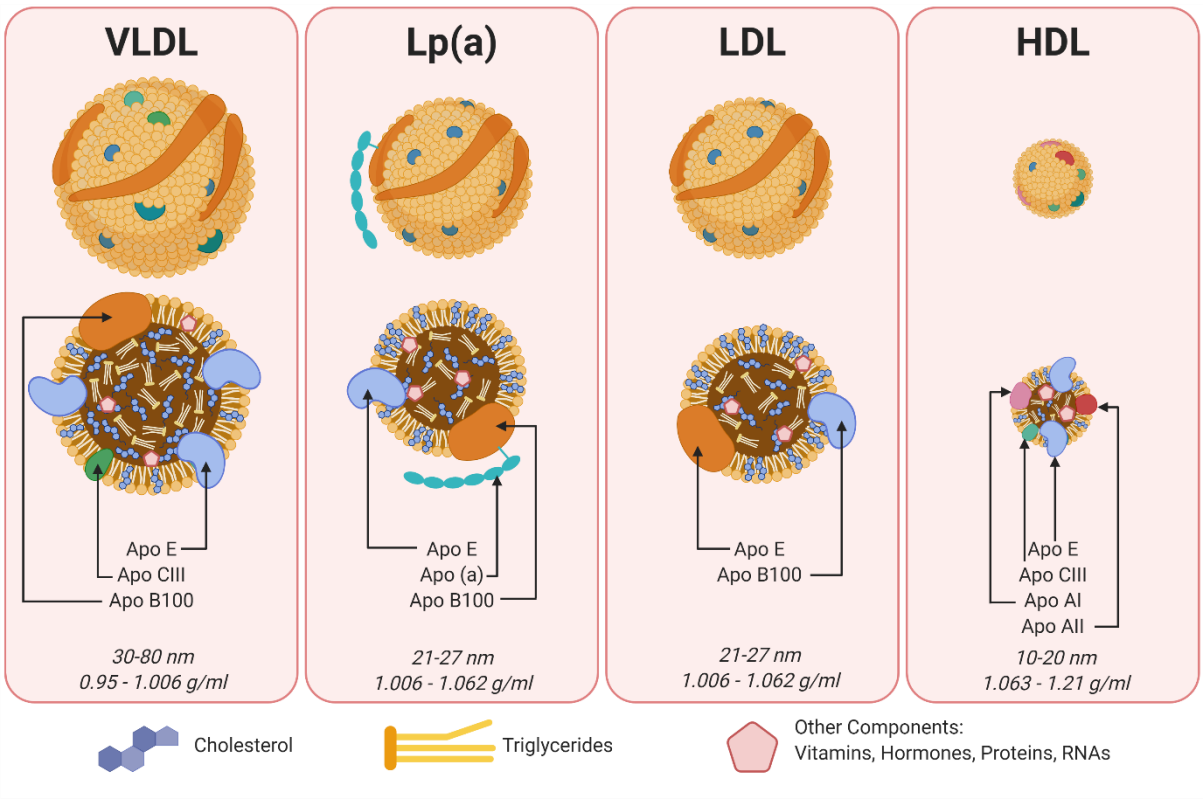

Figure 1.3.1.1 Generalisation schematic of lipoprotein subclasses.

1.3.2 High Density Lipoproteins

High density lipoproteins (HDL) are often referred to as 'good cholesterol' in lay terms due to the particle's role in cholesterol efflux from peripheral tissues and artery wall. The particle itself has a density of approximately 1.063 – 1.21 g/mL and a diameter of approximately 10-20 nm[60]. The known anti-atherogenic[61], anti-oxidative[62] and anti-

inflammatory[63] properties of HDL arise from a combination of components, however, rely heavily upon the primary surface apolipoprotein (apo) AI concentration and bioavailability[64]. Although extremely heterogenous in nature, the HDL particle generally contains 35 – 50% phospholipids, 5 - 10% sphingolipids, 5 - 10% steroids, 5 - 12% triacyl-glycerides and 30 - 40% cholesterol esters[65] as a percentage of total lipid weight. The lipid composition of the HDL particle has a direct effect on the functionality of the particle.

HDLs are released from the liver as pre-β, or discoidal HDLs capable of accepting cholesterols. The particle then transports its cargo to the liver and intestine for excretion. As such, the lipid composition of either discoidal or mature HDL heavily influences its cholesterol efflux capacity[66-68], and even its anti-oxidative[69-71], anti-inflammatory[72] and vasodilatory[73] status, via influence over bilayer fluidity or apolipoprotein bioavailability. As such, the lipid contents of man-made, reconstituted HDLs (rHDLs) typically containing only phospholipid and apo AI can be carefully selected for ideal membrane fluidity[74]. The complexity and variation of HDL can be expanded upon further when considering their ability to carry miRNAs[75]. Although from the discovery of HDL resident miRNAs other small noncoding RNAs, such as small nucleolar RNAs (snoRNAs), small nuclear RNAs (snRNAs) and transport RNA fragments (tRFs), are hypothesised to also be present on the particle, there is currently no experimental data to confirm this, and minimal data exploring the roles of the HDL transcriptome. It is clear however that there are differences in the HDL transcriptome between healthy and diseased subjects[76].

HDL or HDL functionality is associated with a protection from[77-84] and regression of[85] coronary artery disease (CAD). As HDL from CAD patients has impaired anti-inflammatory and antioxidant functionality[86] and has no benefit to CVD [87], the functionality of HDL has a significant role in atherogenesis. In addition to lipids, a number of proteins including apolipoproteins (Apo), such as Apo AI and Apo E, and cholesterol modification proteins,

such as lecithin:cholesterol acyltransferase (LCAT) are present on or in HDL which perform varying tasks influencing coronary artery disease[88]. The primary surface apolipoproteins apo AI and apo AII comprise of 70% and 20% of total HDL particle weight respectively[89], and are responsible for mediating cholesterol efflux into the HDL particle. In humans, the main surface protein Apo AI is also subject to genetic mutations found to increase functionality despite treatment resistant lipid and lipoprotein abnormalities. In particular Apo $AI_{(Milano)}$[90] and Apo $AI_{(Paris)}$[91], named after the cities in which these populations were found. Although *in vivo*[92] and early clinical studies[85] using Apo $AI_{(Milano)}$ in rHDLs highlighted an athero-protective role for the particle, in large scale clinical trials this benefit was not observed above statin therapy[93] and interest in the therapeutic faded. Moreover, other HDL mimetics were not found to benefit plaque burden[94] are yet to demonstrate clinical benefit in addition to statin therapy[95].

To summarise, HDLs are highly variable lipoproteins, with differing lipid efflux functions depending on particle maturity and bioavailability of Apo AI. The anti-atherogenic properties of HDL can also be partly explained by the particle's anti-inflammatory and anti-oxidative effects.

1.3.3 Low Density Lipoprotein

Low density lipoprotein (LDL), conversely to HDL, is often referred to as 'bad cholesterol' as it delivers cholesterol to peripheral tissues via binding to its receptor (LDLR) through interactions with apolipoprotein (apo) E or apo B-100. While this is physiologically important, pathologically high LDL levels contribute to atherosclerosis[96]. As such, LDL cholesterol (LDL-C) accounts for 60-70% of plasma cholesterol and is a major independent risk factor for cardiovascular disease[5], apo B-100 levels predict cardiovascular events[97] and pathologically dysfunctional, oxidised LDL causes increased atherosclerosis[98].

The size of LDL typically ranges from 21-27 nm in diameter and LDL has a density of 1.006-1.062 g/mL[99]. Above general atherogenicity of LDL particles, small LDL particles are particularly atherogenic[100]. The individual LDL particles are extremely heterogeneous in their lipid content and the varying lipid profiles have also been implicated in the atherogenicity of the particle[101, 102]. None-the-less, therapeutics targeting general lowering of LDL-C, including statins, are widely prescribed for their benefits to CVD[103]. A lower LDL level, achieved by either genetics[104] or by lowering therapeutic intervention[105-107] reduces risk of cardiovascular events, with LDL reducing therapies estimated to reduce risk of events by 40-50% per 2-3 mmol/L (approx. 75 – 115 mg/dL) reduction in LDL-C[106]. This LDL lowering effect is however most greatly benefitted by the patients who have high initial levels of LDL-C (higher than 100 mg/dL)[108].

Statins, also 3-hydroxy-3-methylglutaryl-coenzyme A reductase (HMGCoAR) inhibitors, inhibit the *de novo* synthesis of cholesterol[109]. Proprotein convertase subtilisin/kexin type 9 (PCSK9) inhibitors however work by inhibiting the accelerated degradation of the LDLR by its interaction with PSCK9, allowing improved clearance of LDL-C from the plasma[110]. The use of both these therapeutics therefore has such striking effects on CVD by lowering LDL-C. Loss of function genetic mutations in the LDLR cause a disease in humans termed familial hypercholesterolemia (FH) and as the name suggests, is an inherited phenotype of high LDL-C[111]. Patients with FH have an impaired clearance of LDL-C leading to atherosclerosis in the arterial wall and as a result, a significantly increased risk of cardiovascular events[112]. Treatment of these patients from a young age with statins however results in fewer events, even after 20 years of therapy[113]. This disease clearly demonstrates the detrimental effects of high LDL-C on atherosclerosis.

1.3.4 Lipoprotein (a)

Lipoprotein (a) (Lp(a)), pronounced 'L P little A', is an LDL particle, with an apolipoprotein (a) (apo(a)) bound to the surface of its apoB-100 protein and is cleared from the plasma through the LDLR[114]. Apo(a) is only expressed in humans and primates and the hedgehog, presenting difficulties in designing animal studies. The apo(a) gene itself is also highly variable, with over 20 variations per allele. Generally, the shorter the length of the tandem repeat locus, the higher and the more atherogenic the Lp(a) levels[115]. Genome wide association studies (GWASs) identify a causative role for Lp(a) in CVD[116]. While the current hypothesis is that the physiological role of Lp(a) is to scavenge reactive oxygen species (ROS), in pathological conditions this increased ROS on Lp(a) is speculated to exacerbate atherosclerosis[117]. It should be noted however that while this is the current hypothesis, it has not been conclusively proven and the physiological role(s) of Lp(a) remain(s) largely unknown. Moreover, Lp(a) accumulates in atherosclerotic plaques[118-120], supporting the GWAS data.

1.3.5 Triglyceride Rich Lipoproteins

Triglyceride rich lipoproteins (TRLs) are responsible for transporting triglycerides throughout the body and are widely recognised as indicators of CVD. Emerging evidence now suggests a more causative role for these particles in the pathogenesis of atherosclerosis[121], with clinical trials showing additional risk of high TRL levels beyond low density lipoprotein (LDL) levels[122].

TRLs can be divided further into 2 main lipoprotein classes: the very low density lipoproteins (VLDLs) and chylomicrons. VLDL is around 30 - 80 nm in diameter and have a density of 0.95 - 1.006 g/ml, whereas chylomicrons are around 75 – 600 nm in diameter and have a density of <0.95 g/ml. Furthermore, while phospholipids constitute around

20% of VLDL, they only represent 7% of chylomicrons[123]. Although large TRLs, such as large VLDL and chylomicrons are unable to penetrate the artery wall due to their size[124], pathological effects of TRLs in atherosclerosis can be attributed to their smaller remnants[125], often referred to as β-VLDL. These TRL remnants are retained in the arterial wall matrix[126] and have been identified within the atherosclerotic plaques of rabbits[125, 127]. Once in the artery wall, the remnants are implicated in foam cell formation[128, 129], impaired endothelial function[130, 131], activated leukocytes[132], VSMC proliferation[133] and contribute to local inflammation[134, 135]. These effects in combination with epidemiological data[136, 137] suggests a causal role for TRLs in atherosclerosis.

1.3.6 Lipoprotein Modifications

A significant component in the initiation of atherosclerosis is the modification of lipoproteins. Discussed here are the main forms of lipoprotein modifications which affect CVD: oxidation, glycation and acetylation. The roles of specific lipoprotein modifications and their effects of vascular calcification will be discussed in appropriate results chapters.

1.3.6.1 Oxidation

The most discussed lipoprotein modification is oxidation, due to the significant role of oxidised LDL (oxLDL) and oxidised HDL (oxHDL) in atherogenesis. Lipoproteins have varying levels of oxidation. Components including apolipoproteins, phospholipids and core lipids can be oxidised individually or as a combination, and all can have varying oxidative saturation. Lipoproteins typically become oxidised within the arterial wall, however small amounts of oxidation catalysts can be detected in the plasma[138]. As lipoproteins oxidise, they lose oxidation substrates, vitamin E and other particle resident anti-oxidants alongside the emission of oxidative end products. *Ex vivo*, a variety of methods are used to obtain varying degrees of oxidation and its detection.

Copper (II) ion (Cu(II)) mixtures are routinely used to achieve total or partial particle oxidation, the most studied being LDL. 5μM was found to be the optimal Cu(II) concentration[139], with no benefit in lag time or oxidation rate when the concentration was increased to 10μM[139, 140]. The LDL particle has a finite number of copper binding sites[141], enabling partial oxidation by reducing Cu(II) ion concentrations to between 0.1 and 0.5μM[142]. Furthermore, temperature of the Cu(II) ion oxidation influences reaction rate[139, 140]. Due to the 31.1°C melting point of the LDL core[140], a reaction temperature of 37°C is routinely used. In addition, particle concentration, typically between 0.025 and 0.25 g LDL protein/L[139], cholesterol concentration and lipid hydroperoxide content also influence Cu(II)-dependant oxidation[143]. As such, hydrogen peroxide is often added to reactions to stimulate lipid peroxide formation for the induction of oxidation[144, 145]. Other metal ions, such as iron, may also catalyse the oxidation reaction.

The other commonly mentioned and used oxidative catalyst is myeloperoxidase (MPO). Physiologically, MPO is involved in the immune system mostly via the neutrophil network[146] to target and kill pathogens by aiding the conversion of hydrogen peroxide (H_2O_2) into hypochlorous acid (HOCl)[147]. This HOCl then reacts to modify local proteins[148], genetic material[149], lipids[150], sugars[151] and proteoglycans[152] leading to extracellular matrix degradation[152] and releasing radicals in the process[149]. These actions of MPO therefore lead to the leaky junctions characteristic of early atherosclerotic development and MPO remains local to plaques throughout the disease[153], a notion supported by the reduced incidence of myocardial infarctions in MPO deficient human populations[154].

MPO-derived HOCl is also a major requirement for neutrophil extracellular trap (NET) formation[155-157], which are now widely regarded as pro-atherosclerotic and pro-thrombotic compounds[158]. While both the respiratory bi-product H_2O_2 and NET associated MPO generated radicals are vital for immunity, in the context of atherosclerosis NETs can

activate the NLRP3 inflammasome, resulting in IL-1β and IL-18 secretion[159]. In atherosclerosis, while the role of the NLRP3 inflammasome is still debated, it appears as though oxidised LDL also causes activation, leading to an increase in apoptosis, which would then continue to exacerbate plaque progression[160].

The oxidation of HDLs by myeloperoxidase creates a dysfunctional[161], inflammatory[162] particle with profound pro-atherosclerotic effects, including attenuation of endothelial[163] and smooth muscle cell[164] proliferation and migration. MPO is also able to transport on[165] and oxidise[166, 167] LDL, directly[168, 169], or indirectly through local inflammasome activation. It can be converted to an atherogenic form which is more readily scavenged by macrophage CD36 for foam cell formation[170] and induces endothelial dysfunction[171]. As such, MPO oxidised lipoproteins are now widely regarded as heavy contributors to atherogenesis and remain attractive therapeutic targets[172, 173].

1.3.6.2 Glycation

Another important modification, glycated lipoproteins are commonly found in patients with diabetes. The high serum glucose levels lead to the production of advanced glycation end products (AGEs), which through their receptors (RAGEs) have devastating effects on the cardiovascular system. Glycation particularly impacts the extracellular matrix and intracellular signalling molecules, leading to the micro- and macro-vascular complications causative of heart failure, abdominal aortic aneurysms and arterial hardening (vascular calcification)[174].

Glycated HDLs are dysfunctional[175], increase oxidative stress and promote proliferation and migration of VSMCs[176]. Likewise, LDL glycation increases its atherogenicity[177, 178], affecting lipid loading, oxidation and inflammation of VSMCs[179]. Considering that lipoproteins are readily glycated using a simple pathologically high glucose (25 mM) incubation *in vitro*[180], it is not surprising that patients with diabetes have such pronounced

cardiovascular morbidities. Glycaemic control therapies however still leave patients with residual cardiovascular risk[181], confirming that the relationship is more complicated than glycated lipoproteins.

1.3.6.3 Thiolation and Acetylation

Other common modifications, such as thiolation, causing LDL aggregation[182] and acetylation, increasing the affinity of LDL to macrophage scavenger receptors[183] leading to reversible lipid accumulation[184], are also present in the cardiovascular system in diseased states[181]. Through the enormous variations of lipoprotein modifications of specific components, including proteins and lipids, a precise identification is obtained via mass spectrometry[185] or nuclear magnetic resonance (NMR) spectroscopy[186]. As these can be time consuming and costly, typically modifications are measured using either immunochemical techniques (e.g. ELISA, IHC)[187-189] or colorimetric[190] assays. While these assays are less specific as to the modification extent and specifics, they are a speedy and cost effective way to get a snapshot of the lipoprotein's overall modification status.

1.4 Lipoprotein Metabolism

Cholesterol is an essential dietary requirement for higher organisms and has many functions in the human body, including forming dense lipid rafts in cell membranes to enable receptor-mediated signalling[191] and acting as a precursor to formation of bile acids and sterols such as vitamin D. As such, higher organisms have developed finely tuned, complex molecular pathways to regulate the absorption, secretion, transport and removal of cholesterol in the body (figure 1.3.6.1). When these delicate pathways are disturbed, disease pathologies such as atherosclerosis occur.

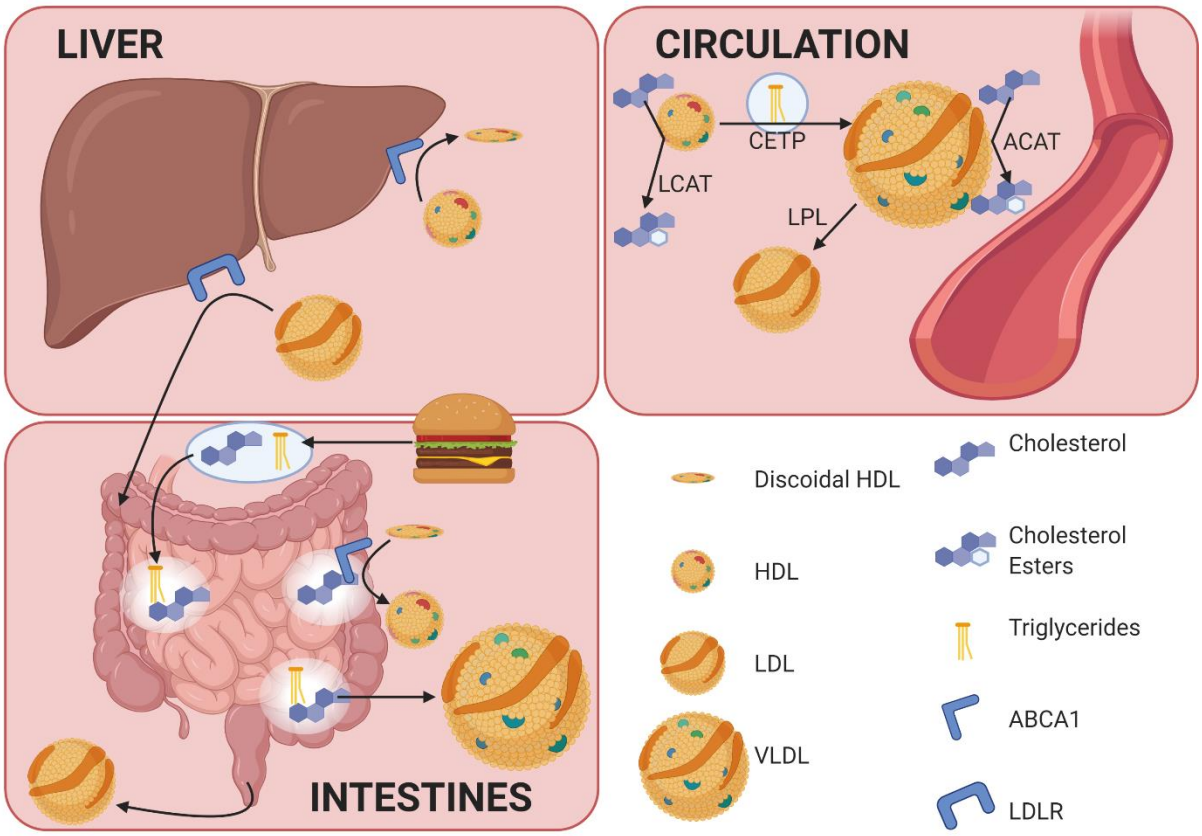

Figure 1.3.6.1 Schematic of lipoprotein metabolism. *Dietary cholesterol and triglycerides enter the intestines after a meal where they are packaged and/or incorporated into VLDL or HDL particles. The particles then enter the circulation, where they undergo modification to enable functional changes in lipoprotein, e.g. VLDL transforming to LDL, or cholesterol transfer. Excess cholesterol from the circulation, or as gathered by HDL from peripheral tissues, may then be delivered back to the liver via HDL recycling. The excess liver cholesterol is then transferred to LDL particles, which may then be excreted by the intestines.*

1.4.1 Lipoprotein Synthesis

After a meal, while there are huge variations between individuals[192] about 50% of the cholesterol consumed enters the body[193], and around 75% of cholesterol absorbed is from intestinal bile secretion of endogenous production[194]. The bile secreted into the intestines

contains mixed micelles, comprising of bile acids and phospholipids, which can solubilise and emulsify dietary lipids. These mixed micelles are then absorbed by the intestinal wall to enter the body, in a process which can be inhibited by administration of ezetimibe[195]. Once in the intestinal walls, cholesterol can be secreted back into the intestinal lumen through the ATP-binding cassette subfamily G member 5 (ABCG5)/G8 transporter or can be incorporated into TRLs or HDL to be secreted into the circulation. Prior to secretion, most of the TRL associated cholesterol is esterified by acetyl-CoA acetyl-transferase 2 (ACAT2)[196], to reduce bioactivity allowing for easier storage and transport. Interestingly, dietary cholesterol influences chylomicron uptake and secretion, whereas HDL secretion is not influenced by intestinal cholesterol changes[197, 198] and mainly absorbs the free cholesterol through ABCA1 binding to Apo AI[199].

In the intestinal cell endoplasmic reticulum (ER), dense apolipoprotein B-48 (apoB-48) vesicles are produced and accumulate triglycerides. As the vesicles move through the ER into the Golgi apparatus, they acquire cholesterol esters and apolipoproteins important for lipid transport before secretion into the lymphatics and then blood stream[199]. Chylomicron triglyceride hydrolysis then leads to the formation of chylomicron remnants, VLDLs, intermediate density lipoproteins (IDLs) and LDLs.

HDLs are secreted from the liver as pre-beta[200] (or nascent) HDL particles, by the combination of apolipoprotein AI with phospholipids, mediated by ATP-binding cassette A1 (ABCA1) [201]. Further modifications of HDL are then regulated within the circulation and peripheral tissues, including cholesterol loading.

1.4.2 Lipoprotein Degradation, Recycling and Excretion

Hepatic uptake of chylomicron remnants, VLDLs, IDLs and LDLs are mainly facilitated through the low-density lipoprotein receptor-related protein 1 (LRP1) and the LDL receptor (LDLR). Once bound, lipoproteins are trafficked to the lysosome for degradation and de-esterification. The free cholesterol is then secreted into the bile in the form of mixed micelles for excretion. The liver is also the likely packaging site for cholesterol in a form that can be delivered to the intestines for excretion[202].

Only a minority of the bound LDLR however is degraded along with the lipoproteins, the majority is recycled for re-capturing the atherogenic lipoproteins[203]. The recycling of the LDLR is a regulated process and is now targetable for treatment by proprotein convertase subtilisin/kexin type 9 (PSCK9) inhibitors and as discovered in the GLAGOV trial, in addition to statin therapy, reduces plaque volume[204].

HDL contents[205, 206] are absorbed in the liver by scavenger receptor, class B type 1 (SR-B1)[207] from lipid laden HDL. Physiologically, in the liver this results in the uptake of the CEs for clearance and recycling of a nascent HDL particle, however pathologically this can result in re-accumulation of lipid.

1.4.3 Lipoproteins in Atherosclerosis and the Plasma

1.4.3.1 Regulation by HDLs

Nascent HDL associated cholesterol is esterified (CE) by (LCAT), forming mature HDL particles, before cholesterol ester transfer protein (CETP) exchange of CE with triglycerides between the mature HDL and LDL or VLDL. As such CETP inhibitors were hypothesised to lower LDL and VLDL cholesterol for athero-protective effects, however promising pre-

clinical results were not observed in large human clinical trials, or were observed in conjunction with other health issues[208].

HDL receives cholesterol from peripheral tissues, such as the artery wall via transfer from ATP-binding cassette A1 (ABCA1) to lipid poor apo AI found on nascent HDL particles[209]. Mutations in ABCA1 lead to an atherosclerotic phenotype termed tangiers disease, whereby patients exhibit deficient HDL levels[210]. Cholesterol accumulates in macrophages[211, 212] and overexpression in mice leads to increased plasma clearance of cholesterol alongside decreased intestinal absorption[211]. Although LDL increases expression of ABCA1 on endothelial cells[213], the failure of nascent HDL to receive lipids leads to their clearance from plasma[214].

ABCG1 is also responsible for the transfer of cholesterol to apo AI associated nascent HDL[215]. ABCG1 cooperates with ABCA1 sequentially, whereby HDL is initially lipidated by ABCA1 then further lipidated by ABCG1[216, 217]. The same ABCA1 and ABCG1 transporters are employed by macrophages for HDL to remove cholesterol from lipid laden macrophages[218] and deficiency of these leads to form foam cells[212]. ABCG1 is also able to prevent inhibition of the beneficial vasodilatory nitric oxide synthesis upon HDL binding[219].

Scavenger receptor, class B type 1 (SR-B1) is a scavenger receptor which accepts esters (cholesterol, vitamins[205], other steroid esters[206]) from lipid laden HDL. Physiologically, in the liver this results in the uptake of the CEs for clearance and recycling of a nascent HDL particle, however pathologically this can result in re-accumulation of lipid. SR-B1 is well conserved between species and is expressed by many of the cells present in the artery wall and plaque, alongside steroidogenic tissues and many others[220]. SR-B1$^{-/-}$ mice therefore have increased lipid laden HDLs[221] and accelerated atherosclerosis[222]. Additionally, SR-B1 is responsible for signalling within the arterial wall[223, 224]. Interestingly,

bone marrow expressed SR-B1 is also protective against atherosclerosis, linking the two tissues and lipoproteins[225].

In addition to its CE uptake properties, binding of apo AI to SR-B1 results in anti-inflammatory gene expression in macrophages[226, 227] and increase phagocytotic activity[227]. Interestingly, in this model of macrophage mediated muscle wound healing, bone marrow SR-B1 expression was necessary[227]. In endothelial cells, it triggers the transcytosis of HDL[228] and LDL[229] into the intimal and medial layers of the artery wall, however HDL inhibits this LDL transcytosis[230]. Endothelial HDL/SR-B1 binding also induces vasodilation via nitric oxide[231] and prostacyclin production[232]. Once in the artery wall, along with its role with the macrophage, SR-B1 mediates travel of HDL through the lymphatics, removing it from the circulation[233]. In addition, HDL reduces the expression of VCAM-1[234], E-selectin[235] and ICAM-1[236] alongside antithrombotic effects[237] in endothelial cells through a variety of mechanisms.

HDL also has associated proteins which modulate its function in addition to LCAT esterifying cholesterols. Paraoxonase 1 (PON1), which prevents oxidation of HDL, aids in the maturation of the lipoprotein[238] and stimulates macrophage cholesterol efflux[239-241]. Upon oxidation of HDL however, PON1 activity is reduced[242], furthering the dysfunctionality of the lipoprotein. Additionally, HDL associated PON1 has been proposed as a link between post-menopausal osteoporosis and CVD[243].

1.4.3.2 Regulation by LDLs and VLDLs

While LDLs and VLDLs can enter the arterial wall via the leaky junctions in the endothelium as described above, they also influence the plaque in an active manner. In conjunction with this, oxidation of lipoproteins, contributes significantly to arterial inflammation and atherosclerosis[244]. This contribution is mostly attributed to scavenger receptor mediated uptake of oxLDL, resulting in foam cell formation[245].

Low density lipoprotein receptor (LDLR), very LDLR (VLDLR) and low density lipoprotein receptor-related proteins (LRPs) are responsible for the transfer of cholesterol to peripheral tissues, including the artery wall. Upon LDLR binding to apo B-100 or apo E, the presenting lipoprotein is endocytosed by the cell, alongside inhibition of HMGCoAR[246, 247] and sterol regulatory element binding proteins (SREBPs)[248], which downregulate LDLR synthesis and activate acyl-CoA cholesterol acyl transferase 1 (ACAT1), which reduces free cholesterol via esterification of excess cholesterol[249].

The apo E portion of binding to LDLR is equally important and is found on both lipoproteins and cells. Apo E on monocytes reduces infiltration into the artery wall[250], is necessary for cholesterol efflux from macrophages[251-253], reduced inflammation[254, 255] and reduced oxidative stress[256-258]. VLDLR is the main receptor for apo E lipoproteins and is expressed in most non-hepatic tissues. As apo-B100 lipoproteins tend to bind to the LDLR, VLDLR primarily accepts and metabolises TRLs[249]. The expression of the VLDLR is regulated by PPAR-γ and overexpression of VLDLR leads to increased storage of TG in epididymal fat[259]. Fasting also leads to VLDLR expression, aiming to scavenge energy rich lipids for tissue usage[260]. VLDLR mediated TRL uptake into endothelial cells[261], up-regulates LPL for TG hydrolysis[261, 262] and storage of TG in adipose tissue[262].

1.5 Vascular Calcification

Vascular calcification (VC) is a feature of atherosclerosis associated with adverse cardiovascular events[263], plaque progression[58] and vulnerability[264]. In patients with diabetes mellitus[265] and chronic kidney disease (CKD)[266], VC is accelerated and contributes to a higher risk of cardiovascular morbidity and mortality. The prevalence of aortic calcification in the general population is 59% for women and 67% for men aged 41-80 years (mean age 61 years)[267]. This increases to 81% in patients with diabetes[268] and to 100% with end-stage renal disease[269] and associates with their cardiovascular co-morbidities and clinical events[270]. As such, measurement of coronary artery calcification (CAC) has been increasingly used to enable accurate cardiovascular risk assessments[271, 272].

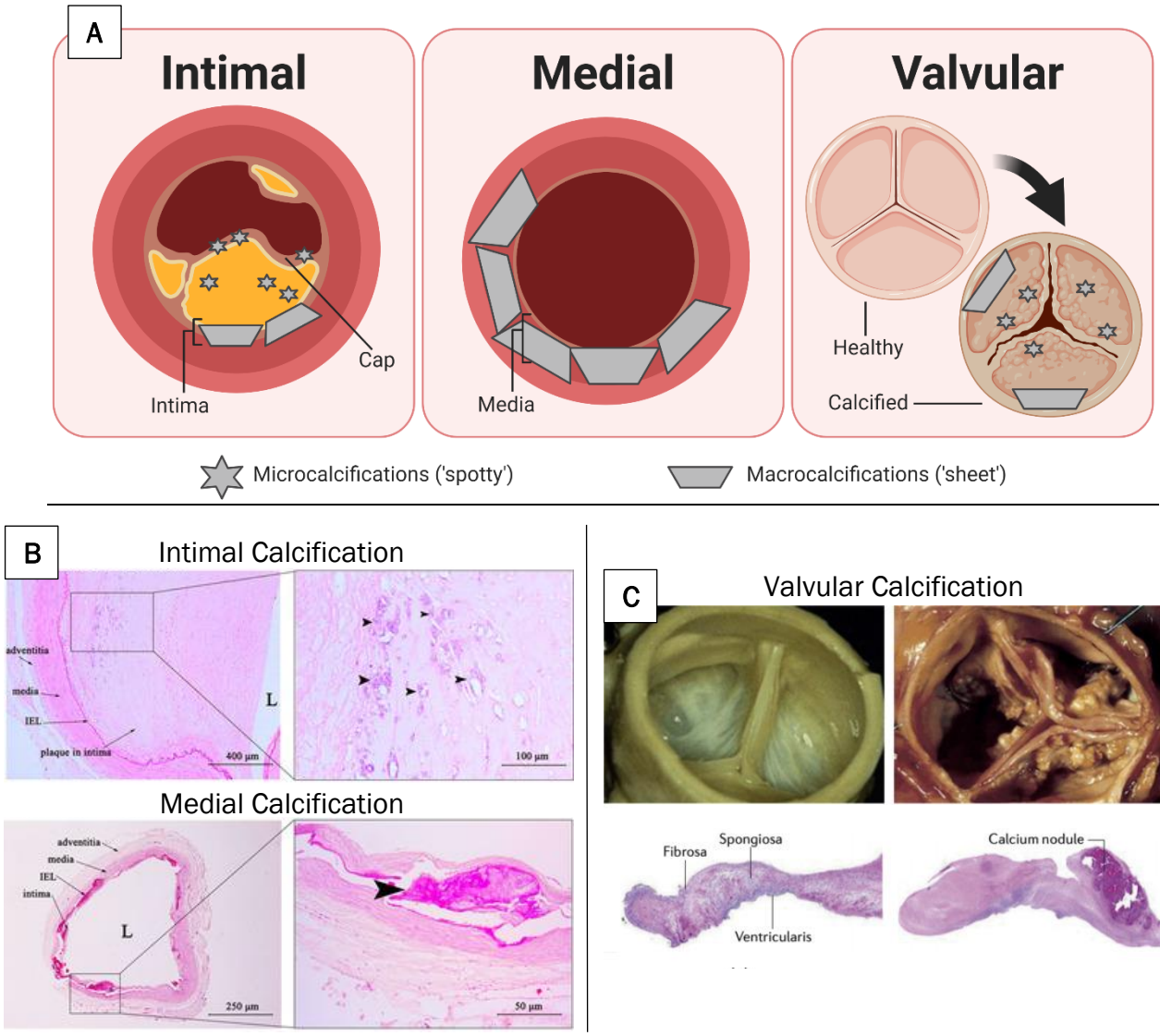

Figure 1.4.3.1 Illustration of the various types of arterial and valvular calcification.

(A) Cartoon diagram of intimal, medial and valvular calcification, (B) modified figure from Yang et al. (2018)[273] showing intimal and medial intracranial artery calcification, (C) modified figure from Fletcher et al. (2021)[274] showing normal and calcified human valves.

Although VC was originally described as having bone-like artery wall morphologies, it was quickly resigned to a passive side-effect of ageing[275]. Recently however, VC has re-emerged as a tightly regulated, complex disease, resembling that of bone mineralisation[276]. There are 2 main types of vascular calcification: atherosclerosis

associated intimal[277, 278] or diabetes and CKD associated medial[279, 280] calcification. Calcification of valves is also able to occur, in a process similar to vascular calcification but with fibrotic undertones, alongside calcification of skin and fat capillaries, termed calciphylaxis. The result is the deposition of calcium phosphate ($CaPO_4$), in particular: hydroxyapatite, crystals into the extracellular matrix via the regulated expression of proteins and calcifying matrix vesicles from VSMCs. This leads to plaque instability in intimal calcification alongside vessel stiffening and reduced compliance in medial calcification[281] (figure 1.5.1).

1.5.1 Atherosclerotic Intimal Calcification and Plaque Stability

Intimal calcification of a plaque occurs in 2 distinct morphologies: 1) micro or 'spotty' early stage calcifications[282] and 2) macro or 'sheet-like' late stage calcifications[283]. The initial release of matrix vesicles surrounding the lipid pools of plaques stimulates microcalcificaiton[282] and debris acts as a nidus for its deposition[283]. These microcalcifications stimulate an inflammatory response and thus lead to plaque instability[284]. Macrocalcifications however have plaque stabilising properties[285]. In the later, healing stages of atherosclerosis, the development of the extracellular matrix to facilitate plaque calcification, leading to a more stable plaque phenotype is mediated by plaque resident cells[286].

1.5.2 Initiation of Vascular Calcification

Inflammation[287-289], vesicle secretion[290-292], apoptotic bodies[293-295] and oxidative stress[296-300] within a plaque, alongside VSMC increased cholesterol content[301], lipotoxicity[302, 303] cholesterol[304-307] and lipogenesis[308] can all contribute to VC, through many different pathways. Furthermore, lipoprotein fragments have also been identified in

both intimal and medial forms of calcification[309], forming the basis for the studies in this thesis.

While there are many cells types involved in VC, including endothelial cells and macrophages, the VSMCs are regarded as having the main role as they can differentiate into osteoblast-like, bone forming cells[310]. VSMCs differentiate easily and are therefore regularly referred to as highly plastic cells, in fact approximately 80% of VSMC origin cells do not stain with traditional smooth muscle markers[311] as they often differentiate into macrophage-like cells and then subsequently foam [312-314] and adipose-like cells[315]. The discoveries of these plastic adipose and macrophage-like VSMC phenotypes are relatively recent, and as such their roles in VC remain unexplored.

Macrophages are also hypothesised to have a significant role in calcification, whereby they in the atherosclerotic milieu have an impaired ability to differentiate into osteoclast-like, bone resorbing cells[316]. It is worth noting that the presence of osteoclasts, when not stained for specifically, is typically determined by histological identification of large, multinucleated cells. There is however another type of monocyte/macrophage lineage multinucleated giant cell that has been identified around many different 'foreign body' settings, that although has strikingly similar bone resorbing properties to the osteoclast and expresses many of the same markers, has an extended, more fibrotic effect[317].

The endothelium is also being increasingly recognised as a major influencer of VC, with evidence showing osteogenic[318, 319] and calcification[320] properties. Until further insight into the specific, non *in vitro* causes of this differentiation however, the endothelium will be typically regarded as a paracrine regulator of VC. Interestingly, free DNA is observed within calcified regions of a plaque and is hypothesised to aid in the precipitation of calcium and phosphate[321]. Although currently the origins of these DNA fragments are unknown, it is well established that DNA traps expelled from neutrophils, called neutrophil

extracellular traps (NETs), have deleterious effects on the vessel wall[322], are associated with larger plaques[323] and increase cardiovascular risk[324].

1.5.3 Regulation of Vascular Calcification: Main Principles

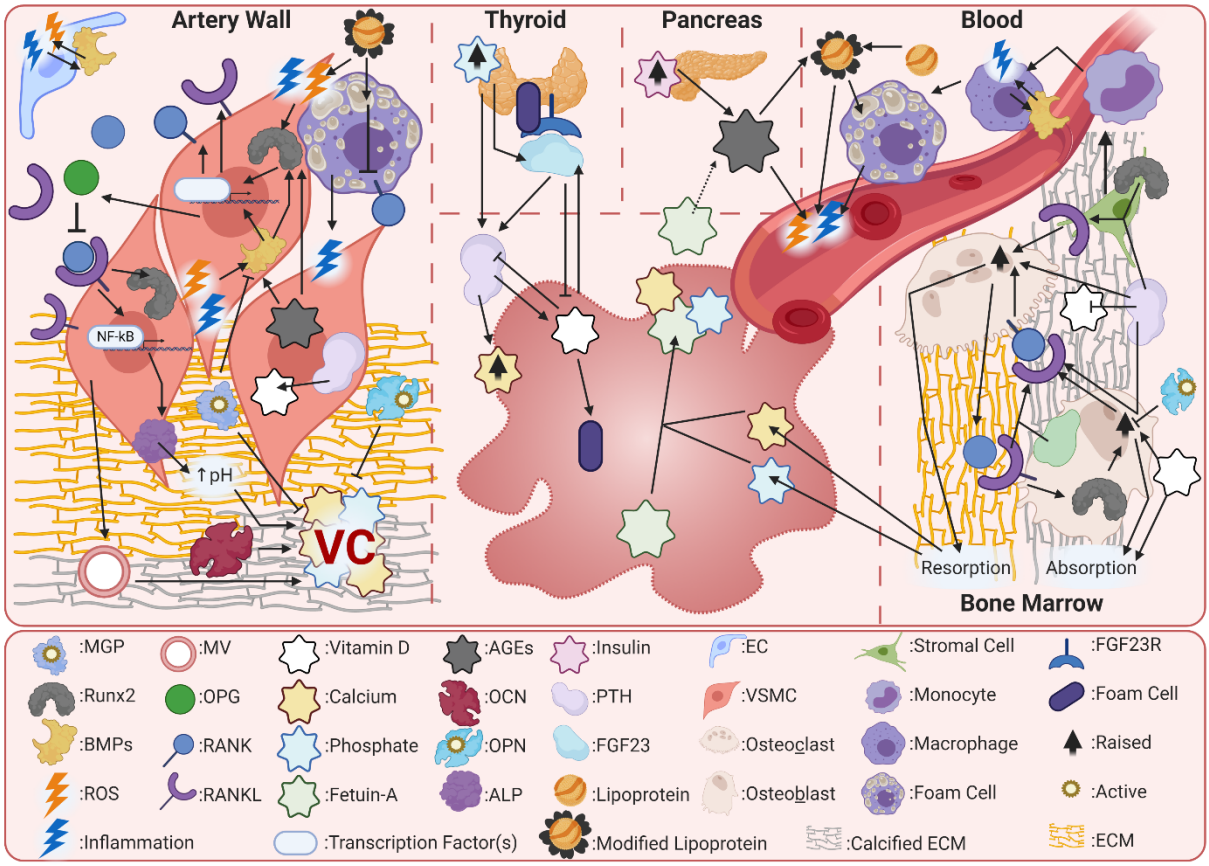

Figure 1.5.3.1 Schematic illustrating the multifaceted, complex nature of the molecular regulation of vascular calcification. *The nature of vascular calcification, while observable in the artery wall, arises from intricate imbalances to any or multiple of many pathways in many calcium and/or phosphate regulatory tissues, including the thyroid, pancreas, circulation, and the bone marrow. Once these pathways have created a suitable calcification environment for the vascular smooth muscle cells (VSMCs). Calcification can commence through Runx2 or BMP mediated RANKL/RANK/OPG/ALP pathways. In this milieu, macrophage foam cells display inhibited osteoclastic activity, allowing the ectopic calcification formations. The role of the other tissues in vascular calcification include increasing the available calcium and phosphate available to the artery wall (bone marrow:*

RANKL/RANK/OPG), regulating serum calcium and phosphate (thyroid: PTH, FGF23, klotho), regulating other factors such as glucose mediated stimulations (pancreas: AGEs) or secreting directly VSMC calcification stimulatory molecules.

In general, there are 4 main hypotheses explaining the occurrence of vascular calcification: 1) cell death leading to a pro-calcification milieu; 2) systemically circulating nucleation complexes or local release of matrix vesicles; 3) loss of both or either systemic or local inhibitory molecules; 4) the differentiation of local cells to actively induce bone formation[278]. In the following sections and as presented in figure 1.5.3, these hypotheses will be introduced and discussed in the context of specific molecules. Furthermore, as the focus of this thesis revolves around the interaction between lipoproteins and VC, the roles of lipoproteins in the context of Runx2, RANKL, RANK, OPG and ALP expression will be discussed and investigated in relevant results chapters.

1.5.4 Transcriptional Regulators

1.5.4.1 Runt Related Transcription Factor 2 (Runx2)

The differentiation of VSMCs into osteoblast-like cells[310] can occur via expression of the calcification regulator runt related transcription factor 2 (Runx2, otherwise known as Cbfa1)[325-329] alongside a reduction in smooth muscle markers such as smooth muscle alpha actin (SMαActin)[328]. The expression of Runx2 can be initiated by inflammation[330], oxidative stress[298, 331] and glucose[332], while P13K/AKT[298], cAMP[329], ERK/MAPK[333] and WNT/β-catenin[325, 334] signalling pathways have been identified as pathways involved in Runx2 regulation. Moreover, Runx2 expression leads to activation of another transcription factor, Osterix, which leads to VC via matrix metalloproteinase mediated matrix degradation and matrix vesicle formation[335]. Specific deletion of Runx2 in murine VSMCs significantly inhibited both chondrocyte formation, which are the osteoblast-like cells

formed by local plaque cells, and the resulting VC[327]. While Runx2 is lowly expressed in the healthy artery, high levels of Runx2 are observed in human atherosclerotic lesions[336, 337].

1.5.4.2 Bone Morphogenic Proteins (BMPs)

Alongside Runx2, bone morphogenic proteins (BMPs) are master regulators of VSMC osteoblastic differentiation[338] and also triggers Runx2 expression[339] highlighting a pro-calcification effect of BMPs. BMP inhibition was also discovered to trigger cholesterol synthesis in the liver, whereby the inhibition of BMP dampened apo B-100 secretion[340].

BMPs are a part of the transforming growth factor-β (TGF-β) superfamily and form subgroups based on their genetic and proteomic codes, of which the signalling BMPs are: BMP-2 and -4; BMP-5, -6, -7 and -8; BMP-9 and -10 and; BMP-12, -13 and -14[341]. These secreted BMPs then bind to a complex of receptors on a cells surface, consisting of type I and type II dimers[342], causing transphosphorylation of the type I receptor, where they then activate SMAD dependant or non-SMAD (Rho-GTPase, ERK, P13K/AKT JNK/p38, MAPK) transcription factors[343, 344]. This complexity of BMP signalling allows co-ordinated regulation, enabling a wide range of functions[344].

While BMP signalling is vital for the initiation of VC[340, 345] and the development of atherosclerosis[340, 346], it also promotes an inflammatory phenotype in atherosclerotic endothelial cells. Inflammatory cytokines such as TNF-α and sheer stress, among inducing adhesion molecules, induced expression of BMP-2[347] and BMP-4[348, 349] in an NF-κB dependant manner[347].This in turn further upregulated inflammation[348, 350] and barrier funtion[351] via ROS production[349] and adhesion molecule (e.g. VCAM-1) expression in a BMP signalling dependant manner[346, 350, 352]. Furthermore, this BMP mediated 'inflammation begets inflammation' pattern is also overserved in atherosclerotic macrophages, whereby, BMP-2 triggers monocyte differentiation into macrophages[353] and M1 macrophages secrete BMP-2[354].

In the atherosclerotic plaque, BMP is expressed[307] and leads to arrest of proliferation[355, 356] and loss of contractile markers in VSMCs[357]. BMP-2, -4, -5, -6, -7 and -9 are the BMPs with the most osteogenic properties[358] and all except BMP-7 have been observed to localise to an atherosclerotic plaque[359]. Interestingly, while BMP-2 and BMP-4 are most frequently associated with VC pathology, there is evidence supporting an inhibitory role for BMP-7 in VC[360]. Both BMP-2 and -7 function by regulating calcification transcription factors Runx2[361-363] and Osterix[364], whereby BMP-2 stimulates and BMP-7 downregulates expression, stimulating osteoblastic differentiation. Interestingly, in committed osteoblasts, BMP-7 inhibits calcification, whereas in uncommitted osteoblast precursors BMP-7 inhibits osteoblastic differentiation and instead redirects it to differentiate into chondrocytes or adipocytes[365]. While it is unclear on the exact roles of BMPs in VC, it is clear that BMP upregulates transcription of osteogenic genes and that this effect increases the effects of other osteogenic signals in VC[366].

.

1.5.5 RANKL/RANK/OPG Triad and ALP Mechanisms of Vascular Calcification

The RANKL/RANK/OPG proteins have complex effects around the body and they are involved in the coordination of calcification, both bone and ectopic, by stimulating differentiation and other effects among multiple cells types around the body. Exploring these systems also highlights the systemic nature of these diseases, providing further support to the hypothesis that a systemic mediator, such as lipoproteins, may be involved. In the setting of vascular calcification however, RANKL/RANK binding stimulates both smooth muscle cell osteoblastic differentiation and macrophage osteoclastic differentiation and can be inhibited via OPG/RANKL binding (figure 1.5.5.1). As will be discussed further however, this process may be accelerated or impaired in the setting of atherosclerosis.

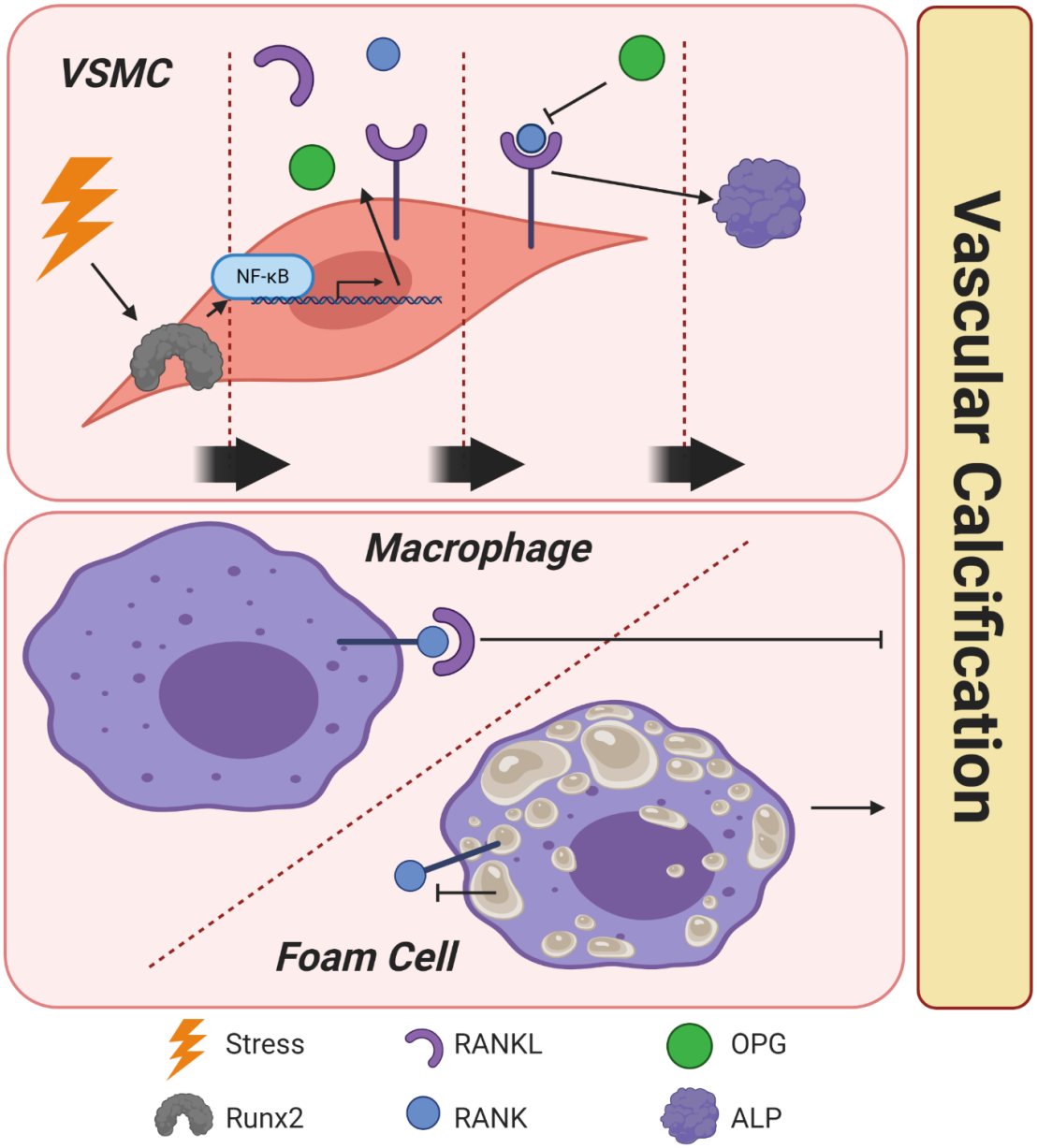

Figure 1.5.5.1 Runx2, RANKL, RANK and OPG regulation of vascular calcification. *Stressors such as inflammation or oxidation stimulate the VSMC to produce Runx2, which activates transcription of RANKL, RANK and OPG. RANKL then binds to free RANK, triggering ALP expression and calcification. Conversely, OPG may bind to RANKL, inhibiting its osteoblastic transcription functionality. Additionally, free RANKL binding to RANK on a macrophage cell surface leads to the expression of osteoclastic genes and inhibition calcification. In foam cells however, this process is faulty, and no osteoclastic activity occurs.*

1.5.5.1 Receptor Activator of NF-κB Ligand (RANKL)

Runx2 upregulates the soluble receptor activator of NF-κB (RANK) ligand (RANKL) expression[367], which then binds to cell surface receptor activator of NF-κB (RANK) for its effects. RANKL in the bone or vasculature is membrane bound on cell types such as T-cells[368], pre-osteoclasts[369] and immune cells[370] and has different effects upon binding to each cell. When RANK is membrane bound osteoclastogenesis (bone resorbing 'chewing' cells) differentiation is triggered, whereas when RANKL is membrane bound osteoblastogenesis (bone 'building' cells) is triggered[371, 372]. Additionally, soluble RANKL can either be secreted from T-cells, or cleaved from its membrane bound form by metalloproteinases[373].

RANKL expression occurs when chromatin histones have already remodelled DNA and is therefore indicative of cell differentiation at the epigenetic DNA level[374]. Furthermore, although RANKL is generally regarded as anti-proliferative, in the presence of macrophage colony stimulating factor (M-CSF) RANKL stimulates DNA synthesis and cell proliferation of osteoclasts[375]. However an atherosclerotic[316] and high inorganic phosphate[376] setting inhibits RANKL/RANK binding stimulated macrophage osteoclast differentiation. Moreover, the M1 skewed, pro-inflammatory phenotype macrophages actively suppress RANKL induced osteoclastogenesis in bone marrow cells[377], an effect which has not yet been investigated in atherosclerosis.

In conjunction with Runx2 upregulation of RANKL, RANKL itself stimulates upregulation of other calcification regulators, namely endothelial cell expression of BMP-2[378, 379], VSMC BMP-4[378, 380], Runx2 itself in a feedback loop[379], and the downregulation of the calcification inhibitor matrix Gla protein (MGP) in VSMCs[379] through RANK binding. Interestingly though, in primary human VSMCs, the addition of RANKL does not enhance inorganic phosphate mediated calcification[381] as studied though 7 different sources of

cells with a wide range of calcification potentials[382], partially explaining how in some studies primary cells were able to calcify via RANKL stimultion[379]. Co-culture of VSMCs with M-CSF bone marrow derived macrophages (BMDMs) also increased calcification, through block-able RANKL stimulation of macrophage TNFα and IL-6 secretion[381].

RANKL can be highly expressed in calcified human[383] and Apo $E^{-/-}$ mouse[379] plaques and these significantly correlated to serum levels of RANKL in humans[383], supporting the hypothesis that circulating pro-calcification factors, potentially released from actively remodelling bone tissue, are partially to blame for VC. The action of RANKL on VSMC calcification is mostly due to its ability to increase ALP expression and activity[379, 384].

RANKL is therefore an attractive target for VC as a therapeutic. Denosumab is a RANKL inhibitor already used to treat osteoporosis and has been hypothesised to continue these beneficial effects into all RANKL/RANK mediated processes, including cancer[385] and immune regulation[386]. In VC, mice treated with denosumab had reduced VC[387], however in humans denosumab did not change aortic calcification levels or cardiovascular risk in post-menopausal women receiving the treatment for osteoporosis[388]. Furthermore, while a 48 participant large clinical trial investigating the efficacy and safety of denosumab found no change to CAC after 12 months in haemodialysis patients[389]. In a case study a patient treated with denosumab for myeloma and hypercalcemia induced by chronic kidney disease co-morbidity, denosumab caused severe hypocalcaemia which was corrected by the clinicians with vitamin D and calcium infusions, leading to rapid progression of vascular and other ectopic calcifications[390]. The use of denosumab as a ‘cure all’ to RANKL/RANK mediated diseases should therefore be closely monitored and administered with caution, particularly in the setting or chronic kidney disease[391].

1.5.5.2 Receptor Activator of NF-κB (RANK)

RANKL binds to its cognate receptor RANK to trigger the calcification process[380]. RANK has a constant expression level throughout both healthy and diseased arteries whereas RANKL is upregulated during the calcification process[392]. It is also interesting to note that RANK gene expression is ubiquitous[393, 394], however RANK protein is only expressed by a select few[393, 395, 396], including endothelial cells in response to VEGF[397], suggesting strong post translational regulation[398].

The binding of RANKL to RANK causes the release of TNF-receptor associated factor 6 (TRAF-6)[399] which then leads to Src/PLCγ , PI3K/AKT/mTOR and MAPK (p38, JNK,ERK1/2) activation which stimulate the translocation of transcription factors such as NF-κB, Fos/Jun or MITF, leading to the expression of bone regulatory genes including cathepsin K and alkaline phosphatase (ALP) alongside cell adhesion molecules including VCAM-1 and ICAM-1[400-404]. As RANK is expressed at the same levels in healthy and diseased arteries[392] alongside having a role in bone density regulation[395, 405, 406], RANK as a target for VC would have implications at multiple sites of the body.

1.5.5.3 Osteoprotegerin (OPG)

Osteoprotegerin is a soluble decoy ligand for RANKL and is generally regarded as protective against VC by blocking RANKL stimulated osteoblastogenesis of VSMCs. Increasing evidence, however, suggests it could actually be the opposite, whereby OPG inhibits osteoclastogenesis. While VSMCs[407-410], endothelial cells[411], monocyte/macrophages (as precursors to osteoclasts)[411] and adventitial cells all express OPG, it is also expressed by circulating leukocytes[412], tumours[413, 414], lymphoid cells[415] and in the bone microenvironment[416]. Interestingly, diet has also been implicated in the expression of OPG, and although the research is preliminary, fatty acid consumption appears to influence the RANKL/RANK/OPG system to benefit CVD and VC[417].

Interestingly, plasma OPG levels in mice increase after about 2 weeks of atherogenic diet[418] or onset of diabetes[419], and humans with coronary artery disease[420] or diabetes[421, 422] also have increased serum OPG levels. High serum OPG levels are correlated with a myriad of metabolic diseases, including obstructive sleep apnea[423], liver fat retention in non-alcoholic fatty liver disease[424], kidney disease[425], heart failure[426], cardiovascular events[420], all-cause mortality[420] and CAC[422]. Further confounding the role of OPG, its administration in $LDLR^{-/-}$ mice, while inhibiting the progression of plaque calcification, did not affect plaque size[418] and while OPG administration to $OPG^{-/-}$ mice was able to rescue osteoporosis, it was not able to reverse medial VC[427]. As RANK protein is regularly expressed in endothelial cells[398] and VEGF increases endothelial RANK expression[397] it has been hypothesised that increased serum OPG levels are an indirect cause of endothelial dysfunction in diabetic and cardiovascular patients[419].

OPG expression is upregulated by several factors, including interleukin (IL)-1α[428], IL-18[429], transforming growth factor-β (TGF-β)[430], bone morphogenic proteins (BMPs)[431], TNF-α[411] and 17β-estradiol[432, 433]. OPG is also downregulated by several factors, including glucocorticoids[434, 435], immunosuppressants[436], parathyroid hormone (PTH)[437], prostaglandin E_2[438], vitamin A[439] and basic fibroblast growth factor[440]. While the studies cited above used a variety of *in vitro* and *in vivo* cells type analyses, there appears to be a strong link between inflammatory mediators and OPG expression. As endothelial cells are front-line regulators of vascular inflammation[441], this again highlights the significant role of intercellular communication in the pathogenesis of VC.

1.5.5.4 *Alkaline Phosphatase (ALP)*

As detailed above, activation of Src/PLCγ, PI3K/Akt/mTOR or MAPK (p38, JNK, ERK1/2) translocates transcription factors such as NF-κB, Fos/Jun or MITF and leads to the expression of the enzyme alkaline phosphatase (ALP)[400]. The action of ALP in VC is to enable the capture of phosphates for mineralisation by the extracellular matrix[442], via the hydrolysis of organic phosphates. ALPs are relevant to many biological systems, ranging from medicine to soil mineral bioavailability and as such, is the sole focus of an entire book[443]. The interest in ALP in general, stems from its differing genetic transcription, post translational modifications and isoforms within the human body and between species, however despite these differences, all ALPs have the same function: hydrolysing organic phosphates for incorporation into the extracellular matrix[444, 445] and inhibition of VC inhibitory inorganic phosphates (PPi)[446, 447]. However, there is conflicting evidence on the precise mechanisms on how ALP has this function[443]. Nonetheless, while ALP is expressed in a majority of tissues, >80% of serum ALP is secreted from the liver and bone[448].

1.5.5.5 *RANKL/RANK/OPG in Bone Regulation*

VC and bone mineralisation share much of their molecular physiology and as such osteoporosis and VC are common co-morbidities[449]. This phenomenon, termed the bone vascular axis, provides insights into VC and increases the difficulty of targeting treatments for the vasculature alone[450-453]. While Runx2, RANKL and ALP are also expressed by bone osteoblasts to stimulate mineralisation there are however some differences, most notably that bone osteoblasts survive in a calcified environment, and rely on ALP for up to 90% of their mineralisation capacity, whereas VSMCs can calcify from ALP independent mechanisms[454].

Runx2 is essential for the differentiation of osteoblasts[455, 456] and then into chondrocytes[457], the interactions between epithelial and mesenchymal stem cells[458] and

for healthy bone[455, 456], tooth[458] and cartilage[459] development, beyond the embryo[460]. Interestingly, overexpression of Runx2 in osteoblasts also inhibits maturation into chondrocytes and causes osteoporosis[461], highlighting the delicate balance required *in situ*.

Binding of RANKL to its receptor RANK on pre-osteoclast cells initiates their differentiation into mature, bone resorbing osteoclasts[395, 405, 406] to fine tune bone mass and to export calcium mineral to the circulation. Osteoclast differentiation is conversely inhibited by secreted OPG[427]. Mice overexpressing soluble RANKL from the liver had accelerated osteoporosis with increased osteoclast count alongside no change in osteoblast count[462]. Any bone loss caused by RANKL deficient mice could also be rescued by soluble RANKL administration[463]. Moreover, OPG deficiency leads to an osteoporotic phenotype via a lack of RANKL inhibition leading to the uncontrolled osteoclastogenesis[427, 464], demonstrating the enormous effect of RANKL/RANK/OPG signalling in the bone.

1.5.6 Other Pro-Calcification Molecules

1.5.6.1 Advanced Glycation End Product (AGE) and their Receptor (RAGE) Signalling

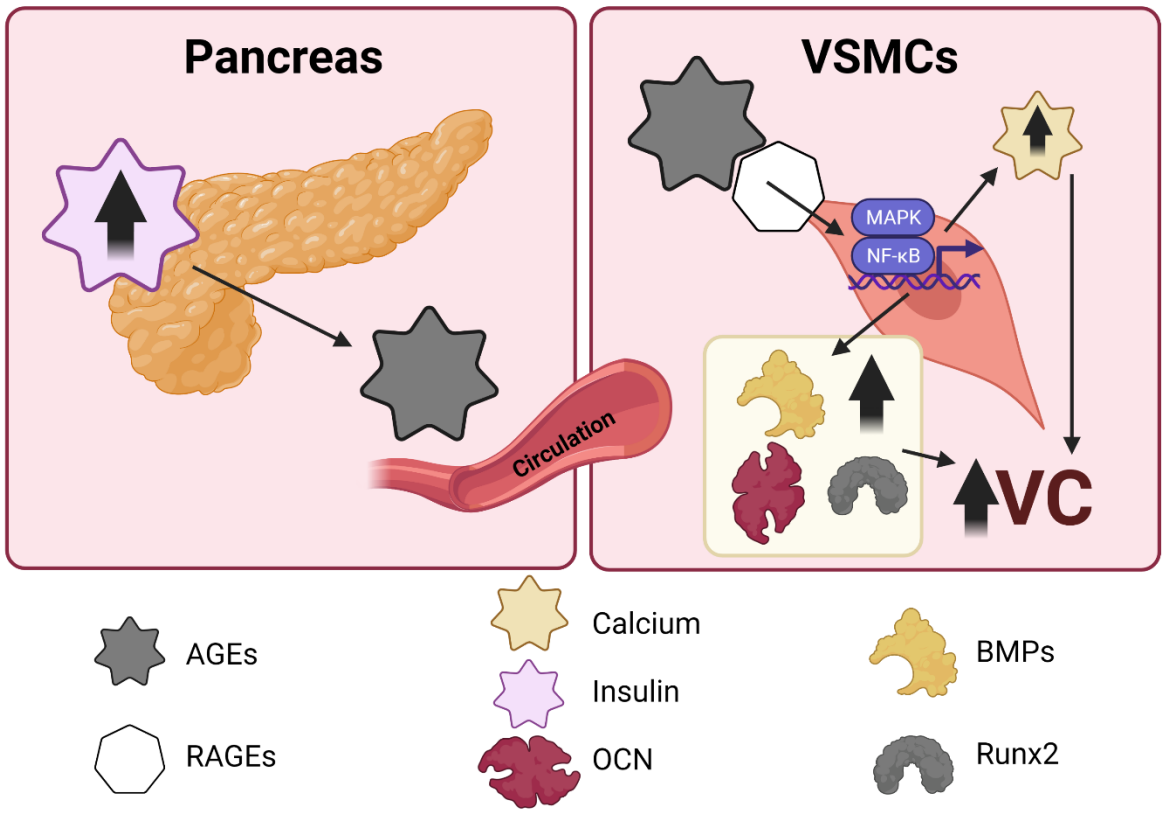

Figure 1.5.6.1 AGE/RAGE regulation of vascular calcification. *In a diabetic, high insulin setting, increased advanced glycation end products (AGEs) are produced, which then travel through the circulation and can bind to AGE receptors (RAGEs) present on the vascular smooth muscle cell (VSMC) surface. This interaction triggers a signalling increase in Runx2, BMPs and OCN expression, alongside increasing intracellular calcium. These effects then lead to increased vascular calcification (VC).*

Diabetes mellitus is a disease characterised by high blood glucose as a result of an inability to use (type 2) or produce (type 1) insulin. Patients with diabetes have a higher risk of cardiovascular mortality[465], largely resulting from their increased progression of VC[466]. In conjunction with other diabetic VC mechanisms, such as preliminary evidence in our laboratory suggesting a stimulatory role for glucose, advanced glycation end products (AGEs) and their receptors (RAGEs) are heavily implicated in diabetes mediated VC[467]. Diabetic high AGE levels are a result of high circulating glucose reacting with amino acid groups and accumulate over time[468]. These AGEs then interact with RAGEs to trigger a variety of pro-VC effects through the activation of the transcriptional regulators MAPK and NF-κB[469, 470].

AGE/RAGE signalling induces osteogenic differentiation of VSMCs by reducing smooth muscle marker expression[471], increasing osteogenic gene expression of BMP[471], Runx2[470], ALP[470, 471] and osteocalcin (OCN)[470 471] and inducing VC[470]. Furthermore, AGEs significantly enhanced intracellular calcium uptake in VSMCs[472], which as introduced further in 1.4.10 also induces VSMC mediated osteoblastic differentiation. Additionally, incubation of VSMCs with AGEs caused upregulation of RAGEs as a result of calcium uptake, leading to the ability of AGEs to cause ALP secretion through receptor binding[472] (figure 1.5.6.1).

1.5.6.2 Osteocalcin (OCN)

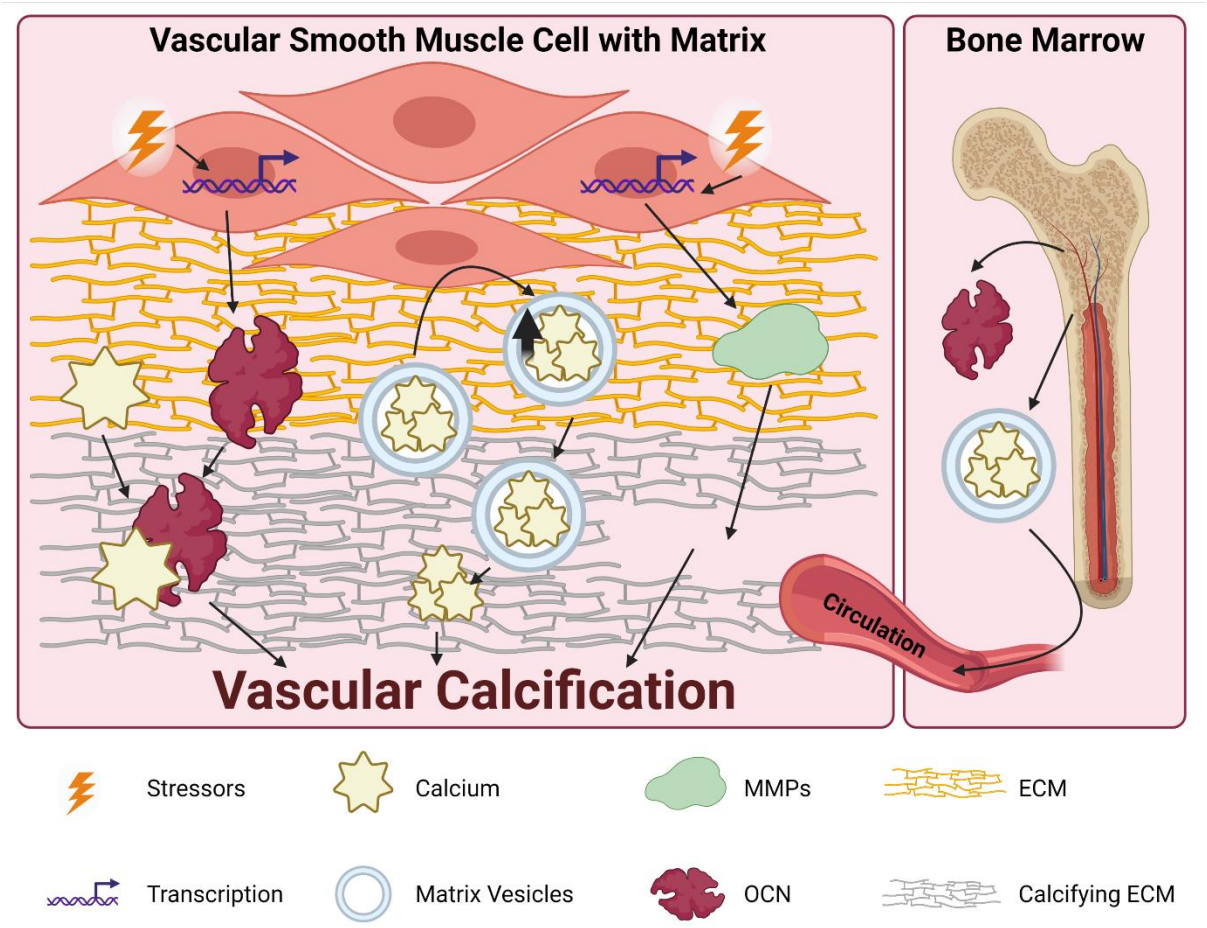

Figure 1.5.6.2 Matrix Pro-Calcification Regulators: OCN, MVs and MMPs. *Either transcribed from stimulated VSMCs or circulated from actively remodelling bone, osteocalcin (OCN) traps calcium to the extracellular matrix (ECM) after carboxylation in a vitamin K dependant manner. Similarly, matrix metalloproteinases degrade elastin in the ECM, allowing calcification to occur. Matrix vesicles (MVs) loaded with calcium stimulate the VSMC release of further loaded MVs, which then embed into the matrix to form the initial nodules of vascular calcification.*

Osteocalcin (OCN) is found in the extracellular matrix, contributes to matrix remodelling and is also found in the circulation post bone resorption. OCN upregulates osteoblastic

activity and contributes to matrix calcification, in a vitamin K dependant manner[473] (figure 1.5.6.2). Interestingly, vitamin K is transported throughout the circulation partially within LDL and mostly VLDL[474], potentially increasing the ability of these particles to contribute to VC.

OCN is post translationally regulated by splicing followed by γ-carboxylation at 3 glutamic residues, giving the protein a high affinity for the bone extracellular matrix and the ability to bind calcium[475] (figure 1.5.6.2). During osteoclast bone resorption however, a low pH level decarboxylates OCN, reducing its bone matrix affinity and releasing it into the circulation[476]. This carboxylation of OCN occurs in a vitamin K dependant manner and the inhibition of vitamin K with diet inadequacy[477] or warfarin[478] triggers this impairment and subsequent release into the plasma.

In the setting of VC and its co-morbidities, calcifying VSMCs upregulated OCN expression following insulin, a signalling molecule with impaired signalling in the diabetic patient, in a RANKL dependant manner[384]. Pathways implicated in VSMC upregulation of OCN include Wnt signalling[479], ERK1/2, MAPK and Akt pathways[384], leading to OCN regulated increased calcification[384, 479] (figure 1.5.6.2). Carboxylated and total OCN, but not uncarboxylated OCN however, associated with improved insulin resistance in a small diabetic cohort[480]. Conversely, uncarboxylated OCN was not found to have any functional effect on the calcification of VSMCs[481], suggesting that carboxylated OCN may have a role in aiding the stabilisation of chronic diseases.

Additionally, general OCN did not significantly correlate to VC in a small cohort of chronic kidney disease patients[481] or to VC in general in a meta-analysis[482], but in the same meta-analysis OCN correlated significantly with VC and atherosclerosis in histologically stained arteries[482]. This suggests that although VSMC OCN may participate in VC, it may not play a central role and may be a result of VC rather than a cause.

1.5.6.3 Matrix Vesicles (MVs)

Matrix vesicles (MVs) are approximately 25-250 nm and are present in the extracellular matrix immediately prior to mineralisation[483] in bone[484] and vascular[485] tissues. The formation of hydroxyapatite begins within the MV, growing in a filamentous morphology until it escapes the bounds of the particle[486]. In atherosclerosis, MVs may be released from aortic resident mesenchymal stem cells[487], macrophages[488, 489], valvular interstitial cells and inflamed VSMCs or are present in the circulation, likely from actively remodelling bone[490] (figure 1.5.6.2). When localised to the fibrous cap, MVs can lead to plaque destabilisation and rupture[491], similar to fibrous cap microcalcifications[492]. In conjunction, MVs also trigger calcification of recipient VSMCs[493].

Counterintuitively however, MVs also contain VC inhibitory proteins such as OPG[494]. Because OPG affects osteoblastic differentiation rather than actual calcium binding however, perhaps this mechanism is a feedback loop to prevent pathological over calcification in the bone.

1.5.6.4 Matrix Metalloproteinases (MMPs) and Elastin

Matrix metalloproteinases (MMPs) have an active role in matrix regulation and as such their inhibition significantly attenuates VC[495]. Alongside their roles in matrix remodelling, metalloproteinases in general also cleave transmembrane proteins, such as klotho (discussed in chapter 1.4.10.1). MMP expression is activated following downstream effects of Runx2 expression[335], where they then degrade the elastin in the extracellular matrix[496], accelerating VC[497, 498] (figure 1.5.6.2). Moreover, elastin degradation is associated with peripheral arterial disease (PAD) independently of VC, despite VC occurring as the major complication of PAD[499]. In an interesting feedback mechanism, calcified elastin triggered osteoblastic differentiation of VSMCs[500], having enormous implications

on a potential role for VC in triggering phonotypic changes or expression profiles in other cells types.

1.5.7 Other Calcification Inhibitory Molecules

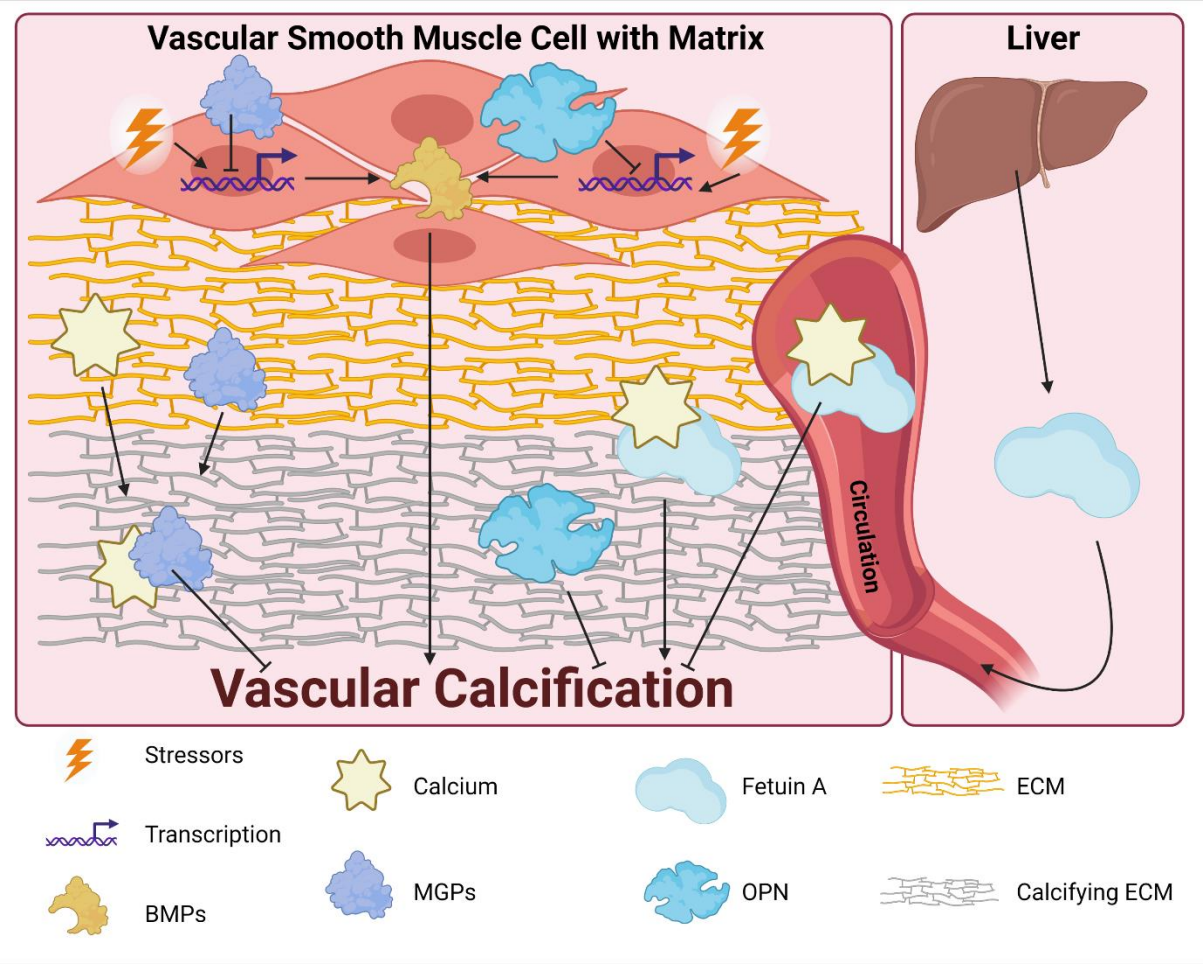

Figure 1.5.7.1 Anti-Calcification Molecules: OPN, MGPs and Fetuin A. *Both matrix GLA proteins (MGPs) and osteopontin (OPN) inhibit vascular calcification (VC) via the inhibition of stimulated vascular smooth muscle cell (VSMC) osteoblastic differentiation. Additionally, MGP binds calcium in the extracellular matrix, inhibiting it from participating in VC. Fetuin A is secreted by the liver and binds to calcium in the circulation. At physiological levels, the complex formation inhibits VC, however when fetuin A is pathologically over secreted, these complexes contribute to VC.*

1.5.7.1 Matrix Gla Protein (MGP)

Matrix Gla protein (MGP) is a VC inhibitory[501, 502], extracellular matrix protein that binds to calcium[503] thereby inhibiting its precipitation to hydroxyapatite and inhibits BMP-2[504-507] mediated osteoblastic differentiation of vascular cells (figure 1.5.7.1). Interestingly, as with the pro-calcification molecule osteocalcin (OCN), MGP needs vitamin K to become active[473] and also binds calcium, yet the effect of this activation and calcium binding has the complete opposite result.

MGP is expressed by bone[501, 508], mesenchymal cells[509, 510], VSMCs[511] and chondrocytes[512, 513]. Furthering its calcification inhibitory effects, its expression in chondrocytes is stimulated by high phosphate concentrations[512]. MGP is post-translationally modified to 2 levels by carboxylation (fully or poorly) by vitamin K and can be phosphorylated. As such, low serum levels of vitamin K, either as a result of disease[514, 515] or warfarin induced[516, 517], are associated with VC phenotypes and reduced MGP functionality. As such, poorly carboxylated MGP has also been identified in calcification regions in atherosclerotic plaques[518] and proposed as a biomarker for calcification in diseased poulations[519]. Additionally, MGP expression has several transcriptional regulators, giving the protein biomarker-like qualities for the prediction of VC.

1.5.7.2 Fetuin A

Fetuin A levels[520-522] and genetics[521] are associated with cardiovascular mortality, chronic kidney disease and atherosclerosis. Fetuin A deficient mice display increased VC[523] and fetuin A levels are well established to be correlated with incidence of VC in patients with kidney diseases[523-526] and CVD[527, 528]. The potency of fetuin A as an inhibitor is so strong, that its effects account for approximately 50% of the anti-calcification ability of whole serum[529]. Fetuin A has these effects by forming calciprotein particles, a serum aggregate of fetuin A, calcium and phosphate[529-531] and occasionally other serum aggregatory

proteins[530]. Even though pathological high levels of calciprotein in the circulation lead to increased calcification[532], physiological levels inhibit the incorporation of these minerals into the extracellular matrix[529] (figure 1.5.7.1).

Fetuin A is mainly produced by the liver and its expression is modified in the presence of endoplasmic reticulum stress[533] or lipids[534], whereby high stress or lipid concentration results in fetuin A overexpression. This is mediated by NF-κB, leading to insulin resistance via impaired adipocyte function[535]. Moreover, liver overload of fats and lipids, in the case of non-alcoholic steatohepatitis and non-alcoholic fatty liver disease causes increased hepatic fetuin A expression[536, 537]. As such, fetuin A has been proposed as a link between obesity and its co-morbidities[538]. During the genesis of VC, as high calciprotein levels associate with increased VC[532], one hypothesis might be that lipoproteins play a role in this over-secretion system. In the setting of low fetuin A levels however, it is unclear where the reduced levels originate.

At the cellular level fetuin A is internalised by VSMCs, where it inhibits apoptosis, enhances matrix vesicle phagocytosis and concentrates within matrix vesicles about to be secreted[539]. Additionally, fetuin A carries calcium ions into the VSMC as it internalises, enhancing its anti-calcification capabilities[540].

Interestingly, in diabetes fetuin A enhances insulin resistance, exacerbating the disease[541, 542]. Adding to its poor properties in the setting of diabetes, although fetuin A inhibits an alternate RAGE ligand in an attempt to inhibit inflammation[543], it thereby enhances AGE binding and vascular osteogenesis[544]. The main systemic calcification effect however is due to the significant increases in oxidative stress and ROS production following AGE/RAGE signalling[545, 546]. Therefore, a reduction in either AGE/RAGE signalling or administration of antioxidant therapies resulted in reduced VC in diabetic rats[547].

1.5.7.3 Osteopontin (OPN)

Osteopontin (OPN) is an interesting secreted protein, due to its differing calcification roles in acute and chronic responses to inflammation in the vascular setting[548]. Moreover, although OPN is a matrix protein, unlike other matrix proteins such as collagen, it has no roles in matrix structure[549]. Instead, OPN serves to modulate cell-matrix interactions by binding to a myriad of functional proteins[550] to have an effect on matrix remodelling[549]. Alongside the 5 isoforms expressed by humans[551], OPN can also be post-transcriptionally regulated via phosphorylation, glycosylation, transglutamination and cleavage by thrombin and matrix metalloproteinases[548].

In physiological settings, arterial OPN expression is low[552] but is important for inhibition of calcification. Upon injury[553, 554], OPN is upregulated by VSMCs, endothelial cells and macrophages[555] to promote cell adhesion[556-559], proliferation[559-561], migration[557-559, 562, 563] and survival[558, 564, 565]. In pre-osteoblastic cells however, OPN negatively regulates proliferation and differentiation[566], adding to potential protective mechanisms of OPN in early VC (figure 1.5.7.1).

In a pathological setting however, OPN levels remain high chronically. OPN is a marker for increased tumour survival capabilities[565, 567-569] and resulting poor clinical outcomes including mortality[567] and metastasis to the bone[568]. High OPN levels are also associated with diseases such as multiple sclerosis[570] and Alzheimers[571]. Furthermore, elevated levels of OPN have several implications in CVD such that it can be a strong predictor of the presence of valvular calcification[572] and indicate clinical outcomes[573].In addition, high levels are implicated in cardiac remodelling[574] and poor long-term outcomes post myocardial infarction[575]. It is also considered a potential therapeutic target[576] or biomarker[577] of brain injury post ischemic stroke and is associated with the presence of peripheral arterial disease[578, 579].

In the setting of vascular calcification, loss of OPN resulted in increased calcification of VSMCs *in vitro*[580] and in murine aortas[502] and aortic valves *in vivo*[581]. Interestingly, both *in vitro* and *in situ* evidence demonstrates that OPN must be phosphorylated to have the VSMC[582] and aortic valve[573] anti-calcification effects alongside biomarker association to aortic valve calcification[572]. Although potentially difficult to target, research seeking to explain the lack of phosphorylation of OPN in chronic pathologies could lead to targetable insights into disease progression.

1.5.8 Regulation of Serum Phosphates

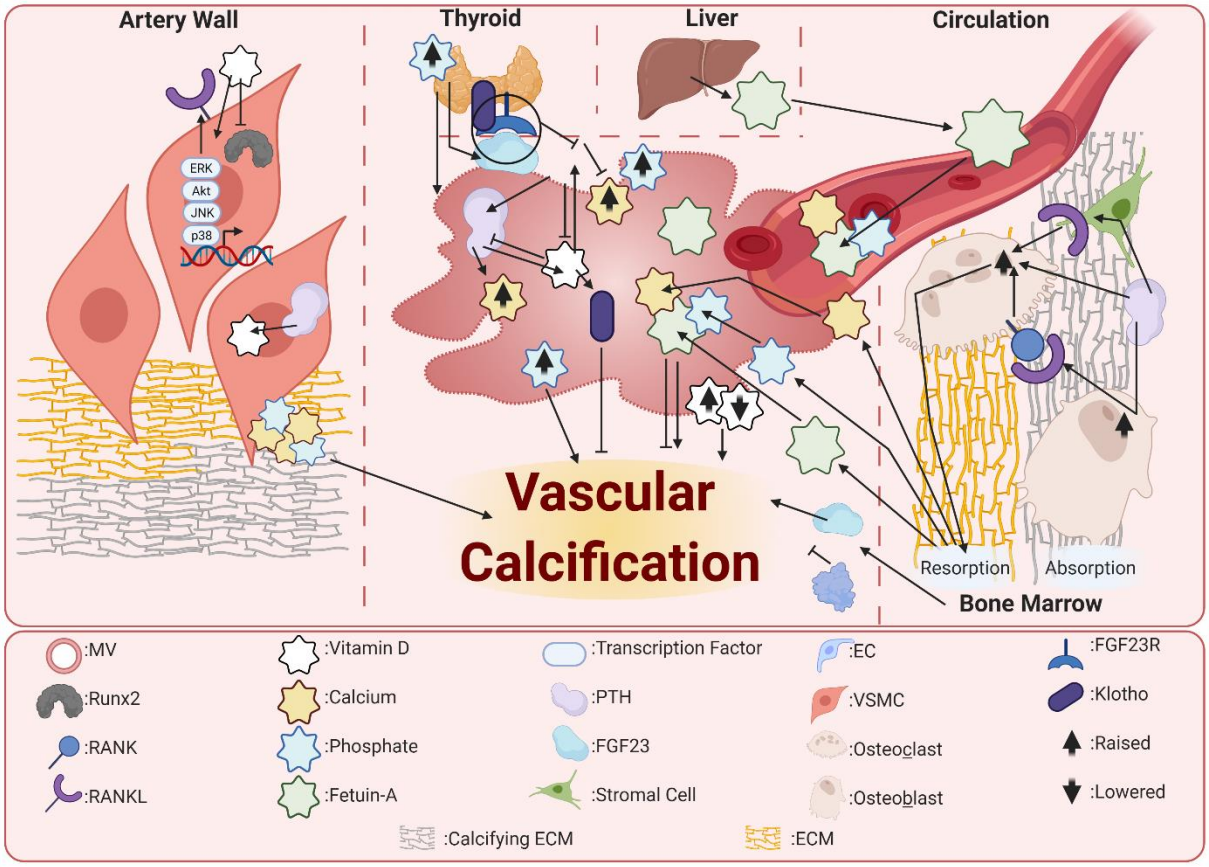

Figure 1.5.8.1 Calcium and Phosphate Regulation and Roles in VC. *Serum calcium and phosphate levels contribute to the development of vascular calcification (VC). Parathyroid hormone (PTH) is pathologically released in response to high serum phosphate, then pathologically increases serum phosphate further by inducing bone resorption. High serum phosphate also triggers thyroid release of fibroblast growth factor 23 (FGF23), which can then bind to it's receptor (FGF23R):Klotho complex to inhibit further raising of serum calcium and phosphate levels. While vitamin D physiologically is VC protective, pathologically high or low vitamin D values increase VC through a variety of mechanisms.*

Elevated serum calcium and phosphate contribute significantly to vascular calcification, particularly medial vascular calcification, and as such high phosphate medium is widely

used as a model for *in vitro* vascular and valvular calcification. Hyperphosphatemia is characterised by higher than normal serum phosphate, where normal levels range from 1.0 to 1.5 mmol/L in human serum, but in chronic kidney disease patient this level exceeds 2.0 mmol/L. Likewise, normal serum calcium levels range between approximately 2.0 -2.7 mmol/L and patients with chronic kidney disease present with serum calcium <2.7mmol/L. As the kidneys have a major role in mineral regulation, the defective kidney leads to higher circulating calcium phosphate mediated VC pathologies. Moreover, the levels of these minerals directly affect calcifying VSMCs.

Phosphates induce VSMC differentiation and VC[583] via sodium mediated internalisation of phosphates[583], through sodium-phosphate channels[584, 585] and induction of matrix vesicle formation[586]. High intracellular calcium also stimulates VC in VSMCs, by reducing inhibitor expression and stimulating matrix vesicle formation[587]. Interestingly, there is evidence to suggest that the initial phases of VC are a passive process, whereby hydroxyapatite forms using dead VSMCs as a nidus[588]. Furthering this, the same authors also discovered an active process of VC from live cells[588], leading to the hypothesis that initial apoptotic or necrotic passive calcification may trigger osteoblastic differentiation of VSMC. Supporting this hypothesis, VSMC incubated with calcified matrix showed increased osteoblastic differentiation[500], revealing that initial hydroxyapatite depositions themselves may lead to vessel wall osteogenesis (figure 1.5.8.1).

Phosphorus is a mineral obtained through the diet, typically bound with oxygen atoms as phosphates, and phosphate homeostasis in the circulation is regulated by 4 main tissues: the small intestine, bone, parathyroid gland and kidneys[589]. The regulation of phosphate uptake is co-ordinated by several endocrine factors but mainly fibroblast growth factor (FGF23), parathyroid hormone (PTH) and vitamin D metabolites, via the regulation of sodium-phosphate channel activity or availability (figure 1.5.8.1). Other endocrine factors

that also contribute to circulating phosphate levels include reabsorption increasers such as growth hormone, insulin and thyroid hormone and reabsorption decreasers such as calcitonin and glucocorticoids[590].

1.5.8.1 Fibroblast Growth Factor 23 (FGF23) and Klotho

During chronic hyperphosphatemia and hypocalcaemia, fibroblast growth factor (FGF23) is over-expressed by the kidneys[591-594] which downregulates expression of sodium-phosphate transporters, supresses vitamin D production[595, 596] and causes excessive parathyroid hormone (PTH) secretion[595, 597], leading to hyperparathyroidism[597, 598]. In chronic kidney disease patients however, as FGF23 production increases, kidney function decreases[594], likely due to the fact that patients with chronic kidney disease have high serum phosphate with pathologically low vitamin D levels[599]. Despite the effort of elevated PTH[600] and FGF23[601] levels however, patients with kidney diseases have high circulating phosphates. In addition, evidence suggests a causative role for FGF23 in tumour induced bone softening (osteomalacia), usually caused by vitamin D deficiency[593], linking it to mineralisation defective pathologies.

Klotho is a transmembrane receptor expressed in the parathyroid gland, kidney, reproductive organs and the brain[602] which can downregulate the expression of sodium-phosphate transporters alongside causing several phenotypes of ageing[603]. By converting multiple FGF receptors into a specific receptors for FGF23[604-606], klotho is essential for the function of FGF23 on sodium-phosphate channels[607]. Klotho as a membrane protein can also be cleaved by metalloproteinases to enter the circulation, in a process which is upregulated by insulin[608]. *In vitro* investigation reveals to need to add both FGF23 and klotho to cells[605] for the resulting effects, through ERK[606], p38, JNK and AKT[589], on sodium-phosphate channels.

While the bone secretes FGF23, it has no detected role in the bone microenvironment, revealing the systemic, endocrine nature of phosphate regulation, involving coordinated participation between FGF23, klotho, PTH and vitamin D and between several organs[589]. Although this may be the case, evidence shows reduced serum levels of klotho in patients, from the early timepoints in chronic kidney disease[609] and that in a small cohort of 114 patients, these low levels associate with arterial stiffness but not vascular calcification[583]. Despite this, *in vivo* evidence suggests that low klotho does lead to VC, however this study was enhanced with *in vitro* data demonstrating a role for circulating klotho on the vasculature itself, whereby klotho inhibited VSMC phosphate uptake through sodium phosphate channels and also inhibited the resulting differentiation and mineralisation[610] (figure 1.5.8.1).

1.5.8.2 Parathyroid Hormone (PTH) and Vitamin D

The role of PTH is to reduce reabsorption of phosphates from the urine and as such hyperphosphatemia and hypocalcaemia stimulate physiological PTH secretion[595]. PTH acts to reduce phosphate levels by reducing sodium phosphate channel activities[611], mobilises phosphate from the bone through osteoblastic[612, 613], stromal cell[614] or osteocyte cell[615] RANKL expression[616] and blocks any beneficial effects of vitamin D on phosphate reabsorption through decreasing the expression of its main receptor[617] (figure 1.5.8.1). PTH increases circulating calcium in a similar manner, by increasing kidney mediated reabsorption, stimulating bone osteoclast activity and increasing vitamin D, which then increases intestinal calcium absorption[618]. PTH hormone associated calcification is often associated with co-morbidities such as renal disease[619-621] and it also significantly correlates to CAC in patients without renal faliure[622]. PTH upregulates RANKL in a Runx2 independent manner in fibroblastic stromal cells[623].

Vitamin D is pro-calcific at pathologically high[624, 625] or low[626] concentrations[627], but because pathologically high concentrations of vitamin D are rare and potentially reversable[625], the focus on vitamin D related disease is on the pathologically low concentrations often observed in patients with renal disease. High vitamin D causes VC by inhibiting PTH expression[628, 629] and increasing intestinal absorption of calcium and phosphate[627]. As a protective mechanisms against pathologically high vitamin D levels, high serum phosphate decreases vitamin D production[595], however the vessel wall has its own mechanisms of vitamin D synthesis.

VSMCs have the machinery to produce active vitamin D in response to PTH[630], where it can then induces an osteoblastic phenotype[631], but can also suppress the Runx2 gene promotor[632]. Alongside vitamin D's influence on osteoblastic differentiation of VSMCs, it is also able to regulate extracellular matrix remodelling via increasing expression of growth factors and stimulating the loading of matrix vesicles with matrix metalloproteinases[633] and causes an atherogenic lipoprotein profile[634], potentially through influencing lipoprotein lipase expression[635] or insulin mediated pathways[636]. Intriguingly, the addition of vitamin D to human VSMCs did not result in increased VC, instead only high phosphate concentrations was able to achieve this[637], suggesting a complex role for vitamin D in VC. With the effect to correct any mineral imbalances caused by vitamin D however, vitamin D itself is a strong inducer of FGF23[596] and Klotho[638] (figure 1.5.8.1).

1.5.9 Studying Vascular Calcification *In Vivo*

To observe atherosclerotic calcification in mice, two plaque prone models are commonly used: the LDL receptor (LDLR) knock out and apolipoprotein E (Apo E) KO mice. Both Apo $E^{-/-}$[639] and $LDLR^{-/-}$[640] mice develop atherosclerosis in a similar way to human arteries[306] and obtain a high LDL phenotype, however Apo $E^{-/-}$ mice have higher plasma cholesterol

and contain larger valvular plaques, with more calcification and higher instability markers than LDLR$^{-/-}$ mice on the same diet, in the same laboratory, in the same time frame[641]. It is therefore important to note that these models, while bringing the lipoprotein profile to a more human phenotype, are still not perfectly aligned.

To study medial calcification, several rodent models are often used. These include: administration of warfarin[547, 642], nicotine[546] or vitamin D[625]; induced chronic kidney disease rodents via genetic knockout of FGF23 or PTH or manipulation of other kidney functionality genes, alongside nephrectomy techniques[465]; induced diabetes by streptozotocin[546, 547] and; genetic deletion of calcification inhibitor OPG[643], MGP[501] and OPN[502]. A combination of any of these in the setting of an atherogenic diet and apo E$^{-/-}$ or LDLR$^{-/-}$ mouse background are therefore hypothesised to increase levels of intimal, atherogenic calcification. In addition to these models, mice transfected with gain of function proprotein convertase subtilisin/kexin type 9 (PCSK9) display hyperlipidaemia and VC above that of LDLR$^{-/-}$ mice[644].

1.6 Treatments of Atherosclerosis and Their Impacts on Vascular Calcifications

1.6.1 Statins

Current *in situ* imaging evidence suggests that statins have pro- macro-calcification, plaque stabilising effects despite lowering cholesterol. Although this is the current hypothesis, there are many pleiotropic effects of statins which may influence vascular calcification and there also exists a body of *in vitro* and *in vivo* evidence suggesting an inhibitory effect of statins. As this thesis will explore the effects of statins on VC in an apo

$E^{-/-}$ mouse model of atherosclerosis, a detailed discussion on the role of statins in VC will be presented in chapter 5.

1.6.2 PCSK9 Inhibitors

Proprotein convertase subtilisin/kexin type 9 (PCSK9) inhibitors have also demonstrated beneficial effects on plasma cholesterol and atheroma volume[204] via modification of the lipoprotein lipidome[645], enabling a new series of studies investigating the role of PCSK9 on vascular calcification. Gain of function (GoF) PCSK9 mutant mice have an LDLR KO lipid profile phenotype[646] and display similarly advanced atherosclerosis[644]. These mice demonstrate more extensive calcification compared to LDLR KO mice, which associates with higher cholesterol levels[644]. PCSK9 has also been shown to influence inflammation, apoptosis, blood pressure, glucose tolerance and adipose tissue metabolism[647], all of which independently modulate calcification pathways. Recent studies of the PCSK9 inhibitor Evolocumab, demonstrate an increase in plaque calcification that associated with LDL cholesterol level lowering [648]. The observation of an increase in plaque calcification in clinical trials of both statins and PCSK9 inhibitors suggests that these effects are likely to result from lowering levels of LDL cholesterol.

1.6.3 High Density Lipoprotein Therapies

Although high density lipoproteins (HDLs) have long been known to be associated with a protection from[77-79] and regression of[85] coronary artery disease (CAD) and initial HDL raising therapies discovered promising clinical trial outcomes[85], large-scale clinical trials have revealed no additional benefit of HDL raising therapies on cardiovascular outcomes[93, 94, 649, 650]. While many therapies, such as lifestyle changes[651], statins[83, 652], fibrates[653, 654], niacin[655, 656], are able to increase HDL levels only some are confirmed to continue this benefit in disease into improved clinical outcomes. As HDL from CAD patients

has impaired anti-inflammatory and antioxidant functionality[86] and has no benefit to CVD[87], HDL raising therapies may just be raising more dysfunctional HDL.

The development of reconstituted HDL particle mimetics permits evaluation of the impact of their protein and lipid components on the artery wall. On the basis of the discovery of the apo AI mutant, apo A1 Milano, and its potentially protective impact on cardiovascular risk, incorporation of this protein in HDL mimetics has demonstrated an inhibitory effect on both aortic plaque and calcification in an atherosclerotic rabbit model[657]. Although infusions of recombinant apo AI Milano reduced plaque burden in a clinical pilot study[85], reconstituted HDL containing apo AI Milano had no additional benefit on top of statin therapy[93]. Furthermore, other HDL mimetics were not found to benefit plaque burden[94]. The impact of HDL mimetics on VC and plaque stabilisation is however yet to be examined.

1.7 Hypothesis and Aims

As currently there are no therapeutic options for plaque stabilisation via the inhibition or stimulation of micro and macro vascular calcifications respectively and as lipoproteins are circulatory factors involved in atherosclerosis, this thesis investigated the links between the two. These studies therefore aim to:

I. Assess and validate a standard *in vitro* calcification assay in VSMCs

II. Investigate the effects of lipoprotein oxidation on VC *in vitro*

III. Investigate the effects lipoprotein modification on VC *in vivo*

   a. The effect of apo CIII deletion on an apo $E^{-/-}$ background in mice

   b. The effect of atorvastatin mediated cholesterol lowering in apo $E^{-/-}$ mice

   c. The effect of rHDL (apo AI and PLPC particles) on VC in mice in

      i. A pro-atherosclerosis apo $E^{-/-}$ model

ii. A pro-atherosclerosis and pro-calcification apo $E^{-/-}$ x $OPG^{-/-}$ model

IV. Investigate the calcification potential of human serum containing various concentrations of lipoproteins

a. The effect of triglyceride level

b. The effect of Lp(a) level

c. The effect of the HDL mimetic CER-001

d. The effect of serum from patients displaying IVUS measured calcification progression

Taken together, the hypothesis of this thesis is that classically atherogenic lipid or lipoproteins will have deleterious effects on VC or VC mediated plaque stabilisation, whereas the classically beneficial HDL and its mimetics will result in a favourable calcification outcome. Individual hypotheses corresponding to the aims above are as follows:

I. Calcification of cells will occur after 2 weeks of calcification

II. Oxidised lipoproteins will progress calcification *in vitro*

III. A change in lipoprotein profile towards a traditionally atherogenic phenotype will increase VC *in vivo*

a. Apo CIII deletion on an apo $E^{-/-}$ background in mice will result in less VC

b. Atorvastatin in apo $E^{-/-}$ mice will decrease VC

c. rHDL (apo AI and PLPC particles) will decrease VC in mice in

i. A pro-atherosclerosis apo $E^{-/-}$ model

ii. A pro-atherosclerosis and pro-calcification apo $E^{-/-}$ x $OPG^{-/-}$ model

IV. Human serum with a traditionally atherogenic profile will increase VC of HAoSMCs *ex vivo*

   a. Serum with high triglyceride levels will increase VC *ex vivo*

   b. Serum with high Lp(a) levels will increase VC *ex vivo*

   c. Subjects receiving the HDL mimetic CER-001 will have reduced calcification progression

   d. Serum from patients displaying the greatest IVUS measured calcification progression will stimulate VC *ex vivo*, and this will be positively correlated with serum markers for VC

To briefly summarise the introductory chapter, vascular calcification is a complex process involving several molecular pathways and arising from a wide variety of complications, including atherosclerosis. Moreover, the natural history of calcification progression or regression, alongside its clinical relevance over varying morphologies are understudied or unknown. Lipoproteins are also highly complex particles, which due to their heavy involvement in atherosclerosis, may also be involved in the modulation of vascular calcification. The overall aim of this thesis is therefore to examine the role of lipoproteins in a range of standardised settings, to gain a broad picture of what may be occurring and the generate a starting point for future investigations.

2 : Chapter Two

Materials and Methods

2.1 Isolation of Lipoproteins

Lipoproteins were prepared from pooled, expired, autologously donated human plasma kindly donated by the Red Cross Blood Bank, Adelaide, South Australia. Native VLDL, LDL and HDL were isolated from the plasma by serial density gradient ultracentrifugation in a Beckman Optima XPN ultracentrifuge using a Type 50.2 Ti rotor (Beckman Coulter, Fullarton, CA, USA). Briefly, plasma density was adjusted using potassium bromide (KBr) to 1.019 g/ml and centrifuged at 50,000 rpm for 18 hours. The top fraction was collected and dialysed against 3 changes of 1 L 1X PBS solution to obtain VLDL. The bottom fraction was pooled, density adjusted to 1.063 g/ml with KBr and centrifuged at 50,000 rpm for 18 hours. The top fraction containing HDL was collected, pooled and adjusted to 1.21 g/ml while the bottom, LDL fraction was pooled and adjusted to 1.055 g/ml using a KBr dialysis density solution (1 L H_2O, 79.52 g KBr, 200 mg NAN_3, 100 mg EDTA-NA_2). Both the HDL and LDL fractions were then centrifuged at 50,000 rpm for 18 hours. The top fraction of each spin was pooled separately and dialysed against 3 changes of 1 L 1X PBS solution over 72 h to obtain LDL and native HDL.

2.2 Isolation of Apolipoprotein AI from Native HDL

To prepare apoA-I, a portion of the native HDL obtained from the isolation protocol described here in method 2.1 was reserved for further processing. Native HDL was re-adjusted to 1.21 g/ml using a KBr dialysis density solution (1 L H_2O, 332.96 g KBr, 200 mg NAN_3, 100 mg EDTA-NA_2) overnight and centrifuged at 70,000 rpm using a Beckman type 70 Ti rotor for 18 hours. The top fraction was pooled a dialysed against 3 changes of 5 L 5 mM Ammonium bicarbonate solution (5 L H_2O, 1.98 g NH_4HCO_3, 1.86 g EDTA-NA_2), lyophilised for 4 hours, then delipidated as previously described[658]. All steps were performed at 4^{o}C and each dialysis step was incubated overnight. The resulting protein

fraction of the HDL was then dried under N_2 gas, dissolved in 20 mM Tris-HCl (pH 8.2), lyophilised completely and stored at -20°C.

Apo AI was isolated from the HDL protein fraction by anion exchange fast paced liquid chromatography (FPLC), using a xk 26/20 column (cytiva) packed with Q Sepharose Fast Flow beads (Amersham Pharmacia Biotech) attached to a Bio-Rad FPLC system (Bio-Rad). The column was pre-equilibrated with 20 mM Tris-HCl, 6 M Urea (pH 8.5). The apo AI protein was separated using a modification of the Weisweiler method[659] as described by Rye (1990)[660]. Protein elution was monitored at A_{280} nm, fractions corresponding to the apo AI elution times were collected, then confirmed using coomassie stained SDS-PAGE gels (described in Methods 2.9.2) and pooled for dialysis against 3 changes, for 24 hours, at 4°C, of 5 L 20 mM Ammonium bicarbonate solution (5 L H_2O, 7.92 g NH_4HCO_3, 1.86 g EDTA-NA_2). The Apo AI fraction was then completely lyophilised and stored at -20°C.

2.3 Preparation of rHDL, Containing Apo AI and PLPC

10 mg/ml of Apo AI was reconstituted in reconstitution buffer (50 mL H_2O, 0.006 g Tris-HCl, 14.329 g guanidine-HCl, 5 mg EDTA-Na_2, pH 8.2), then dialysed against 5 changes of Tris-buffered saline (TBS) (1 L H_2O, 1.244 g Tris-HCl, 8.766 g $NaCl_2$, 0.06 g NaN_3, 0.05 g EDTA-Na_2, Ph 7.4). Lyophilised 1-Palmitoyl-2-linoeoyl-sn-glycero-3-phosphocholine (16:0-18:2 PC) (PLPC) (Avanti Polar Lipids) was reconstituted in a chloroform:methanol (2:1) solution and stored at -80°C until required. Apo AI was complexed with PLPC to obtain discoidal rHDL using the cholate dialysis method[661]. Briefly, 99 moles of PLPC were added to glass tubes and dried under N_2 gas, then lyophilised overnight to ensure complete drying. 99 moles of sodium cholate (30 mg/ml sodium cholate in TBS solution) were added to the tubes, vortexed, then the tubes were filled to 0.5 ml with TBS and vortexed at 15-minute intervals until optically clear. Protein concentration of apo AI was measured using

the Pierce BCA Assay (Life Technologies), then 1 mole of apo AI was added to each tube and incubated in the dark on ice for 2 hours. Tube contents were pooled and dialysed against 5 changes of 1L TBS followed by 2 changes of 1L endotoxin free phosphate buffered saline (Sigma) (PBS). The Pierce BCA assay (Life Technologies) was used to estimate the final concentration of the rHDL discs before storing 1 mL aliquots at 4^{o}C, under N_2 gas, wrapped in parafilm, for no longer than 4 weeks.

2.4 Human Aortic Smooth Muscle Cell (HAoSMC) Calcification

2.4.1 Cell Line Maintenance, Culture and Replicate Layout

Human aortic smooth muscle cells (HAoSMCs, Lonza) were cultured between passage 3 to 10 in Lonza Clonetics® Smooth Muscle Cell Medium BulletKit® SmGM®-2 BulletKit® media at 37^{o}C under 5% CO_2. Cells were passaged at 90% confluency by washing twice with 1XPBS (Sigma), incubating in trypsin (Life Technologies) for 1-5 minutes then re-plated into 3 new T-75 flasks. The media on these cells was replaced 2-3 times per week and HAoSMCs were passaged 1-4 times per fortnight, with the growth rate corresponding to cell passage. Cell morphology was monitored via light microscopy and elongated cells were discarded. Cells for experiments were plated in 6-well plates at 1x10_5 cells/ml. Any excess cells were frozen for storage by washing twice with PBS, detaching cells using trypsin, centrifuging at 500 rcf for 5 minutes, resuspending the cell pellet in 10% (v/v) DMSO in foetal bovine serum then freezing using a Mr. Frosty (Corning) slow freeze container. Cells from 6 well plates to be used in experiments did not have wells combined. Triplicate wells were used as technical triplicates and multiple plates with receiving lipoproteins from different combined donors were used as biological triplicates.

2.4.2 HAoSMC Calcification

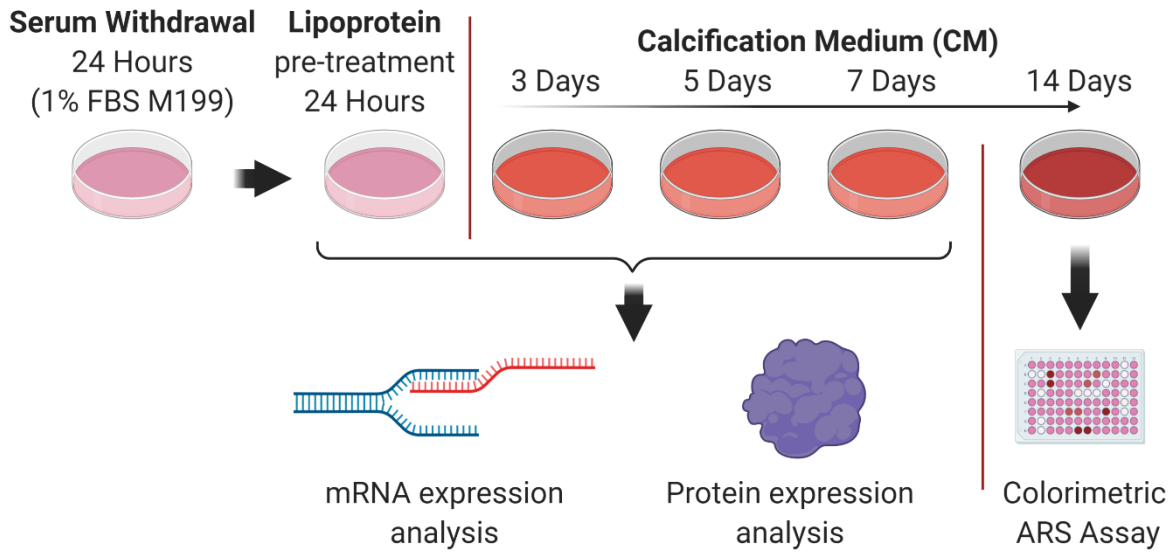

Figure 2.4.2.1 *In vitro* experimental timeline.

After a 24 hour incubation in low serum media, HAoSMCs were either left untreated (NT) or treated with CM, native lipoproteins, or oxidised lipoproteins (200 µg/ml) for 24 hours before undergoing calcification. Cells and media were harvested either pre-calcification (immediately after lipoprotein exposure), or 5 or 7 days post calcification for mRNA and protein expression analysis. Additionally, cells were harvested after 15 days of calcification to assess changes in mineralisation caused by pre-treatments using the alizarin red s (ARS) calcification stain.

HAoSMCs were serum starved in 6-well plates in M199 media (Sigma) supplemented with 1% pen/strep, 1% L-glutamine and 1%FBS (starvation medium), then treated with $CaPO_4$ supplemented media (calcification medium (CM): M199 media: 2.7 mM $CaCl_2$, 2.0 mM $NaPO_4$) for up to 15 days. The media was changed 3 times per week on alternate days and cells were harvested at indicated timepoints. All experiments performed in this thesis used passage 7 HAoSMCs.

Figure 2.4.2.1.1 shows a timeline for *in vitro* cell calcification experiments. To study the effects of lipoproteins on these cells 200µg/mL rHDL, oxrHDL, HDL, oxHDL, LDL, oxLDL, VLDL or oxVLDL were applied to the cells for 24 hours after 1 day in low serum media and before the application of CM. Cells were washed twice briefly with 2 mL of PBS between removing the lipoproteins and applying the CM. The cells or cell culture supernatants were used after 5 or 7 days of calcification for RNA or Protein analysis or after 15 days for calcification deposition analysis as detailed below.

2.4.2.1 HAoSMC Calcification – Human Serum Pre-Treatments

10% human serum diluted in M199 media (Sigma), supplemented with 1% pen/strep, 1% L-glutamine and 1%FBS, was applied to cells immediately following a 24 hour serum starvation period in low serum media. Cells then incubated in the 10% serum for 24 hours and were rinsed twice with 1XPBS before incubating in CM for 15 days. Cell calcification was measured by ARS assay as described below. Relevant protocols and ethics approval numbers are presented in their respective results chapters.

2.4.3 Alizarin Red S Stain Calcification Identification *in vitro*

2.4.3.1 Methods Used in Experimental Analysis

Fully calcified HAoSMCs were harvested after 15 days of calcification media (CM) for the detection of calcification via Alizarin Red S (ARS) staining as previously described[662]. Briefly, cells were fixed using 10% (v/v) formaldehyde (ProSciTech) for 15 minutes at room temperature, washed twice with 2 mL RO water, then stained using 1 mL 40mM pH 4.1 ARS (Chem-Supply) by incubating shaking at room temperature for 20 minutes. The plate was then washed twice with 2 mL RO water and stored at -20^{o}C until further use, or immediately dissolved in 800 µL 10% (v/v) acetic acid (Univar) gently shaking at room temperature for 15 minutes. Cells and acetic acid were scraped into Eppendorfs and incubated at 85^{o}C for 10 minutes with 500 µL mineral oil (Sigma), then spun at 20,000 x *g* in an Eppendorf 5424R centrifuge to remove cell debris. 200 µL 10% (v/v) ammonium hydroxide (Sigma) was added to the bottom layer to neutralise the pH, then read on a Promega GloMax Discover spectrophotometer at the wavelength 405 nm.

2.4.3.2 Methods Used in Optimisation of Assay

For the optimisation assay presented in chapter 3, cells calcified in medium for various timeframes were stained as per methods above (2.4.3.1). Plates were then photographed using an Oppo R11 phone and opened using Image J (FIJI) software. The images were thresholded for the distinctive red colour of the alizarin red s stain present on calcified tissue, and a percentage of area calcified was obtained.

2.5 RNA Extraction

2.5.1 RNA Extraction from Cells

To extract RNA, cells were washed once with cold PBS before adding 500 µl cold Tri Reagent (Sigma), scraping cells and transferring to a 1.5 ml Eppendorf. 100 µl of 1-bromo-

3-cholropropane (Sigma) was added to each Eppendorf, which were then vortexed, centrifuged at 14,000 x *g* for 15 minutes at 4°C to separate the RNA, DNA and protein into different phases. The top, RNA containing layer was collected into a new Eppendorf tube with 250 µl of isopropanol, then stored at -20°C overnight. Precipitated RNA was pellet by centrifugation at 14,000 x *g* for 15 minutes at 4°C and the supernatant was removed. The pellet was then washed with ethanol by vortexing and centrifuged again at 14,000 x *g* for 10 minutes at 4°C. The supernatant was removed, and the RNA pellet was dried until clear of ethanol. 20 µl of nuclease free water was used to dissolve the RNA pellet by using a 10-minute incubation at 60°C on an Eppendorf shaker then stored at -80°C. RNA was quantified using a Thermo Scientific NanoDrop 8000 Spectrophotometer nanodrop and normalised using nuclease free water to 100 ng/µl.

2.5.2 RNA Extraction from Tissue

The commercially available AllPrep DNA/RNA/Protein Mini Kit (Qiagen) was used to extract protein, DNA and RNA simultaneously from animal tissues as per kit instructions. RNA was quantified using a Thermo Scientific NanoDrop 8000 Spectrophotometer nanodrop and normalised using nuclease free water to 100 ng/µl.

2.6 Reverse Transcription

cDNA from normalised RNA was generated by performing reverse transcription polymerase chain reaction (RT-PCR). 500 ng RNA was aliquoted to PCR tubes with 2 µl of 5x iScript Supermix (BioRad) reaction buffer and 3 µl of nuclease free water to total 10 µl per reaction. The tubes were then primed for 5 minutes at 25°C, reverse transcribed at 42°C for 30 minutes, inactivated at 95°C for 5 minutes and held at 15°C for no longer than 10 minutes. cDNA was stored at -20°C.

2.7 Polymerase Chain Reaction

2.7.1 Primer Design and Sequences

Primers were found in the literature and assessed using both the NCBI BLAST software and the Sigma software for acceptable binding, melting temperatures and secondary structure likelihood limits. Primers used are outlined in table 2.7.1.1 and 2.7.1.2.

Table 2.7.1.1 List of Human Primers

Primer Label	Primer Sequence
GAPDH Forward	GAAGGCTGGGGCTCATTT
GAPDH Reverse	CAGGAGGCATTGCTGATGAT
Runx2 Forward	TGGTTACTGTCATGGCGGGTA
Runx2 Reverse	TCTCAGATCGTTGAACCTTGCTA
RANKL Forward	CACTATTAATGCCACCGAC
RANKL Reverse	GGGTATGAGAACTTGGGATT
RANK Forward	ATGCGGTTTGCAGTTCTTCTC
RANK Reverse	ACTCCTTATCTCCACTTAGG
OPG Forward	TCTATACTGCAGCCCCGTGT
OPG Reverse	AGGAGGGCAGCTCCTATGTT
ALP Forward	ACCACCACGAGAGTGAACCA
ALP Reverse	CGTTGTCTGAGTACCAGTCCC
SmαActin Forward	CAGGGCTGTTTTCCCATCCAT
SmαActin Reverse	ACGTAGCTGTCTTTTTGTCCC

Table 2.7.1.2 List of Mouse Primers

Primer Label	Primer Sequence
β-Actin Forward	AACCGTGAAAAGATGACCCAGAT
β-Actin Reverse	CACAGCCTGGATGGCTACGTA
Runx2 Forward	AACGATCTGAGATTTGTGGGC
Runx2 Reverse	CCTGCGTGGGATTTCTTGGTT
RANKL Forward	TGTACTTTCGAGCGCAGATG
RANKL Reverse	AGGCTTGTTTCATCCTCCTG
ALP Forward	GTGACTACCACTCGGGTGAAC
ALP Reverse	CTCTGGTGGCATCTCGTTATC
OPG Forward	ATCAGAGCCTCATCACCTT
OPG Reverse	CTTAGGTCCAACTACAGAGGAAC
HMGCOAR Forward	AGCTTGCCCGAATTGTATGTG
HMGCOAR Reverse	TCTGTTGTGAACCATGTGACTTC
SREBP1 Forward	AGCAGCCCCTAGAACAAACAC
SREBP1 Reverse	CAGCAGTGAGTCTGCCTTGAT
GLUT2 Forward	GGCTAATTTCAGGACTGGTT
GLUT2 Reverse	TTTCTTTGCCCTGACTTCCT
LDLR Forward	AGCCATGTACGTAGCCATCC
LDLR Reverse	CTCTCAGCTGTGGTGGTGAA

2.7.2 Real-Time PCR

Real-time PCR was performed on either a BioRad CFX Connect or a QuantStudio 7. 0.4 µM of each primer pair, iQ SYBR Green Super Mix and nuclease free water were prepared in a master mix appropriate for final well volumes of either 10 or 15 µl. Regardless of final volume, 1500 ng of cDNA was added to each reaction. The reaction was activated at 95°C for 3 minutes, then amplified using a cycle of 10 seconds denaturation at 95°C, 10 seconds annealing at 60°C then 30 seconds of extension at 72°C, with an absorbance read after each cycle. The PCR was followed by a melt curve reading to identify incomplete or contaminated samples, briefly, samples had absorbance measured at 5 second intervals with a temperature increase of 0.5°C per 5 seconds between 65°C and 95°C. Quantification of the gene of interest was calculated relative to the GAPDH control gene by the comparative ($\Delta\Delta C_T$) method[663].

2.8 Protein Extraction

2.8.1 Protein Extraction from Cells

To extract protein, cells from individual wells (9.6 cm^2) of a 6 well plate were washed once with cold PBS before adding 100 µl cold radioimmunoprecipitation assay (RIPA) buffer (Sigma) to each well. Phenylmethylsulfonyl fluoride (PMSF) protease inhibitor cocktail (1:100) (Sigma) were added to the RIPA buffer immediately prior to application to the cells and plates were stored in RIPA buffer at -80°C overnight. Cells were then thawed on ice, gently scraped, transferred to Eppendorf tubes and sonicated at 20% amplitude for 3 seconds. The samples were centrifuged at 440 rcf for 4 minutes to remove bubbles and cell debris. The supernatant was collected, transferred to a new Eppendorf tube and stored at -80°C. The Pierce BCA Assay (Life Technologies) was used to estimate protein

concentration from each well to normalise samples to indicated concentrations. Protein from individual wells were not combined.

2.9 Electrophoresis

2.9.1 SDS-Polyacrylamide Gel Electrophoresis

Sodium dodecyl sulphate polyacrylamide gel electrophoresis (SDS-PAGE) was performed using Life Technology running tanks, Bolt™ 4-12% Bis-Tris Plus Gels and Bolt™ MES SDS Running Buffer with a Bio-Rad Precision Plus Dual Colour molecular weight ladder. 30 µl of samples at 1 µg/30 µl were incubated at 95°C for 5 minutes with 3 µl 1X Bolt™ Sample Reducing Agent and 8 µl 4X Bolt™ LDS Sample Buffer before cooling on ice and loading into wells. The gel was then run for 1 hour at 120 V on a Bio-Rad PowerPac™ HC.

2.9.2 Coomassie Blue Stain

A coomassie blue stain was used to confirm the presence of apo AI in fraction samples from FPLC. The gel was incubated under agitation at room temperature for 1 – 2 hours in 10 ml coomassie blue solution (500 ml H_2O, 100 ml acetic acid, 400 ml methanol, 1 g coomassie brilliant blue R-250), then de-stained using several 15 minute changes of de-stain solution (500 ml H_2O, 100 ml acetic acid, 400 ml methanol) under agitation at room temperature until protein negative areas were clear. Fractions that were identified at apo AI at 25 - 30 kDa were pooled and progressed through method 2.2.

2.9.3 Western Blot

The protein from SDS-PAGE gels were transferred to nitrocellulose membranes using Life Technology iBlot™ Transfer Stacks and iBlot™ Transfer System at 20 V for 1 minute, 23 V for 4 minutes then 25 V for 2 minutes. The membrane was briefly incubated with ponceau solution (Sigma) to confirm protein transfer. The membrane was then washed with RO water and blocked using 10% (w/v) skim milk in TBS-Tween (TBS-T) solution (20X TBS: fill to 2L H_2O, 4.8 g Tris Base, 350.6 g $NaCl_2$, pH 7.4. TBS-T: 1900 ml H_2O, 100 ml 20X TBS,

2 ml Tween20), for at least 1 hour. The membrane was washed using 3 changes of 5 minutes each TBS-T before incubating at 4°C over 4 nights (unless otherwise indicated) in primary antibody diluted with TBS-T at indicated concentrations (see table 2.9.3.1). Membranes were washed again, then incubated with appropriate secondary antibodies diluted in TBS-T at indicated concentrations for 2 hours (see table 2.9.3.1). The membranes were then washed again and visualised using a Pierce ECL reagent kit (Life Technologies) as per protocol, Bio-Rad ChemiDoc systems and ImageLab 6.0 (Bio-Rad, 2017) software. All incubations were performed with agitation at room temperature. Band densities were normalised to a standard sample to allow inter-blot normalisation and β-Actin was used as the housekeeper protein. Data is presented in this thesis as fold change from the cells receiving no treatment.

Table 2.9.3.1 List of Antibodies Used for Western Blots

Antibodies	Company	Dilution
Mouse anti Human Runx2 Primary	Jomar Life Research D130-3	1:600
Mouse anti Human RANKL Primary	Metagene sc-377079	1:250
Rabbit anti β-Actin (incubated over 1 night only) Primary	Abcam ab8227	1:5000
Mouse IgG VisUCyte HRP Polymer Secondary	In Vitro Tech RDSVC001025	1:2000
Rabbit IgG VisUCyte HRP Polymer Secondary	In Vitro Tech RDSVC003025	1:2000

2.10 Cell Culture Supernatant Protein Analysis

Total protein in the cell culture supernatant collected from cell experiments at indicated timepoints during the calcification assay were measured using the Pierce BCA Assay (Life Technologies) with a bovine serum albumin standard. Enzyme-linked immunosorbent assays (ELISAs) for RANKL (In Vitro Tech, R&D Systems DuoSet kit: cat# RDSDY626 and RDSDY008) and OPG (Abcam: cat# ab100617) were the used as per protocol to find cell culture supernatant protein concentrations of RANKL and OPG with quality control and negative controls included on each plate. The results from the ELISA were then normalised to the total protein results.

2.11 General Mouse Study Protocols

2.11.1 Animal husbandry

Mice were housed at the South Australian Health and Medical Research Institute (SAHMRI) under the animal ethics approval number SAM186 (studies in chapter 4) and SAM188 (studies in chapter 6). Mice were kept in accordance with the Australian code for the care and use of animals for scientific purposes (National Health and Medical Research Council, 2013). International Biosafety committee (IBC) approval number is BC 029/2014.

Up to 5 sibling mice of the same gender were housed in each cage, which had bedding changed twice per week and were given fresh water and food ad libitum. Upon commencement of the experiment, the food available was the atherogenic, 22% fat and 0.15% cholesterol diet SF00-219 (Specialty Feeds). Prior to entering the study, mice were fed a standard rodent diet (Teklad Global 18% Protein Rodent Diet, Harlan Laboratories) containing 18.6% protein, 6.2% fat, 44.2% carbohydrates, and 0% cholesterol. Mice were weighed weekly and monitored daily.

Mice were obtained from the Jackson Laboratory (USA) and genetic knock out lines were confirmed either on site using the Genetic Engineering and Archiving Services (GENEAS)

or off site using the mouse genotyping services at the Garvan Institute of Medical Research (Australia).

2.11.2 Mouse Terminal Cardiac Puncture

Mice were humanely killed under isoflurane anaesthesia by both terminal cardiac puncture and lung harvest. After anaesthesia was confirmed, ethanol was applied to the chest and abdomen before making a small incision in the skin immediately below the centre of the rib cage. Terminal cardiac puncture was performed by identifying the heart through the incision, then using a 25-gauge needle attached to a 1 mL syringe and inserting into the left ventricle of the heart until flashback was observed. Complete exsanguination of blood from the ventricle was completed before opening the chest cavity completely, making a small incision in both atria, then injecting 2 mL of saline into the right ventricle to flush the blood from the mouse. The lungs were then completely removed, and isoflurane was ceased.

2.11.3 Mouse Tissue Collection

Immediately following cardiac puncture, blood was collected in EDTA blood collection tubes for plasma isolation, the liver was collected and weighed, then the left ventricle was flushed with 3 mL of normal saline. Tissues were then collected and weighed then either snap frozen in liquid N_2 or fixed in 10% neutral buffered formalin overnight for morphological analysis.

2.12 Staining

2.12.1 Sample and Slide Preparation

Tissues collected in 3 ml 10% formalin were incubated at room temperature overnight then stored in cassettes submerged in a beaker of 70% ethanol until tissue processing. Tissues were processed using a Shanson Excelsior ES® Tissue Processor (ThermoFischer Scientific), by using automated ethanol gradient concentrations to xylene and then paraffin in an 11 hour run. The tissues were then embedded into paraffin was blocks using a HistoStar™ Embedding Workstation (ThermoFisher Scientific). Blocks where stored at room temperature and placed on ice 1 hour prior to microtome sectioning.

5 µm sections of formalin fixed, paraffin embedded tissues were cut, mounted on Thermo Fisher SuperFrost™ Plus Adhesive Slides and dried at 60°C overnight. On the day of staining, slides were de-paraffinised by immersion in two changes of xylene (5 mins) followed by re-hydration in 4 changes of decreasing concentrations of ethanol (2x 100% ethanol, 2x 95% ethanol and 1x 70% ethanol, 1 minute each), then immersed in RO water for at least 1 minute.

2.12.2 Immunohistochemical Staining

2.12.2.1 Slide Preparation

Antigen retrieval was performed by microwaving slides for 2x 10 minutes at 70% power in sodium citrate buffer (fill to 1L H_2O, 2.94 g tri-sodium citrate (dehydrate), pH 6.0, 0.5 ml Tween20), maintaining a temperature of 95 – 99°C after the solution reached boiling point. Slides were then rinsed with RO water until cooled and then with 5 minutes of PBS-T (1L PBS, 1 mL Tween20). Endogenous peroxidase activity was blocked by incubation with 0.3% (v/v) H_2O_2 in methanol for 20 minutes at room temperature, then washed again for 5 minutes in PBS-T. The sections were then blocked in 10% (v/v) goat serum for at least 4 hours at room temperature.

2.12.2.2 CD68 Staining

The primary antibody, rat anti mouse CD68 (Bio-Rad), was diluted 1:100 in 5% BSA (in PBS-T), applied to the slides and incubated overnight at 4°C. The slides were then washed with 2x changes of PBS-T for 5 minutes each before incubating with biotinylated goat anti-rat antibodies (Abacus, VEBA9401) diluted in 10% horse serum for 2 hours at room temperature. Slides were then washed three times, 5 minutes each wash, with PBS-T before developing colour with DAB kit (Abacus, VESK4105) for 12 minutes, as per protocol. Colour change was inhibited by dipping the slides in water.

2.12.2.3 SMαActin Staining

Sections were incubated in monoclonal mouse α-mouse SMαActin conjugated to alkaline phosphatase (1:50, Sigma, A5691) in 1% BSA, covered overnight at 4°C. Slides were then washed twice for 5 minutes each in PBS-T before developing colour with Vector Red Alkaline Phosphatase Substrate Kit (Abacus, VESK5100) for 12 minutes, as per protocol. Colour change was inhibited by dipping the slides in water.

2.12.2.4 Slide Imaging

All immunohistochemically stained slides were counterstained with Meyer's haematoxylin then dehydrated through increasing ethanol (1x 70%, 2x 95%, 2x 100%) concentrations to xylene (1 minute each) and mounted in DPX (Sigma) with coverslips. Slides were imaged using a Zeiss Axio Lab.A1 microscope at 5X – 10X magnification and a Zeiss AxioCam ERc 5s camera. Images were analysed using FIJI is just ImageJ 1.52h (FIJI) software (National Institutes of Health, USA). Briefly, colour thresholds were determined using 5 sample images and applied to all images. Colour positive areas were measured and presented as a percentage of plaque area.

2.12.3 Special Staining

2.12.3.1 Alizarin Red S Slide Stain

Rehydrated slides were incubated in 2% ARS (Chem-Supply, AL080-25G) solution, pH4.2 (diluted in MilliQ water) for 2 minutes. Slides were allowed to drain before 20 dips of acetone (Thermo, FSBA/0600/17), then 20 dips of acetone:xylene (1:1). Slides were incubated for 1 minute in xylene 2 times, then mounted using DPX mounting media (Sigma) and coverslips (Thermo).

2.12.3.2 H&E Stain

Rehydrated slides were submerged in Meyer's Haematoxylin (Australian Biostain) for 45 seconds, followed by a 1 minute wash in running water. Slides were then dipped twice in 0.3% acid ethanol (36% HCl (Univar) 3 ml, 70% ethanol (LabServ) 100ml), Scott's tap water (2 L water, sodium bicarbonate (sigma) 7 g, magnesium sulphate (sigma) 40 g), for 1 minute. The slides were then washed with 3 dips of water before staining with eosin (eosin (Sigma) 100 mg, calcium chloride (Univar) 2 g, water 100 ml), for 1 minute. Slides were washed with running tap water for 1 minute, then dehydrated through increasing ethanol (1x 70%, 2x 95%, 2x 100%) concentrations to xylene (1 minute each) and mounted in DPX (Sigma) with coverslips.

2.12.3.3 Masson's Trichrome Stain

A Masson's trichrome stain was performed per manufacturer's instructions (Abcam). Briefly, rehydrated sections were incubated with Weigert's haematoxylin for 5 minutes before washing under running tap water for an additional 5 minutes. Sections were then incubated in Beibrich Scarlet/Acid Fuchsin solution for 5 minutes, washed in tap water for 1 minute before being differentiated in phosphomolybdic/phosphotungstic acid solution for 5 minutes and then aniline for a further 5 minutes., Sections were then rinsed briefly in tap water, incubated in 1% acetic acid for 2 minutes, rinsed briefly in tap water then

dehydrated by 2 quick dips through an ethanol gradient (1x 70%, 2x 95%, 2x 100%) then 1x 2 minute incubations in xylene. Slides were then dried and then mounted using DPX mounting media (Sigma) and coverslips (Thermo).

2.13 Blood Plasma Analysis

2.13.1 Mouse Plasma Processing

Blood was collected from animals prior to diet commencement and throughout the study at regular intervals via tail vein incision, with blood allowed to drip into EDTA-Na_2 coated tubes, then centrifuged at 1500 rcf in an Eppendorf Centrifuge 5810 R for 15 minutes at 4^{o}C to obtain plasma, which was stored at -80^{o}C until analysis.

2.13.2 Mouse Plasma Analysis

All chemical assays were measured on a Promega GloMax Discover spectrophotometer. Concentrations of triglycerides (WAKO: Novachem cat# 439-17501) (2µl plasma used per mouse, in duplicate), total cholesterol (WAKO: Novachem cat# 432-40201) (2µl plasma used per mouse, in duplicate), calcium (Cayman Chemical) (5µl plasma used per mouse, in duplicate) and ALP protein (WAKO: Novachem cat# 291-58601) (5µl plasma used per mouse, in duplicate) were quantified using commercially available colourimetric assay kits. OPG protein concentration was analysed using a commercially available ELISA assay (Abcam: cat# ab203365) (50µl plasma used per mouse, in duplicate) as per manufacturer's instructions.

2.13.3 Human Plasma or Serum Analysis

Human plasma total cholesterol, HDL-cholesterol and triglyceride content was measured by ClinPath Services, Adelaide. Serum calcium (Cayman Chemical) and ALP protein (WAKO) levels were measured using commercially available colourimetric assay kits as per manufacturer's instructions.

2.14 Statistical Analyses

All data in this thesis are expressed as mean± SEM. GraphPad Prism Version 8 (San Diego, CA) was used to analyse results using the tests as appropriate in table 2.14.1. A p value of <0.05 was considered statistically significant.

Table 2.14.1 Statistical tests and rationale

Test	Rationale
D'Agostino-Pearson's omnibus normality test	Tested all data sets larger than n=3 for normal (Gaussian) distribution
Unpaired t-test (t-test)	Used to test the difference in 1 variable between 2 groups, of parametrically distributed data or cell experiments of n=3
Mann-Whitney test	Used to test the difference in 1 variable between 2 groups, of nonparametrically distributed data or mouse experiments of n=3
One-way ANOVA with Bonferroni's correction	Used to test the difference in 1 outcome measurement between 3 or more groups with 1 variable, of parametrically distributed data or cell experiments of n=3
Kruskal-Wallis test with Dunn's correction	Used to test the difference in 1 outcome measurement between 3 or more groups with 1 variable, of nonparametrically distributed data or mouse experiments of n=3
Two-way ANOVA	Used to test the difference in 1 outcome measurement between 2 groups with 2 variables

Pearson correlation coefficients	Used to test the r value correlation and p value significance by plotting 2 measured outcomes of individuals within a population

3 : Chapter Three

Vascular Smooth Muscle Cell Calcification

3.1 Introduction

It is now widely accepted that calcification associates with plaque progression[58] and vulnerability[264] in different settings and measurement of CAC has been increasingly used for more accurate cardiovascular risk assessments[271, 272]. Despite the clear need to understand this disease, research into calcification triggers and mechanisms however has been hindered in part due to a lack of *in vitro* model standardisation.

As detailed in chapter 1, the calcification process involves the differentiation of vascular smooth muscle cells (VSMC) into osteoblast-like cells which express calcification markers, such as runt related transcription factor 2 (Runx2) and receptor activator of NF-κB ligand (RANKL), followed by raised alkaline phosphatase (ALP) expression and excretion of calcifying matrix vesicles[664]. Additionally, inhibition of local and circulating calcification inhibitory proteins, such as MGP and OPG contribute significantly to the formation of VC[665]. Although Runx2 expression regulates RANKL and OPG expression[666] an exact time point of when these molecules are expressed depends on the type of cell. Moreover, RANKL and OPG have biphasic expression patterns[667], adding to the time-dependant complexity of measuring calcification markers *in vitro*.

Within the literature however, there is a lack of standardisation creating difficulties when comparing results. Table 3.1.1 below outlines most common potential variables in these assays.

Table 2.13.3.1 Common variables present in the literature for *in vitro* calcification assays

Variables	Common Variants
Donor Species	Human, Mouse, Rat, Cow, Pig
Donor Artery	Aortic, Carotid, Coronary, Umbilical, Valvular
Donor Cell Variety	Regular, Calcification Prone, Passage
Donor Calcification Susceptibility	Age, Gender
Growth Medium	With or without growth hormones
Calcification Medium	Mineral concentration (e.g. Ca and PO_4), FBS concentration, Additives (e.g. dexamethasone)
Calcification End-Point	Nodule formation, Mineral formation, expression of mRNAs or proteins involved in differentiation or mineralisation

When studying vascular calcification *in vitro*, 2 main media types for calcification tend to be used: media which contains either organic or inorganic phosphates. The first of which containing organic phosphate (β-glycerophosphate), allows ALP to be secreted from the differentiated VSMCs to hydrolyse the β-glycerophosphate into inorganic phosphate, which is now able to incorporate into the calcifying nodules in the extracellular matrix[668]. Although the initial use of inorganic phosphate may promote mineralisation by 'skipping' this hydrolysation step, ALP is still needed to inhibit potent calcification inhibitors (namely, inorganic pyrophosphate)[668], therefore it remains unclear which pathology is more relevant.

Many studies also use media containing a synthetic glucocorticoid, a family of molecules known to induce osteoblastic differentiation in bone cells[669] and VSMCs[670], called

dexamethasone. Although VSMCs do not need dexamethasone to differentiate or calcify, the molecule reduces the time needed for the cells to differentiate[670].

The aim of this study therefore has 2 parts: the first is to design an assay which allows the exploration of the experimental questions of this thesis, and the second is to characterise the likeness of our assay to the literature by showing progressive differentiation and calcification of VSMCs over time. To achieve this, human aortic smooth muscle cells (HAoSMCs) were incubated with high inorganic phosphate and calcium levels and assessed for calcification potential using the alizarin red s assay, mRNA expression using PCR and protein expression using western blotting and ELISA assays.

3.2 Methods

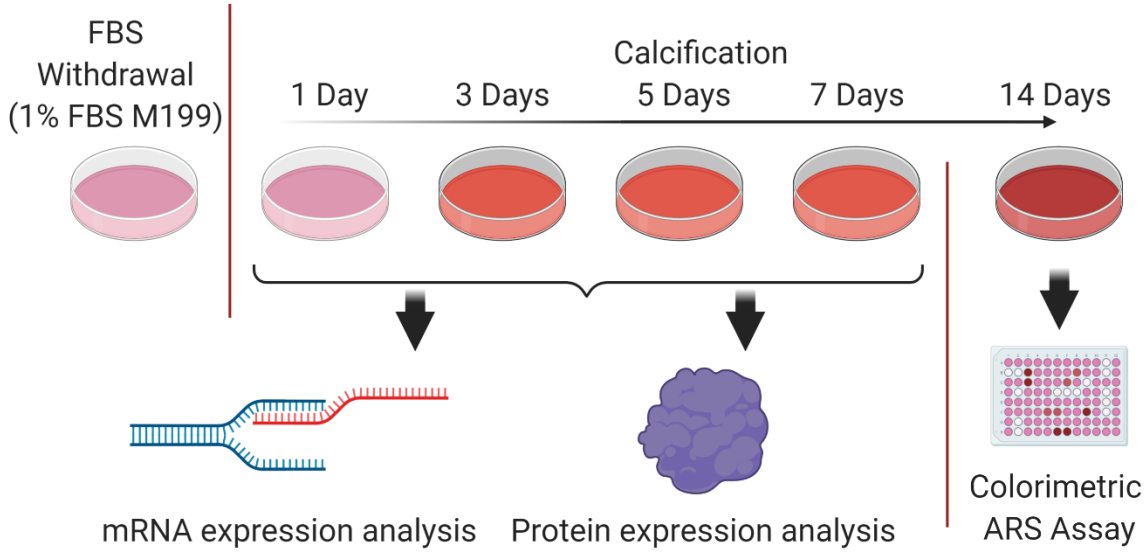

Figure 2.13.3.1 Schematic of the *in vitro* calcification assay.

HAoSMCs were treated with $CaPO_4$ (Ca 2.7 mM, PO_4 2.0 mM) medium (CM) for up to 15 days. Cells were then analysed at various timepoints with PCR, western blot and stained with Alizarin Red S (ARS) stain to monitor calcium deposition and molecule expression.

Cells were maintained and calcified as per methods chapter 2.4. After 1,3,5 and 7 days of calcification medium (CM), cell mRNA was harvested and transformed to cDNA for PCR analysis as per methods chapter 2.5.1, 2.6 and 2.7 respectively. Cells were harvested after 5 and 7 days of calcification for protein expression analysis via methods in chapter 2.8 and 2.9. Additionally, media also was collected after the 5 and 7 day CM timepoints and analysed for protein secretion using ELISA assays as per methods chapter 2.10. A timeline of the *in vitro* calcification assay is presented in figure 3.2.1. Cells receiving no treatment were collected at all timepoints, experimented separately and combined for analysis.

3.3 Results

3.3.1 Development of the Alizarin Red S (ARS) Functional Assay

All smooth muscle cells behave differently, and this is reflected throughout multiple studies[382, 671] with varying times required for SMCs to calcify. In order to establish the length of time required for calcification, HAoSMCs were subjected to treatment with calcification medium (CM) (M199 supplemented with 2.7 mM Ca, 2.0 mM PO_4 and 1% FBS). It was determined that these cells required 15 days of CM to present with significant calcification as determined by an Alizarin Red S stain (figure 3.3.1.1). Upon analysis of the stain using image J software, the 15 day timepoint was observed to be significantly more calcified than all other timepoints (0 Days: 0.0±0.0, $p<0.0001$; 8 Days: 0.0±0.0, $p<0.0001$; 11 Days: 4.25±1.64, $p<0.0001$; 13 Days: 20.81±12.56, $p<0.001$; vs 15 Days: 74.94±1.25) (figure 3.3.1.1).

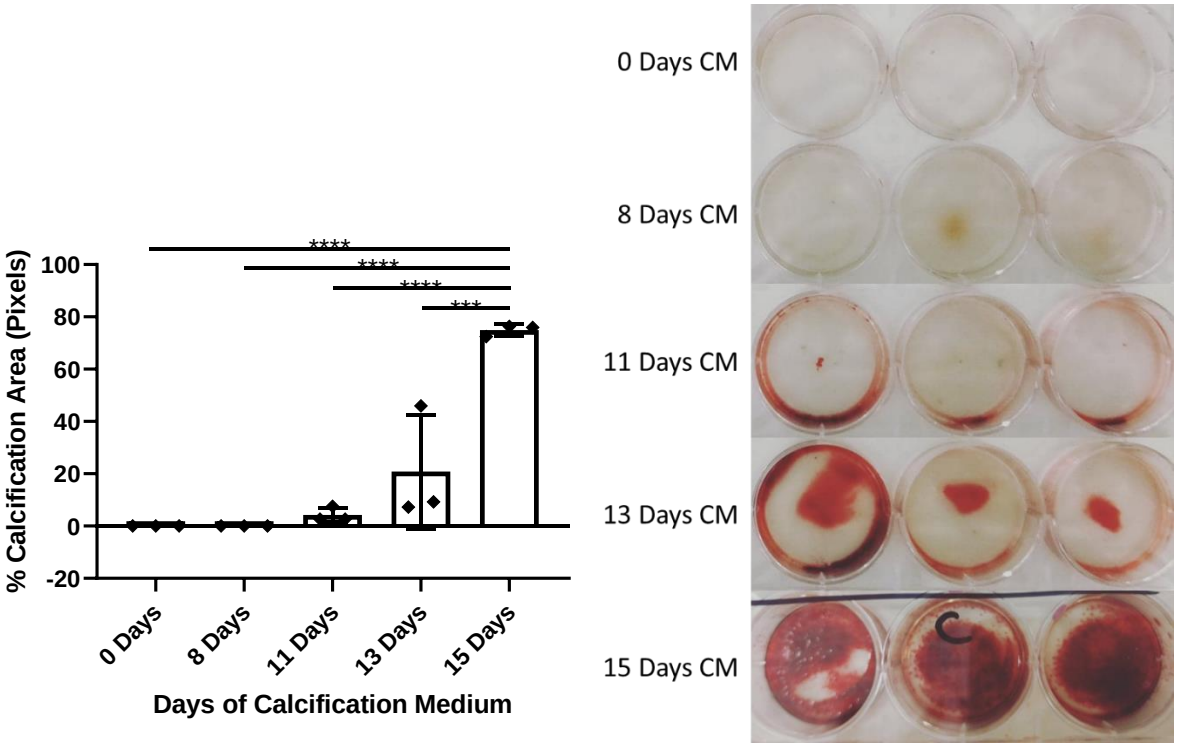

Figure 3.3.1.1 The effect of calcification medium on calcification of over time.

*HAoSMCs were treated with $CaPO_4$ (Ca 2.7 mM, PO_4 2.0 mM) medium (CM) for up to 15 days and stained with Alizarin Red S (ARS) stain to visualise calcium deposition. Images presented in figure 3.3.1 were analysed using image J software and presented as % of total well area. ***p<0.001, ****p<0.0001, ANOVA with Bonferroni's correction. Data represented mean± SEM, n=3.*

3.3.2 Vascular Calcification Markers

Based on the presence of advanced calcification determined by the Alizarin Red S stain at 15 days, the cells were then assessed at the mRNA level over a period of 1 to 7 days to determine the optimal timepoint for expression of calcification markers in HAoSMCs. Subsequently cells were then probed at the protein level at days 5 and 7 of calcification, to capture differentiation of HAoSMCs towards osteoblast expression.

Runx2 – Runx2, the master regulator of differentiation, had significantly increased mRNA expression (figure 3.3.2.1) after 7 days of calcification compared to all other timepoints and the cells with no treatment (NT) ($p<0.0001$. NT: 105.2±1.58; 1 day: 84.18±9.39; 3 days: 112.2±32.51; 5 days: 157.5±87.89; 7 days: 1440±269.5). Figure 3.3.2.1 illustrates the effects of calcification on Runx2 levels over time. After 5 days of calcification there was no difference in Runx2 protein levels, however after 7 days of calcification Runx2 was significantly increased (100±14.72 vs 1014±286.7, $p<0.001$).

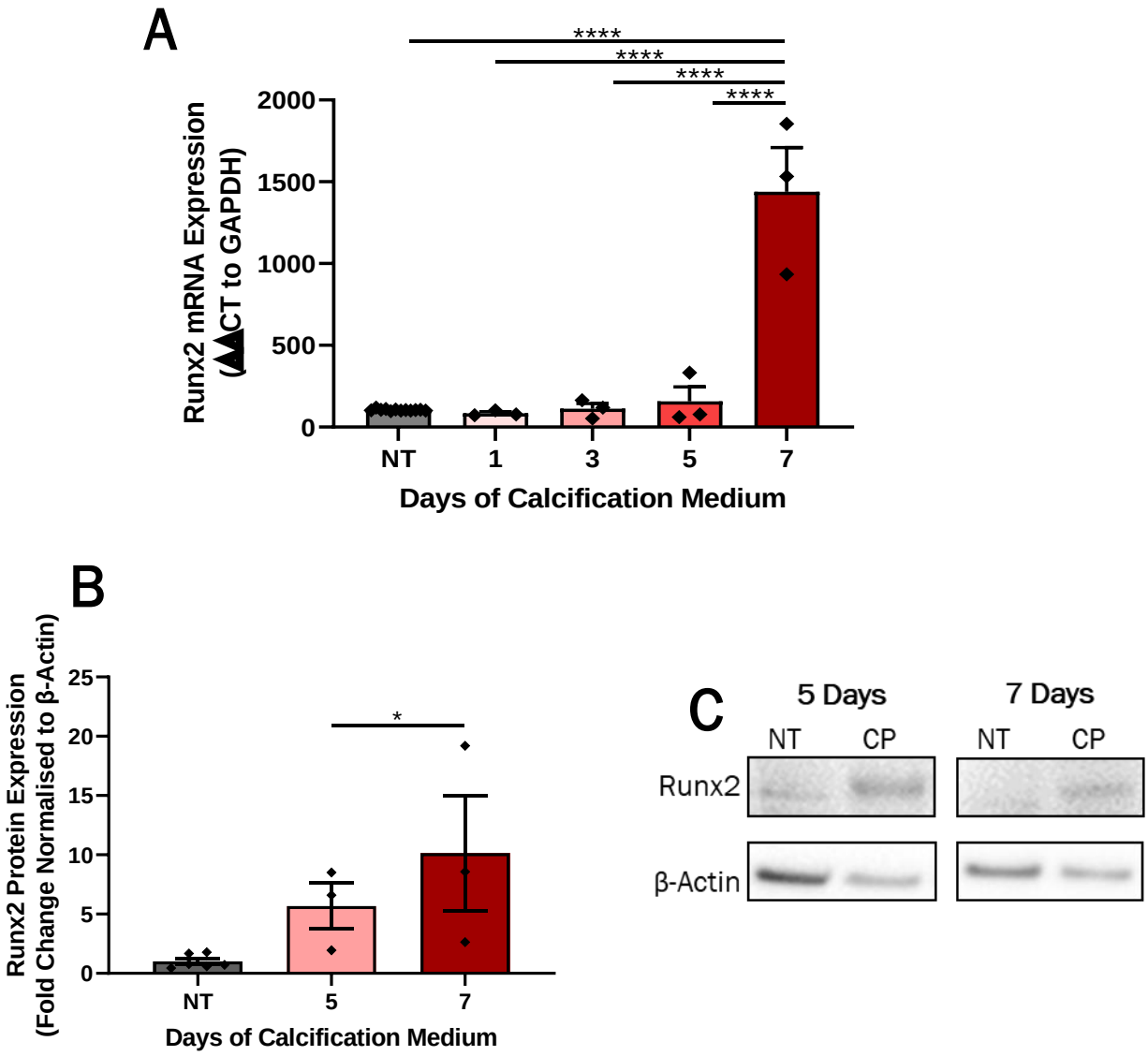

Figure 3.3.2.1 The effect of calcification medium on Runx2 expression.

*HAoSMCs were treated with $CaPO_4$ (Ca 2.7 mM, PO_4 2.0 mM) medium (CM) for indicated time points. (A) Runx2 mRNA expression was measured by qPCR using GAPDH as the internal control. (B-C) Runx2 protein expression was measured by western blotting using β-Actin and a standard sample as internal controls *p<0.05; ****p<0.0001 compared to all other conditions, ANOVA with Bonferroni's correction. Data represented as % of NT, mean± SEM, n=3.*

RANKL – The expression of RANKL can be directly influenced by activation of Runx2. Given the effects of stimulating calcification on Runx2 in the previous section, it is unsurprising to see the same pattern for RANKL as calcification occurs over time (figure 3.3.2.2 A). Similar to Runx2 mRNA expression, RANKL mRNA expression was significantly upregulated after 7 days of calcification when compared to all other timepoints (7 Days: 3174±714.0 vs NT: 110±1.84, $p<0.0001$; 1 day: 205.2±8.08, $p<0.0001$; 3 days: 469.5±20.87, $p=0.003$; 5 days: 1235±603.1, $p<0.05$). Additionally, 5 days of calcification caused a significant upregulation in RANKL mRNA expression when compared to the NT group (110±1.84 vs 1235±603.1, $p<0.05$). To confirm that the expression of RANKL protein will correspond to that of the upstream Runx2 patterns we also probed the cellular protein for RANKL. While there was an increased expression of RANKL over time, this increase was not significantly different from the NT group (figure 3.3.2.2).

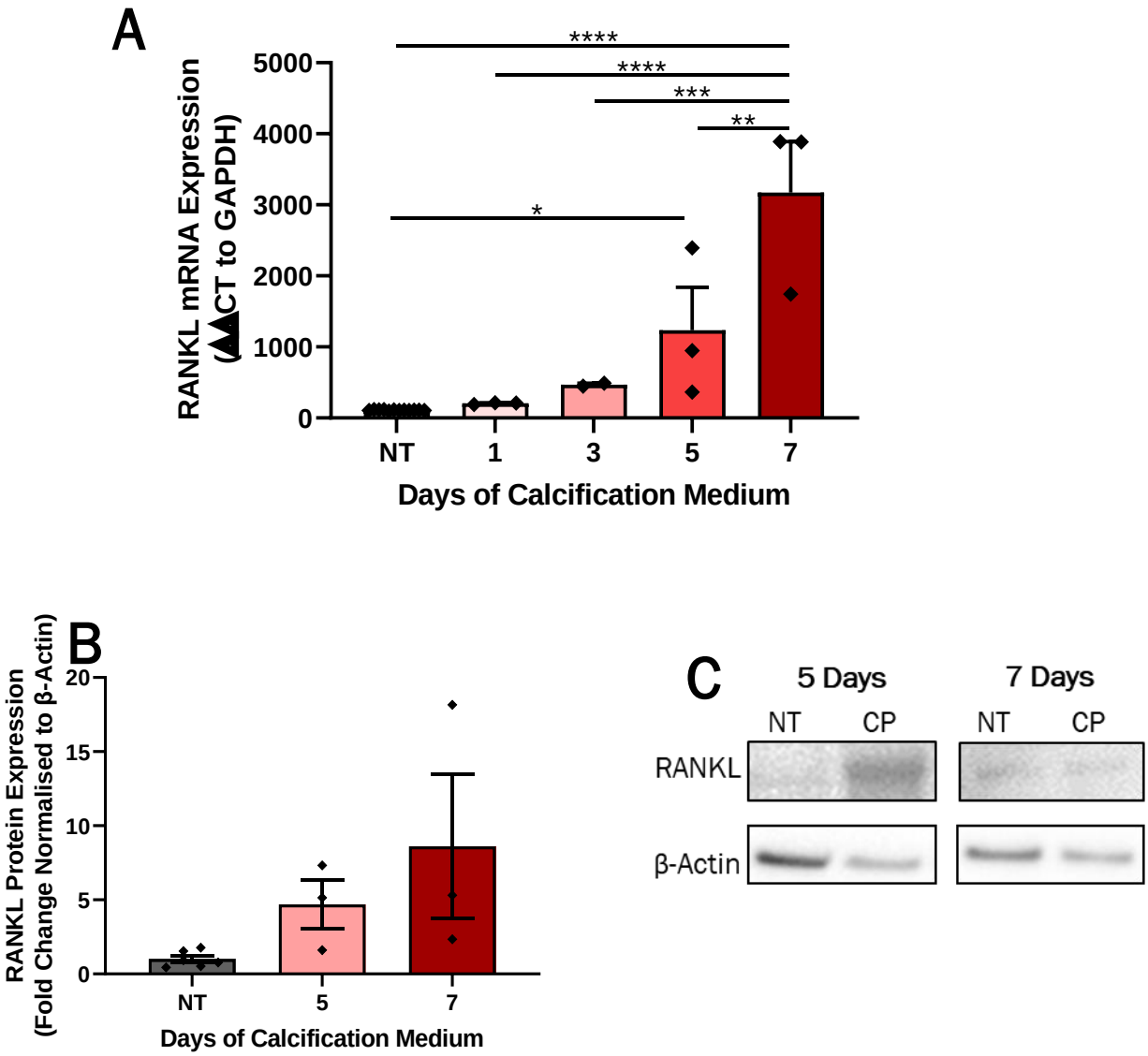

Figure 3.3.2.2 The effect of calcification medium on RANKL mRNA expression over time.

*HAoSMCs were treated with $CaPO_4$ (Ca 2.7 mM, PO_4 2.0 mM) medium (CM) for indicated time points. (A) RANKL mRNA expression was measured by qPCR using GAPDH as the internal control. (B-C) RANKL protein expression was measured by western blotting using β-Actin and a standard sample as internal controls *p<0.05, **p<0.01, ***p<0.001, ****p<0.0001, ANOVA with Bonferroni's correction. Data represented as % of NT, mean± SEM, n=3.*

In addition to membrane bound RANKL, RANKL can also be secreted to have autocrine and paracrine functions. An ELISA was used to assess levels in cell culture media from calcification stimulated HAoSMCs, normalised to total protein present (figure 3.3.2.3). After either 5 or 7 days of calcification, there was no difference in RANKL secreted when compared to the no treatment control, however after 7 days of calcification there were significantly higher RANKL levels when compared to media from cells undergoing 5 days of calcification (0.87±0.02 vs 1.068±0.03, $p<0.05$).

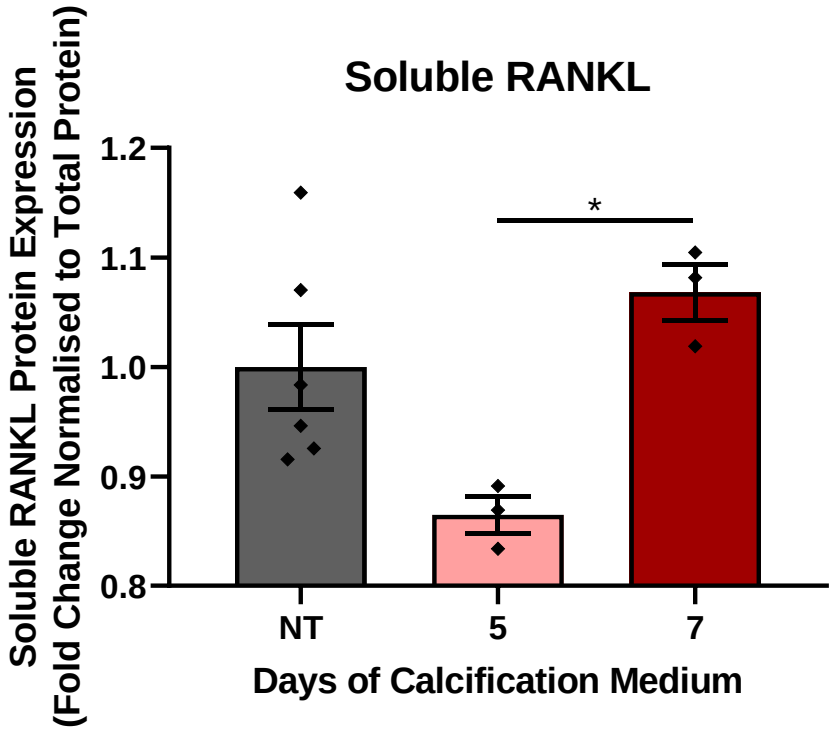

Figure 3.3.2.3 The effect of calcification medium on soluble RANKL levels.

*HAoSMCs were treated with $CaPO_4$ (Ca 2.7 mM, PO_4 2.0 mM) medium (CM) for indicated time points. Soluble RANKL protein levels were measured by ELISA using BCA measured total protein as a control. *p<0.05, ANOVA with Bonferroni's correction. Data represented as fold change of NT, mean± SEM, n=3.*

Alkaline Phosphatase – During vascular calcification mineral is deposited in the blood vessel. Immediately prior to this deposition ALP mRNA expression is upregulated due to the elevations in pH levels. Following a similar expression pattern as the previous results (figures 3.3.2.1, 3.3.2.2 and 3.3.2.3), after 7 days of calcification ALP mRNA expression (figure 3.3.2.4) was significantly increased from the NT baseline and all other timepoints (7 Days: 3174±714.0 vs NT: 110±1.84, p<0.0001; 1 day: 205.2±8.08, p<0.0001; 3 days: 469.5±20.87, p<0.01; 5 days: 1235±603.1, p<0.05).

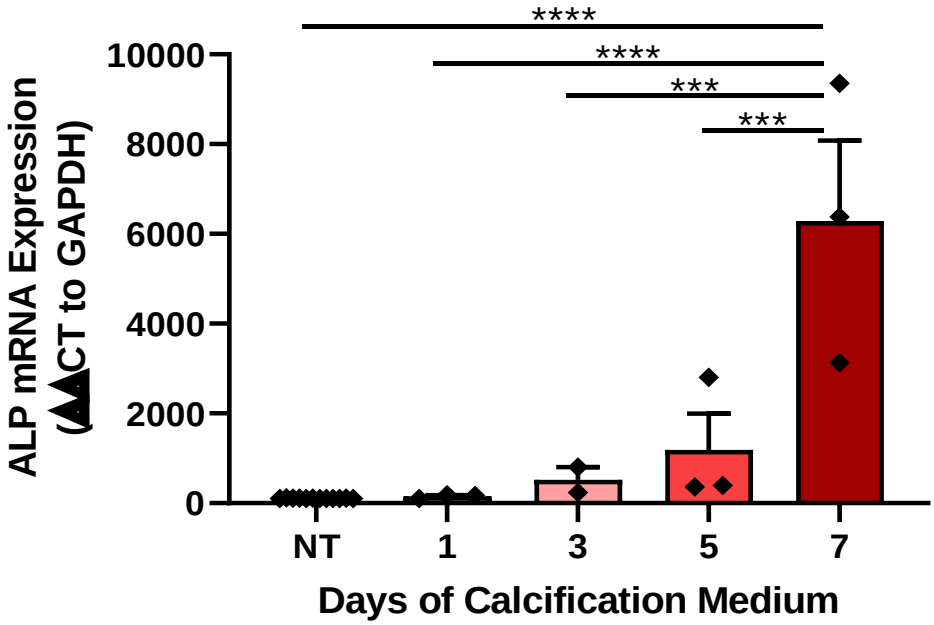

Figure 3.3.2.4 The effect of calcification medium on ALP mRNA expression.

*HAoSMCs were treated with $CaPO_4$ (Ca 2.7 mM, PO_4 2.0 mM) medium (CM) for indicated time points. ALP mRNA expression was measured by qPCR using GAPDH as the internal control. ****p<0.0001, ANOVA with Bonferroni's correction. Data represented as % of NT, mean± SEM, n=3.*

Smooth muscle alpha actin – When VSMCs differentiate they undergo a transformation from their contractile state to a more synthetic, osteoblastic phenotype[328]. A crucial identifier of this process is the presence of SMα actin. As shown in figure 3.3.2.5, SMα actin mRNA expression was reduced over time, reaching significantly lower levels after 7 days when compared to the NT group (103.6±0.52 vs 28.13±10.31, p<0.001).

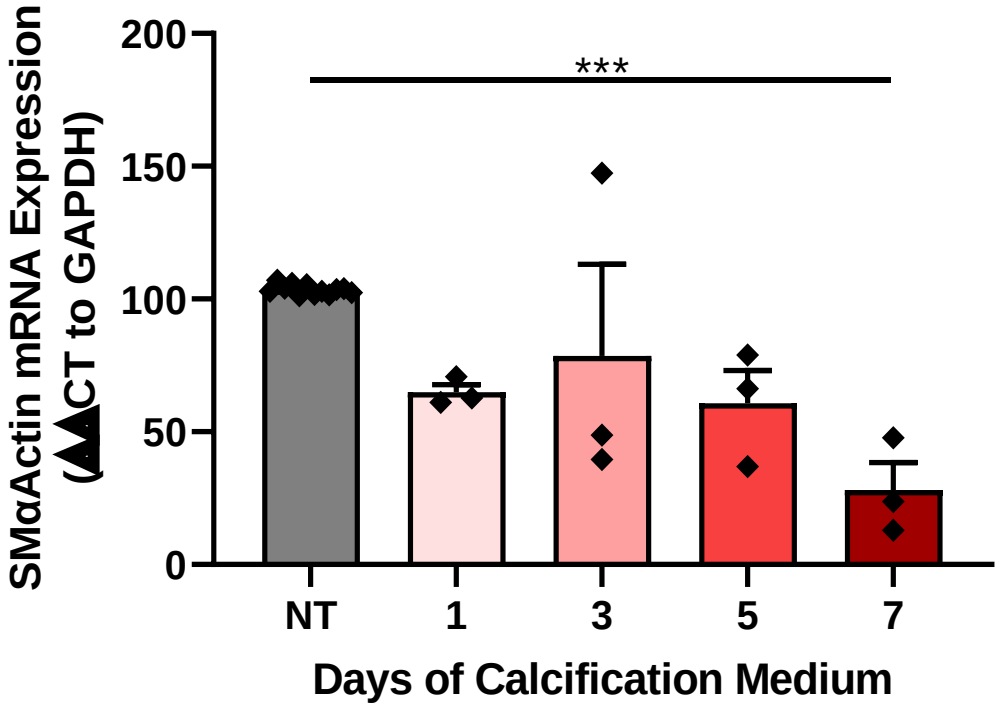

Figure 3.3.2.5 The effect of calcification medium on SMαActin mRNA expression.

*HAoSMCs were treated with $CaPO_4$ (Ca 2.7 mM, PO_4 2.0 mM) medium (CM) for indicated time points. SMαActin mRNA expression was measured by qPCR using GAPDH as the internal control. ***p<0.001, ANOVA with Bonferroni's correction. Data represented as % of NT, mean± SEM, n=3.*

Osteoprotegerin – As described in chapter 1, OPG inhibits the differentiation of VSMCs into an osteogenic phenotype providing a defence mechanism of VC. In addition to the reduced SMα actin mRNA levels observed in figure 3.3.2.5, the calcification inhibitory molecule, OPG was also reduced (figure 3.3.2.6). Stimulation of HAoSMCs with calcification medium significantly reduced OPG mRNA expression at days 5 and 7 compared to NT (NT: 104.5±1.22 vs 5 days: 53.89±30.84, $p<0.05$; 7 days: 8.5±2.15, $p<0.0001$). It was clear that expression of OPG decreased over time with levels at days 3, 5 and 7 significantly lower than day 1 (1 day: 124.6±21.91 vs 3 days: 65.32±13.37, $p<0.05$; 1 day: 124.6±21.91 vs 5 days: : 53.89±30.84, $p<0.05$; 7 days: 8.5±2.15, $p<0.0001$). Cells secrete OPG as a decoy protein, binding RANK to inhibit RANK:RANKL binding to activate calcification. Figure 3.3.4.6 A describes the effects of calcification on soluble OPG levels over time, showing that both 5 (100±3.15 vs 52.1±8.89, $p<0.001$) and 7 days (100±3.15 vs 56.44±4.71 $p<0.001$) of treatment significantly reduced OPG protein secretion.

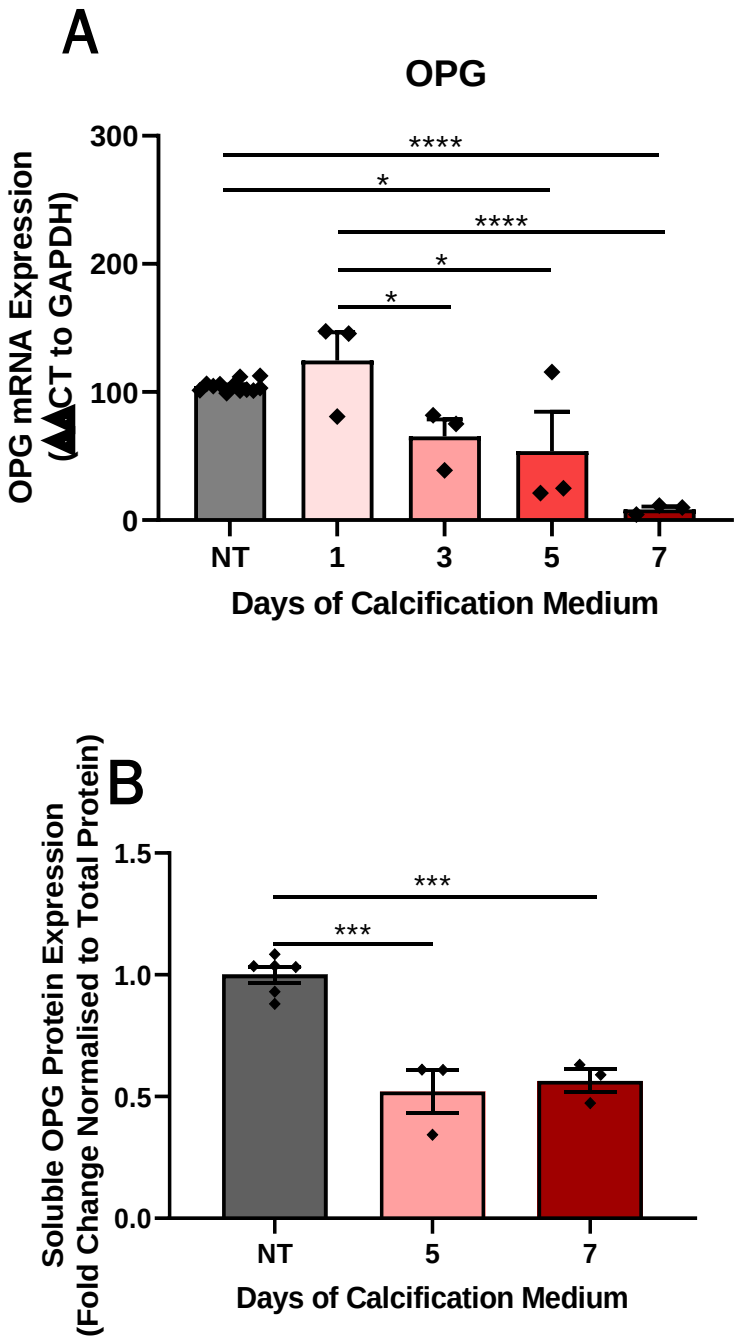

Figure 3.3.2.6 The effect of calcification medium on OPG expression.

*HAoSMCs were treated with $CaPO_4$ (Ca 2.7 mM, PO_4 2.0 mM) medium (CM) for indicated time points. (A) OPG mRNA expression was measured by qPCR using GAPDH as the internal control. (B) Soluble OPG levels were measured by ELISA using BCA measured total protein as a control. *p<0.05, ***p<0.001, ****p<0.0001, ANOVA with Bonferroni's correction. Data represented as % of NT, mean± SEM, n=3.*

3.4 Discussion

Here in chapter 3, the assay to be used in all further chapters was developed and characterised by identifying the expression levels of molecules typically involved in VSMC calcification. Figure 3.3.1.1 shows that these cells take 15 days to almost completely calcify and have raised expression mRNA and protein levels of the pro-calcification molecules Runx2, RANKL and ALP at the 7 day timepoint and in some cases as early as the 5 day timepoint. Additionally, the VSMC marker SMα actin and the anti-calcification molecule, OPG had decreased expression at the 5 and 7 day timepoints.

As the calcification potential of cells can change between donor, subset and species[382, 671], for these studies, the use of human aortic smooth muscle cells (HAoSMCs) ensured relevance to a human population. Furthermore, a regular, non-calcification-prone phenotype and demographic was selected to ensure the detection of early changes: the donor is a 31 year old female and the cells were used at passage 7, to avoid senescence phenotypes. While the use of a single donor provides a clear indication of what is happening in healthy cells, in the future the experiments in this thesis would benefit from adding different donor cells, from a range of demographics, to thoroughly examine VC over a population of cells more similar to the general population, or the populations experiencing VC.

The calcification medium used in this thesis employed calcium and inorganic phosphate (PO_4) at concentrations replicating the upper limits of observed human plasma concentrations (Ca 2.7 mM and NaH_2PO_4 2.0 mM). The use of inorganic phosphate allowed a greater flexibility of passage number in the cells, as it has been previously reported that valvular calcification can slow past passage 4 when using organic phosphate[672]. Additionally, cells were supplemented with 1% FBS during the calcification process to prevent cell death, which is another stimulator of calcification[293-295]. For these

reasons, the study presented here shows strengths over the previous literature presented in the introduction chapter 3.1.

The *in vitro* studies performed in this entire thesis were also all done simultaneously, adding to the standardisation of these experiments. Cells were grown to passage 6, then combined, split to passage 7 and plated on the same day, in the same hood and rotated within the same incubator. As such, all PCR, western blot and calcification assays were performed on cells harvested from the same batches and on the same days, with the same reagents, allowing for direct comparison between treatment groups in a standardised model. As presented here in chapter 3, this *in vitro* calcification assay allows the detection of early changes in calcification in a pathologically relevant manner and convers a range of markers, allowing for easier comparison to the literature.

The data presented here not only corresponds to the described patterns of calcification, identified from runx2, RANKL and OPG expression[666, 667], but applies it to a standardised human model for the detection of VSMC differentiation and calcification. From the data in chapter 3.3, the timepoint of 5 and 7 days were chosen to examine mRNA and PCR expression changes post exposure to lipoproteins, whereas for the calcification assay the 15 day timepoint was selected.

4 : Chapter Four

Investigating the role of triglyceride rich lipoproteins on vascular calcification

4.1 Introduction

Triglyceride rich lipoproteins (TRLs) are responsible for transporting triglycerides throughout the body and are widely recognised as indicators of CVD. Emerging evidence now suggests a more causative role for these particles in the pathogenesis of atherosclerosis[121], with clinical trials showing additional risk of high TRL levels beyond low density lipoprotein (LDL) levels[122].

Although large TRLs, such as large very low-density lipoprotein (VLDL) and chylomicrons, are unable to penetrate the artery wall due to their size[124], the pathological effects of TRLs in atherosclerosis can be attributed to their smaller remnants[125], often referred to as β-VLDL. These TRL remnants are retained in the arterial wall matrix[126] and have been identified within the atherosclerotic plaques of rabbits[125, 127]. Once in the artery wall, the remnants are able to participate in foam cell formation[128, 129], impair endothelial function[130, 131], activate leukocytes[132], promote VSMC proliferation[133] and contribute to local inflammation[134, 135]. These effects in combination with epidemiological data[136, 137] suggests a causal role for TRLs in atherosclerosis.

The retention of TRLs in the plasma are coordinated via the ability of apolipoprotein CIII (apo CIII) to inhibit lipoprotein lipase (LPL)[673] and hepatic VLDL uptake[674, 675]. Conversely, apo CII activates LPL activity and mimetic peptides of apo CII can be used to treat hypertriglyceridemia of CII deficient patients[676]. As such, treatments targeting LPL, apo CII and apo CIII are attractive options for the management of atherosclerosis[676-680]. Interestingly, in humans the genes for apo AI, CIII and AIV are linked in a clustered tandem organisation[681], and that genetic variants of their allele can result in elevated apo CIII alone and the correlating raised TG levels[682] and atherosclerosis[683]. There are also human populations containing genetically coded reduced apo CIII levels, including the Lancaster Amish[684], resulting in a favourable lipid and atherogenic profile[680, 684-686].

A similar phenotype occurs in animals, where apo CIII deficiency protects against atherosclerosis[687, 688], lowers TG levels[680, 689, 690] and protects against postprandial hypertriglyceridemia[689]. Conversely, apo CIII overexpression or human transgenic expression leads to hypertriglyceridemia[691], diet induced obesity[692, 693] and increased early atherosclerosis[158]. Mice expressing both cholesterol ester transfer protein (CETP), a protein which facilitates the transfer of cholesterol esters from HDL to TRLs, and apo CIII however did not have diet induced weight gain[692] and have reduced early plaque volume[694].

Apo CIII-containing HDL particles account for approximately half of lipoprotein associated apo CIII, modulating the severity of hypertriglyceridemia[695], changing the structure and functionality of the HDL and promoting metabolic activation of brown adipose tissue[696]. Upregulation of apo CIII transcript expression can also be achieved by high plasma glucose levels, potentially contributing to diabetic dyslipidaemia[697] and therefore diabetic cardiovascular risk[698, 699]. Moreover, apo CIII has the pro-atherogenic property of enhancing leukocyte-endothelial activation and binding[700], an interaction which can be suppressed by statins[701].

In the arterial wall, VSMCs are capable of triglyceride uptake, storage and *de novo* synthesis, implicating a role for TRLs in smooth muscle plasticity into adipose-like cells. The VSMCs also interact with apo CIII, which causes proliferation, migration and inflammation of VSMCs through the NF-κB pathway[702]. Raised cholesterol content of VLDL particles highly associated with coronary artery calcification (CAC)[703] and elevated plasma triglyceride levels associated with calcification of the mitral annulus[311], suggesting a relationship between VLDL uptake and VC. Interestingly, a paradox exists whereby small VLDL particles and remnants correlate to atherosclerosis, but large VLDL particles are associated with CAC and chronic kidney disease (CKD)[100]. For *APOC3* loss-of-function

heterozygosity in humans, reduced triglycerides and remnant cholesterol had a parallel association with reduced CAC[684], linking apo CIII's effects on lipoproteins to vascular calcification.

As it is now somewhat established that TRLs interact with the vessel wall to encourage atherosclerotic plaque development, we hypothesise that it continues to have a role in the progression of vascular calcification. While there appears to be some evidence to implicate a role for VLDL in VC, to date there have been no studies aiming to further examine these findings *in vitro* or *in vivo*. The studies presented in this chapter therefore aim to determine potential roles for VLDL and oxVLDL in the function and regulation of calcification *in vitro*. Additionally, this study aims to identify an *in vivo* relationship between triglycerides, apo CIII and atherosclerotic markers, and examine the calcification potential of human serum containing high levels of TG.

4.2 Methods

4.2.1 *In Vitro Study Design*

Cells were maintained and calcified as per methods chapter 2.4 after 24 hours of pre-treatment with VLDL or oxVLDL at 200µg/ml. After 1,3,5 and 7 days of calcification medium (CM), cell mRNA was harvested and transformed to cDNA for PCR analysis as per methods chapter 2.5.1, 2.6 and 2.7 respectively. Cells were harvested after 5 and 7 days of calcification for protein expression analysis via methods in chapter 2.8 and 2.9. Additionally, media also was collected after the 5 and 7 day CM timepoints and analysed for protein secretion using ELISA assays as per methods chapter 2.10. A timeline of the *in vitro* calcification assay is presented in figure 4.2.1.

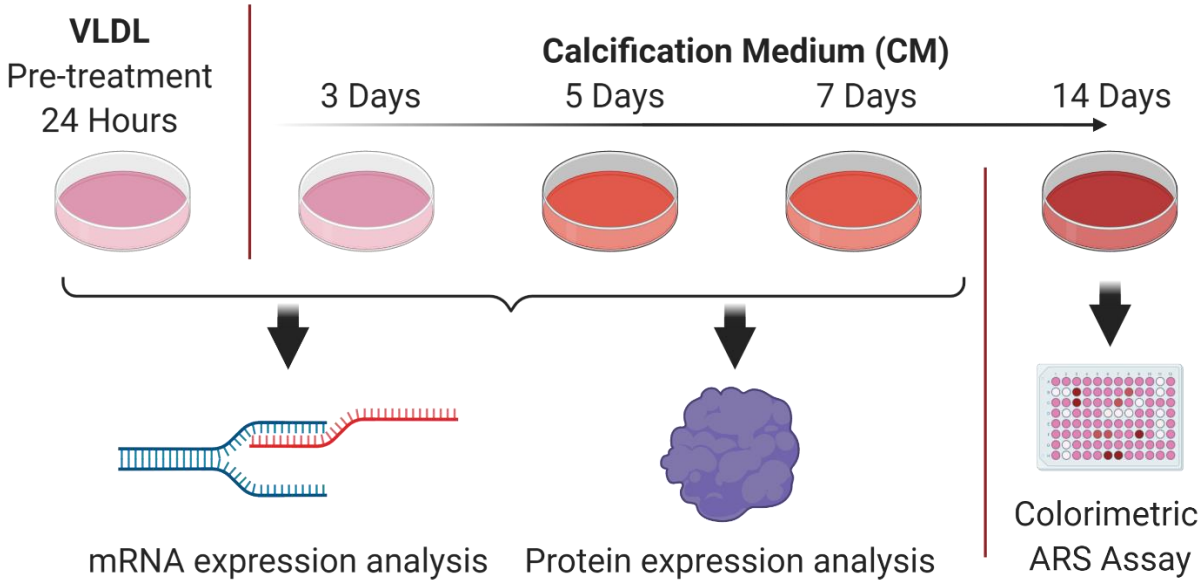

Figure 4.2.1.1 Schematic of the VLDL *in vitro* calcification assay.

HAoSMCs were pre-treated with VLDL or oxVLDL at 200µg/ml for 24 hours, then treated with $CaPO_4$ (Ca 2.7 mM, PO_4 2.0 mM) medium (CM) for up to 15 days. Cells were then analysed at various timepoints with PCR, western blot and stained with Alizarin Red S (ARS) stain to monitor calcium deposition and molecule expression.

4.2.2 *In Vivo Study Design*

Forty one 8-week-old Apo $E^{-/-}$ x Apo $CIII^{-/-}$ and Apo $E^{-/-}$ mice on a C57Bl/6 background were randomized to either 8 or 16 weeks of atherogenic diet (AD) (22% fat, 0.15% cholesterol, irradiation at min 25kGy, SF00-219, Specialty Feeds, WA, Australia), corresponding to early-mid stage atherosclerosis and early VC in humans (figure 4.2.1.1). Mice were weighed weekly and bedding changed twice per week. Blood was collected for triglyceride, total cholesterol, calcium and ALP analysis immediately prior to commencing the atherogenic diet and upon terminal cardiac puncture when completing the study. This study was approved by the South Australian Health and Medical Research Institute Animal Ethics Committee (SAM186).

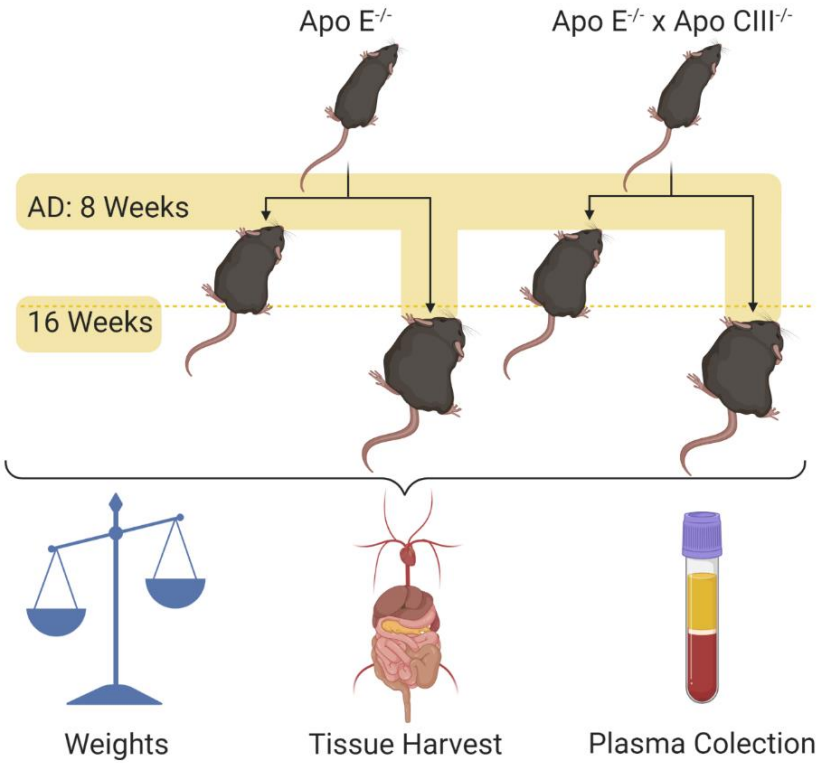

Figure 4.2.2.1 *In vivo* experimental timeline.

8-week-old Apo E$^{-/-}$ x Apo CIII$^{-/-}$ and Apo E$^{-/-}$ mice on a C57Bl/6 background were randomized to either 8 or 16 weeks of atherogenic diet (AD). Upon completion of AD, mice were weighed and harvested for tissues and blood plasma.

4.2.3 *Human Study Design*

45 adult volunteers with varying triglyceride (TG) levels (<2 mM n=15, 2 - 6 mM n=15, >6 mM n=15) were recruited from outpatient clinics by RAH treating clinicians or patients who were referred by other clinicians according to their lipid profile. Normal (<2 mM TG), hyper triglyceridemic (2 – 6 mM TG) and super-hyper triglyceridemic (>6 mM) patient serum samples were age based propensity matched (n=5 per group) and analysed for lipid content, VC biomarker content (Calcium and ALP) and calcification potential (ARS assay on calcifying VSMCs). This study was approved by the Central Adelaide Local Health Network Human Research Ethics Committee (CALHN HREC) and CALHN Research Governance, under the ethics number HREC/15/RAH/282.

Volunteers who satisfied the eligibility criteria then had a basic health assessment recorded, including the measurement of height, weight and blood pressure. 20 mL of blood was withdrawn by venepuncture and transferred to heparin or Z serum clot activator coated tubes. Serum and plasma were collected via centrifugation at 1500 rcf for 15 minutes and stored at -80^{o}C until use.

Table 4.2.3.1 Eligibility criteria of clinical study.

Criteria	Eligibility
Gender and Age	Male or female aged 18-85 years
General Health	No bleeding tendency or significant health problems
Pregnancy Status	Not currently pregnant or breastfeeding

Ability to Give Informed Consent	Good command of the English language and able to provide informed consent

In Vitro Results

The role of VLDL and oxVLDL in VSMC calcification

4.3 Results

4.3.1 The Functional Effects of VLDL and oxVLDL on HAoSMC Calcification

While there is currently a limited number of studies investigating the role of VLDL in calcification *in vitro*, there is some data demonstrating the presence of VLDL receptors in the artery wall[704] and that VLDL can dose dependently promote VSMC proliferation[133], suggesting an active role in plaque progression.

The influence of VLDL and oxVLDL pre-treatment on the calcification potential of HAoSMCs was assessed using the ARS assay. HAoSMC calcification was significantly increased in response to oxVLDL pre-treatment (1±0.03 vs 1.23±0.044, $p<0.0001$). Moreover, oxVLDL pre-treatment augmented HAoSMC calcification significantly more than VLDL (1.09±0.015 vs 1.23±0.044, $p<0.01$) (figure 4.3.1.1), demonstrating a functional effect for oxVLDL in progressing vascular calcification.

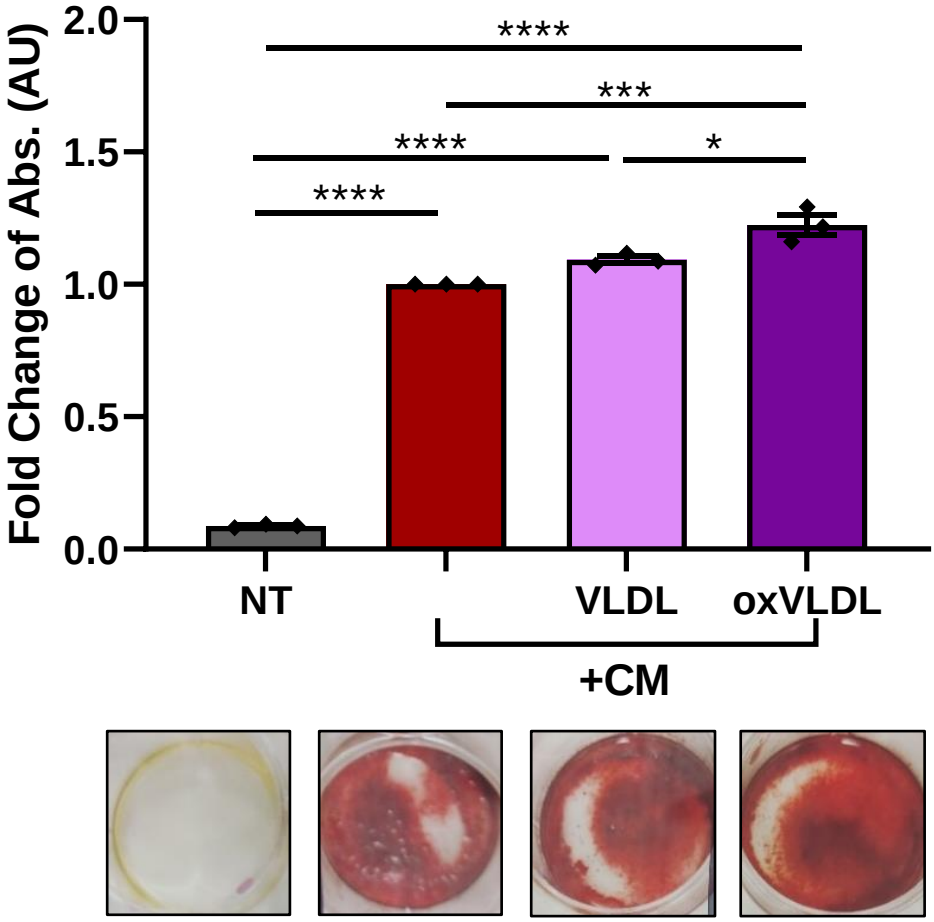

Figure 4.3.1.1 The effect of VLDL and oxVLDL on calcification.

*HAoSMCs were pre-treated with VLDL or oxVLDL (200 µg/ml) for 24 hours then treated with CM (Ca 2.7 mM, PO_4 2.0 mM) for 15 days. Calcification was measured by ARS assay with no treatment (NT) and CM alone and expressed as fold change from CM. NT ****p<0.0001 compared to all other treatments. *p<0.05, ***p<0.001, ANOVA with Bonferroni's correction. Data represented as mean± SEM, n=3.*

4.3.2 The Effects of VLDL and oxVLDL on HAoSMC Calcification Gene Expression

While it is well established that oxidative stress has a role in VC[296-300] by inducing osteoblastic differentiation of VSMCs, the specific effects of VLDL and its oxidative form on HAoSMC calcification remain unknown. Gene expression profiling of calcification markers was utilised to investigate the effects of calcification medium (CM) (Ca 2.7 mM, PO_4 2.0 mM), VLDL or oxVLDL treatment individually. After 24 hours of exposure to CM, an increase in the pro-calcification marker RANKL (106.2±5.8 vs 204.1±20.54, $p<0.0001$) was observed. Correspondingly there was a decrease in SMαActin (103.4±3.84 vs 65.09±4.43, $p<0.0001$) mRNA expression when compared to the NT baseline controls. No changes were observed in the pro-calcific marker Runx2 (A), ALP (C), and the calcification protective OPG (E) genes (figure 4.3.2.1).

Treatment with VLDL and oxVLDL downregulated pro-calcific gene expression after 24 hours. Runx2, the master regulator of calcification gene transcription, was significantly reduced when cells were treated with VLDL (NT: 110.6±12.37 vs 51.45±4.81, $p<0.0001$; CM: 84.18±7.28 vs 51.45±4.81, $p<0.05$) and oxVLDL (NT: 110.6±12.37 vs 5.49±0.62, $p<0.0001$, CM: 84.18±7.28 vs 5.49±0.62, $p<0.0001$). Additionally, oxVLDL reduced Runx2 mRNA levels further when directly compared to VLDL (51.45±4.81 vs 5.49±0.62, $p<0.01$) (figure 4.3.2.1 A). VLDL also significantly reduced the expression of RANKL, the mediator of osteoblastic differentiation, when compared to both NT and CP controls (NT: 106.2±5.8 vs 40.98±6.05, $p<0.01$; CP: 204.1±20.54 vs 40.98±6.05, $p<0.0001$) and oxVLDL (NT: 106.2±5.8 vs 14.35±4.27, $p<0.0001$; CP: 204.1±20.54 vs 14.35±4.27, $p<0.0001$). (figure 4.3.2.1 B). Interestingly however, the expression of ALP, the final pH regulator for effective calcium deposition, was unchanged by any treatment compared to control cells (figure 4.3.2.1 C).

Differential results were observed when SMαActin and OPG were assessed. The VSMC marker SMαActin was significantly reduced by oxVLDL (103.4±3.84 vs 17.81±2.01, $p<0.0001$) when compared to the NT control while its native form had no effect. There was, however, a significant reduction following oxVLDL treatment compared to VLDL (65.09±4.43 vs 17.81±2.01, $p<0.0001$) (figure 4.3.2.1 D). When measuring OPG, the RANKL decoy protein, mRNA levels were significantly reduced following 24 hours of treatment with both VLDL (NT: 107.1±11.09 vs 49.24±8.1, $p<0.01$; CM: 122±13.99 vs 49.24±8.1, $p<0.0001$) and oxVLDL (NT: 107.1±11.09 vs 1.64±0.21, $p<0.0001$; CM: 122±13.99 vs 1.64±0.21, $p<0.0001$) treatment. In addition, cells treated with oxVLDL had almost abolished OPG mRNA levels completely even more than cells treated with VLDL (49.24±8.1 vs 1.64±0.21, $p<0.01$) (figure 4.3.2.1 E).

Given that the current data on VLDL is pro-atherogenic it was surprising to see that in this assay both the native and oxidised forms reduced not only the calcification inhibitors but also the pro-calcific genes. Understandably this was only a 24 hour treatment of the lipoproteins themselves, therefore in the next section an environment more similar to pathological VC will be assessed and at longer timepoints.

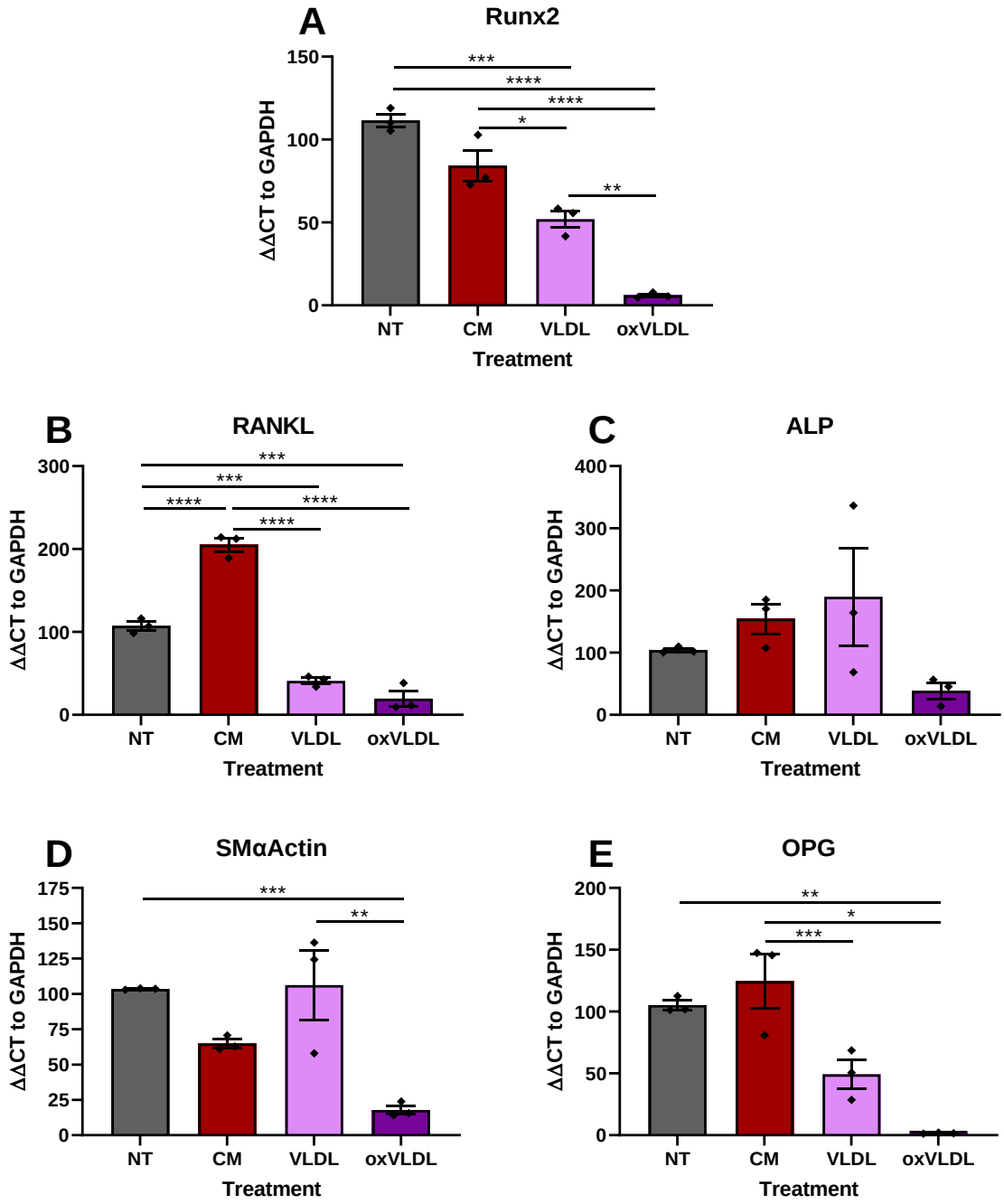

Figure 4.3.2.1 The effect of VLDL and oxVLDL on mRNA expression.

*HAoSMCs were treated with CM (Ca 2.7 mM, PO_4 2.0 mM) VLDL or oxVLDL (200 µg/ml) for 24 hours. mRNA expression was measured by qPCR using GAPDH as the internal control. *p<0.05, **p<0.01, ***p<0.001, ****p<0.0001, ANOVA with Bonferroni's correction. Data represented as % of NT, mean± SEM, n=3.*

4.3.3 The effects of VLDL and oxVLDL Pre-Treatment on HAoSMC Gene expression

After discovering an effect for oxVLDL on the global reduction of HAoSMC calcification-involved gene expression after 24 hours of treatment, we investigated the influence of VLDL and oxVLDL on the expression of these calcification markers at the 5 and 7 day timepoints established earlier in Chapter 3.

When pre-treating cells for 24 hours with VLDL before 5 days of calcification, there were no differences in Runx2 mRNA expression compared to untreated cells (NT), or CM treated cells. Despite this, compared to oxVLDL, VLDL appeared to exert a protection against the induced calcification which was lost when the VLDL was oxidised (VLDL: 208.6±52.86 vs 929.7±93.87; $p<0.01$). Even when increasing the length of calcification to 7 days, VLDL treatment was still able to prevent the significant increase in Runx2 observed by both CM and oxVLDL treatment. (figure 4.3.3.1). Pre-treating the cells with oxVLDL prior to calcification induction markedly enhanced Runx2 expression compared to all other treatments at day 5 (NT: 103.4±6.47 vs 929.7±93.87, $p<0.0001$; CM: 146.2±52.23 vs 929.7±93.87, $p<0.0001$; VLDL: 208.6±52.86 vs 929.7±93.87, $p<0.01$), however by day 7 the induction was comparable to cells stimulated with CM alone (figure 4.3.3.1).

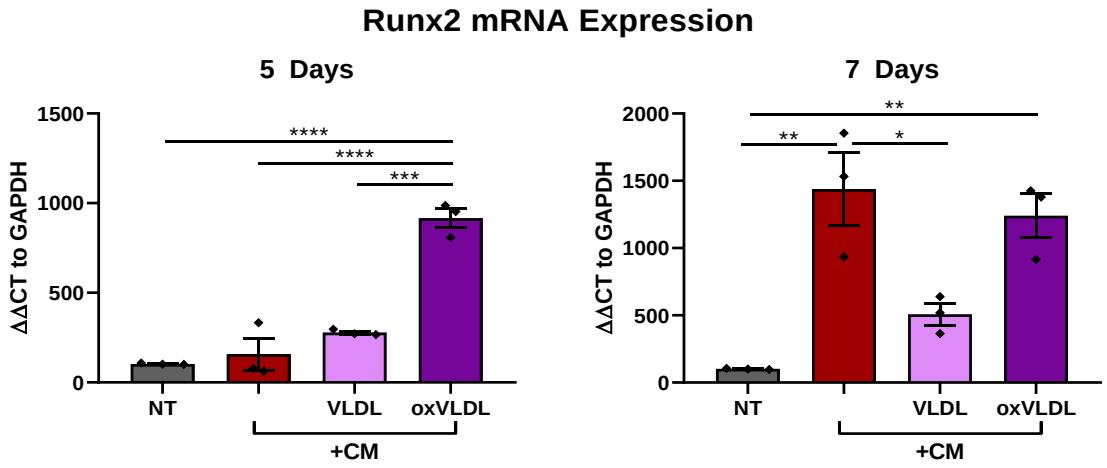

Figure 4.3.3.1 The effect of VLDL and oxVLDL on Runx2 mRNA expression.

*HAoSMCs were pre-treated with VLDL or oxVLDL (200 µg/ml) for 24 hours then treated with CM (Ca 2.7 mM, PO_4 2.0 mM) for 5 or 7 days. A no treatment (NT) baseline and a CM alone positive control were used. Runx2 mRNA expression was measured by qPCR using GAPDH as the internal control. *p<0.05, **p<0.01, ***p<0.001, ****p<0.0001, ANOVA with Bonferroni's correction. Data represented as % of NT, mean± SEM, n=3.*

Based on earlier data where RANKL expression corresponded with what was observed for Runx2 (figure 4.3.2.1), it was interesting that VLDL treatment did not appear to follow the same trend. RANKL mRNA levels were unchanged regardless of treatment groups after 5 days of calcification. By day 7 however, pre-treatment with both VLDL (CM: 358±800.7 vs 429.5±111.5, p<0.0001) and oxVLDL (CM: 3582±800.7 vs 284.6±69.81, p<0.0001) significantly reduced RANKL mRNA expression levels compared to CM (figure 4.3.3.2).

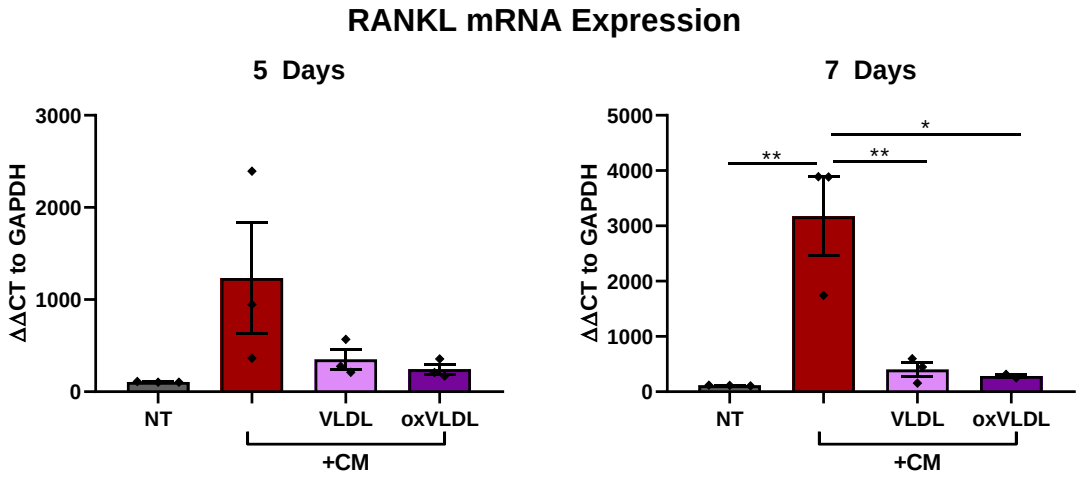

Figure 4.3.3.2 The effect of VLDL and oxVLDL on RANKL mRNA expression.

*HAoSMCs were pre-treated with VLDL or oxVLDL (200 µg/ml) for 24 hours then treated with CM (Ca 2.7 mM, PO_4 2.0 mM) for 5 or 7 days. A no treatment (NT) baseline and a CM alone positive control were used. RANKL mRNA expression was measured by qPCR using GAPDH as the internal control. *p<0.05, **p<0.01, ANOVA with Bonferroni's correction. Data represented as % of NT, mean± SEM, n=3.*

ALP mRNA expression is upregulated immediately prior to the mineral deposition in VC. After 5 days of calcification, oxVLDL pre-treatment significantly raised ALP mRNA expression when compared to NT (110.3±4.066 vs 5692±344.5, p<0.001), CM (1188±808.0 vs 5692±344.5, p<0.01) and VLDL (1165±213.3 vs 5692±344.5, p<0.01) pre-treated cells (figure 4.3.3.3). After 7 days of calcification VLDL pre-treatment did not affect ALP mRNA expression when compared to either NT or CP alone. However, oxVLDL pre-treated cells had significantly raised expression levels when compared to the NT baseline (108.8±2.0 vs 12123±40.48, p<0.05) (figure 4.3.3.3).

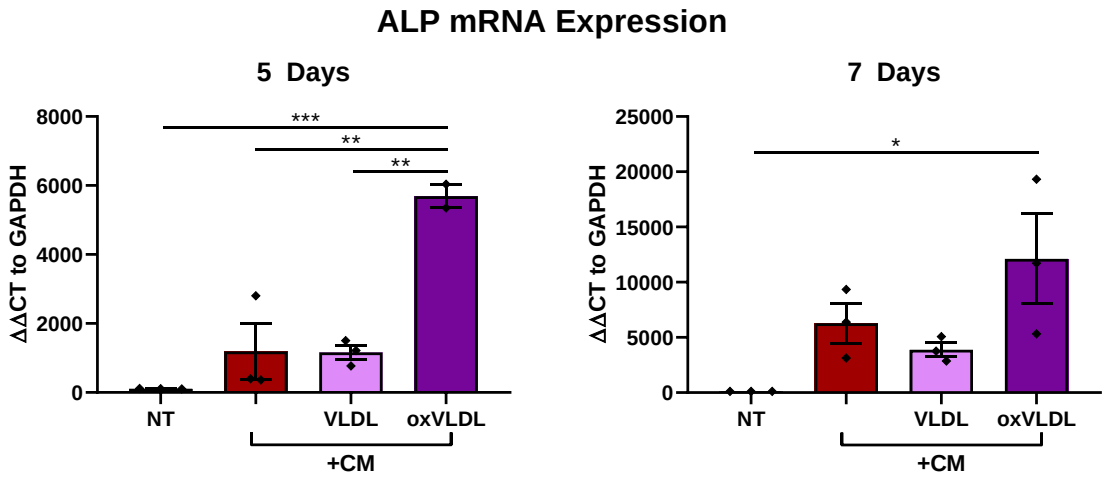

Figure 4.3.3.3 The effect of VLDL and oxVLDL on ALP mRNA expression.

*HAoSMCs were pre-treated with VLDL or oxVLDL (200 µg/ml) for 24 hours then treated with CM (Ca 2.7 mM, PO_4 2.0 mM) for 5 or 7 days. A no treatment (NT) baseline and a CM alone positive control were used. ALP mRNA expression was measured by qPCR using GAPDH as the internal control. *p<0.05, **p<0.01, ***p<0.001, ANOVA with Bonferroni's correction. Data represented as % of NT, mean± SEM, n=3.*

When VSMCs differentiate they can undergo a transformation from their contractile state to a more synthetic phenotype. A crucial identifier of this process is the presence of SMα actin. The effects of VLDL and oxVLDL on subsequent expression of SMα actin after calcification stimulus were assessed (figure 4.3.3.4). After 5 days of calcification VLDL significantly reduced levels of SMα actin compared to both NT (103.1±7.22 vs 17.8±2.82, p<0.0001) and CM (46.72±8.04 vs 17.8±2.82, p<0.001) controls and by day 7 levels were still reduced. oxVLDL continued to reduce expression of SMα actin (day 5: 46.72±8.04 vs 4.34±0.57, p=ns; day 7: 19.97±3.32 vs 3.29±0.49, p=ns) compared to CM, suggesting a detrimental effect of oxidation on the maintenance of contractile SMC phenotype.

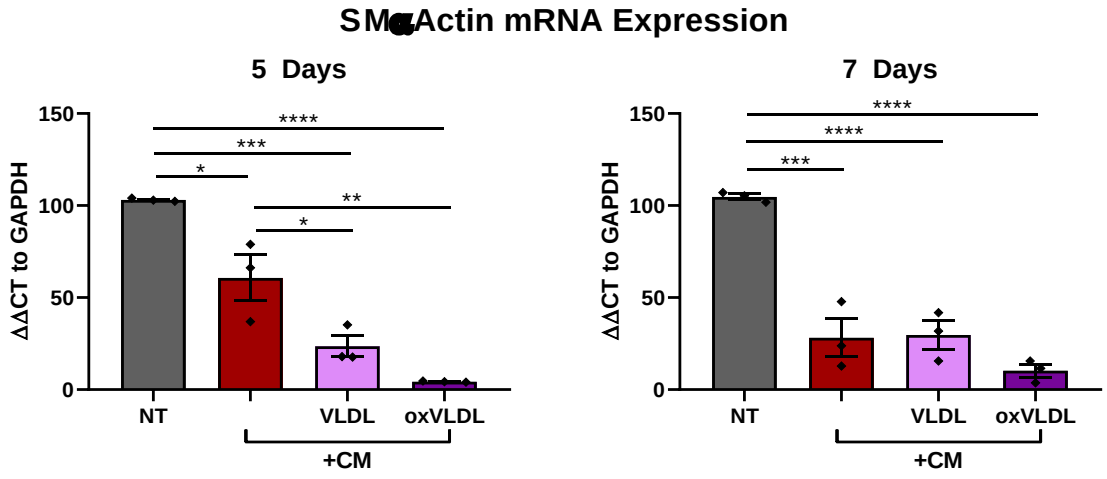

Figure 4.3.3.4 The effect of VLDL and oxVLDL on SMαActin expression.

*HAoSMCs were pre-treated with VLDL or oxVLDL (200 µg/ml) for 24 hours then treated with CM (Ca 2.7 mM, PO_4 2.0 mM) for 5 or 7 days. A no treatment (NT) baseline and a CM alone positive control were used. SMαActin mRNA expression was measured by qPCR using GAPDH as the internal control. *p<0.05, **p<0.01, ***p<0.001, ANOVA with Bonferroni's correction. Data represented as % of NT, mean± SEM, n=3.*

Osteoprotegerin (OPG) acts as a decoy receptor for RANKL to block the bone deposition. In VSMCs lack of OPG triggers differentiation towards an osteogenic phenotype and the addition of OPG demonstrates direct proliferative and survival effects[705]. In this study, after 5 days of calcification, both VLDL and oxVLDL significantly lowered OPG mRNA expression when compared to CM treatment (VLDL: 23.1±1.92 vs 4.9±1.1, p<0.01; oxVLDL: 23.1±1.92 vs 1.7±0.83, p<0.01). Additionally, compared to NT, VLDL at day 5 (106.5±12.63 vs 4.9±1.34, p<0.0001) and day 7 (102.1±11.3 vs 7.43±1.63, p<0.0001) and oxVLDL at day 5 (106.5±12.63 vs 1.79±0.49, p<0.0001) and day 7 (102.1±11.3 vs 4.26±1.46, p<0.0001) all significantly reduced OPG mRNA expression (figure 4.3.3.5).

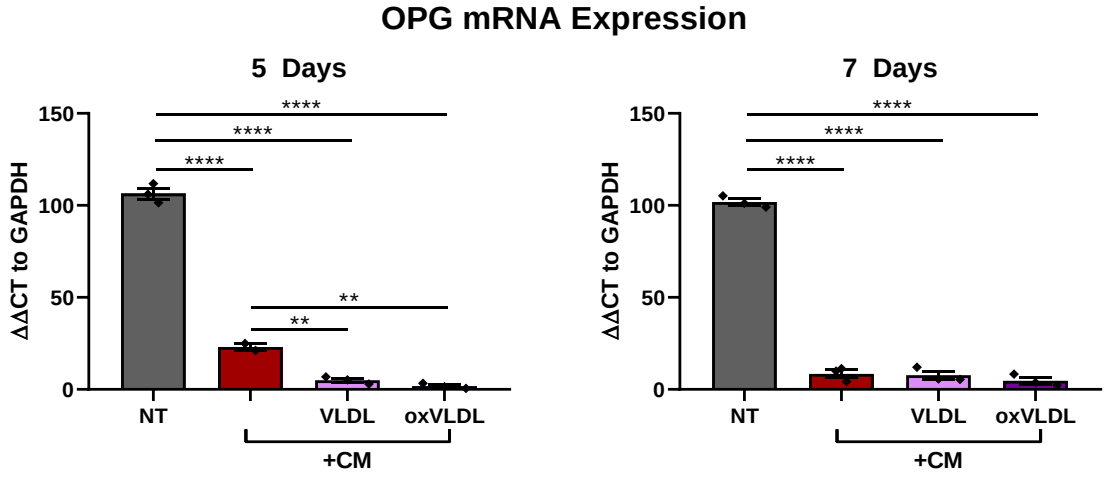

Figure 4.3.3.5 The effect of VLDL and oxVLDL on OPG expression.

*HAoSMCs were pre-treated with VLDL or oxVLDL (200 µg/ml) for 24 hours then treated with CM (Ca 2.7 mM, PO_4 2.0 mM) for 5 or 7 days. A no treatment (NT) baseline and a CM alone positive control were used. OPG mRNA expression was measured by qPCR using GAPDH as the internal control. *p<0.05, **p<0.01, ***p<0.001, ANOVA with Bonferroni's correction. Data represented as % of NT, mean± SEM, n=3.*

4.3.4 The effects of VLDL on HAoSMC Calcification Protein Expression and Secretion

Based on the results presented in chapter 3.3.3 , that VLDL and particularly oxVLDL influence the expression of Runx2, RANKL, ALP and OPG mRNA expression at 5 and 7 days of calcification, we performed western blots, ELISAs and colorimetric assays to identify whether the effects of VLDL continued at the protein level.

oxVLDL significantly increased Runx2 protein expression compared to the NT baseline (1±0.3445 vs 44.19±3.156, $p<0.001$), CM alone control (5.678±1.948 vs 44.19±3.156, $p<0.001$) and VLDL pre-treatment (10.44±5.592 vs 44.19±3.156, $p<0.001$). While after 7 days the same pattern was observed, there were no significant differences between treatments (figure 4.3.4.1). Combined with the ARS data presented in figure 3.3.1.1 and the gene expression data presented in figure 3.3.3.1, we see a consistent role for oxVLDL in the stimulation of vascular calcification when examining Runx2.

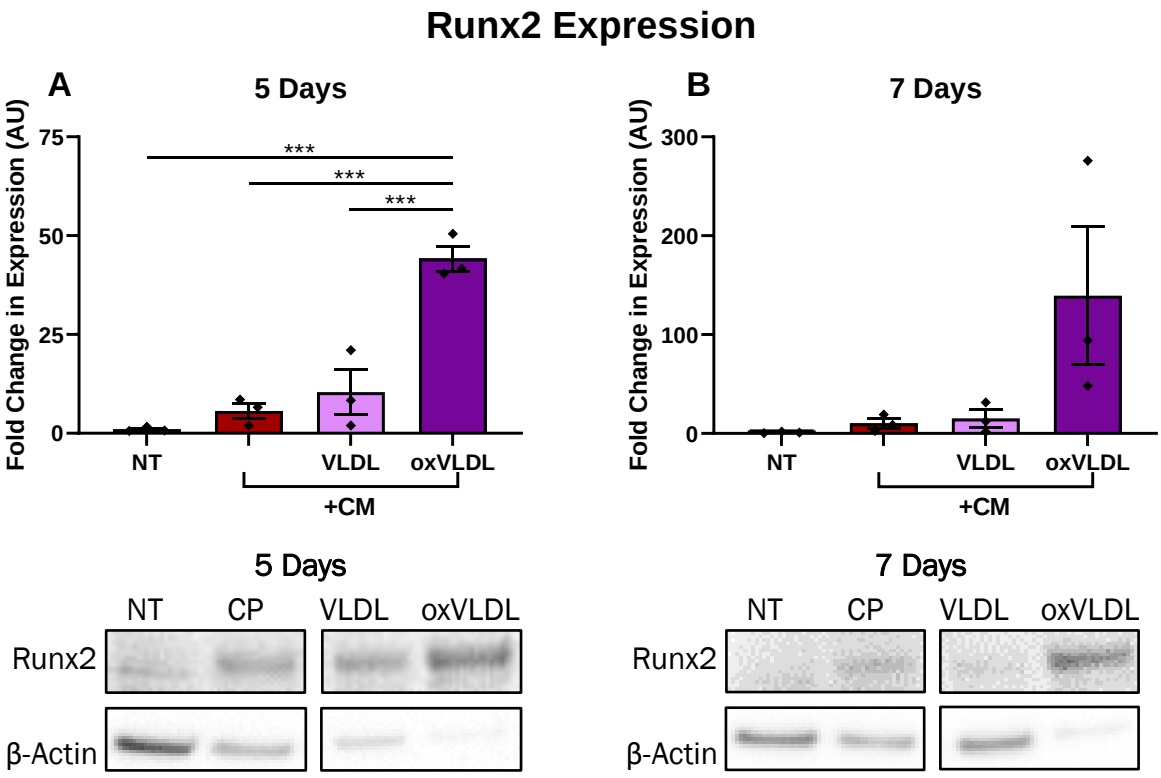

Figure 4.3.4.1 The effect of VLDL and oxVLDL on Runx2 protein expression.

*HAoSMCs were pre-treated with VLDL or oxVLDL (200 µg/ml) for 24 hours then treated with CM (Ca 2.7 mM, PO_4 2.0 mM) for 15 days. A no treatment (NT) baseline and a CM positive control were used. Runx2 protein expression was measured by western blotting using β-Actin and a standard sample as internal controls. *p<0.05, ***p<0.001, ****p<0.0001, ANOVA with Bonferroni's correction. Data represented as % of NT, mean± SEM, n=3. Representative blots of 5 days and 7 days CP treatment shown below graphs.*

Next, we probed for cellular RANKL protein, hypothesising a similar pattern to the observations for Runx2 protein expression in figure 4.3.4.1. After both 5 and 7 days of CM treatment, oxVLDL pre-treated cells had significantly higher RANKL protein levels than untreated cells (5 days: 100±32.85 vs 3777±402.4, $p<0.001$; 7 days: 100±20.02 vs 9407±2680), CM (5 days: 469.3±135.3 vs 3777±402.4, $p<0.0001$; 7 days: 860.4±252.4 vs 9407±2680, $p<0.0001$) (figure 4.3.4.2). While the protein expression of RANKL presented here in figure 4.3.4.2 complements the effect observed in the ARS assay in figure 4.3.1.1, the profile differs from that observed for the gene expression data (figure 4.3.3.2). While further experimental data is needed to explain these effects in detail, ultimately, RANKL protein levels indicate that the VSMCs are undergoing osteogenic phenotype switching resulting in calcification. As RANKL is expressed biphasically[667], it is possible that the discrepancies between the mRNA and protein expression levels could be due to this effect.

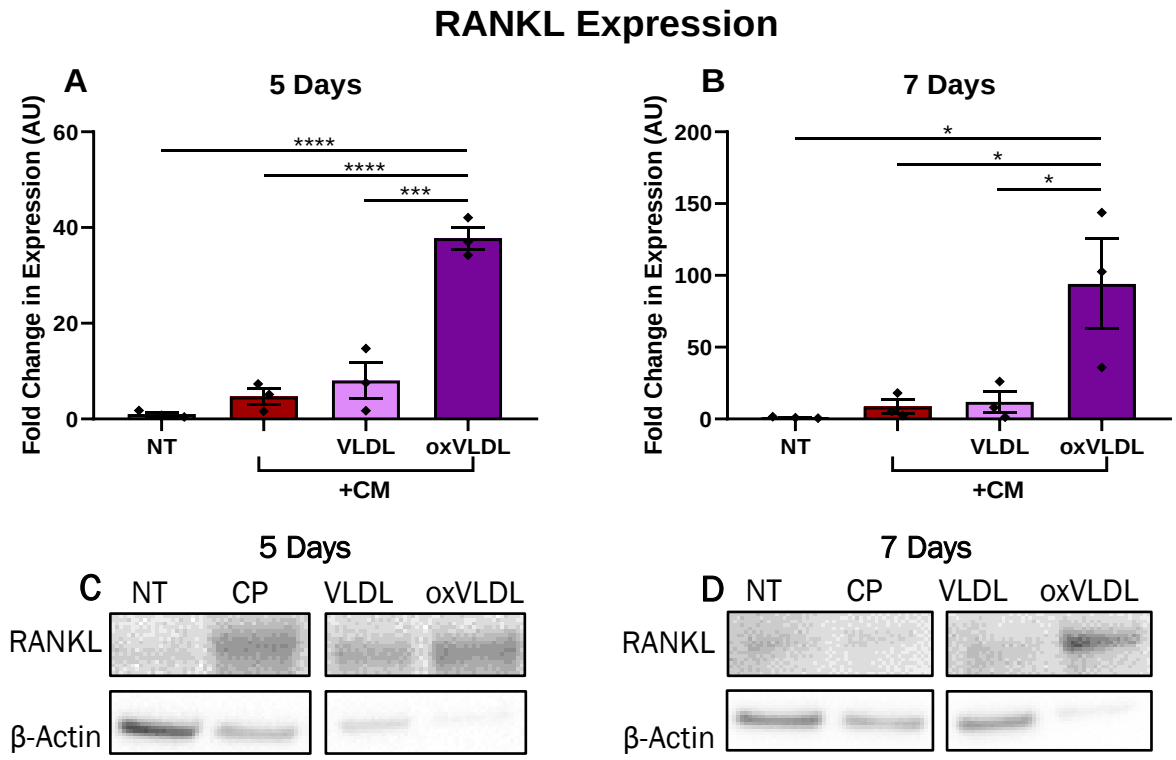

Figure 4.3.4.2 The effect of VLDL and oxVLDL on RANKL protein expression.

*HAoSMCs were pre-treated with VLDL or oxVLDL (200 µg/ml) for 24 hours then treated with CM (Ca 2.7 mM, PO_4 2.0 mM) for 15 days. A no treatment (NT) baseline and a CM positive control were used. RANKL protein expression was measured by western blotting using β-Actin and a standard sample as internal controls. **p<0.01, ***p<0.001, ****p<0.0001, ANOVA with Bonferroni's correction. Data represented as % of NT, mean± SEM, n=3. Representative blots of 5 days (D) and 7 days (E) CP treatment shown below graphs.*

As RANKL can also be secreted to have autocrine and paracrine functions, soluble levels were assessed in the cell culture media, normalised to total protein present (figure 4.3.4.3). In contrast to the RANKL expression observed in the cell membrane soluble RANKL was significantly decreased after both 5 and 7 days of calcification when compared to both the NT and CM treated cells (VLDL - 5 days: 1±0.04 or 0.86±0.02 vs 0.24±0.003, $p<0.0001$; 7 days: 1±0.08 or 1.07±0.03 vs 0.27±0.03, $p<0.0001$ and oxVLDL - 5 days: 1±0.04 or 0.86±0.02 vs 0.23±0.01, $p<0.0001$; 7 days: 1±0.08 or 1.07±0.03 vs 0.27±0.02, $p<0.0001$) (figure 4.3.4.3). This contrast is unexpected as the retention of RANKL then RANK binding leads to osteoblast-like phenotypic switching. Moreover, free RANKL can trigger macrophage osteoclastogenesis, thereby soluble RANKL could act to decrease VC.

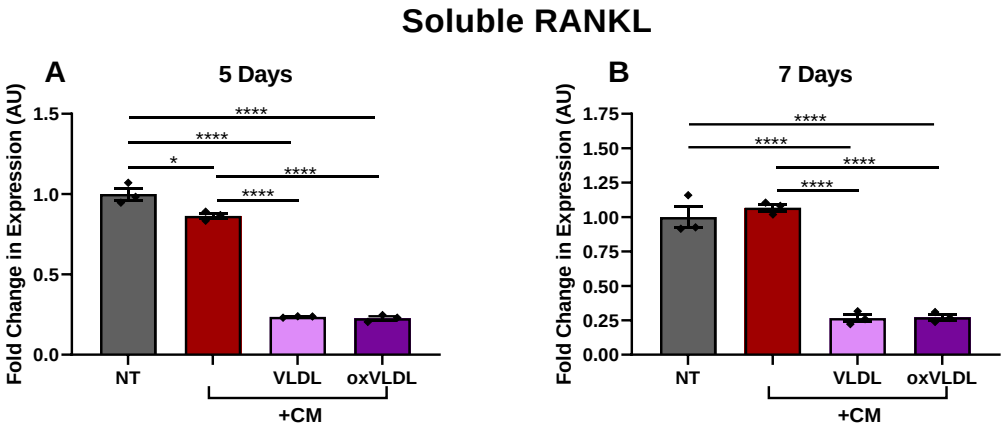

Figure 4.3.4.3 The effect of VLDL and oxVLDL on soluble RANKL.

*HAoSMCs were pre-treated with VLDL or oxVLDL (200 µg/ml) for 24 hours then treated with CM (Ca 2.7 mM, PO_4 2.0 mM) for 15 days. A no treatment (NT) baseline and a CM positive control were used. RANKL protein secretion was measured by ELISA using BCA measured total protein as a control. *p<0.05, ****p<0.0001, ANOVA with Bonferroni's correction. Data represented as fold change of NT, mean± SEM, n=3.*

As described in chapter 1, OPG inhibits the differentiation of VSMCs into an osteogenic phenotype providing a defence mechanism against VC. Soluble OPG acts as a decoy protein, binding to RANK to inhibit RANK:RANKL binding to activate calcification. VLDL pre-treatment had no effect on soluble levels of OPG compared to either NT or CP treatment after 5 days of calcification however by day 7 there was a significant reduction in OPG when compared to NT (100± 6.13 vs 76.02±3.28, $p<0.0001$). In comparison, oxVLDL pre-treatment caused a significant reduction in OPG as early as day 5 when compared to NT (100±3.48 vs 11.05±2.23, $p<0.0001$), CM (52.1±3.48 vs 11.05±2.23, $p<0.01$) or VLDL pre-treated cells (76.79±6.77 vs 11.05±2.23, $p<0.001$) which was maintained after 7 days of calcification compared to NT (100±6.13 vs 14.03±4.56, $p<0.0001$), CM (56.44±4.71 vs 14.03±4.56, $p<0.01$) or VLDL pre-treated cells (76.02±3.28 vs 14.03±4.56, $p<0.0001$) (figure 3.3.4.4). These results, in combination with mRNA expression observed in figure 4.3.3.5, demonstrate a more translational effect for oxVLDL in the reduction of OPG, and further support the functional ARS assay results presented in figure 4.3.1.1.

The data presented here demonstrates a role for TRLs and their modifications in vascular calcification *in vitro*, whereby oxVLDL, but not VLDL, causes an increase in VSMC calcification through modification of calcification regulatory factors both at an mRNA and protein level. In order to observe whether these effects of TRLs also occur *in vivo*, a hyperlipidemic Apo $E^{-/-}$ mouse model was utilised and compared to a novel hyperlipidemic, low triglyceride Apo $E^{-/-}$ x Apo $CIII^{-/-}$ mouse model.

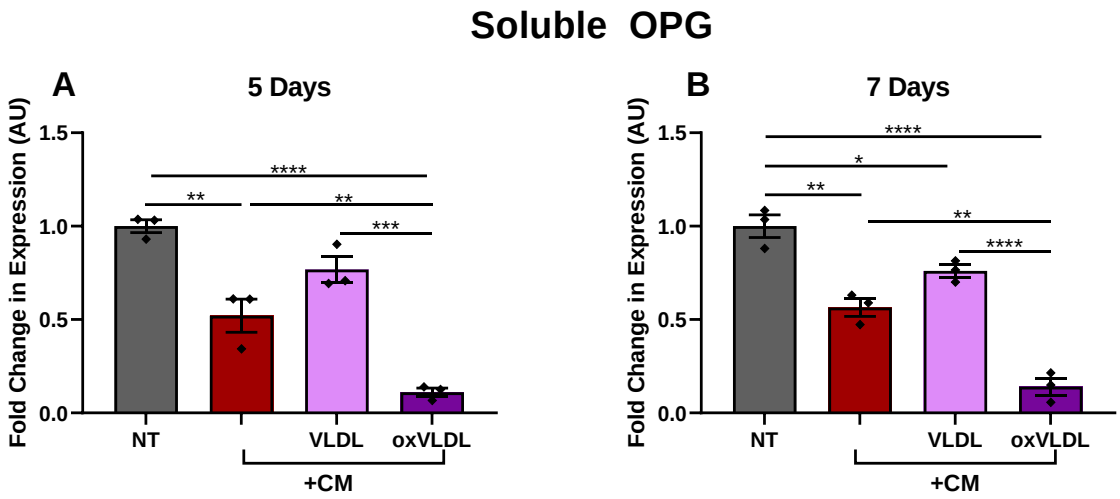

Figure 4.3.4.4 The effect of VLDL and oxVLDL on soluble OPG.

*HAoSMCs were pre-treated with VLDL or oxVLDL (200 µg/ml) for 24 hours then treated with CM (Ca 2.7 mM, PO_4 2.0 mM) for 15 days. A no treatment (NT) baseline and a CM positive control were used. OPG protein expression was measured by ELISA and normalised to total protein. *p<0.05, **p<0.01, ***p<0.001, ****p<0.0001, ANOVA with Bonferroni's correction. Data represented as % of NT, mean± SEM, n=3.*

In Vivo Results

The role of Apo CIII in plaque calcification of Apo $E^{-/-}$ mice

4.3.5 The Effects of Apo CIII deficiency on plasma biomarkers

The *in vitro* data presented in this chapter revealed a pronounced role for oxVLDL in the initiation and progression of calcification in VSMCs. The role of triglycerides in vascular calcification *in vivo* however has yet to be explored. To investigate these roles, a high cholesterol apolipoprotein (Apo) E knock out (Apo $E^{-/-}$) mouse was crossed with an Apo $CIII^{-/-}$ mouse and placed on an atherogenic diet to assess the effects of lowered triglycerides on plaque development and vascular calcification, for the first time in the literature. As Apo CIII is known to increase plasma triglyceride levels, the effects of Apo CIII deficiency in Apo $E^{-/-}$ mice before and after HFD on cholesterol and triglycerides levels were assessed in addition to calcification markers ALP and calcium. As expected, the Apo $E^{-/-}$ x Apo $CIII^{-/-}$ mice on a regular chow diet had significantly lower circulating triglyceride levels than Apo $E^{-/-}$ mice (Figure 4.3.5.1 A: 157.4±17.99 vs 99.21±15.39, $p<0.05$). Additionally, these Apo $E^{-/-}$ x Apo $CIII^{-/-}$ mice also had significantly less total cholesterol than the Apo $E^{-/-}$ mice (Figure 4.4.5.1. B: 219.3±10.44 vs 155.4±14.7, $p<0.001$). At baseline however there were no differences in either plasma ALP (2.59±0.32 vs 2.02±0.24, $p>0.05$) or calcium (2.28±0.28 vs 2.31±0.32, $p>0.05$) (figure 4.3.5.1). Upon completion of the 8 and 16 week atherogenic diet plasma cholesterol levels between Apo $E^{-/-}$ and Apo $E^{-/-}$ x Apo $CIII^{-/-}$ mouse were observed to be significantly different at the 8 week timepoint (table 4.3.5.1).

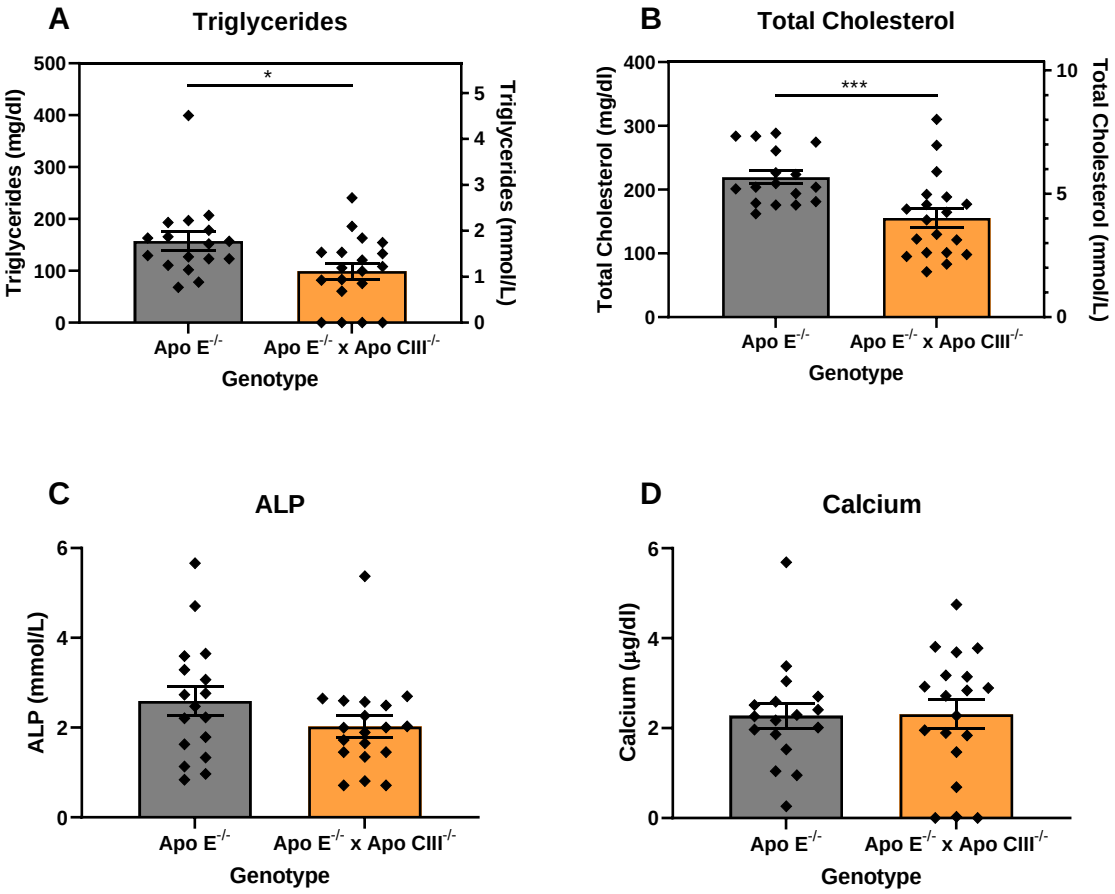

Figure 4.3.5.1 Circulating plasma markers of Apo E-/- and Apo E-/- x Apo CIII-/- mice prior to commencing an atherogenic diet.

*Mouse blood was collected from the tail vein and plasma was extracted from 8 week old mice. Mouse plasma was then assessed for triglyceride (Wako), total cholesterol (Wako), ALP (Wako) and calcium (Cayman) levels as per manufacturer's instructions. *p<0.05, ***p<0.001, Mann-Whitney t-test. Data represented as mean± SEM, n=17-19.*

Table 4.3.5.1 Circulating plasma markers of atherosclerosis and calcification in Apo $E^{-/-}$ and Apo $E^{-/-}$ x Apo $CIII^{-/-}$ mice.

Mean (±SEM), 2-way-ANOVA, n=10-11.

	8 Weeks Atherogenic Diet			16 Weeks Atherogenic Diet			p-value (8 weeks vs 16 weeks AD)	
	Apo $E^{-/-}$	Apo $E^{-/-}$ x Apo $CIII^{-/-}$	p-value	Apo $E^{-/-}$	Apo $E^{-/-}$ x Apo $CIII^{-/-}$	p-value	Apo $E^{-/-}$	Apo $E^{-/-}$ x Apo $CIII^{-/-}$
Final Triglyceride (mg/dl)	413.6 (±26.1)	397.3 (±49.9)	**>0.99**	450.6 (±42.5)	346.6 (±25.9)	**0.4**	>0.99	>0.99
Triglyceride Change (mg/dl)	262.4 (±23.7)	283.5 (±58.2)	**>0.99**	286.4 (±42.6)	272.6 (±41.0)	**>0.99**	>0.99	>0.99
Final Total Cholesterol (mg/dl)	642.8 (±49.4)	452.1 (±32.7)	**0.0064**	608.6 (±37.8)	538.1 (±32.1)	**>0.99**	>0.99	0.71
Total Cholesterol Change (mg/dl)	398.1 (±45.1)	298.4 (±35.4)	**0.63**	402.3 (±37.9)	382.8 (±40.2)	**>0.99**	>0.99	0.79
Final ALP (mmol/L)	2.72 (±0.18)	4.18 (±1.46)	**>0.99**	2.70 (±0.27)	3.17 (±0.34)	**>0.99**	>0.99	>0.99
ALP Change (mmol/L)	0.44 (±0.31)	0.57 (±0.39)	**>0.99**	-0.20 (±0.50)	1.07 (±0.30)	**0.14**	>0.99	>0.99
Final Calcium (mmol/L)	8.06 (±0.43)	7.15 (±0.62)	**>0.99**	9.46 (±1.10)	7.77 (±0.81)	**0.81**	>0.99	>0.99
Calcium Change (mmol/L)	5.53 (±0.45)	3.72 (±0.64)	**>0.99**	7.23 (±1.10)	6.04 (±0.91)	**>0.99**	>0.99	0.39

4.3.6 The Effects of Apo CIII$^{-/-}$ on Body Weight

Assessment of body weight is a clear indicator of diet-induced metabolic changes, particularly in the liver and fat deposits. After 8 weeks of atherogenic diet there were no changes observed either in body weight or the weight of internal organs between Apo E$^{-/-}$ and Apo E$^{-/-}$ x Apo CIII$^{-/-}$ mice (Table 4.3.6.1). After 16 weeks of AD Apo E$^{-/-}$ x Apo CIII$^{-/-}$ mice were significantly heavier than their 8 week counterparts ($p<0.05$) and had significantly heavier livers ($p<0.001$) and retroperitoneal fat deposits ($p<0.05$) compared to Apo E$^{-/-}$ mice. Although Apo E$^{-/-}$ mice gained total body weight between the 8 and 16 week AD timepoints, all the organs remained similar weights. The Apo E$^{-/-}$ x Apo CIII$^{-/-}$ mice however had significantly heavier epidydimal fat ($p<0.05$), livers ($p<0.01$) and retroperitoneal fat ($p<0.05$) after 16 weeks of atherogenic diet compared to mice only fed for 8 weeks.

Table 4.3.6.1 Weights Apo E-/- and Apo E-/- x Apo CIII-/- mice and their tissues. *Grams or % of total body weight (grams), mean (±SEM), 2-way-ANOVA, n=10-11.*

	8 Weeks Atherogenic Diet			16 Weeks Atherogenic Diet			p-value (8 weeks vs 16 weeks AD)	
	Apo $E^{-/-}$	Apo $E^{-/-}$ x Apo $CIII^{-/-}$	p-value	Apo $E^{-/-}$	Apo $E^{-/-}$ x Apo $CIII^{-/-}$	p-value	Apo $E^{-/-}$	Apo $E^{-/-}$ x Apo $CIII^{-/-}$
Final body weight	39.6 (±1.1)	40.8 (±2.3)	**>0.99**	44.6 (±1.4)	49.1 (±2.4)	**0.69**	0.46	**0.024**
Weight Change	10.7 (±0.8)	14.2 (±2.2)	**0.92**	17.9 (±1.4)	23.3 (±2.0)	**0.21**	**0.035**	**0.0033**
% Epididymal Fat	1.8 (±0.1)	1.8 (±0.2)	**>0.99**	2.0 (±0.1)	2.5 (±0.2)	**0.21**	>0.99	**0.024**
% Liver	6.1 (±0.3)	6.8 (±0.4)	**>0.99**	6.5 (±0.4)	9.5 (±0.8)	**0.0006**	>0.99	**0.0023**
% Spleen	0.3 (±0.02)	0.3 (±0.02)	**>0.99**	0.4 (±0.07)	0.3 (±0.02)	**>0.99**	>0.99	>0.99
% Kidney	0.5 (±0.03)	0.5 (±0.02)	**>0.99**	0.5 (±0.03)	0.5 (±0.02)	**0.3**	>0.99	>0.99
% Retro-peritoneal Fat	0.6 (±0.06)	0.8 (±0.07)	**0.85**	0.8 (±0.07)	1.1 (±0.08)	**0.032**	>0.99	**0.039**
% Epicardial Fat	0.095 (±0.005)	0.13 (±0.016)	**0.34**	0.11 (±0.006)	0.15 (0.026)	**0.62**	>0.99	>0.99
% Calf Muscle	0.5 (±0.02)	0.4 (±0.02)	**>0.99**	0.5 (±0.01)	0.4 (±0.03)	**>0.99**	>0.99	>0.99
% Sub-Cutaneous Fat	0.3 (±0.02)	0.3 (±0.02)	**>0.99**	0.3 (±0.02)	0.3 (±0.02)	**>0.99**	>0.99	>0.99

4.3.7 The Effects of Apo CIII$^{-/-}$ on atherosclerotic plaques

Next, as Apo CIII influences lipoprotein lipid contents, we assessed the effect of Apo CIII$^{-/-}$ on atherosclerosis in these mice. The changes observed in weight of the mice and increased liver and fat alongside increases in plasma triglyceride and total cholesterol levels suggest that Apo E$^{-/-}$ x Apo CIII$^{-/-}$ mice could be less susceptible to atherosclerosis, as the lipids look to be stored in fat tissues (table 4.3.6.1). The brachiocephalic artery and the aortic root were examined for atherosclerosis plaque development using an H&E stain (figure 4.3.7.1). After either 8 or 16 weeks of AD, there was no difference between the genotypes in plaque size. In the aortic roots both Apo E$^{-/-}$ (25785.3±2738.1 vs 61064.7±4331.5, $p<0.001$) and Apo E$^{-/-}$ x Apo CIII$^{-/-}$ (14224.9±2461.1 vs 40464.4±10604.4, $p<0.05$) mice fed an AD for 16 weeks had increased plaques compared to their 8 week counterparts. Between genotypes however there was only a trend in a reduction in plaque size in Apo E$^{-/-}$ x Apo CIII$^{-/-}$ mice compared to Apo E$^{-/-}$ mice at either the 8 week (14224.9±2461.1 vs 25785.3±2738.1, $p<0.05$) or 16 week (40464.4±10604.4 vs 61064.7±4331.5, $p>0.05$) AD timepoints.

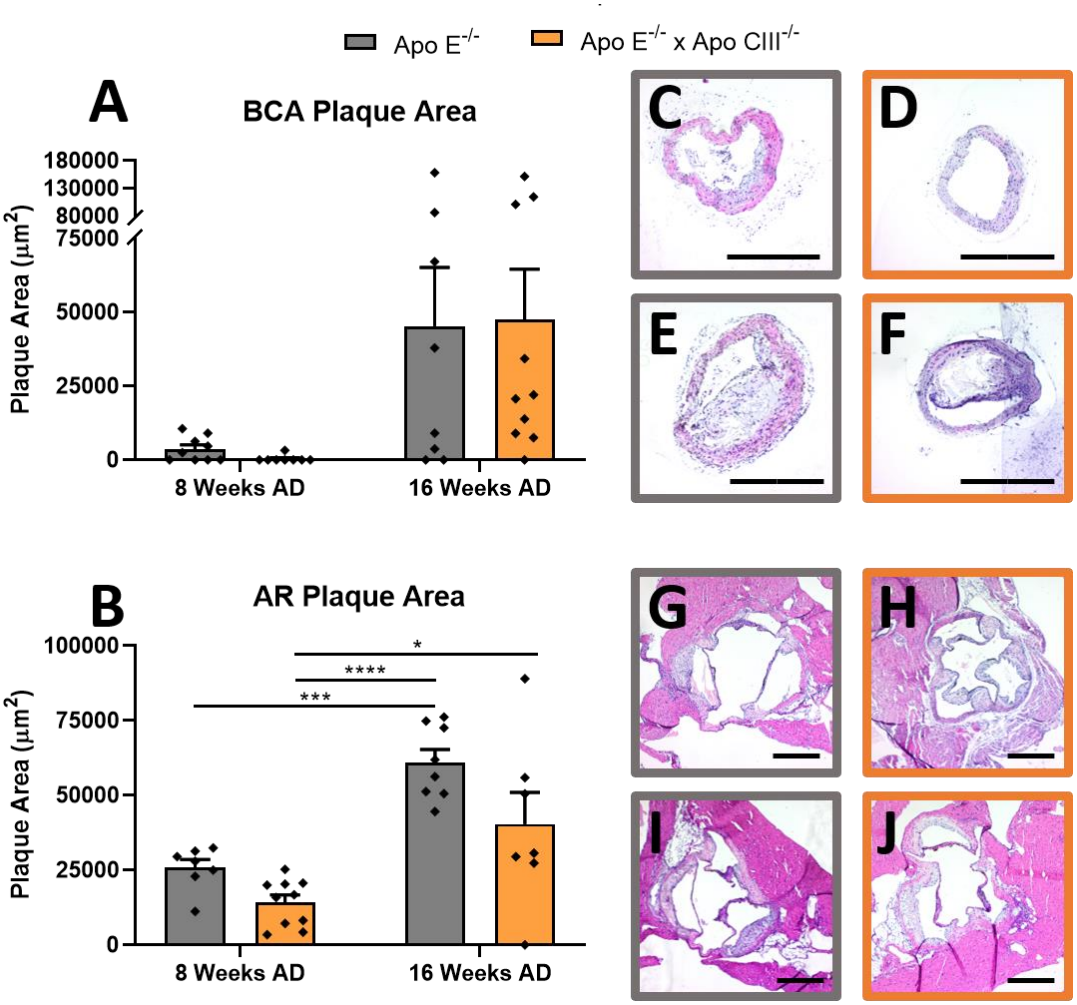

Figure 4.3.7.1 Plaque burden in Apo E-/- mice compared to Apo E-/- x Apo CIII-/- mice.

8 week old Apo E$^{-/-}$ and Apo E$^{-/-}$ x Apo CIII$^{-/-}$ mice were fed an atherogenic diet (AD) for 8 or 16 weeks. Tissues were collected post cardiac puncture and saline flush in formalin and embedded in paraffin. Arteries and valves were sectioned at 5µm thickness and stained with H&E. Images were captured using a Zeiss Axio Lab A.1 microscope with a Zeiss AxioCam ERc 5s camera and analysed using image J software. 2-Way-ANOVA. Data represented as mean± SEM, n=10-11. (A) brachiocephalic artery (BCA) plaque area, (B) aortic root leaflet (AR) plaque area. Representative images: (C) BCA Apo E$^{-/-}$ 8 week AD, (D) BCA Apo E$^{-/-}$ x Apo CIII$^{-/-}$ 8 week AD, (E) BCA Apo E$^{-/-}$ 16 week AD, (F) BCA Apo E$^{-/-}$ x Apo CIII$^{-/-}$ 16 week AD, (G) AR Apo E$^{-/-}$ 8 week AD, (H) AR Apo E$^{-/-}$ x Apo CIII$^{-/-}$ 8 week AD, (I) AR Apo E$^{-/-}$ 16 week AD, (J) AR Apo E$^{-/-}$ x Apo CIII$^{-/-}$ 16 week AD.

As described in chapter 1, depending on morphology, plaque calcification is a useful tool to indicate plaque stability. As these mice are in early-mid stages of plaque development, the ARS calcium stain appears purple in regions about to calcify due to the increased local alkalinity rather than actual calcium deposition. Only 1 of the Apo $E^{-/-}$ x Apo $CIII^{-/-}$ mice after 8 weeks on an atherogenic diet developed plaque and overall, none of the plaques in the 8 week cohort were advanced enough to contain any calcification, therefore no statistical analyses could be performed for this timepoint. After 16 weeks on an atherogenic diet however, Apo $E^{-/-}$ x Apo $CIII^{-/-}$ mice had reduced arterial plaque calcification compared to Apo $E^{-/-}$ mice (2.84±1.47 vs 0.14±0.13, $p<0.05$: t-test) (figure 4.3.7.2 A). In the aortic root, ARS staining revealed no significant difference between genotypes after both 8 weeks and 16 weeks on an atherogenic diet. The aortic roots of Apo $E^{-/-}$ x Apo $CIII^{-/-}$ mice after 16 weeks on an atherogenic diet did however have significantly raised calcification compared to their 8 week AD (0.002±0.002 vs 0.844±0.411, $p<0.05$) counterparts (figure 4.3.7.2 B).

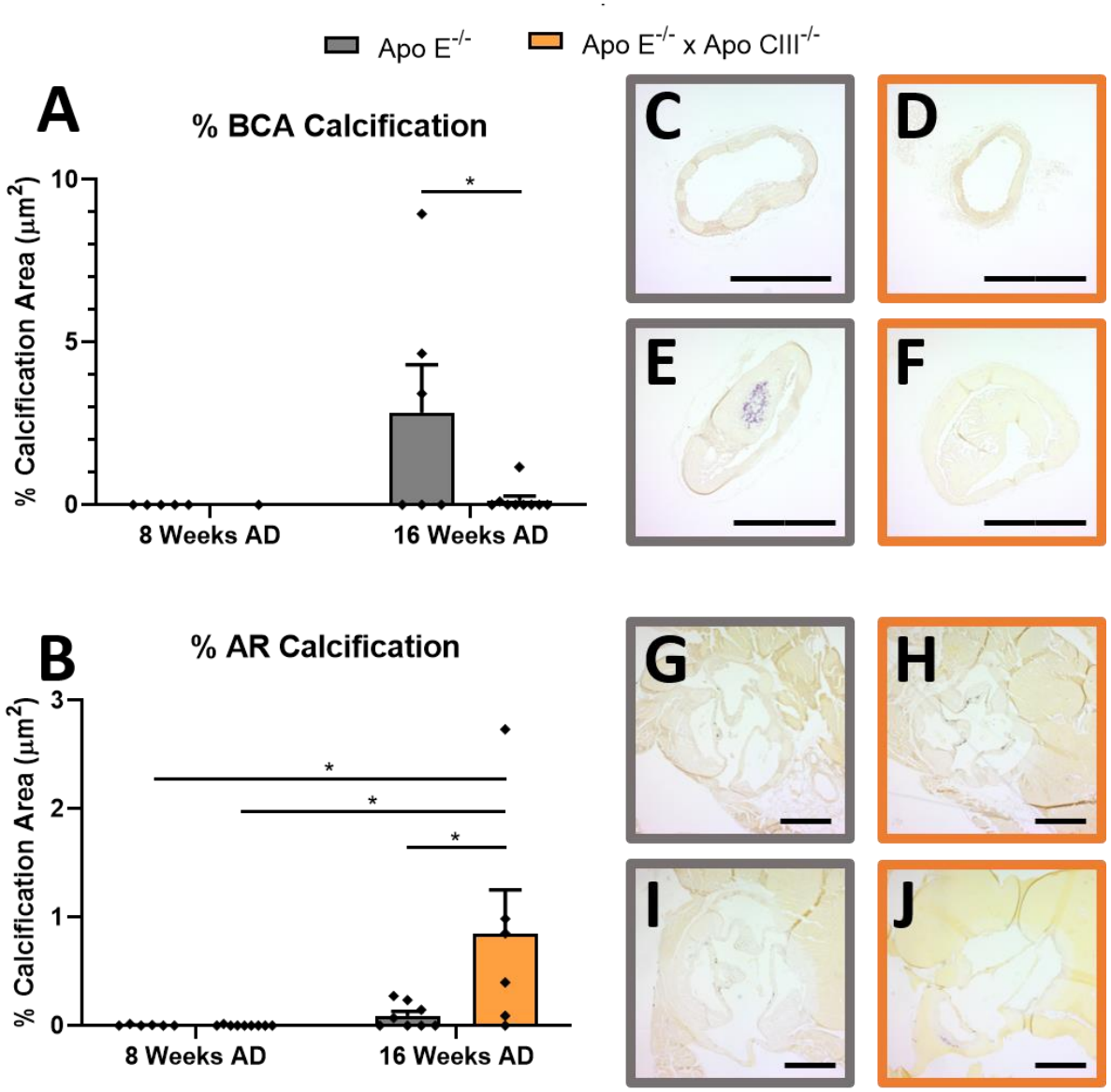

Figure 4.3.7.2 The effect of atherogenic diet on the brachiocephalic artery plaque calcium content of Apo E-/- mice compared to Apo E-/- x Apo CIII-/- mice.

(A) 8 week old Apo E$^{-/-}$ and Apo E$^{-/-}$ x Apo CIII$^{-/-}$ mice were fed an atherogenic diet (AD) for 8 or 16 weeks. Tissues were collected post cardiac puncture and saline flush in formalin and embedded in paraffin. Arteries were sectioned at 5µm thickness and stained with Alizarin Red S (ARS). Images were captured using a Zeiss Axio Lab A.1 microscope with a Zeiss AxioCam ERc 5s camera and analysed using image J software. 2-Way-ANOVA. Data represented as mean± SEM, n=10-11. Representative images: (B) Apo E$^{-/-}$ 8 week AD, (C) Apo E$^{-/-}$ x Apo CIII$^{-/-}$ 8 week AD, (D) Apo E$^{-/-}$ 16 week AD, (E) Apo E$^{-/-}$ x Apo CIII$^{-/-}$ 16 week AD.

Given the increased plaque development and observed changes in calcification in the Apo $E^{-/-}$ x Apo $CIII^{-/-}$ mice it was important to assess the plaques for additional structural components to determine the effect of apo CIII deficiency. In the BCA of Apo $E^{-/-}$ mice, there was a marked reduction in plaque SMα Actin after 16 weeks of AD compared to 8 weeks (Table 4.3.7.1). This is most likely due to the stage of plaque development, where at 8 weeks the plaques are smaller and VSMCs that have migrated into the plaque may not have yet differentiated into foam or osteoblast-like cells.

In the BCA or AR, there were no other significant differences in medial area, plaque collagen, chondrocyte count, CD68 or SMα Actin content between genotypes or AD timepoints (Table 4.3.7.1). The only exception to this was a significant increase in AR plaque collagen in Apo $E^{-/-}$ x Apo $CIII^{-/-}$ mice between the 8 and 16 week AD timepoints ($p<0.05$). These assessments of plaque composition suggest a stabilising effect of Apo $CIII^{-/-}$ in the plaques present in the aortic root.

Table 4.3.7.1 Plaque composition of Apo E-/- and Apo E-/- x Apo CIII-/- mice. *Mean (±SEM), 2-way-ANOVA, n=10-11.*

	8 Weeks Atherogenic Diet			16 Weeks Atherogenic Diet			p-value (8 weeks vs 16 weeks AD)	
	Apo $E^{-/-}$	Apo $E^{-/-}$ x Apo $CIII^{-/-}$	p-value	Apo $E^{-/-}$	Apo $E^{-/-}$ x Apo $CIII^{-/-}$	p-value	Apo $E^{-/-}$	Apo $E^{-/-}$ x Apo $CIII^{-/-}$
BCA Medial Area (µm)	65263.3 (±6886.6)	48520.9 (±4151.0)	**0.96**	55667.3 (±10851.5)	65030.4 (±8661.2)	**>0.99**	**>0.99**	**0.93**
AR Medial Area (µm)	93819.2 (±9892.4)	79607.2 (±7098.8)	**>0.99**	82339.5 (±7999.6)	84345.7 (±12548.1)	**>0.99**	**>0.99**	**>0.99**
BCA % Collagen (µm)	35.0 (±15.8)	11.1 (1 Plaque Only)	**>0.99**	45.4 (±8.6)	35.2 (±6.6)	**>0.99**	**>0.99**	**>0.99**
AR % Collagen (µm)	34.8 (±6.3)	27.9 (±3.4)	**>0.99**	50.4 (±2.3)	49.6 (±8.0)	**>0.99**	**0.33**	**0.037**
BCA Chondrocytes /mm²	201.3 (±100.6)	0 (1 Plaque Only)	**>0.99**	490.4 (±223.5)	202.9 (±86.8)	**>0.99**	**>0.99**	**>0.99**
AR Chondrocytes /mm²	2416.1 (±1748.2)	349.9 (±349.9)	**0.53**	609.3 (±138.0)	905.6 (±185.6)	**>0.99**	**0.94**	**>0.99**
BCA % CD68 (µm)	31.8 (±8.4)	40.4 (1 Plaque Only)	**>0.99**	21.9 (±10.0)	18.7 (±4.7)	**>0.99**	**>0.99**	**>0.99**
AR % CD68 (µm)	28.1 (±3.8)	26.0 (±3.5)	**>0.99**	18.3 (±3.5)	19.1 (±2.6)	**>0.99**	**0.36**	**0.93**
BCA % SMαActin (µm)	33.8 (±13.4)	8.5 (1 Plaque Only)	**>0.99**	0.75 (±0.62)	5.3 (±1.9)	**>0.99**	**0.0033**	**>0.99**
AR % SMαActin (µm)	2.8 (±0.9)	4.8 (±1.2)	**>0.99**	6.1 (±1.8)	9.2 (±3.6)	**>0.99**	**>0.99**	**0.78**

4.3.8 The Effects of Apo CIII$^{-/-}$ on calcification markers

Next, we sought to identify if Apo CIII deficiency effects markers of vascular calcification namely Runx2, RANKL, ALP, OPG and SMαActin. In figure 4.3.8.1 we show that there was no change in aortic calcification gene expression in Apo E$^{-/-}$ x Apo CIII$^{-/-}$ mice compared to Apo E$^{-/-}$ mice at the 8 week and 16 week AD timepoints. Although there appeared to be slight increases, the changes are slight and most likely arise from low n values and high variation in expression.

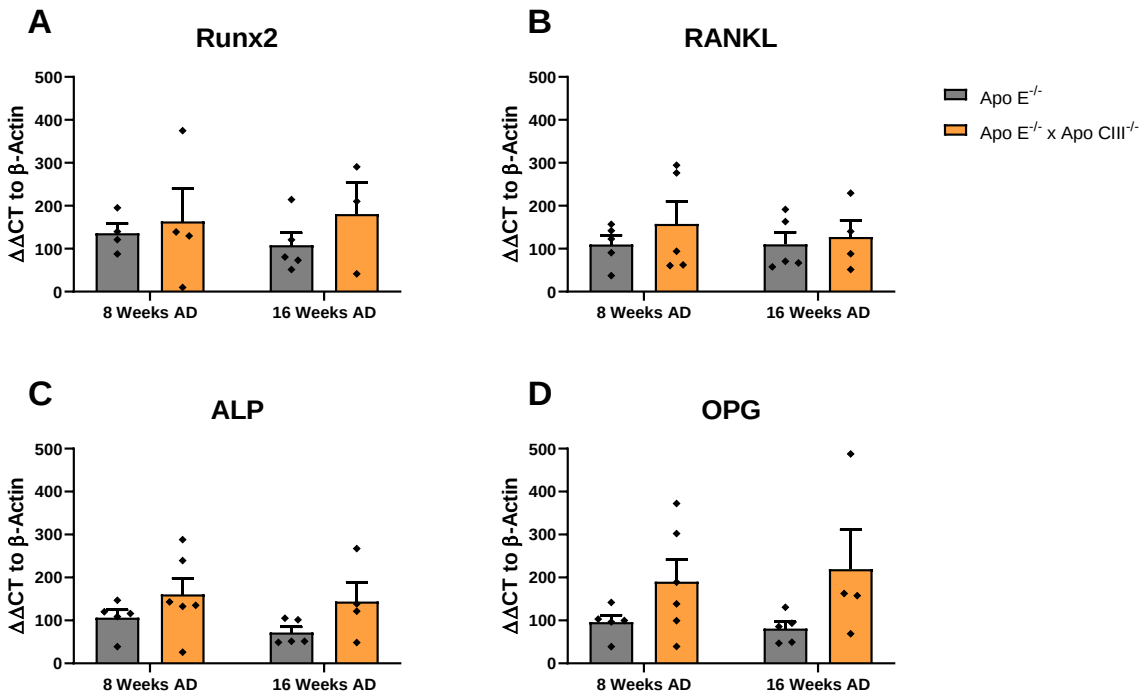

Figure 4.3.8.1 Expression of aortic calcification markers in Apo E-/- compared to Apo E-/- x Apo CIII-/- mouse. *8 week old Apo E$^{-/-}$ and Apo E$^{-/-}$ x Apo CIII$^{-/-}$ mice were fed an atherogenic diet for 8 or 16 weeks. Mice were euthanised via cardiac puncture and flushed with sterile saline before the collection of tissues. Aortas were snap frozen in $N_{2(l)}$ and RNA was extracted using an AllPrep DNA/RNA/Protein Mini Kit (Qiagen). mRNA expression was measured by qPCR using β-Actin as the internal control. 2-way-ANOVA. Data represented as mean± SEM, n=3-6.*

4.3.9 The Effects of Apo CIII$^{-/-}$ on Lipoprotein-Regulatory Gene Expression

As Apo CIII$^{-/-}$ mice thus far exhibit altered lipid profiles initially and altered lipid storage when challenged with an atherogenic diet, the role of Apo CIII was therefore investigated for the potential to regulate proteins involved in lipid or glucose metabolism, namely 3-hydroxy-3-methyl-glutaryl-coenzyme A reductase (HMGCoAR), the rate limiting protein for *de novo* cholesterol synthesis, sterol regulatory element-binding transcription factor 1 (SREBP1), a protein which increases TG storage, low density lipoprotein receptor (LDLR), a membrane protein for capture of Apo B-100 and Apo E lipoproteins and glucose transporter 2 (GLUT2), which facilitates glucose uptake. As Apo CIII is known to influence lipoprotein lipid levels and uptake (particularly with VLDL)[706], we sought to identify differences between Apo E$^{-/-}$ x Apo CIII$^{-/-}$ and Apo E$^{-/-}$ mice in the mRNA expression of these regulatory genes, in the liver and duodenum: the main sites of lipoprotein regulation.

When assessing the liver for changes in gene expression of HMGCoAR, GLUT2, SREBP1 or the LDLR there was no difference between either the genotypes or the length of time on atherogenic diet (figure 4.3.9.1). Similarly, figure 4.3.9.2 shows that there were no differences in the mRNA levels of HMGCoAR, GLUT2, SREBP1 or the LDLR between Apo E$^{-/-}$ or Apo E$^{-/-}$ x Apo CIII$^{-/-}$ mice at either AD timepoint in the duodenums of these mice. Together this data shows that any alteration in lipoprotein regulation is not likely due to a lack of CIII having influence over the expression of these particular genes.

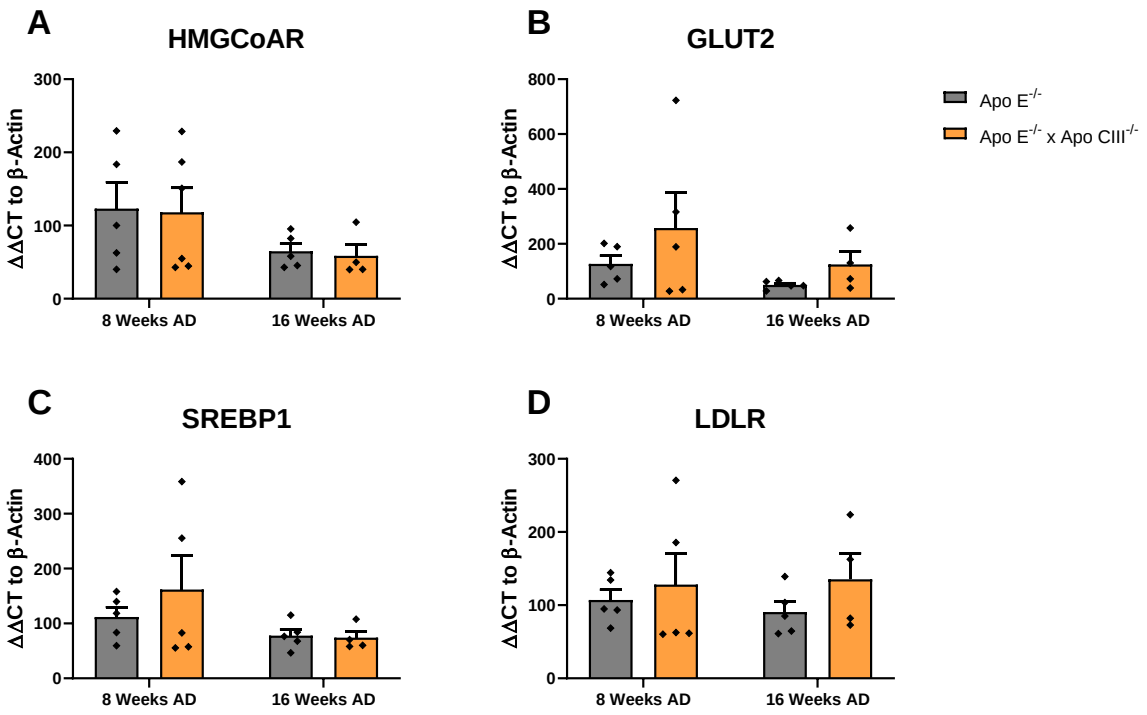

Figure 4.3.9.1 Expression of hepatic lipid metabolism markers in Apo E-/- mouse compared to Apo E-/- x Apo CIII-/- mouse.

8 week old Apo E$^{-/-}$ and Apo E$^{-/-}$ x Apo CIII$^{-/-}$ mice were fed an atherogenic diet for 8 or 16 weeks. Mice were euthanised via cardiac puncture and flushed with sterile saline before the collection of tissues. Livers were snap frozen in $N_{2(l)}$ and RNA was extracted using an AllPrep DNA/RNA/Protein Mini Kit (Qiagen). mRNA expression was measured by qPCR using β-Actin as the internal control. 2-way-ANOVA. Data represented as mean± SEM, n=5-6.

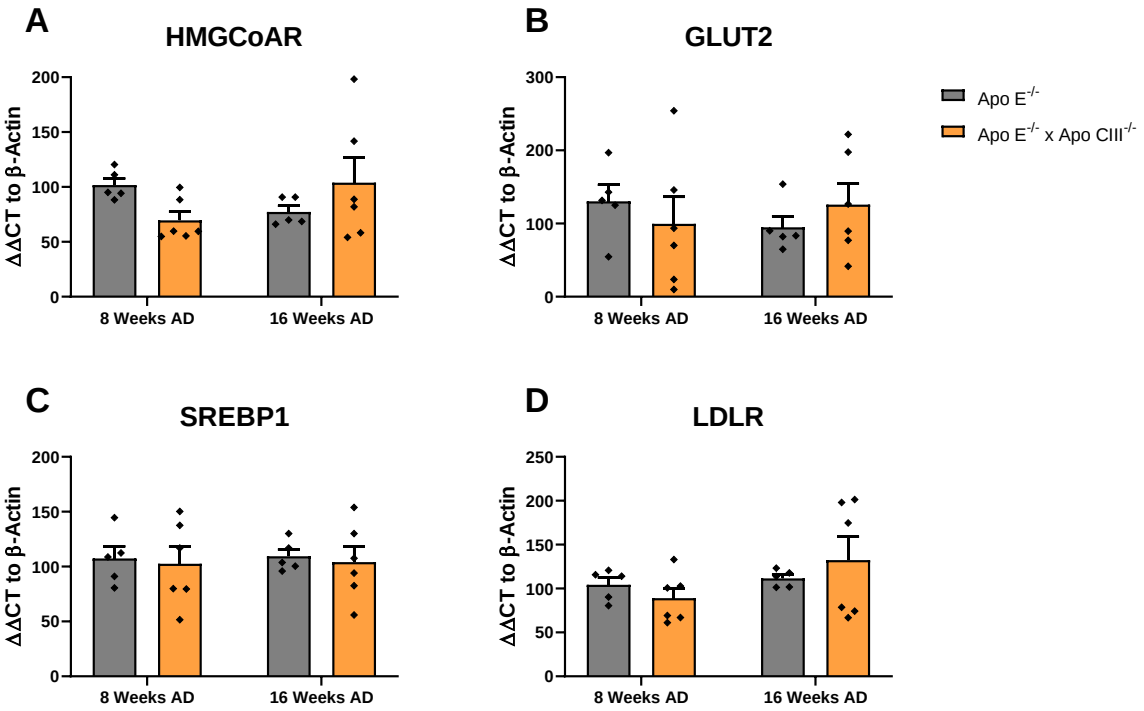

Figure 4.3.9.2 Expression of intestinal lipid metabolism markers in Apo E-/- mouse compared to Apo E-/- x Apo CIII-/- mouse.

8 week old Apo E$^{-/-}$ and Apo E$^{-/-}$ x Apo CIII$^{-/-}$ mice were fed an atherogenic diet for 8 or 16 weeks. Mice were euthanised via cardiac puncture and flushed with sterile saline before the collection of tissues. Duodenums were snap frozen in $N_{2(l)}$ and RNA was extracted using an AllPrep DNA/RNA/Protein Mini Kit (Qiagen). mRNA expression was measured by qPCR using β-Actin as the internal control. 2-way-ANOVA. Data represented as mean± SEM, n=5-6.

4.3.10 Correlations Between Atherogenic and VC Characteristics in Apo E$^{-/-}$ and Apo E$^{-/-}$ x Apo CIII$^{-/-}$ Mice

As a result of the differences observed in plaque characteristics between the two sites, the brachiocephalic artery (BCA) and aortic root (AR), correlation analyses were performed to investigate similarities.

Figure 4.3.10.1 shows the correlation between BCA and AR plaque areas, regardless of AD feeding time or genotype. We observed a significant positive correlation between the 2 sites, showing that as expected both plaques grow simultaneously ($r=0.52$, $p<0.01$).

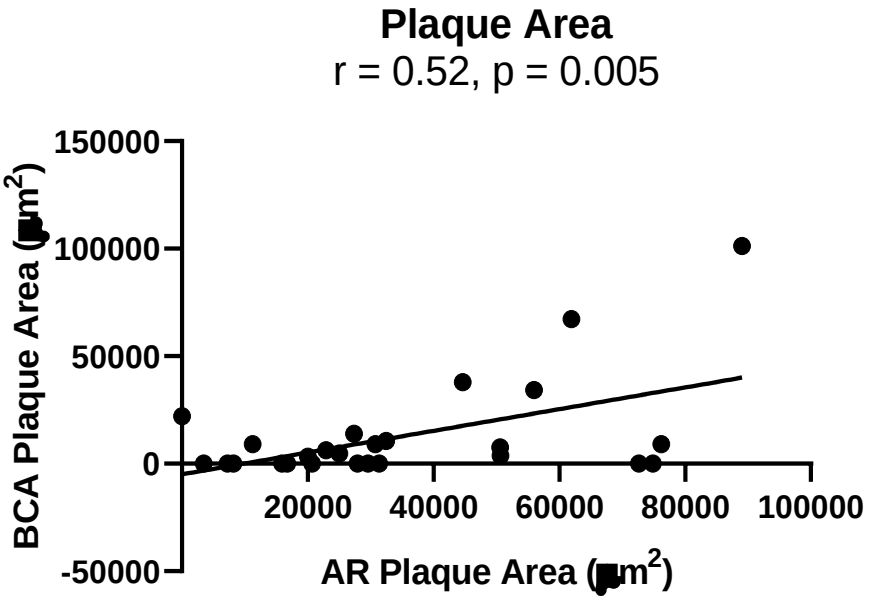

Figure 4.3.10.1 The correlation between aortic root and brachiocephalic artery plaque in mice fed an atherogenic diet.

Pearson's correlation of brachiocephalic artery (BCA) plaque area vs aortic root (AR) plaque area. Data represented as exact values per mouse fed an atherogenic diet for 8 or 16 weeks, n=27.

Continuing the investigation, correlations between plaque area and plaque calcification where assessed at 16 weeks of AD regardless of genotype. This 16 week timepoint was chosen, as there were not enough plaques in the 8 week cohort to do these analyses. There were no significant correlations between the BCA and AR plaque areas, BCA and AR plaque calcification or the plaque area and plaque calcification of the BCA in 16 week AD fed mice (figure 4.3.10.2). In the AR however there was a significant negative correlation between plaque calcification and plaque area of these mice ($r=-0.65$, $p<0.05$), showing that the smaller plaques tend to have more calcification and therefore potentially have increased stability.

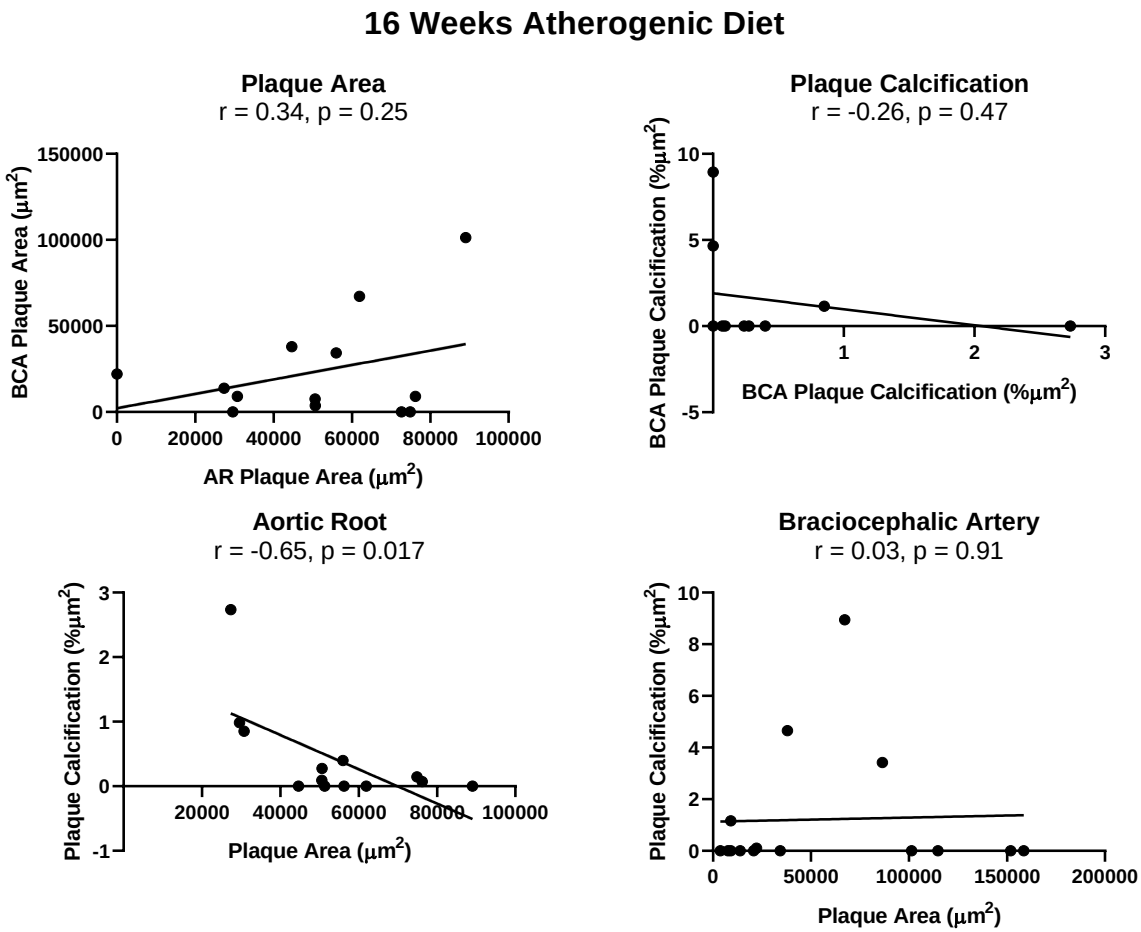

Figure 4.3.10.2 The correlations between aortic root and brachiocephalic artery plaque calcification of mice on an atherogenic diet for 16 weeks.

Pearson's correlation of brachiocephalic artery (BCA) plaque area vs aortic root (AR) plaque area. Data represented as exact values per mouse fed an atherogenic diet for 16 weeks, n=14-18.

The relationships between plaque calcification and either collagen or chondrocyte count were investigated in both the BCA and AR of these mice to assess whether these 'plaque stabilisation markers' were correlated in this cohort. In figure 4.3.10.3 we observed a significant correlation between plaque calcification and collagen. Interestingly, the correlations were opposite in the different plaque sites: in the AR, there was a significant negative correlation ($r=-0.76$, $p<0.01$) whereas; in the BCA there was a significant positive correlation ($r=0.55$, $P<0.5$). When examining the correlation between plaque calcification and chondrocyte count, there was a significant positive correlation in the BCA ($r=0.73$, $p<0.01$). This data suggests that in the BCA, the more collagen and chondrocytes a plaque has, the more calcification it will contain, aligning with the hypothesis that large calcifications create a stable plaque. In the AR however, we see that the more collagen a plaque had, the less calcification it contained. As the valves require increased flexibility compared to the arteries, calcifies in a more 'fibrotic' nature[707, 708] and disruption of valvular collagen leads to calcification[709], this indicates a pattern of self-protection. The mechanisms behind these interactions between calcification and collagen contents of plaques could yield some interesting insights with further investigations.

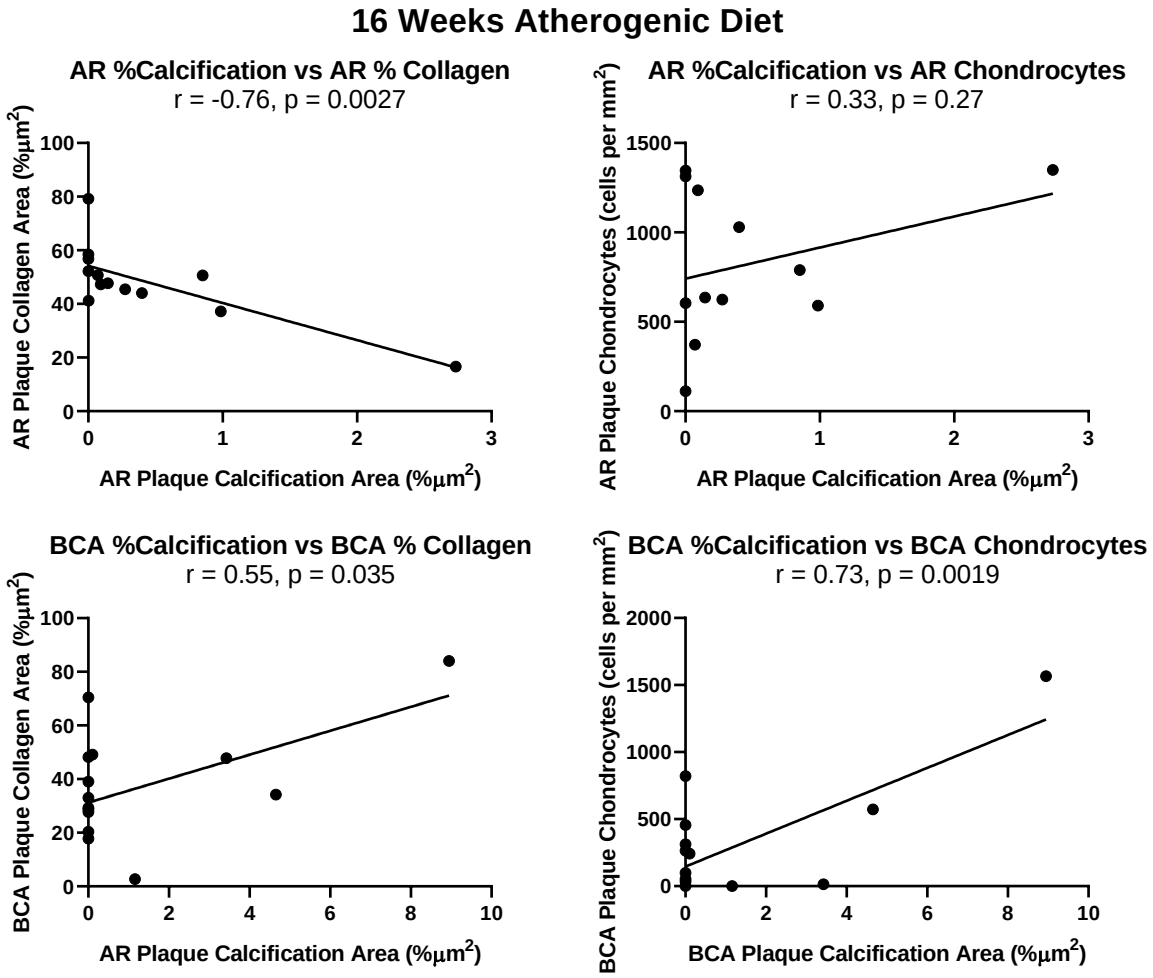

Figure 4.3.10.3 The correlations between aortic root or brachiocephalic artery plaque calcification characteristics.

Pearson's correlation of brachiocephalic artery (BCA) or aortic root (AR) % calcification area vs % collagen area or chondrocyte count per mm^2 of plaque. Data represented as exact values per mouse fed an atherogenic diet for 16 weeks, n=13-15.

As triglycerides have been indicated to play a causal role in atherosclerosis[136, 137] and are associated with increased valve calcification[311], we investigated the correlations between triglycerides, plaque area and plaque calcification in our BCA and AR sites. There was a significant negative correlation between triglyceride level at time of death and plaque calcification ($r=-0.62$, $p<0.05$), but no significant correlations between these triglycerides and AR plaque area (figure 4.3.10.4). There were no significant correlations between these characteristics for the BCA plaques.

Increased VLDL particle size in humans associates with coronary artery calcification[100] and mice overexpressing Apo CIII have larger VLDL particles[706]. Based on this we could speculate that the Apo $E^{-/-}$ x Apo $CII^{-/-}$ mice may have smaller, more atherogenic particles. From table 4.3.5.1 however we see that AD nullifies changes in triglyceride levels, and therefore potentially VLDL levels. While the increase in AR plaque calcification could be due to an influence of Apo CIII deletion in some of the mice on physical VLDL characteristics rather than a molecular characteristic, it is also important to note that Apo CIII over expression in mice reduces lipoprotein bound Apo E levels[706], an effect which we are unable to study in this thesis due to the Apo $E^{-/-}$ background of these mice.

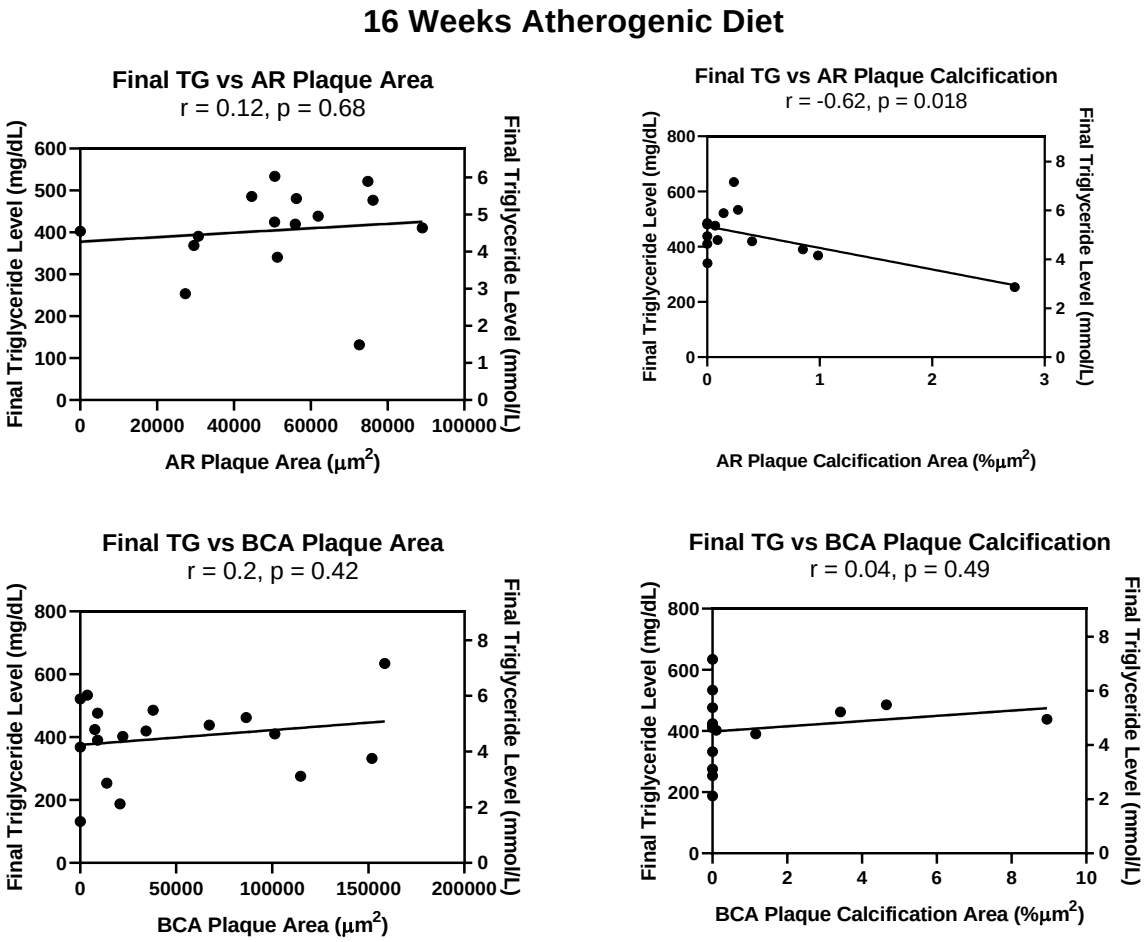

Figure 4.3.10.4 Correlations between triglyceride levels and plaque.

Pearson's correlation of final triglyceride levels and brachiocephalic artery (BCA) or aortic root (AR) plaque or % plaque calcification area. Data represented as exact values per mouse fed an atherogenic diet for 16 weeks, n=10-15.

Continuing the exploration into the relationship between triglycerides and calcification, we investigated the correlations between circulating plasma triglycerides, calcium or ALP levels at the end of the study figure 4.3.10.5 shows significant positive correlations between plasma calcium levels ($r=0.76$, $p<0.0001$), ALP levels ($r=0.22$, $p<0.05$) and triglyceride levels. While this may suggest a relationship between triglyceride rich lipoproteins (TRLs) and expression or mobilisation of these molecules in the artery wall for calcification, it may also suggest an increased mobilisation of calcium and ALP from the bone marrow. Triglyceride levels have been positively correlated with bone mineral density in a healthy population[710, 711], but also create a mobile layer within bone capable of interacting with bone metabolism and mineralisation[712, 713], therefore it would not be unreasonable to hypothesise a relationship between the bone, artery wall and triglyceride levels.

Since research into VC is still relatively understudied *in vivo*, investigations into correlations between plaque characteristics within each site could lend insight into the nature of the disease, leading to improved identification techniques or therapeutic development.

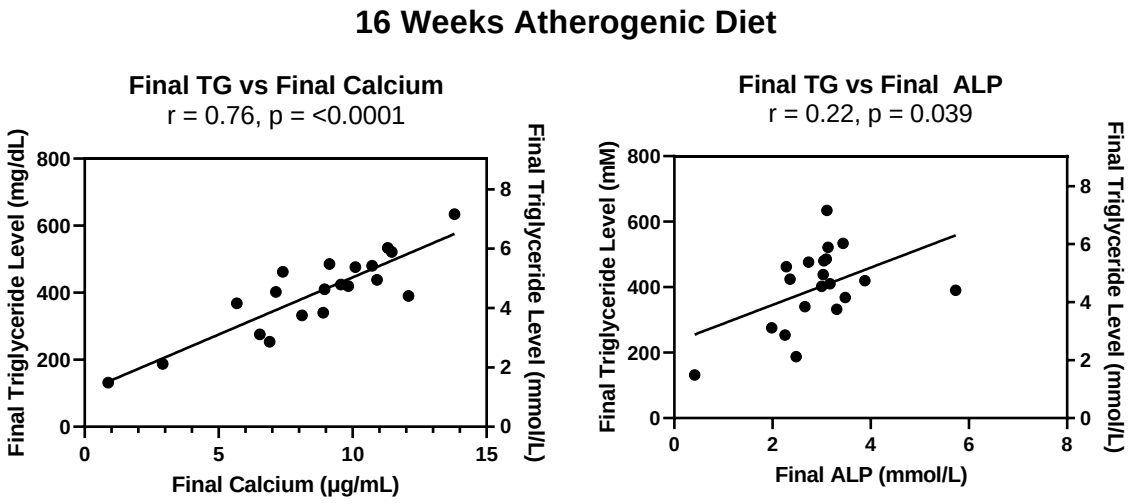

Figure 4.3.10.5 Correlations between triglyceride levels and plasma calcium or ALP of Apo E-/- and Apo E-/- x Apo CIII-/- mice fed an atherogenic diet for 16 weeks.

Pearson's correlation of brachiocephalic artery (BCA) plaque area vs aortic root (AR) plaque area. Data represented as exact values per mouse fed an atherogenic diet for 16 weeks, n=20.

Ex Vivo Results

The role of VLDL and oxVLDL in VSMC calcification

4.3.11 The Effects of Human Plasma Triglyceride Level on Vascular Calcification

After examining the roles of VLDL and oxVLDL *in vitro* alongside the effects of Apo CIII deletion on an atherosclerotic background *in vivo*, we progressed to expanding these results to include using whole human serum with varying levels of triglycerides in an *ex vivo* pilot study. The patient characteristics of the samples used are as shown below in table 4.3.11.1. There were no significant differences between groups in any characteristic, except the plasma triglyceride levels (Kruskal-Wallis, $p<0.01$) and total cholesterol levels between the low TG (<2mM) and high TG (>6mM) groups (Dunn's test, $p<0.05$).

Table 4.3.11.1 Donor characteristics for entire cohort and for samples used in the human triglyceride (TG) study.

*One-Way ANOVA or Kruskal-Wallis test. Expressed as mean (±SEM) or incidence %. *p<0.05, **p<0.01 when compared to the >6 mM TG group with Dunn's multiple comparisons test.*

	All Samples	Samples by Triglyceride (TG) Level			
	All TG levels (n=15)	TG <2 mM (n=5)	TG 2-6 mM (n=5)	TG >6 mM (n=5)	p-value
Age (Years)	63.7 (±3.5)	74.2 (±4.4)	60 (±4.5)	57 (±6.8)	0.19
Female (%)	40%	60%	20%	40%	0.64
BMI	29.8 (±1.9)	26.9 (±4.3)	31.9 (±1.7)	30.7 (±3.6)	0.41
Diabetes Mellitus (%)	53.3%	60%	40%	60%	0.91
Hypertension (%)	86.6%	100%	60%	100%	0.2
Triglyceride (mM)	4.41 (±0.96)	1.18 (±0.17) **	3.04 (±0.47)	9.02 (±1.03)	0.0047
Total Cholesterol (mM)	5.67 (±0.97)	3.5 (±0.35) *	4.74 (±0.68)	8.78 (±2.33)	0.058
LDL (mM)	2.92 (±0.66)	1.84 (±0.28)	2.49 (±0.56)	4.18 (±2.06)	0.44
HDL (mM)	0.99 (±0.07)	1.12 (±0.14)	0.88 (±0.06)	0.98 (±0.13)	0.54

Patient serum was assessed for circulating calcium and ALP to investigate the calcification potential of the patient serum. Figure 4.3.11.1 shows that human serum with extremely high triglyceride concentrations had trending, but not significantly higher levels of the circulating calcium (9.77±0.51 vs 12.68±2.29, p>0.05) and ALP (0.59±0.06 vs 1.46±0.51, p>0.05).

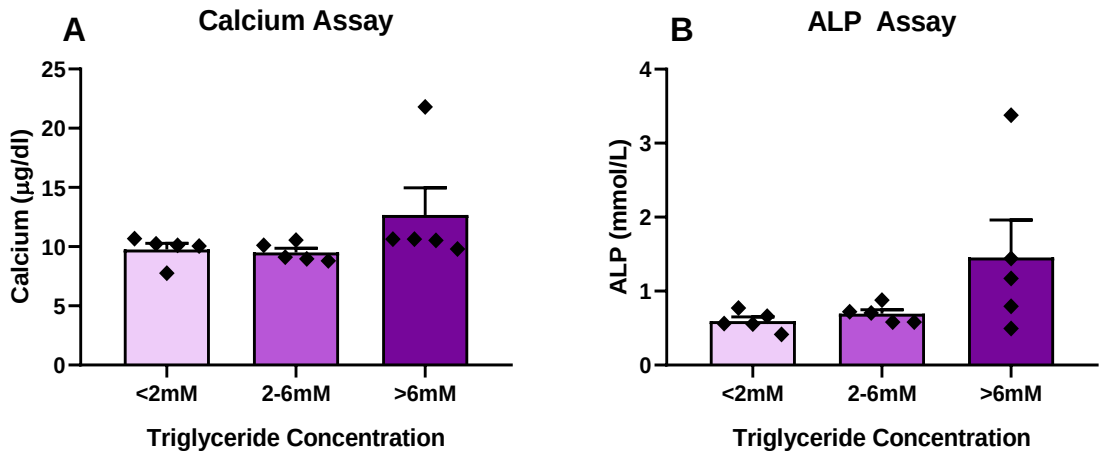

Figure 4.3.11.1 The effect of human serum triglyceride levels on human serum calcification marker levels.

Serum at various triglyceride levels was tested using either the Wako ALP assay or the Cayman calcium assay as per protocol. Welsh's T-test. Data represented as mean± SEM, n=5.

To further assess the calcification potential of serum with high TGs, a calcification ARS assay was performed as described in chapter 4.2. The triglyceride concentration of human serum did not affect the calcification potential of HAoSMCs. The cells with no treatment or calcification medium (CM) had significantly less calcification than all other treatment groups ($p<0.0001$). There were no other significant differences between any other treatments (figure 4.3.11.2).

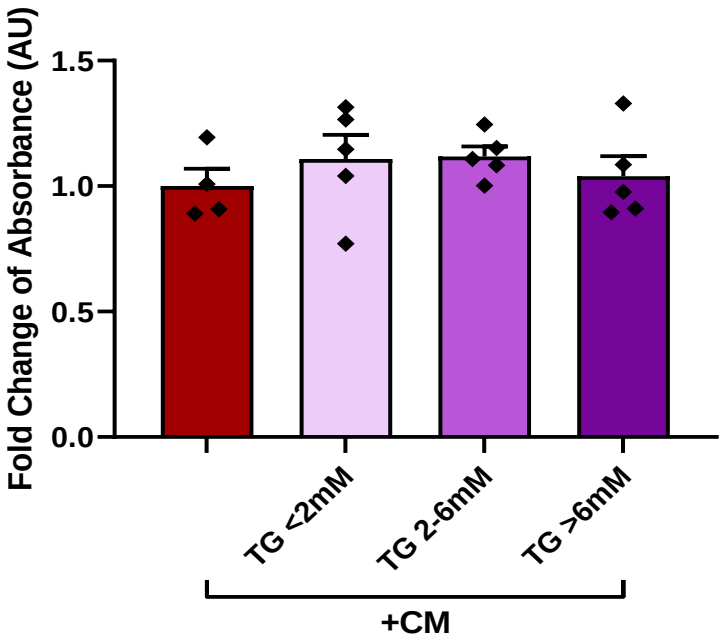

Figure 4.3.11.2 The effect of human serum triglyceride concentration on HAoSMC calcification.

HAoSMCs were pre-treated with human serum for 24 hours then treated with $CaPO_4$ (Ca 2.7 mM, PO_4 2.0 mM) for 15 days. Calcification was measured by ARS assay with no treatment (NT) and $CaPO_4$ medium alone (CM) controls and expressed as fold change from CM. ANOVA with Bonferroni's correction. Data represented as mean± SEM, n=5.

We then used the values from the ARS, calcium and ALP assays to analyse any correlations between these values and the lipid data. The calcification potential of serum on HAoSMC was not significantly correlated to serum TG (F), total cholesterol (TC) (I), HDL (L), calcium (B) or ALP (A) levels (figure 4.3.11.3). Both TG and TC levels were however both significantly correlated to serum markers of VC, namely circulating calcium (TG (E): $r=0.6$, $p<0.05$, TC (H): $r=0.86$, $p<0.0001$) and ALP (TG (D): $r=0.75$, $p<0.01$, TC (G): $r=0.93$, $p<0.0001$). HDL did not correlate to either calcium (K) or ALP (J) in this cohort (figure 4.3.11.3).

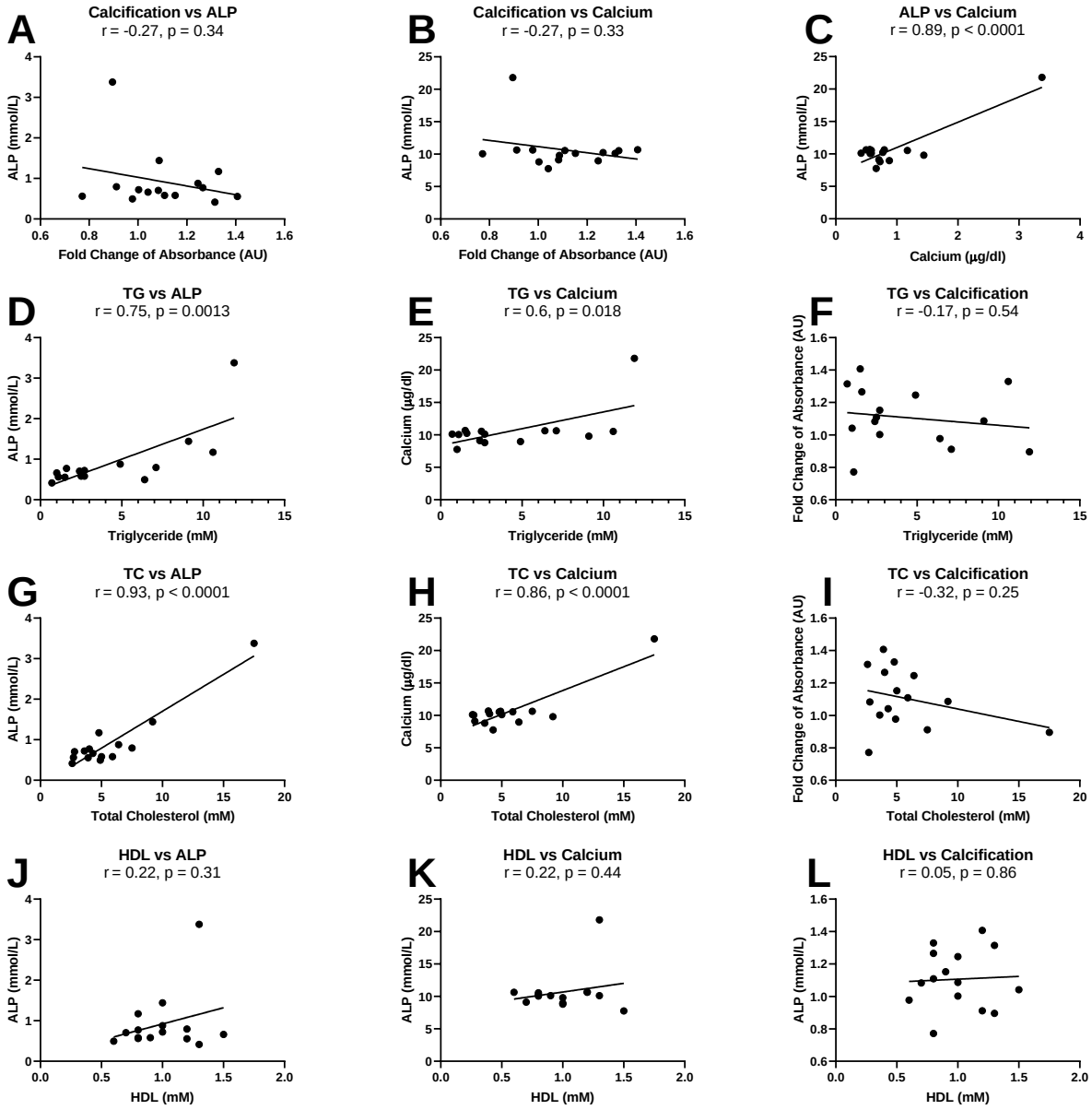

Figure 4.3.11.3 The correlations between lipid data and vascular calcification in the triglyceride human serum study.

Serum marker level and calcification data from chapter 4.3.11 was correlated using Pearson's r correlations. Data represented as mean vs mean, n=15.

4.4 Discussion

The *in vitro* study compares the effects of native VLDL and oxVLDL on vascular calcification (VC) and known calcification regulators. This study suggests a moderate effect of VLDL in the initiation and regulation of VC and a more dramatic stimulatory effect from oxVLDL treatment. For VLDL, the majority of changes were observed at the earlier timepoints, whereas the effects of ox VLDL became apparent later on in the calcification process. In addition, the impact of Apo CIII deficiency in an atherosclerotic mouse model was investigated, revealing a significant positive correlation between TG level, circulating calcification markers but a negative correlation to AR plaque calcification. When examining the calcification potential of human serum, we also identified significant positive correlations between triglycerides and circulating calcium or ALP, but not calcification of VSMCs treated with the serum.

VC occurs due to delicate imbalances in the expression of VSMC regulators. In this study, we examined the changes of Runx2, RANKL, ALP, OPG and SMαActin in response to VLDL or oxVLDL treatments. While the 0, 3, 5 and 7 day timepoints reflect early, mid and late timepoints in calcification initiation, the expression of these regulators are prone to compensation from the cells to normalise the disease and are biphasically and time-dependently expressed[667]. Ideally, as the calcification process takes 15 days in these cells, assessing alterations in gene expression would be more optimal at this later timepoints, however due to the apoptotic nature of VC when mineralising this causes difficulties in preserving cellular RNA and protein.

When challenged with VLDL, we observed a pattern in the HAoSMC suggesting the use of a compensatory mechanism. Gene expression of Runx2, RANKL, ALP, OPG and SMαActin (figures 4.3.3.1 – 4.3.3.5) were time dependently increased or decreased in expression when treated with VLDL compared to CP alone. Although by 5 to 7 days, the expression of

all these genes followed the expected patterns, as extrapolated from the increased VC formation in figure 4.3.1.1, the early timepoints did not reflect the expected pattern of expression indicating that these cells could be responding to environmental cues to exert a protective effect against the initiation of calcification.

As oxidative stress causes both apoptosis[714-717] and VC[296-300], it is possible the observed effects are a direct result. Cells looked visibly stressed under the microscope within the first few days of treatment. These two observations combined with the reduced expression in all genes after 24 hours treatment (figure 4.3.2.1) suggest that oxVLDL could be increasing calcification on these cells not only via the Runx2 regulatory system, but also via apoptotic pathways. While there is some evidence for the role of apoptosis in VC[293-295], the role of VLDL and oxVLDL in this system is unknown and warrants further investigation.

Larger lipoprotein particles are typically not associated with increased risk of atherosclerosis due to the physical difficulty infiltrating the endothelium and entering the artery wall[124, 125]. Interestingly however, these larger particles are highly associated with increased calcification[100]. This highlights that the role of VLDL in calcification is more complex than simply cholesterol or triglyceride content. It is hypothesised that intimal and medial calcifications may have subtly different mechanisms, similar to the minute differences between arterial and valvular calcifications[707]. It could be speculated that VLDL and oxVLDL are influencing a more medial plaque calcification pathology, or modifying plaque composition to a pro-calcification phenotype, rather than the assumed regular intimal morphologies.

In addition to particle size, particle composition could be playing a role in the calcification process. The oxidation status or apolipoprotein content of VLDL could have a significant effect on the calcification process, via potential non-lipid transfer related effects on the artery wall. Supporting this, in the *in vivo* studies apo $E^{-/-}$ x apo $CIII^{-/-}$ mice had a significant

increase in valvular collagen and maintained brachiocephalic SMαActin content over time, whereas apo $E^{-/-}$ mice had no increase in collagen content and had significantly reduced SMαActin content over time (table 4.3.7.1). Altogether, this shows that apo CIII may have a role in the reduction of VSMCs and the inhibition of collagen formation, both important components of VC.

Apo CIII is a major component of VLDL functionality via inhibition of lipoprotein lipase and impairment of Apo E binding, causing increased blood triglyceride concentration. Utilising an Apo CIII deficient mouse model on an atherosclerotic background the ability of apo CIII to modify plaque composition and VC was assessed. As expected, the baseline triglyceride levels of Apo $E^{-/-}$ x Apo $CIII^{-/-}$ mice were significantly lower than the Apo $E^{-/-}$ mice. Interestingly, the total cholesterol of the Apo $E^{-/-}$ x Apo $CIII^{-/-}$ mice was also lower at baseline, however after 8 and 16 weeks of an atherogenic diet these differences in triglycerides and cholesterol had balanced out. While this could potentially be due to oversaturation from the atherogenic diet, it could also be a result of the loss of Apo E mediated clearance of these particles.

Calcification is often overlooked in early stage atherosclerotic plaque progression however there is evidence that VSMC differentiation into chondrocytes occurs as early as <8 weeks in $MGP^{-/-}$ mice[501] or 12 weeks of atherogenic diet in Apo $E^{-/-}$ mice[718] and calcium deposits were visible in these mice at <8 weeks and 20 weeks of atherogenic diet respectively. While at 8 weeks calcification was not visible due to small or absent plaques, by 16 weeks of atherogenic diet there were changes observed in both the BCA and aortic root, albeit in opposite directions.

Evidence in human studies have outlined differing pathologies of calcification in varying blood vessels, including differences in matrix composition, sheer stress levels and presence of an adventitial layer. None the less, aortic valve calcification is observed to

associate with coronary artery calcification[719] and plaque burden[720]. In the studies in this chapter however, we observe that although when examining plaques over different timepoints the plaque area between the AR and BCA are correlated, the significance is lost when examining only the 16 week AD timepoint, suggesting either a need for a variation in plaque sizes to reach significance, or a higher n value. Moreover, in these studies we observed no significant correlation between plaque sites with regards to VC and no correlation between plaque size and VC in the BCA. Interestingly, in the AR of these mice after 16 weeks of AD, VC was significantly negatively correlated with plaque size, opposing the literature. Because these studies were performed in a short-medium term mouse model with some begging the study with low TG and total cholesterol levels, this data might suggest a site specific role for Apo CIII or TRLs in plaque calcification.

The vessel wall is a collagenous environment, capable of trapping TG[721]. Although the larger VLDL particles may be unable to pass the endothelial layer, a wide distribution of TGs have been identified in the arterial intima an impact adventitial cell adiposity[722]. Correspondingly, therapeutic reduction of TGs increased the stability of diabetes induced atherosclerosis *in vivo*[723] and large VLDL particle size associated with increased VC[100], suggesting that the role of TGs in atherosclerosis could be facilitated through adventitial access to medial VSMCs for differentiation and calcification. Interestingly, Apo CIII over expression in mice leads to large VLDL particle size[706], however in this Apo CIII$^{-/-}$ study, we see no change in atheroma volumes. This study differs from the human population and mouse overexpression population by being on an Apo E$^{-/-}$ background, potentially skewing the results seen here. Not only does Apo CIII influence lipoprotein bound Apo E in mice[706], but mice with both Apo CIII and CETP expression also have different cardiovascular profiles[692]. The influence of all these factors may explain some of the inconsistencies with the literature in this study.

As triglycerides are found in the mobile phase of the bone[712], investigations into the role of TRLs in bone metabolism simultaneously with VC could provide insight into the relationships between the sites and co-morbidities. One potential mechanism worth exploring is the interaction between fetuin A and TGs, as circulating fetuin A correlates to metabolic disease[724] and TG levels significantly correlate to fetuin A[725]. Interestingly, fetuin A inhibits BMP signalling, which modulates matrix mineralisation in the bone[726], but can also stimulate cellular triglyceride synthesis from external fatty acids[727] and associates with cholesterol, CEs and partially with TGs, forming a HDL-like lipoprotein particle[728]. With this evidence, it is therefore worth hypothesising an interplay between the two particles, potentially whereby TRLs may facilitate the transfer of calcium to lipoproteins through fetuin scavenging.

The effect of high TG levels in the patient serum highlighted a potential correlative role in calcification. Significant positive correlations were identified between triglycerides and circulating calcium or ALP, but not calcification of VSMCs treated with the serum. While ALP[729, 730] and calcium[731] concentrations are both linked to VC, there are multiple other components of serum which can contribute to the inhibition of VC, such as fetuin-A complexes[539, 732, 733]. Although there was no relationship between serum triglyceride levels and their calcification potential on VSMCs, the sample size was small with 5 participants per group, which may have influenced the significance of the results obtained. As the *in vitro* data suggests that oxidation of VLDL increases its potential to calcify these cells via the Runx2 pathway, it would be worth assessing serum oxidation levels in both the human study population and animal study mice.

In conclusion, the data from this chapter suggests that the role of VLDL in VC is due to the readily oxidised nature of VLDL. While it appears that initially Apo CIII$^{-/-}$ on an Apo E$^{-/-}$ background may provide early lipid profile benefit, when challenged with an AD these mice

had heavier fatty tissue weights and increased AR calcification. Interestingly, both *in* vivo and *ex vivo*, TG levels correlated to calcification markers, suggesting an influence of TRLs in the progression of calcification. Moving forward with VC research into VLDL and its components, it would be interesting to consider different pathways of calcification, such as oxidative or apoptotic routes and explore the relationships between fat metabolism and calcification.

5 : Chapter Five

Investigating the role of low-density lipoproteins on vascular calcification

5.1 Introduction

During the late-1990's a series of clinical studies correlated LDL to coronary artery calcification (CAC) using CT imaging: high LDL associated with increased calcification progression in patients with known aortic calcification[734] and lipid lowering treatments significantly reduced CAC progression[735]. Furthermore, LDL cholesterol is still the only correlating and significant risk factor for CAC[736] and calcification progression[737].

Upon further investigation, the quality and size of the LDL particle was important, with small particles associating with macrocalcifcation[100] and general lipoprotein modifications, such as oxidation, glycation[294, 738], acetylation, enzymatic[739] and aggregation have all been implicated in calcification development. In particular, modification of human LDL via iron oxidation significantly increased cellular ALP activity in calcifying bovine aortic VSMC, whereas native human LDL did not[740]. Interestingly, the same study found the reverse for bone pre-osteoblasts cells, where iron oxidised LDL significantly inhibited cellular ALP activity, suggesting a role for oxLDL in mediating these co-morbidities.

In VSMCs, incubation with oxLDL triggers the TLR4/NF-κB/Ceramide[741], Wnt/β-catenin[742], Runx2[743] and BMP-2[744] signalling pathways of VC. Interestingly, endothelial cell upregulation of Runx2[320] and BMP-2[745] mRNA expression, or even calcifying themselves[320] after oxLDL stimulation, adds to the pro-calcification effects of oxLDL *in situ*. Enzyme modified non-oxidised LDL (ELDL), a type of LDL with cleaved or dysfunctional apo B100, also significantly induced calcification *in vitro* via upregulation of BMP-2 mRNA, alongside loss of the protective MGP mRNA expression[746] and is preferentially absorbed by the VSMCs to cause macrophage-like differentiation (expression of CD68 and Mac2 with loss of smooth muscle alpha actin)[315]. As oxLDL stimulates inflammatory M1

polarised foam-cell macrophages which then may stimulate micro-calcifcations[206], oxLDL may also stimulate the initiation of VC through macrophage and VSMC interactions.

Statins, an LDL and cholesterol lowering therapy, are known to stimulate polarisation of macrophages to an M2, calcification progressive phenotype[747] and disrupt macrophage Rac1 regulation, leading to increased calcification[748]. Furthermore, in VSMCs, statins increase VC[749], potentially by inhibition of matrix metalloproteinase secretion[750], modulation of fibrinolytic balance of vascular cells[751] and regulation of VSMC inflammatory transcription factors[752]. Exemplifying these effects, statin treated mice display increased aortic calcification[748], in relation to their IL-1β levels[753]. Furthermore, statins are now widely accepted as calcification promotors independent of their plaque-regressive effects[285], with the same effect observed in non-diabetic[754], type 2 diabetic[755] and CKD[756] populations. Taken together, these data suggest a role for statins in the stabilisation of plaques via macrocalcification stimulation.

Lipoprotein (a) (Lp(a)), an LDL particle with apolipoprotein (a) attached to its apo B100, as identified by *in vivo*, imaging and genome wide association studies, is significantly correlated to, or causative of CVD[116], inflammation driven[757] calcific aortic valve disease[758, 759] and is an independent risk factor for CAC[760], particularly in women with type 2 diabetes[761]. Lp(a) accumulates in atherosclerotic plaques[118-120] and delivers scavenged oxidised phospholipids[762, 763], stimulating VSMC osteoblastic differentiation[764]. Potential treatments for high Lp(a) however, including PCSK9 inhibitors, niacin and the CETP inhibitor anacetrapib, have yet to demonstrate, or be investigated for, any benefit correlating Lp(a) lowering to VC. Interestingly, statins have been shown to both lower[765] and raise[766] Lp(a) levels in clinical trials and although the Lp(a) raising effects of statins are now being debated[767, 768], statin induced changes in Lp(a) were not investigated for their correlation to VC in either study. As more specific Lp(a) lowering therapies undergo

clinical evaluation they will provide the opportunity to investigate the impact of Lp(a) lowering on VC.

Although the literature suggests an important role for LDL, oxLDL, Lp(a) and their regulation by statins in VC, there remains a paucity of specific, functional research on these effects. In this chapter, we describe the influence of these particles on VSMCs in the context of calcification *in vitro*. Furthermore, we examine the role of statins, on VC on Apo $E^{-/-}$ mice *in vivo* and Lp(a) *ex vivo*.

5.2 Methods

5.2.1 *In Vitro Study Design*

Cells were maintained and calcified as per methods chapter 2.4 after 24 hours of pre-treatment with LDL or oxLDL at 200µg/ml. After 1,3,5 and 7 days of calcification medium (CM), cell mRNA was harvested and transformed to cDNA for PCR analysis as per methods chapter 2.5.1, 2.6 and 2.7 respectively. Cells were harvested after 5 and 7 days of calcification for protein analysis via methods in chapter 2.8 and 2.9. Additionally, media also was collected after the 5 and 7 day CM timepoints and analysed for protein secretion using ELISA assays as per methods chapter 2.10. A timeline of the *in vitro* calcification assay is presented in figure 5.2.1.

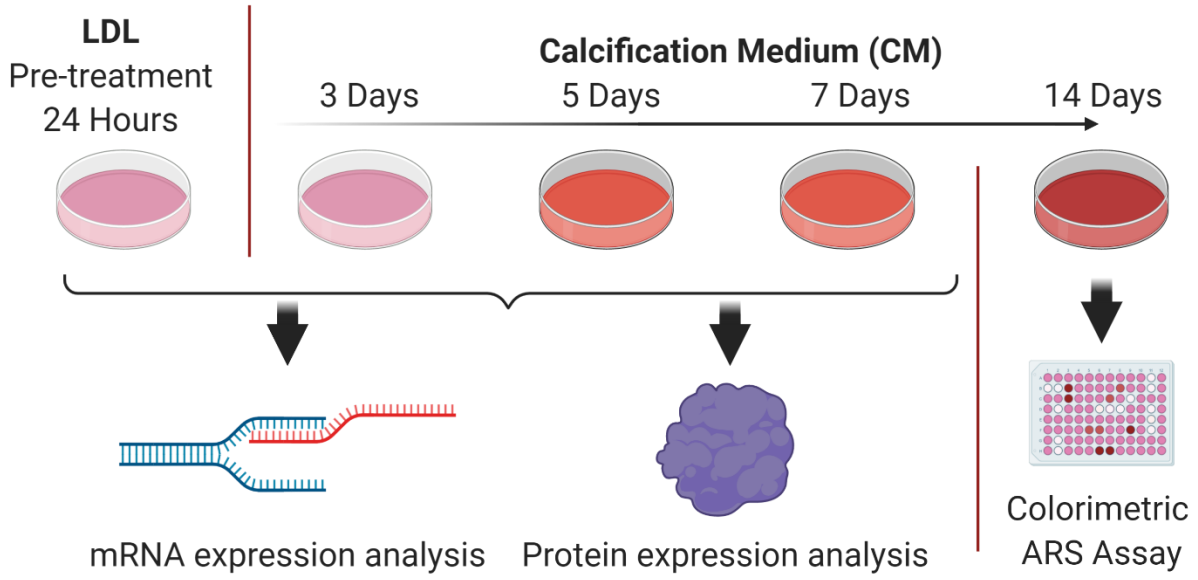

Figure 5.2.1.1 Schematic of the LDL *in vitro* calcification assay.

HAoSMCs were pre-treated with LDL or oxLDL at 200µg/ml for 24 hours, then treated with $CaPO_4$ (Ca 2.7 mM, PO_4 2.0 mM) medium (CM) for up to 15 days. Cells were then analysed at various timepoints with PCR, western blot and stained with Alizarin Red S (ARS) stain to monitor calcium deposition and molecule expression.

5.2.2 *In Vivo* Study Design

This study was performed in the Psaltis laboratory within the Vascular Research Centre at SAHMRI. Samples were kindly made available for this assessment of calcification and inclusion in this thesis. Briefly, 8-week-old Apo $E^{-/-}$ mice were fed an atherogenic diet (SF 219-0012) for 4 weeks, then randomized to either saline or atorvastatin (~2 mg/kg) treatment via daily oral gavage in addition to an atherogenic diet for 12 weeks. Atorvastatin was dissolved incrementally in NaCl via vigorous vortexing. The solution was vortexed again immediately prior to gavage. Mice were weighed weekly and had a change of bedding twice per week. Blood was harvested for lipid analysis immediately prior to commencing the atherogenic diet (HFD). Upon completion of the HFD period, mice were humanely sacrificed via cardiac puncture. This study was approved by the South Australian Health and Medical Research Institute Animal Ethics Committee (SAM182).

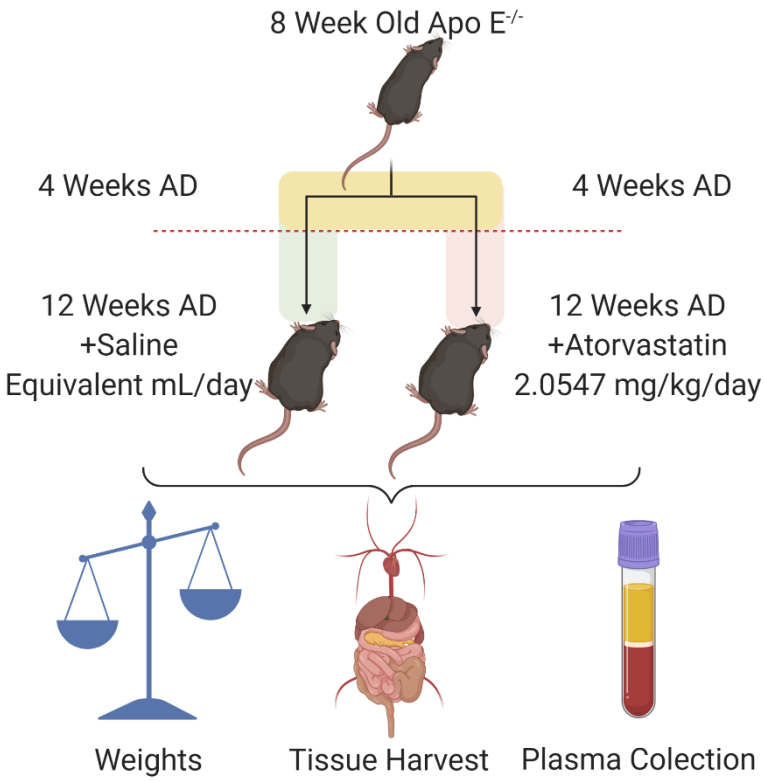

Figure 5.2.2.1 Atorvastatin study *in vivo* experimental timeline.

8-week-old Apo E$^{-/-}$ mice were fed an atherogenic diet (SF 219-0012) for 4 weeks, then randomized to either saline or atorvastatin (~2 mg/kg) treatment via daily oral gavage in addition to an atherogenic diet for 12 weeks. After the 16 week total feeding period, mice were humanely sacrificed via cardiac puncture. Valves and plasma were collected and used for experiments.

5.2.3 *Patient Study Outline and Design*

To study the role of Lp(a), a particularly atherogenic form of LDL, serum was collected from 64 patients with coronary artery disease (CAD). Male or female patients ≥18 years with CAD on a stable dose of statins (≥4 weeks) identified in outpatient clinics by RAH treating clinicians were invited to participate in this study. Volunteer samples selected were propensity matched to age and gender. Based on a previous study, we expected to see 50% normal (<0.5g/L), 40% high (0.5 g/L – 1 g/L) and 10% super high (>1 g/L) Lp(a) concentrations in this population. The Lp(a) concentrations were used as the categories to analyse differences between varying Lp(a) levels. This study was approved by the Central Adelaide Local Health Network Human Research Ethics Committee (CALHN HREC) and CALHN Research Governance, under the ethics number HREC/18/CALHN/111.

Table 5.2.3.1 List of eligibility criteria of clinical study.

Criteria	Eligibility
Gender and Age	Male or female aged over 18 years
Cardiovascular Health	Diagnosed coronary artery disease on stable statin dose for ≥4 weeks
General Health	No bleeding tendency or significant health problems
Pregnancy Status	Not currently pregnant or breastfeeding
Ability to Give Informed Consent	Good command of the English language and able to provide independent informed consent

Volunteers who satisfied the eligibility criteria then had a basic health assessment recorded, including the measurement of height, weight and blood pressure. 20mL of blood was withdrawn by venepuncture and transferred to heparin or Z serum clot activator coated tubes. Serum and plasma were collected via centrifugation at 1500 rcf for 15 minutes and stored at -80^{o}C until use. Serum and plasma sample aliquots were sent to Clinpath for lipid analysis.

5.2.3.1 Data Analysis and Statistics

A study with a cohort of similar demographics found that 38% of serum samples had an Lp(a) concentration ≥50 mg/dl[769]. Additionally, the interquartile range of these patients was 0.1 – 0.795 g/L and the mean was 0.53 (± 0.62) g/L Lp(a). From this, it is likely that approximately 10% of our cohort will have an Lp(a) plasma concentration of above 1 g/L. A cohort of 64 therefore has an expected yield of approximately 6 samples above 1 g/L Lp(a).

Data collected via blood sample analysis and questionnaires were analysed using the statistical methods detailed in methods chapter 2.14.

In Vitro Results

The role of LDL and oxLDL in VSMC calcification

5.3 Results

5.3.1 The Functional Effects of LDL and oxLDL on HAoSMC Calcification

In previous studies *in vitro*, oxLDL has stimulated human VSMC calcification using a co-culture of beta-glycerophosphate and oxLDL[741] which induces an osteogenic type differentiation. In this study, cells are stimulated with calcium phosphate (calcification medium; CM) to elicit a phenotype closely resembling what occurs in human CVD. Pre-treating HAoSMCs with LDL (1.0±0.0 vs 0.937±0.004, $p>0.99$) or oxLDL (1.0±0.0 vs 1.126±0.069, $p<0.2$) did not induce further calcification above the CM control (figure 5.3.1.1), however oxLDL significantly increased calcification above LDL (0.937±0.004 vs 1.126±0.069, $p=0.0295$).

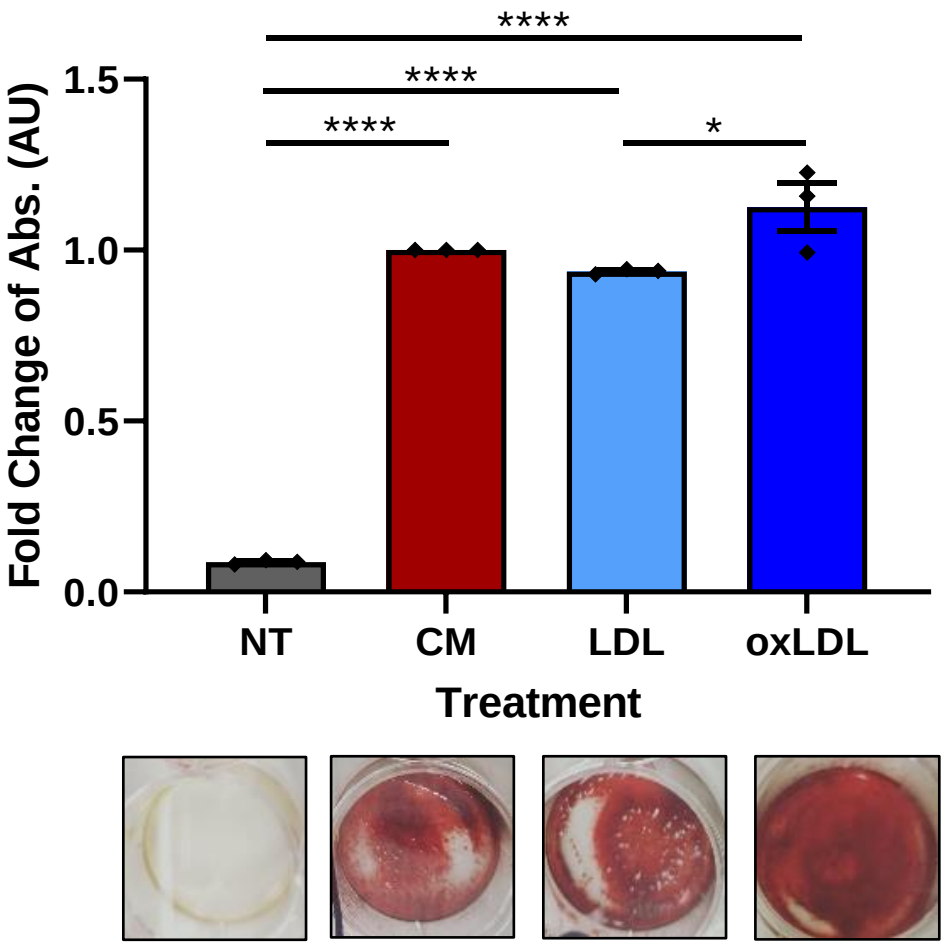

Figure 5.3.1.1 The effect of LDL and oxLDL on calcification.

*HAoSMCs were pre-treated with LDL or oxLDL (200 µg/ml) for 24 hours then treated with CM (Ca 2.7 mM, PO_4 2.0 mM) for 15 days. Calcification was measured by ARS assay with no treatment (NT) and CM and expressed as fold change from CM. Representative images of stain immediately prior to dissolving shown below graph. Data represented as mean± SEM, n=3. *p<0.05, ****p<0.0001 compared to all other treatments, ANOVA with Bonferroni's correction.*

5.3.2 The Effects of LDL and oxLDL on Calcification Gene Expression

While it is well established that oxidative stress has a role in VC[296-300], the early effects of oxLDL on HAoSMC calcification gene expression, in relation to native LDL remain unknown. After 24 hours of incubation with oxLDL, there was a significant reduction, compared to CM only, in mRNA expression of Runx2 (84.18±9.39 vs 19.04±4.99, p=0.0067), RANKL (205.2±8.08 vs 62.46±21.22, p=0.0005) and ALP (154.5±23.85 vs 28.76±19.11, p=0.024) pro-calcification markers. There were also reductions in the smooth muscle marker SMαActin (64.83±2.99 vs 32.78±5.44, p=0.0069) and anti-calcification marker OPG (124.6±21.91 vs 44.3±12.35, p=0.0147). In addition, oxLDL also reduced Runx2 and SMαActin mRNA expression when compared to NT (Runx2: 111.5±3.98 vs 19.04±4.99, p=0.0007; SMαActin: 103.4±0.32 vs 32.78±5.44, p<0.0001) and LDL (Runx2: 68.49±14.72 vs 19.04±4.99, p=0.033; SMαActin: 86.77±6.78 vs 32.78±5.44, p=0.0002) treatments. Furthermore, LDL significantly reduced RANKL mRNA expression compared to the CM control (205.2±8.08 vs 80.36±14.44, p=0.0012) (figure 5.3.2.1).

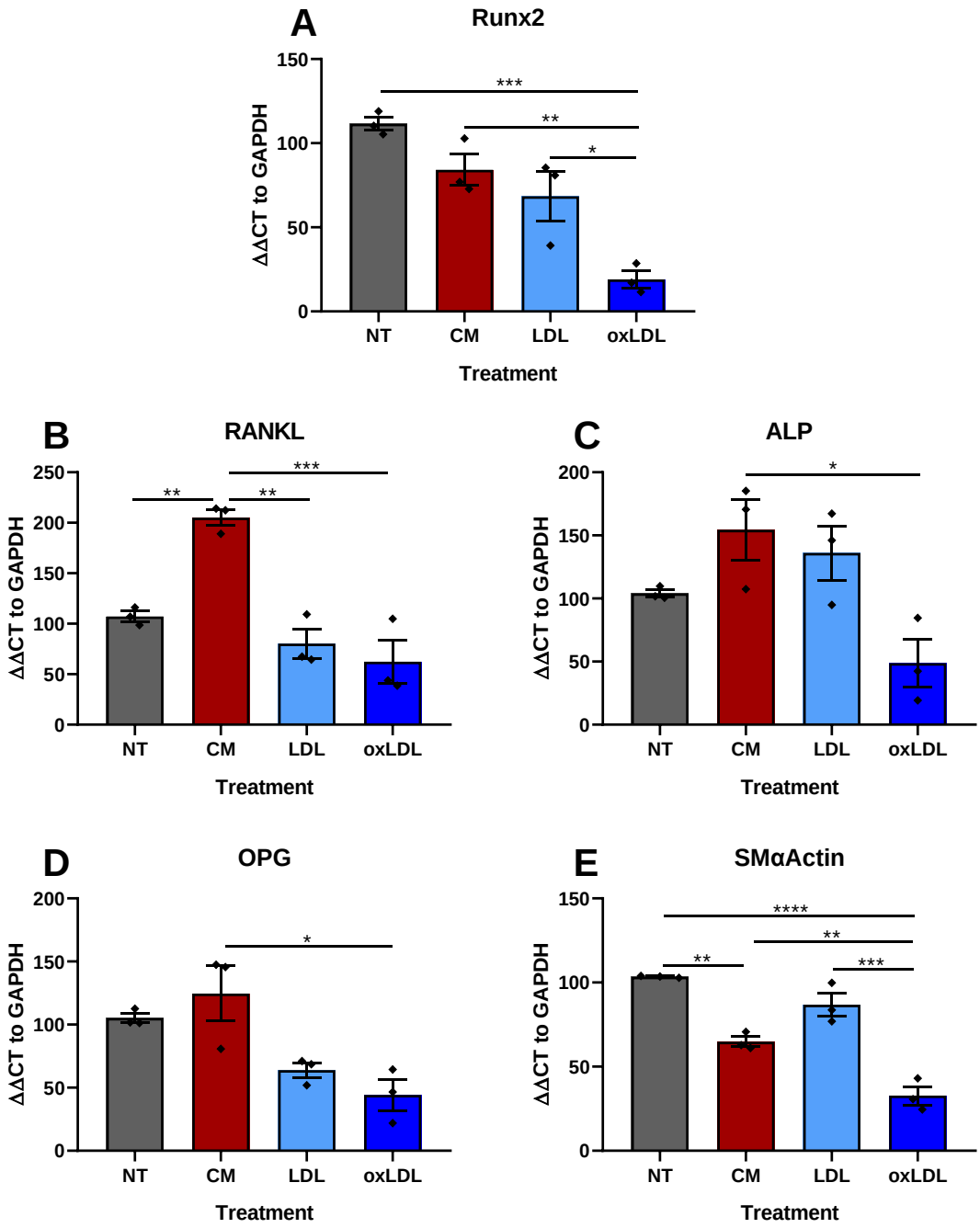

Figure 5.3.2.1 The effect of LDL and oxLDL on mRNA expression.

*HAoSMCs were treated with no treatment (NT), $CaPO_4$ (Ca 2.7 mM, PO_4 2.0 mM) medium (CM), LDL or oxLDL (200 µg/ml) for 24 hours. mRNA expression was measured by qPCR using GAPDH as the internal control. Data represented as % of NT, mean± SEM, n=3. *p<0.05, **p<0.01, ***p<0.001, ****p<0.0001, ANOVA with Bonferroni's correction*

5.3.3 The effects of LDL Pre-Treatment on Calcification Gene expression

After discovering an effect for oxLDL on the global reduction of calcification markers after 24 hours of treatment, the effect of LDL and oxLDL was assessed over 5 and 7 days of calcification. Pre-treating cells with either LDL or oxLDL resulted in no change in Runx2 expression when compared with the NT controls at either 5 or 7 days of calcification (Figure 5.3.3.1). After 7 days of calcification however both LDL (1440±269.5 vs 73.17±22.59, p=0.0006) and oxLDL (1440±269.5 vs 57.88±9.312, p=0.0005) significantly reduced Runx2 mRNA expression compared to the CM alone , back to the level of NT baseline (1440±269.5 vs 101.9±2.469, p=0.0007) . Also, after 7 days of calcification, LDL significantly lowered RANKL expression when compared to CM (NT vs CM: 113.1±3.81 vs 3174±714.0, p=0.006; NT vs LDL: 113.1±3.81 vs 978.9±418.1, p=0.042). There were no significant differences between any treatments at the 5 day timepoint (figure 5.3.3.1).

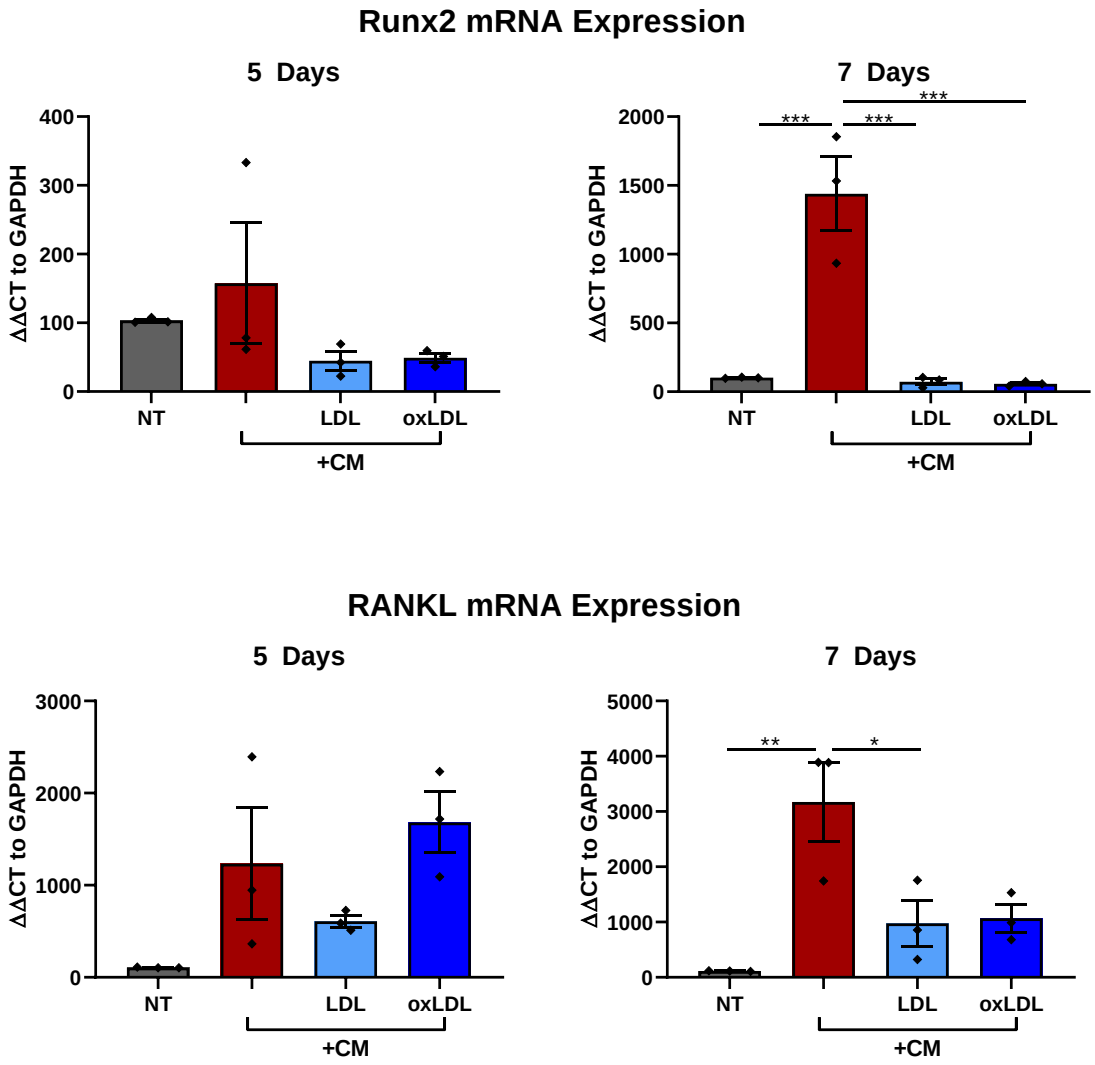

Figure 5.3.3.1 The effect of LDL and oxLDL on Runx2 and RANKL mRNA expression.

*HAoSMCs were pre-treated with LDL or oxLDL (200 µg/ml) for 24 hours then treated with $CaPO_4$ (Ca 2.7 mM, PO_4 2.0 mM) for 15 days. A no treatment (NT) baseline and a $CaPO_4$ medium alone positive control (CM) were used. Runx2 mRNA expression was measured by qPCR using GAPDH as the internal control. ***p<0.001 compared to all other treatments, ANOVA with Bonferroni's correction. Data represented as % of NT, mean± SEM, n=3.*

ALP mRNA levels are upregulated immediately prior to the mineral deposition in VC. After 7 days of calcification, LDL significantly lowered ALP expression back to the NT baseline when compared to cells treated with CM alone (CM vs LDL: 6286±1797 vs 1045±174.8, p=0.021). The same trend was observed for oxLDL (CM vs LDL: 6286±1797 vs 860.8±107.8, p=0.017). There were no other significant differences between LDL or oxLDL and the NT or CM controls at the 5 day timepoint (figure 5.3.3.2).

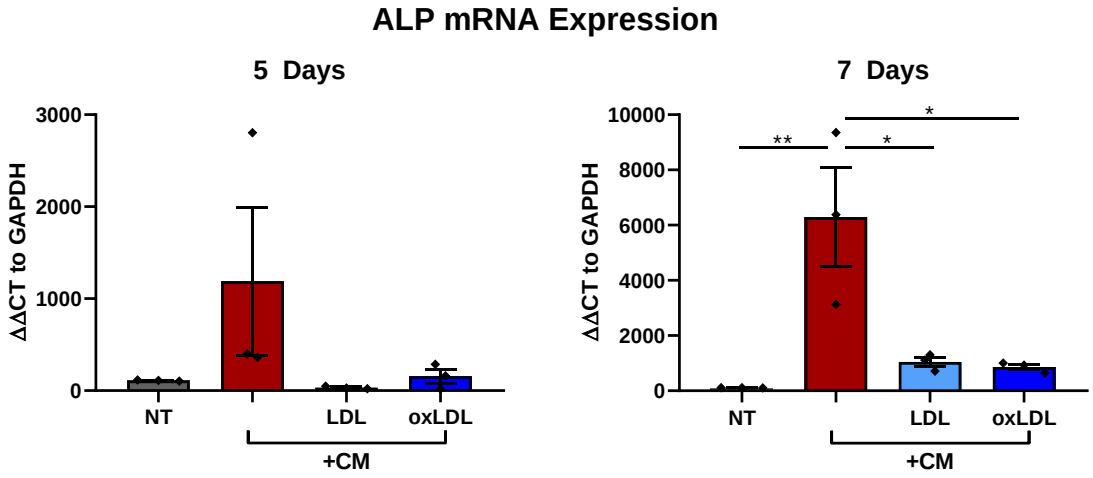

Figure 5.3.3.2 The effect of LDL and oxLDL on ALP mRNA expression.

*HAoSMCs were pre-treated with LDL or oxLDL (200 µg/ml) for 24 hours then treated with $CaPO_4$ (Ca 2.7 mM, PO_4 2.0 mM) for 15 days. A no treatment (NT) baseline and a $CaPO_4$ medium alone positive control (CM) were used. ALP mRNA expression was measured by qPCR using GAPDH as the internal control. *p<0.05, **p<0.01, ANOVA with Bonferroni's correction. Data represented as % of NT, mean± SEM, n=3.*

Next, we tested for the smooth muscle cell (SMC) marker, SMαActin to identify potential effects of LDL and oxLDL on cell type conservation. After 5 days of calcification, CM (103.1±0.5 vs 53.2±8.91, p=0.0168), LDL (103.1±0.5 vs 52.94±11.52, p=0.163) and oxLDL (103.1±0.5 vs 45.09±7.98, p=0.0068) treated cells had significantly lower SMαActin expression than the NT control. After 7 days of calcification, this effect persisted with CM (104.7±1.55 vs 17.45±3.26, p=0.0003), LDL (104.7±1.55 vs 47.6±14.36, p=0.0058) and oxLDL (104.7±1.55 vs 57.77±5.87, p=0.043) treated cells. Interestingly, oxLDL appeared to elevate levels of SMαActin in comparison to cells treated with CM alone (figure 5.3.3.3).

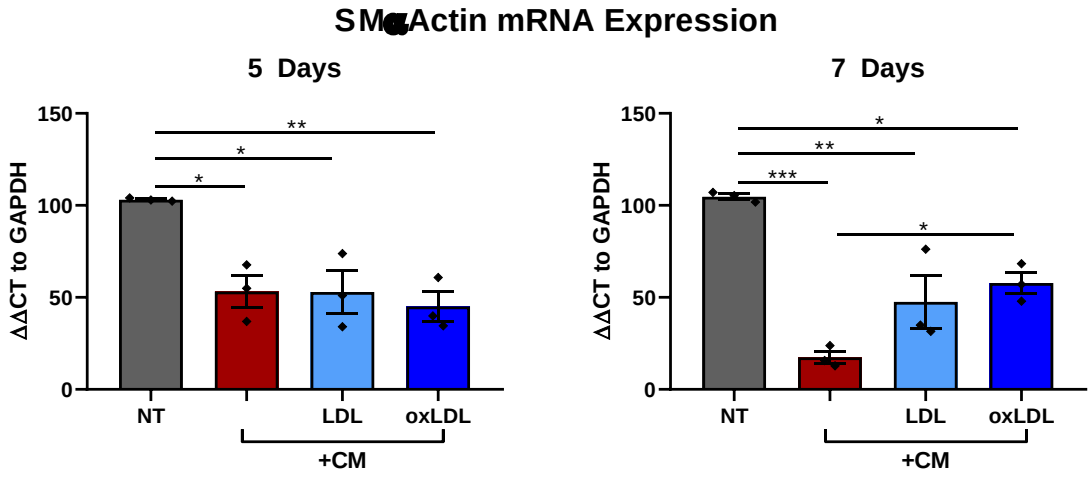

Figure 5.3.3.3 The effect of LDL and oxLDL on SMαActin expression.

*HAoSMCs were pre-treated with LDL or oxLDL (200 µg/ml) for 24 hours then treated with $CaPO_4$ (Ca 2.7 mM, PO_4 2.0 mM) for 15 days. A no treatment (NT) baseline and a $CaPO_4$ medium alone positive control (CM) were used. SMαActin mRNA expression was measured by qPCR using GAPDH as the internal control. *p<0.05, **p<0.01, ***p<0.001, ANOVA with Bonferroni's correction. Data represented as % of NT, mean± SEM, n=3.*

To test whether the cells were expressing anti calcification markers after treatment with LDL or oxLDL, OPG expression was examined. After 5 days of calcification, oxLDL significantly increased OPG mRNA expression above the CM control (53.89±30.84 vs 178.2±15.79, p=0.0086) and the LDL pre-treated cells (53.38±12.59 vs 178.2±15.79, p=0.0084). The same effect was observed after 7 days of calcification (CM vs oxLDL: 8.5±2.15 vs 116.8±27.77, p=0.0092; LDL vs oxLDL: 36.47±16.81 vs 116.8±27.77, p=0.0493) (figure 5.3.3.4) highlighting a potential compensatory effect of the cells in response to calcification.

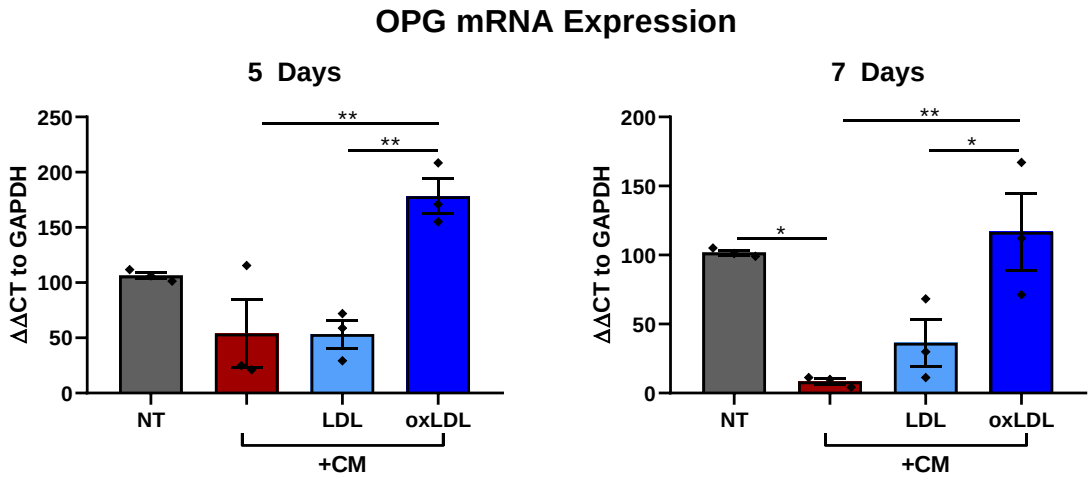

Figure 5.3.3.4 The effect of LDL and oxLDL on OPG expression.

*HAoSMCs were pre-treated with LDL or oxLDL (200 µg/ml) for 24 hours then treated with $CaPO_4$ (Ca 2.7 mM, PO_4 2.0 mM) for 15 days. A no treatment (NT) baseline and a $CaPO_4$ medium alone positive control (CM) were used. OPG mRNA expression was measured by qPCR using GAPDH as the internal control. *p<0.05, **p<0.01, ANOVA with Bonferroni's correction. Data represented as % of NT, mean± SEM, n=3.*

5.3.4 The effects of LDL on Calcification Protein Expression and Secretion

Based on the results presented in chapter 5.3.3 , that LDL and particularly oxLDL influence the expression of Runx2, RANKL, ALP and OPG mRNAs after 5 and 7 days of calcification, western blots, ELISAs and colorimetric assays were performed to identify whether the influence of these lipoproteins continued at the protein level. Although oxLDL appears to raise Runx2 protein expression after both 5 (A) and 7 (B) days of calcification, this effect was not significant. There were no significant differences between either LDL or oxLDL and NT or CM controls (figure 5.3.4.1). RANKL protein expression followed a similar pattern to that of the upstream Runx2 protein expression, with no effect (figure 5.3.4.1 C and D).

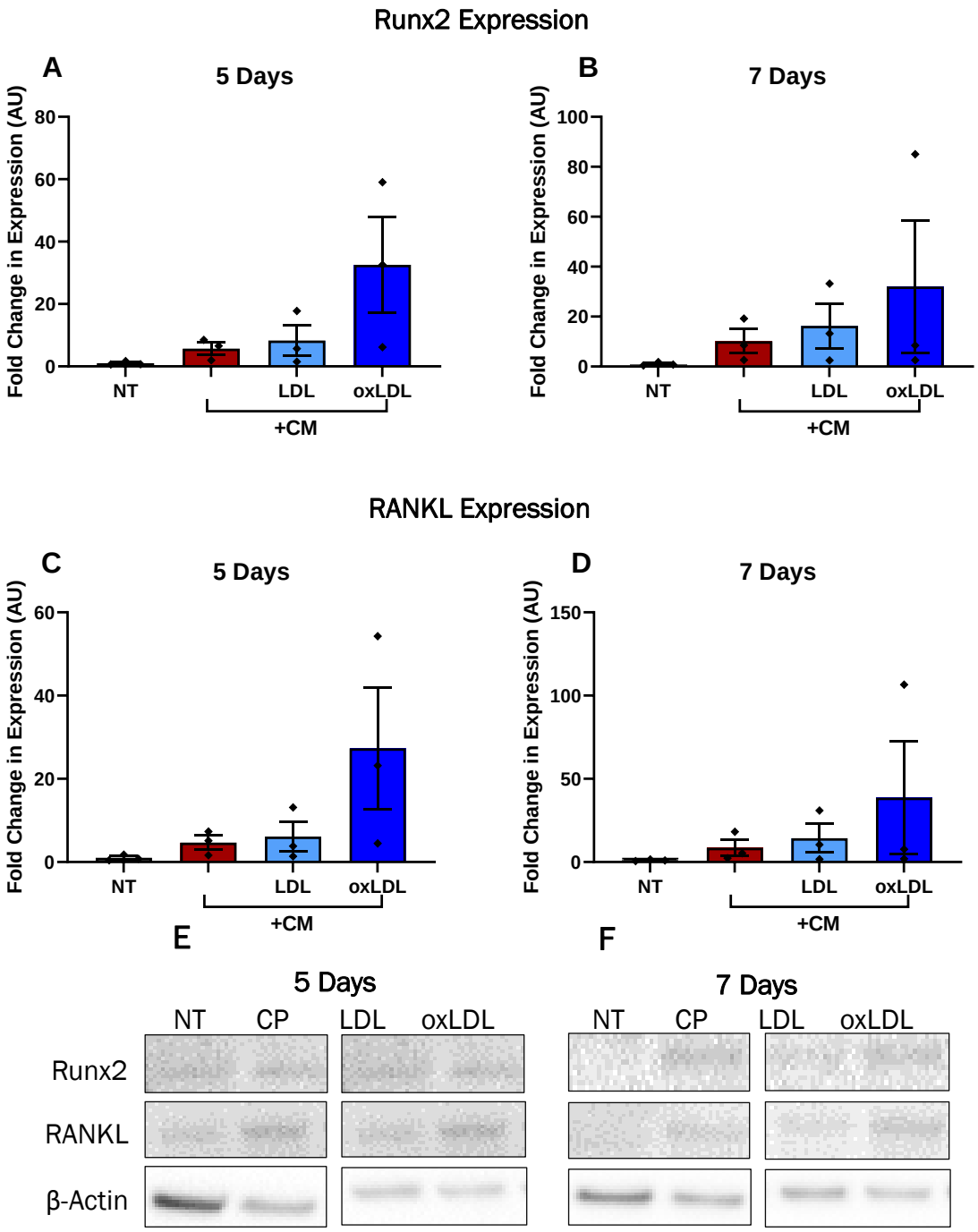

Figure 5.3.4.1 The effect of LDL and oxLDL on Runx2 and RANKL protein expression.

HAoSMCs were pre-treated with LDL or oxLDL (200 µg/ml) for 24 hours then treated with $CaPO_4$ (Ca 2.7 mM, PO_4 2.0 mM) for 15 days. A no treatment (NT) baseline and a $CaPO_4$ medium alone positive control (CM) were used. Runx2 protein expression was measured by western blotting using β-Actin and a standard sample as internal controls. ANOVA with Bonferroni's correction. Data represented as fold change of NT, mean± SEM, n=3.

As RANKL can also be secreted to have autocrine and paracrine functions, an ELISA was used to assess protein levels in culture media. After 5 days of calcification, both LDL and oxLDL significantly increased soluble RANKL when compared to the NT (LDL: 1.0±0.04 vs 1.27±0.03, p=0.0006; oxLDL: 1.0±0.04 vs 1.29±0.02, p=0.0004) and CM (0.86±0.02 vs 1.27±0.03, p<0.0001; oxLDL: 0.86±0.02 vs 1.29±0.02, p<0.0001) controls (figure 4.3.4.2 A). The same effect was observed at the 7 day (4.3.4.2 B) timepoint (NT vs LDL: 1.0±0.08 vs 1.38±0.06, p=0.0075; CM vs LDL: 1.07±0.03 vs 1.38±0.06, p=0.0237; NT vs oxLDL: 1.0±0.08 vs 1.35±0.04, p=0.0142; CM vs oxLDL: 1.07±0.03 vs 1.35±0.04, p=0.0477) (figure 5.3.4.2).

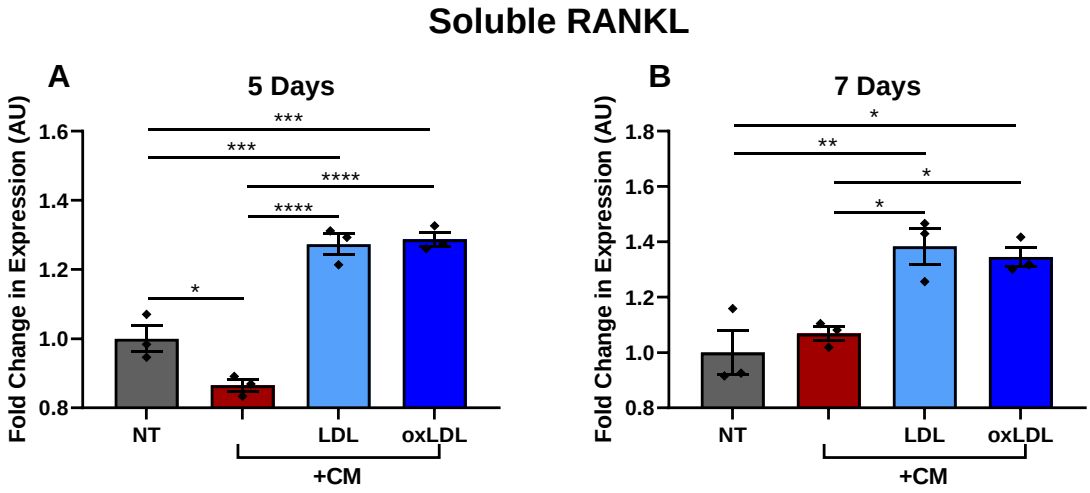

Figure 5.3.4.2 The effect of LDL and oxLDL on soluble RANKL.

*HAoSMCs were pre-treated with LDL or oxLDL (200 µg/ml) for 24 hours then treated with $CaPO_4$ (Ca 2.7 mM, PO_4 2.0 mM) for 15 days. A no treatment (NT) baseline and a $CaPO_4$ medium alone positive control (CM) were used. Soluble RANKL protein secretion was measured by ELISA using BCA measured total protein as a control. *p<0.05, **p<0.01, ***p<0.001, ****p<0.0001, ANOVA with Bonferroni's correction. Data represented as fold change of NT, mean± SEM, n=3.*

To assess the effect of LDL and oxLDL on OPG protein secretion an OPG ELISA was performed. Figure 5.3.4.3 shows no significant differences between treatment groups at the 5 day timepoint. However, after 7 days of calcification oxLDL pre-treated cells had secreted significantly less OPG than the NT control (1.0±0.06 vs 0.59±0.13, p=0.0359) (figure 5.3.4.3). Overall, the data presented here suggests a modest involvement of oxLDL in the initiation of VC, in contrast to the current literature[741-744] whereby oxLDL stimulates VSMC calcification.

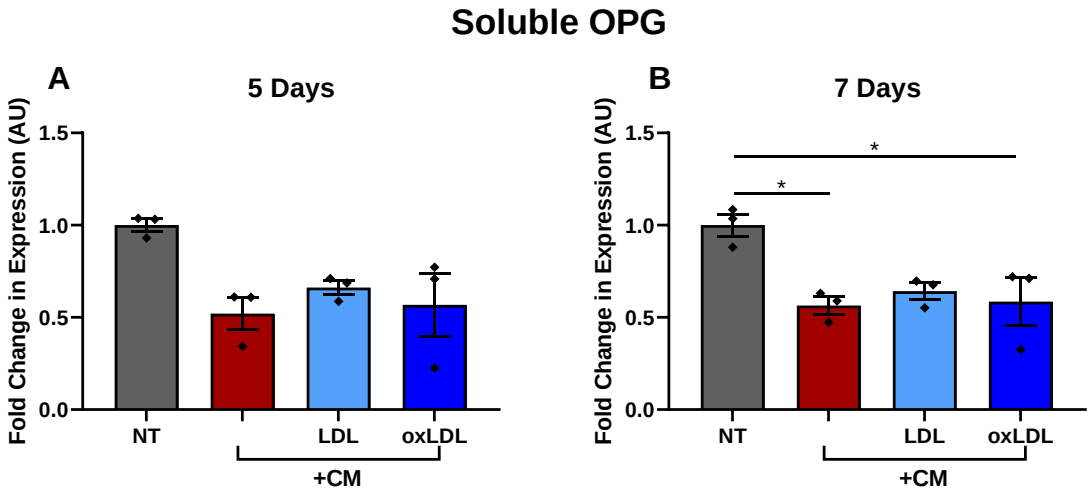

Figure 5.3.4.3 The effect of LDL and oxLDL on soluble OPG protein.

*HAoSMCs were pre-treated with LDL or oxLDL (200 µg/ml) for 24 hours then treated with $CaPO_4$ (Ca 2.7 mM, PO_4 2.0 mM) for 15 days. A no treatment (NT) baseline and a $CaPO_4$ medium alone positive control (CM) were used. Soluble OPG protein secretion was measured by ELISA and normalised to total protein. *p<0.05, ANOVA with Bonferroni's correction. Data represented as fold change of NT, mean± SEM, n=3.*

In Vivo Results

The role of atorvastatin treatment on early stage plaque calcification

5.3.5 The Effects of Statin Treatment on Apo $E^{-/-}$ Mouse Valvular Calcification

To study the effects of LDL lowering therapies on VC *in vivo*, we employed an atherosclerotic Apo $E^{-/-}$ mouse on an atherogenic diet treated with atorvastatin from the early stages of disease. The data from this study models what may happen in early, non-culprit plaques in patients taking statins. This *in vivo* mouse study was performed by Prof Psaltis and his team in collaboration with my supervisors. A portion of this study was made available for me for calcification analysis and this data is presented here.

Although atorvastatin has known cholesterol lowering effects in both humans and mice, the data presented in figure 5.3.5.1 A shows that in this particular mouse cohort there was no reduction (536.5±45.06 vs 439±59.48, p=0.2395). In addition to total cholesterol, neither triglyceride (figure 5.3.6.1 B) (464±40.26 vs 345.2±74.81, p=0.2141), ALP (figure 5.3.5.1 C) (2.89±0.71 vs 1.98±0.69, p=0.4091) nor circulating calcium (figure 5.3.5.1 D) (14.3±3.312 vs 8.95±2.98, p=0.2844) levels were significantly changed with atorvastatin treatment.

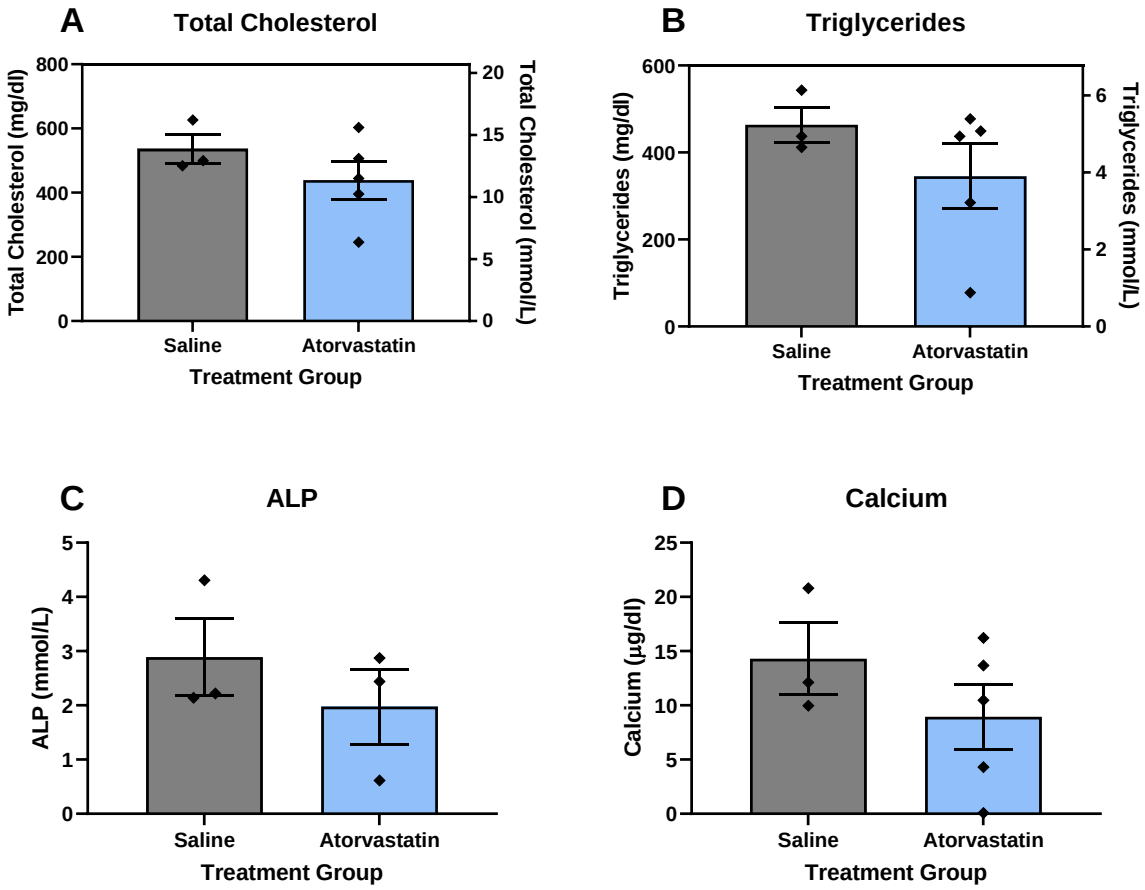

Figure 5.3.5.1 The effect of atorvastatin treatment on circulating lipids and calcification markers.

8 week old Apo E$^{-/-}$ mice were fed an atherogenic diet for 16 weeks and gavaged daily with atorvastatin (2.0547 mg/kg) during the final 10 weeks of the study. Blood plasma was harvested upon completion of the treatment period. Lipid markers and ALP were measured using WAKO colorimetric assays. Calcium was measured using the Cayman colorimetric assay. Mann Whitney test. Data represented as mean± SEM, n=3-5.

Although atorvastatin treatment appeared not to affect circulating lipids and calcification markers, when the aortic valves of these mice were examined atorvastatin was significantly associated with reduced plaque vascular calcification (3.15±1.76 vs 0.31±0.16%, $p<0.05$) (figure 5.3.5.2). This suggests either a role for lipoprotein associated cholesterol, or a pleiotropic effect of atorvastatin on vascular calcification.

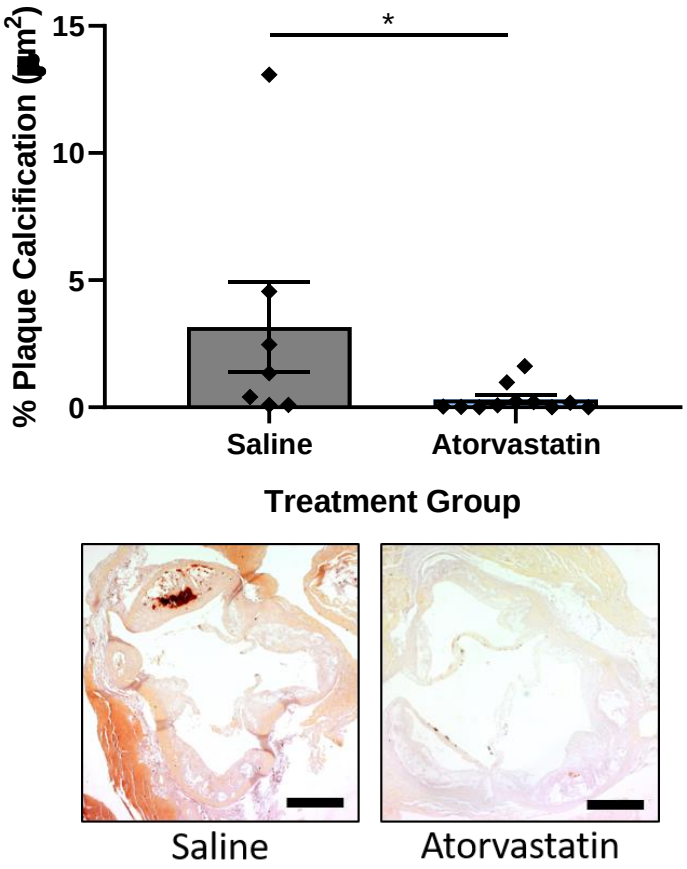

Figure 5.3.5.2 The effect of atorvastatin treatment on aortic valve calcification.

*8 week old Apo E$^{-/-}$ mice were fed an atherogenic diet for 16 weeks and gavaged daily with atorvastatin (2.0547 mg/kg) during the final 10 weeks of the study. Mouse aortic roots were formalin fixed, paraffin embedded and sliced at 5 μm thickness. Slides were stained with alizarin red s (ARS) stain, imaged using a Zeiss Axio Lab A.1 microscope with a Zeiss AxioCam ERc 5s camera and quantified using Image J software. *p<0.05, Mann-Whitney test. Data represented as mean± SEM, n=3.*

Correlations between plasma markers and vascular calcification were assessed and are presented in Figure 5.3.5.3 A. The data shows a significant positive correlation between total cholesterol and triglycerides (r=0.758, p=0.029), triglycerides and ALP (p=0.017), triglycerides and calcium (r=0.919, p=0.001) and ALP and calcium (r=0.97,p=0.001).

When examining the saline treated mice separately (figure 5.3.5.3 B), there was a strong, significant, positive correlation between triglyceride levels and circulating calcium (r=1.000, p=0.001). Atorvastatin mice, however, demonstrated positive correlations between calcium and both total cholesterol (r=0.969, p=0.007) and triglyceride (r=0.921, p=0.027) levels (figure 5.3.5.3 C).

This data presented in chapter 5.3.5 shows that atorvastatin, although having no effect on total cholesterol levels, significantly reduced aortic valve calcification in these mice. Furthermore, the correlation matrices suggest that while triglycerides and cholesterol correlates to circulating calcium in most cases, calcification was not correlated to any blood plasma markers in these mice. Interestingly, triglycerides correlated to circulating calcium in all groups.

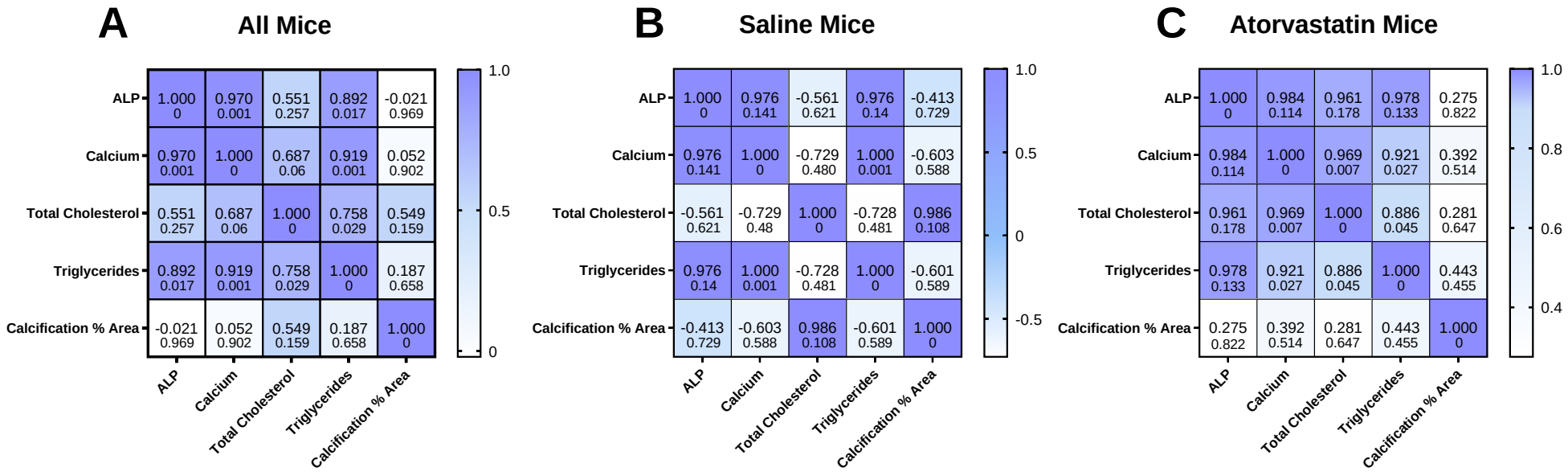

Figure 5.3.5.3 Correlations between calcification and circulating lipids or calcification markers in saline or atorvastatin treated mice.

Data on circulating lipids and calcification markers from figure 5.3.5.1 was correlated to the corresponding vascular calcification values presented in figure 5.3.5.2 using a correlation matrix to calculate Pearson's r values (top number) and p values (bottom number). n=3-8.

Ex Vivo Results

The role of Lp(a) concentration on VSMC calcification

5.3.6 The Effects of Human Plasma Lp(a) Level on Vascular Calcification Potential

Lp(a) has been strongly linked to increased cholesterol levels, vascular calcification and cardiovascular risk. Although it has recently been discovered that Lp(a) induces mRNA expression of Runx2, BMP-2 and IL-6 via the delivery of apo(a) attached oxidised phospholipids[764], there is currently no data demonstrating functional or mechanistic effects of Lp(a) on VC. In this chapter, the effects of elevated levels of Lp(a) in human serum was assessed for calcification potential *in vitro*.

Human serum samples containing different Lp(a) concentrations were obtained from outpatient clinics at the RAH. Donor samples were then selected from the entire cohort by propensity matching low (<0.5 g/L) Lp(a) samples to moderate (0.5 – 1 g/L) and high (>1 g/L) Lp(a) samples. In table 5.3.6.1, donor characteristics show a significant difference in incidence of type 2 diabetes mellitus (T2DM) ($p=0.035$) and Lp(a) ($p=0.0002$). Donors with T2DM were excluded from the study due to the known effects of glucose on VC. As such, upon further investigation there were no significant differences between the donor samples used in the study. As would be assumed, the samples in the high Lp(a) group had significantly higher Lp(a) levels than the entire cohort of samples used (1.57 ± 0.19 vs 0.44 ± 0.07, $p<0.01$) and the samples in the low Lp(a) group (1.57 ± 0.19 vs 0.14 ± 0.02, $p<0.001$).

Table 5.3.6.1 Donor characteristics for entire cohort and for samples used in the human Lp(a) study.

*Expressed as mean (±SEM) or incidence %. **p<0.01, ***p<0.001 when compared to the High Lp(a) group. (CAD) Coronary Artery Disease.*

	All Samples	Propensity Matched Samples			
	Lp(a) 0-3.0 g/L (Entire Cohort n=60)	Lp(a) <0.5 g/L (Low: n=11)	Lp(a) 0.5-1.0 g/L (Moderate: n=5)	Lp(a) >1 g/L (High: n=6)	p-value
Lp(a) (g/L)	0.44±0.07**	0.14±0.02***	0.67±0.08	1.57±0.19	**0.0002**
Age (Years)	63.73±1.61	62.36±3.54	56.4±3.56	61.5±6.18	**0.63**
Female (%)	21.67%	27.27%	20.00%	33.33%	**0.91**
BMI	29.61±0.94	26.48±2.88	29.92±2.19	27.62±2.38	**0.74**
Diabetes Mellitus (%)	30.51%	0%	0%	0%	**0.035**
CAD (%)	98.31%	100%	100%	100%	**0.94**
Hyperlipidemic (%)	64.41%	72.72%	100%	50%	**0.31**
Hypertension (%)	59.32%	63.63%	80%	50%	**0.77**

To assess calcification potential, serum from the low, moderate and high Lp(a) groups were added to HAoSMCs. Serum samples were added at a concentration of 10% final volume in HAoSMC media and applied to cells for 24 hours, before undergoing 15 days of calcification treatment. Figure 5.3.6.1 shows that the total Lp(a) concentration of the donor serum pre-treatments did not significantly affect the calcification potential of HAoSMCs.

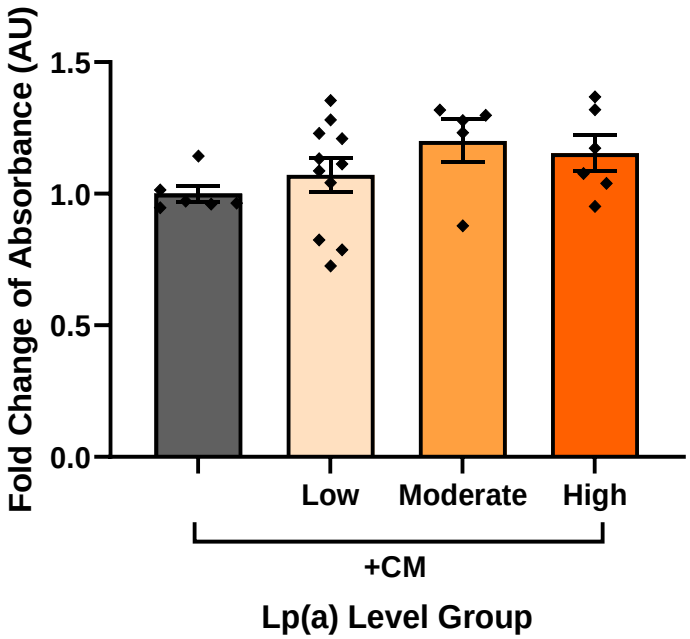

Figure 5.3.6.1 The effect of human serum Lp(a) concentration on calcification.

HAoSMCs were pre-treated with human serum (10%) for 24 hours then treated with $CaPO_4$ (Ca 2.7 mM, PO_4 2.0 mM) for 15 days. Calcification was measured by ARS assay with a $CaPO_4$ medium alone (CM) control and expressed as fold change from CM. Kruskal-Wallis test with Dunn's multiple comparisons test. Data represented as mean± SEM, n=5-11.

To follow up, donor serum was serially diluted prior to applying to cells in order to control for potential isoform differences. The isoform of Lp(a) refers to the length of the attached apo(a), whereby small isoforms (as seen in high Lp(a) levels) bind easier to cells. High Lp(a) donor serum samples were serially diluted with media to final Lp(a) concentrations of 0.5, 0.25, 0.125 and 0.0625 g/L and applied to cells for 24 hours, before undergoing 15 days of calcification. Figure 5.3.6.2 A shows that when analysed together, there was no significant difference between pre-treatment with any concentration of Lp(a) and calcification medium alone (CM). Furthermore, figure 5.3.6.2 B shows that there was no significant trend between donors when observing the average of all donors. Although donor 5 had a significant negative correlation between calcification and Lp(a) concentration (r^2=0.91, p=0.046), there were no other significant correlations observed for individual donors. A significant difference between slopes was observed (p=0.048), showing that there was a differential effect of Lp(a) concentration within each sample on VC.

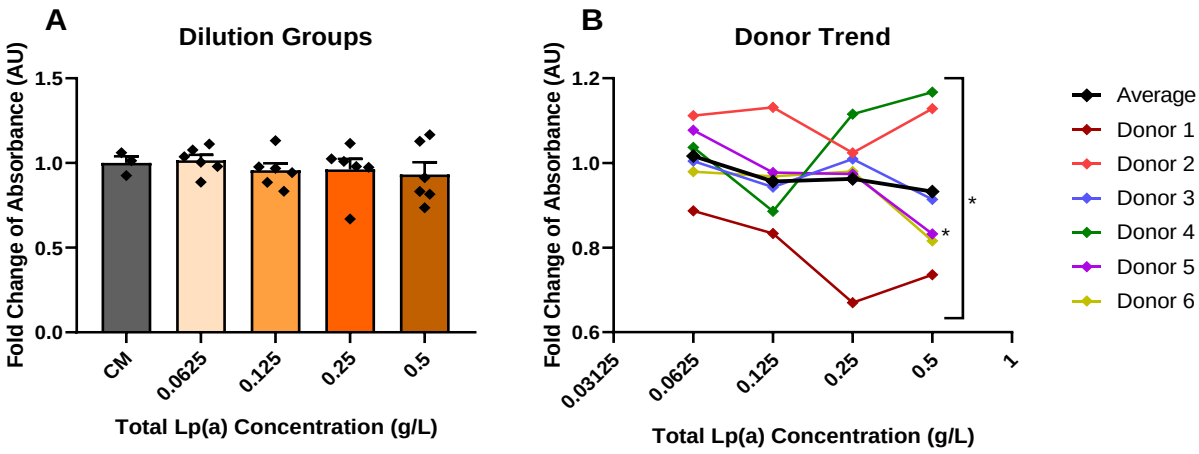

Figure 5.3.6.2 The effect of serially diluted human serum Lp(a) concentration on calcification.

*HAoSMCs were pre-treated with serial dilutions of donor serum for 24 hours then treated with $CaPO_4$ (Ca 2.7 mM, PO_4 2.0 mM) for 15 days. Calcification was measured by ARS assay with a $CaPO_4$ medium alone (CM) controls and expressed as fold change from CM. A: ANOVA with Bonferroni's correction, data represented as mean± SEM, n=6 forma samples and 3 for control (CM). B: Linear regression, data represented as exact values. *p<0.05.*

To test whether there were effects of Lp(a) levels on circulating calcification factors, calcium and ALP levels were measured in the donor serum via colorimetric assays. Human serum Lp(a) concentration had no significant effect on circulating calcium or ALP levels (figure 5.3.6.3), corresponding with the ARS data presented in figure 5.3.6.1 and 5.3.6.2.

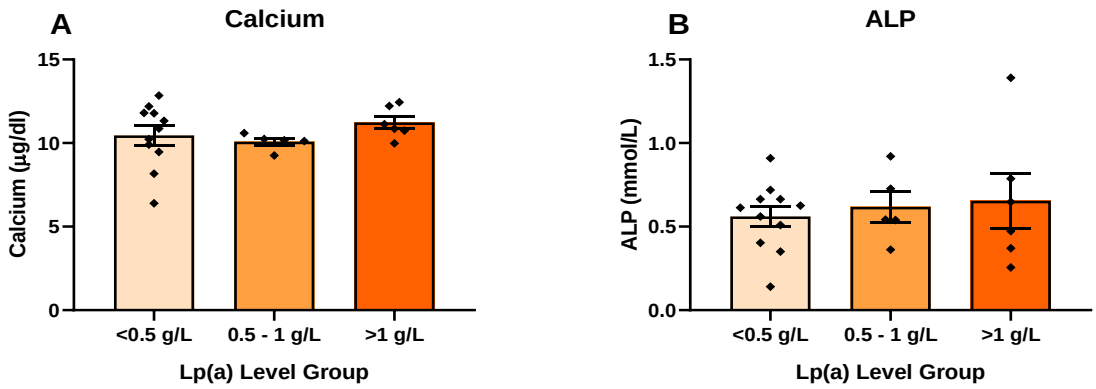

Figure 5.3.6.3 The effect of human serum Lp(a) levels on human serum calcification marker levels.

Serum at various Lp(a) levels was tested using either the Wako ALP assay or the Cayman calcium assay as per protocol. ANOVA. Data represented as mean± SEM, n=5-11.

To fully assess the relationships between Lp(a) levels and the markers assessed here a correlation matrix using data from all Lp(a) level groups was calculated. There were no significant correlations between Lp(a), calcification, calcium or ALP levels (figure 5.3.6.4).

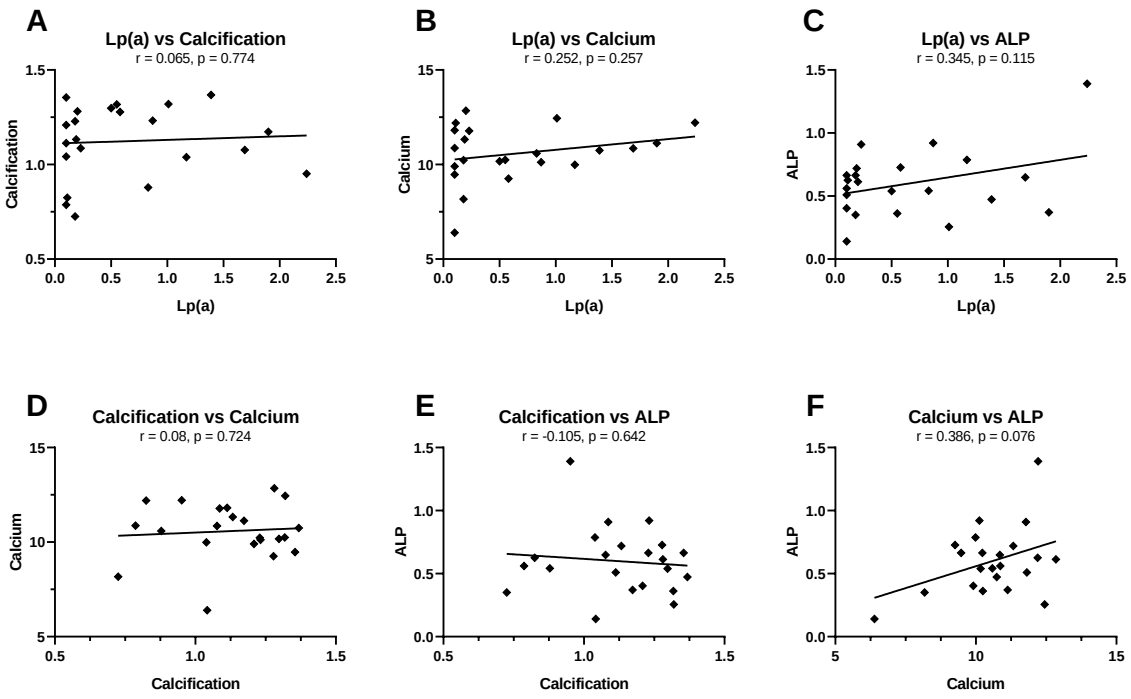

Figure 5.3.6.4 Correlation matrix between vascular calcification and serum Lp(a), calcium or ALP levels in the Lp(a) human serum study.

Data from figures 5.3.6.1 and 5.3.6.3 were compared to investigate correlations between serum calcium, serum ALP, Lp(a) level and VSMC calcification potential. Pearson's Correlations. n=22.

To further assess these relationships, correlations were performed between the specific Lp(a) cohorts, calcification, calcium and ALP levels. Figure 5.3.6.5 A shows a significant positive correlation between calcium and ALP levels in donors with low Lp(a) levels ($r = 0.745$, $p = 0.009$), however in donors with moderate and high Lp(a) levels (figure 5.3.6.5 B and C) this correlation between circulating calcification factors was lost. In the high Lp(a) level cohort (figure 5.3.6.5 C) there was a significant negative correlation between calcification and ALP levels ($r = -0.822$, $p = 0.045$). In samples with moderate Lp(a) levels there were no significant correlations between Lp(a) level, calcification, serum calcium or serum ALP levels (figure 5.3.6.6). In the high Lp(a) (>1g/L) serum level cohort however, we observed a significant negative correlation between serum ALP levels and VSMC calcification ($r=-0.822$, $p=0.045$). There were no other significant correlations between Lp(a) level, calcification, serum calcium or serum ALP levels in donors with high Lp(a) levels (figure 5.3.6.7).

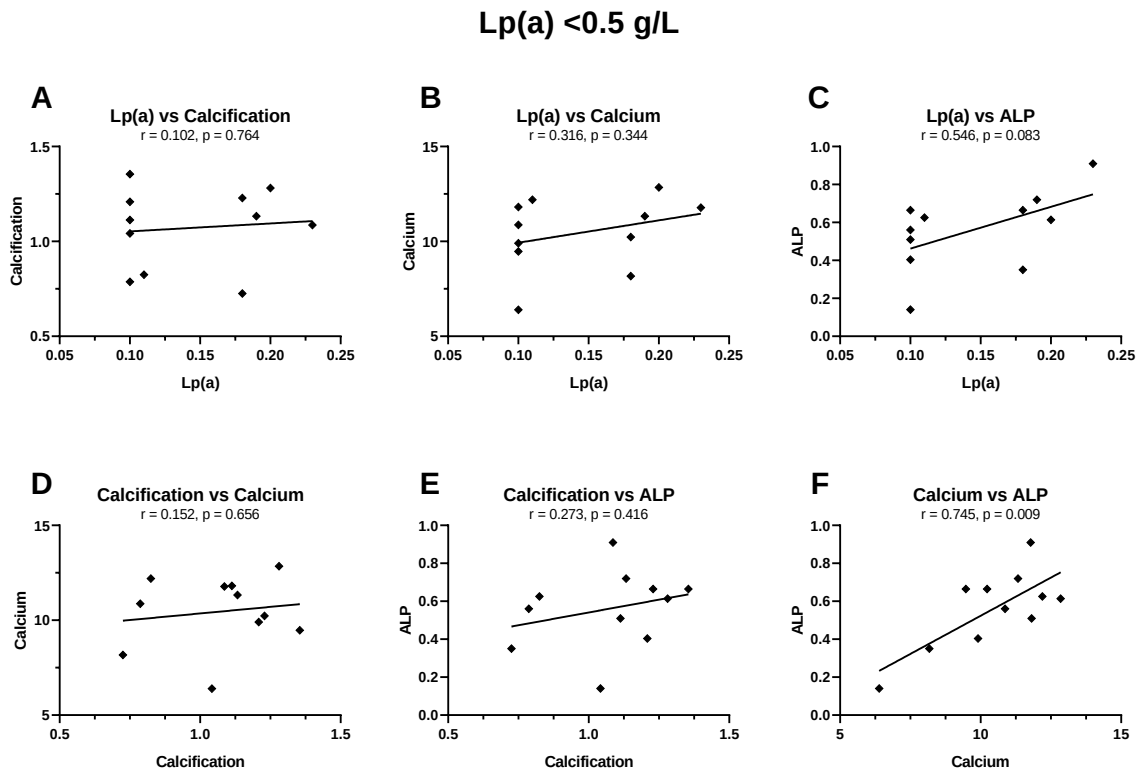

Figure 5.3.6.5 Correlation matrix between vascular calcification and low serum Lp(a), calcium or ALP levels in the Lp(a) human serum study.

Data from figures 5.3.6.1 and 5.3.6.3 were compared to investigate correlations between serum calcium, serum ALP, low Lp(a) levels and VSMC calcification potential. Pearson's Correlations. n=11.

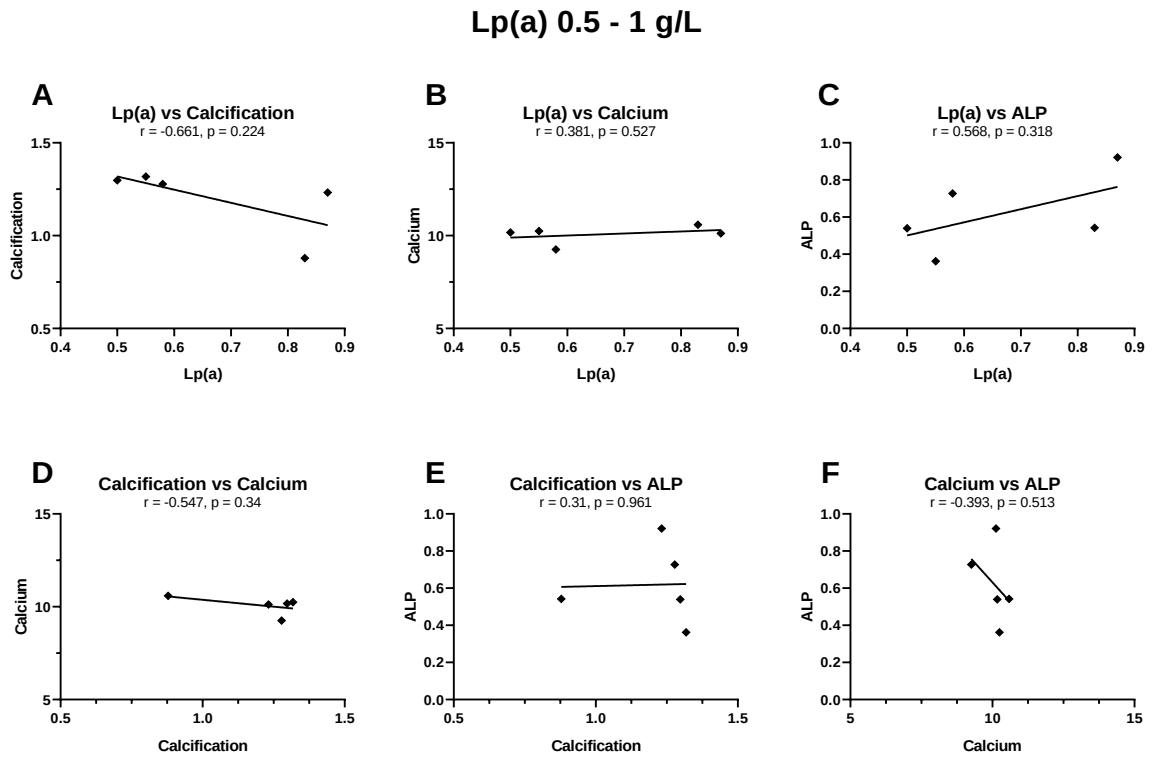

Figure 5.3.6.6 Correlation matrix between vascular calcification and moderate serum Lp(a), calcium or ALP levels in the Lp(a) human serum study.

Data from figures 5.3.6.1 and 5.3.6.3 were compared to investigate correlations between serum calcium, serum ALP, moderate Lp(a) levels and VSMC calcification potential. Pearson's Correlations. n=5.

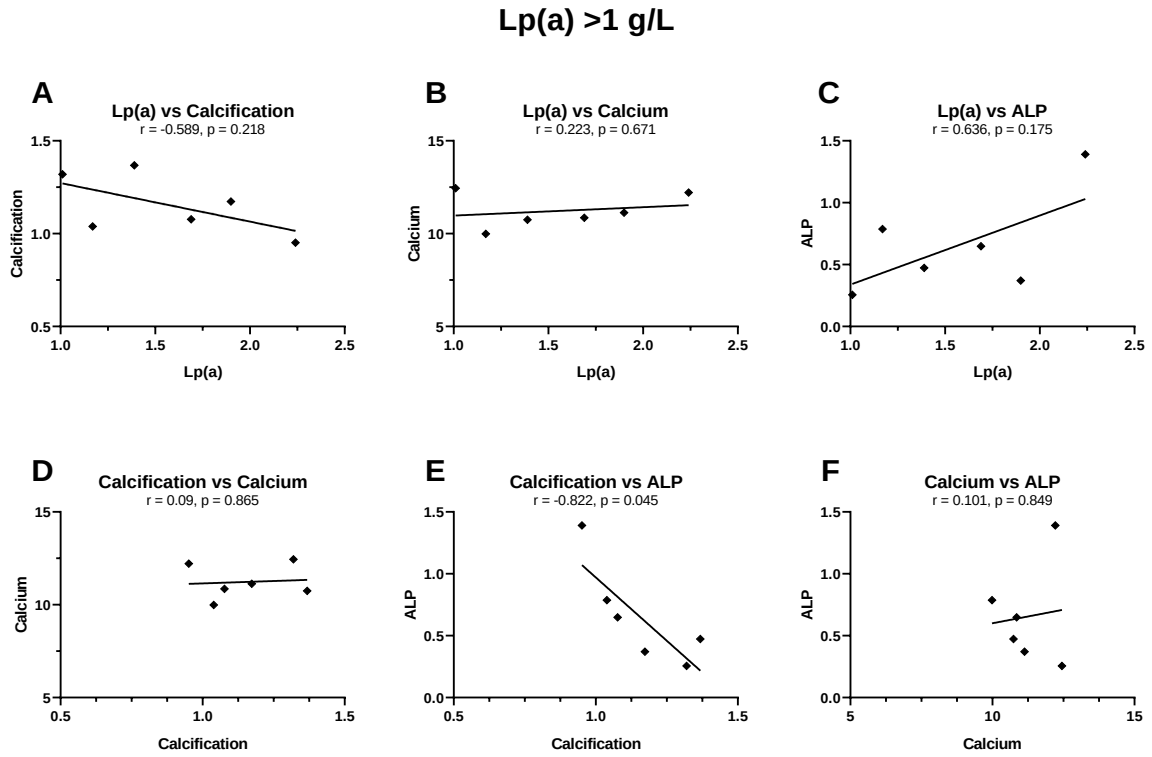

Figure 5.3.6.7 Correlation matrix between vascular calcification and high serum Lp(a), calcium or ALP levels in the Lp(a) human serum study.

Data from figures 5.3.6.1 and 5.3.6.3 were compared to investigate correlations between serum calcium, serum ALP, high Lp(a) levels and VSMC calcification potential. Pearson's Correlations. n=6.

5.4 Discussion

This study compares the effects of LDL, its variants on vascular calcification and known calcification regulators over time *in vitro*, *in vivo* and *ex vivo*. The data suggests that the oxidation status of LDL particles, in conjunction with the stage of plaque assessed, are important factors when investigating the roles of LDL, Lp(a) and their lowering therapeutics on VC.

The *in vitro* data demonstrates that oxLDL significantly increases VSMC calcification above that of LDL, but not the CM control. Although the gene expression data shows results conflicting with the mild increase in calcification gene by oxLDL pre-treatment, the protein secretion of RANKL was significantly increased by oxLDL pre-treatment. Furthermore, the *in vitro* data presented here does not fully align with the current literature on oxLDL and VC, but it also doesn't show the expected effects from oxidative stress alone, whereby oxidation is a VC progressor and initiator through the RANKL pathway[770].

Although this study focused on the Runx2, RANKL, OPG pathway, other pathways of calcification exist, such as BMP-2 regulation[744]. BMP-2 and Runx2 are considered the master regulators of VC, whereby increased expression of either molecule suggests early differentiation into osteoblast-like cells. BMP-2 itself has also been shown to reduce oxLDL induced endothelial ROS secretion, and even inhibit HEPG2 apo B100 secretion to altogether reduce plaque volume and VC[340]. Future studies will therefore require RANKL or Runx2 inhibition, in conjunction with BMP-2 expression analysis, to investigate the importance of this pathway regarding oxLDL induced VC.

Interestingly, VSMC secreted RANKL during the calcification process causes migration and differentiation of macrophages into osteoclast-like cells[367]. As VSMCs are highly plastic and can transdifferentiate into macrophage-like cells after cholesterol loading in an atherosclerotic setting themselves[771], investigating the roles of these cell types would be

beneficial. The same focus can be applied in animal models. While it is now established that M1 and M2 type macrophages play roles in both micro and macro calcifications[747], information on the underlying molecular pathways, and how they are modulated with oxLDL particles, could provide opportunities for local VC targets.

Atorvastatin, an LDL lowering agent, has been shown to disrupt macrophage Rac1 regulation, leading to increased calcification[748], however, in murine models of atherosclerotic calcification – statins in general have had varied results. Atorvastatin has been shown to increase valve calcification[748], or have no effect[772], whereas simvastatin reduced the frequency of calcification in the brachiocephalic artery[773] and calcification area in the aorta[774]. Furthermore, *in vitro* statins have inhibited VC[308, 775-778] via restoration of the Gas6-Axl apoptosis survival pathway[775] and by decreasing lipogenesis[308].

In contrast, statin administration in humans significantly promotes calcification[285] which is hypothesised to be a plaque stabilising effect. Results from this study found a significant reduction in plaque calcification following statin treatment, regardless of the lack of lipid lowering effect, or any decreases in circulating calcium and ALP. Although the difference in results could be contributed to differences in vivarium, species, statin used and method of calcification, the discord between the effects of statins *in vitro*, *in vivo* and in clinical trials requires further investigation in a standardised manner.

Although the overall result of the *in vivo* statin study was that atorvastatin reduced valve calcification despite no change in blood plasma markers, limited numbers were available for plasma measurements giving an indication of what may be happening in a larger population. Interestingly, the trend for total cholesterol, triglyceride, ALP and calcium levels were all suggestive of a lowering effect of atorvastatin treatment. Given that this is a murine study, larger n values would be needed to make any sound conclusions.

The reduction in aortic valve calcification however in the atorvastatin treated mice conflicts with previous literature where atorvastatin increased arterial calcification *in vivo*[748].Additionally it does not correspond with clinical trial evidence[285], but supports *in vivo* mouse[779] and rabbit[780] studies that showed an inhibition of valvular calcification and *in vitro* literature showing an inhibition of calcification induction *in vitro*[775-778]. Conversely, atorvastatin has been found to dose dependently raise *in vitro* calcification[749], further showcasing the varied nature and results in VSMC calcification research.

In this study, mice were gavaged with somewhat precise doses of atorvastatin daily, as opposed to ad libitum atorvastatin containing high fat diet. Additionally, although the dose of ~2mg/ml mg/kg/day atorvastatin per day is around 10x higher than the diet administered doses (predicted ingestion of 0.15[773] - 0.18[748] mg/kg/day), it is drastically lower than other gavage studies which administered 100 mg/kg 6/7 days per week[774]. To date, there are no studies examining a dose dependant effect of statins on VC *in vivo*.

This study however has reduced experimental power, arising from the unavailability of mice for correlative analysis. As these studies were a secondary outcome from the study, these experiments were not prioritised for available plasma. Although this renders the correlative data presented as speculative, rather than indicative, the results still warrant further investigation. These future studies will need to be appropriately powered and, ideally, matched with *in vitro* and human data to comprehensively investigate the use of and mechanisms behind atorvastatin modulated VC.

As discussed earlier, Lp(a) is another, individual human lipoprotein similar to LDL but with an attached apo (a), that genetically predisposes an individual's susceptibility to CVD. Because of Lp(a)'s clear link to atherosclerotic development and emerging link to VC, we sought to identify a functional role for Lp(a) in VC. Unfortunately, the generation of mice with elevated Lp(a), or even any Lp(a), is a possible but complicated process which may

not even yield meaningful data, due to natural differences between human and mouse lipoprotein and cardiovascular systems. We therefore investigated the link between Lp(a) and VC using human serum and calcifying human VSMCs.

The current literature examining the *ex vivo* roles of Lp(a) in VC suggests that Lp(a) plays a causal role in VC via the delivery of oxidised phospholipids to the artery wall. This interaction then upregulates Runx2 and BMP-2 mRNA expression, in valvular interstitial cells[764]. Although this study found an upregulation of Runx2 and BMP-2, they did not conduct any functional calcification assays, or examine additional timepoints beyond 3 days. Additionally, they used concentrated (to 1 g/L), isolated Lp(a), free from the influence of other serum factors, separated from healthy patients with <0.5 g/L Lp(a). The serum used here was from patients with CAD and has not had Lp(a) concentrated or isolated, thus providing a snapshot of the total serum effects on VC, as opposed to a concentrated, isolated effect of the Lp(a) itself. Furthermore, both experimental designs do not consider isoform variation and can be referred to most accurately as 'small sample pilot data'. It is also important to remember that serum components, such as feutin-a[539, 781, 782], inhibit VC *in vitro*, therefore using diluted whole serum is not ideal but benefits a more realistic *in vitro* modelling of complex *in situ* interactions with VSMCs.

Considering the strong correlations between Lp(a) and VC in the clinical trial data[120, 760, 761], together with the initial findings that isolated Lp(a) causes osteoblastic differentiation[764], the results here highlight the complex nature of Lp(a)'s involvement in VC and the need for more precise experimentation in this field. While we found no induction of VSMC calcification following varying Lp(a) concentrations there was a significant correlation between ALP and Lp(a) levels in the cohort of patients with <1 g/L plasma Lp(a). In patients with high levels of Lp(a), ALP was negatively correlated to VSMC calcification despite having similar levels of ALP to other groups. This indicates a

potentially interesting and targetable interaction between small Lp(a) isoforms and ALP production or liberation from the bone for future studies. Before the continuation of these studies however, it is worth strengthening the current study by increasing n values, looking at differences between whole serum and isolated Lp(a) and including isoform analysis, as isoform plays an important role in the atherogenicity of the particle.

As Lp(a) is an oxidative molecule scavenger, it is unsurprising that a previous study showed a role for Lp(a) in calcification[764]. This supports the data from this study and others where VSMC calcification was increased following oxLDL pre-treatment, showing a stimulatory role of oxidative stress in VC[296-300]. It is surprising then that the Lp(a) study in this chapter produced no significant changes or correlations between Lp(a) levels, calcification or serum markers. This suggests that there might be a more isoform focused relationship between Lp(a).

The same ethos can be applied to the small cohort atorvastatin *in vivo* study, whereby conflicting literature presents difficulties for finding meaningful trends in their roles in VC. Particularly for *in vivo* studies, opportunities to replicate the treatment process for early, mid and late stages of atherosclerosis or calcification are available. Here we present that in the early stages of atorvastatin treatment, in conjunction with mild, non-significant lipid lowering, there is a significant inhibition of valvular calcification development. As atorvastatin has been previously shown to downregulate BMP-2 expression caused by oxLDL[783], in future studies, it would be interesting to investigate the oxidation status of the plasma and plaques of these mice, or in clinical trials.

Although statins have not been shown to lower Lp(a) levels in clinical trials[765] and their Lp(a) raising properties are hotly debated[766-768], it would also be interesting to examine any pleiotropic effects of statins in the inhibition or stimulation of Lp(a) induced calcification. Additionally, investigating the effects of Lp(a) lowering therapeutics such as

PCSK9 inhibitors[784-786] or fibrates[787] could also provide interesting data on potential VC treatments. Already, PCSK9 and elevated Lp(a) levels have been associated with increased CAC scores[788] and combination therapies including statins and PCSK9 inhibitors were identified to slow the progression of calcification[789].

In conclusion, the data from this chapter suggests that the role of LDL in VC is due to the readily oxidised nature of LDL and its lipoprotein sibling Lp(a). While it appears that statins reduce calcification in the early stages of disease *in vivo*, supporting the 'statins stabilise as well as reduce plaques' hypothesis, the literature on statin research *in vivo* and *in vitro* has conflicting results. Moving forward with VC research into LDL, Lp(a) and their lowering therapeutic agents, a standard testing format, considering the stage of plaque, oxidation status, multiple molecular pathways (i.e. Runx2 and BMP-2), apo(a) isoform and other serum components (such as fetuin-a) should be considered.

6 : Chapter Six

Investigating the role of high-density lipoproteins on vascular calcification

6.1 Introduction

Despite the fact the HDL has been identified to play a significant role in atherosclerosis, as discussed in chapter 1, we only know a small amount on its potential role in vascular calcification (VC), despite growing evidence that HDL influences its development. Patients with calcific valvular stenosis have less Apo AI in the valve and the Apo AI that is present is found to co-localise with areas of calcification and osteoprotegerin (OPG), potentially interfering with the mechanisms of valvular calcification[790]. Additionally, epicardial fat expression of osteopontin[791], a protein which prevents calcium crystal growth and induces cellular mineral resorption[792], and osteoprotegerin (OPG) is associated with certain HDL subclasses[791]. Moreover, while smaller HDLs are associated with less coronary artery calcification[793], dysfunctional oxHDL levels are independently associated with valvular calcification[794].

As HDL raising therapeutics may only be raising levels of the dysfunctional HDLs observed in CAD patients[86], current HDL therapeutics are focused on HDL mimetic or reconstituted HDL (rHDL) infusions. Although early clinical trials demonstrated plaque regression[85], there is no information on the influence of HDL mimetic therapy on the status of VC or stability within these plaques. In rabbits however, incorporation of Apo AI-Milano in a HDL mimetic demonstrated an inhibitory effect on both aortic plaque and calcification in an atherosclerotic rabbit model[657, 795].

The first *in vitro* study examining the direct influence of HDL on calcification identified HDL as an inhibitor of ALP expression in calcification prone VSMCs[796]. This was followed by the demonstration that modified HDL by oxidation reduced its favourable effects on inflammation, oxidative stress and cholesterol efflux[797]. It is therefore possible that dysfunctional HDL may have a deleterious effect on inflammatory-induced

microcalcification. The observation that HDL subspecies differentially associates with the presence or absence of VC may further reflect the impact of HDL functionality[100].

Given that similar mechanisms underscore both VC and bone formation and that HDL mediated cholesterol efflux from pre-osteoclasts inhibits their maturation, stimulates their apoptosis and inhibits osteoblast RANKL expression[798], we hypothesised that HDL would have similar effects in the vessel wall. Here in chapter 6, we present *in vitro* experiments examining the role of HDL, oxHDL, rHDL and oxrHDL in calcification of human aortic smooth muscle cells (HAoSMCs). In continuing our investigations into the role of HDLs in VC, we infused atherosclerotic prone mice with rHDL and also assessed the calcification potential of serum from patients receiving an HDL mimetic as part of a clinical trial (CARAT). We hypothesised that functional HDLs would lead to a stabilisation phenotype, by increasing macrocalcifications and decreasing microcalcifications.

6.2 Methods

6.2.1 *In Vitro Study Design*

Cells were maintained and calcified as described earlier (chapter 2.4) with HDL, oxHDL, rHDL or oxrHDL at 200µg/ml for 24 hours prior to calcification stimulus. After 1,3,5 and 7 days of calcification medium (CM), mRNA was harvested and transformed to cDNA for PCR analysis as per methods chapter 2.5.1, 2.6 and 2.7 respectively. Cells were harvested after 5 and 7 days of calcification for protein expression analysis using methods described in chapter 2.8 and 2.9. Additionally, media also was collected after the 5 and 7 day CM timepoints and analysed for protein secretion using ELISA. A timeline of the *in vitro* calcification assay is presented in figure 6.2.1.1.

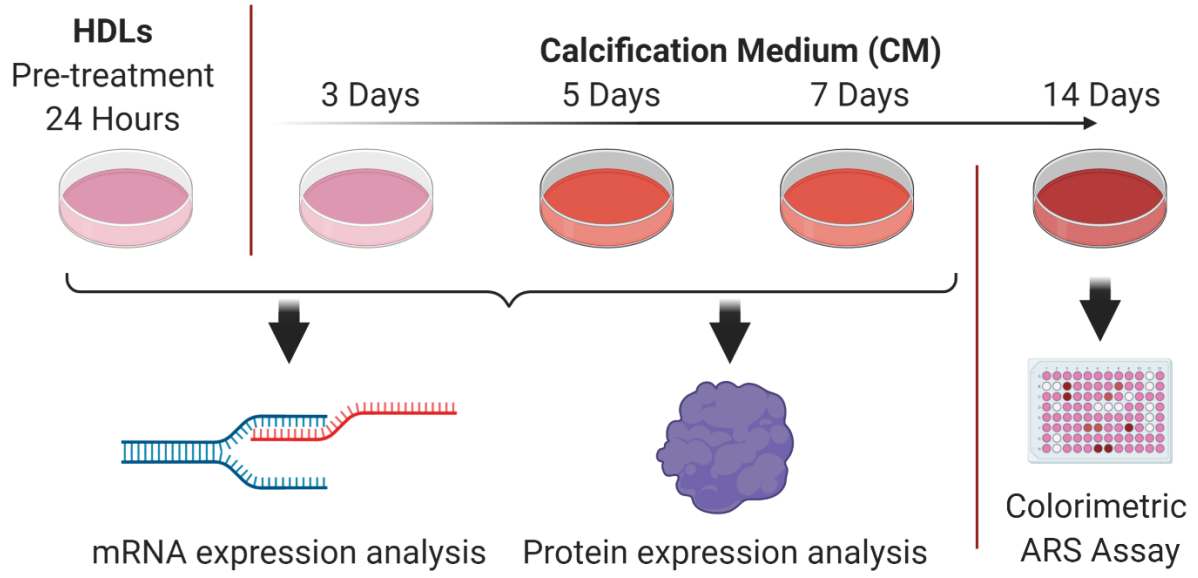

Figure 6.2.1.1 Schematic of the HDL or rHDL *in vitro* calcification assay.

HAoSMCs were pre-treated with HDL, oxHDL, rHDL or oxrHDL at 200µg/ml for 24 hours, then treated with $CaPO_4$ (Ca 2.7 mM, PO_4 2.0 mM) medium (CM) for up to 15 days. Cells were then analysed at various timepoints with PCR, western blot and stained with Alizarin Red S (ARS) stain to monitor calcium deposition and molecule expression.

6.2.2 *In Vivo* Methods

6.2.2.1 Study Design

OPG$^{-/-}$ mice on an Apo E$^{-/-}$ background were utilised in this study to examine the effects of the loss of inhibitory OPG on atherosclerotic VC and if rHDL infusions are able to influence these results. OPG$^{-/-}$ mice exhibit early arterial calcification and osteoporotic phenotypes[643] and Apo E$^{-/-}$ x OPG$^{-/-}$ mice have been observed to have atherosclerotic calcifications[799].

8-week-old Apo E$^{-/-}$ x OPG$^{-/-}$ and Apo E$^{-/-}$ mice on a C57Bl/6 background were fed an atherogenic diet (AD) (22% fat and 0.15% cholesterol diet SF00-219 (Specialty Feeds)) ad libitum for 36 weeks. Additional cohorts were then randomized to either rHDL or saline infusions 3 times weekly for 4 additional weeks of a 40 week in total AD ad libitum. Mice were weighed weekly and had a change of bedding twice per week. Blood was collected, using EDTA coated collection tubes spun at 1500 rcf for 15 minutes, at baseline, at 8 week intervals and during euthanasia via cardiac puncture. This study was approved by the South Australian Health and Medical Research Institute Animal Ethics Committee (SAM188). Study schematic is presented in figure 6.2.2.1.

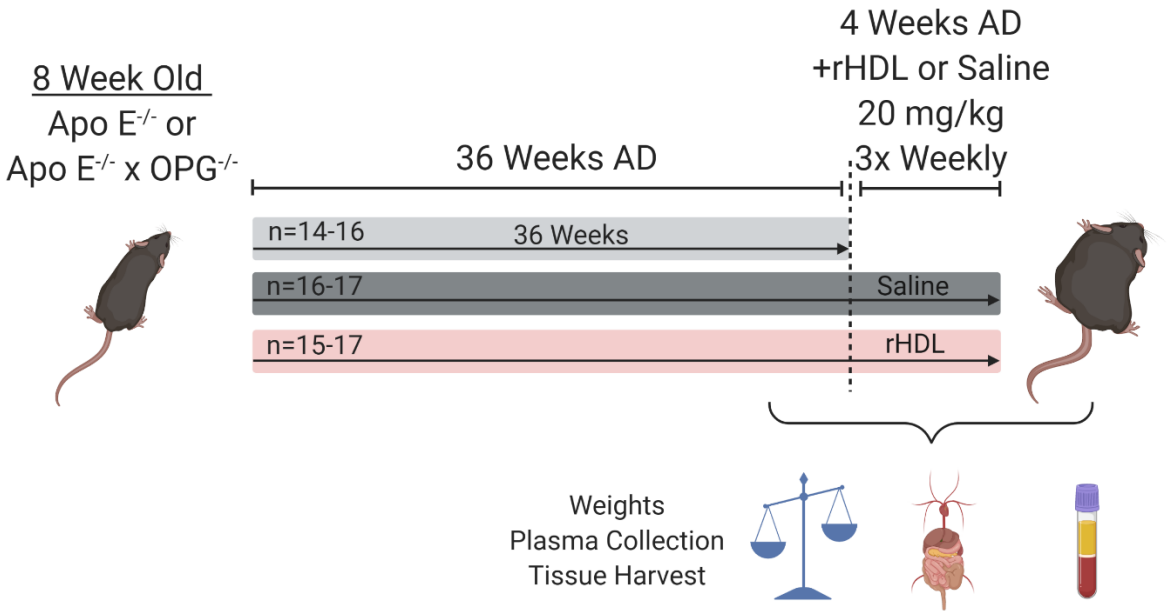

Figure 6.2.2.1 Study design for the investigation of rHDL effects of VC in Apo E-/- and Apo E /- x OPG-/- mice.

Apo E$^{-/-}$ and Apo E$^{-/-}$ x OPG$^{-/-}$ mice were fed an atherogenic diet (AD) ad libitum for 36 weeks. One group of mice was euthanised at this point for a pre-treatment group, whereas the other 2 groups continued eating AD ad libitum for 4 more weeks (totalling 40 weeks) while receiving 20 mg/kg infusions of saline or rHDL 3 times per week. Mice were weighed weekly and plasma was collected at 8 week intervals from the beginning of the study. Mice were euthanised via cardiac puncture and tissues were collected in either formalin or snap frozen in liquid nitrogen for further processing. This study was approved by the South Australian Health and Medical Research Institute Animal Ethics Committee (SAM188).

6.2.3 *Patient Study*

6.2.3.1 Study Outline and Design

This chapter utilises human serum samples collected from the CER-001 Atherosclerosis Regression Acute Coronary Syndrome Trial (CARAT)[800]. Briefly, CARAT is a double-blind randomised, multicentre trial aiming to evaluate the potential of 10 weekly intravenous infusions of CER-001 at 3 mg/kg. Patients with acute coronary syndrome and percent atheroma volume above 30% in the proximal segment of an epicardial artery, identified using intravascular ultrasonography (IVUS), were randomised to either CER-001 treatment or placebo and final numbers at follow up were 135 and 137 respectively.

In this thesis, we examined the entire trial cohort to detect significant differences between CER-001 and placebo treatments in plaque calcification detected via intravascular ultrasound (IVUS) imaging. Briefly, each image in the IVUS pull-back was assigned a value from 0-4, to describe the amount of calcification observed in the vessel. A calculation was then performed to obtain a calcium index, indicative of the average calcification observed in the entire artery imaged [285]..

Patient samples corresponding to the largest increases in plaque calcification were assessed. Out of the 257 participants with available calcium indices at baseline and follow up, the top 11 calcification progressors were selected for further examination, to assess what might be causing this change in these patients. 4 samples were from participants receiving placebo and 7 were from participants receiving CER-001. While the change in calcium index between baseline and follow up ranged from -0.14 – 0.23 in the entire 257 participant large cohort, in our top calcification progressor cohort the calcium index change ranged from 0.14-0.23.

The serum from these patients (10% in M199 medium) was used to pre-treat HAoSMCs for 24 hours and subsequently assess calcification (as outlined in chapter 2.4.22).

6.2.4 Statistics

Statistics for all data collected in this chapter were calculated as per methods chapter 2.14 unless otherwise stated in the figure or table legend.

In Vitro Results

The role of native HDL and oxHDL in VSMC calcification

6.3 Results

6.3.1 The Functional Effects of HDL and oxHDL on HAoSMC Calcification

Although HDL was shown to upregulate the expression of vascular calcification (VC) markers by Parhami *et al*. in 2002[801], since then no studies have further explored these anti-calcification effects of HDL. The alizarin red s (ARS) assay was used in this study to confirm the functional effect of native HDL, oxHDL, rHDL and oxrHDL on HAoSMC VC. In figure 6.3.1.1 A, we show that HDL pre-treatment significantly reduces VC on HAoSMCs compared to treatment with calcification medium (CM) alone (1.0±0.0 vs 0.78±0.03, $p<0.05$). Conversely, oxidised HDL (oxHDL) maintained the level calcification similar to CM alone which was significantly higher than HDL treated cells (0.78±0.03 vs 1.02±0.06, $p<0.01$), demonstrating that oxidation of HDL negates its ability to reduce VC.

When moving forward with HDL therapeutics, a lab made, reconstituted HDL (rHDL) is an attractive option due to its consistency in functionality. For this reason, as well as identifying whether the specific Apo AI and PLPC components of the rHDL discs are responsible for any effects of native HDL, that we repeated the analysis using both lipoprotein particles. Although the pattern was the same for rHDLs and HDLs, we observed no significant effects from rHDL or oxrHDL pre-treatment on the calcification of HAoSMCs. From this ARS assay, we find that rHDL does not match the same pattern as native HDL in figure 6.3.1.1 B, showing a role for an element of HDL other than Apo AI or PLPC.

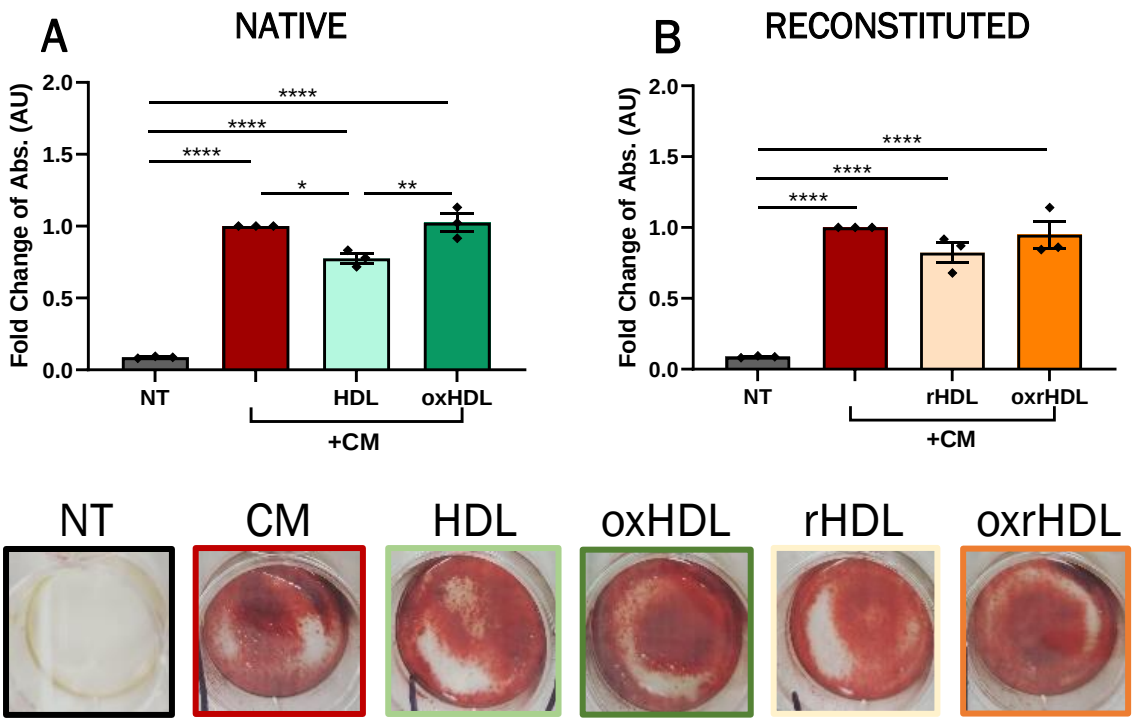

Figure 6.3.1.1 The effect of HDL and oxHDL on calcification.

*HAoSMCs were pre-treated with (A) HDL or oxHDL or (B) rHDL or oxrHDL (200 µg/ml) for 24 hours then treated with calcification medium (CM; Ca 2.7 mM, PO_4 2.0 mM) for 15 days. Calcification was measured by ARS assay with no treatment (NT) and CM alone controls and expressed as fold change from CM. Representative images of stain immediately prior to dissolving shown below graph. NT ****p<0.0001 compared to all other treatments. *p<0.05, **p<0.01, ****p<0.0001 as indicated, ANOVA with Bonferroni's correction. Data represented as mean± SEM, n=3.*

6.3.2 The Effects of HDL and oxHDL on Calcification Gene Expression

To further investigate the interactions between HDL, oxHDL and calcification induction, we used quantitative PCR assays. HAoSMCs were exposed to HDL and oxHDL for 24 hours to identify the effects of on the cells prior to calcification. Treatment with HDL for 24 hours significantly lowered Runx2 (111.5±4.0 vs 60.2±11.7, $p<0.05$) and OPG (124.6±21.9 vs 52.7±6.0, $p<0.05$) compared to the NT baseline, while raising SMαActin (64.8±3.0 vs 103.7±7.3, $p<0.01$) mRNA expression compared to the CM. A similar trend was observed following oxHDL treatment when assessing Runx2 compared to the NT baseline (111.5±4.0 vs 51.3±3.98 vs 10.61, $p<0.05$) and OPG compared to the CM control (124.6±21.91 vs 48.66±7.802, $p<0.05$) mRNA expression. Interestingly, SMαActin expression remained at a similar level to CM treatment which was also and significantly reduced compared to NT (103.4±0.3 vs 58.7±2.9, $p<0.001$) and HDL (103.7±7.3 vs 58.7±2.8, $p<0.001$) (figure 6.3.2.1).

Next, the immediate effects of rHDL and oxrHDL on mRNA expression of genes involved in VSMC calcification were assessed via qPCR after 24 hours of incubation. oxrHDL treatment for 24 hours significantly increased RANKL (107.3±5.04 vs 355.7±62.68, $p<0.01$) and ALP (104.1±2.9 vs 267.4±60.28, $p=0.0489$) mRNA expression above the NT baseline and increased RANKL mRNA expression compared to the rHDL treatment (113.1±6.66 vs 355.7±62.68, $p<0.01$). While there were no observed differences between either rHDL or oxrHDL treatments and CM alone both rHDL (103.4±0.32 vs 68.37±4.71, $p<0.05$) and oxrHDL (103.4±0.32 vs 61.54±12.48, $p<0.05$) significantly reduced SMαActin mRNA expression below the NT baseline, similar to the effects of CM treatment (NT vs CM: 103.4±0.32 vs 64.83±2.99, $p<0.05$; figure 6.3.2.2).

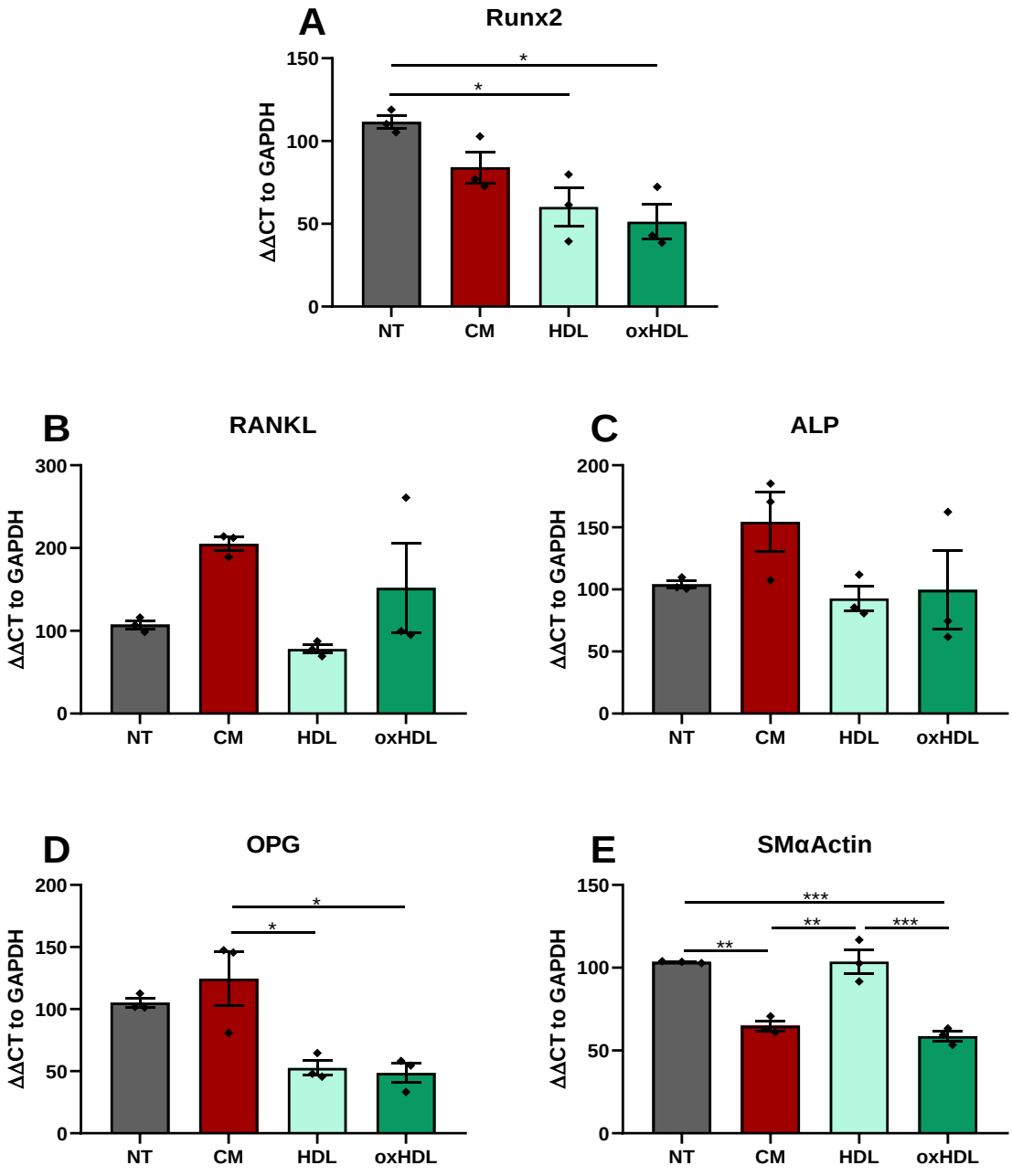

Figure 6.3.2.1 The effect of HDL and oxHDL on mRNA expression.

*HAoSMCs were treated with calcification medium (CM; Ca 2.7 mM, PO_4 2.0 mM) HDL or oxHDL (200 µg/ml) for 24 hours. mRNA expression was measured by qPCR using GAPDH as the internal control. *p<0.05, **p<0.01, ***p<0.001, ANOVA with Bonferroni's correction. Data represented as % of NT, mean± SEM, n=3.*

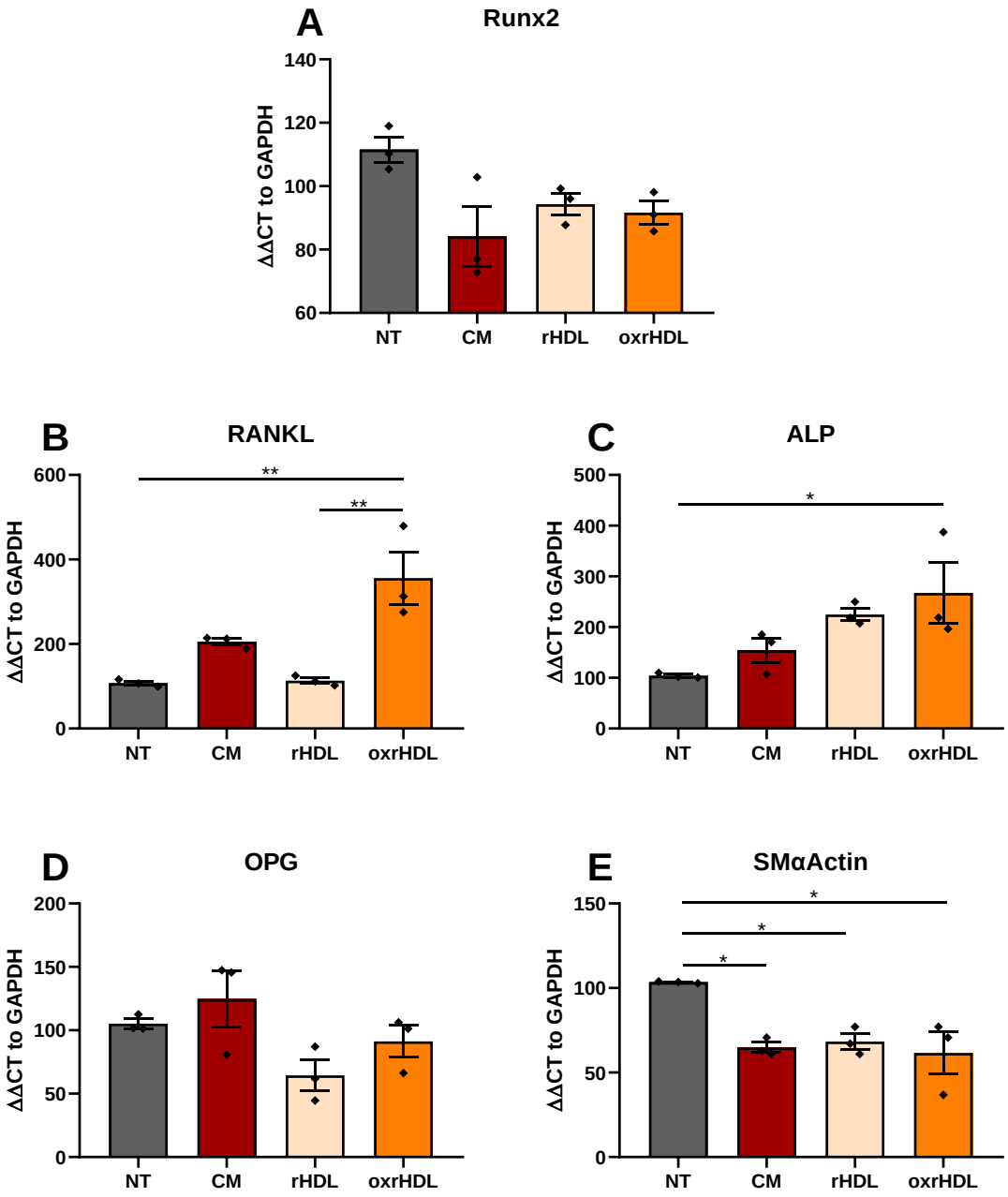

Figure 6.3.2.2 The effect of rHDL and oxrHDL on mRNA expression.

*HAoSMCs were treated with calcification medium (CM; Ca 2.7 mM, PO_4 2.0 mM) rHDL or oxrHDL (200 µg/ml) for 24 hours. mRNA expression was measured by qPCR using GAPDH as the internal control. *p<0.05, **p<0.01, ANOVA with Bonferroni's correction. Data represented as % of NT, mean± SEM, n=3.*

6.3.3 The effects of HDL Pre-Treatment on Calcification Gene expression

After discovering effects of native HDL and oxHDL in the initial regulation of calcification genes, a PCR time course experiment was conducted to examine the role of HDL and oxHDL as calcification progresses. Figure 6.3.3.1 A & C shows that neither HDL nor oxHDL pre-treatment influenced Runx2 mRNA expression at either 5 or 7 days into calcification with CM.

The reconstituted HDL forms demonstrated no significant effects on Runx2 gene expression (figure 6.3.3.1 B & D). This was keeping with the expression profile for HDL and oxHDL presented in figure 6.3.3.1 A & C and fits with the early timepoints for Runx2 expression.

Although not significant, after 5 days of calcification in CM, HDL pre-treatment reduced RANKL mRNA expression below that CM alone control, whereas the dysfunctional oxHDL did not. After 7 days in calcification medium however, this effect was lost. (figure 6.3.3.2 A & C). In a similar fashion to the measures with native HDL in A & C, the reconstituted forms demonstrated no significant effects on RANKL gene expression (figure 6.3.3.1 B & D).

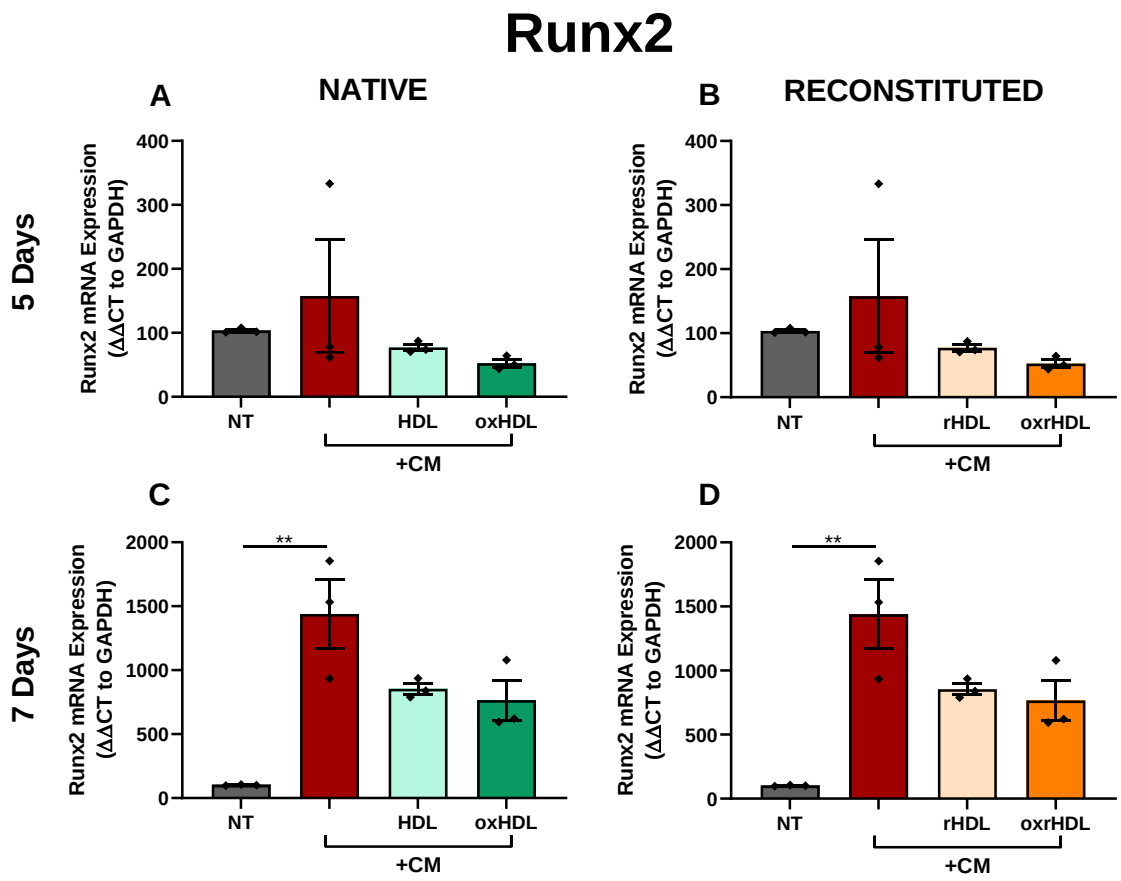

Figure 6.3.3.1 The effect of HDL, oxHDL, rHDL and oxrHDL on Runx2 mRNA expression.

*HAoSMCs were pre-treated with HDL, oxHDL, rHDL or oxrHDL (200 µg/ml) for 24 hours then treated with calcification medium (CM; Ca 2.7 mM, PO_4 2.0 mM) for 15 days. A no treatment (NT) baseline and a CM alone positive control were used. Runx2 mRNA expression was measured by qPCR using GAPDH as the internal control. *p<0.05, **p<0.01, ***p<0.001, ****p<0.0001, ANOVA with Bonferroni's correction. Data represented as % of NT, mean± SEM, n=3.*

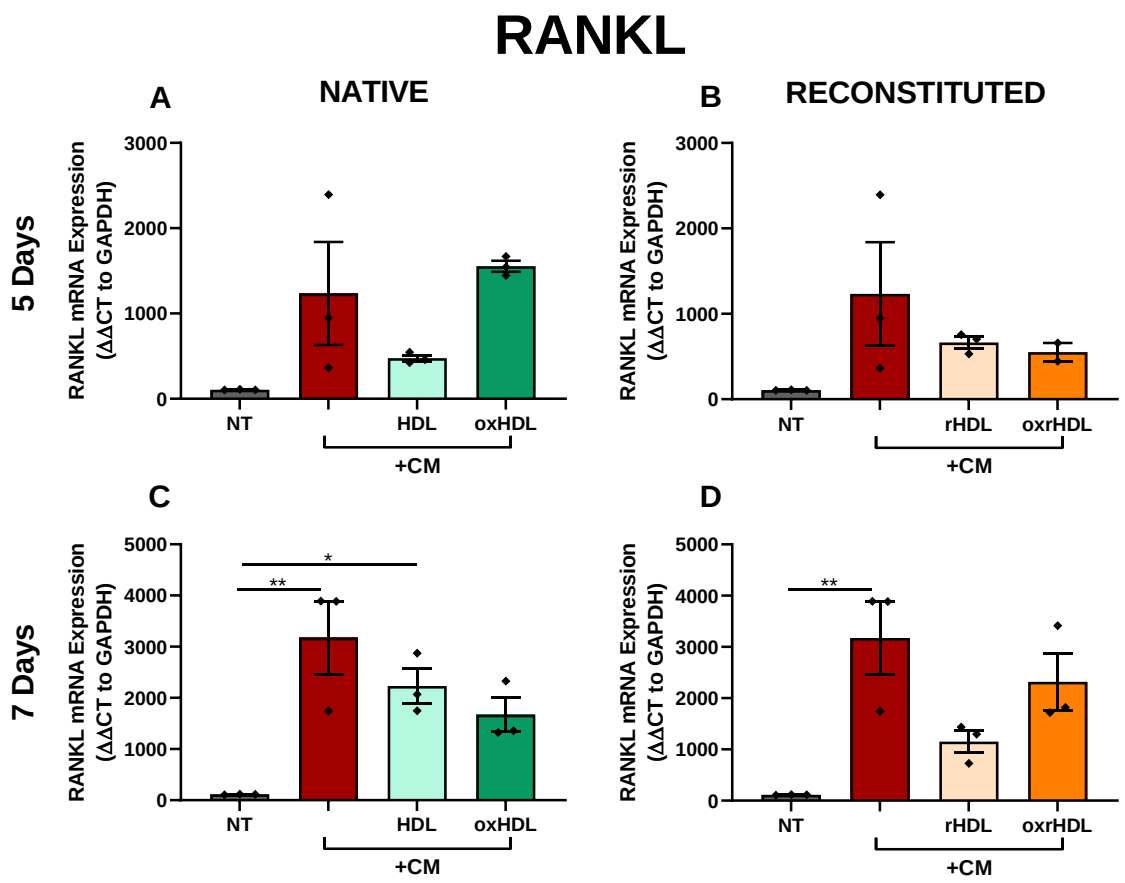

Figure 6.3.3.2 The effect of HDL, oxHDL, rHDL and oxrHDL on RANKL mRNA expression.

*HAoSMCs were pre-treated with HDL, oxHDL, rHDL or oxrHDL (200 µg/ml) for 24 hours then treated with calcification medium (CM; Ca 2.7 mM, PO_4 2.0 mM) for 15 days. A no treatment (NT) baseline and a CM positive control were used. RANKL mRNA expression was measured by qPCR using GAPDH as the internal control. **p<0.01, ANOVA with Bonferroni's correction. Data represented as % of NT, mean± SEM, n=3.*

When assessing the effects of HDL on ALP it was observed that neither HDL nor oxHDL had any significant effect after 5 or 7 days of calcification (figure 6.3.3.3 A & C). Although there were no significant effects, HDL and oxHDL pre-treatments did appear to lower ALP mRNA expression back to the NT baseline compared to the CM alone treated cells. Similar to HDL and oxHDL, for the reconstituted forms rHDL and oxrHDL pre-treatments also had no significant effects on ALP mRNA expression (figure 6.3.3.3 B & D).

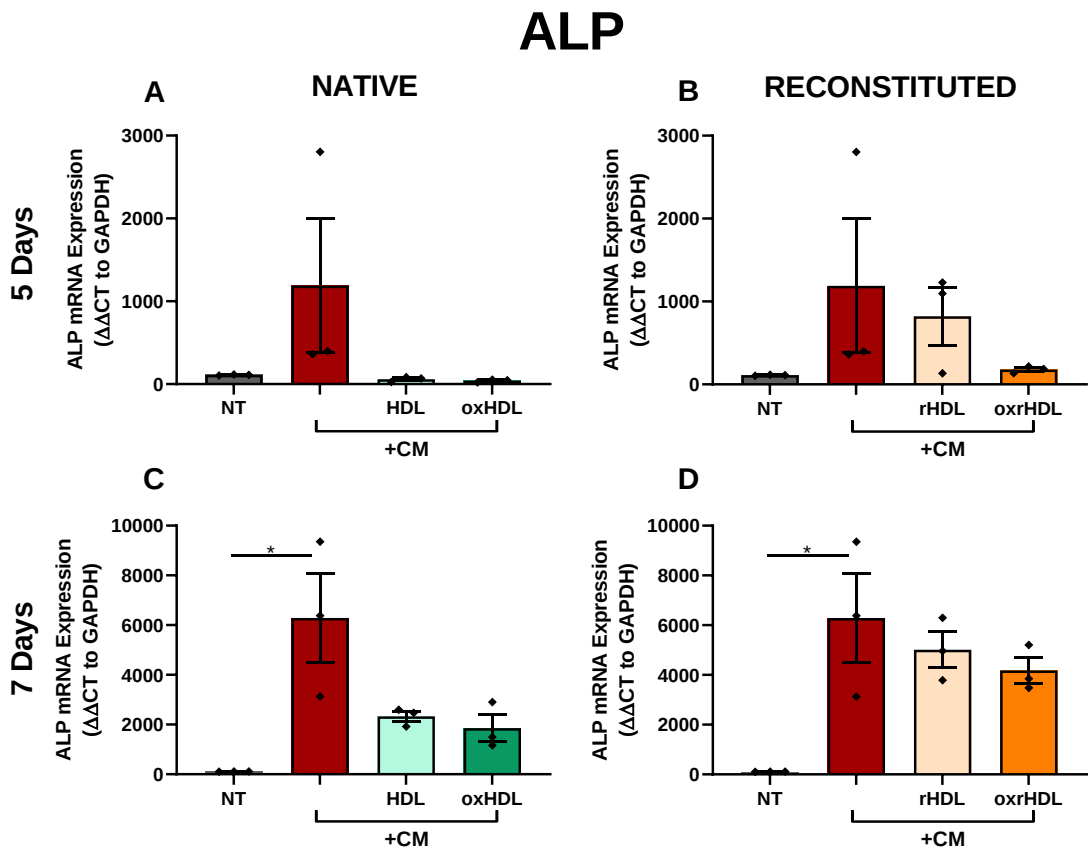

Figure 6.3.3.3 The effect of HDL, oxHDL, rHDL and oxrHDL on ALP mRNA expression.

*HAoSMCs were pre-treated with HDL, oxHDL, rHDL or oxrHDL (200 µg/ml) for 24 hours then treated with calcification medium (CM; Ca 2.7 mM, PO_4 2.0 mM) for 15 days. A no treatment (NT) baseline and a CM positive control were used. ALP mRNA expression was measured by qPCR using GAPDH as the internal control. *p<0.05, ANOVA with Bonferroni's correction. Data represented as % of NT, mean± SEM, n=3.*

We tested for the smooth muscle cell identifier gene SMαActin to identify potential effects of HDL and oxHDL on cell type conservation. Although there were no significant differences between cells pre-treated with HDL or oxHDL and the cells treated with CM alone, at both the 5 and 7 days of CM timepoints HDL modestly raised SMαActin mRNA levels (figure 6.3.3.4 A & C). While at 24 hours there was a significant increase in SMαActin expression compared to CM (figure 6.3.2.1) by 5 or 7 days of calcification this initial effect was lost.

While there were no significant differences following rHDL or oxrHDL pre-treatments after 5 days of CM, both rHDL (104.7±1.55 vs 22.53±6.98, $p<0.001$) and oxrHDL (104.7±1.55 vs 29.16±12.42, $p<0.001$) pre-treatments significantly reduced SMαActin mRNA expression from the NT baseline, to match that of the CM alone control (NT vs CM: 104.7±1.55 vs 17.45±3.259, $p<0.001$) thereby showing no additional effects above the CM treatment (figure 6.3.3.4 B & D). Conversely, there were no significant effects at either timepoint after HDL or oxHDL pre-treatments as shown in figure 6.3.3.4 A & C for SMαActin mRNA expression.

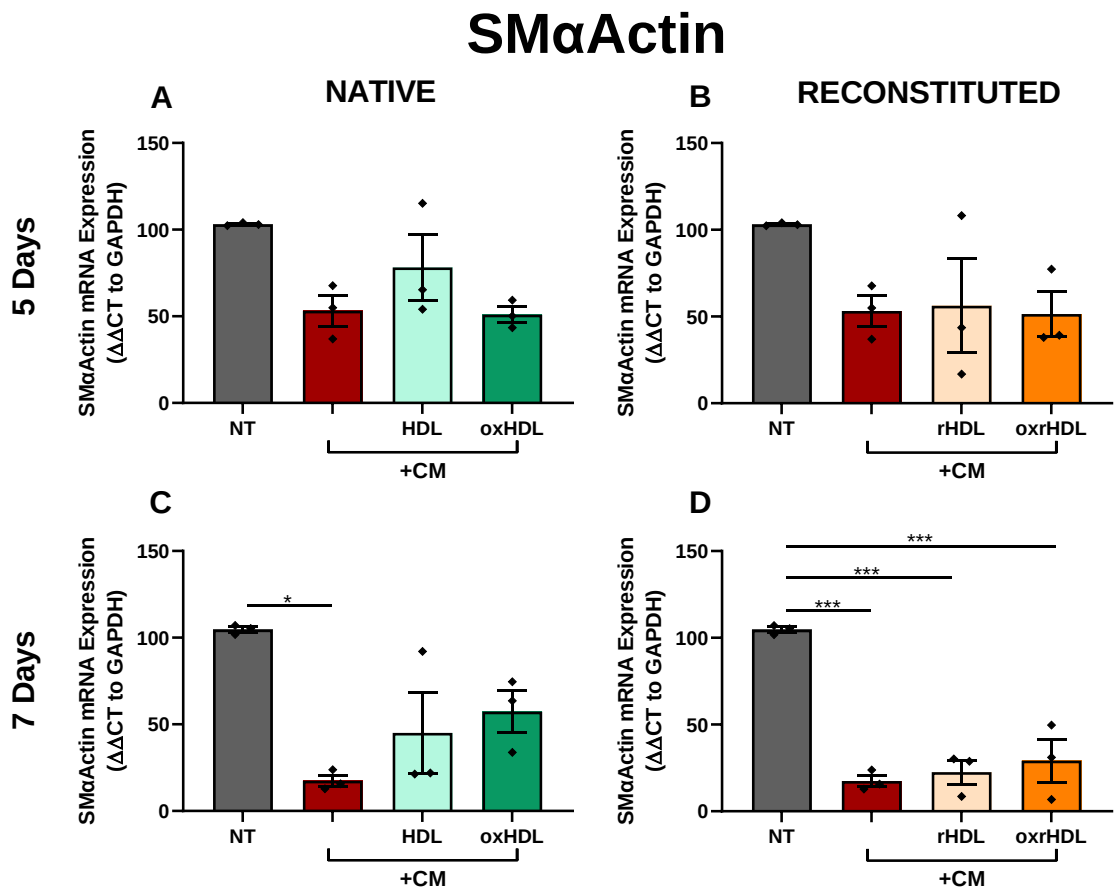

Figure 6.3.3.4 The effect of HDL, oxHDL, rHDL and oxrHDL on SMαActin expression.

*HAoSMCs were pre-treated with HDL, oxHDL, rHDL or oxrHDL (200 µg/ml) for 24 hours then treated with calcification medium (CM; Ca 2.7 mM, PO_4 2.0 mM) for 15 days. A no treatment (NT) baseline and a CM alone control were used. SMαActin mRNA expression was measured by qPCR using GAPDH as the internal control. *p<0.05, ANOVA with Bonferroni's correction. Data represented as % of NT, mean± SEM, n=3.*

The cell's defence mechanism to VC, OPG expression, was assessed via qPCR. Like the SMαActin expression patterns in figure 6.3.3.4 A & C, there was a trend towards increased expression with HDL However, the observed results were not significant (figure 6.3.3.5 A & C). When treating with reconstituted forms of HDL, neither rHDL or oxrHDL had any effect on OPG mRNA expression either at the 5 or 7 day timepoint. rHDL and oxrHDL also had no additional effects above CM treatments (figure 6.3.3.5 B & D).

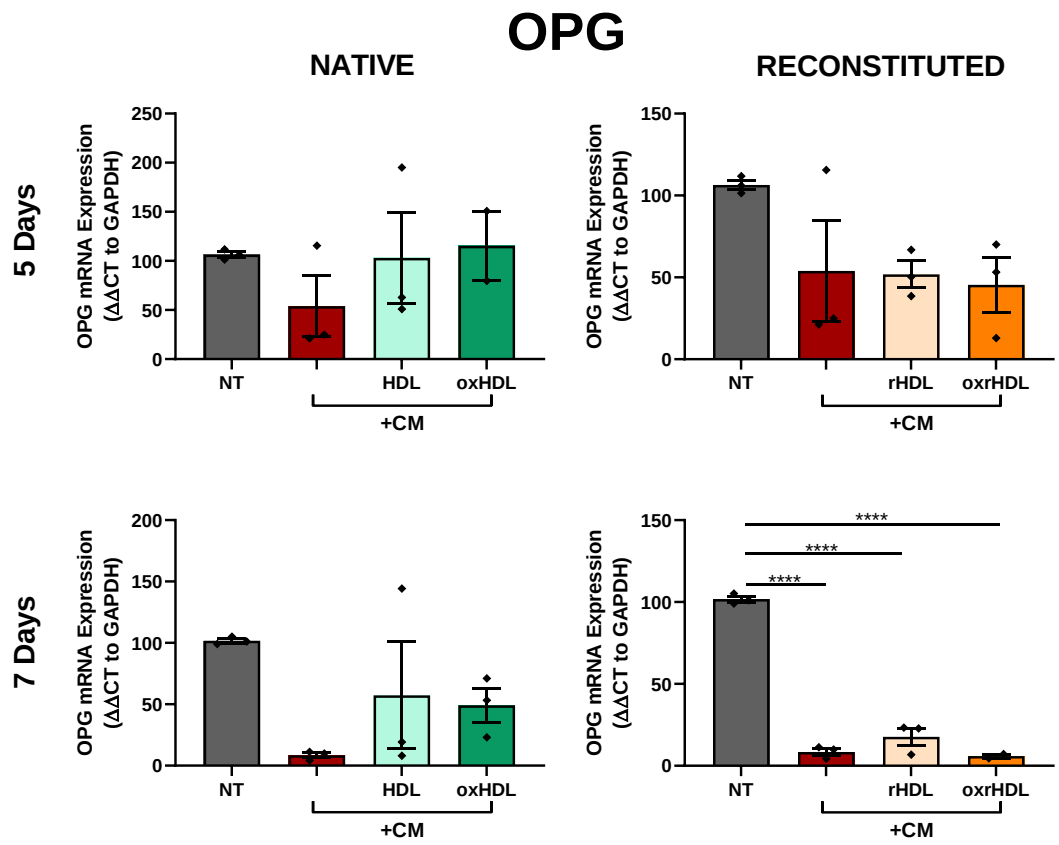

Figure 6.3.3.5 The effect of HDL, oxHDL, rHDL and oxrHDL on OPG expression.

*HAoSMCs were pre-treated with HDL, oxHDL, rHDL or oxrHDL (200 µg/ml) for 24 hours then treated with calcification medium (CM: Ca 2.7 mM, PO_4 2.0 mM) for 15 days. A no treatment (NT) baseline and a CM alone control were used. OPG mRNA expression was measured by qPCR using GAPDH as the internal control. ****p<0.0001, ANOVA with Bonferroni's correction. Data represented as % of NT, mean± SEM, n=3.*

6.3.4 The effects of HDL on Calcification Protein Expression and Secretion

While looking at mRNA expression profiles identified potential expression patterns following HDL and oxHDL pre-treatment, we sought to confirm these results at the protein level. To examine the protein levels, we used western blotting techniques on cell lysates for intercellular proteins and ELISA assays on cell culture media for secreted proteins.

After both 5 (A) and 7 (B) days of CM neither HDL nor oxHDL cased any significant differences in Runx2 protein levels (figure 6.3.4.1). As reported earlier, Runx2 mRNA is primarily influenced by HDL at the early 24 hour timepoint, so this result for the Runx2 protein levels is not surprising (figure 6.3.4.1). Similarly, cells pre-treated with the reconstituted forms of HDL also had no effect on Runx2 protein levels either at day 5 or day 7.

Similar to the Runx2 patterns post HDL, oxHDL, rHDL and oxrHDL pre-treatments, RANKL protein expression was not significantly changed HDL, oxHDL, rHDL or oxrHDL pre-treatments (figure 6.3.4.2).

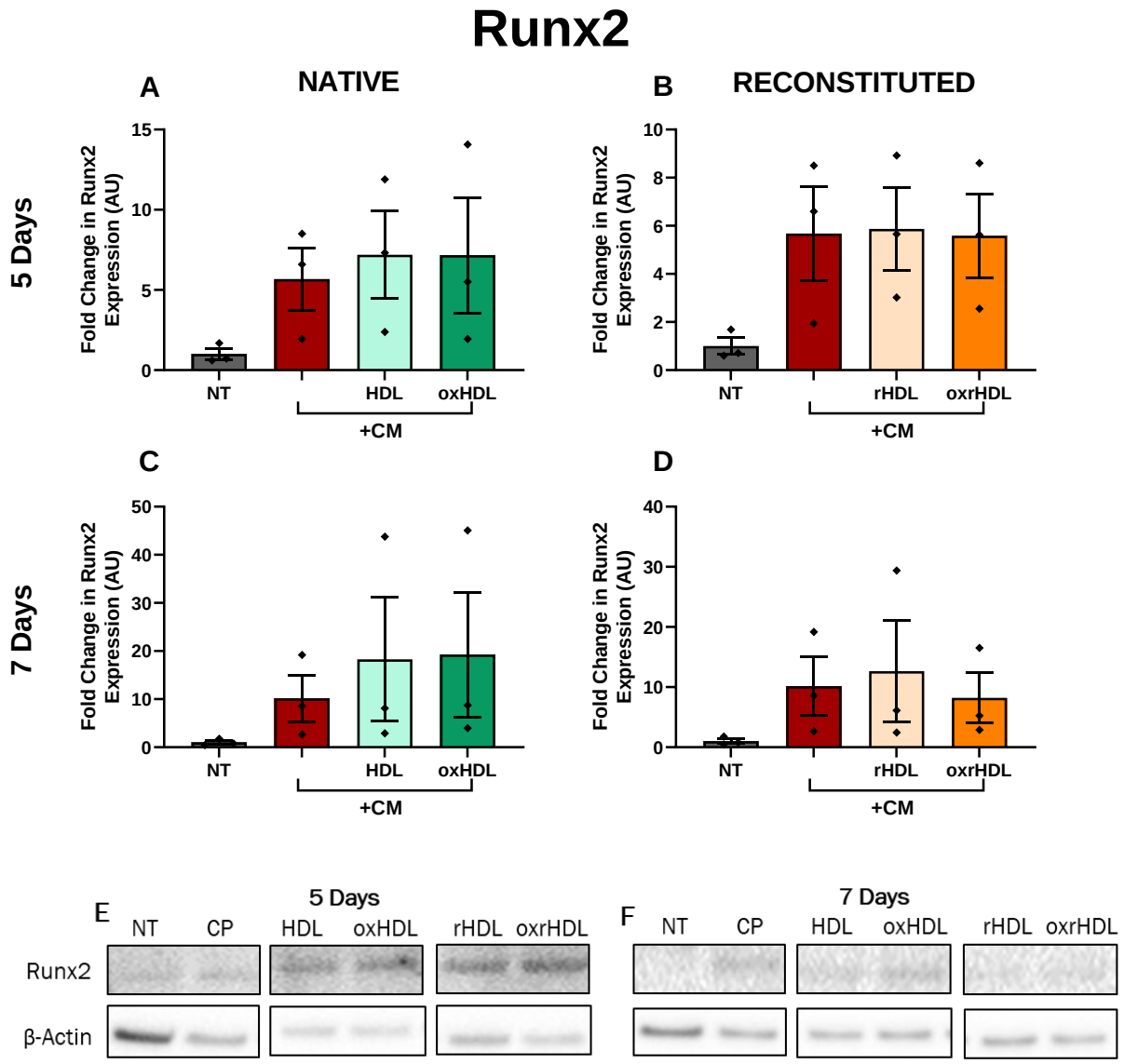

Figure 6.3.4.1 The effect of HDL, oxHDL, rHDL and oxrHDL on Runx2 and RANKL protein expression.

HAoSMCs were pre-treated with HDL, oxHDL, rHDL or oxrHDL (200 µg/ml) for 24 hours then treated with calcification medium (CM; Ca 2.7 mM, PO_4 2.0 mM) for 15 days. A no treatment (NT) baseline and a CM positive control were used. Runx2 protein expression was measured by western blotting using β-Actin and a standard sample as internal controls. ANOVA with Bonferroni's correction. Data represented as % of NT, mean± SEM, n=3.

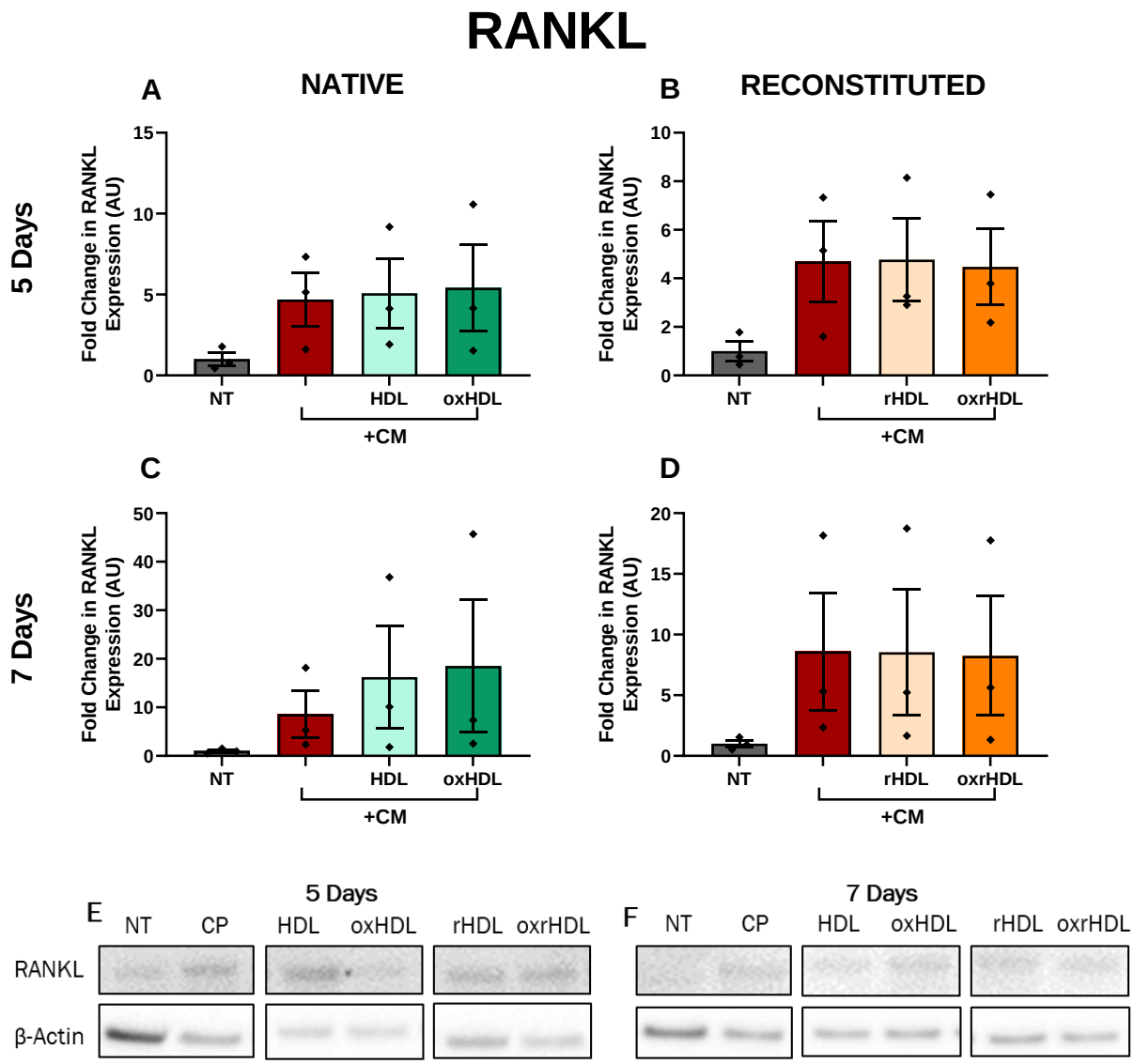

Figure 6.3.4.2 The effect of HDL, oxHDL, rHDL and oxrHDL on RANKL protein expression.

HAoSMCs were pre-treated with HDL, oxHDL, rHDL or oxrHDL (200 µg/ml) for 24 hours then treated with calcification medium (CM; Ca 2.7 mM, PO_4 2.0 mM) for 15 days. A no treatment (NT) baseline and a CM positive control were used. RANKL protein expression was measured by western blotting using β-Actin and a standard sample as internal controls. ANOVA with Bonferroni's correction. Data represented as % of NT, mean± SEM, n=3.

As RANKL can have autocrine and paracrine effects, cellular expression (figure 6.3.4.2) was measured by western blotting, whereas RANKL secretion was measured in the cell culture supernatant using an ELISA (figure 6.3.4.3). After 5 days of CM, the native forms of HDL (0.86±0.017 vs 1.25±0.067, $p<0.01$) and oxHDL (0.86±0.017 vs 1.23±0.071, $p<0.01$) significantly raised RANKL secretion above the CM alone control, while the reconstituted forms had no effect. After 7 days of CM however, this elevation was only maintained by oxHDL (1.0±0.08 vs 1.4±0.11, $p<0.05$) (figure 6.3.4.3 C), demonstrating that the dysfunctional oxHDL particles can maintain a pro-VC phenotype in these cells over time.

Similarly, OPG is a secreted protein and was measured in the cell culture supernatant using an ELISA. After 5 or 7 days of CM, pre-treatment with neither HDL nor oxHDL had any additional effect on OPG secretion compared to the CM control. This result was also observed with reconstituted HDL (figure 6.3.4.4).

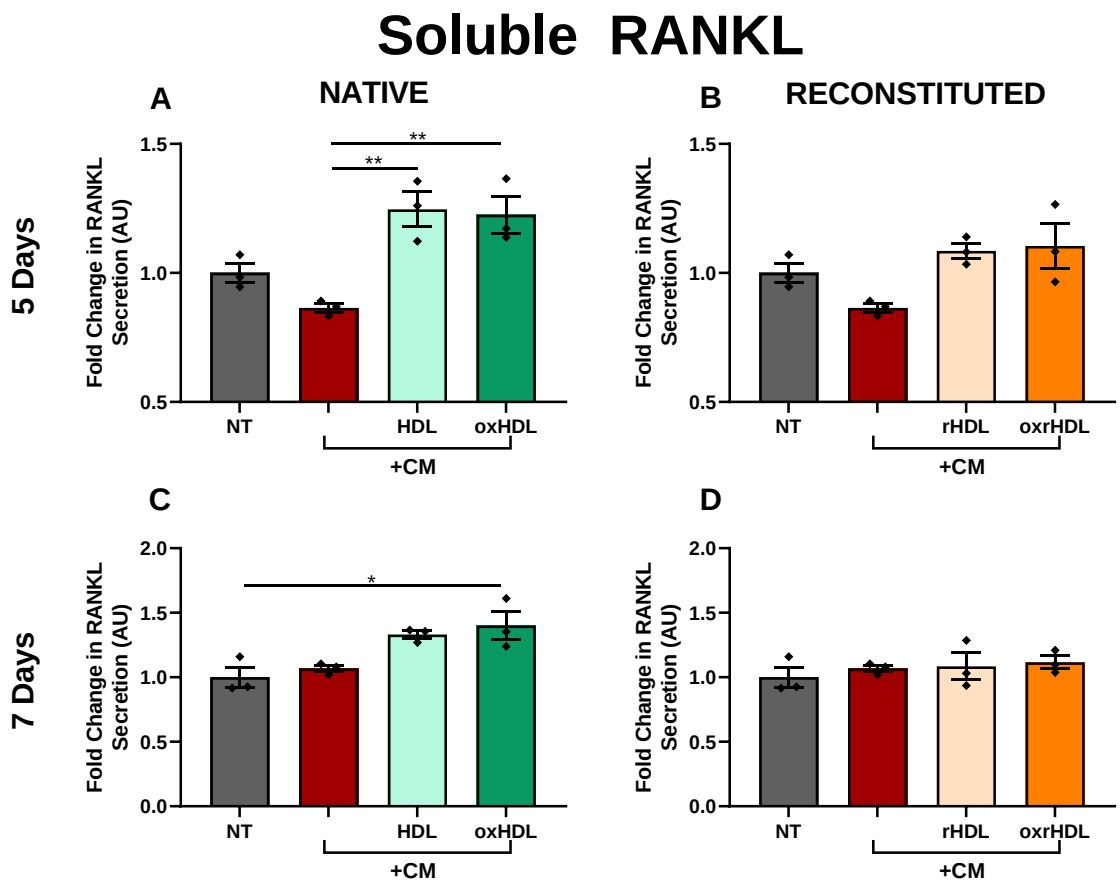

Figure 6.3.4.3 The effect of HDL, oxHDL, rHDL and oxrHDL on soluble RANKL protein.

*HAoSMCs were pre-treated with HDL, oxHDL, rHDL or oxrHDL (200 µg/ml) for 24 hours then treated with calcification medium (CM; Ca 2.7 mM, PO_4 2.0 mM) for 15 days. A no treatment (NT) baseline and a CM positive control were used. Soluble RANKL protein secretion was measured by ELISA using BCA measured total protein as a control. *p<0.05, **p<0.01, ANOVA with Bonferroni's correction. Data represented as fold change of NT, mean± SEM, n=3.*

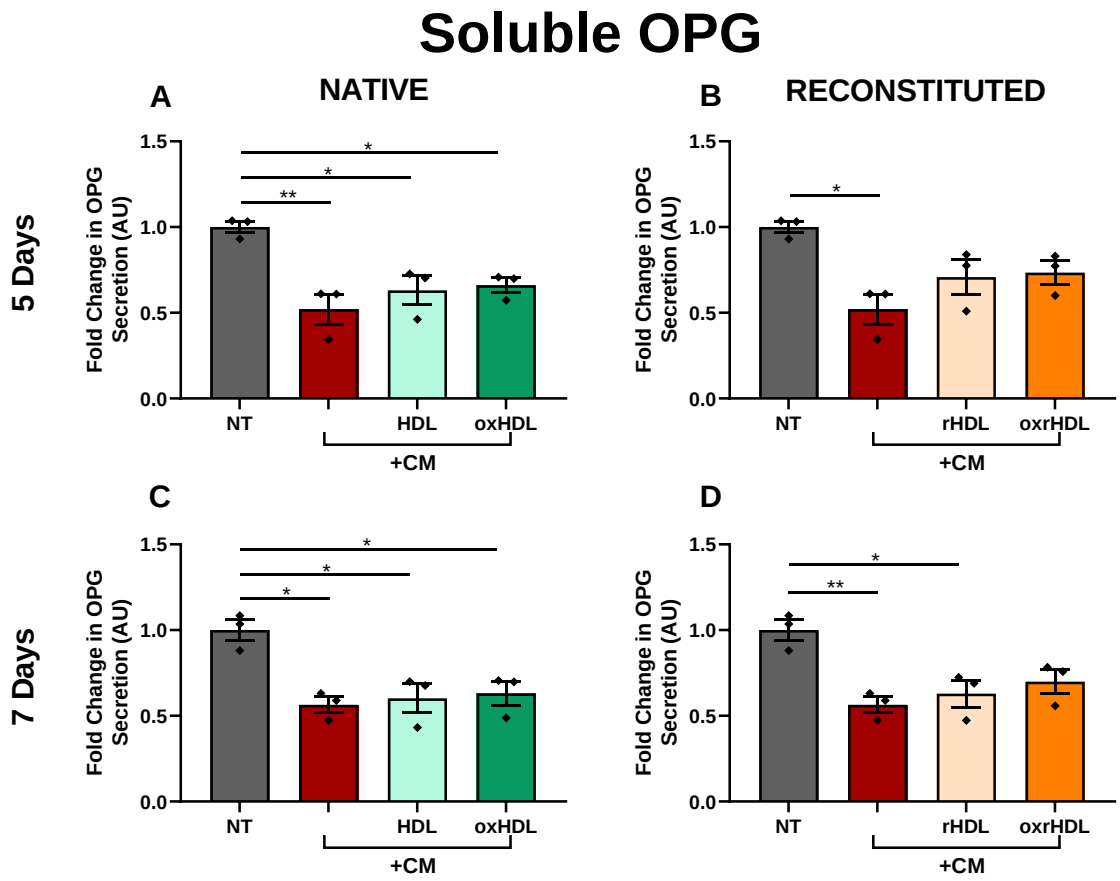

Figure 6.3.4.4 The effect of HDL, oxHDL, rHDL and oxrHDL on Soluble OPG protein.

*HAoSMCs were pre-treated with HDL, oxHDL, rHDL or oxrHDL (200 µg/ml) for 24 hours then treated with calcification medium (CM; Ca 2.7 mM, PO_4 2.0 mM) for 15 days. A no treatment (NT) baseline and a CM positive control were used. Soluble OPG protein expression was measured by ELISA and normalised to total protein. *p<0.05, **p<0.01, ANOVA with Bonferroni's correction. Data represented as % of NT, mean± SEM, n=3.*

The cellular data presented here demonstrates a role for HDL and its oxidised form in vascular calcification, whereby HDL, but not oxHDL, reduced VSMC calcification through alteration of calcification regulatory gene and protein levels. We have also shown a small role for rHDL and oxrHDL in VC *in vitro* which does not match the data presented for native HDL and native oxHDL. The effects from rHDL and oxrHDL on VC appear at earlier timepoints and with a different expression pattern after 24 hours of treatments compared to HDL and oxHDL and neither rHDL nor oxrHDL pre-treatments had any effect on HAoSMC calcification, suggesting that the effects of HDL on VC may be from a component other than Apo AI or PLPC. Next, in order to study the effects of rHDL *in vivo*, we examined the effects of rHDL infusions on atherogenic and pro-VC mice in a late-stage plaque model.

In human trials reconstituted HDL (rHDL) is commonly used as it is a standardised particle with only 2 components of typical HDL. Human HDL has many variables including, but not limited to, lipid species and content, protein species and content, RNA molecules, size, vitamin and mineral contents. The rHDL used in the *in vitro* and *in vivo* chapters of this thesis have only 1 lipid: 1-Palmitoyl-2-linoeoyl-sn-glycero-3-phosphocholine (PLPC: 16:0-18:2 PC), and 1 protein: Apo AI. Next, we aimed to investigate the role of rHDL *in vivo*, assessing whether any effects will be maintained in a full system.

In Vivo Results

The role of reconstituted HDL infusions in a late stage plaque and calcification mouse model

6.3.5 Plasma biomarkers assessed at baseline

Although the plaque regressive effects of rHDL on Apo $E^{-/-}$ mice has been extensively examined[92, 802-809], the effect of OPG deficiency has yet to be assessed. Prior to commencing the study, 8 week old Apo $E^{-/-}$ and Apo $E^{-/-}$ x $OPG^{-/-}$ mice had a blood sample measured for total cholesterol, triglycerides, ALP and calcium levels. At baseline, Apo $E^{-/-}$ mice had significantly higher total cholesterol than Apo $E^{-/-}$ x $OPG^{-/-}$ mice (165.0±8.093 vs 136.0±6.96, $p<0.01$) (figure 6.3.5.1).

In table 6.3.5.1 the differences between the final plasma measurements of each of these groups in both genotypes are presented. The 36 week cohort had a significantly higher change in total cholesterol compared to the saline ($p<0.05$) or rHDL ($p<0.001$) treated Apo $E^{-/-}$ x $OPG^{-/-}$ mice. There were no other significant differences between groups or genotypes of mice in final total cholesterol, change in total cholesterol, final triglycerides or change in triglycerides.

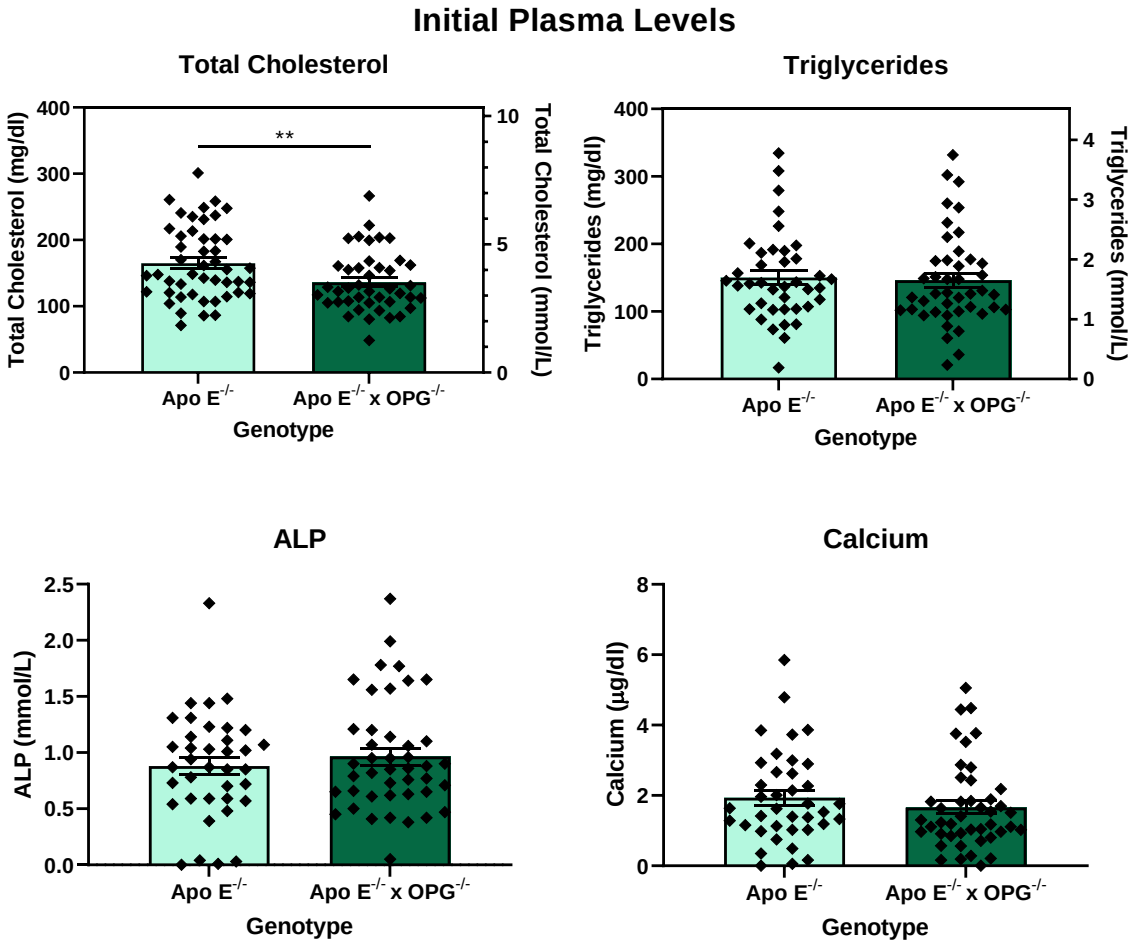

Figure 6.3.5.1 Plasma biomarkers assessed at baseline.

*Mouse blood was collected from the tail vein and plasma was extracted from 8 week old mice. Mouse plasma was then tested for triglyceride, total cholesterol and ALP levels using WAKO kits as per protocol. Circulating calcium was measured from plasma using the Cayman calcium assay kit as per protocol. **p<0.01, t-test with Welch's correction. Data represented as mean± SEM, n=37-50.*

Table 6.3.5.1 Circulating plasma lipids in Apo $E^{-/-}$ and Apo $E^{-/-}$ x $OPG^{-/-}$ mice. *Mean (±SEM), 2-way-ANOVA, n=9-17.*

Final Total Cholesterol (mg/dl)	Mean (±SEM)			P-Value		
	36 w	Saline (40w)	rHDL (40w)	36w vs. Saline	36w vs. rHDL	Saline vs. rHDL
Apo $E^{-/-}$	257.9 (±382.6)	378.5 (±22.03)	355.4 (±17.04)	>0.9999	>0.9999	>0.9999
Apo $E^{-/-}$ x $OPG^{-/-}$	358.1 (±17.85)	303.4 (±17.18)	311.6 (±10.55)	0.5447	0.5630	>0.9999
P-value	>0.9999	0.0772	0.8205			
Total Cholesterol Change (mg/dl)	**Mean (±SEM)**			**P-Value**		
	36 w	Saline (40w)	rHDL (40w)	36w vs. Saline	36w vs. rHDL	Saline vs. rHDL
Apo $E^{-/-}$	240.5 (±16.03)	211.1 (±17.47)	217.1 (±13.23)	>0.9999	>0.9999	>0.9999
Apo $E^{-/-}$ x $OPG^{-/-}$	253.2 (±18.16)	154.5 (±24.61)	146.0 (±21.62)	0.0176	0.0009	>0.9999
P-value	>0.9999	0.9106	0.0912			
Final Triglyceride (mg/dl)	**Mean (±SEM)**			**P-Value**		
	36 w	Saline (40w)	rHDL (40w)	36w vs. Saline	36w vs. rHDL	Saline vs. rHDL
Apo $E^{-/-}$	292.1 (±23.83)	263.6 (±27.1)	248.4 (±22.04)	>0.9999	>0.9999	>0.9999
Apo $E^{-/-}$ x $OPG^{-/-}$	320.2 (±24.76)	320.2 (±24.76)	287.2 (±17.59)	0.4901	>0.9999	>0.9999
P-value	>0.9999	>0.9999	>0.9999			
Triglyceride Change (mg/dl)	**Mean (±SEM)**			**P-Value**		
	36 w	Saline (40w)	rHDL (40w)	36w vs. Saline	36w vs. rHDL	Saline vs. rHDL
Apo $E^{-/-}$	151.7 (±22.88)	76.59 (±32.8)	105.7 (±29.12)	0.9622	>0.9999	>0.9999
Apo $E^{-/-}$ x $OPG^{-/-}$	222.1 (±24.33)	97.47 (±40.19)	109.6 (±25.28)	0.0840	0.0734	>0.9999
P-value	>0.9999	>0.9999	>0.9999			

Next, we measured the mouse plasma for circulating markers that influence VC, alkaline phosphatase (ALP) and calcium (table 6.3.5.2). Saline treated Apo $E^{-/-}$ mice had significantly higher final ALP ($p<0.01$), final calcium ($p<0.0001$) and change in calcium since commencement of the atherogenic diet ($p<0.0001$) compared to the Apo $E^{-/-}$ x $OPG^{-/-}$ saline treated mice. Additionally, rHDL treated Apo $E^{-/-}$ mice also had significantly higher final calcium levels ($p<0.001$) and a higher change in calcium ($p<0.001$) than the Apo $E^{-/-}$ x $OPG^{-/-}$ mice. This shows that at the end of 40 weeks of atherogenic diet, but not at 36 weeks, the Apo $E^{-/-}$ x $OPG^{-/-}$ mice had significantly less circulating calcium, regardless of treatment.

The 36 week cohort of Apo $E^{-/-}$ mice had significantly less calcium than both the saline ($p<0.0001$) and rHDL ($p<0.0001$) treated mice. When examining the change in calcium levels since commencing the atherogenic diet, 36 week Apo $E^{-/-}$ mice had a significantly lower increase in calcium than Apo $E^{-/-}$ mice treated with rHDL ($p<0.01$). The 36 week cohort of Apo $E^{-/-}$ x $OPG^{-/-}$ mice had significantly higher ALP levels ($p<0.001$) and change in ALP ($p<0.001$) compared to the saline treated Apo $E^{-/-}$ x $OPG^{-/-}$ mice. In rHDL treated Apo $E^{-/-}$ x $OPG^{-/-}$ mice, there were significantly higher final calcium levels ($p<0.05$) than the saline treated Apo $E^{-/-}$ x $OPG^{-/-}$ mice. Overall, rHDL treatment did not appear to significantly change ALP or calcium levels, instead the amount of time on atherogenic diet and genotype of the mouse had the greater influence.

Table 6.3.5.2 Circulating plasma calcification markers in Apo $E^{-/-}$ and Apo $E^{-/-}$ x $OPG^{-/-}$ mice. *Mean (±SEM), 2-way-ANOVA, n=9-17.*

Final ALP (mmol/L)	Mean (±SEM)			P-Value		
	36 w	Saline (40w)	rHDL (40w)	36w vs. Saline	36w vs. rHDL	Saline vs. rHDL
Apo $E^{-/-}$	2.101 (±0.209)	2.364 (±0.204)	2.243 (±2.23)	>0.9999	>0.9999	>0.9999
Apo $E^{-/-}$ x $OPG^{-/-}$	2.505 (±0.158)	1.101 (±0.263)	1.888 (±0.169)	0.0001	0.5131	0.1121
P-value	>0.9999	0.0015	>0.9999			
ALP Change (mmol/L)	**Mean (±SEM)**			**P-Value**		
	36 w	Saline (40w)	rHDL (40w)	36w vs. Saline	36w vs. rHDL	Saline vs. rHDL
Apo $E^{-/-}$	1.017 (±0.223)	1.14 (±0.452)	1.389 (±0.23)	>0.9999	>0.9999	>0.9999
Apo $E^{-/-}$ x $OPG^{-/-}$	1.62 (±0.213)	0.031 (±0.306)	0.816 (±0.186)	0.0009	0.4379	0.4941
P-value	>0.9999	0.1005	>0.9999			
Final Calcium (µg/dl)	**Mean (±SEM)**			**P-Value**		
	36 w	Saline (40w)	rHDL (40w)	36w vs. Saline	36w vs. rHDL	Saline vs. rHDL
Apo $E^{-/-}$	4.81 (±0.621)	11.28 (±0.953)	9.768 (±0.74)	<0.0001	<0.0001	>0.9999
Apo $E^{-/-}$ x $OPG^{-/-}$	5.563 (±0.479)	2.805 (±0.8)	5.696 (±0.493)	0.0860	>0.9999	0.0434
P-value	>0.9999	<0.0001	0.0005			
Calcium Change (µg/dl)	**Mean (±SEM)**			**P-Value**		
	36 w	Saline (40w)	rHDL (40w)	36w vs. Saline	36w vs. rHDL	Saline vs. rHDL
Apo $E^{-/-}$	3.512 (±0.629)	6.831 (±1.348)	7.943 (±0.701)	0.0726	0.0015	>0.9999
Apo $E^{-/-}$ x $OPG^{-/-}$	4.341 (±0.588)	1.107 (±0.773)	3.419 (±0.583)	0.0557	>0.9999	0.4939
P-value	>0.9999	<0.0001	0.0007			

6.3.6 Body weight of mice at baseline and end of the study.

Mice were weighed at 8 weeks of age, immediately prior to commencing the atherogenic diet. There was observed difference in the initial weights between Apo $E^{-/-}$ and Apo $E^{-/-}$ x $OPG^{-/-}$ mice. At the end of the study we investigated any changes in weight in these mice due to time on diet, genotype or treatment received. Although no difference in the final weight or change in weight was observed in the 36 week cohort, upon completion of 40 weeks of atherogenic diet, Apo $E^{-/-}$ mice had significantly higher body weights (Saline: $p<0.01$; rHDL: $p<0.001$) and had gained significantly more weight (Saline: $p<0.001$; rHDL: $p<0.001$) than Apo $E^{-/-}$ x $OPG^{-/-}$ mice, regardless of treatment. Additionally, although there was no significant differences in weight gain between the 36 week Apo $E^{-/-}$ mice and the saline treated Apo $E^{-/-}$ mice, the rHDL treated Apo $E^{-/-}$ mice had gained significantly more weight than the 36 week Apo $E^{-/-}$ mice ($p<0.05$)(table 6.3.6.1).

As an initial investigation into potential changes in tissues caused by genotype or rHDL treatment, we weighed several tissues which can be influenced by lipoproteins or lipid levels and expressed them as a % of total final body weight. We observed that after 40 weeks of atherogenic diet, Apo $E^{-/-}$ mice had significantly larger epididymal (Saline: $p<0.0001$; rHDL: $P<0.01$) and retroperitoneal (Saline: $p<0.001$; rHDL $p<0.0001$) fat deposits compared to Apo $E^{-/-}$ x $OPG^{-/-}$ mice, regardless of treatment type. Additionally, Apo $E^{-/-}$ mice receiving saline had significantly heavier epidydimal fat deposits ($p<0.01$) compared to their 36 week counterparts, whereas the rHDL treated Apo $E^{-/-}$ did not. There were no other significant differences between any genotype or treatment when measuring the epidydimal fat, liver, spleen, kidney or retroperitoneal fat tissues (table 6.3.6.2).

Table 6.3.6.1 Final and change of weight in treated Apo $E^{-/-}$ and Apo $E^{-/-}$ x $OPG^{-/-}$ mice. *Mean (±SEM), 2-way-ANOVA, n=9-17.*

Initial Weight	**Mean (±SEM)**			**P-Value**		
Apo $E^{-/-}$	22.10 (±0.5303)					
Apo $E^{-/-}$ x $OPG^{-/-}$	21.12 (±0.5099)					
P-value	**0.1883**					
Final Weight	**Mean (±SEM)**			**P-Value**		
	36 w	Saline (40w)	rHDL (40w)	36w vs. Saline	36w vs. rHDL	Saline vs. rHDL
Apo $E^{-/-}$	39.99 (±1.44)	42.02 (±1.84)	42.54 (±2.45)	**>0.9999**	**>0.9999**	**>0.9999**
Apo $E^{-/-}$ x $OPG^{-/-}$	33.38 (±1.21)	32.53 (±0.9)	32.85 (1.32)	**>0.9999**	**>0.9999**	**>0.9999**
P-value	**0.1154**	**0.0017**	**0.0009**			
Weight Change	**Mean (±SEM)**			**P-Value**		
	36 w	Saline (40w)	rHDL (40w)	36w vs. Saline	36w vs. rHDL	Saline vs. rHDL
Apo $E^{-/-}$	15.12 (±1.62)	20.99 (±1.76)	21.97 (± 2.27)	**0.1256**	**0.0334**	**>0.9999**
Apo $E^{-/-}$ x $OPG^{-/-}$	12.09 (±0.88)	11.63 (±1.04)	11.67 (±0.98)	**>0.9999**	**>0.9999**	**>0.9999**
P-value	**>0.9999**	**0.0009**	**0.0001**			

Table 6.3.6.2 Tissue weights in treated Apo $E^{-/-}$ and Apo $E^{-/-}$ x $OPG^{-/-}$ mice. *% of total body weight, Mean (±SEM), 2-way-ANOVA, n=9-17.*

% Epididymal Fat	Mean (±SEM)			P-Value		
	36 w	Saline (40w)	rHDL (40w)	36w vs. Saline	36w vs. rHDL	Saline vs. rHDL
Apo $E^{-/-}$	1.65 (±0.14)	2.60 (±0.23)	2.20 (±0.19)	0.0014	0.2948	>0.9999
Apo $E^{-/-}$ x $OPG^{-/-}$	0.48 (±0.05)	0.46 (±0.06)	0.43 (±0.06)	>0.9999	>0.9999	>0.9999
P-value	>0.9999	<0.0001	0.0013			
% Liver	Mean (±SEM)			P-Value		
	36 w	Saline (40w)	rHDL (40w)	36w vs. Saline	36w vs. rHDL	Saline vs. rHDL
Apo $E^{-/-}$	8.03 (±0.73)	6.46 (±0.60)	6.62 (±0.45)	0.3297	0.5799	>0.9999
Apo $E^{-/-}$ x $OPG^{-/-}$	7.09 (±0.25)	6.81 (±0.34)	6.50 (±0.26)	>0.9999	0.4539	>0.9999
P-value	>0.9999	>0.9999	>0.9999			
% Spleen	Mean (±SEM)			P-Value		
	36 w	Saline (40w)	rHDL (40w)	36w vs. Saline	36w vs. rHDL	Saline vs. rHDL
Apo $E^{-/-}$	0.51 (±0.06)	0.5 (±0.07)	0.47 (±0.04)	>0.9999	>0.9999	>0.9999
Apo $E^{-/-}$ x $OPG^{-/-}$	0.41 (±0.02)	0.50 (±0.05)	0.43 (±0.03)	>0.9999	>0.9999	>0.9999
P-value	>0.9999	>0.9999	>0.9999			
% Kidney	Mean (±SEM)			P-Value		
	36 w	Saline (40w)	rHDL (40w)	36w vs. Saline	36w vs. rHDL	Saline vs. rHDL
Apo $E^{-/-}$	0.49 (±0.02)	0.49 (± 0.03)	0.51 (±0.04)	>0.9999	>0.9999	>0.9999
Apo $E^{-/-}$ x $OPG^{-/-}$	0.54 (±0.02)	0.56 (±0.02)	0.59 (±0.02)	>0.9999	>0.9999	>0.9999
P-value	>0.9999	>0.9999	0.5258			
% Retroperitoneal Fat	Mean (±SEM)			P-Value		
	36 w	Saline (40w)	rHDL (40w)	36w vs. Saline	36w vs. rHDL	Saline vs. rHDL
Apo $E^{-/-}$	1.44 (±0.25)	2.03 (±0.22)	2.19 (±0.27)	0.5500	0.1260	>0.9999
Apo $E^{-/-}$ x $OPG^{-/-}$	0.82 (±0.12)	0.81 (±0.13)	0.76 (±0.11)	>0.9999	>0.9999	>0.9999
P-value	0.5369	0.0007	<0.0001			

6.3.7 The Effects of rHDL Infusions on Arterial Plaque Characteristics

In Apo $E^{-/-}$ mice it is well established that rHDL infusions does not reduce plaque size in late stage atherosclerotic mice[807-809], however there is little information regarding the effects of infusion on plaque stabilisation. Culprit plaques, causing heart attack, stroke and tissue ischemia, arise from highly unstable plaques, therefore discovering therapies to increase stability will result in fewer cardiovascular mortalities while patients work towards plaque size reduction. We show in figure 6.3.7.1, consistent with the literature, that rHDL infusions has no effect on late stage plaque size in Apo $E^{-/-}$ mice. We additionally find that rHDL does not reduce plaque size in Apo $E^{-/-}$ x $OPG^{-/-}$ mice. While plaque size was generally larger in Apo $E^{-/-}$ x $OPG^{-/-}$ mice compared to Apo $E^{-/-}$ mice, this comparison was only significant in the 36 week cohort mice (133493±15095 vs 204551±14324, $p<0.01$).

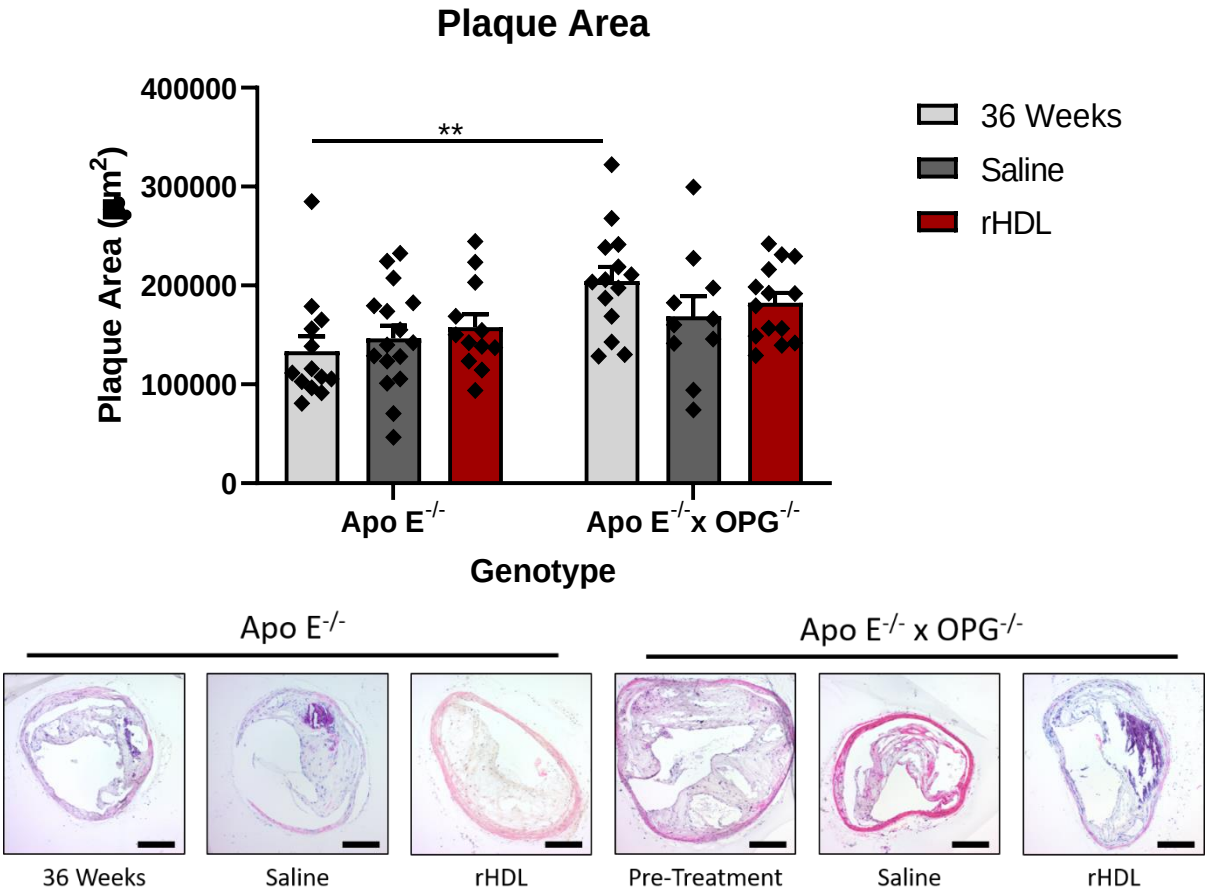

Figure 6.3.7.1 The effect of rHDL on atherosclerotic plaque area.

*8 week old Apo E$^{-/-}$ and Apo E$^{-/-}$ x OPG$^{-/-}$ mice were fed an atherogenic diet for 36-40 weeks. Mice on the AD for 40 weeks received either saline or 20 mg/kg rHDL infusions 3x per week until completion of the study (4 weeks of treatment total). Tissues were collected post cardiac puncture and saline flush in 10% buffered formalin and embedded in paraffin. Arteries were sectioned at 5μm thickness and stained with H&E from sigma as per protocol. Images were captured using a Zeiss Axio Lab A.1 microscope with a Zeiss AxioCam ERc 5s camera and analysed using image J software. **p<0.01, 2-Way-ANOVA. Data represented as mean± SEM, n=10-16. Representative images are displayed below.*

One major focus of this thesis is to investigate the ability of rHDL in plaque stabilisation, specifically through effects on plaque calcification. Here in figure 6.3.7.2 we show the % of total plaque calcification, % of calcification in the fibrous cap and the number (#) of calcifications at these plaque sites in the brachiocephalic artery (BCA). Because calcifications can be macro ('sheet like') or micro ('spotty'), the number of calcifications at a site gives insight into plaque instability. Likewise, calcification measured in the fibrous cap area are hypothesised to influence plaque instability[282, 284, 492, 810].

In figure 6.3.7.2 we show that treatment or genotype has no influence over total BCA plaque % calcification (A), however saline (24.46±9.064 vs 92.0±30.52, $p<0.05$) and rHDL (24.46±9.064 vs 83.85±18.43, $p<0.05$) treated Apo $E^{-/-}$ x $OPG^{-/-}$ mice have significantly more calcifications than the 36 week cohort of Apo $E^{-/-}$ x $OPG^{-/-}$ mice (C). Additionally, while the Apo $E^{-/-}$ x $OPG^{-/-}$ mice on an atherogenic diet for 40 weeks had a greater number of calcifications than the Apo $E^{-/-}$ mice, this was only significant when comparing the saline treated mice (20.64±5.59 vs 92.0±30.52, $p<0.05$). This shows that although the total % of calcification in these mice are the same, the Apo $E^{-/-}$ x $OPG^{-/-}$ mice fed an atherogenic diet for 40 weeks had a spottier calcification phenotype, regardless of treatment.

When observing the levels of BCA plaque cap calcification, Apo $E^{-/-}$ x $OPG^{-/-}$ mice treated with saline had a significantly higher percentage of cap calcification (B)(0.03±0.013 vs 3.015±1.53, $p<0.05$) and number of cap calcifications (D)(1.0±0.34 vs 10.9±3.46, $p<0.05$) than the Apo $E^{-/-}$ saline treated mice. rHDL treated Apo $E^{-/-}$ x $OPG^{-/-}$ mice also had significantly more cap calcifications than the 36 week Apo $E^{-/-}$ x $OPG^{-/-}$ mice (1.25±0.63 vs 8.46±2.5, $p<0.05$), showing that Apo $E^{-/-}$ x $OPG^{-/-}$ mice fed an atherogenic diet for 40 weeks also have more cap calcifications than the other mice.

Figure 6.3.7.2 The effect of rHDL on brachiocephalic artery plaque and cap calcification.

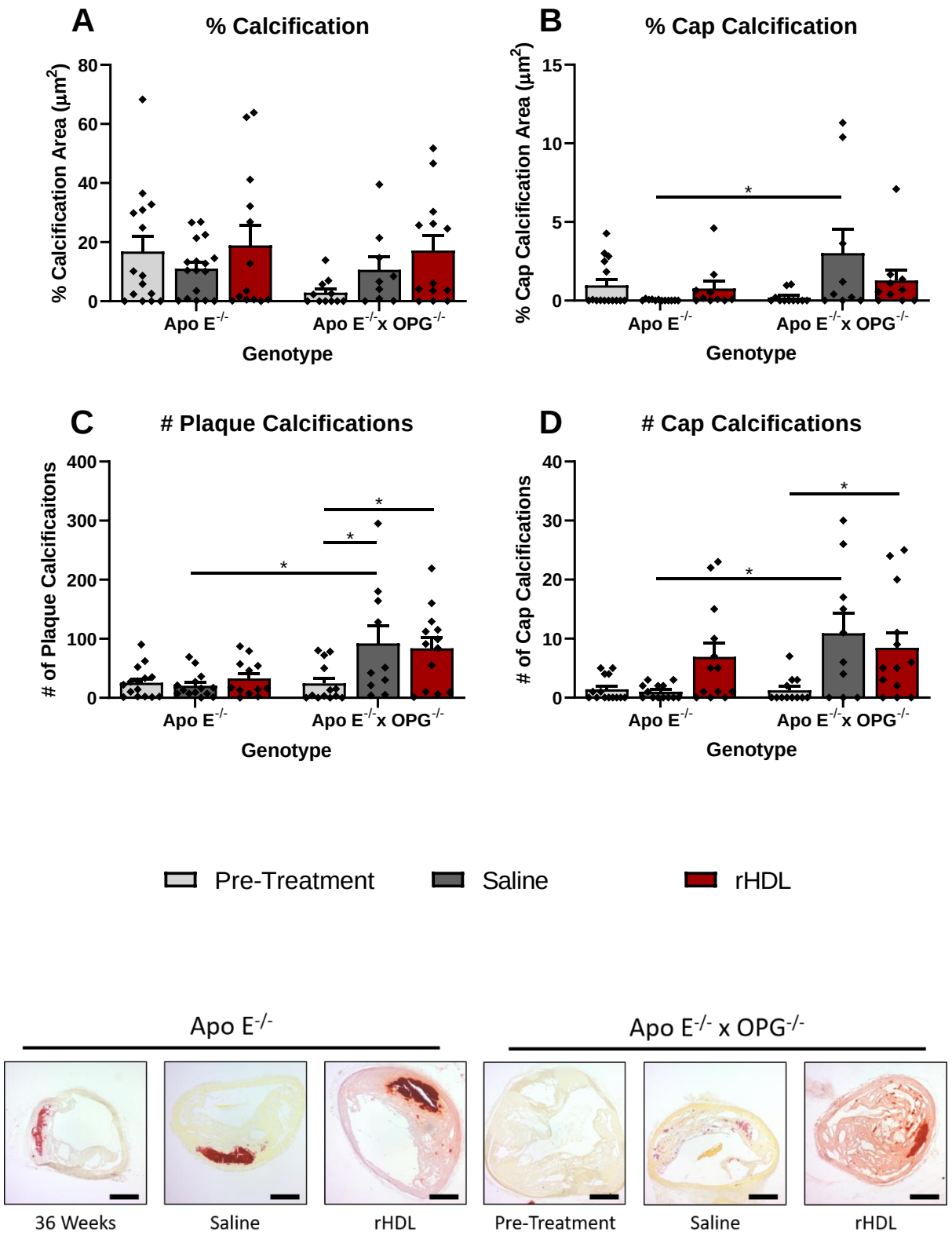

Figure 6.3.7.2 The effect of rHDL on brachiocephalic artery plaque and cap calcification.

*8 week old Apo E$^{-/-}$ and Apo E$^{-/-}$ x OPG$^{-/-}$ mice were fed an atherogenic diet for 36-40 weeks. Mice on the AD for 40 weeks received either saline or 20 mg/kg rHDL infusions 3x per week until completion of the study (4 weeks of treatment total). Tissues were collected post cardiac puncture and saline flush in 10% buffered formalin and embedded in paraffin. Arteries were sectioned at 5µm thickness and stained with H&E from sigma as per protocol. Images were captured using a Zeiss Axio Lab A.1 microscope with a Zeiss AxioCam ERc 5s camera and analysed using image J software. *p<0.05, 2-Way-ANOVA. Data represented as mean± SEM, n=9-17. Representative images are displayed beneath respective bars.*

To continue our measurements into BCA plaque stability, we used Masson's, H&E and immunohistochemical staining to identify BCA plaque characteristics as shown in table 6.3.7.1. The medial area of a plaque identifies the level of arterial thickening and VSMC expansion, leading to increased plaque vulnerability. Generally, the Apo $E^{-/-}$ mice had larger medial areas than the Apo $E^{-/-}$ x $OPG^{-/-}$ mice, however this was only significant between the saline treated mice ($p<0.01$).

The % of collagen within a plaque indicates plaque stability, with plaques containing higher levels of collagen being more stable. Saline treated Apo $E^{-/-}$ mice had a significantly higher % of BCA plaque collagen levels than saline treated Apo $E^{-/-}$ x $OPG^{-/-}$ mice ($p<0.01$). Additionally, the 36 week cohort of Apo $E^{-/-}$ mice had a significantly lower % of BCA plaque collagen than the saline ($p<0.0001$) or rHDL (<0.0001) treated Apo $E^{-/-}$ mice, showing an increase in BCA plaque stability over time, regardless of treatment. Interestingly, the Apo $E^{-/-}$ x $OPG^{-/-}$ did not show the same improvements.

The presence of chondrocytes in a plaque indicate that initiation of calcification. Here in table 6.3.7.1 we show that although the Apo $E^{-/-}$ mice have increased chondrocytes per mm^2 of BCA plaque, particularly after 40 weeks of atherogenic diet, compared to the Apo $E^{-/-}$ x $OPG^{-/-}$ mice, this comparison only reached significance in the saline treated mice ($p<0.05$). Although chondrocytes are precursors to plaque calcification, it is unclear whether these cells promote macro or micro calcifications and the resulting effect on plaque stability.

The amount of CD68 present in a plaque indicates the level of macrophage infiltration, and therefore plaque instability. Here we see no effect of genotype or treatment on the % of CD68 in the BCA plaques of these mice.

The % of SMαActin present in a plaque represents the amount of VSMC migration. After the VSMCs have migrated into the plaque, they may form new vascular layers, differentiate into macrophages, differentiate into chondrocytes or differentiate into a myriad of other mixtures of cell types. It is therefore an indication of plaque instability to have VSMC migration into the plaque. Here in table 6.3.7.1 we show that in the Apo $E^{-/-}$ 36 week mice there was a significantly higher % of SMαActin in the BCA plaques than in the 36 week pre-treatment Apo $E^{-/-}$ x $OPG^{-/-}$ mice ($p<0.05$). This significance between genotypes was lost in both saline and rHDL treatments after the 40 weeks of atherogenic diet, potentially due to the VSMCs losing their SMαActin expressing phenotype. Additionally, this data may suggest that VSMC migration occurs earlier in Apo $E^{-/-}$ x $OPG^{-/-}$ mice, causing the initial significant difference to the Apo $E^{-/-}$ mice in the 36 week groups.

This hypothesis may be further supported by the 36 week cohort of Apo $E^{-/-}$ mice showing a significantly higher % of BCA plaque SMαActin than the saline ($p<0.05$) or rHDL ($p<0.05$) treated Apo $E^{-/-}$ mice. This pattern of reduction in SMαActin staining may suggest that the Apo $E^{-/-}$ mouse BCA plaques have differentiating VSMCs between the 36 week and 40 week timepoints and that this differentiation is not affected by rHDL treatment.

Taken together, the data presented in table 6.3.7.1 suggests that the BCA plaques of Apo $E^{-/-}$ mice are generally more stable than the Apo $E^{-/-}$ x $OPG^{-/-}$ mice, and increase in stability over time on the atherogenic diet unlike the Apo $E^{-/-}$ x $OPG^{-/-}$ mice.

Table 6.3.7.1 BCA plaque characteristics in treated Apo $E^{-/-}$ and Apo $E^{-/-}$ x $OPG^{-/-}$ mice. *Mean (±SEM), 2-way-ANOVA, n=9-17.*

Medial Area (µm²)	Mean (±SEM)			P-Value		
	36 w	Saline (40w)	rHDL (40w)	36w vs. Saline	36w vs. rHDL	Saline vs. rHDL
Apo $E^{-/-}$	70104 (±5221)	88099 (±8163)	75673 (±7405)	0.5692	>0.9999	>0.9999
Apo $E^{-/-}$ x $OPG^{-/-}$	65407 (±4247)	52573 (±6338)	61160 (±4423)	>0.9999	>0.9999	>0.9999
P-value	>0.9999	0.0036	>0.9999			
% Collagen (µm²)	**Mean (±SEM)**			**P-Value**		
	36 w	Saline (40w)	rHDL (40w)	36w vs. Saline	36w vs. rHDL	Saline vs. rHDL
Apo $E^{-/-}$	31.44 (±3.055)	59.17 (±2.396)	49.4 (±1.979)	<0.0001	<0.0001	0.0629
Apo $E^{-/-}$ x $OPG^{-/-}$	40.56 (±1.963)	45.61 (±2.99)	45.12 (±2.28)	>0.9999	>0.9999	>0.9999
P-value	0.1852	0.0057	>0.9999			
Chondrocytes per mm² Plaque	**Mean (±SEM)**			**P-Value**		
	36 w	Saline (40w)	rHDL (40w)	36w vs. Saline	36w vs. rHDL	Saline vs. rHDL
Apo $E^{-/-}$	337.4 (±44.05)	558.8 (±82.53)	465.5 (±52.98)	0.1361	>0.9999	>0.9999
Apo $E^{-/-}$ x $OPG^{-/-}$	321.1 (±48.02)	268.9 (±85.8)	208.6 (±40.13)	>0.9999	>0.9999	>0.9999
P-value	>0.9999	0.0318	0.0630			
% CD68 Area (µm²)	**Mean (±SEM)**			**P-Value**		
	36 w	Saline (40w)	rHDL (40w)	36w vs. Saline	36w vs. rHDL	Saline vs. rHDL
Apo $E^{-/-}$	16.22 (±1.965)	14.45 (±1.568)	13.51 (±1.773)	>0.9999	>0.9999	>0.9999
Apo $E^{-/-}$ x $OPG^{-/-}$	18.08 (±1.72)	12.47 (±1.68)	13.47 (±1.95)	0.6140	>0.9999	>0.9999
P-value	>0.9999	>0.9999	>0.9999			
% SMαActin Area (µm²)	**Mean (±SEM)**			**P-Value**		
	36 w	Saline (40w)	rHDL (40w)	36w vs. Saline	36w vs. rHDL	Saline vs. rHDL
Apo $E^{-/-}$	5.598 (±1.298)	2.363 (±0.5309)	2.101 (±0.5737)	0.0303	0.0209	>0.9999
Apo $E^{-/-}$ x $OPG^{-/-}$	1.937 (±0.5261)	1.462 (±0.459)	1.859 (±0.645)	>0.9999	>0.9999	>0.9999
P-value	0.0101	>0.9999	>0.9999			

6.3.8 The Effects of rHDL Infusions on Aortic Root Plaque Characteristics

In 6.3.7, we show the effects of rHDL infusions and global OPG$^{-/-}$ on brachiocephalic plaque characteristics of Apo E$^{-/-}$ and Apo E$^{-/-}$ x OPG$^{-/-}$ mice. Next, we investigated the plaque characteristics of the atherosclerotic aortic root leaflets (AR). While there are many similarities between plaques of the two sites, plaque development at this site have increased susceptibility to fibrosis and calcification. To get a more complete picture of the effects of rHDL and global OPG$^{-/-}$ on plaque calcification and stability, were therefore repeated the staining and analysis in the AR of these mice. We show in figure 6.8.3.1, consistent with the literature, that rHDL infusions has no effect on late stage plaque size in the ARs of Apo E$^{-/-}$ mice. We additionally find that rHDL has no effect on AR plaque size in Apo E$^{-/-}$ x OPG$^{-/-}$ mice and that AR plaque sizes between the two genotypes are statistically similar (figure 6.3.8.1).

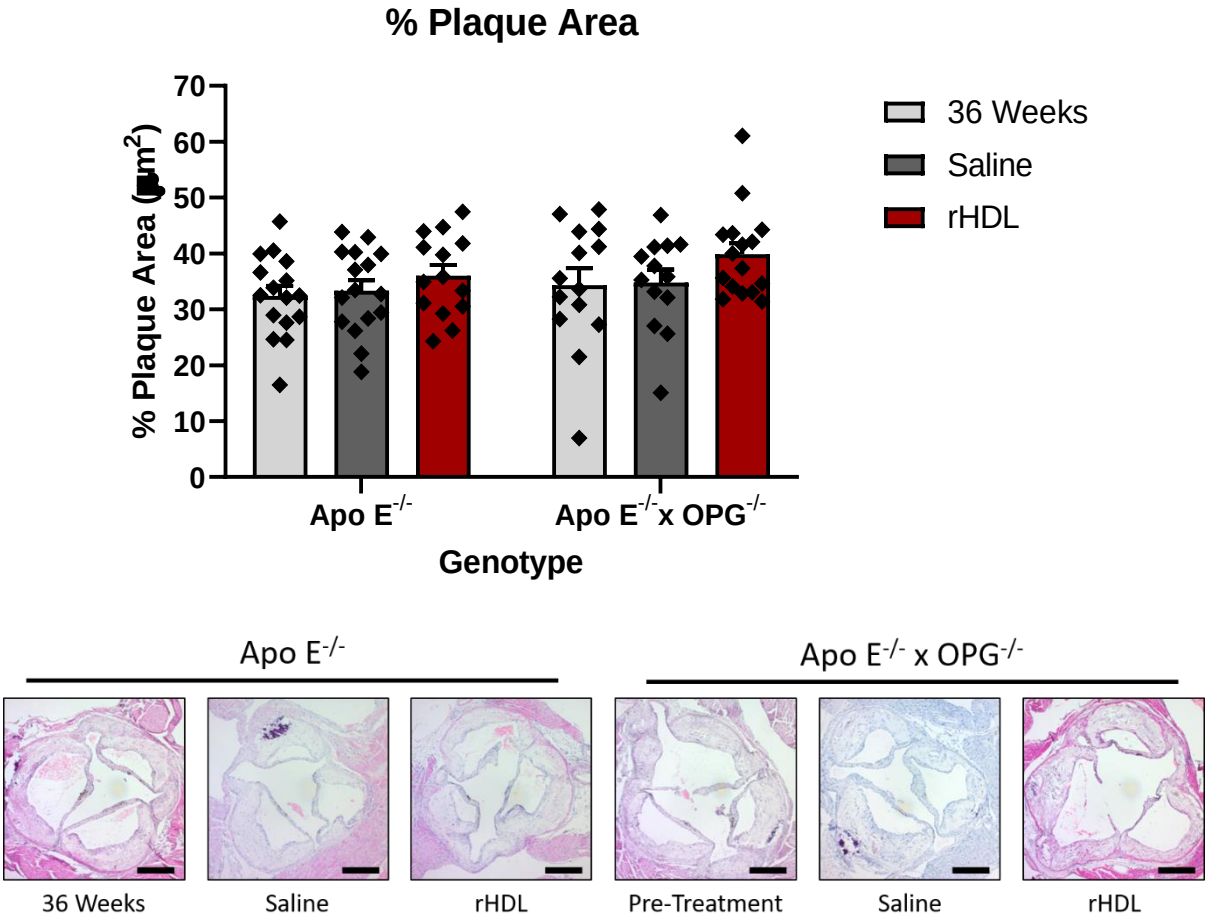

Figure 6.3.8.1 The effect of rHDL on aortic root atherosclerotic plaque area.

8 week old Apo E$^{-/-}$ and Apo E$^{-/-}$ x OPG$^{-/-}$ mice were fed an atherogenic diet for 36-40 weeks. Mice on the AD for 40 weeks received either saline or 20 mg/kg rHDL infusions 3x per week until completion of the study (4 weeks of treatment total). Tissues were collected post cardiac puncture and saline flush in 10% buffered formalin and embedded in paraffin. Arteries were sectioned at 5μm thickness and stained with H&E from sigma as per protocol. Images were captured using a Zeiss Axio Lab A.1 microscope with a Zeiss AxioCam ERc 5s camera and analysed using image J software. 2-Way-ANOVA. Data represented as mean± SEM, n=10-16. Representative images are displayed beneath respective bars.

The AR plaques of Apo $E^{-/-}$ x $OPG^{-/-}$ mice had a significantly higher % of plaque calcification than Apo $E^{-/-}$ mice (36 w: 0.36±0.11 vs 9.4±1.41, $p<0.05$; Saline: 2.19±1.26 vs 18.92±2.43, $p<0.01$; rHDL: 4.28±1.26 vs 14.79±3.09, $p<0.01$) (A) and after 40 weeks of atherogenic diet had significantly more calcifications in the total plaque area (Saline: 171.4±34.81 vs 450.1±70.21, $p<0.01$; rHDL: 224.0±45.91 vs 423.8±76.76, $p<0.05$) regardless of treatment (C). Additionally, Apo $E^{-/-}$ x $OPG^{-/-}$ mice fed an atherogenic diet for 40 weeks had a significantly higher % of cap calcification (Saline: 0.12±0.04 vs 0.96±0.22, $p<0.01$; rHDL: 0.11±0.03 vs 0.74±0.21, $p<0.05$) than Apo $E^{-/-}$ mice, regardless of treatment (B) and rHDL treated Apo $E^{-/-}$ x $OPG^{-/-}$ mice had a significantly higher number of cap calcifications (4.2±1.15 vs 18.13±4.39, $p<0.05$) than Apo $E^{-/-}$ rHDL treated mice (D).

Altogether, the data in figure 6.3.8.2 shows that the Apo $E^{-/-}$ x $OPG^{-/-}$ mice on an atherogenic diet for 40 weeks had a higher % of AR plaque or cap calcification and a higher number of plaque or cap calcifications than their Apo $E^{-/-}$ counterparts, regardless of treatment. This data in figure 6.3.8.2 suggests that the Apo $E^{-/-}$ x $OPG^{-/-}$ mice fed an atherogenic diet have many micro calcifications and therefore have decreased AR plaque stability.

Figure 6.3.8.2 The effect of rHDL on aortic root plaque and cap calcification.

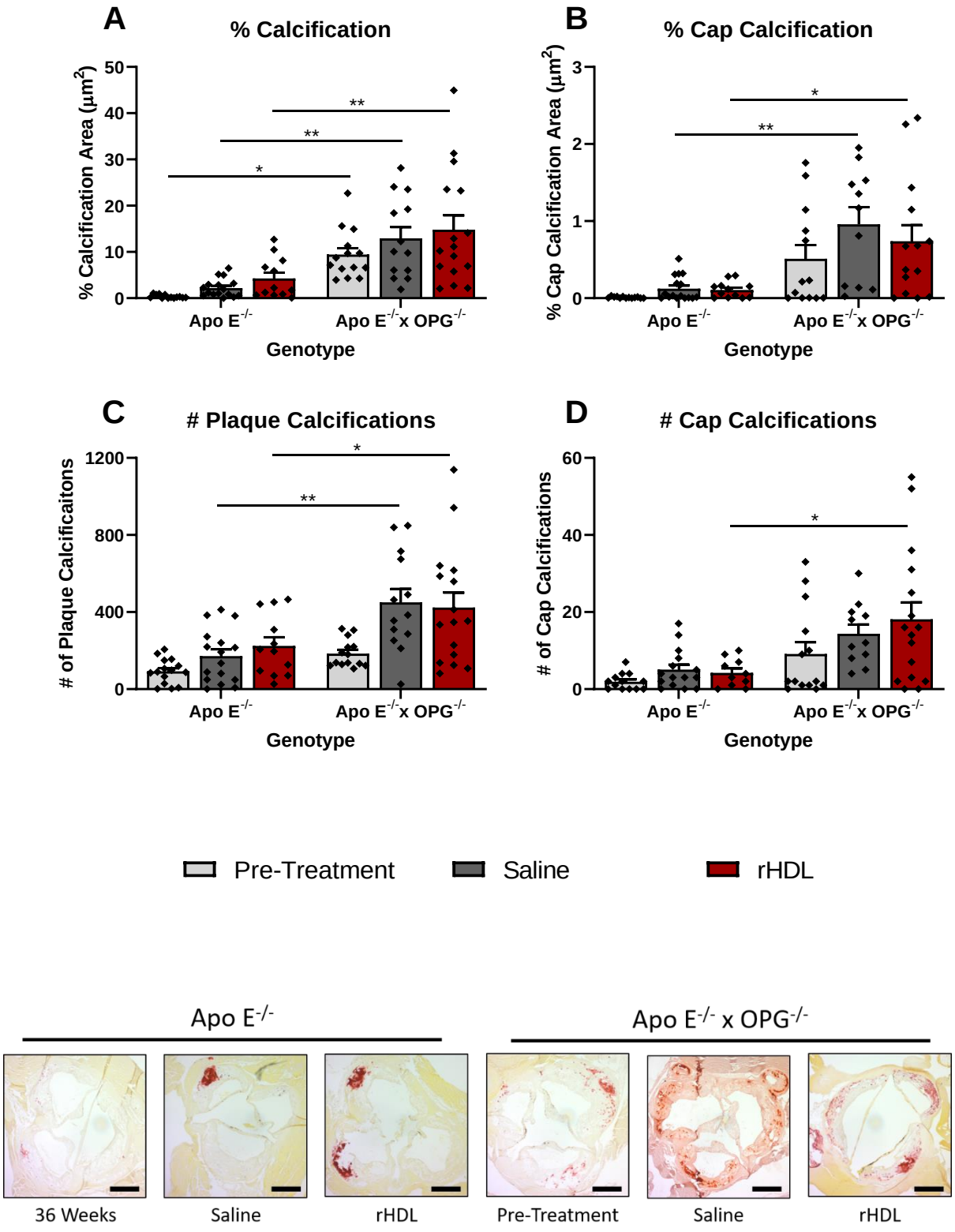

Figure 6.3.8.2 The effect of rHDL on aortic root plaque and cap calcification.

*8 week old Apo E$^{-/-}$ and Apo E$^{-/-}$ x OPG$^{-/-}$ mice were fed an atherogenic diet for 36-40 weeks. Mice on the AD for 40 weeks received either saline or 20 mg/kg rHDL infusions 3x per week until completion of the study (4 weeks of treatment total). Tissues were collected post cardiac puncture and saline flush in 10% buffered formalin and embedded in paraffin. Arteries were sectioned at 5µm thickness and stained with H&E from sigma as per protocol. Images were captured using Zeiss Axio Lab A.1 microscope with a Zeiss AxioCam ERc 5s camera and analysed using image J software. *p<0.05, **p<0.01, 2-Way-ANOVA. Data represented as mean± SEM, n=9-17. Representative images are displayed beneath respective bars.*

In continuing our assessment of AR plaque characteristics, AR sections were stained with Masson's, H&E or immunohistochemically to identify markers of instability. In table 6.3.8.1 we show that after 40 weeks of atherogenic diet, regardless of treatment, Apo $E^{-/-}$ have a significantly larger medial area than Apo $E^{-/-}$ x $OPG^{-/-}$ mice (Saline: $p<0.001$; rHDL $p<0.05$). Additionally, Apo $E^{-/-}$ had more chondrocytes per mm^2 of AR plaque than Apo $E^{-/-}$ x $OPG^{-/-}$ mice after 36 weeks of atherogenic diet ($p<0.01$). There were no other significant differences between Apo $E^{-/-}$ and Apo $E^{-/-}$ x $OPG^{-/-}$ mice.

36 week Apo $E^{-/-}$ had significantly less chondrocytes per mm^2 of AR plaque ($p<0.05$) and a significantly higher % of SMαActin in AR plaques ($p<0.05$) than saline treated Apo $E^{-/-}$ mice. Additionally, 36 week pre-treatment Apo $E^{-/-}$ x $OPG^{-/-}$ mice had a significantly higher % of SMαActin in their AR plaques than the saline treated Apo $E^{-/-}$ x $OPG^{-/-}$ mice ($p<0.05$). Neither saline nor rHDL treatments had any other significant effects in these mice. This is consistent with the SMαActin data from table 6.3.8.1 showing a decline in SMαActin over time, potentially due to the differentiation of the VSMC into other cell types.

Here in table 6.3.8.1 we show that although after 40 weeks of atherogenic diet Apo $E^{-/-}$ mice have a significantly larger AR medial area than Apo $E^{-/-}$ x $OPG^{-/-}$ mice, there are no other differing factors between genotypes in plaque stability measures at this timepoint. We also show no effect of rHDL on the stability of AR plaques in these mice.

Table 6.3.8.1 AR plaque characteristics in treated Apo $E^{-/-}$ and Apo $E^{-/-}$ x $OPG^{-/-}$ mice. *Mean (±SEM), 2-way-ANOVA, n=9-17.*

Medial Area (µm²)	Mean (±SEM)			P-Value		
	36 w	Saline (40w)	rHDL (40w)	36w vs. Saline	36w vs. rHDL	Saline vs. rHDL
Apo $E^{-/-}$	230983 (±10698)	284571 (±19090)	257294 (±17995)	0.1298	>0.9999	>0.9999
Apo $E^{-/-}$ x $OPG^{-/-}$	232990 (±16364)	187283 (±12170)	182108 (±8240)	0.6171	0.3200	>0.9999
P-value	>0.9999	0.0002	0.0116			
% Collagen (µm²)	**Mean (±SEM)**			**P-Value**		
	36 w	Saline (40w)	rHDL (40w)	36w vs. Saline	36w vs. rHDL	Saline vs. rHDL
Apo $E^{-/-}$	28.42 (±2.212)	26.65 (±2.509)	27.47 (±1.801)	>0.9999	>0.9999	>0.9999
Apo $E^{-/-}$ x $OPG^{-/-}$	33.45 (±2.964)	30.0 (±2.964)	32.39 (±1.714)	>0.9999	>0.9999	>0.9999
P-value	>0.9999	>0.9999	>0.9999			
Chondrocytes per mm² Plaque	**Mean (±SEM)**			**P-Value**		
	36 w	Saline (40w)	rHDL (40w)	36w vs. Saline	36w vs. rHDL	Saline vs. rHDL
Apo $E^{-/-}$	1.103 (±0.764)	2.217 (±1.698)	3.736 (±1.885)	0.0490	0.3463	>0.9999
Apo $E^{-/-}$ x $OPG^{-/-}$	0.4277 (±0.3098)	1.366 (±0.9612)	1.446 (±0.5497)	>0.9999	>0.9999	>0.9999
P-value	0.0054	>0.9999	>0.9999			
% CD68 Area (µm²)	**Mean (±SEM)**			**P-Value**		
	36 w	Saline (40w)	rHDL (40w)	36w vs. Saline	36w vs. rHDL	Saline vs. rHDL
Apo $E^{-/-}$	12.36 (±1.661)	6.39 (±1.81)	13.01 (±3.557)	>0.9999	>0.9999	>0.9999
Apo $E^{-/-}$ x $OPG^{-/-}$	19.56 (±1.673)	14.1 (±1.82)	16.38 (±3.244)	>0.9999	>0.9999	>0.9999
P-value	0.2606	0.5740	>0.9999			
% SMαActin Area (µm²)	**Mean (±SEM)**			**P-Value**		
	36 w	Saline (40w)	rHDL (40w)	36w vs. Saline	36w vs. rHDL	Saline vs. rHDL
Apo $E^{-/-}$	2.162 (±0.4245)	0.5929 (±1479)	1.101 (±0.2595)	0.0181	0.3861	>0.9999
Apo $E^{-/-}$ x $OPG^{-/-}$	1.72 (±0.5939)	0.1991 (±0.0695)	0.3514 (±0.1238)	0.0483	0.0985	>0.9999
P-value	>0.9999	>0.9999	>0.9999			

6.3.9 The Effects of rHDL Infusions on the Expression of Aortic Calcification Markers

To begin assessing links between calcification at sites in these mice, we measured their aortas for mRNA expression of the calcification genes Runx2, RANKL, ALP and OPG. Interestingly, the Apo $E^{-/-}$ x $OPG^{-/-}$ mice treated with rHDL had significantly higher aortic ALP and OPG mRNA expression than their 36 week cohort (ALP: 118.4±21.96 vs 352.2±80.0, $p<0.001$; OPG: 95.81±23.39 vs 258.2±62.65, $p<0.05$), saline (ALP: 124.7±23.09 vs 352.2±80.0, $p<0.01$; OPG: 80.7±16.27 vs 258.2±62.65, $p<0.05$) and rHDL treated Apo $E^{-/-}$ (ALP: 69.82±16.68 vs 352.2±80.0, $p<0.0001$; OPG: 113.0±20.27 vs 258.2±62.65, $p<0.05$) counterparts (figure 6.3.9.1). This suggests that while there may be higher levels of calcification in this group, the cells are actively trying to counteract this. Because these mice are OPG deficient, the mRNA expression here does not translate into protein expression as shown via ELISA (appendix 1, chapter 9.1).

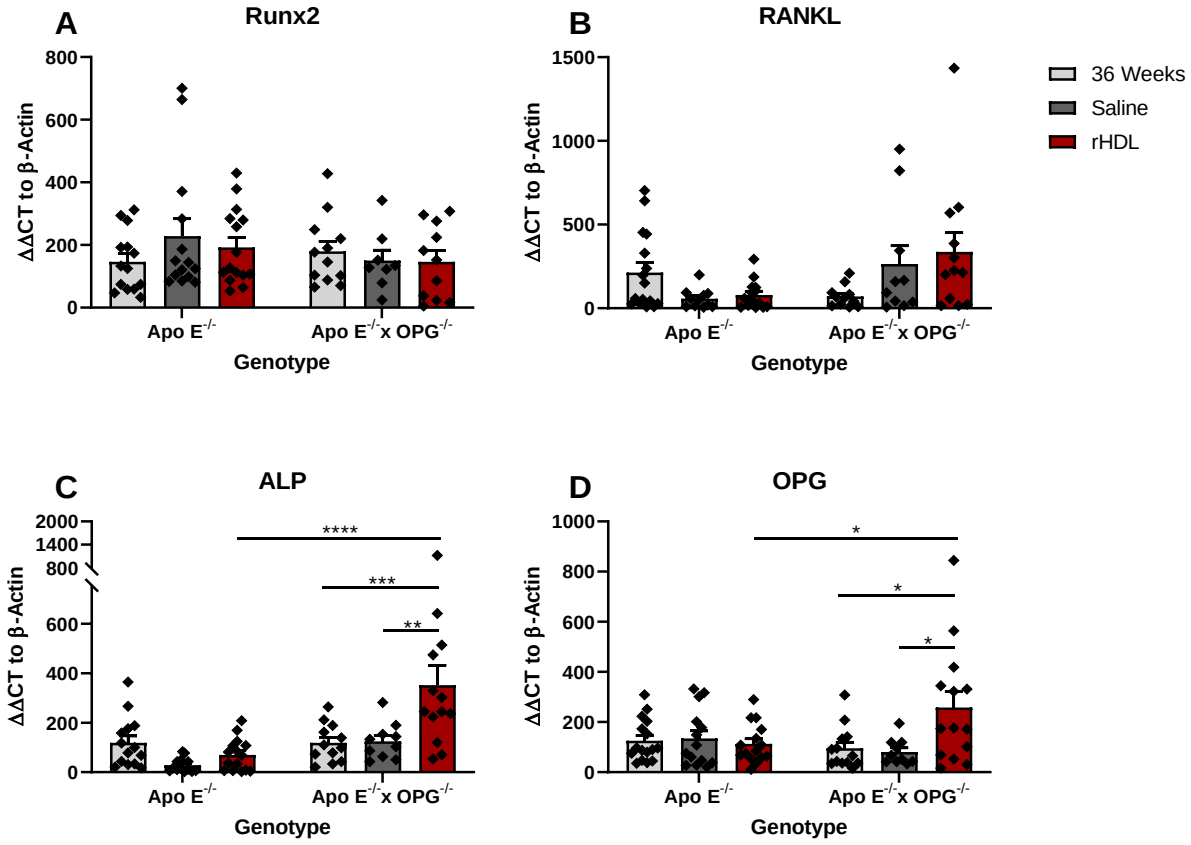

Figure 6.3.9.1 The effect of rHDL on aortic calcification gene expression.

8 week old Apo E$^{-/-}$ and Apo E$^{-/-}$ x OPG$^{-/-}$ mice were fed an atherogenic diet for 36-40 weeks. Mice on the AD for 40 weeks received either saline or 20 mg/kg rHDL infusions 3x per week until completion of the study (4 weeks of treatment total). Mice were euthanised via cardiac puncture and flushed with sterile saline before the collection of tissues. Aortas were snap frozen in $N_{2(l)}$ and RNA was extracted using an AllPrep DNA/RNA/Protein Mini Kit (Qiagen). mRNA expression of Runx2 (A), RANKL (B), ALP (C) and OPG (D) was measured by qPCR using β-Actin as the internal control and expressed as % expression of Apo E$^{-/-}$ pre-treated mice. 2-way-ANOVA. Data represented as mean± SEM, n=8-16.

6.3.10 Correlations Between Apo E$^{-/-}$ and Apo E$^{-/-}$ x OPG$^{-/-}$ Mouse Plasma and Tissue

To investigate potential relationships between the plaques in the brachiocephalic artery (BCA) and aortic root leaflet (AR) we performed Pearson's correlations between the sites for plaque size, plaque calcification (VC) % and the number of calcifications (VC) within these plaques, regardless of mouse genotype or treatment group (figure 6.3.10.1). Although we identified no relationships between plaque area (A) or % of plaque VC (B), there was a significant positive correlation between the number of plaques in the BCA and the AR (C: r=0.375, p<0.001). This suggests that although plaque size or % VC are not correlated the morphology of the plaque may be linked.

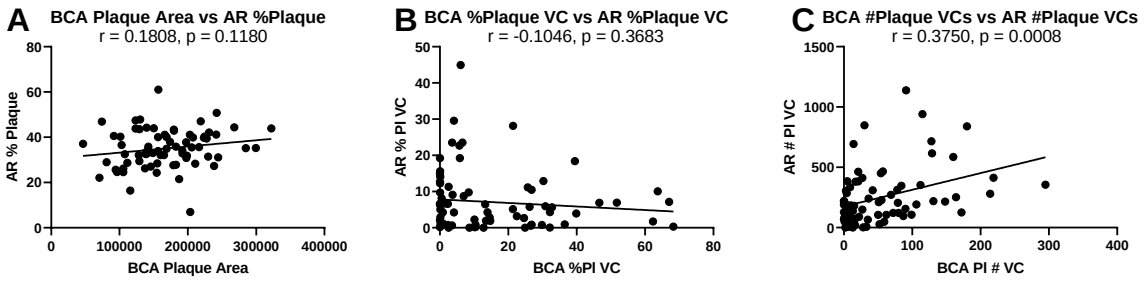

Figure 6.3.10.1 The correlations between BCA and AR in plaque volume, % VC or # of VC.

Pearson's correlation between brachiocephalic artery (BCA) and aortic root (AR) in plaque volume, % vascular calcification (VC) or # of VCs. Data represented as exact values (μm^2) per mouse, n=76-77.

To further examine the relationship between the % of plaque VC and other circulating calcification markers, we calculated a correlation matrix between the % of BCA or of AR plaque VC and final levels of total cholesterol, triglycerides, ALP or calcium (figure 6.3.10.2). We see here that although there were no significant correlations between plasma markers and the % of BCA plaque VC, there was a significant negative correlation between final total cholesterol levels and the % of VC in the AR plaques of these mice ($r=-0.256$, $p<0.05$). Additionally, there were significant positive correlations between final triglyceride levels and final total cholesterol ($r=0.3711$, $p<0.01$), final calcium ($r=0.4221$, $p<0.001$) and final ALP ($r=0.4572$, $p<0.0001$) levels. There was also a significant positive correlation between calcium and ALP levels in these mice ($r=6028$, $p<0.0001$).

Figure 6.3.10.2 altogether suggests that in this population of advanced atherosclerotic mice, regardless of genotype or treatment group, only total cholesterol and % of VC in the AR plaques were correlated. Triglycerides however were significantly correlated with other plasma calcification markers, similarly to the data presented previously in chapters 4 and 5.

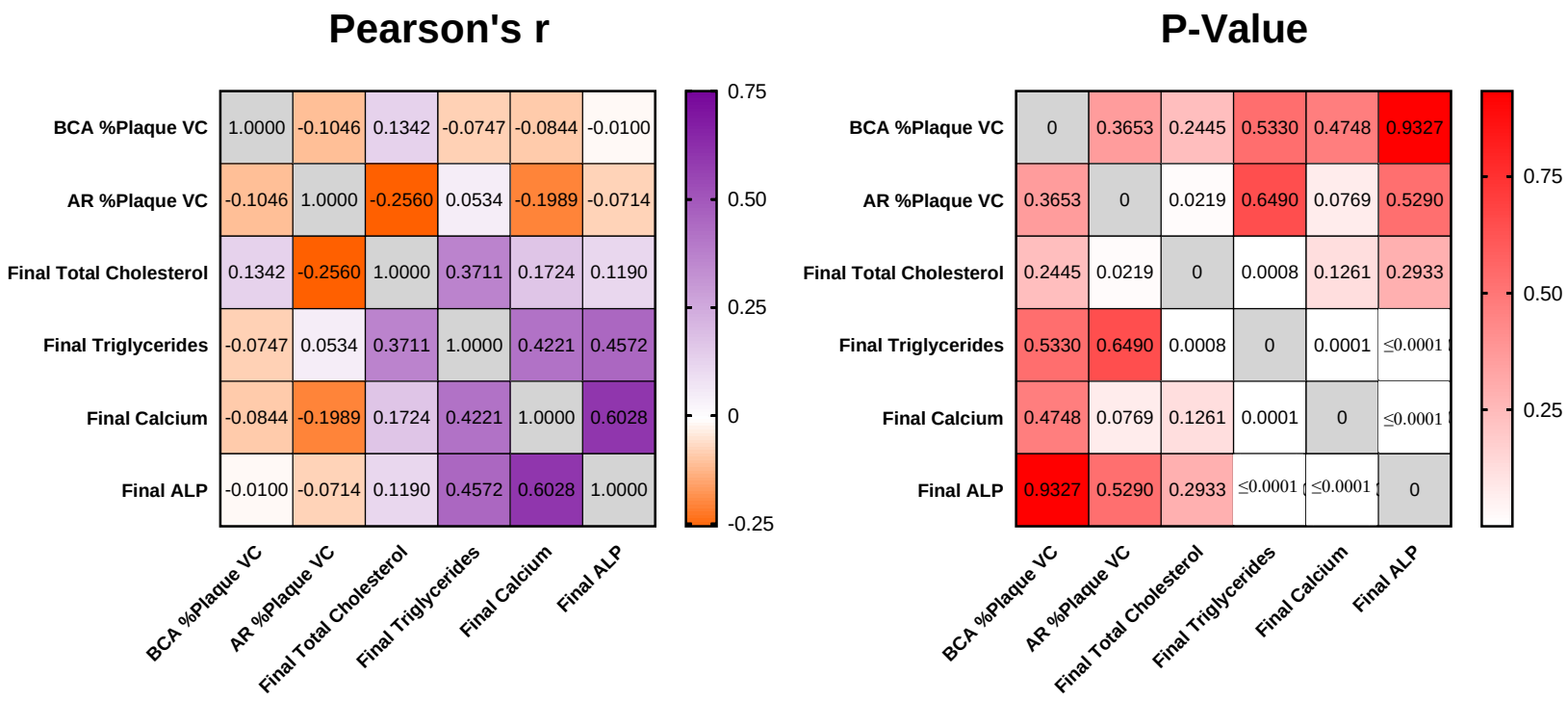

Figure 6.3.10.2 The correlations between plaque vascular calcification, plasma total cholesterol, triglyceride, calcium and ALP levels in the brachiocephalic arteries and aortic root leaflets of all mice completing the rHDL study.

Pearson's correlation of brachiocephalic artery (BCA) or aortic root leaflet (AR) plaque vascular calcification (VC), plasma total cholesterol, triglyceride, calcium and alkaline phosphatase (ALP) levels in all mice completing the rHDL study regardless of treatment group or weeks on atherogenic diet. Data represented as a heat map of the Pearson's r and p-values of exact values per sample, n=80-87.

Next, we correlated the % of BCA or AR plaque VC to Aortic (Ao) expression levels of Runx2, RANKL, ALP or OPG mRNA to identify any patterns between sites, regardless of genotype or treatment group. In figure 6.3.10.3 we show a significant positive correlation between the % VC in the BCA plaques and Ao ALP mRNA expression ($r=0.228$, $p<0.05$), but no other significant correlations between BCA or AR % plaque VC. As could be expected however, we see a significant positive correlations between Ao ALP mRNA expression and Ao Runx2 ($r=0.2319$, $p<0.05$), Ao RANKL ($r=0.4951$, $p<0.0001$) and Ao OPG ($r=0.4715$, $p<0.0001$) mRNA expression and a significant positive correlation between Ao RANKL and Ao OPG ($r=0.4929$, $p<0.0001$) mRNA expression.

Here in figures 6.3.5 to 6.3.10 we show no significant effect of rHDL on advanced atherosclerosis, or plaque calcification. What we did see however, was a decrease in plaque stability in the Apo $E^{-/-}$ x $OPG^{-/-}$ mice, particularly in the mice fed an atherogenic diet for the full 40 weeks. We additionally identified correlations between total cholesterol, triglycerides or aortic mRNA expression profiles and the % of plaque vascular calcifications or calcification markers.

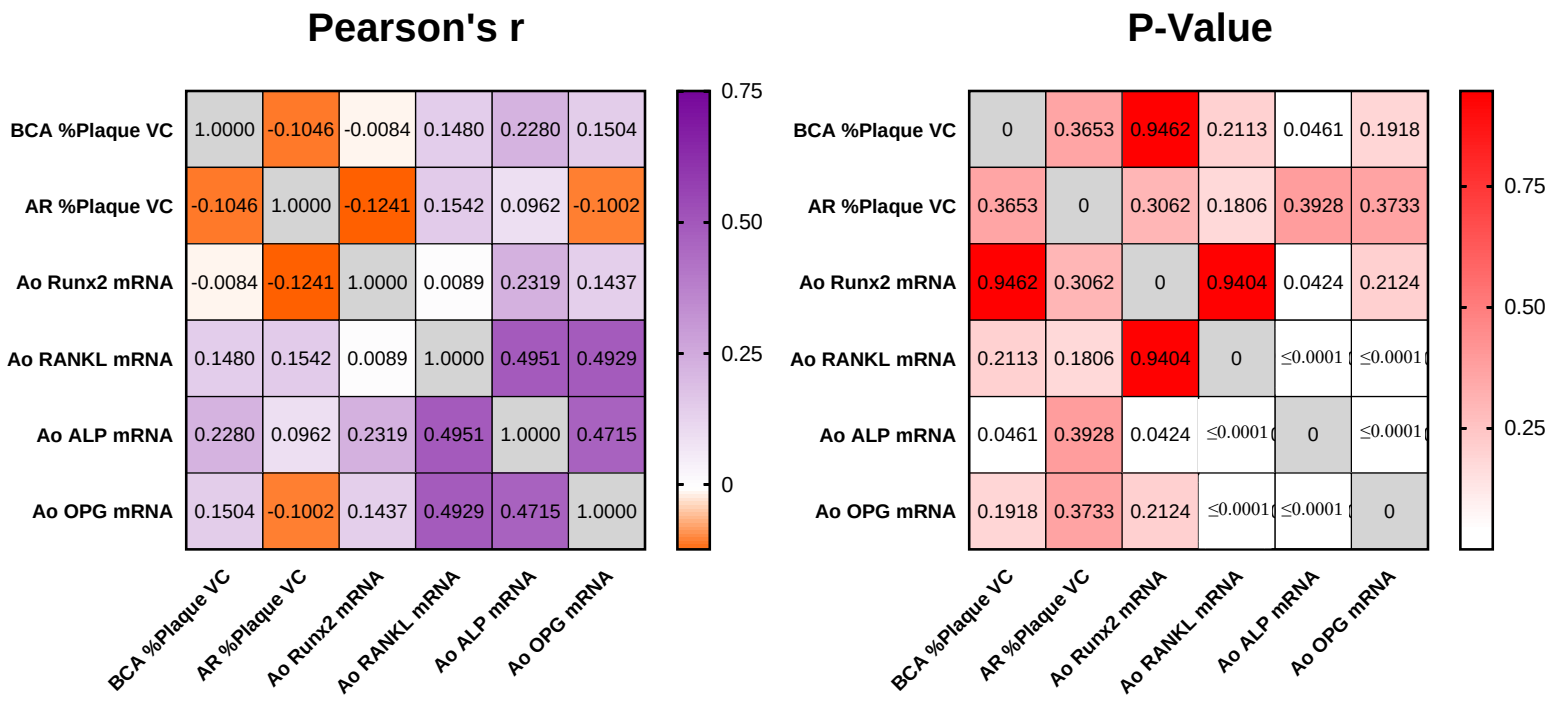

Figure 6.3.10.3 The correlations between plaque vascular calcification and aortic mRNA levels of Runx2, RANKL, ALP and OPG in the brachiocephalic arteries and aortic root leaflets of all mice completing the rHDL study.

Pearson's correlation of brachiocephalic artery (BCA) and aortic root leaflet (AR) plaque vascular calcification (VC) and aortic mRNA levels of Runx2, RANKL, ALP and OPG in all mice completing the rHDL study regardless of treatment group or weeks on atherogenic diet. Data represented as a heat map of the Pearson's r and p-values of exact values per sample, n=77-89.

Results from the CARAT Clinical Trial

The role of reconstituted HDL infusions on calcification *in situ* and *ex vivo* on calcifying VSMCs

6.3.11 The Effects of rHDL infusions on Human Vascular Calcification – CARAT Study

After examining the roles of rHDL and oxrHDL *in vitro* and *in vivo*, we progressed to expanding upon these results using whole human serum from patients receiving CER-001, an HDL mimetic similar to our rHDL particle. Table 6.3.11.1 shows the baseline characteristics of these subjects to have no significant differences between treatment groups, except in the BMI whereby participants receiving placebo had a slightly but significantly larger BMI than the participants receiving CER-001 ($p<0.05$).

Table 6.3.11.1 CARAT Patient characteristics at baseline.

P-value for the difference between treatment groups at the baseline is calculated using the Mann-Whitney test. Significance set to $p<0.05$.

Parameter	Placebo (n=137)	CER-001 (n=135)	P-value
Age, Mean (SD)	59.06 (9.37)	60.60 (9.51)	**0.18**
White, n (%)	131 (95.6%)	130 (96.3%)	**0.78**
BMI, Median (IQR)	29.28 (26.32, 32.41)	28.40 (25.16, 30.68)	**0.042**
Hypertension, n (%)	94 (68.6%)	87 (64.4%)	**0.47**
Previous PCI, n (%)	26 (19.0%)	13 (9.6%)	**0.028**
Previous MI, n (%)	15 (10.9%)	12 (8.9%)	**0.57**
Smoking, n (%)	47 (34.3%)	52 (38.5%)	**0.47**
Diabetes, n (%)	32 (23.4%)	21 (15.6%)	**0.10**
Baseline statin use, n (%)	130 (94.9%)	128 (94.8%)	**0.98**
Statin Intensity			
High, n (%)	84 (61.3%)	94 (69.6%)	**0.15**
Moderate, n (%)	46 (33.6%)	34 (25.2%)	**0.13**
New to Statin, n (%)	92 (67.2%)	91 (67.4%)	**0.96**
Antiplatelet, n (%)	42 (30.7%)	34 (25.2%)	**0.31**
Anti-hypertensive, n (%)	81 (59.1%)	75 (55.6%)	**0.55**

To assess the effect of CER-001 on vascular calcification progression or regression, calcification data was obtained through IVUS image analysis for the entire cohort by other members of the Nicholls laboratory, then the average individual vessel calcium index was calculated as per protocol outlined previously[285] and was used to analyse the effects of placebo or CER-001 on global change in coronary artery calcification.

Table 6.3.11.2 shows that while there is no change in the calcification of coronary arteries in placebo treated patients, the CER-001 treated patients had a significant increase in plaque calcification ($p<0.05$). The difference in changes between placebo and CER-001 however was not significant.

Table 6.3.11.2 Change in average calcium score with placebo or CER-001 treatments.

Data is presented as average calcium score median (IQR).

Group	Baseline	Follow-up	Change	P-value
Placebo (n=137)	0.263 (0.111-0.458)	0.257 (0.130-0.486)	0.000 (-0.021-0.038)	**0.132**
CER-001 (n=135)	0.284 (0.157-0.507)	0.292 (0.155-0.557)	0.010 (-0.027-0.052)	**0.016**
P-value	**0.314**		**0.267**	

Investigations of Serum Calcification Potential in a Calcification Progressive Human Cohort

The participants from the CARAT study with the highest levels of calcification progression were identified via IVUS imaging. After selection of the top calcification progressors, there were 4 samples from participants receiving placebo and 7 from participants receiving CER-001. All samples progressed in calcium index score between 0.14 and 0.23. The entire CARAT cohort with available calcium index scores was 257 participants and the index change ranged from -0.14 – 0.23. The serum from these patients was analysed for calcification potential by measuring serum characteristics and using the serum as a pre-treatment in a HAoSMC calcification ARS assay.

The participant characteristics of the samples used are as shown below in table 6.3.12.1. There were no significant differences between placebo or CER-001 treated participant serum total cholesterol, LDL cholesterol (LDL-C), HDL cholesterol (HDL-C), triglyceride, Apo AI, Apo B, calcium or ALP levels.

Table 6.3.11.3 Levels of circulating atherosclerosis and calcification markers in the human serum samples used to treat HAoSMCs.

Data expressed as mean (±SEM). t-test, n=4-7.

Blood Serum Data		Placebo (n=4)	CER-001 (n=7)	P-value
Total Cholesterol (mg/dL)	Baseline	138.0 (±12.51)	141.6 (±9.95)	0.83
	Follow-Up	144.8 (±17.85)	151.9 (±14.52)	0.77
	Change	6.75 (±11.82)	10.29 (±8.66)	0.81
	P-value	0.77	0.57	
LDL-C (mg/dL)	Baseline	80 (±8.05)	71.71 (±7.38)	0.49
	Follow-Up	69 (±8.74)	69 (±8.07)	>0.99
	Change	-11 (±2.68)	0 (±5.81)	0.18
	P-value	0.39	0.81	
HDL-C (mg/dL)	Baseline	38.5 (±5.56)	43.14 (±5.11)	0.58
	Follow-Up	49.75 (±14.97)	45.71 (±5.96)	0.77
	Change	11.25 (±9.95)	2.571 (±1.89)	0.29
	P-value	0.51	0.75	
Triglyceride (mg/dL)	Baseline	98.5 (±4.35)	134.7 (±30.78)	0.41
	Follow-Up	130.8 (±27.51)	175.9 (±69.53)	0.65
	Change	32.25 (±31.81)	41.14 (±39.57)	0.88
	P-value	0.29	0.60	
Apo AI	Baseline	120.5 (±13.76)	129.1 (±7.03)	0.55
	Follow-Up	147.3 (±31.85)	138.3 (±11.52)	0.75
	Change	26.75 (±21.41)	9.143 (±8.3)	0.38
	P-value	0.47	0.51	
Apo B	Baseline	69.5 (±4.05)	68.29 (±7.4)	0.91
	Follow-Up	66.75 (±5.12)	72.57 (±6.99)	0.58
	Change	-2.75 (±1.75)	4.286 (±3.14)	0.15
	P-value	0.69	0.68	
Calcium (µg/dL)	Baseline	9.388 (±0.46)	9.597 (±0.24)	0.67
	Follow-Up	10.02 (±0.25)	9.971 (±0.38)	0.92
	Change	0.6366 (±0.42)	0.3747 (±0.31)	0.62
	P-value	0.27	0.42	
ALP (mmol/L)	Baseline	0.4079 (±0.05)	0.5666 (±0.07)	0.17
	Follow-Up	0.3861 (±0.03)	0.6533 (±0.12)	0.14
	Change	-0.02174 (±0.05)	0.08677 (0.09)	0.40
	P-value	0.74	0.55	

To investigate whether the serum of calcification progressor participants also upregulates calcification of HAoSMCs *ex vivo*, serum from these participants was applied to the cells as a 24 hour pre-treatment. We see in figure 6.3.12.1 that the cells pre-treated with serum either before (1.019±0.048 vs 1.272±0.05, $p<0.05$) or after (1.019±0.048 vs 1.29±0.044, $p<0.05$) placebo or CER-001 treatments had significantly more calcification compared to the cells with CM alone. This shows that the serum from these participants has a high calcification potential both *in situ* and *ex vivo*.

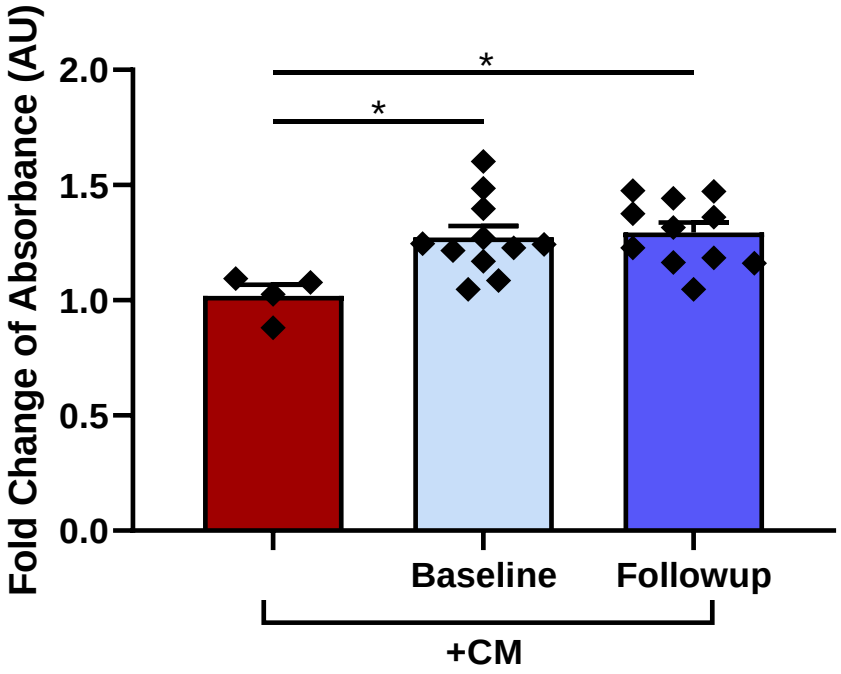

Figure 6.3.11.1 The effect of actively calcifying human serum on calcification potential.

*HAoSMCs were pre-treated with human serum (10%) for 24 hours then treated with calcification medium (CM; Ca 2.7 mM, PO_4 2.0 mM) for 15 days. Calcification was measured by ARS assay with no treatment (NT) and CM alone and expressed as fold change from CM. *p<0.05. ANOVA with Bonferroni's correction. Data represented as mean± SEM, fold change from the CM alone control, n=4-11.*

Next, we looked at the correlations between HDL-C or Apo AI and the calcification potential of the serum as measured by the ARS calcification assay at both baseline and follow up and identified that both HDL-C ($r=-0.4337$, $p<0.05$) and Apo AI ($r=-0.5714$, $p<0.01$) significantly negatively correlated with *ex vivo* calcification potential (figure 6.3.12.3). This supports findings that HDL or its components correlate to vascular or valvular calcification *in situ*[790, 791, 793, 794], however this is the first demonstration of its link to calcification potential *ex vivo*.

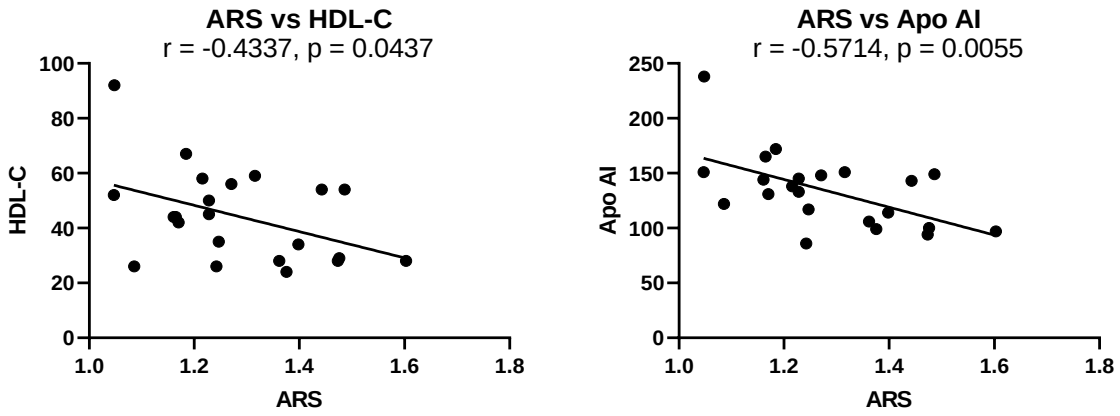

Figure 6.3.11.2 The correlations between serum calcification potential (ARS) and HDL-C or Apo AI levels in human serum.

Pearson's correlation of serum calcification potential (ARS) and HDL-C or Apo AI levels at baseline or follow up, regardless of treatment group. Data represented as exact values per sample, n=22.

Finally, we investigated the correlations between ARS values and circulating calcification factors or lipids in this cohort. We present in table 6.3.12.2 that in participants receiving CER-001, there was a significant negative correlation between ALP and both HDL-C ($r=-0.6559$, $p<0.05$) or Apo AI ($r=-0.6621$, $p<0.01$). Although this is somewhat contradictory to the non-significant correlations between ARS and HDL-C or Apo AI, and again with further investigation could aid in explaining rHDL mimetic clinical trial outcomes.

Here in chapter 6.3.11 – 6.3.12 we show that participants of the CARAT clinical trial receiving CER-001 had a significant increase in vascular calcification and that the serum from the participants with the highest change in calcium index, regardless of treatment, significantly increased the calcification potential of HAoSMCs *ex vivo*. We also show that high levels of HDL-C and Apo AI in the high calcification potential serum was correlated with lower levels of ALP in the CER-001 treated participants, but not ARS measured HAoSMC calcification. Conversely in the placebo group high HDL-C and Apo AI levels correlated with reduced calcification potential as measured by ARS.

Table 6.3.11.4 Correlations between ARS and circulating factors of highly calcification CARAT participant serum.

Pearson's r and p-value, n=4-7.

	Comparison	All Samples (n=11)		Placebo (n=4)		CER-001 (n=7)	
		Pearson's r	p-value	Pearson's r	p-value	Pearson's r	p-value
vs. ARS	Total Cholesterol	-0.221	0.3229	-0.5788	0.1328	-0.07311	0.8038
	LDL-Cholesterol	-0.01477	0.9493	-0.1119	0.792	0.06497	0.833
	Triglycerides	0.0256	0.91	0.1749	0.6787	-0.03843	0.8962
	Calcium	0.3412	0.1202	0.6917	0.0574	0.1586	0.588
	ALP	0.2913	0.1884	-0.2925	0.482	0.359	0.2074
vs. HDL-C	Calcium	-0.3402	0.1213	-0.307	0.4595	-0.3869	0.1717
	ALP	-0.292	0.1873	0.5467	0.1608	-0.6559	0.0109
vs. Apo AI	Calcium	-0.3573	0.1026	-0.2738	0.5117	-0.4862	0.0779
	ALP	-0.2372	0.2878	0.5831	0.1292	-0.6621	0.0099

6.4 Discussion

To begin our analysis on the roles of HDL particles in atherosclerosis and vascular calcification (VC), we investigated the role of native HDL, the clinically used reconstituted HDL particle (rHDL) and their oxidised forms in the setting of calcification initiation using a calcification assay with HAoSMCs *in vitro*. We initially discovered that native HDL and not rHDL significantly reduced calcification on these cells using an ARS assay and that this effect was not observed in the cells pre-treated with the oxidised forms of these HDLs.

This effect from the native HDL could possibly have been from the ability to maintain the initial levels of SMαActin and significantly reduce Runx2 mRNA, alongside a non-significant reduction in RANKL and ALP mRNA, as shown after 24 hours of incubation. Conversely, rHDL showed no trends at the 24 hour timepoint in gene expression of markers of VC. There were also no clear trends for either HDL or rHDL at the 5 or 7 day timepoints of calcification, suggesting that HDL or an HDL component may influence calcification through another mechanism. As HDL modification by oxidation reduces its favourable effects on inflammation, oxidative stress and cholesterol efflux[797], one of these effects may be influencing the results presented in this chapter.

Calcification can also be influenced by lipoproteins through mechanisms other than the Runx2/RANKL/OPG pathway. One in particular is the BMP-2 or Msx2 calcification pathway. It was recently shown by Sun *et al*. (2019)[794] that oxHDL also increases valvular interstitial cell calcification and raises BMP-2, Msx2 and Runx2 in a dose-mediated fashion. This study uses a similar timeframe to the studies in this thesis however the HDL in their study was incubated for 14 days in combination with β-glycerophosphate supplemented medium. Additionally, oxidised phospholipids have been shown to regulate osteoblast expression of ALP and osteocalcin in a pre-treatment study[811], showing that the oxHDL and oxrHDL loss of benefit may also be due to BMP-2 signalling.

A similar remark could be made for the animal study in this chapter, where although rHDL treatment significantly upregulated ALP and OPG mRNA expression in Apo $E^{-/-}$ x $OPG^{-/-}$ mice there were so significant changes in calcification suggesting alternate mechanisms. However, there was no effect of rHDL on the expression levels of Runx2 and RANKL mRNA in the aortas of these mice suggesting either using a timepoint too late in the disease progression for these markers, or a more BMP-2 regulated model. In $LDLR^{-/-}$ mice, pharmacological BMP-2 inhibition significantly inhibited both plaque growth and plaque VC[340]. Additionally, matrix Gla Protein (MGP), an inhibitor of BMPs, deficiency in Apo $E^{-/-}$ mice led to an increase in diffuse aortic calcification whereas MGP overexpression in Apo $E^{-/-}$ mice resulted in reduced VC and inflammation[345]. Although these rHDL infusions may have been affecting the expression of BMPs or MPG, the lack of treatment effect in conjunction with increased effects for rHDL at the earliest timepoints *in vitro*, suggest that the time frame in which rHDL may have an effect is likely earlier than what was used in this late stage plaque model.

Interestingly, there was a significant negative correlation between total final cholesterol and % valvular calcification in all the mice completing the study, regardless of treatment type or timepoint (between 36 and 40 weeks). Although this goes against the hypothesis generated from previous literature[812], the experiments here are carried out in different mouse models. The differences in models could be having a significant impact, due to the changes in macrophage and lipoproteins biology, which as mentioned in the introduction chapter 1 both influence atherosclerosis and calcification development. In addition, the timepoint of 9 months may be having an impact, as protective mechanisms of calcification, such as calciprotein particles, may be triggered after certain amounts of calcium has been deposited. As there is little knowledge on the natural history of VC however this last statement is purely speculative. As OPG is expressed biphasically, future experiments

examining the progression of calcification are needed to explain why in these mice total cholesterol was negatively correlated to valvular calcification.

This is the first study to investigate the change of plaque characteristics following late stage rHDL infusions in aged Apo $E^{-/-}$ or Apo $E^{-/-}$ x $OPG^{-/-}$ mice. While rHDL infusions or raising therapies demonstrate early effects on plaque regression in animal models[92, 802-806], they demonstrate no regressive effects on the plaque volume in aged Apo $E^{-/-}$ or $LDLR^{-/-}$ mice on an atherogenic diet[807-809], but instead inhibit further growth[808]. We therefore hypothesised that if rHDL has any benefit to aged plaques, it may be through a measure of plaque stabilisation. What we discovered however is that rHDL appears to have no benefit to these late stage plaques in stabilisations markers, including VC. We do however see many changes between our Apo $E^{-/-}$ mice and our Apo $E^{-/-}$ x $OPG^{-/-}$ mice, including circulating calcium or ALP levels, fat deposit or total weights and plaque levels of calcification or stability markers. $OPG^{-/-}$ mice have an osteoporotic phenotype, with aortic and renal artery medial calcifications[643], while Apo $E^{-/-}$ x $OPG^{-/-}$ mice have been observed to have increased late stage brachiocephalic artery plaque size by 40 weeks of age and calcium content by 60 weeks of age compared to their Apo $E^{-/-}$ x $OPG^{+/+}$ littermates[799]. Additionally, bone marrow transplants from 10 week old Apo $E^{-/-}$ mice to 10-12 week old Apo $E^{-/-}$ x $OPG^{-/-}$ mice significantly inhibited brachiocephalic artery plaque calcification by 34 weeks[813]. It is also interesting to note that 4 weeks of infusions of recombinant OPG in $OPG^{-/-}$ mice was not able to inhibit or reverse aortic VC in 12 week old mice[427]. None of these experiments however were performed in the setting of an atherogenic diet, making our study unique to the current literature and potentially causing the overserved lack of effects: the atherogenicity of the diet may be overwhelming many of the usually pronounced effects of $OPG^{-/-}$.

When examining the effects of rHDL infusions in humans from the CARAT trial, we see that although there was no difference between participants receiving placebo or CER-001 in calcium index values, there was a significant increase in calcium index between participants receiving CER-001 at baseline and follow up. Furthermore, participants whose calcium index increased substantially had serum which increased the calcification potential of HAoSMCs *ex vivo*, but CER-001 treatment had no additional effect. While this may be the case, it should be noted that the nature of the study did not include low progressor or regressor controls and had a low number of samples. This study also had a low sample size for the *ex vivo* experiments, as it was intended as an exploratory pilot study, which may have led to missed signification differences. Before examining further, follow up experiments addressing these weaknesses should be performed.

As outlined earlier, the effect of rHDL on plaque calcification seems to appear earlier on in disease progression *in vitro*, as presented in this chapter, and *in vivo*[803, 814, 815]. While interesting and worth studying for more targeted effects, inhibiting growth of plaques early in their development is not as clinically relevant as muting culprit and late stage plaques. The CARAT study presented here however is in later stage plaques, in participants receiving a high dose of satins on top of their rHDL infusions. It could therefore be that the effect of statins is somewhat overwhelming the response of the plaque to the CER-001 infusions.

Moreover, it is well established that dysfunctional HDL has no benefit to CVD[87] and we see here in this chapter that oxHDL has no benefit to calcifying HAoSMCs *in vitro*. In humans, high oxHDL is associated with calcific aortic valve disease severity[794] and a decrease in oxHDL is associated with reduced progression of coronary artery calcification[816], supporting our *in vitro* findings. Furthermore osteopontin and OPG expressed in epicardial fat is associated with certain HDL subclasses[791]. Therefore, a detailed analysis into the HDLs present and any remodelling occurring on the CER-001 particle could provide further

insights into the role of HDL infusions in modifying plaque characteristics in this cohort. These further examinations into HDL subclasses and any CER-001 modifications may also help to explain the correlation data describing significant negative correlations between HDL-C or Apo AI levels and *ex vivo* calcification potential of whole serum samples, but not in participants treated with CER-001. As CER-001 is designed with a special coating to protect against modification, investigation into the native lipoprotein subclasses may yield more insight.

The discovery that HDL-C or Apo AI levels significantly negatively correlated with the *ex vivo* calcification potential of whole serum however connects well with our *in vitro* data, where HDL and rHDL significantly reduced calcification potential on the same HAoSMCs. CER-001 infusions however had no effect on the *ex vivo* calcification potential of the whole serum and significantly raised the calcification in these participants *in situ*. Although this may seem to be further complicating the effect of HDL raising therapies on VC, all these experiments have occurred in very different models of atherosclerosis or vascular calcification and therefore all show different aspects of HDL potential.

In chapter 6, we studied the effect of both native and reconstituted HDL and their oxidised forms on VC *in vitro* and extended the study of rHDL into late stage plaque *in vivo* and *ex vivo* studies. Although we find a role for HDLs in the early stages of calcification *in vitro* and correlation between HDL components and circulating factors *in vivo* and *ex vivo*, we find no definitive role for HDLs in late stage plaque calcification *in vivo* and a modest role for HDLs in the progression of calcification *in situ*. Further investigation is required to identify the precise components responsible for these varying effects.

7 : Chapter Seven

Discussion

The genesis of this thesis came about from the need to discover new targets for the treatments of vascular calcification (VC). VC is a common feature of atherosclerosis that is associated with adverse events[263], with prevalence of aortic calcification in the general population at 59% for women and 67% for men aged 41-80 years (mean age 61 years)[267]. This increases to 81% in patients with diabetes[268] and 100% with end-stage renal disease[269], associating with their co-morbidities and clinical sequelae[270]. Moreover, VC is such a strong indicator of plaque progression[58] and vunerability[264], that is it routinely used as a marker, such as in PET scans for coronary artery calcification (CAC) scores, to aid cardiologists in designing cardiovascular treatment plans[271, 272]. Although VC is so common and so strikingly linked to poor cardiovascular health, we are still only recently learning that morphology specific outcomes may exist, let alone nearing the development of a specific VC treatment to adjust these morphologies.

Moreover, the ability of scientists and medical professionals to generate a therapeutic is greatly inhibited by the similarities between VC development and bone metabolism[391, 642, 817-819] and moreover by a reduction in bone marrow leading to decreased haematopoietic production with a focus on the production of inflammatory cells[820]. This phenomenon, termed the bone-vascular axis, is clinically relevant, with patients often displaying both VC and osteoporosis co-morbidities. This arises from both similarities and differences in mineralisation in the very same proteins this thesis focuses on, Runx2, RANKL, OPG and ALP, as they form an essential pathway to VC. Given this information and the knowledge that lipoproteins are systemic and interact with both the bone and artery wall, we sought to investigate the impact of the major lipoprotein classes, high density (HDL), low density (LDL) and very low density (VLDL) lipoproteins and their oxidised, dysfunctional forms, on the vascular smooth muscle cells (VSMCs) responsible for vessel calcification.

Although lipoproteins have been extensively studied regarding atherosclerotic plaque size, there are relatively few studies showing their relationships with plaque composition as discussed in chapter 1 and fewer again for vascular calcification (VC) as discussed in relevant results chapters for each lipoprotein. Here we identified through the data in chapters 4-6, that oxidation of lipoproteins increases whereas HDL decreases onset of VC *in vitro* and that these oxidised lipoproteins, specifically oxLDL and oxVLDL, were affecting the Runx2/RANKL/OPG pathway (chapter 3).

When studying triglycerides (TG) (chapter 4) *in vivo* and *ex vivo*, we found that TG levels significantly correlated to the circulating calcification markers ALP and calcium and in the Apo $E^{-/-}$ x Apo $CIII^{-/-}$ mice, with low TG levels immediately prior to an atherogenic diet, TGs negatively correlated to aortic root leaflet (AR) calcification. The differences in plaque composition between the brachiocephalic artery (BCA) and AR sites suggest 2 different roles for TG that warrants further exploration.

Upon *in vivo* exploration, we find that while atorvastatin in atherogenic diet fed Apo $E^{-/-}$ mice significantly reduced AR VC, it did this independently of total cholesterol (TC) levels, whereas *ex vivo* we found no relationship between Lp(a) and VC in a human cohort. As many studies have identified a causal link between Lp(a), osteoblastic differentiation[764] and calcification[120, 760, 761], we hypothesised that Lp(a) pre-treatment in whole serum would increase *ex vivo* calcification of HAoSMCs in a dose dependant manner, however this was not the case, contradicting early findings of Lp(a) raising calcification markers in valvular interstitial cells[764]. This result however may have arisen from the lack of isoform specification or Lp(a) isolation, both of which should be performed to investigate specific interactions between Lp(a) and VC.

Although HDL levels are correlated to coronary heart disease[77] and there is evidence to suggest a role for HDL in inhibiting calcification[801]. In chapter 6 there was no observed

role for HDL infusions in the modification of VC in late stage plaques. While there is a reported link between HDL characteristics and *ex vivo* calcification potential or circulating ALP levels in humans, it appears from the *in vitro* data presented here and *in vivo* elsewhere that the benefit of HDL occurs earlier in the natural history of VC. Furthermore, this may occur through a mechanism partially independent of the Runx2/RANKL/OPG pathway.

VSMCs readily differentiate into many different types of cells, including but not limited to osteoblast-like, macrophage-like and adipose-like cell types[312]. Through lineage tracing in mice, it is now widely accepted that VSMCs migrate into the plaque and lose their VSMC identification markers, such as SMαActin, so much so that it is estimated that most of plaque VSMC content is incorrectly identified as macrophage content[313, 314]. Additionally, in human coronary lesions it is estimated that around 34-40% of foam cells are from VSMC origin[821]. Moreover, it has recently been discovered that VSMCs overtake a plaque in a cancer-like fashion, likely arriving from 1 'stem cell' source[822] and that this takeover leads to unstable necrotic core formation[823]. With all these differences in VSMC involvement alone, it would be interesting and likely fruitful to investigate the roles of differentiated VSMCs in VC.

In conjunction with VSMCs, macrophage (or macrophage-like VSMCs) cells have known roles in VC. Cell-cell interactions between monocyte/macrophages and VSMCs[824] in conjunction with release of inflammatory cytokines such as IL-6 and TNFα[381], lead to the phenotype conversion of vascular cells into osteogenic cells[825]. Additionally oxLDL stimulates[826] polarisation of macrophages to the M1 phenotype[354], which secrete BMP-2 leading to upregulation of Runx2[827]. M2 polarised macrophages however can reduce VC *in vitro* via an increase in the calcification inhibitor pyrophosphate (PPi)/ATP[828] and indirectly through the efferocytosis of mineral nucleating apoptotic bodies[829]. Additionally,

VSMC secreted RANKL stimulates the differentiation of plaque macrophages into osteoclast-like cells[367], however in local plaque macrophages this process is impaired[316]. Given that native and oxidised atherogenic lipoprotein loading of VSMCs results in their differentiation to macrophage-like[830] foam[821, 831, 832] cells, it would be interesting to see if these macrophage/VSMC/foam hybrid cells skew towards an osteoblast or osteoclast like phenotype during the calcification process.

The endothelial layer of these plaques may also contribute to calcification through oxLDL induced BMP-2[745] and other calcification regulatory gene[833] expression, or even calcify themselves in response to oxLDL[320]. Moreover, TG rich lipoproteins (TRLs) causes endothelial inflammation[134, 135], oxLDL causes endothelial dysfunction[171] and increases interactions with monocytes[185], oxHDL blocks endothelial cell proliferation and migration[185] whereas HDL induces angiogenesis through endothelial Ras/MAP Kinase activation[834] or in the setting of ischemia, rHDL gathers endothelial progenitors to enhance blood vessel formation[835]. Altogether, these data suggest a potential secondary role for lipoproteins in the regulation of atherosclerotic calcification through non-VSMC mediated mechanisms.

Lipoproteins are complex particles, so complex that it is fair to assume slight differences in composition between each individual particle. Moreover, the presence of extracellular vesicles in the plasma further convolute these analyses[836]. In moving forward with lipoprotein research, many laboratories now use sophisticated phenotyping technologies including genomic (for RNA molecules trafficked by lipoproteins, found to be of mostly microbiome origin)[837], proteomic[838-841] and lipidomic[645, 842, 843] analyses to examine specific interactions between targets. Even small differences, such as rough size of each particle[100, 793] and oxidative status[763, 764, 794, 797, 816, 844] has been shown to correlate to differences in VC in humans. As the bone-vascular axis is laden with similarities, finding

any specific differences between interactions of lipoproteins with the bone and vessel wall may lead to targeted treatments. It would also strengthen the studies presented here in this thesis to profile the lipoproteins more robustly, for example examining HDL and LDL level changes in mice alongside their composition.

Further investigation into the natural history of VC would provide researchers with a better context of the disease. While we know that generally microcalcification generate plaque instability whereas macrocalcifications do the reverse, it is unknown whether microcalcification grow into macrocalcifications or whether macrocalcifications arise from differing plaque conditions. In New Zealand, researchers are currently developing a new imaging system, called MARS (Medipex All Resolution System)[845-847], which they aim to use to map the natural history of VC (discussed formally and informally at the Australian Atherosclerosis Society meetings).

Additional to the role of lipoproteins on individual plaque cell types and their interactions with each other on VC, the role of the calcification itself on these cells is unknown and would be an important future direction for this project. Could a small amount of calcification in the plaque be stimulating other local calcifications? It is clear from the literature that there are still many questions regarding VC research which when answered could lead to therapeutic development.

Future directions of this project could also include addressing the limitations of this thesis. The impact of these preliminary results could be increased via more robust exploration, including expanding of n value from 3 to 6+ for the variable *in vitro* PCR and western blot data, alongside employing other *in vitro* calcification methodologies, lipoprotein oxidation techniques and a greater variety of donor VSMCs, rather than exclusively using 31 year old female donor cells. Additionally, the use of inhibitors to RANKL, Runx2, OPG or other proteins involved in this pathway would yield insight into the importance of this pathway in

lipoprotein mediated vascular calcification. Of note for RANKL, exploring the potential involvement of lipoproteins in RANKL post translational regulation may also yield insights into disease treatments and explain any discrepancies between PCR, western blot and ELISA data.

After these limitations have been addressed, PCR and western blot analysis of other calcification markers such as OPN, BMPs and MGP could yield interesting data from both *in vitro* and *in vivo* calcification sources. Moreover, examining other pathways of calcification such as apoptosis could provide insights. This thesis also focuses exclusively on VSMC related calcification, however a focus on macrophage involvement would be another interesting future direction. Moreover, the focus on VSMC was as a whole, rather than the individual cancer- or macrophage-like VSMC populations.

The *in vivo* studies in this thesis were also limited by only exploring the early or late phases of calcification and only in the aorta, valve and brachycephalic artery. Expanding the scope of arteries would provide other useful insights, for example the coronary artery for insights into myocardial infarctions. Additionally, not only would additional early timepoints have provided insight into the potential of using rHDL or triglyceride therapeutics as a preventative for future cardiovascular events on non-culprit plaques, but it may have provided insight into the natural history of calcification. As it is currently unknown whether macrocalcifications for from microcalcifications or as a separate process, addressing this limitation would be a worthwhile future direction for this project.

Another limitation both *in vivo* and in the human trials is that the extent of calcification was only measured in small areas of artery and *ex vivo*. Ideally, for imaging calcification, it would be beneficial to have a study using multiple imaging techniques over a large area of the body. This future direction would enable researchers to characterise the extent of both micro and macro calcifications, as well as seeing the effects of target molecules over a

wide range of arteries. As examples: does rHDL have an effect in the peripheral arteries but not the coronary or; does Lp(a) level effect VC in only certain artery types. Moreover, if a time course for these images could be established, it would provide insight into both the natural history of VC alongside how different arteries change in response to therapies or lipid levels over time.

Another important factor and future direction when considering lipoproteins and CVD is of course estrogen. HDL associated oestradiol influence on vasodilation occurs through SR-B1 binding[848], confirming a roles for lipoprotein bound sterols in atherogenesis but raising questions about their influence in calcification and differences in lipoprotein composition between genders. Estrogen also raises Apo E mRNA translation, an important molecule in CVD[849]. Moreover, lipoproteins carry vitamins which also have a variety of known roles in atherosclerosis, VC and other calcification inducive conditions, most notably the heavy influence of vitamin D[300, 600, 630, 850-860] and K[451, 453, 474, 517, 861, 862] on bone and vascular mineralisation. Although many of these interactions are more relevant to medial, or non-plaque associated VC, there appears to be links between calcium, phosphate, estrogen, vitamin D, vitamin K, parathyroid hormone and fibroblast growth factor 23 levels altogether creating a delicate molecular balance, and VC[600, 630, 850, 855, 863-870]. These balances may also explain the gender differences we see in CVD and VC.

The mouse models used in this thesis creates increased atherosclerosis via the deletion of the lipoprotein component Apo E to raise LDL and VLDL levels while decreasing HDL. Apo E is necessary not only for lipoprotein clearance from the plasma but it's deletion also increases bone formation in mice[871] and modifies macrophage biology. Atherosclerosis can be improved by Apo E expressing macrophages[872, 873] whereas Apo $E^{-/-}$ mouse macrophages tend to polarise to the inflammatory M1 phenotype[874] and have increased leucocytosis[250]. As Apo E also has antioxidative properties, the lipoproteins in Apo $E^{-/-}$ mice

are more oxidised[875] and as shown in this thesis, the oxidised forms of LDL and VLDL that accumulate in the Apo $E^{-/-}$ mouse plasma may increase VSMC calcification potential. Furthermore, the isoform of Apo E influence atherogenesis[876] and interestingly Alzheimer's[877, 878] in humans. As the rHDL studies in chapter 6 only contained Apo AI as the protein component, this could potentially explain why we see significant early changes for HDL treatment *in vitro*, with no changes in VC following rHDL treatment *in vitro*, *in vivo*, *ex vivo* or *in situ*, instead having changes correlate to the HDL-C and Apo AI levels: perhaps any ability for HDL to influence calcification at any timepoint is not due to Apo AI, but due to Apo E or Apo E mediated effects. In improving HDL mimetics as treatments, it could therefore be beneficial to create a more complex particle containing more than just Apo AI and phospholipids by either adding components or loading the lipoprotein with a therapeutic, such as denosumab, a RANKL inhibitor used to improve osteoporosis and potentially vascular calcification[391].

In conclusion, we find that the oxidation status of a lipoprotein is important for VC, triglyceride levels are correlated to VC markers and that although any role for HDL in VC may be preventative at the early stages, like in atherosclerosis, HDL-C and Apo AI correlated to *ex vivo* calcification potential of whole serum from patients with increasing VC *in situ*. While altogether this thesis supports the literature, this is the first study to examine the role of lipoproteins in a standardised manner across a range of VC settings. Therefore, the data from this thesis provides an essential base for further investigation into the impact of lipoproteins and their components on VC, in order to identify potential targets aiming to stabilise late stage atherosclerosis.

8 : Chapter Eight

Bibliography

1. Colantonio LD and Muntner P. It Is Time for Reducing Global Cardiovascular Mortality. 2019.
2. ReFaey K, Tripathi S, Grewal SS, Quinones DJ, Chaichana KL, Antwi SO, Cooper LT, Meyer FB, Dronca RS and Diasio RB. Current Leading Cause of Death in the World: Cancer versus Cardiovascular Disease. *Available at SSRN 3396025*. 2019.
3. Joseph P, Leong D, McKee M, Anand SS, Schwalm J-D, Teo K, Mente A and Yusuf S. Reducing the global burden of cardiovascular disease, part 1: the epidemiology and risk factors. *Circulation research*. 2017;121:677-694.
4. Sniderman AD, Williams K, Contois JH, Monroe HM, McQueen MJ, de Graaf J and Furberg CD. A meta-analysis of low-density lipoprotein cholesterol, non-high-density lipoprotein cholesterol, and apolipoprotein B as markers of cardiovascular risk. *Circulation: Cardiovascular Quality and Outcomes*. 2011;4:337-345.
5. Assmann G, Cullen P and Schulte H. Simple scoring scheme for calculating the risk of acute coronary events based on the 10-year follow-up of the prospective cardiovascular Munster (PROCAM) study. *Circulation*. 2002;105:310-315.
6. Barquera S, Pedroza-Tobías A, Medina C, Hernández-Barrera L, Bibbins-Domingo K, Lozano R and Moran AE. Global overview of the epidemiology of atherosclerotic cardiovascular disease. *Archives of medical research*. 2015;46:328-338.
7. Organization WH. Global Health Observatory (GHO) data. Raised cholesterol: situation and trends. *Available at:)(Accessed:)* *http://wwwwhoint/gho/ncd/risk_factors/cholesterol_text/en/*. 2008.
8. Kjeldsen SE. Hypertension and cardiovascular risk: general aspects. *Pharmacological research*. 2018;129:95-99.
9. Haapala EA, Lankhorst K, de Groot J, Zwinkels M, Verschuren O, Wittink H, Backx FJ, Visser-Meily A and Takken T. The associations of cardiorespiratory fitness, adiposity and sports participation with arterial stiffness in youth with chronic diseases or physical disabilities. *European journal of preventive cardiology*. 2017;24:1102-1111.
10. Gorostegi-Anduaga I, Corres P, MartinezAguirre-Betolaza A, Perez-Asenjo J, Aispuru GR, Fryer SM and Maldonado-Martin S. Effects of different aerobic exercise programmes with nutritional intervention in sedentary adults with overweight/obesity and hypertension: EXERDIET-HTA study. *European journal of preventive cardiology*. 2018;25:343-353.
11. Gui Y-j, Liao C-x, Liu Q, Guo Y, Yang T, Chen J-y, Wang Y-t, Hu J-h and Xu D-y. Efficacy and safety of statins and exercise combination therapy compared to statin monotherapy in patients with dyslipidaemia: a systematic review and meta-analysis. *European journal of preventive cardiology*. 2017;24:907-916.
12. Piepoli MF. Editor's Presentation Benefit of healthy lifestyle on cardiovascular risk factor control: Focus on body weight, exercise and sleep quality. 2019.
13. De Geest B, Aboumsallem JP and Mishra M. Racial/ethnic differences in hypertension prevalence: Public health impact versus clinical importance of baseline data of the HELIUS study. 2018.
14. Mercuro G, Deidda M, Piras A, Dessalvi CC, Maffei S and Rosano GM. Gender determinants of cardiovascular risk factors and diseases. *Journal of Cardiovascular Medicine*. 2010;11:207-220.
15. Erhardt L. Cigarette smoking: an undertreated risk factor for cardiovascular disease. *Atherosclerosis*. 2009;205:23-32.
16. Gawlik KS, Melnyk BM and Tan A. An epidemiological study of population health reveals social smoking as a major cardiovascular risk factor. *American Journal of Health Promotion*. 2018;32:1221-1227.
17. Eichstaedt JC, Schwartz HA, Kern ML, Park G, Labarthe DR, Merchant RM, Jha S, Agrawal M, Dziurzynski LA and Sap M. Psychological language on Twitter predicts county-level heart disease mortality. *Psychological science*. 2015;26:159-169.

18. Berenson GS, Wattigney WA, Tracy RE, Newman III WP, Srinivasan SR, Webber LS, Dalferes Jr ER and Strong JP. Atherosclerosis of the aorta and coronary arteries and cardiovascular risk factors in persons aged 6 to 30 years and studied at necropsy (The Bogalusa Heart Study). *The American journal of cardiology*. 1992;70:851-858.
19. Berenson GS, Srinivasan SR, Bao W, Newman WP, Tracy RE and Wattigney WA. Association between multiple cardiovascular risk factors and atherosclerosis in children and young adults. *New England journal of medicine*. 1998;338:1650-1656.
20. P MCAHEEMGTTRESJ. Origin of atherosclerosis in childhood and adolescence. *The American journal of clinical nutrition*. 2000;72:1307s-1315s.
21. Sandoo A, van Zanten JJV, Metsios GS, Carroll D and Kitas GD. The endothelium and its role in regulating vascular tone. *The open cardiovascular medicine journal*. 2010;4:302.
22. Chien S. Mechanotransduction and endothelial cell homeostasis: the wisdom of the cell. *American Journal of Physiology-Heart and Circulatory Physiology*. 2007;292:H1209-H1224.
23. Bazzoni G and Dejana E. Endothelial cell-to-cell junctions: molecular organization and role in vascular homeostasis. *Physiological reviews*. 2004;84:869-901.
24. Stevens T, Garcia JG, Shasby DM, Bhattacharya J and Malik AB. Mechanisms regulating endothelial cell barrier function. *American Journal of Physiology-Lung Cellular and Molecular Physiology*. 2000;279:L419-L422.
25. Tarbell JM. Shear stress and the endothelial transport barrier. *Cardiovascular research*. 2010;87:320-330.
26. Muller WA. Leukocyte–endothelial-cell interactions in leukocyte transmigration and the inflammatory response. *Trends in immunology*. 2003;24:326-333.
27. Ley K, Laudanna C, Cybulsky MI and Nourshargh S. Getting to the site of inflammation: the leukocyte adhesion cascade updated. *Nature Reviews Immunology*. 2007;7:678.
28. Dessì M, Noce A, Bertucci P, Manca di Villahermosa S, Zenobi R, Castagnola V, Addessi E and Di Daniele N. Atherosclerosis, dyslipidemia, and inflammation: the significant role of polyunsaturated fatty acids. *ISRN inflammation*. 2013;2013.
29. Arndt H, Smith CW and Granger DN. Leukocyte-endothelial cell adhesion in spontaneously hypertensive and normotensive rats. *Hypertension*. 1993;21:667-673.
30. Prescott MF, McBride CK and Court M. Development of intimal lesions after leukocyte migration into the vascular wall. *The American journal of pathology*. 1989;135:835.
31. Bou-Gharios G, Ponticos M, Rajkumar V and Abraham D. Extra-cellular matrix in vascular networks. *Cell proliferation*. 2004;37:207-220.
32. Nahar NN, Missana LR, Garimella R, Tague SE and Anderson HC. Matrix vesicles are carriers of bone morphogenetic proteins (BMPs), vascular endothelial growth factor (VEGF), and noncollagenous matrix proteins. *Journal of bone and mineral metabolism*. 2008;26:514-519.
33. Sukhova GK, Wang B, Libby P, Pan J-H, Zhang Y, Grubb A, Fang K, Chapman HA and Shi G-P. Cystatin C deficiency increases elastic lamina degradation and aortic dilatation in apolipoprotein E–null mice. *Circulation research*. 2005;96:368-375.
34. Stenmark KR, Davie N, Frid M, Gerasimovskaya E and Das M. Role of the adventitia in pulmonary vascular remodeling. *Physiology*. 2006;21:134-145.
35. Barger AC, Beeuwkes III R, Lainey LL and Silverman KJ. Hypothesis: vasa vasorum and neovascularization of human coronary arteries: a possible role in the pathophysiology of atherosclerosis. *New England Journal of Medicine*. 1984;310:175-177.

36. Corselli M, Chen C-W, Sun B, Yap S, Rubin JP and Péault B. The tunica adventitia of human arteries and veins as a source of mesenchymal stem cells. *Stem cells and development*. 2011;21:1299-1308.
37. Morigi M, Zoja C, Figliuzzi M, Foppolo M, Micheletti G, Bontempelli M, Saronni M, Remuzzi G and Remuzzi A. Fluid shear stress modulates surface expression of adhesion molecules by endothelial cells. 1995.
38. Bevilacqua MP. Endothelial-leukocyte adhesion molecules. *Annual review of immunology*. 1993;11:767-804.
39. Lingen MW. Role of leukocytes and endothelial cells in the development of angiogenesis in inflammation and wound healing. *Archives of pathology & laboratory medicine*. 2001;125:67-71.
40. Bevilacqua M, Ph. D, Michael P, Nelson PD, Richard M, Mannori M, Ph. D, Gianna and Cecconi M, Oliviero. Endothelial-leukocyte adhesion molecules in human disease. *Annual review of medicine*. 1994;45:361-378.
41. Fogelstrand P and Boren J. Retention of atherogenic lipoproteins in the artery wall and its role in atherogenesis. *Nutrition, metabolism and cardiovascular diseases*. 2012;22:1-7.
42. Feng C, Chen Q, Fan M, Guo J, Liu Y, Ji T, Zhu J and Zhao X. Platelet-derived microparticles promote phagocytosis of oxidized low-density lipoprotein by macrophages, potentially enhancing foam cell formation. *Annals of translational medicine*. 2019;7.
43. Schrijvers DM, De Meyer GR, Herman AG and Martinet W. Phagocytosis in atherosclerosis: molecular mechanisms and implications for plaque progression and stability. *Cardiovascular research*. 2007;73:470-480.
44. Vainio S and Ikonen E. Macrophage cholesterol transport: a critical player in foam cell formation. *Annals of medicine*. 2003;35:146-155.
45. Italiani P and Boraschi D. From monocytes to M1/M2 macrophages: phenotypical vs. functional differentiation. *Frontiers in immunology*. 2014;5:514.
46. Dushkin M. Macrophage/foam cell is an attribute of inflammation: mechanisms of formation and functional role. *Biochemistry (Moscow)*. 2012;77:327-338.
47. Sakakura K, Nakano M, Otsuka F, Ladich E, Kolodgie FD and Virmani R. Pathophysiology of atherosclerosis plaque progression. *Heart, Lung and Circulation*. 2013;22:399-411.
48. Shah PK. Mechanisms of plaque vulnerability and rupture. *Journal of the American college of cardiology*. 2003;41:S15-S22.
49. Furie B and Furie BC. Mechanisms of thrombus formation. *New England Journal of Medicine*. 2008;359:938-949.
50. Virmani R, Burke AP and Farb A. Plaque rupture and plaque erosion. *Thrombosis and haemostasis*. 2000;82:1-3.
51. Ohayon J, Finet G, Gharib AM, Herzka DA, Tracqui P, Heroux J, Rioufol G, Kotys MS, Elagha A and Pettigrew RI. Necrotic core thickness and positive arterial remodeling index: emergent biomechanical factors for evaluating the risk of plaque rupture. *American journal of physiology-heart and circulatory physiology*. 2008;295:H717-H727.
52. Shekhonin BV, Domogatsky SP, Muzykantov VR, Idelson GL and Rukosuev VS. Distribution of type I, III, IV and V collagen in normal and atherosclerotic human arterial wall: immunomorphological characteristics. *Collagen and related research*. 1985;5:355-368.
53. Berillis P. The role of collagen in the aorta's structure. *The Open Circulation and Vascular Journal*. 2013;6.
54. Bot PT, Grundmann S, Goumans M-J, de Kleijn D, Moll F, de Boer O, van der Wal AC, van Soest A, de Vries J-P and van Royen N. Forkhead box protein P1 as a downstream

target of transforming growth factor-β induces collagen synthesis and correlates with a more stable plaque phenotype. *Atherosclerosis*. 2011;218:33-43.
55. Libby P and Aikawa M. New insights into plaque stabilisation by lipid lowering. *Drug*s. 1998;56:9-13.
56. Geng Y-J, Phillips JE, Mason RP and Casscells SW. Cholesterol crystallization and macrophage apoptosis: implication for atherosclerotic plaque instability and rupture. *Biochemical pharmacology*. 2003;66:1485-1492.
57. Kwon HM, Sangiorgi G, Ritman EL, McKenna C, Holmes DR, Schwartz RS and Lerman A. Enhanced coronary vasa vasorum neovascularization in experimental hypercholesterolemia. *The Journal of clinical investigation*. 1998;101:1551-1556.
58. Kataoka Y, Wolski K, Uno K, Puri R, Tuzcu EM, Nissen SE and Nicholls SJ. Spotty calcification as a marker of accelerated progression of coronary atherosclerosis: insights from serial intravascular ultrasound. *Journal of the American College of Cardiology*. 2012;59:1592-1597.
59. Maldonado N, Kelly-Arnold A, Vengrenyuk Y, Laudier D, Fallon JT, Virmani R, Cardoso L and Weinbaum S. A mechanistic analysis of the role of microcalcifications in atherosclerotic plaque stability: potential implications for plaque rupture. *American Journal of Physiology-Heart and Circulatory Physiology*. 2012;303:H619-H628.
60. El Harchaoui K, Arsenault BJ, Franssen R, Després J-P, Hovingh GK, Stroes ES, Otvos JD, Wareham NJ, Kastelein JJ and Khaw K-T. High-density lipoprotein particle size and concentration and coronary risk. *Annals of internal medicine*. 2009;150:84-93.
61. Kwiterovich Jr PO. The antiatherogenic role of high-density lipoprotein cholesterol. *The American journal of cardiology*. 1998;82:13-21.
62. Podrez EA. Anti-oxidant properties of high-density lipoprotein and atherosclerosis. *Clinical and Experimental Pharmacology and Physiology*. 2010;37:719-725.
63. Murphy A, Chin-Dusting J, Sviridov D and Woollard KJ. The anti inflammatory effects of high density lipoproteins. *Current medicinal chemistry*. 2009;16:667-675.
64. Rosales C, Gillard BK, Xu B, Gotto Jr AM and Pownall HJ. Revisiting Reverse Cholesterol Transport in the Context of High-Density Lipoprotein Free Cholesterol Bioavailability. *Methodist DeBakey cardiovascular journal*. 2019;15:47.
65. Kontush A, Lhomme M and Chapman MJ. Unraveling the complexities of the HDL lipidome. *Journal of lipid research*. 2013;54:2950-2963.
66. Yancey PG, de la Llera-Moya M, Swarnakar S, Monzo P, Klein SM, Connelly MA, Johnson WJ, Williams DL and Rothblat GH. High density lipoprotein phospholipid composition is a major determinant of the bi-directional flux and net movement of cellular free cholesterol mediated by scavenger receptor BI. *Journal of Biological Chemistry*. 2000;275:36596-36604.
67. Guha M, Gao X, Jayaraman S and Gursky O. Correlation of structural stability with functional remodeling of high-density lipoproteins: the importance of being disordered. *Biochemistry*. 2008;47:11393-11397.
68. Ma C-IJ, Beckstead JA, Thompson A, Hafiane A, Wang RHL, Ryan RO and Kiss RS. Tweaking the cholesterol efflux capacity of reconstituted HDL. *Biochemistry and Cell Biology*. 2012;90:636-645.
69. Zerrad-Saadi A, Therond P, Chantepie S, Couturier M, Rye K-A, Chapman MJ and Kontush A. HDL3-mediated inactivation of LDL-associated phospholipid hydroperoxides is determined by the redox status of apolipoprotein AI and HDL particle surface lipid rigidity: relevance to inflammation and atherogenesis. *Arteriosclerosis, thrombosis, and vascular biology*. 2009;29:2169-2175.
70. Vila A, Korytowski W and Girotti AW. Spontaneous transfer of phospholipid and cholesterol hydroperoxides between cell membranes and low-density lipoprotein:

assessment of reaction kinetics and prooxidant effects. *Biochemistry*. 2002;41:13705-13716.
71. Curtiss LK, Bonnet DJ and Rye K-A. The conformation of apolipoprotein AI in high-density lipoproteins is influenced by core lipid composition and particle size: a surface plasmon resonance study. *Biochemistry*. 2000;39:5712-5721.
72. Balstad T, Holven K, Ottestad I, Otterdal K, Halvorsen B, Myhre A, Ose L and Nenseter M. Altered composition of HDL3 in FH subjects causing a HDL subfraction with less atheroprotective function. *Clinica chimica acta*. 2005;359:171-178.
73. Persegol L, Verges B, Foissac M, Gambert P and Duvillard L. Inability of HDL from type 2 diabetic patients to counteract the inhibitory effect of oxidised LDL on endothelium-dependent vasorelaxation. *Diabetologia*. 2006;49:1380.
74. Baker PW, Rye K-A, Gamble JR, Vadas MA and Barter PJ. Phospholipid composition of reconstituted high density lipoproteins influences their ability to inhibit endothelial cell adhesion molecule expression. *Journal of lipid research*. 2000;41:1261-1267.
75. Vickers KC, Palmisano BT, Shoucri BM, Shamburek RD and Remaley AT. MicroRNAs are transported in plasma and delivered to recipient cells by high-density lipoproteins. *Nature cell biology*. 2011;13:423-433.
76. Vickers KC and Remaley AT. HDL and cholesterol: life after the divorce? *Journal of lipid research*. 2014;55:4-12.
77. Gordon T, Castelli WP, Hjortland MC, Kannel WB and Dawber TR. High density lipoprotein as a protective factor against coronary heart disease: the Framingham Study. *The American journal of medicine*. 1977;62:707-714.
78. Gordon DJ, Probstfield JL, Garrison RJ, Neaton JD, Castelli WP, Knoke JD, Jacobs Jr DR, Bangdiwala S and Tyroler HA. High-density lipoprotein cholesterol and cardiovascular disease. Four prospective American studies. *Circulation*. 1989;79:8-15.
79. Annema W and von Eckardstein A. High-density lipoproteins. *Circulation Journal*. 2013;77:2432-2448.
80. Barter P, Gotto AM, LaRosa JC, Maroni J, Szarek M, Grundy SM, Kastelein JJ, Bittner V and Fruchart J-C. HDL cholesterol, very low levels of LDL cholesterol, and cardiovascular events. *New England Journal of Medicine*. 2007;357:1301-1310.
81. Gordon DJ and Rifkind BM. High-density lipoprotein—the clinical implications of recent studies. *New England Journal of Medicine*. 1989;321:1311-1316.
82. Takagi H, Umemoto T and Group A. A meta-analysis of randomized head-to-head trials for effects of rosuvastatin versus atorvastatin on apolipoprotein profiles. *The American Journal of Cardiology*. 2014;113:292-301.
83. Nicholls SJ, Tuzcu EM, Sipahi I, Grasso AW, Schoenhagen P, Hu T, Wolski K, Crowe T, Desai MY and Hazen SL. Statins, high-density lipoprotein cholesterol, and regression of coronary atherosclerosis. *Jama*. 2007;297:499-508.
84. Nicholls SJ, Tuzcu EM, Wolski K, Bayturan O, Lavoie A, Uno K, Kupfer S, Perez A, Nesto R and Nissen SE. Lowering the triglyceride/high-density lipoprotein cholesterol ratio is associated with the beneficial impact of pioglitazone on progression of coronary atherosclerosis in diabetic patients: insights from the PERISCOPE (Pioglitazone Effect on Regression of Intravascular Sonographic Coronary Obstruction Prospective Evaluation) study. *Journal of the American College of Cardiology*. 2011;57:153-159.
85. Nissen SE, Tsunoda T, Tuzcu EM, Schoenhagen P, Cooper CJ, Yasin M, Eaton GM, Lauer MA, Sheldon WS and Grines CL. Effect of recombinant ApoA-I Milano on coronary atherosclerosis in patients with acute coronary syndromes: a randomized controlled trial. *Jama*. 2003;290:2292-2300.
86. Besler C, Heinrich K, Rohrer L, Doerries C, Riwanto M, Shih DM, Chroni A, Yonekawa K, Stein S and Schaefer N. Mechanisms underlying adverse effects of HDL on eNOS-

activating pathways in patients with coronary artery disease. *The Journal of clinical investigation*. 2011;121:2693-2708.
87. Rosenson RS, Brewer HB, Ansell BJ, Barter P, Chapman MJ, Heinecke JW, Kontush A, Tall AR and Webb NR. Dysfunctional HDL and atherosclerotic cardiovascular disease. *Nature reviews cardiology*. 2016;13:48-60.
88. Heinecke JW. The HDL proteome: a marker–and perhaps mediator–of coronary artery disease. *Journal of lipid research*. 2009;50:S167-S171.
89. Schultz JR, Verstuyft JG, Gong EL, Nichols AV and Rubin EM. Protein composition determines the anti-atherogenic properties of HDL in transgenic mice. *Nature*. 1993;365:762-764.
90. Sirtori CR and Franceschini G. Apolipoprotein AI Milano. *Ricerca in clinica e in laboratorio*. 1982;12:83-86.
91. Bruckert E, von Eckardstein A, Funke H, Beucler I, Wiebusch H, Turpin G and Assmann G. The replacement of arginine by cysteine at residue 151 in apolipoprotein AI produces a phenotype similar to that of apolipoprotein A-IMilano. *Atherosclerosis*. 1997;128:121-128.
92. Shah PK, Yano J, Reyes O, Chyu K-Y, Kaul S, Bisgaier CL, Drake S and Cercek B. High-Dose Recombinant Apolipoprotein A-IMilano Mobilizes Tissue Cholesterol and Rapidly Reduces Plaque Lipid and Macrophage Content in Apolipoprotein E–Deficient Mice: Potential Implications for Acute Plaque Stabilization. *Circulation*. 2001;103:3047-3050.
93. Nicholls SJ, Puri R, Ballantyne CM, Jukema JW, Kastelein JJ, Koenig W, Wright RS, Kallend D, Wijngaard P and Borgman M. Effect of infusion of high-density lipoprotein mimetic containing recombinant apolipoprotein AI Milano on coronary disease in patients with an acute coronary syndrome in the MILANO-PILOT trial: a randomized clinical trial. *JAMA cardiology*. 2018;3:806-814.
94. Nicholls SJ, Andrews J, Kastelein JJ, Merkely B, Nissen SE, Ray KK, Schwartz GG, Worthley SG, Keyserling C and Dasseux J-L. Effect of serial infusions of CER-001, a pre-β high-density lipoprotein mimetic, on coronary atherosclerosis in patients following acute coronary syndromes in the CER-001 Atherosclerosis Regression Acute Coronary Syndrome Trial: a randomized clinical trial. *JAMA cardiology*. 2018.
95. Di Bartolo BA, Psaltis PJ, Bursill CA and Nicholls SJ. Translating evidence of HDL and plaque regression. *Arteriosclerosis, thrombosis, and vascular biology*. 2018;38:1961-1968.
96. Mora S, Szklo M, Otvos JD, Greenland P, Psaty BM, Goff Jr DC, O'Leary DH, Saad MF, Tsai MY and Sharrett AR. LDL particle subclasses, LDL particle size, and carotid atherosclerosis in the Multi-Ethnic Study of Atherosclerosis (MESA). *Atherosclerosis*. 2007;192:211-217.
97. Benn M. Apolipoprotein B levels, APOB alleles, and risk of ischemic cardiovascular disease in the general population, a review. *Atherosclerosis*. 2009;206:17-30.
98. Kita T, Kume N, Minami M, Hayashida K, Murayama T, Sano H, Moriwaki H, Kataoka H, Nishi E and Horiuchi H. Role of oxidized LDL in atherosclerosis. *Annals of the New York Academy of Sciences*. 2001;947:199-206.
99. St-Pierre A, Ruel I, Cantin B, Dagenais G, Bernard P-M, Després J-P and Lamarche B. Comparison of various electrophoretic characteristics of LDL particles and their relationship to the risk of ischemic heart disease. *Circulation*. 2001;104:2295-2299.
100. Colhoun HM, Otvos JD, Rubens MB, Taskinen M, Underwood SR and Fuller JH. Lipoprotein subclasses and particle sizes and their relationship with coronary artery calcification in men and women with and without type 1 diabetes. *Diabetes*. 2002;51:1949-1956.
101. Laufs U and Weinga O. Pathological phenotypes of LDL particles. 2018.

102. Berneis KK and Krauss RM. Metabolic origins and clinical significance of LDL heterogeneity. *Journal of lipid research*. 2002;43:1363-1379.
103. O'Keeffe AG, Nazareth I and Petersen I. Time trends in the prescription of statins for the primary prevention of cardiovascular disease in the United Kingdom: a cohort study using The Health Improvement Network primary care data. *Clinical epidemiology*. 2016;8:123.
104. Sandhu MS, Waterworth DM, Debenham SL, Wheeler E, Papadakis K, Zhao JH, Song K, Yuan X, Johnson T and Ashford S. LDL-cholesterol concentrations: a genome-wide association study. *The Lancet*. 2008;371:483-491.
105. Silverman MG, Ference BA, Im K, Wiviott SD, Giugliano RP, Grundy SM, Braunwald E and Sabatine MS. Association between lowering LDL-C and cardiovascular risk reduction among different therapeutic interventions: a systematic review and meta-analysis. *Jama*. 2016;316:1289-1297.
106. Trialists CT. Efficacy and safety of more intensive lowering of LDL cholesterol: a meta-analysis of data from 170 000 participants in 26 randomised trials. *The Lancet*. 2010;376:1670-1681.
107. Nissen SE, Tuzcu EM, Schoenhagen P, Crowe T, Sasiela WJ, Tsai J, Orazem J, Magorien RD, O'Shaughnessy C and Ganz P. Statin therapy, LDL cholesterol, C-reactive protein, and coronary artery disease. *New England Journal of Medicine*. 2005;352:29-38.
108. Navarese EP, Robinson JG, Kowalewski M, Kołodziejczak M, Andreotti F, Bliden K, Tantry U, Kubica J, Raggi P and Gurbel PA. Association between baseline LDL-C level and total and cardiovascular mortality after LDL-C lowering: a systematic review and meta-analysis. *Jama*. 2018;319:1566-1579.
109. Stancu C and Sima A. Statins: mechanism of action and effects. *Journal of cellular and molecular medicine*. 2001;5:378-387.
110. Glerup S, Schulz R, Laufs U and Schlüter K-D. Physiological and therapeutic regulation of PCSK9 activity in cardiovascular disease. *Basic research in cardiology*. 2017;112:32.
111. Goldstein JL. Familial hypercholesterolemia. 1974.
112. Wiegman A, Rodenburg J, de Jongh S, Defesche JC, Bakker HD, Kastelein JJ and Sijbrands EJ. Family history and cardiovascular risk in familial hypercholesterolemia: data in more than 1000 children. *Circulation*. 2003;107:1473-1478.
113. Luirink IK, Wiegman A, Kusters DM, Hof MH, Groothoff JW, de Groot E, Kastelein JJ and Hutten BA. 20-Year follow-up of statins in children with familial hypercholesterolemia. *New England Journal of Medicine*. 2019.
114. Hofmann SL, Eaton DL, Brown MS, McConathy WJ, Goldstein JL and Hammer RE. Overexpression of human low density lipoprotein receptors leads to accelerated catabolism of Lp (a) lipoprotein in transgenic mice. *The Journal of clinical investigation*. 1990;85:1542-1547.
115. Clarke R, Peden JF, Hopewell JC, Kyriakou T, Goel A, Heath SC, Parish S, Barlera S, Franzosi MG and Rust S. Genetic variants associated with Lp (a) lipoprotein level and coronary disease. *New England Journal of Medicine*. 2009;361:2518-2528.
116. Consortium IKC. Large-scale gene-centric analysis identifies novel variants for coronary artery disease. *PLoS genetics*. 2011;7:e1002260.
117. Tsimikas S, Brilakis ES, Miller ER, McConnell JP, Lennon RJ, Kornman KS, Witztum JL and Berger PB. Oxidized phospholipids, Lp (a) lipoprotein, and coronary artery disease. *New England Journal of Medicine*. 2005;353:46-57.
118. Rath M and Pauling L. Immunological evidence for the accumulation of lipoprotein (a) in the atherosclerotic lesion of the hypoascorbemic guinea pig. *Proceedings of the National Academy of Sciences*. 1990;87:9388-9390.

119. Smith EB and Cochran S. Factors influencing the accumulation in fibrous plaques of lipid derived from low density lipoprotein: II. Preferential immobilization of lipoprotein (a)(Lp (a)). *Atherosclerosis*. 1990;84:173-181.
120. Sun H, Unoki H, Wang X, Liang J, Ichikawa T, Arai Y, Shiomi M, Marcovina SM, Watanabe T and Fan J. Lipoprotein (a) enhances advanced atherosclerosis in WHHL transgenic rabbits expressing human apolipoprotein (a). *Journal of Biological Chemistry*. 2002.
121. Chapman MJ, Ginsberg HN, Amarenco P, Andreotti F, Borén J, Catapano AL, Descamps OS, Fisher E, Kovanen PT and Kuivenhoven JA. Triglyceride-rich lipoproteins and high-density lipoprotein cholesterol in patients at high risk of cardiovascular disease: evidence and guidance for management. *European heart journal*. 2011;32:1345-1361.
122. Miller M, Cannon CP, Murphy SA, Qin J, Ray KK, Braunwald E and Investigators PI-T. Impact of triglyceride levels beyond low-density lipoprotein cholesterol after acute coronary syndrome in the PROVE IT-TIMI 22 trial. *Journal of the American College of Cardiology*. 2008;51:724-730.
123. Mathews CK, Van Holde KE and Ahern KG. Biochemistry. *Add Wesley Longman, San Francisco*. 2000.
124. Nordestgaard B, Stender S and Kjeldsen K. Reduced atherogenesis in cholesterol-fed diabetic rabbits. Giant lipoproteins do not enter the arterial wall. *Arteriosclerosis: An Official Journal of the American Heart Association, Inc*. 1988;8:421-428.
125. Mamo L. Retention of fluorescent-labelled chylomicron remnants within the intima of the arterial wall—evidence that plaque cholesterol may be derived from post-prandial lipoproteins. *European journal of clinical investigation*. 1998;28:497-503.
126. Rapp JH, Lespine A, Hamilton RL, Colyvas N, Chaumeton AH, Tweedie-Hardman J, Kotite L, Kunitake ST, Havel RJ and Kane JP. Triglyceride-rich lipoproteins isolated by selected-affinity anti-apolipoprotein B immunosorption from human atherosclerotic plaque. *Arteriosclerosis and thrombosis: a journal of vascular biology*. 1994;14:1767-1774.
127. Daugherty A, Lange LG, Sobel BE and Schonfeld G. Aortic accumulation and plasma clearance of beta-VLDL and HDL: effects of diet-induced hypercholesterolemia in rabbits. *Journal of lipid research*. 1985;26:955-963.
128. Pitas RE, Innerarity TL and Mahley RW. Foam cells in explants of atherosclerotic rabbit aortas have receptors for beta-very low density lipoproteins and modified low density lipoproteins. *Arteriosclerosis: An Official Journal of the American Heart Association, Inc*. 1983;3:2-12.
129. Goldstein JL, Ho Y, Brown M, Innerarity T and Mahley R. Cholesteryl ester accumulation in macrophages resulting from receptor-mediated uptake and degradation of hypercholesterolemic canine beta-very low density lipoproteins. *Journal of Biological Chemistry*. 1980;255:1839-1848.
130. Zheng X-Y and Liu L. Remnant-like lipoprotein particles impair endothelial function: direct and indirect effects on nitric oxide synthase. *Journal of lipid research*. 2007;48:1673-1680.
131. Giannattasio C, Zoppo A, Gentile G, Failla M, Capra A, Maggi F, Catapano A and Mancia G. Acute effect of high-fat meal on endothelial function in moderately dyslipidemic subjects. *Arteriosclerosis, thrombosis, and vascular biology*. 2005;25:406-410.
132. Alipour A, van Oostrom AJ, Izraeljan A, Verseyden C, Collins JM, Frayn KN, Plokker TW, Elte JWF and Castro Cabezas M. Leukocyte activation by triglyceride-rich lipoproteins. *Arteriosclerosis, thrombosis, and vascular biology*. 2008;28:792-797.
133. Lipskaia L, Pourci M-L, Deloménie C, Combettes L, Goudounèche D, Paul J-L, Capiod T and Lompré A-M. Phosphatidylinositol 3-kinase and calcium-activated transcription

pathways are required for VLDL-induced smooth muscle cell proliferation. *Circulation research*. 2003;92:1115-1122.
134. Ting HJ, Stice JP, Schaff UY, Hui DY, Rutledge JC, Knowlton AA, Passerini AG and Simon SI. Triglyceride-rich lipoproteins prime aortic endothelium for an enhanced inflammatory response to tumor necrosis factor-α. *Circulation research*. 2007;100:381-390.
135. Wang L, Gill R, Pedersen TL, Higgins LJ, Newman JW and Rutledge JC. Triglyceride-rich lipoprotein lipolysis releases neutral and oxidized FFAs that induce endothelial cell inflammation. *Journal of lipid research*. 2009;50:204-213.
136. Budoff M. Triglycerides and triglyceride-rich lipoproteins in the causal pathway of cardiovascular disease. *The American journal of cardiology*. 2016;118:138-145.
137. Nordestgaard BG. Triglyceride-rich lipoproteins and atherosclerotic cardiovascular disease: new insights from epidemiology, genetics, and biology. *Circulation research*. 2016;118:547-563.
138. Gutteridge J. Copper-phenanthroline-induced site-specific oxygen-radical damage to DNA. Detection of loosely bound trace copper in biological fluids. *Biochemical Journal*. 1984;218:983.
139. Kleinveld HA, Hak-Lemmers H, Stalenhoef A and Demacker P. Improved measurement of low-density-lipoprotein susceptibility to copper-induced oxidation: application of a short procedure for isolating low-density lipoprotein. *Clinical chemistry*. 1992;38:2066-2072.
140. Ramos P, Gieseg S, Schuster B and Esterbauer H. Effect of temperature and phase transition on oxidation resistance of low density lipoprotein. *Journal of lipid research*. 1995;36:2113-2128.
141. Gieseg SP and Esterbauer H. Low density lipoprotein is saturable by pro-oxidant copper. *FEBS letters*. 1994;343:188-194.
142. Ziouzenkova O, Sevanian A, Abuja PM, Ramos P and Esterbauer H. Copper can promote oxidation of LDL by markedly different mechanisms. *Free radical biology and medicine*. 1998;24:607-623.
143. Thomas CE and Jackson RL. Lipid hydroperoxide involvement in copper-dependent and independent oxidation of low density lipoproteins. *Journal of Pharmacology and Experimental Therapeutics*. 1991;256:1182-1188.
144. Frei B and Gaziano J. Content of antioxidants, preformed lipid hydroperoxides, and cholesterol as predictors of the susceptibility of human LDL to metal ion-dependent and-independent oxidation. *Journal of lipid research*. 1993;34:2135-2145.
145. O'leary V, Darley-Usmar V, Russell L and Stone D. Pro-oxidant effects of lipoxygenase-derived peroxides on the copper-initiated oxidation of low-density lipoprotein. *Biochemical journal*. 1992;282:631-634.
146. Nichols B and Bainton D. Differentiation of human monocytes in bone marrow and blood. Sequential formation of two granule populations. *Laboratory investigation; a journal of technical methods and pathology*. 1973;29:27.
147. Harrison J and Schultz J. Studies on the chlorinating activity of myeloperoxidase. *Journal of Biological Chemistry*. 1976;251:1371-1374.
148. HAWKINS CL and DAVIES MJ. Hypochlorite-induced damage to proteins: formation of nitrogen-centred radicals from lysine residues and their role in protein fragmentation. *Biochemical journal*. 1998;332:617-625.
149. Hawkins CL and Davies MJ. Hypochlorite-induced damage to nucleosides: formation of chloramines and nitrogen-centered radicals. *Chemical Research in Toxicology*. 2001;14:1071-1081.
150. Zhang R, Brennan M-L, Shen Z, MacPherson JC, Schmitt D, Molenda CE and Hazen SL. Myeloperoxidase functions as a major enzymatic catalyst for initiation of lipid

peroxidation at sites of inflammation. *Journal of Biological Chemistry*. 2002;277:46116-46122.
151. Rees MD, Hawkins CL and Davies MJ. Hypochlorite-mediated fragmentation of hyaluronan, chondroitin sulfates, and related N-acetyl glycosamines: evidence for chloramide intermediates, free radical transfer reactions, and site-specific fragmentation. *Journal of the American Chemical Society*. 2003;125:13719-13733.
152. McGowan SE. Mechanisms of extracellular matrix proteoglycan degradation by human neutrophils. *Am J Respir Cell Mol Biol*. 1990;2:271-279.
153. Daugherty A, Dunn JL, Rateri DL and Heinecke JW. Myeloperoxidase, a catalyst for lipoprotein oxidation, is expressed in human atherosclerotic lesions. *The Journal of clinical investigation*. 1994;94:437-444.
154. Kutter D, Devaquet P, Vanderstocken G, Paulus J-M, Marchal V and Gothot A. Consequences of total and subtotal myeloperoxidase deficiency: risk or benefit? *Acta haematologica*. 2000;104:10-15.
155. Akong-Moore K, Chow OA, von Köckritz-Blickwede M and Nizet V. Influences of chloride and hypochlorite on neutrophil extracellular trap formation. *PloS one*. 2012;7.
156. Metzler KD, Fuchs TA, Nauseef WM, Reumaux D, Roesler J, Schulze I, Wahn V, Papayannopoulos V and Zychlinsky A. Myeloperoxidase is required for neutrophil extracellular trap formation: implications for innate immunity. *Blood, The Journal of the American Society of Hematology*. 2011;117:953-959.
157. Parker H, Dragunow M, Hampton MB, Kettle AJ and Winterbourn CC. Requirements for NADPH oxidase and myeloperoxidase in neutrophil extracellular trap formation differ depending on the stimulus. *Journal of leukocyte biology*. 2012;92:841-849.
158. Gaul DS, Stein S and Matter CM. Neutrophils in cardiovascular disease. 2017.
159. Kahlenberg JM, Carmona-Rivera C, Smith CK and Kaplan MJ. Neutrophil extracellular trap–associated protein activation of the NLRP3 inflammasome is enhanced in lupus macrophages. *The journal of immunology*. 2013;190:1217-1226.
160. Hoseini Z, Sepahvand F, Rashidi B, Sahebkar A, Masoudifar A and Mirzaei H. NLRP3 inflammasome: its regulation and involvement in atherosclerosis. *Journal of Cellular Physiology*. 2018;233:2116-2132.
161. Nicholls SJ, Zheng L and Hazen SL. Formation of dysfunctional high-density lipoprotein by myeloperoxidase. *Trends in cardiovascular medicine*. 2005;15:212-219.
162. Undurti A, Huang Y, Lupica JA, Smith JD, DiDonato JA and Hazen SL. Modification of high density lipoprotein by myeloperoxidase generates a pro-inflammatory particle. *Journal of Biological Chemistry*. 2009;284:30825-30835.
163. Chen X, Duong M-N, Nicholls SJ and Bursill C. Myeloperoxidase modification of high-density lipoprotein suppresses human endothelial cell proliferation and migration via inhibition of ERK1/2 and Akt activation. *Atherosclerosis*. 2018;273:75-83.
164. Zhou B, Zu L, Chen Y, Zheng X, Wang Y, Pan B, Dong M, Zhou E, Zhao M and Zhang Y. Myeloperoxidase-oxidized high density lipoprotein impairs atherosclerotic plaque stability by inhibiting smooth muscle cell migration. *Lipids in health and disease*. 2017;16:3.
165. Carr AC, Myzak MC, Stocker R, McCall MR and Frei B. Myeloperoxidase binds to low-density lipoprotein: potential implications for atherosclerosis. *FEBS letters*. 2000;487:176-180.
166. Savenkova M, Mueller DM and Heinecke JW. Tyrosyl radical generated by myeloperoxidase is a physiological catalyst for the initiation of lipid peroxidation in low density lipoprotein. *Journal of Biological Chemistry*. 1994;269:20394-20400.
167. Malle E, Marsche G, Arnhold J and Davies MJ. Modification of low-density lipoprotein by myeloperoxidase-derived oxidants and reagent hypochlorous acid.

Biochimica et Biophysica Acta (BBA)-Molecular and Cell Biology of Lipids. 2006;1761:392-415.
168. Podrez EA, Schmitt D, Hoff HF and Hazen SL. Myeloperoxidase-generated reactive nitrogen species convert LDL into an atherogenic form in vitro. *The Journal of clinical investigation*. 1999;103:1547-1560.
169. Liu Q, Liu Y, Shi J, Gao M, Liu Y, Cong Y, Li Y, Wang Y, Yu M and Lu Y. Entire peroxidation reaction system of Myeloperoxidase correlates with progressive Low-Density Lipoprotein modifications via reactive aldehydes in atherosclerotic patients with hypertension. *Cellular Physiology and Biochemistry*. 2018;50:1245-1254.
170. Podrez EA, Febbraio M, Sheibani N, Schmitt D, Silverstein RL, Hajjar DP, Cohen PA, Frazier WA, Hoff HF and Hazen SL. Macrophage scavenger receptor CD36 is the major receptor for LDL modified by monocyte-generated reactive nitrogen species. *The Journal of clinical investigation*. 2000;105:1095-1108.
171. Abdo AI, Rayner BS, van Reyk DM and Hawkins CL. Low-density lipoprotein modified by myeloperoxidase oxidants induces endothelial dysfunction. *Redox biology*. 2017;13:623-632.
172. Nicholls SJ and Hazen SL. Myeloperoxidase, modified lipoproteins, and atherogenesis. *Journal of lipid research*. 2009;50:S346-S351.
173. Davies MD and Hawkins CL. The role of myeloperoxidase (MPO) in biomolecule modification, chronic inflammation and disease. *Antioxidants and Redox Signaling*. 2019.
174. Fukami K, Yamagishi S-i and Okuda S. Role of AGEs-RAGE system in cardiovascular disease. *Current pharmaceutical design*. 2014;20:2395-2402.
175. Hedrick C, Thorpe S, Fu M-X, Harper C, Yoo J, Kim S-M, Wong H and Peters A. Glycation impairs high-density lipoprotein function. *Diabetologia*. 2000;43:312-320.
176. Du Q, Qian M-M, Liu P-L, Zhang L, Wang Y and Liu D-H. Glycation of high-density lipoprotein triggers oxidative stress and promotes the proliferation and migration of vascular smooth muscle cells. *Journal of geriatric cardiology: JGC*. 2017;14:473.
177. Rabbani N, Godfrey L, Xue M, Shaheen F, Geoffrion M, Milne R and Thornalley PJ. Glycation of LDL by methylglyoxal increases arterial atherogenicity: a possible contributor to increased risk of cardiovascular disease in diabetes. *Diabetes*. 2011;60:1973-1980.
178. Lopes-Virella MF, Hunt KJ, Baker NL, Lachin J, Nathan DM, Virella G, Control D, Trial C, Interventions EoD and Group CR. Levels of oxidized LDL and advanced glycation end products–modified LDL in circulating immune complexes are strongly associated with increased levels of carotid intima-media thickness and its progression in type 1 diabetes. *Diabetes*. 2011;60:582-589.
179. Sima AV, Botez GM, Stancu CS, Manea A, Raicu M and Simionescu M. Effect of irreversibly glycated LDL in human vascular smooth muscle cells: lipid loading, oxidative and inflammatory stress. *Journal of cellular and molecular medicine*. 2010;14:2790-2802.
180. Knott HM, Brown BE, Davies MJ and Dean RT. Glycation and glycoxidation of low-density lipoproteins by glucose and low-molecular mass aldehydes: Formation of modified and oxidized particles. *European Journal of Biochemistry*. 2003;270:3572-3582.
181. Purmalek MM, Carlucci PM, Dey AK, Sampson M, Temesgen-Oyelakin Y, Sakhardande S, Lerman JB, Fike A, Davis M and Chung JH. Association of lipoprotein subfractions and glycoprotein acetylation with coronary plaque burden in SLE. *Lupus Science & Medicine*. 2019;6.
182. Naruszewicz M, Mirkiewicz E, Olszewski AJ and McCully KS. Thiolation of low-density lipoprotein by homocysteine thiolactone causes increased aggregation and altered interaction with cultured macrophages. *Nutrition Metabolism and Cardiovascular Diseases*. 1994;4:70-70.

183. Goldstein JL, Ho Y, Basu SK and Brown MS. Binding site on macrophages that mediates uptake and degradation of acetylated low density lipoprotein, producing massive cholesterol deposition. *Proceedings of the National Academy of Sciences*. 1979;76:333-337.
184. Brown MS, Goldstein JL, Krieger M, Ho Y and Anderson R. Reversible accumulation of cholesteryl esters in macrophages incubated with acetylated lipoproteins. *The Journal of cell biology*. 1979;82:597-613.
185. Watson AD, Leitinger N, Navab M, Faull KF, Hörkkö S, Witztum JL, Palinski W, Schwenke D, Salomon RG and Sha W. Structural identification by mass spectrometry of oxidized phospholipids in minimally oxidized low density lipoprotein that induce monocyte/endothelial interactions and evidence for their presence in vivo. *Journal of Biological Chemistry*. 1997;272:13597-13607.
186. Liokatis S, Dose A, Schwarzer D and Selenko P. Simultaneous detection of protein phosphorylation and acetylation by high-resolution NMR spectroscopy. *Journal of the American Chemical Society*. 2010;132:14704-14705.
187. Craig WY, Poulin SE, Nelson CP and Ritchie RF. ELISA of IgG antibody to oxidized low-density lipoprotein: effects of blocking buffer and method of data expression. *Clinical chemistry*. 1994;40:882-888.
188. Podrez EA, O'Neil J, Salomon RG, Schreiber MJ and Hoff HF. Measurement of oxidation in plasma Lp (a) in CAPD patients using a novel ELISA. *Kidney international*. 1998;54:637-645.
189. Takeuchi M, Yanase Y, Matsuura N, Yamagishi S-i, Kameda Y, Bucala R and Makita Z. Immunological detection of a novel advanced glycation end-product. *Molecular Medicine*. 2001;7:783-791.
190. Rael LT, Thomas GW, Craun ML, Curtis CG, Bar-Or R and Bar-Or D. Lipid peroxidation and the thiobarbituric acid assay: standardization of the assay when using saturated and unsaturated fatty acids. *BMB Reports*. 2004;37:749-752.
191. Lajoie P, Goetz JG, Dennis JW and Nabi IR. Lattices, rafts, and scaffolds: domain regulation of receptor signaling at the plasma membrane. *Journal of Cell Biology*. 2009;185:381-385.
192. Stellaard F and Lütjohann D. Fractional cholesterol absorption measurements in humans: determinants of the blood-based dual stable isotope tracer technique. *Journal of clinical lipidology*. 2015;9:14-25.
193. Bosner MS, Lange LG, Stenson WF and Ostlund RE. Percent cholesterol absorption in normal women and men quantified with dual stable isotopic tracers and negative ion mass spectrometry. *Journal of lipid research*. 1999;40:302-308.
194. Mitchell J, Stone B, Logan G and Duane W. Role of cholesterol synthesis in regulation of bile acid synthesis and biliary cholesterol secretion in humans. *Journal of lipid research*. 1991;32:1143-1149.
195. Garcia-Calvo M, Lisnock J, Bull HG, Hawes BE, Burnett DA, Braun MP, Crona JH, Davis HR, Dean DC and Detmers PA. The target of ezetimibe is Niemann-Pick C1-Like 1 (NPC1L1). *Proceedings of the National Academy of Sciences*. 2005;102:8132-8137.
196. Nguyen TM, Sawyer JK, Kelley KL, Davis MA and Rudel LL. Cholesterol esterification by ACAT2 is essential for efficient intestinal cholesterol absorption: evidence from thoracic lymph duct cannulation. *Journal of lipid research*. 2012;53:95-104.
197. Iqbal J, Anwar K and Hussain MM. Multiple, independently regulated pathways of cholesterol transport across the intestinal epithelial cells. *Journal of Biological Chemistry*. 2003;278:31610-31620.
198. Nordestgaard BG and Varbo A. Triglycerides and cardiovascular disease. *The Lancet*. 2014;384:626-635.

199. Abumrad NA and Davidson NO. Role of the gut in lipid homeostasis. *Physiological reviews*. 2012;92:1061-1085.
200. Chau P, Nakamura Y, Fielding CJ and Fielding PE. Mechanism of prebeta-HDL formation and activation. *Biochemistry*. 2006;45:3981-3987.
201. Barrans A, Jaspard B, Barbaras R, Chap H, Perret B and Collet X. Pre-β HDL: structure and metabolism. *Biochimica et Biophysica Acta (BBA)-Lipids and Lipid Metabolism*. 1996;1300:73-85.
202. de Boer JF, Kuipers F and Groen AK. Cholesterol transport revisited: a new turbo mechanism to drive cholesterol excretion. *Trends in Endocrinology & Metabolism*. 2018;29:123-133.
203. Leren TP. Sorting an LDL receptor with bound PCSK9 to intracellular degradation. *Atherosclerosis*. 2014;237:76-81.
204. Nicholls SJ, Puri R, Anderson T, Ballantyne CM, Cho L, Kastelein JJ, Koenig W, Somaratne R, Kassahun H and Yang J. Effect of evolocumab on progression of coronary disease in statin-treated patients: the GLAGOV randomized clinical trial. *Jama*. 2016;316:2373-2384.
205. Reboul E, Klein A, Bietrix F, Gleize B, Malezet-Desmoulins C, Schneider M, Margotat A, Lagrost L, Collet X and Borel P. Scavenger receptor class B type I (SR-BI) is involved in vitamin E transport across the enterocyte. *Journal of Biological Chemistry*. 2006;281:4739-4745.
206. Saddar S, Carriere V, Lee W-R, Tanigaki K, Yuhanna IS, Parathath S, Morel E, Warrier M, Sawyer JK and Gerard RD. Scavenger receptor class B type I is a plasma membrane cholesterol sensor. *Circulation research*. 2013;112:140-151.
207. Out R, Hoekstra M, Spijkers JA, Kruijt JK, Van Eck M, Bos IS, Twisk J and Van Berkel TJ. Scavenger receptor class B type I is solely responsible for the selective uptake of cholesteryl esters from HDL by the liver and the adrenals in mice. *Journal of lipid research*. 2004;45:2088-2095.
208. Nicholls SJ and Bubb K. The mystery of evacetrapib-why are CETP inhibitors failing? 2020.
209. Hafiane A and Genest J. ATP binding cassette A1 (ABCA1) mediates microparticle formation during high-density lipoprotein (HDL) biogenesis. *Atherosclerosis*. 2017;257:90-99.
210. Hayden MR, Clee SM, Brooks-Wilson A, Genest Jr J, Attie A and Kastelein JJ. Cholesterol efflux regulatory protein, Tangier disease and familial high-density lipoprotein deficiency. *Current opinion in lipidology*. 2000;11:117-122.
211. McNeish J, Aiello RJ, Guyot D, Turi T, Gabel C, Aldinger C, Hoppe KL, Roach ML, Royer LJ and de Wet J. High density lipoprotein deficiency and foam cell accumulation in mice with targeted disruption of ATP-binding cassette transporter-1. *Proceedings of the National Academy of Sciences*. 2000;97:4245-4250.
212. Yvan-Charvet L, Ranalletta M, Wang N, Han S, Terasaka N, Li R, Welch C and Tall AR. Combined deficiency of ABCA1 and ABCG1 promotes foam cell accumulation and accelerates atherosclerosis in mice. *The Journal of clinical investigation*. 2007;117:3900-3908.
213. Liao H, Langmann T, Schmitz G and Zhu Y. Native LDL upregulation of ATP-binding cassette transporter-1 in human vascular endothelial cells. *Arteriosclerosis, thrombosis, and vascular biology*. 2002;22:127-132.
214. Schaefer EJ, Blum CB, Levy RI, Jenkins LL, Alaupovic P, Foster DM and Brewer Jr HB. Metabolism of high-density lipoprotein apolipoproteins in Tangier disease. *New England Journal of Medicine*. 1978;299:905-910.

215. Kennedy MA, Barrera GC, Nakamura K, Baldán Á, Tarr P, Fishbein MC, Frank J, Francone OL and Edwards PA. ABCG1 has a critical role in mediating cholesterol efflux to HDL and preventing cellular lipid accumulation. *Cell metabolism*. 2005;1:121-131.
216. Gelissen IC, Harris M, Rye K-A, Quinn C, Brown AJ, Kockx M, Cartland S, Packianathan M, Kritharides L and Jessup W. ABCA1 and ABCG1 synergize to mediate cholesterol export to apoA-I. *Arteriosclerosis, thrombosis, and vascular biology*. 2006;26:534-540.
217. Vaughan AM and Oram JF. ABCA1 and ABCG1 or ABCG4 act sequentially to remove cellular cholesterol and generate cholesterol-rich HDL. *Journal of lipid research*. 2006;47:2433-2443.
218. Wang X, Collins HL, Ranalletta M, Fuki IV, Billheimer JT, Rothblat GH, Tall AR and Rader DJ. Macrophage ABCA1 and ABCG1, but not SR-BI, promote macrophage reverse cholesterol transport in vivo. *The Journal of clinical investigation*. 2007;117:2216-2224.
219. Terasaka N, Yu S, Yvan-Charvet L, Wang N, Mzhavia N, Langlois R, Pagler T, Li R, Welch CL and Goldberg IJ. ABCG1 and HDL protect against endothelial dysfunction in mice fed a high-cholesterol diet. *The Journal of clinical investigation*. 2008;118:3701-3713.
220. Shen W-J, Azhar S and Kraemer FB. SR-B1: a unique multifunctional receptor for cholesterol influx and efflux. *Annual review of physiology*. 2018;80:95-116.
221. Rigotti A, Trigatti BL, Penman M, Rayburn H, Herz J and Krieger M. A targeted mutation in the murine gene encoding the high density lipoprotein (HDL) receptor scavenger receptor class B type I reveals its key role in HDL metabolism. *Proceedings of the National Academy of Sciences*. 1997;94:12610-12615.
222. Van Eck M, Twisk J, Hoekstra M, Van Rij BT, Van der Lans CA, Bos IST, Kruijt JK, Kuipers F and Van Berkel TJ. Differential effects of scavenger receptor BI deficiency on lipid metabolism in cells of the arterial wall and in the liver. *Journal of Biological Chemistry*. 2003;278:23699-23705.
223. Al-Jarallah A and Trigatti BL. A role for the scavenger receptor, class B type I in high density lipoprotein dependent activation of cellular signaling pathways. *Biochimica et Biophysica Acta (BBA)-Molecular and Cell Biology of Lipids*. 2010;1801:1239-1248.
224. Saddar S, Mineo C and Shaul PW. Signaling by the high-affinity HDL receptor scavenger receptor B type I. *Arteriosclerosis, thrombosis, and vascular biology*. 2010;30:144-150.
225. Pei Y, Chen X, Aboutouk D, Fuller MT, Dadoo O, Yu P, White EJ, Igdoura SA and Trigatti BL. SR-BI in bone marrow derived cells protects mice from diet induced coronary artery atherosclerosis and myocardial infarction. *PloS one*. 2013;8:e72492.
226. Song GJ, Kim S-M, Park K-H, Kim J, Choi I and Cho K-H. SR-BI mediates high density lipoprotein (HDL)-induced anti-inflammatory effect in macrophages. *Biochemical and biophysical research communications*. 2015;457:112-118.
227. Zhang J, Qu C, Li T, Cui W, Wang X and Du J. Phagocytosis mediated by scavenger receptor class BI promotes macrophage transition during skeletal muscle regeneration. *Journal of Biological Chemistry*. 2019;294:15672-15685.
228. Zhang X, Sessa WC and Fernández-Hernando C. Endothelial transcytosis of lipoproteins in atherosclerosis. *Frontiers in cardiovascular medicine*. 2018;5:130.
229. Huang L, Chambliss KL, Gao X, Yuhanna IS, Behling-Kelly E, Bergaya S, Ahmed M, Michaely P, Luby-Phelps K and Darehshouri A. SR-B1 drives endothelial cell LDL transcytosis via DOCK4 to promote atherosclerosis. *Nature*. 2019;569:565-569.
230. Fung KYY, Lee W and Fairn G. Inhibition of Low density Lipoprotein Internalization and Transcytosis by HDL; an alternative role for “good” cholesterol. *The FASEB Journal*. 2020;34:1-1.
231. Yuhanna IS, Zhu Y, Cox BE, Hahner LD, Osborne-Lawrence S, Lu P, Marcel YL, Anderson RG, Mendelsohn ME and Hobbs HH. High-density lipoprotein binding to

scavenger receptor-BI activates endothelial nitric oxide synthase. *Nature medicine*. 2001;7:853-857.
232. Zhang Q-H, Zu X-Y, Cao R-X, Liu J-H, Mo Z-C, Zeng Y, Li Y-B, Xiong S-L, Liu X and Liao D-F. An involvement of SR-B1 mediated PI3K–Akt–eNOS signaling in HDL-induced cyclooxygenase 2 expression and prostacyclin production in endothelial cells. *Biochemical and biophysical research communications*. 2012;420:17-23.
233. Lim HY, Thiam CH, Yeo KP, Bisoendial R, Hii CS, McGrath KC, Tan KW, Heather A, Alexander JSJ and Angeli V. Lymphatic vessels are essential for the removal of cholesterol from peripheral tissues by SR-BI-mediated transport of HDL. *Cell metabolism*. 2013;17:671-684.
234. Ashby DT, Rye K-A, Clay MA, Vadas MA, Gamble JR and Barter PJ. Factors influencing the ability of HDL to inhibit expression of vascular cell adhesion molecule-1 in endothelial cells. *Arteriosclerosis, thrombosis, and vascular biology*. 1998;18:1450-1455.
235. Nofer J-R, Geigenmüller S, Göpfert C, Assmann G, Buddecke E and Schmidt A. High density lipoprotein-associated lysosphingolipids reduce E-selectin expression in human endothelial cells. *Biochemical and biophysical research communications*. 2003;310:98-103.
236. Tabet F, Vickers KC, Torres LFC, Wiese CB, Shoucri BM, Lambert G, Catherinet C, Prado-Lourenco L, Levin MG and Thacker S. HDL-transferred microRNA-223 regulates ICAM-1 expression in endothelial cells. *Nature communications*. 2014;5:1-14.
237. Mineo C, Deguchi H, Griffin JH and Shaul PW. Endothelial and antithrombotic actions of HDL. *Circulation research*. 2006;98:1352-1364.
238. Gugliucci A and Menini T. Paraoxonase 1 and HDL maturation. *Clinica Chimica Acta*. 2015;439:5-13.
239. Rosenblat M, Karry R and Aviram M. Paraoxonase 1 (PON1) is a more potent antioxidant and stimulant of macrophage cholesterol efflux, when present in HDL than in lipoprotein-deficient serum: Relevance to diabetes. *Atherosclerosis*. 2006;187:74.e1-74.e10.
240. Rosenblat M, Vaya J, Shih D and Aviram M. Paraoxonase 1 (PON1) enhances HDL-mediated macrophage cholesterol efflux via the ABCA1 transporter in association with increased HDL binding to the cells: a possible role for lysophosphatidylcholine. *Atherosclerosis*. 2005;179:69-77.
241. Efrat M and Aviram M. Paraoxonase 1 Interactions with HDL, Antioxidants and Macrophages Regulate Atherogenesis – A Protective Role for HDL Phospholipids. In: T. S. Reddy, ed. *Paraoxonases in Inflammation, Infection, and Toxicology* Totowa, NJ: Humana Press; 2010: 153-166.
242. Jaouad L, Milochevitch C and Khalil A. PON1 paraoxonase activity is reduced during HDL oxidation and is an indicator of HDL antioxidant capacity. *Free radical research*. 2003;37:77-83.
243. Eren E, Ellidag HY, Aydin O and Yılmaz N. HDL-associated paraoxonase 1 as a bridge between postmenopausal osteoporosis and cardiovascular disease. *Chonnam medical journal*. 2014;50:75-81.
244. Pentikäinen M, Öörni K, Ala-Korpela M and Kovanen P. Modified LDL–trigger of atherosclerosis and inflammation in the arterial intima. *Journal of internal medicine*. 2000;247:359-370.
245. Kzhyshkowska J, Neyen C and Gordon S. Role of macrophage scavenger receptors in atherosclerosis. *Immunobiology*. 2012;217:492-502.
246. Caruso MG, Notarnicola M, Santillo M, Cavallini A and Di AL. Enhanced 3-hydroxy-3-methyl-glutaryl coenzyme A reductase activity in human colorectal cancer not expressing low density lipoprotein receptor. *Anticancer research*. 1999;19:451-454.

247. Powell EE and Kroon PA. Low density lipoprotein receptor and 3-hydroxy-3-methylglutaryl coenzyme A reductase gene expression in human mononuclear leukocytes is regulated coordinately and parallels gene expression in human liver. *The Journal of clinical investigation*. 1994;93:2168-2174.
248. Shimomura I, Bashmakov Y, Shimano H, Horton JD, Goldstein JL and Brown MS. Cholesterol feeding reduces nuclear forms of sterol regulatory element binding proteins in hamster liver. *Proceedings of the National Academy of Sciences*. 1997;94:12354-12359.
249. Go G-w and Mani A. Low-density lipoprotein receptor (LDLR) family orchestrates cholesterol homeostasis. *The Yale journal of biology and medicine*. 2012;85:19.
250. Murphy AJ, Akhtari M, Tolani S, Pagler T, Bijl N, Kuo C-L, Wang M, Sanson M, Abramowicz S and Welch C. ApoE regulates hematopoietic stem cell proliferation, monocytosis, and monocyte accumulation in atherosclerotic lesions in mice. *The Journal of clinical investigation*. 2011;121:4138-4149.
251. Yancey PG, Yu H, Linton MF and Fazio S. A pathway-dependent on apoE, ApoAI, and ABCA1 determines formation of buoyant high-density lipoprotein by macrophage foam cells. *Arteriosclerosis, thrombosis, and vascular biology*. 2007;27:1123-1131.
252. Mazzone T and Reardon C. Expression of heterologous human apolipoprotein E by J774 macrophages enhances cholesterol efflux to HDL3. *Journal of lipid research*. 1994;35:1345-1353.
253. Zanotti I, Pedrelli M, Potì F, Stomeo G, Gomaraschi M, Calabresi L and Bernini F. Macrophage, but not systemic, apolipoprotein E is necessary for macrophage reverse cholesterol transport in vivo. *Arteriosclerosis, thrombosis, and vascular biology*. 2011;31:74-80.
254. Ali K, Middleton M, Puré E and Rader DJ. Apolipoprotein E suppresses the type I inflammatory response in vivo. *Circulation research*. 2005;97:922-927.
255. Li K, Ching D, Luk FS and Raffai RL. Apolipoprotein E enhances microRNA-146a in monocytes and macrophages to suppress nuclear factor-κB–driven inflammation and atherosclerosis. *Circulation research*. 2015;117:e1-e11.
256. Maor I, Kaplan M, Hayek T, Vaya J, Hoffman A and Aviram M. Oxidized monocyte-derived macrophages in aortic atherosclerotic lesion from apolipoprotein E-deficient mice and from human carotid artery contain lipid peroxides and oxysterols. *Biochemical and biophysical research communications*. 2000;269:775-780.
257. Rosenblat M, Coleman R and Aviram M. Increased macrophage glutathione content reduces cell-mediated oxidation of LDL and atherosclerosis in apolipoprotein E-deficient mice. *Atherosclerosis*. 2002;163:17-28.
258. Miyata M and Smith JD. Apolipoprotein E allele–specific antioxidant activity and effects on cytotoxicity by oxidative insults and β–amyloid peptides. *Nature genetics*. 1996;14:55-61.
259. Tao H, Aakula S, Abumrad NN and Hajri T. Peroxisome proliferator-activated receptor-γ regulates the expression and function of very-low-density lipoprotein receptor. *American Journal of Physiology-Endocrinology and Metabolism*. 2010;298:E68-E79.
260. Kwok S, Singh-Bist A, Natu V and Kraemer F. Dietary regulation of the very low density lipoprotein receptor in mouse heart and fat. *Hormone and metabolic research*. 1997;29:524-529.
261. Goudriaan JR, Santo SME, Voshol PJ, Teusink B, van Dijk KW, van Vlijmen BJ, Romijn JA, Havekes LM and Rensen PC. The VLDL receptor plays a major role in chylomicron metabolism by enhancing LPL-mediated triglyceride hydrolysis. *Journal of lipid research*. 2004;45:1475-1481.
262. Yagyu H, Lutz EP, Kako Y, Marks S, Hu Y, Choi SY, Bensadoun A and Goldberg IJ. Very low density lipoprotein (VLDL) receptor-deficient mice have reduced lipoprotein lipase

activity possible causes of hypertriglyceridemia and reduced body mass with VLDL receptor deficiency. *Journal of Biological Chemistry*. 2002;277:10037-10043.
263. Polonsky TS, McClelland RL, Jorgensen NW, Bild DE, Burke GL, Guerci AD and Greenland P. Coronary artery calcium score and risk classification for coronary heart disease prediction. *Jama*. 2010;303:1610-1616.
264. Kataoka Y, Puri R, Hammadah M, Duggal B, Uno K, Kapadia SR, Tuzcu EM, Nissen SE and Nicholls SJ. Spotty calcification and plaque vulnerability in vivo: frequency-domain optical coherence tomography analysis. *Cardiovascular diagnosis and therapy*. 2014;4:460.
265. Yahagi K, Kolodgie FD, Lutter C, Mori H, Romero ME, Finn AV and Virmani R. Pathology of human coronary and carotid artery atherosclerosis and vascular calcification in diabetes mellitus. *Arteriosclerosis, thrombosis, and vascular biology*. 2017;37:191-204.
266. Chen J, Budoff MJ, Reilly MP, Yang W, Rosas SE, Rahman M, Zhang X, Roy JA, Lustigova E and Nessel L. Coronary artery calcification and risk of cardiovascular disease and death among patients with chronic kidney disease. *JAMA cardiology*. 2017;2:635-643.
267. Samelson EJ, Cupples LA, Broe KE, Hannan MT, O'Donnell CJ and Kiel DP. Vascular calcification in middle age and long-term risk of hip fracture: the Framingham Study. *Journal of Bone and Mineral Research*. 2007;22:1449-1454.
268. Reaven P and Sacks J. Coronary artery and abdominal aortic calcification are associated with cardiovascular disease in type 2 diabetes. *Diabetologia*. 2005;48:379-385.
269. Kraus MA, Kalra PA, Hunter J, Menoyo J and Stankus N. The prevalence of vascular calcification in patients with end-stage renal disease on hemodialysis: a cross-sectional observational study. *Therapeutic advances in chronic disease*. 2015;6:84-96.
270. Rocha-Singh KJ, Zeller T and Jaff MR. Peripheral arterial calcification: prevalence, mechanism, detection, and clinical implications. *Catheterization and Cardiovascular Interventions*. 2014;83:E212-E220.
271. Sangiorgi G, Rumberger JA, Severson A, Edwards WD, Gregoire J, Fitzpatrick LA and Schwartz RS. Arterial calcification and not lumen stenosis is highly correlated with atherosclerotic plaque burden in humans: a histologic study of 723 coronary artery segments using nondecalcifying methodology. *Journal of the American College of Cardiology*. 1998;31:126-133.
272. Arad Y, Goodman KJ, Roth M, Newstein D and Guerci AD. Coronary calcification, coronary disease risk factors, C-reactive protein, and atherosclerotic cardiovascular disease events: the St. Francis Heart Study. *Journal of the American College of Cardiology*. 2005;46:158-165.
273. Yang W-J, Zheng L, Wu X-H, Huang Z-Q, Niu C-B, Zhao H-L, Leung TW-H, Wong LK-S and Chen X-Y. Postmortem study exploring distribution and patterns of intracranial artery calcification. *Stroke*. 2018;49:2767-2769.
274. Fletcher A, Singh T, Syed M and Dweck M. Imaging aortic valve calcification: Significance, approach and implications. *Clinical Radiology*. 2021;76:15-26.
275. Virchow R. As based upon physiological and pathological histology. *Nutrition reviews*. 1989;47:23-25.
276. Duer MJ, Friščić T, Proudfoot D, Reid DG, Schoppet M, Shanahan CM, Skepper JN and Wise ER. Mineral surface in calcified plaque is like that of bone: further evidence for regulated mineralization. *Arteriosclerosis, thrombosis, and vascular biology*. 2008;28:2030-2034.

277. Chistiakov DA, Myasoedova VA, Melnichenko AA, Grechko AV and Orekhov AN. Calcifying Matrix Vesicles and Atherosclerosis. *BioMed research international*. 2017;2017.
278. Otsuka F, Sakakura K, Yahagi K, Joner M and Virmani R. Has our understanding of calcification in human coronary atherosclerosis progressed? *Arteriosclerosis, thrombosis, and vascular biology*. 2014;34:724-736.
279. Proudfoot D and Shanahan CM. Biology of calcification in vascular cells: intima versus media. *Herz*. 2001;26:245-251.
280. Leopold JA. Vascular Calcification: Mechanisms of Vascular Smooth Muscle Cell Calcification. *Trends in cardiovascular medicine*. 2015;25:267-274.
281. Sutliff RL, Walp ER, El-Ali AM, Elkhatib S, Lomashvili KA and O'Neill WC. Effect of medial calcification on vascular function in uremia. *American Journal of Physiology-Renal Physiology*. 2011;301:F78-F83.
282. Hutcheson JD, Goettsch C, Bertazzo S, Maldonado N, Ruiz JL, Goh W, Yabusaki K, Faits T, Bouten C and Franck G. Genesis and growth of extracellular-vesicle-derived microcalcification in atherosclerotic plaques. *Nature materials*. 2016;15:335.
283. Vattikuti R and Towler DA. Osteogenic regulation of vascular calcification: an early perspective. *American Journal of Physiology-Endocrinology And Metabolism*. 2004;286:E686-E696.
284. Cardoso L and Weinbaum S. Microcalcifications, Their Genesis, Growth, and Biomechanical Stability in Fibrous Cap Rupture *Molecular, Cellular, and Tissue Engineering of the Vascular System*: Springer; 2018: 129-155.
285. Puri R, Nicholls SJ, Shao M, Kataoka Y, Uno K, Kapadia SR, Tuzcu EM and Nissen SE. Impact of statins on serial coronary calcification during atheroma progression and regression. *Journal of the American College of Cardiology*. 2015;65:1273-1282.
286. Karlöf E, Seime T, Dias N, Lengquist M, Witasp A, Almqvist H, Kronqvist M, Gådin JR, Odeberg J and Maegdefessel L. Correlation of computed tomography with carotid plaque transcriptomes associates calcification with lesion-stabilization. *Atherosclerosis*. 2019.
287. Bessueille L and Magne D. Inflammation: a culprit for vascular calcification in atherosclerosis and diabetes. *Cellular and Molecular Life Sciences*. 2015;72:2475-2489.
288. Aghagolzadeh P, Bachtler M, Bijarnia R, Jackson C, Smith ER, Odermatt A, Radpour R and Pasch A. Calcification of vascular smooth muscle cells is induced by secondary calciprotein particles and enhanced by tumor necrosis factor-α. *Atherosclerosis*. 2016;251:404-414.
289. Zickler D, Luecht C, Willy K, Chen L, Witowski J, Girndt M, Fiedler R, Storr M, Kamhieh-Milz J and Schoon J. Tumour necrosis factor-alpha in uraemic serum promotes osteoblastic transition and calcification of vascular smooth muscle cells via extracellular signal-regulated kinases and activator protein 1/c-FOS-mediated induction of interleukin 6 expression. *Nephrology Dialysis Transplantation*. 2017;33:574-585.
290. Kapustin AN, Chatrou ML, Drozdov I, Zheng Y, Davidson SM, Soong DY, Furmanik M, Sanchis P, de Rosales RT and Alvarez-Hernandez D. Vascular smooth muscle cell calcification is mediated by regulated exosome secretion. *Circulation research*. 2015:CIRCRESAHA. 114.305012.
291. Dusso A, Colombo MI and Shanahan CM. Not all vascular smooth muscle cell exosomes calcify equally in chronic kidney disease. *Kidney international*. 2018;93:298-301.
292. Reynolds JL, Joannides AJ, Skepper JN, McNair R, Schurgers LJ, Proudfoot D, Jahnen-Dechent W, Weissberg PL and Shanahan CM. Human vascular smooth muscle cells undergo vesicle-mediated calcification in response to changes in extracellular calcium and phosphate concentrations: a potential mechanism for accelerated vascular

calcification in ESRD. *Journal of the American Society of Nephrology*. 2004;15:2857-2867.
293. Proudfoot D, Skepper J, Hegyi L, Farzaneh-Far A, Shanahan C and Weissberg P. The role of apoptosis in the initiation of vascular calcification. *Zeitschrift für Kardiologie*. 2001;90:43-46.
294. Koike S, Yano S, Tanaka S, Sheikh AM, Nagai A and Sugimoto T. Advanced glycation end-products induce apoptosis of vascular smooth muscle cells: a mechanism for vascular calcification. *International journal of molecular sciences*. 2016;17:1567.
295. Proudfoot D, Skepper JN, Hegyi L, Bennett MR, Shanahan CM and Weissberg PL. Apoptosis regulates human vascular calcification in vitro: evidence for initiation of vascular calcification by apoptotic bodies. *Circulation research*. 2000;87:1055-1062.
296. Nyitrai M, Balla G and Balla J. Oxidative stress: one of the major causes of vascular calcification in chronic kidney disease patients. *Orvosi hetilap*. 2015;156:1926-1931.
297. Mody N, Parhami F, Sarafian TA and Demer LL. Oxidative stress modulates osteoblastic differentiation of vascular and bone cells. *Free Radical Biology and Medicine*. 2001;31:509-519.
298. Byon CH, Javed A, Dai Q, Kappes JC, Clemens TL, Darley-Usmar VM, McDonald JM and Chen Y. Oxidative stress induces vascular calcification through modulation of the osteogenic transcription factor Runx2 by AKT signaling. *Journal of Biological Chemistry*. 2008;283:15319-15327.
299. Shao J-S, Aly ZA, Lai C-F, Cheng S-L, Cai JUN, Huang E, Behrmann ABE and Towler DA. Vascular Bmp–Msx2–Wnt Signaling and Oxidative Stress in Arterial Calcification. *Annals of the New York Academy of Sciences*. 2007;1117:40-50.
300. Tang F, Chen S, Wu X, Wang T, Chen J, Li J, Bao L, Huang H and Liu P. Hypercholesterolemia accelerates vascular calcification induced by excessive vitamin D via oxidative stress. *Calcified tissue international*. 2006;79:326-339.
301. Geng Y, Hsu JJ, Lu J, Ting TC, Miyazaki M, Demer LL and Tintut Y. The role of cellular cholesterol metabolism in vascular cell calcification. *Journal of Biological Chemistry*. 2011:jbc. M111. 269639.
302. Listenberger LL, Han X, Lewis SE, Cases S, Farese RV, Ory DS and Schaffer JE. Triglyceride accumulation protects against fatty acid-induced lipotoxicity. *Proceedings of the National Academy of Sciences*. 2003;100:3077-3082.
303. Masuda M, Miyazaki-Anzai S, Keenan AL, Okamura K, Kendrick J, Chonchol M, Offermanns S, Ntambi JM, Kuro-o M and Miyazaki M. Saturated phosphatidic acids mediate saturated fatty acid–induced vascular calcification and lipotoxicity. *The Journal of Clinical Investigation*. 2015;125:4544-4558.
304. Watson KE, Boström K, Ravindranath R, Lam T, Norton B and Demer LL. TGF-beta 1 and 25-hydroxycholesterol stimulate osteoblast-like vascular cells to calcify. *The Journal of clinical investigation*. 1994;93:2106-2113.
305. Sarig S, Weiss TA, Katz I, Kahana F, Azoury R, Okon E and Kruth HS. Detection of cholesterol associated with calcium mineral using confocal fluorescence microscopy. *Lab Invest*. 1994;71:782-7.
306. Bobryshev YV. Transdifferentiation of smooth muscle cells into chondrocytes in atherosclerotic arteries in situ: implications for diffuse intimal calcification. *The Journal of pathology*. 2005;205:641-650.
307. Boström K, Watson K, Horn S, Wortham C, Herman I and Demer L. Bone morphogenetic protein expression in human atherosclerotic lesions. *Journal of Clinical Investigation*. 1993;91:1800.
308. Ting TC, Miyazaki-Anzai S, Masuda M, Levi M, Demer LL, Tintut Y and Miyazaki M. Increased lipogenesis and stearate accelerate vascular calcification in calcifying vascular cells. *Journal of Biological Chemistry*. 2011:jbc. M111. 237065.

309. Reid DG, Shanahan CM, Duer MJ, Arroyo LG, Schoppet M, Brooks RA and Murray RC. Lipids in biocalcification: contrasts and similarities between intimal and medial vascular calcification and bone by NMR. *Journal of Lipid Research*. 2012;53:1569-1575.
310. Speer MY, Yang H-Y, Brabb T, Leaf E, Look A, Lin W-L, Frutkin A, Dichek D and Giachelli CM. Smooth muscle cells give rise to osteochondrogenic precursors and chondrocytes in calcifying arteries. *Circulation research*. 2009;104:733-741.
311. Afshar M, Luk K, Do R, Dufresne L, Owens DS, Harris TB, Peloso GM, Kerr KF, Wong Q and Smith AV. Association of triglyceride-related genetic variants with mitral annular calcification. *Journal of the American College of Cardiology*. 2017;69:2941-2948.
312. Allahverdian S, Chaabane C, Boukais K, Francis GA and Bochaton-Piallat M-L. Smooth muscle cell fate and plasticity in atherosclerosis. *Cardiovascular research*. 2018;114:540-550.
313. Albarrán-Juárez J, Kaur H, Grimm M, Offermanns S and Wettschureck N. Lineage tracing of cells involved in atherosclerosis. *Atherosclerosis*. 2016;251:445-453.
314. Wang Y, Dubland JA, Allahverdian S, Asonye E, Sahin B, Jaw JE, Sin DD, Seidman MA, Leeper NJ and Francis GA. Smooth muscle cells contribute the majority of foam cells in ApoE (apolipoprotein E)-deficient mouse atherosclerosis. *Arteriosclerosis, thrombosis, and vascular biology*. 2019;39:876-887.
315. Rong JX, Shapiro M, Trogan E and Fisher EA. Transdifferentiation of mouse aortic smooth muscle cells to a macrophage-like state after cholesterol loading. *Proceedings of the National Academy of Sciences*. 2003;100:13531-13536.
316. Chinetti-Gbaguidi G, Daoudi M, Mickael R, Vinod M, Louvet L, Copin C, Fanchon M, Vanhoutte J, Derudas B and Belloy L. Human Alternative Macrophages Populate Calcified Areas of Atherosclerotic Lesions and Display Impaired RANKL-Induced Osteoclastic Bone Resorption Activity. *Circulation Research*. 2017:CIRCRESAHA. 116.310262.
317. Miron RJ, Zohdi H, Fujioka-Kobayashi M and Bosshardt DD. Giant cells around bone biomaterials: Osteoclasts or multi-nucleated giant cells? *Acta biomaterialia*. 2016;46:15-28.
318. Medici D, Shore EM, Lounev VY, Kaplan FS, Kalluri R and Olsen BR. Conversion of vascular endothelial cells into multipotent stem-like cells. *Nature medicine*. 2010;16:1400.
319. Yao Y, Jumabay M, Ly A, Radparvar M, Cubberly MR and Boström KI. A role for the endothelium in vascular calcification. *Circulation research*. 2013;113:495-504.
320. Yung L-M, Sánchez-Duffhues G, ten Dijke P and Yu PB. Bone morphogenetic protein 6 and oxidized low-density lipoprotein synergistically recruit osteogenic differentiation in endothelial cells. *Cardiovascular research*. 2015;108:278-287.
321. Coscas R, Bensussan M, Jacob M-P, Louedec L, Massy Z, Sadoine J, Daudon M, Chaussain C, Bazin D and Michel J-B. Free DNA precipitates calcium phosphate apatite crystals in the arterial wall in vivo. *Atherosclerosis*. 2017;259:60-67.
322. O'Neil LJ, Kaplan MJ and Carmona-Rivera C. The role of neutrophils and neutrophil extracellular traps in vascular damage in systemic lupus erythematosus. *Journal of clinical medicine*. 2019;8:1325.
323. Mangold A, Hofbauer TM, Ondracek AS, Artner T, Scherz T, Speidl WS, Krychtiuk KA, Sadushi-Kolici R, Jakowitsch J and Lang IM. Neutrophil extracellular traps and monocyte subsets at the culprit lesion site of myocardial infarction patients. *Scientific reports*. 2019;9:1-10.
324. Döring Y, Weber C and Soehnlein O. Footprints of neutrophil extracellular traps as predictors of cardiovascular risk. 2013.
325. Cai T, Sun D, Duan Y, Wen P, Dai C, Yang J and He W. WNT/β-catenin signaling promotes VSMCs to osteogenic transdifferentiation and calcification through directly modulating Runx2 gene expression. *Experimental cell research*. 2016;345:206-217.

326. Speer MY, Li X, Hiremath PG and Giachelli CM. Runx2/Cbfa1, but not loss of myocardin, is required for smooth muscle cell lineage reprogramming toward osteochondrogenesis. *Journal of cellular biochemistry*. 2010;110:935-947.
327. Lin M-E, Chen TM, Wallingford MC, Nguyen NB, Yamada S, Sawangmake C, Zhang J, Speer MY and Giachelli CM. Runx2 deletion in smooth muscle cells inhibits vascular osteochondrogenesis and calcification but not atherosclerotic lesion formation. *Cardiovascular Research*. 2016;112:606-616.
328. Steitz SA, Speer MY, Curinga G, Yang H-Y, Haynes P, Aebersold R, Schinke T, Karsenty G and Giachelli CM. Smooth muscle cell phenotypic transition associated with calcification: upregulation of Cbfa1 and downregulation of smooth muscle lineage markers. *Circulation research*. 2001;89:1147-1154.
329. Tintut Y, Parhami F, Boström K, Jackson SM and Demer LL. cAMP Stimulates Osteoblast-like Differentiation of Calcifying Vascular Cells POTENTIAL SIGNALING PATHWAY FOR VASCULAR CALCIFICATION. *Journal of Biological Chemistry*. 1998;273:7547-7553.
330. Lee H-L, Woo KM, Ryoo H-M and Baek J-H. Tumor necrosis factor-α increases alkaline phosphatase expression in vascular smooth muscle cells via MSX2 induction. *Biochemical and biophysical research communications*. 2010;391:1087-1092.
331. Byon CH, Heath JM and Chen Y. Redox signaling in cardiovascular pathophysiology: A focus on hydrogen peroxide and vascular smooth muscle cells. *Redox Biology*. 2016;9:244-253.
332. Sinha A and Vyavahare NR. High-glucose levels and elastin degradation products accelerate osteogenesis in vascular smooth muscle cells. *Diabetes and Vascular Disease Research*. 2013;10:410-419.
333. Ge C, Xiao G, Jiang D, Yang Q, Hatch NE, Roca H and Franceschi RT. Identification and functional characterization of ERK/MAPK phosphorylation sites in the Runx2 transcription factor. *Journal of Biological Chemistry*. 2009;284:32533-32543.
334. Li S-J, Kao Y-H, Chung C-C, Cheng W-L and Chen Y-J. HDAC I inhibitor regulates RUNX2 transactivation through canonical and non-canonical Wnt signaling in aortic valvular interstitial cells. *American journal of translational research*. 2019;11:744.
335. Nishimura R, Wakabayashi M, Hata K, Matsubara T, Honma S, Wakisaka S, Kiyonari H, Shioi G, Yamaguchi A and Tsumaki N. Osterix regulates calcification and degradation of chondrogenic matrices through matrix metalloproteinase 13 (MMP13) expression in association with transcription factor Runx2 during endochondral ossification. *Journal of Biological Chemistry*. 2012;287:33179-33190.
336. Engelse MA, Neele JM, Bronckers AL, Pannekoek H and de Vries CJ. Vascular calcification: expression patterns of the osteoblast-specific gene core binding factor α-1 and the protective factor matrix gla protein in human atherogenesis. *Cardiovascular research*. 2001;52:281-289.
337. Tyson KL, Reynolds JL, McNair R, Zhang Q, Weissberg PL and Shanahan CM. Osteo/chondrocytic transcription factors and their target genes exhibit distinct patterns of expression in human arterial calcification. *Arteriosclerosis, thrombosis, and vascular biology*. 2003;23:489-494.
338. Leboy PS. Regulating bone growth and development with bone morphogenetic proteins. *Annals of the New York Academy of Sciences*. 2006;1068:14-18.
339. Li X, Yang H-Y and Giachelli CM. BMP-2 promotes phosphate uptake, phenotypic modulation, and calcification of human vascular smooth muscle cells. *Atherosclerosis*. 2008;199:271-277.
340. Derwall M, Malhotra R, Lai CS, Beppu Y, Aikawa E, Seehra JS, Zapol WM, Bloch KD and Yu PB. Inhibition of bone morphogenetic protein signaling reduces vascular

calcification and atherosclerosis. *Arteriosclerosis, thrombosis, and vascular biology*. 2012;32:613-622.
341. Salazar VS, Gamer LW and Rosen V. BMP signalling in skeletal development, disease and repair. *Nature Reviews Endocrinology*. 2016;12:203.
342. Rahman MS, Akhtar N, Jamil HM, Banik RS and Asaduzzaman SM. TGF-β/BMP signaling and other molecular events: regulation of osteoblastogenesis and bone formation. *Bone research*. 2015;3:15005.
343. Gomez-Puerto MC, Iyengar PV, García de Vinuesa A, Ten Dijke P and Sanchez-Duffhues G. Bone morphogenetic protein receptor signal transduction in human disease. *The journal of pathology*. 2019;247:9-20.
344. Wu DH and Hatzopoulos AK. Bone morphogenetic protein signaling in inflammation. *Experimental Biology and Medicine*. 2019;244:147-156.
345. Yao Y, Bennett BJ, Wang X, Rosenfeld ME, Giachelli C, Lusis AJ and Boström KI. Inhibition of bone morphogenetic proteins protects against atherosclerosis and vascular calcification. *Circulation research*. 2010;107:485-494.
346. Pi X, Lockyer P, Dyer LA, Schisler JC, Russell B, Carey S, Sweet DT, Chen Z, Tzima E and Willis MS. Bmper inhibits endothelial expression of inflammatory adhesion molecules and protects against atherosclerosis. *Arteriosclerosis, thrombosis, and vascular biology*. 2012;32:2214-2222.
347. Csiszar A, Smith KE, Koller A, Kaley G, Edwards JG and Ungvari Z. Regulation of Bone Morphogenetic Protein-2 Expression in Endothelial Cells: Role of Nuclear Factor-κB Activation by Tumor Necrosis Factor-α, H2O2, and High Intravascular Pressure. *Circulation*. 2005;111:2364-2372.
348. Sorescu GP, Sykes M, Weiss D, Platt MO, Saha A, Hwang J, Boyd N, Boo YC, Vega JD and Taylor WR. Bone morphogenic protein 4 produced in endothelial cells by oscillatory shear stress stimulates an inflammatory response. *Journal of Biological Chemistry*. 2003;278:31128-31135.
349. Sorescu GP, Song H, Tressel SL, Hwang J, Dikalov S, Smith DA, Boyd NL, Platt MO, Lassegue B and Griendling KK. Bone morphogenic protein 4 produced in endothelial cells by oscillatory shear stress induces monocyte adhesion by stimulating reactive oxygen species production from a nox1-based NADPH oxidase. *Circulation research*. 2004;95:773-779.
350. Helbing T, Rothweiler R, Ketterer E, Goetz L, Heinke J, Grundmann S, Duerschmied D, Patterson C, Bode C and Moser M. BMP activity controlled by BMPER regulates the proinflammatory phenotype of endothelium. *Blood, The Journal of the American Society of Hematology*. 2011;118:5040-5049.
351. Helbing T, Wiltgen G, Hornstein A, Brauers EZ, Arnold L, Bauer A, Esser JS, Diehl P, Grundmann S and Fink K. Bone morphogenetic protein-modulator BMPER regulates endothelial barrier function. *Inflammation*. 2017;40:442-453.
352. Sucosky P, Balachandran K, Elhammali A, Jo H and Yoganathan AP. Altered shear stress stimulates upregulation of endothelial VCAM-1 and ICAM-1 in a BMP-4–and TGF-β1–dependent pathway. *Arteriosclerosis, thrombosis, and vascular biology*. 2009;29:254-260.
353. Pardali E, Makowski LM, Leffers M, Borgscheiper A and Waltenberger J. BMP-2 induces human mononuclear cell chemotaxis and adhesion and modulates monocyte-to-macrophage differentiation. *Journal of cellular and molecular medicine*. 2018;22:5429-5438.
354. Dube PR, Birnbaumer L and Vazquez G. Evidence for constitutive bone morphogenetic protein-2 secretion by M1 macrophages: Constitutive auto/paracrine osteogenic signaling by BMP-2 in M1 macrophages. *Biochemical and biophysical research communications*. 2017;491:154-158.

355. Nakaoka T, Gonda K, Ogita T, Otawara-Hamamoto Y, Okabe F, Kira Y, Harii K, Miyazono K, Takuwa Y and Fujita T. Inhibition of rat vascular smooth muscle proliferation in vitro and in vivo by bone morphogenetic protein-2. *The Journal of clinical investigation*. 1997;100:2824-2832.
356. Wong GA, Tang V, El-Sabeawy F and Weiss RH. BMP-2 inhibits proliferation of human aortic smooth muscle cells via p21Cip1/Waf1. *American Journal of Physiology-Endocrinology and Metabolism*. 2003;284:E972-E979.
357. King KE, Iyemere VP, Weissberg PL and Shanahan CM. Krüppel-like factor 4 (KLF4/GKLF) is a target of bone morphogenetic proteins and transforming growth factor β1 in the regulation of vascular smooth muscle cell phenotype. *Journal of Biological Chemistry*. 2003;278:11661-11669.
358. Rosen V and Wozney JM. Bone morphogenetic proteins *Principles of bone biology*: Elsevier; 2002: 919-928.
359. Hruska KA, Mathew S and Saab G. Bone morphogenetic proteins in vascular calcification. *Circulation research*. 2005;97:105-114.
360. Mathew S, Tustison K and Hruska K. Bone morphogenetic protein-7 (BMP-7) restores human aortic vascular smooth muscle cell (HAoSMC) phenotype and inhibits calcification in vitro. *J Am Soc Nephrol*. 2004;15:7A.
361. Spinella-Jaegle S, Roman-Roman S, Faucheu C, Dunn F-W, Kawai S, Gallea S, Stiot V, Blanchet A, Courtois B and Baron R. Opposite effects of bone morphogenetic protein-2 and transforming growth factor-β1 on osteoblast differentiation. *Bone*. 2001;29:323-330.
362. Lee M-H, Kim Y-J, Kim H-J, Park H-D, Kang A-R, Kyung H-M, Sung J-H, Wozney JM and Ryoo H-M. BMP-2-induced Runx2 expression is mediated by Dlx5, and TGF-β1 opposes the BMP-2-induced osteoblast differentiation by suppression of Dlx5 expression. *Journal of Biological Chemistry*. 2003;278:34387-34394.
363. Chaudhary L, Hofmeister A and Hruska K. Differential growth factor control of bone formation through osteoprogenitor differentiation. *Bone*. 2004;34:402-411.
364. Lee M-H, Kwon T-G, Park H-S, Wozney JM and Ryoo H-M. BMP-2-induced Osterix expression is mediated by Dlx5 but is independent of Runx2. *Biochemical and biophysical research communications*. 2003;309:689-694.
365. Zohar R, Mcculloch CA, Sampath K and Sodek J. Flow cytometric analysis of recombinant human osteogenic protein-1 (BMP-7) responsive subpopulations from fetal rat calvaria based on intracellular osteopontin content. *Matrix biology*. 1998;16:295-306.
366. Mikhaylova L, Malmquist J and Nurminskaya M. Regulation of in vitro vascular calcification by BMP4, VEGF and Wnt3a. *Calcified tissue international*. 2007;81:372-381.
367. Byon CH, Sun Y, Chen J, Yuan K, Mao X, Heath JM, Anderson PG, Tintut Y, Demer LL, Wang D and Chen Y. Runx2-Upregulated Receptor Activator of Nuclear Factor κB Ligand in Calcifying Smooth Muscle Cells Promotes Migration and Osteoclastic Differentiation of Macrophages. *Arteriosclerosis, Thrombosis, and Vascular Biology*. 2011;31:1387-1396.
368. Kanamaru F, Iwai H, Ikeda T, Nakajima A, Ishikawa I and Azuma M. Expression of membrane-bound and soluble receptor activator of NF-κB ligand (RANKL) in human T cells. *Immunology letters*. 2004;94:239-246.
369. Martin A, Xiong J, Koromila T, Ji JS, Chang S, Song YS, Miller JL, Han C-Y, Kostenuik P and Krum SA. Estrogens antagonize RUNX2-mediated osteoblast-driven osteoclastogenesis through regulating RANKL membrane association. *Bone*. 2015;75:96-104.
370. Ogasawara N, Poposki JA, Klingler AI, Tan BK, Hulse KE, Stevens WW, Peters AT, Grammer LC, Welch KC and Smith SS. Role of RANK-L as a potential inducer of ILC2-mediated type 2 inflammation in chronic rhinosinusitis with nasal polyps. *Mucosal Immunology*. 2020;13:86-95.

371. Zhang S, Wang X, Li G, Chong Y, Zhang J, Guo X, Li B and Bi Z. Osteoclast regulation of osteoblasts via RANK-RANKL reverse signal transduction in vitro. *Molecular medicine reports*. 2017;16:3994-4000.
372. Nakashima T, Kobayashi Y, Yamasaki S, Kawakami A, Eguchi K, Sasaki H and Sakai H. Protein expression and functional difference of membrane-bound and soluble receptor activator of NF-κB ligand: modulation of the expression by osteotropic factors and cytokines. *Biochemical and biophysical research communications*. 2000;275:768-775.
373. Hofbauer LC and Heufelder AE. Role of receptor activator of nuclear factor-κB ligand and osteoprotegerin in bone cell biology. *Journal of molecular medicine*. 2001;79:243-253.
374. Fan X, Roy EM, Murphy TC, Nanes MS, Kim S, Pike JW and Rubin J. Regulation of RANKL promoter activity is associated with histone remodeling in murine bone stromal cells. *Journal of cellular biochemistry*. 2004;93:807-818.
375. Rahman MM, Takeshita S, Matsuoka K, Kaneko K, Naoe Y, Sakaue-Sawano A, Miyawaki A and Ikeda K. Proliferation-coupled osteoclast differentiation by RANKL: cell density as a determinant of osteoclast formation. *Bone*. 2015;81:392-399.
376. Mozar A, Haren N, Chasseraud M, Louvet L, Mazière C, Wattel A, Mentaverri R, Morlière P, Kamel S and Brazier M. High extracellular inorganic phosphate concentration inhibits RANK–RANKL signaling in osteoclast-like cells. *Journal of cellular physiology*. 2008;215:47-54.
377. Yamaguchi T, Movila A, Kataoka S, Wisitrasameewong W, Torruella MR, Murakoshi M, Murakami S and Kawai T. Proinflammatory M1 macrophages inhibit RANKL-induced osteoclastogenesis. *Infection and immunity*. 2016;84:2802-2812.
378. Davenport C, Harper E, Forde H, Rochfort KD, Murphy RP, Smith D and Cummins PM. RANKL promotes osteoblastic activity in vascular smooth muscle cells by upregulating endothelial BMP-2 release. *The International Journal of Biochemistry & Cell Biology*. 2016;77:171-180.
379. Osako MK, Nakagami H, Koibuchi N, Shimizu H, Nakagami F, Koriyama H, Shimamura M, Miyake T, Rakugi H and Morishita R. Estrogen inhibits vascular calcification via vascular RANKL system: common mechanism of osteoporosis and vascular calcification. *Circulation research*. 2010;107:466-475.
380. Panizo S, Cardus A, Encinas M, Parisi E, Valcheva P, López-Ongil S, Coll B, Fernandez E and Valdivielso JM. RANKL increases vascular smooth muscle cell calcification through a RANK-BMP4–dependent pathway. *Circulation research*. 2009;104:1041-1048.
381. Deuell KA, Callegari A, Giachelli CM, Rosenfeld ME and Scatena M. RANKL enhances macrophage paracrine pro-calcific activity in high phosphate-treated smooth muscle cells: dependence on IL-6 and TNF-α. *Journal of vascular research*. 2012;49:510-521.
382. Olesen M, Skov V, Mechta M, Mumm BH and Rasmussen LM. No influence of OPG and its ligands, RANKL and TRAIL, on proliferation and regulation of the calcification process in primary human vascular smooth muscle cells. *Molecular and cellular endocrinology*. 2012;362:149-156.
383. Higgins CL, Isbilir S, Basto P, Chen IY, Vaduganathan M, Vaduganathan P, Reardon MJ, Lawrie G, Peterson L and Morrisett JD. Distribution of alkaline phosphatase, osteopontin, RANK ligand and osteoprotegerin in calcified human carotid atheroma. *The protein journal*. 2015;34:315-328.
384. Yuan L-Q, Zhu J-H, Wang H-W, Liang Q-H, Xie H, Wu X-P, Zhou H, Cui R-R, Sheng Z-F and Zhou H-D. RANKL is a downstream mediator for insulin-induced osteoblastic differentiation of vascular smooth muscle cells. *PloS one*. 2011;6:e29037.

385. Renema N, Navet B, Heymann M-F, Lezot F and Heymann D. RANK–RANKL signalling in cancer. *Bioscience reports*. 2016;36:e00366.
386. Sobacchi C, Menale C and Villa A. The RANKL-RANK axis: A bone to thymus round trip. *Frontiers in immunology*. 2019;10:629.
387. Helas S, Goettsch C, Schoppet M, Zeitz U, Hempel U, Morawietz H, Kostenuik PJ, Erben RG and Hofbauer LC. Inhibition of receptor activator of NF-κB ligand by denosumab attenuates vascular calcium deposition in mice. *The American journal of pathology*. 2009;175:473-478.
388. Samelson EJ, Miller PD, Christiansen C, Daizadeh NS, Grazette L, Anthony MS, Egbuna O, Wang A, Siddhanti SR and Cheung AM. RANKL inhibition with denosumab does not influence 3-year progression of aortic calcification or incidence of adverse cardiovascular events in postmenopausal women with osteoporosis and high cardiovascular risk. *Journal of Bone and Mineral Research*. 2014;29:450-457.
389. Iseri K, Watanabe M, Yoshikawa H, Mitsui H, Endo T, Yamamoto Y, Iyoda M, Ryu K, Inaba T and Shibata T. Effects of denosumab and alendronate on bone health and vascular function in hemodialysis patients: a randomized, controlled trial. *Journal of Bone and Mineral Research*. 2019;34:1014-1024.
390. Ueki K, Yamada S, Tsuchimoto A, Tokumoto M, Kumano T, Kitazono T and Tsuruya K. Rapid progression of vascular and soft tissue calcification while being managed for severe and persistent hypocalcemia induced by denosumab treatment in a patient with multiple myeloma and chronic kidney disease. *Internal Medicine*. 2015;54:2637-2642.
391. Westenfeld R, Ketteler M and Brandenburg VM. Anti-RANKL therapy—implications for the bone-vascular-axis in CKD? Denosumab in post-menopausal women with low bone mineral density. *Nephrology Dialysis Transplantation*. 2006;21:2075-2077.
392. Oštrić M, Kukuljan M, Markić D, Gršković A, Ivančić A, Bobinac D, Španjol J, Maroević J, Šoša I and Ćelić T. Expression of bone-related proteins in vascular calcification and its serum correlations with coronary artery calcification score. *Journal of biological regulators and homeostatic agents*. 2019;33:29.
393. Anderson DM, Maraskovsky E, Billingsley WL, Dougall WC, Tometsko ME, Roux ER, Teepe MC, DuBose RF, Cosman D and Galibert L. A homologue of the TNF receptor and its ligand enhance T-cell growth and dendritic-cell function. *Nature*. 1997;390:175-179.
394. Nakagawa N, Kinosaki M, Yamaguchi K, Shima N, Yasuda H, Yano K, Morinaga T and Higashio K. RANK is the essential signaling receptor for osteoclast differentiation factor in osteoclastogenesis. *Biochemical and biophysical research communications*. 1998;253:395-400.
395. Lacey D, Timms E, Tan H-L, Kelley M, Dunstan C, Burgess T, Elliott R, Colombero A, Elliott G and Scully S. Osteoprotegerin ligand is a cytokine that regulates osteoclast differentiation and activation. *cell*. 1998;93:165-176.
396. Wong BR, Josien R, Lee SY, Sauter B, Li H-L, Steinman RM and Choi Y. TRANCE (tumor necrosis factor [TNF]-related activation-induced cytokine), a new TNF family member predominantly expressed in T cells, is a dendritic cell–specific survival factor. *The Journal of experimental medicine*. 1997;186:2075-2080.
397. Min J-K, Kim Y-M, Kim Y-M, Kim E-C, Gho YS, Kang I-J, Lee S-Y, Kong Y-Y and Kwon Y-G. Vascular Endothelial Growth Factor Up-regulates Expression of Receptor Activator of NF-κB (RANK) in Endothelial Cells Concomitant Increase of Angiogenic Responses to RANK Ligand. *Journal of Biological Chemistry*. 2003;278:39548-39557.
398. Wong BR, Josien R and Choi Y. TRANCE is a TNF family member that regulates dendritic cell and osteoclast function. *Journal of Leukocyte Biology*. 1999;65:715-724.
399. Lomaga MA, Yeh W-C, Sarosi I, Duncan GS, Furlonger C, Ho A, Morony S, Capparelli C, Van G and Kaufman S. TRAF6 deficiency results in osteopetrosis and defective interleukin-1, CD40, and LPS signaling. *Genes & development*. 1999;13:1015-1024.

400. Raju R, Balakrishnan L, Nanjappa V, Bhattacharjee M, Getnet D, Muthusamy B, Kurian Thomas J, Sharma J, Rahiman BA and Harsha H. A comprehensive manually curated reaction map of RANKL/RANK-signaling pathway. *Database*. 2011;2011.
401. Gohda J, Akiyama T, Koga T, Takayanagi H, Tanaka S and Inoue Ji. RANK-mediated amplification of TRAF6 signaling leads to NFATc1 induction during osteoclastogenesis. *The EMBO journal*. 2005;24:790-799.
402. Darnay BG, Ni J, Moore PA and Aggarwal BB. Activation of NF-κB by rank requires tumor necrosis factor receptor-associated factor (TRAF) 6 and NF-κB-inducing kinase identification of a novel TRAF6 interaction motif. *Journal of Biological Chemistry*. 1999;274:7724-7731.
403. Kim H-H, Shin JN, Lee YS, Jeon YM, Chung C-H, Ni J, Kwon BS and Lee ZH. Receptor activator of NF-κB recruits multiple TRAF family adaptors and activates c-Jun N-terminal kinase. *FEBS letters*. 1999;443:297-302.
404. Galibert L, Tometsko ME, Anderson DM, Cosman D and Dougall WC. The involvement of multiple tumor necrosis factor receptor (TNFR)-associated factors in the signaling mechanisms of receptor activator of NF-κB, a member of the TNFR superfamily. *Journal of Biological Chemistry*. 1998;273:34120-34127.
405. Matsumoto Y, Larose J, Kent OA, Lim M, Changoor A, Zhang L, Storozhuk Y, Mao X, Grynpas MD, Cong F and Rottapel R. RANKL coordinates multiple osteoclastogenic pathways by regulating expression of ubiquitin ligase RNF146. *The Journal of Clinical Investigation*. 2017;127:1303-1315.
406. Enomoto H, Shiojiri S, Hoshi K, Furuichi T, Fukuyama R, Yoshida CA, Kanatani N, Nakamura R, Mizuno A, Zanma A, Yano K, Yasuda H, Higashio K, Takada K and Komori T. Induction of Osteoclast Differentiation by Runx2 through Receptor Activator of Nuclear Factor-κB Ligand (RANKL) and Osteoprotegerin Regulation and Partial Rescue of Osteoclastogenesis in Runx2−/− Mice by RANKL Transgene. *Journal of Biological Chemistry*. 2003;278:23971-23977.
407. Candido R, Toffoli B, Corallini F, Bernardi S, Zella D, Voltan R, Grill V, Celeghini C and Fabris B. Human full-length osteoprotegerin induces the proliferation of rodent vascular smooth muscle cells both in vitro and in vivo. *Journal of vascular research*. 2010;47:252-261.
408. Olesen P, Ledet T and Rasmussen LM. Arterial osteoprotegerin: increased amounts in diabetes and modifiable synthesis from vascular smooth muscle cells by insulin and TNF-α. *Diabetologia*. 2005;48:561-568.
409. Olesen P, Nguyen K, Wogensen L, Ledet T and Rasmussen LM. Calcification of human vascular smooth muscle cells: associations with osteoprotegerin expression and acceleration by high-dose insulin. *American Journal of Physiology-Heart and Circulatory Physiology*. 2007;292:H1058-H1064.
410. Nybo M and Rasmussen LM. Osteoprotegerin released from the vascular wall by heparin mainly derives from vascular smooth muscle cells. *Atherosclerosis*. 2008;201:33-35.
411. Collin-Osdoby P, Rothe L, Anderson F, Nelson M, Maloney W and Osdoby P. Receptor activator of NF-κB and osteoprotegerin expression by human microvascular endothelial cells, regulation by inflammatory cytokines, and role in human osteoclastogenesis. *Journal of Biological Chemistry*. 2001;276:20659-20672.
412. Loureiro MB, Ururahy MA, Freire-Neto FP, Oliveira GH, Duarte VM, Luchessi AD, Brandão-Neto J, Hirata RD, Hirata MH and Maciel-Neto JJ. Low bone mineral density is associated to poor glycemic control and increased OPG expression in children and adolescents with type 1 diabetes. *Diabetes research and clinical practice*. 2014;103:452-457.

413. Holen I, Cross SS, Neville-Webbe HL, Cross NA, Balasubramanian SP, Croucher PI, Evans CA, Lippitt JM, Coleman RE and Eaton CL. Osteoprotegerin (OPG) expression by breast cancer cells in vitro and breast tumours in vivo–a role in tumour cell survival? *Breast cancer research and treatment*. 2005;92:207-215.
414. Peng X, Guo W, Ren T, Lou Z, Lu X, Zhang S, Lu Q and Sun Y. Differential expression of the RANKL/RANK/OPG system is associated with bone metastasis in human non-small cell lung cancer. *PLoS One*. 2013;8:e58361.
415. Yun TJ, Chaudhary PM, Shu GL, Frazer JK, Ewings MK, Schwartz SM, Pascual V, Hood LE and Clark EA. OPG/FDCR-1, a TNF receptor family member, is expressed in lymphoid cells and is up-regulated by ligating CD40. *The Journal of Immunology*. 1998;161:6113-6121.
416. Schoppet M, Preissner KT and Hofbauer LC. RANK ligand and osteoprotegerin paracrine regulators of bone metabolism and vascular function. *Arteriosclerosis, thrombosis, and vascular biology*. 2002;22:549-553.
417. Tamtaji OR, Borzabadi S, Ghayour-Mobarhan M, Ferns G and Asemi Z. The effects of fatty acids consumption on OPG/RANKL/RANK system in cardiovascular diseases: Current status and future perspectives for the impact of diet-gene interaction. *Journal of cellular biochemistry*. 2019;120:2774-2781.
418. Morony S, Tintut Y, Zhang Z, Cattley RC, Van G, Dwyer D, Stolina M, Kostenuik PJ and Demer LL. Osteoprotegerin inhibits vascular calcification without affecting atherosclerosis in ldlr (−/−) mice. *Circulation*. 2008;117:411-420.
419. Secchiero P, Corallini F, Pandolfi A, Consoli A, Candido R, Fabris B, Celeghini C, Capitani S and Zauli G. An increased osteoprotegerin serum release characterizes the early onset of diabetes mellitus and may contribute to endothelial cell dysfunction. *The American journal of pathology*. 2006;169:2236-2244.
420. Bjerre M, Hilden J, Winkel P, Jensen GB, Kjøller E, Sajadieh A, Kastrup J, Kolmos HJ, Larsson A and Ärnlöv J. Serum osteoprotegerin as a long-term predictor for patients with stable coronary artery disease and its association with diabetes and statin treatment: A CLARICOR trial 10-year follow-up substudy. *Atherosclerosis*. 2020.
421. Avignon A, Sultan A, Piot C, Elaerts S, Cristol JP and Dupuy AM. Osteoprotegerin is associated with silent coronary artery disease in high-risk but asymptomatic type 2 diabetic patients. *Diabetes Care*. 2005;28:2176-2180.
422. Anand DV, Lahiri A, Lim E, Hopkins D and Corder R. The relationship between plasma osteoprotegerin levels and coronary artery calcification in uncomplicated type 2 diabetic subjects. *Journal of the American College of Cardiology*. 2006;47:1850-1857.
423. Wen W-W, Ning Y, Zhang Q, Yang Y-X, Jia Y-F, Sun H-L, Qin Y-W, Fang F, Zhang M and Wei Y-X. TNFRSF11B: a potential plasma biomarker for diagnosis of obstructive sleep apnea. *Clinica Chimica Acta*. 2019;490:39-45.
424. Zhang C, Luo X, Chen J, Zhou B, Yang M, Liu R, Liu D, Gu HF, Zhu Z and Zheng H. Osteoprotegerin promotes liver steatosis by targeting the ERK–PPAR-γ–CD36 pathway. *Diabetes*. 2019;68:1902-1914.
425. Bernardi S, Voltan R, Rimondi E, Melloni E, Milani D, Cervellati C, Gemmati D, Celeghini C, Secchiero P and Zauli G. TRAIL, OPG, and TWEAK in kidney disease: biomarkers or therapeutic targets? *Clinical Science*. 2019;133:1145-1166.
426. Ueland T, Jemtland R, Godang K, Kjekshus J, Hognestad A, Omland T, Squire IB, Gullestad L, Bollerslev J and Dickstein K. Prognostic value of osteoprotegerin in heart failure after acute myocardial infarction. *Journal of the American College of Cardiology*. 2004;44:1970-1976.
427. Min H, Morony S, Sarosi I, Dunstan CR, Capparelli C, Scully S, Van G, Kaufman S, Kostenuik PJ and Lacey DL. Osteoprotegerin reverses osteoporosis by inhibiting endosteal

osteoclasts and prevents vascular calcification by blocking a process resembling osteoclastogenesis. *Journal of Experimental Medicine*. 2000;192:463-474.
428. Vidal ON, Sjögren K, Eriksson BI, Ljunggren Ö and Ohlsson C. Osteoprotegerin mRNA is increased by interleukin-1α in the human osteosarcoma cell line MG-63 and in human osteoblast-like cells. *Biochemical and biophysical research communications*. 1998;248:696-700.
429. Makiishi-Shimobayashi C, Tsujimura T, Iwasaki T, Yamada N, Sugihara A, Okamura H, Hayashi S-i and Terada N. Interleukin-18 up-regulates osteoprotegerin expression in stromal/osteoblastic cells. *Biochemical and Biophysical Research Communications*. 2001;281:361-366.
430. Takai H, Kanematsu M, Yano K, Tsuda E, Higashio K, Ikeda K, Watanabe K and Yamada Y. Transforming growth factor-β stimulates the production of osteoprotegerin/osteoclastogenesis inhibitory factor by bone marrow stromal cells. *Journal of Biological Chemistry*. 1998;273:27091-27096.
431. Wan M, Shi X, Feng X and Cao X. Transcriptional mechanisms of bone morphogenetic protein-induced osteoprotegrin gene expression. *Journal of Biological Chemistry*. 2001;276:10119-10125.
432. Saika M, Inoue D, Kido S and Matsumoto T. 17β-estradiol stimulates expression of osteoprotegerin by a mouse stromal cell line, ST-2, via estrogen receptor-α. *Endocrinology*. 2001;142:2205-2212.
433. Hofbauer LC, Khosla S, Dunstan CR, Lacey DL, Spelsberg TC and Riggs BL. Estrogen stimulates gene expression and protein production of osteoprotegerin in human osteoblastic cells. *Endocrinology*. 1999;140:4367-4370.
434. Vidal N, Brandstrom H, Jonsson K and Ohlsson C. Osteoprotegerin mRNA is expressed in primary human osteoblast-like cells: down-regulation by glucocorticoids. *Journal of Endocrinology*. 1998;159:191.
435. Hofbauer LC, Gori F, Riggs BL, Lacey DL, Dunstan CR, Spelsberg TC and Khosla S. Stimulation of osteoprotegerin ligand and inhibition of osteoprotegerin production by glucocorticoids in human osteoblastic lineage cells: potential paracrine mechanisms of glucocorticoid-induced osteoporosis. *Endocrinology*. 1999;140:4382-4389.
436. Hofbauer LC, Shui C, Riggs BL, Dunstan CR, Spelsberg TC, O'Brien T and Khosla S. Effects of immunosuppressants on receptor activator of NF-κB ligand and osteoprotegerin production by human osteoblastic and coronary artery smooth muscle cells. *Biochemical and biophysical research communications*. 2001;280:334-339.
437. Onyia J, Miles R, Yang X, Halladay D, Hale J, Glasebrook A, McClure D, Seno G, Churgay L and Chandrasekhar S. In vivo demonstration that human parathyroid hormone 1–38 inhibits the expression of osteoprotegerin in bone with the kinetics of an immediate early gene. *Journal of Bone and Mineral Research*. 2000;15:863-871.
438. Brändström H, Jonsson KB, Ohlsson C, Vidal O, Ljunghall S and Ljunggren Ö. Regulation of osteoprotegerin mRNA levels by prostaglandin E2in human bone marrow stroma cells. *Biochemical and biophysical research communications*. 1998;247:338-341.
439. Jacobson A, Johansson S, Branting M and Melhus H. Vitamin A differentially regulates RANKL and OPG expression in human osteoblasts. *Biochemical and biophysical research communications*. 2004;322:162-167.
440. Nakagawa N, Yasuda H, Yano K, Mochizuki S-i, Kobayashi N, Fujimoto H, Shima N, Morinaga T, Chikazu D and Kawaguchi H. Basic fibroblast growth factor induces osteoclast formation by reciprocally regulating the production of osteoclast differentiation factor and osteoclastogenesis inhibitory factor in mouse osteoblastic cells. *Biochemical and biophysical research communications*. 1999;265:158-163.
441. van Hinsbergh VW. Endothelium—role in regulation of coagulation and inflammation. *Seminars in immunopathology*. 2012;34:93-106.

442. Štefková K, Procházková J and Pacherník J. Alkaline phosphatase in stem cells. *Stem cells international*. 2015;2015.
443. McComb RB, Bowers Jr GN and Posen S. *Alkaline phosphatase*: Springer Science & Business Media; 2013.
444. Bellows C, Aubin J and Heersche J. Initiation and progression of mineralization of bone nodules formed in vitro: the role of alkaline phosphatase and organic phosphate. *Bone and mineral*. 1991;14:27-40.
445. Abd-Alla M. Phosphatases and the utilization of organic phosphorus by Rhizobium leguminosarum biovar viceae. *Letters in Applied Microbiology*. 1994;18:294-296.
446. Moss D, Eaton RH, Smith J and Whitby L. Association of inorganic-pyrophosphatase activity with human alkaline-phosphatase preparations. *Biochemical Journal*. 1967;102:53-57.
447. Lomashvili KA, Cobbs S, Hennigar RA, Hardcastle KI and O'Neill WC. Phosphate-induced vascular calcification: role of pyrophosphate and osteopontin. *Journal of the American Society of Nephrology*. 2004;15:1392-1401.
448. Lowe D and John S. Alkaline phosphatase. 2017.
449. Hofbauer L, Brueck C, Shanahan C, Schoppet M and Dobnig H. Vascular calcification and osteoporosis—from clinical observation towards molecular understanding. *Osteoporosis International*. 2007;18:251-259.
450. Hjortnaes J, Butcher J, Figueiredo JL, Riccio M, Kohler RH, Kozloff KM, Weissleder R and Aikawa E. Arterial and aortic valve calcification inversely correlates with osteoporotic bone remodelling: a role for inflammation. *Eur Heart J*. 2010;31:1975-84.
451. Wasilewski G, Vervloet M and Schurgers LJ. The bone–vasculature axis: calcium supplementation and the role of vitamin K. *Frontiers in cardiovascular medicine*. 2019;6:6.
452. Rattazzi M, Faggin E, Buso R, Di Virgilio R, Puato M, Plebani M, Zaninotto M, Palmosi T, Bertacco E and Fadini GP. Atorvastatin Reduces Circulating Osteoprogenitor Cells and T-Cell RANKL Expression in Osteoporotic Women: Implications for the Bone–Vascular Axis. *Cardiovascular therapeutics*. 2016;34:13-20.
453. Villa JKD, Diaz MAN, Pizziolo VR and Martino HSD. Effect of vitamin K in bone metabolism and vascular calcification: a review of mechanisms of action and evidences. *Critical reviews in food science and nutrition*. 2017;57:3959-3970.
454. Patel JJ, Bourne LE, Davies BK, Arnett TR, MacRae VE, Wheeler-Jones CP and Orriss IR. Differing calcification processes in cultured vascular smooth muscle cells and osteoblasts. *Experimental cell research*. 2019;380:100-113.
455. Otto F, Thornell AP, Crompton T, Denzel A, Gilmour KC, Rosewell IR, Stamp GW, Beddington RS, Mundlos S and Olsen BR. Cbfa1, a candidate gene for cleidocranial dysplasia syndrome, is essential for osteoblast differentiation and bone development. *Cell*. 1997;89:765-771.
456. Komori T, Yagi H, Nomura S, Yamaguchi A, Sasaki K, Deguchi K, Shimizu Y, Bronson R, Gao Y-H and Inada M. Targeted disruption of Cbfa1 results in a complete lack of bone formation owing to maturational arrest of osteoblasts. *cell*. 1997;89:755-764.
457. Inada M, Yasui T, Nomura S, Miyake S, Deguchi K, Himeno M, Sato M, Yamagiwa H, Kimura T and Yasui N. Maturational disturbance of chondrocytes in Cbfa1-deficient mice. *Developmental dynamics: an official publication of the American Association of Anatomists*. 1999;214:279-290.
458. D'Souza RN, Aberg T, Gaikwad J, Cavender A, Owen M, Karsenty G and Thesleff I. Cbfa1 is required for epithelial-mesenchymal interactions regulating tooth development in mice. *Development*. 1999;126:2911-2920.
459. Komori T. A fundamental transcription factor for bone and cartilage. *Biochemical and biophysical research communications*. 2000;276:813-816.

460. Ducy P, Starbuck M, Priemel M, Shen J, Pinero G, Geoffroy V, Amling M and Karsenty G. A Cbfa1-dependent genetic pathway controls bone formation beyond embryonic development. *Genes & development*. 1999;13:1025-1036.
461. Liu W, Toyosawa S, Furuichi T, Kanatani N, Yoshida C, Liu Y, Himeno M, Narai S, Yamaguchi A and Komori T. Overexpression of Cbfa1 in osteoblasts inhibits osteoblast maturation and causes osteopenia with multiple fractures. *Journal of Cell Biology*. 2001;155:157-166.
462. Mizuno A, Kanno T, Hoshi M, Shibata O, Yano K, Fujise N, Kinosaki M, Yamaguchi K, Tsuda E and Murakami A. Transgenic mice overexpressing soluble osteoclast differentiation factor (sODF) exhibit severe osteoporosis. *Journal of bone and mineral metabolism*. 2002;20:337-344.
463. Lo Iacono N, Blair HC, Poliani PL, Marrella V, Ficara F, Cassani B, Facchetti F, Fontana E, Guerrini MM and Traggiai E. Osteopetrosis rescue upon RANKL administration to Rankl−/− mice: A new therapy for human RANKL-dependent ARO. *Journal of Bone and Mineral Research*. 2012;27:2501-2510.
464. Kanzaki H, Chiba M, Shimizu Y and Mitani H. Dual regulation of osteoclast differentiation by periodontal ligament cells through RANKL stimulation and OPG inhibition. *Journal of dental research*. 2001;80:887-891.
465. Neven E and D'Haese PC. Vascular calcification in chronic renal failure: what have we learned from animal studies? *Circulation research*. 2011;108:249-264.
466. Snell-Bergeon JK, Budoff MJ and Hokanson JE. Vascular calcification in diabetes: mechanisms and implications. *Current diabetes reports*. 2013;13:391-402.
467. Soman S, Raju R, Sandhya VK, Advani J, Khan AA, Harsha H, Prasad TK, Sudhakaran P, Pandey A and Adishesha PK. A multicellular signal transduction network of AGE/RAGE signaling. *Journal of cell communication and signaling*. 2013;7:19-23.
468. Singh R, Barden A, Mori T and Beilin L. Advanced glycation end-products: a review. *Diabetologia*. 2001;44:129-146.
469. Geraldes P and King GL. Activation of protein kinase C isoforms and its impact on diabetic complications. *Circulation research*. 2010;106:1319-1331.
470. Tanikawa T, Okada Y, Tanikawa R and Tanaka Y. Advanced glycation end products induce calcification of vascular smooth muscle cells through RAGE/p38 MAPK. *Journal of vascular research*. 2009;46:572-580.
471. Suga T, Iso T, Shimizu T, Tanaka T, Yamagishi S-i, Takeuchi M, Imaizumi T and Kurabayashi M. Activation of receptor for advanced glycation end products induces osteogenic differentiation of vascular smooth muscle cells. *Journal of atherosclerosis and thrombosis*. 2011:1104200368-1104200368.
472. Ren X, Shao H, Wei Q, Sun Z and Liu N. Advanced glycation end-products enhance calcification in vascular smooth muscle cells. *Journal of International Medical Research*. 2009;37:847-854.
473. Hauschka PV, Lian JB, Cole D and Gundberg CM. Osteocalcin and matrix Gla protein: vitamin K-dependent proteins in bone. *Physiological reviews*. 1989;69:990-1047.
474. Lamon-Fava S, Sadowski JA, Davidson KW, O'Brien ME, McNamara JR and Schaefer EJ. Plasma lipoproteins as carriers of phylloquinone (vitamin K1) in humans. *The American journal of clinical nutrition*. 1998;67:1226-1231.
475. Poser JW, Esch FS, Ling NC and Price PA. Isolation and sequence of the vitamin K-dependent protein from human bone. Undercarboxylation of the first glutamic acid residue. *Journal of Biological Chemistry*. 1980;255:8685-8691.
476. Malashkevich VN, Almo SC and Dowd TL. X-ray crystal structure of bovine 3 Glu-osteocalcin. *Biochemistry*. 2013;52:8387-8392.
477. Haffa A, Krueger D, Bruner J, Engelke J, Gundberg C, Akhter M and Binkley N. Diet- or warfarin-induced vitamin K insufficiency elevates circulating undercarboxylated

osteocalcin without altering skeletal status in growing female rats. *Journal of Bone and Mineral Research*. 2000;15:872-878.
478. Menon R, Gill D, Thomas M, Kernoff P and Dandona P. Impaired carboxylation of osteocalcin in warfarin-treated patients. *The Journal of Clinical Endocrinology & Metabolism*. 1987;64:59-61.
479. Rashdan NA, Sim AM, Cui L, Phadwal K, Roberts FL, Carter R, Ozdemir DD, Hohenstein P, Hung J and Kaczynski J. Osteocalcin regulates arterial calcification via altered Wnt signaling and glucose metabolism. *Journal of Bone and Mineral Research*. 2020;35:357-367.
480. Shea MK, Gundberg CM, Meigs JB, Dallal GE, Saltzman E, Yoshida M, Jacques PF and Booth SL. γ-Carboxylation of osteocalcin and insulin resistance in older men and women. *The American journal of clinical nutrition*. 2009;90:1230-1235.
481. Millar SA, John SG, McIntyre CW, Ralevic V, Anderson SI and O'Sullivan SE. An Investigation Into the Role of Osteocalcin in Human Arterial Smooth Muscle Cell Calcification. *Frontiers in Endocrinology*. 2020;11:369.
482. Millar SA, Patel H, Anderson SI, England TJ and O'Sullivan SE. Osteocalcin, vascular calcification, and atherosclerosis: a systematic review and meta-analysis. *Frontiers in Endocrinology*. 2017;8:183.
483. Bonucci E. Bone mineralization. *Front Biosci (Landmark Ed)*. 2012;17:100-28.
484. Cui L, Houston D, Farquharson C and MacRae V. Characterisation of matrix vesicles in skeletal and soft tissue mineralisation. *Bone*. 2016;87:147-158.
485. Boström K, Watson KE, Stanford WP and Demer LL. Atherosclerotic calcification: relation to developmental osteogenesis. *The American journal of cardiology*. 1995;75:88B-91B.
486. Zazzeroni L, Faggioli G and Pasquinelli G. Mechanisms of arterial calcification: the role of matrix vesicles. *European Journal of Vascular and Endovascular Surgery*. 2018;55:425-432.
487. Pasquinelli G and Valente S. Ultrastructural assessment of the differentiation potential of human multipotent mesenchymal stromal cells. *Ultrastructural Pathology*. 2013;37:318-327.
488. Chen Q, Bei J-J, Liu C, Feng S-B, Zhao W-B, Zhou Z, Yu Z-P, Du X-J and Hu H-Y. HMGB1 induces secretion of matrix vesicles by macrophages to enhance ectopic mineralization. *PLoS One*. 2016;11:e0156686.
489. New SE, Goettsch C, Aikawa M, Marchini JF, Shibasaki M, Yabusaki K, Libby P, Shanahan CM, Croce K and Aikawa E. Macrophage-derived matrix vesicles: an alternative novel mechanism for microcalcification in atherosclerotic plaques. *Circulation research*. 2013:CIRCRESAHA. 113.301036.
490. Viegas CS, Santos L, Macedo AL, Matos AA, Silva AP, Neves PL, Staes A, Gevaert K, Morais R and Vermeer C. Chronic kidney disease circulating calciprotein particles and extracellular vesicles promote vascular calcification: a role for GRP (Gla-Rich Protein). *Arteriosclerosis, thrombosis, and vascular biology*. 2018;38:575-587.
491. Bobryshev Y, Killingsworth M, Lord R and Grabs A. Matrix vesicles in the fibrous cap of atherosclerotic plaque: possible contribution to plaque rupture. *Journal of cellular and molecular medicine*. 2008;12:2073-2082.
492. Kelly-Arnold A, Maldonado N, Laudier D, Aikawa E, Cardoso L and Weinbaum S. Revised microcalcification hypothesis for fibrous cap rupture in human coronary arteries. *Proceedings of the National Academy of Sciences*. 2013;110:10741-10746.
493. Chen NX, O'Neill KD and Moe SM. Matrix vesicles induce calcification of recipient vascular smooth muscle cells through multiple signaling pathways. *Kidney international*. 2018;93:343-354.

494. Schoppet M, Kavurma MM, Hofbauer LC and Shanahan CM. Crystallizing nanoparticles derived from vascular smooth muscle cells contain the calcification inhibitor osteoprotegerin. *Biochemical and Biophysical Research Communications*. 2011;407:103-107.
495. Qin X, Corriere MA, Matrisian LM and Guzman RJ. Matrix metalloproteinase inhibition attenuates aortic calcification. *Arteriosclerosis, thrombosis, and vascular biology*. 2006;26:1510-1516.
496. Basalyga DM, Simionescu DT, Xiong W, Baxter BT, Starcher BC and Vyavahare NR. Elastin degradation and calcification in an abdominal aorta injury model: role of matrix metalloproteinases. *Circulation*. 2004;110:3480-3487.
497. Hosaka N, Mizobuchi M, Ogata H, Kumata C, Kondo F, Koiwa F, Kinugasa E and Akizawa T. Elastin degradation accelerates phosphate-induced mineralization of vascular smooth muscle cells. *Calcified tissue international*. 2009;85:523.
498. Pai A, Leaf EM, El-Abbadi M and Giachelli CM. Elastin degradation and vascular smooth muscle cell phenotype change precede cell loss and arterial medial calcification in a uremic mouse model of chronic kidney disease. *The American journal of pathology*. 2011;178:764-773.
499. Bartstra JW, Spiering W, van den Ouweland JM, Mali WP, Janssen R and de Jong PA. Increased Elastin Degradation in Pseudoxanthoma Elasticum Is Associated with Peripheral Arterial Disease Independent of Calcification. *Journal of clinical medicine*. 2020;9:2771.
500. Lei Y, Sinha A, Nosoudi N, Grover A and Vyavahare N. Hydroxyapatite and calcified elastin induce osteoblast-like differentiation in rat aortic smooth muscle cells. *Experimental cell research*. 2014;323:198-208.
501. Luo G, Ducy P, McKee MD, Pinero GJ, Loyer E, Behringer RR and Karsenty G. Spontaneous calcification of arteries and cartilage in mice lacking matrix GLA protein. 1997.
502. Speer MY, McKee MD, Guldberg RE, Liaw L, Yang H-Y, Tung E, Karsenty G and Giachelli CM. Inactivation of the osteopontin gene enhances vascular calcification of matrix Gla Protein–deficient mice evidence for osteopontin as an inducible inhibitor of vascular calcification in vivo. *The Journal of experimental medicine*. 2002;196:1047-1055.
503. Roy M and Nishimoto S. Matrix Gla protein binding to hydroxyapatite is dependent on the ionic environment: calcium enhances binding affinity but phosphate and magnesium decrease affinity. *Bone*. 2002;31:296-302.
504. Boström K, Tsao D, Shen S, Wang Y and Demer LL. Matrix GLA protein modulates differentiation induced by bone morphogenetic protein-2 in C3H10T1/2 cells. *Journal of Biological Chemistry*. 2001;276:14044-14052.
505. Sweatt A, Sane D, Hutson S and Wallin R. Matrix Gla protein (MGP) and bone morphogenetic protein-2 in aortic calcified lesions of aging rats. *Journal of Thrombosis and Haemostasis*. 2003;1:178-185.
506. Zebboudj AF, Imura M and Boström K. Matrix GLA protein, a regulatory protein for bone morphogenetic protein-2. *Journal of Biological Chemistry*. 2002;277:4388-4394.
507. Zebboudj AF, Shin V and Boström K. Matrix GLA protein and BMP-2 regulate osteoinduction in calcifying vascular cells. *Journal of cellular biochemistry*. 2003;90:756-765.
508. Young MF, Kerr JM, Ibaraki K, Heegaard A-M and Robey PG. Structure, expression, and regulation of the major noncollagenous matrix proteins of bone. *Clinical orthopaedics and related research*. 1992:275-294.

509. Feng Y, Liao Y, Huang W, Lai X, Luo J, Du C, Lin J, Zhang Z, Qiu D and Liu Q. Mesenchymal stromal cells-derived matrix Gla protein contribute to the alleviation of experimental colitis. *Cell death & disease*. 2018;9:1-14.
510. Mertsch S, Schurgers LJ, Weber K, Paulus W and Senner V. Matrix gla protein (MGP): an overexpressed and migration-promoting mesenchymal component in glioblastoma. *BMC cancer*. 2009;9:302.
511. Proudfoot D, Skepper JN, Shanahan CM and Weissberg PL. Calcification of human vascular cells in vitro is correlated with high levels of matrix Gla protein and low levels of osteopontin expression. *Arteriosclerosis, thrombosis, and vascular biology*. 1998;18:379-388.
512. Julien M, Magne D, Masson M, Rolli-Derkinderen M, Chassande O, Cario-Toumaniantz C, Cherel Y, Weiss P and Guicheux J. Phosphate stimulates matrix Gla protein expression in chondrocytes through the extracellular signal regulated kinase signaling pathway. *Endocrinology*. 2007;148:530-537.
513. Luo G, D'Souza R, Hogue D and Karsenty G. The matrix Gla protein gene is a marker of the chondrogenesis cell lineage during mouse development. *Journal of Bone and Mineral Research*. 1995;10:325-334.
514. Roumeliotis S, Dounousi E, Eleftheriadis T and Liakopoulos V. Association of the inactive circulating matrix Gla protein with vitamin K intake, calcification, mortality, and cardiovascular disease: a review. *International journal of molecular sciences*. 2019;20:628.
515. Nigwekar SU, Bloch DB, Nazarian RM, Vermeer C, Booth SL, Xu D, Thadhani RI and Malhotra R. Vitamin K–dependent carboxylation of matrix Gla protein influences the risk of calciphylaxis. *Journal of the American Society of Nephrology*. 2017;28:1717-1722.
516. Demer LL and Boström KI. Conflicting Forces of Warfarin and Matrix Gla Protein in the Artery Wall. *Arteriosclerosis, thrombosis, and vascular biology*. 2015;35:9-10.
517. Schurgers LJ, Joosen IA, Laufer EM, Chatrou ML, Herfs M, Winkens MH, Westenfeld R, Veulemans V, Krueger T and Shanahan CM. Vitamin K-antagonists accelerate atherosclerotic calcification and induce a vulnerable plaque phenotype. *PloS one*. 2012;7:e43229.
518. Schurgers LJ, Teunissen KJ, Knapen MH, Kwaijtaal M, van Diest R, Appels A, Reutelingsperger CP, Cleutjens JP and Vermeer C. Novel conformation-specific antibodies against matrix γ-carboxyglutamic acid (Gla) protein: undercarboxylated matrix Gla protein as marker for vascular calcification. *Arteriosclerosis, thrombosis, and vascular biology*. 2005;25:1629-1633.
519. Cranenburg EC, Brandenburg VM, Vermeer C, Stenger M, Mühlenbruch G, Mahnken AH, Gladziwa U, Ketteler M and Schurgers LJ. Uncarboxylated matrix Gla protein (ucMGP) is associated with coronary artery calcification in haemodialysis patients. *Thrombosis and haemostasis*. 2009;101:359-366.
520. Ketteler M, Bongartz P, Westenfeld R, Wildberger JE, Mahnken AH, Böhm R, Metzger T, Wanner C, Jahnen-Dechent W and Floege J. Association of low fetuin-A (AHSG) concentrations in serum with cardiovascular mortality in patients on dialysis: a cross-sectional study. *The Lancet*. 2003;361:827-833.
521. Stenvinkel P, Wang K, Qureshi AR, Axelsson J, Pecoits-Filho R, Gao P, Barany P, Lindholm B, Jogestrand T and Heimberger O. Low fetuin-A levels are associated with cardiovascular death: impact of variations in the gene encoding fetuin. *Kidney international*. 2005;67:2383-2392.
522. Hermans M, Brandenburg V, Ketteler M, Kooman J, Van der Sande F, Boeschoten E, Leunissen K, Krediet R, Dekker F and Dialysis Ncsotao. Association of serum fetuin-A levels with mortality in dialysis patients. *Kidney international*. 2007;72:202-207.

523. Westenfeld R, Schäfer C, Krüger T, Haarmann C, Schurgers LJ, Reutelingsperger C, Ivanovski O, Drueke T, Massy ZA and Ketteler M. Fetuin-A protects against atherosclerotic calcification in CKD. *Journal of the American Society of Nephrology*. 2009;20:1264-1274.
524. Chen HY, Chiu YL, Hsu SP, Pai MF, Yang JY and Peng YS. Relationship between fetuin A, vascular calcification and fracture risk in dialysis patients. *PloS one*. 2016;11:e0158789.
525. Westenfeld R, Jahnen-Dechent W and Ketteler M. Vascular calcification and fetuin-A deficiency in chronic kidney disease. *Trends in cardiovascular medicine*. 2007;17:124-128.
526. Jung H, Baek H and Kim S. Fetuin-A, coronary artery calcification and outcome in maintenance hemodialysis patients. *Clinical nephrology*. 2011;75:391.
527. Lehtinen AB, Burdon KP, Lewis JP, Langefeld CD, Ziegler JT, Rich SS, Register TC, Carr JJ, Freedman BI and Bowden DW. Association of α2-heremans-schmid glycoprotein polymorphisms with subclinical atherosclerosis. *The Journal of Clinical Endocrinology & Metabolism*. 2007;92:345-352.
528. Ix JH, Chertow GM, Shlipak MG, Brandenburg VM, Ketteler M and Whooley MA. Association of fetuin-A with mitral annular calcification and aortic stenosis among persons with coronary heart disease: data from the Heart and Soul Study. *Circulation*. 2007;115:2533.
529. Schinke T, Amendt C, Trindl A, Pöschke O, Müller-Esterl W and Jahnen-Dechent W. The serum protein α2-HS glycoprotein/fetuin inhibits apatite formation in vitro and in mineralizing calvaria cells a possible role in mineralization and calcium homeostasis. *Journal of Biological Chemistry*. 1996;271:20789-20796.
530. Heiss A, Eckert T, Aretz A, Richtering W, Van Dorp W, Schäfer C and Jahnen-Dechent W. Hierarchical role of fetuin-A and acidic serum proteins in the formation and stabilization of calcium phosphate particles. *Journal of biological chemistry*. 2008;283:14815-14825.
531. Heiss A, Jahnen-Dechent W, Endo H and Schwahn D. Structural dynamics of a colloidal protein-mineral complex bestowing on calcium phosphate a high solubility in biological fluids. *Biointerphases*. 2007;2:16-20.
532. Pasch A, Jahnen-Dechent W and Smith ER. Phosphate, calcification in blood, and mineral stress: the physiologic blood mineral buffering system and its association with cardiovascular risk. *International journal of nephrology*. 2018;2018.
533. Ou H-Y, Wu H-T, Hung H-C, Yang Y-C, Wu J-S and Chang C-J. Endoplasmic reticulum stress induces the expression of fetuin-A to develop insulin resistance. *Endocrinology*. 2012;153:2974-2984.
534. Dasgupta S, Bhattacharya S, Biswas A, Majumdar SS, Mukhopadhyay S, Ray S and Bhattacharya S. NF-κB mediates lipid-induced fetuin-A expression in hepatocytes that impairs adipocyte function effecting insulin resistance. *Biochemical journal*. 2010;429:451-462.
535. Chatterjee P, Seal S, Mukherjee S, Kundu R, Mukherjee S, Ray S, Mukhopadhyay S, Majumdar SS and Bhattacharya S. Adipocyte fetuin-A contributes to macrophage migration into adipose tissue and polarization of macrophages. *Journal of Biological Chemistry*. 2013;288:28324-28330.
536. Kahraman A, Sowa J-P, Schlattjan M, Sydor S, Pronadl M, Wree A, Beilfuss A, Kilicarslan A, Altinbaş A and Bechmann LP. Fetuin-A mRNA expression is elevated in NASH compared with NAFL patients. *Clinical science*. 2013;125:391-400.
537. Peter A, Kovarova M, Staiger H, Machann J, Schick F, Königsrainer A, Koenigsrainer I, Schleicher E, Fritsche A and Häring H-U. The hepatokines fetuin-A and fetuin-B are upregulated in the state of hepatic steatosis and may differently impact on glucose homeostasis in humans. *American Journal of Physiology-Endocrinology and Metabolism*. 2018;314:E266-E273.

538. Trepanowski J, Mey J and Varady K. Fetuin-A: a novel link between obesity and related complications. *International journal of obesity*. 2015;39:734-741.
539. Reynolds JL, Skepper JN, McNair R, Kasama T, Gupta K, Weissberg PL, Jahnen-Dechent W and Shanahan CM. Multifunctional roles for serum protein fetuin-a in inhibition of human vascular smooth muscle cell calcification. *Journal of the American Society of Nephrology*. 2005;16:2920-2930.
540. Chen NX, O'Neill KD, Chen X, Duan D, Wang E, Sturek MS, Edwards JM and Moe SM. Fetuin-A uptake in bovine vascular smooth muscle cells is calcium dependent and mediated by annexins. *American Journal of Physiology-Renal Physiology*. 2007;292:F599-F606.
541. Song A, Xu M, Bi Y, Xu Y, Huang Y, Li M, Wang T, Wu Y, Liu Y and Li X. Serum fetuin-A associates with type 2 diabetes and insulin resistance in Chinese adults. *PLoS One*. 2011;6:e19228.
542. Stefan N, Fritsche A, Weikert C, Boeing H, Joost H-G, Häring H-U and Schulze MB. Plasma fetuin-A levels and the risk of type 2 diabetes. *Diabetes*. 2008;57:2762-2767.
543. Wang H and E Sama A. Anti-inflammatory role of fetuin-A in injury and infection. *Current molecular medicine*. 2012;12:625-633.
544. Kay AM, Simpson CL and Stewart JA. The role of AGE/RAGE signaling in diabetes-mediated vascular calcification. *Journal of diabetes research*. 2016;2016.
545. Daffu G, Del Pozo CH, O'Shea KM, Ananthakrishnan R, Ramasamy R and Schmidt AM. Radical roles for RAGE in the pathogenesis of oxidative stress in cardiovascular diseases and beyond. *International journal of molecular sciences*. 2013;14:19891-19910.
546. Wei Q, Ren X, Jiang Y, Jin H, Liu N and Li J. Advanced glycation end products accelerate rat vascular calcification through RAGE/oxidative stress. *BMC cardiovascular disorders*. 2013;13:13.
547. Brodeur MR, Bouvet C, Bouchard S, Moreau S, Leblond J, deBlois D and Moreau P. Reduction of advanced-glycation end products levels and inhibition of RAGE signaling decreases rat vascular calcification induced by diabetes. *PloS one*. 2014;9:e85922.
548. Lok ZSY and Lyle AN. Osteopontin in Vascular Disease: Friend or Foe? *Arteriosclerosis, thrombosis, and vascular biology*. 2019;39:613-622.
549. Murphy-Ullrich JE and Sage EH. Revisiting the matricellular concept. *Matrix Biology*. 2014;37:1-14.
550. Bornstein P. Matricellular proteins: an overview. *Journal of cell communication and signaling*. 2009;3:163.
551. Saitoh Y, Kuratsu J-i, Takeshima H, Yamamoto S and Ushio Y. Expression of osteopontin in human glioma. Its correlation with the malignancy. *Laboratory investigation; a journal of technical methods and pathology*. 1995;72:55.
552. Myers DL, Harmon KJ, Lindner V and Liaw L. Alterations of arterial physiology in osteopontin-null mice. *Arteriosclerosis, thrombosis, and vascular biology*. 2003;23:1021-1028.
553. Lyle AN, Joseph G, Fan AE, Weiss D, Landázuri N and Taylor WR. Reactive oxygen species regulate osteopontin expression in a murine model of postischemic neovascularization. *Arteriosclerosis, thrombosis, and vascular biology*. 2012;32:1383-1391.
554. Wang X, Louden C, Yue T-L, Ellison JA, Barone FC, Solleveld HA and Feuerstein GZ. Delayed expression of osteopontin after focal stroke in the rat. *Journal of Neuroscience*. 1998;18:2075-2083.
555. O'Brien ER, Garvin MR, Stewart DK, Hinohara T, Simpson JB, Schwartz SM and Giachelli CM. Osteopontin is synthesized by macrophage, smooth muscle, and endothelial

cells in primary and restenotic human coronary atherosclerotic plaques. *Arteriosclerosis and Thrombosis: A Journal of Vascular Biology*. 1994;14:1648-1656.
556. Liaw L, Almeida M, Hart CE, Schwartz SM and Giachelli CM. Osteopontin promotes vascular cell adhesion and spreading and is chemotactic for smooth muscle cells in vitro. *Circulation Research*. 1994;74:214-224.
557. Liaw L, Skinner MP, Raines EW, Ross R, Cheresh DA, Schwartz SM and Giachelli CM. The adhesive and migratory effects of osteopontin are mediated via distinct cell surface integrins. Role of alpha v beta 3 in smooth muscle cell migration to osteopontin in vitro. *The Journal of clinical investigation*. 1995;95:713-724.
558. Standal T, Borset M and Sundan A. Role of osteopontin in adhesion, migration, cell survival and bone remodeling. *Exp Oncol*. 2004;26:179-84.
559. Shin H, Zygourakis K, Farach-Carson MC, Yaszemski MJ and Mikos AG. Attachment, proliferation, and migration of marrow stromal osteoblasts cultured on biomimetic hydrogels modified with an osteopontin-derived peptide. *Biomaterials*. 2004;25:895-906.
560. Gadeau A-P, Campan M, Millet D, Candresse T and Desgranges C. Osteopontin overexpression is associated with arterial smooth muscle cell proliferation in vitro. *Arteriosclerosis and Thrombosis: A Journal of Vascular Biology*. 1993;13:120-125.
561. Tardelli M, Zeyda K, Moreno-Viedma V, Wanko B, Grün NG, Staffler G, Zeyda M and Stulnig TM. Osteopontin is a key player for local adipose tissue macrophage proliferation in obesity. *Molecular metabolism*. 2016;5:1131-1137.
562. Weber GF, Zawaideh S, Hikita S, Kumar VA, Cantor H and Ashkar S. Phosphorylation-dependent interaction of osteopontin with its receptors regulates macrophage migration and activation. *Journal of leukocyte biology*. 2002;72:752-761.
563. Senger DR, Ledbetter SR, Claffey KP, Papadopoulos-Sergiou A, Peruzzi C and Detmar M. Stimulation of endothelial cell migration by vascular permeability factor/vascular endothelial growth factor through cooperative mechanisms involving the alphavbeta3 integrin, osteopontin, and thrombin. *The American journal of pathology*. 1996;149:293.
564. Lin Y-H and Yang-Yen H-F. The osteopontin-CD44 survival signal involves activation of the phosphatidylinositol 3-kinase/Akt signaling pathway. *Journal of Biological Chemistry*. 2001;276:46024-46030.
565. Hur EM, Youssef S, Haws ME, Zhang SY, Sobel RA and Steinman L. Osteopontin-induced relapse and progression of autoimmune brain disease through enhanced survival of activated T cells. *Nature immunology*. 2007;8:74-83.
566. Huang W, Carlsen B, Rudkin G, Berry M, Ishida K, Yamaguchi DT and Miller TA. Osteopontin is a negative regulator of proliferation and differentiation in MC3T3-E1 pre-osteoblastic cells. *Bone*. 2004;34:799-808.
567. Singhal H, Bautista DS, Tonkin KS, O'Malley FP, Tuck AB, Chambers AF and Harris JF. Elevated plasma osteopontin in metastatic breast cancer associated with increased tumor burden and decreased survival. *Clinical Cancer Research*. 1997;3:605-611.
568. Hotte SJ, Winquist EW, Stitt L, Wilson SM and Chambers AF. Plasma osteopontin: associations with survival and metastasis to bone in men with hormone-refractory prostate carcinoma. *Cancer: Interdisciplinary International Journal of the American Cancer Society*. 2002;95:506-512.
569. Kim J-H, Skates SJ, Uede T, Wong K-k, Schorge JO, Feltmate CM, Berkowitz RS, Cramer DW and Mok SC. Osteopontin as a potential diagnostic biomarker for ovarian cancer. *Jama*. 2002;287:1671-1679.
570. Agah E, Zardoui A, Saghazadeh A, Ahmadi M, Tafakhori A and Rezaei N. Osteopontin (OPN) as a CSF and blood biomarker for multiple sclerosis: A systematic review and meta-analysis. *PloS one*. 2018;13:e0190252.

571. Heywood WE, Galimberti D, Bliss E, Sirka E, Paterson RW, Magdalinou NK, Carecchio M, Reid E, Heslegrave A and Fenoglio C. Identification of novel CSF biomarkers for neurodegeneration and their validation by a high-throughput multiplexed targeted proteomic assay. *Molecular neurodegeneration*. 2015;10:64.
572. Sainger R, Grau JB, Poggio P, Branchetti E, Bavaria JE, Gorman III JH, Gorman RC and Ferrari G. Dephosphorylation of circulating human osteopontin correlates with severe valvular calcification in patients with calcific aortic valve disease. *Biomarkers*. 2012;17:111-118.
573. Grau JB, Poggio P, Sainger R, Vernick WJ, Seefried WF, Branchetti E, Field BC, Bavaria JE, Acker MA and Ferrari G. Analysis of osteopontin levels for the identification of asymptomatic patients with calcific aortic valve disease. *The Annals of thoracic surgery*. 2012;93:79-86.
574. Singh M, Foster CR, Dalal S and Singh K. Osteopontin: role in extracellular matrix deposition and myocardial remodeling post-MI. *Journal of molecular and cellular cardiology*. 2010;48:538-543.
575. Bjerre M, Pedersen SH, Møgelvang R, Lindberg S, Jensen JS, Galatius S and Flyvbjerg A. High osteopontin levels predict long-term outcome after STEMI and primary percutaneous coronary intervention. *European journal of preventive cardiology*. 2013;20:922-929.
576. Zhu Q, Luo X, Zhang J, Liu Y, Luo H, Huang Q, Cheng Y and Xie Z. Osteopontin as a potential therapeutic target for ischemic stroke. *Current Drug Delivery*. 2017;14:766-772.
577. Li Y, Dammer EB, Zhang-Brotzge X, Chen S, Duong DM, Seyfried NT, Kuan C-Y and Sun Y-Y. Osteopontin is a blood biomarker for microglial activation and brain injury in experimental hypoxic-ischemic encephalopathy. *Eneuro*. 2017;4.
578. Koshikawa M, Aizawa K, Kasai H, Izawa A, Tomita T, Kumazaki S, Tsutsui H, Koyama J, Shimodaira S and Takahashi M. Elevated osteopontin levels in patients with peripheral arterial disease. *Angiology*. 2009;60:42-45.
579. Kapetanios D, Karkos C, Giagtzidis I, Papazoglou K, Kiroplastis K and Spyridis C. Vascular calcification biomarkers and peripheral arterial disease. *International angiology: a journal of the International Union of Angiology*. 2015;35:455-459.
580. Speer MY, Chien Y-C, Quan M, Yang H-Y, Vali H, McKee MD and Giachelli CM. Smooth muscle cells deficient in osteopontin have enhanced susceptibility to calcification in vitro. *Cardiovascular research*. 2005;66:324-333.
581. Steitz SA, Speer MY, McKee MD, Liaw L, Almeida M, Yang H and Giachelli CM. Osteopontin inhibits mineral deposition and promotes regression of ectopic calcification. *The American journal of pathology*. 2002;161:2035-2046.
582. Jono S, Peinado C and Giachelli CM. Phosphorylation of osteopontin is required for inhibition of vascular smooth muscle cell calcification. *Journal of Biological Chemistry*. 2000;275:20197-20203.
583. Kitagawa M, Sugiyama H, Morinaga H, Inoue T, Takiue K, Ogawa A, Yamanari T, Kikumoto Y, Uchida HA and Kitamura S. A decreased level of serum soluble Klotho is an independent biomarker associated with arterial stiffness in patients with chronic kidney disease. *PloS one*. 2013;8:e56695.
584. Jono S, McKee MD, Murry CE, Shioi A, Nishizawa Y, Mori K, Morii H and Giachelli CM. Phosphate regulation of vascular smooth muscle cell calcification. *Circulation research*. 2000;87:e10-e17.
585. Li X, Yang H-Y and Giachelli CM. Role of the sodium-dependent phosphate cotransporter, Pit-1, in vascular smooth muscle cell calcification. *Circulation research*. 2006;98:905-912.

586. Chaudhary SC, Kuzynski M, Bottini M, Beniash E, Dokland T, Mobley CG, Yadav MC, Poliard A, Kellermann O and Millán JL. Phosphate induces formation of matrix vesicles during odontoblast-initiated mineralization in vitro. *Matrix Biology*. 2016;52:284-300.
587. Kapustin AN, Davies JD, Reynolds JL, McNair R, Jones GT, Sidibe A, Schurgers LJ, Skepper JN, Proudfoot D and Mayr M. Calcium regulates key components of vascular smooth muscle cell–derived matrix vesicles to enhance mineralization. *Circulation research*. 2011;109:e1-e12.
588. Villa-Bellosta R, Millan A and Sorribas V. Role of calcium-phosphate deposition in vascular smooth muscle cell calcification. *American Journal of Physiology-Cell Physiology*. 2011;300:C210-C220.
589. Razzaque MS. The FGF23–Klotho axis: endocrine regulation of phosphate homeostasis. *Nature Reviews Endocrinology*. 2009;5:611-619.
590. Murer H, Hernando N, Forster I and Biber Jr. Proximal tubular phosphate reabsorption: molecular mechanisms. *Physiological reviews*. 2000;80:1373-1409.
591. Antoniucci DM, Yamashita T and Portale AA. Dietary phosphorus regulates serum fibroblast growth factor-23 concentrations in healthy men. *The Journal of Clinical Endocrinology & Metabolism*. 2006;91:3144-3149.
592. Imel EA and Econs MJ. Fibroblast growth factor 23: roles in health and disease. *Journal of the American Society of Nephrology*. 2005;16:2565-2575.
593. Shimada T, Mizutani S, Muto T, Yoneya T, Hino R, Takeda S, Takeuchi Y, Fujita T, Fukumoto S and Yamashita T. Cloning and characterization of FGF23 as a causative factor of tumor-induced osteomalacia. *Proceedings of the National Academy of Sciences*. 2001;98:6500-6505.
594. Ferrari SL, Bonjour J-P and Rizzoli R. Fibroblast growth factor-23 relationship to dietary phosphate and renal phosphate handling in healthy young men. *The Journal of Clinical Endocrinology & Metabolism*. 2005;90:1519-1524.
595. Portale AA, Booth BE, Halloran BP and Morris RC. Effect of dietary phosphorus on circulating concentrations of 1, 25-dihydroxyvitamin D and immunoreactive parathyroid hormone in children with moderate renal insufficiency. *The Journal of clinical investigation*. 1984;73:1580-1589.
596. Shimada T, Yamazaki Y, Takahashi M, Hasegawa H, Urakawa I, Oshima T, Ono K, Kakitani M, Tomizuka K and Fujita T. Vitamin D receptor-independent FGF23 actions in regulating phosphate and vitamin D metabolism. *American Journal of Physiology-Renal Physiology*. 2005;289:F1088-F1095.
597. Shalhoub V, Shatzen EM, Ward SC, Davis J, Stevens J, Bi V, Renshaw L, Hawkins N, Wang W and Chen C. FGF23 neutralization improves chronic kidney disease–associated hyperparathyroidism yet increases mortality. *The Journal of clinical investigation*. 2012;122:2543-2553.
598. Slatopolsky E, Finch J, Denda M, Ritter C, Zhong M, Dusso A, MacDonald PN and Brown AJ. Phosphorus restriction prevents parathyroid gland growth. High phosphorus directly stimulates PTH secretion in vitro. *The Journal of clinical investigation*. 1996;97:2534-2540.
599. Dusso A, González EA and Martin KJ. Vitamin D in chronic kidney disease. *Best practice & research Clinical endocrinology & metabolism*. 2011;25:647-655.
600. Levin A, Bakris G, Molitch M, Smulders M, Tian J, Williams L and Andress D. Prevalence of abnormal serum vitamin D, PTH, calcium, and phosphorus in patients with chronic kidney disease: results of the study to evaluate early kidney disease. *Kidney international*. 2007;71:31-38.
601. Isakova T, Wahl P, Vargas GS, Gutiérrez OM, Scialla J, Xie H, Appleby D, Nessel L, Bellovich K and Chen J. Fibroblast growth factor 23 is elevated before parathyroid hormone and phosphate in chronic kidney disease. *Kidney international*. 2011;79:1370-1378.

602. Li S-A, Watanabe M, Yamada H, Nagai A, Kinuta M and Takei K. Immunohistochemical localization of Klotho protein in brain, kidney, and reproductive organs of mice. *Cell structure and function*. 2004;29:91-99.
603. Kuro-o M, Matsumura Y, Aizawa H, Kawaguchi H, Suga T, Utsugi T, Ohyama Y, Kurabayashi M, Kaname T and Kume E. Mutation of the mouse klotho gene leads to a syndrome resembling ageing. *nature*. 1997;390:45-51.
604. Urakawa I, Yamazaki Y, Shimada T, Iijima K, Hasegawa H, Okawa K, Fujita T, Fukumoto S and Yamashita T. Klotho converts canonical FGF receptor into a specific receptor for FGF23. *Nature*. 2006;444:770-774.
605. Yamazaki Y, Tamada T, Kasai N, Urakawa I, Aono Y, Hasegawa H, Fujita T, Kuroki R, Yamashita T and Fukumoto S. Anti-FGF23 neutralizing antibodies show the physiological role and structural features of FGF23. *Journal of Bone and Mineral Research*. 2008;23:1509-1518.
606. Kurosu H, Ogawa Y, Miyoshi M, Yamamoto M, Nandi A, Rosenblatt KP, Baum MG, Schiavi S, Hu M-C and Moe OW. Regulation of fibroblast growth factor-23 signaling by klotho. *Journal of Biological Chemistry*. 2006;281:6120-6123.
607. Nakatani T, Sarraj B, Ohnishi M, Densmore MJ, Taguchi T, Goetz R, Mohammadi M, Lanske B and Razzaque MS. In vivo genetic evidence for klotho-dependent, fibroblast growth factor 23 (Fgf23)-mediated regulation of systemic phosphate homeostasis. *The FASEB Journal*. 2009;23:433-441.
608. Chen C-D, Podvin S, Gillespie E, Leeman SE and Abraham CR. Insulin stimulates the cleavage and release of the extracellular domain of Klotho by ADAM10 and ADAM17. *Proceedings of the National Academy of Sciences*. 2007;104:19796-19801.
609. Shimamura Y, Hamada K, Inoue K, Ogata K, Ishihara M, Kagawa T, Inoue M, Fujimoto S, Ikebe M and Yuasa K. Serum levels of soluble secreted α-Klotho are decreased in the early stages of chronic kidney disease, making it a probable novel biomarker for early diagnosis. *Clinical and experimental nephrology*. 2012;16:722-729.
610. Hu MC, Shi M, Zhang J, Quiñones H, Griffith C, Kuro-o M and Moe OW. Klotho deficiency causes vascular calcification in chronic kidney disease. *Journal of the American Society of Nephrology*. 2011;22:124-136.
611. Keusch I, Traebert M, Lötscher M, Kaissling B, Murer H and Biber J. Parathyroid hormone and dietary phosphate provoke a lysosomal routing of the proximal tubular Na/Pi-cotransporter type II. *Kidney international*. 1998;54:1224-1232.
612. Coetzee M, Haag M and Kruger MC. Effects of arachidonic acid, docosahexaenoic acid, prostaglandin E2 and parathyroid hormone on osteoprotegerin and RANKL secretion by MC3T3-E1 osteoblast-like cells. *The Journal of nutritional biochemistry*. 2007;18:54-63.
613. Walker EC, Poulton IJ, McGregor NE, Ho PW, Allan EH, Quach JM, Martin TJ and Sims NA. Sustained RANKL response to parathyroid hormone in oncostatin M receptor-deficient osteoblasts converts anabolic treatment to a catabolic effect in vivo. *Journal of Bone and Mineral Research*. 2012;27:902-912.
614. Kondo H, Guo J and Bringhurst FR. Cyclic adenosine monophosphate/protein kinase A mediates parathyroid hormone/parathyroid hormone-related protein receptor regulation of osteoclastogenesis and expression of RANKL and osteoprotegerin mRNAs by marrow stromal cells. *Journal of Bone and Mineral Research*. 2002;17:1667-1679.
615. Ben-awadh AN, Delgado-Calle J, Tu X, Kuhlenschmidt K, Allen MR, Plotkin LI and Bellido T. Parathyroid hormone receptor signaling induces bone resorption in the adult skeleton by directly regulating the RANKL gene in osteocytes. *Endocrinology*. 2014;155:2797-2809.
616. Ricarte FR, Le Henaff C, Kolupaeva VG, Gardella TJ and Partridge NC. Parathyroid hormone (1–34) and its analogs differentially modulate osteoblastic Rankl expression via

PKA/SIK2/SIK3 and PP1/PP2A–CRTC3 signaling. *Journal of Biological Chemistry*. 2018;293:20200-20213.
617. Healy KD, Vanhooke JL, Prahl JM and DeLuca HF. Parathyroid hormone decreases renal vitamin D receptor expression in vivo. *Proceedings of the National Academy of Sciences*. 2005;102:4724-4728.
618. Gallant KMH and Spiegel DM. Calcium balance in chronic kidney disease. *Current Osteoporosis Reports*. 2017;15:214-221.
619. Gao Z, Li X, Miao J and Lun L. Impacts of parathyroidectomy on calcium and phosphorus metabolism disorder, arterial calcification and arterial stiffness in haemodialysis patients. *Asian journal of surgery*. 2019;42:6-10.
620. Evenepoel P, Bover J and Torres PU. Parathyroid hormone metabolism and signaling in health and chronic kidney disease. *Kidney international*. 2016;90:1184-1190.
621. Carrillo-López N, Panizo S, Alonso-Montes C, Martínez-Arias L, Avello N, Sosa P, Dusso AS, Cannata-Andía JB and Naves-Díaz M. High-serum phosphate and parathyroid hormone distinctly regulate bone loss and vascular calcification in experimental chronic kidney disease. *Nephrology Dialysis Transplantation*. 2019;34:934-941.
622. Wu GY, Xu BD, Wu T, Wang XY, Wang TX, Zhang X, Wang X, Xia Y and Zong GJ. Correlation between serum parathyroid hormone levels and coronary artery calcification in patients without renal failure. *Biomedical Reports*. 2016;5:601-606.
623. Galli C, Fu Q, Wang W, Olsen BR, Manolagas SC, Jilka RL and O'Brien CA. Commitment to the osteoblast lineage is not required for RANKL gene expression. *Journal of Biological Chemistry*. 2009;284:12654-12662.
624. Briese S, Wiesner S, Will JC, Lembcke A, Opgen-Rhein B, Nissel R, Wernecke K-D, Andreae J, Haffner D and Querfeld U. Arterial and cardiac disease in young adults with childhood-onset end-stage renal disease—impact of calcium and vitamin D therapy. *Nephrology Dialysis Transplantation*. 2006;21:1906-1914.
625. Bas A, Lopez I, Perez J, Rodriguez M and Aguilera-Tejero E. Reversibility of calcitriol-induced medial artery calcification in rats with intact renal function. *Journal of Bone and Mineral Research*. 2006;21:484-490.
626. Mizobuchi M, Finch J, Martin D and Slatopolsky E. Differential effects of vitamin D receptor activators on vascular calcification in uremic rats. *Kidney international*. 2007;72:709-715.
627. Razzaque MS. The dualistic role of vitamin D in vascular calcifications. *Kidney international*. 2011;79:708-714.
628. Silver J, Naveh-Many T, Mayer H, Schmelzer H and Popovtzer M. Regulation by vitamin D metabolites of parathyroid hormone gene transcription in vivo in the rat. *The Journal of clinical investigation*. 1986;78:1296-1301.
629. Silver J, Yalcindag C, Sela-Brown A, Kilav R and Naveh-Many T. Regulation of the parathyroid hormone gene by vitamin D, calcium and phosphate. *Kidney international*. 1999;56:S2-S7.
630. Somjen D, Weisman Y, Kohen F, Gayer B, Limor R, Sharon O, Jaccard N, Knoll E and Stern N. 25-Hydroxyvitamin D3-1α-Hydroxylase Is Expressed in Human Vascular Smooth Muscle Cells and Is Upregulated by Parathyroid Hormone and Estrogenic Compounds. *Circulation*. 2005;111:1666-1671.
631. Tukaj C, Kubasik-Juraniec J and Kraszpulski M. Morphological changes of aortal smooth muscle cells exposed to calcitriol in culture. *Medical Science Monitor*. 2000;6:668-674.
632. Drissi H, Pouliot A, Koolloos C, Stein JL, Lian JB, Stein GS and Van Wijnen AJ. 1, 25-(OH) 2-vitamin D3 suppresses the bone-related Runx2/Cbfa1 gene promoter. *Experimental cell research*. 2002;274:323-333.

633. Boyan BD, Wong KL, Fang M and Schwartz Z. 1α, 25 (OH) 2D3 is an autocrine regulator of extracellular matrix turnover and growth factor release via ERp60 activated matrix vesicle metalloproteinases. *The Journal of steroid biochemistry and molecular biology*. 2007;103:467-472.
634. Schwetz V, Scharnagl H, Trummer C, Stojakovic T, Pandis M, Gruebler MR, Verheyen N, Gaksch M, Zittermann A and Aberer F. Vitamin D supplementation and lipoprotein metabolism: a randomized controlled trial. *Journal of clinical lipidology*. 2018;12:588-596. e4.
635. Querfeld U, Hoffmann MM, KLAUS G, Eifinger F, Ackerschott M, Michalk D and Kern PA. Antagonistic effects of vitamin D and parathyroid hormone on lipoprotein lipase in cultured adipocytes. *Journal of the American Society of Nephrology*. 1999;10:2158-2164.
636. Huang Y, Li X, Wang M, Ning H, Lima A, Li Y and Sun C. Lipoprotein lipase links vitamin D, insulin resistance, and type 2 diabetes: a cross-sectional epidemiological study. *Cardiovascular diabetology*. 2013;12:17.
637. Wu-Wong JR, Noonan W, Ma J, Dixon D, Nakane M, Bolin AL, Koch KA, Postl S, Morgan SJ and Reinhart GA. Role of phosphorus and vitamin D analogs in the pathogenesis of vascular calcification. *Journal of pharmacology and experimental therapeutics*. 2006;318:90-98.
638. Ohnishi M, Nakatani T, Lanske B and Razzaque MS. Reversal of mineral ion homeostasis and soft-tissue calcification of klotho knockout mice by deletion of vitamin D 1α-hydroxylase. *Kidney international*. 2009;75:1166-1172.
639. Rattazzi M, Bennett BJ, Bea F, Kirk EA, Ricks JL, Speer M, Schwartz SM, Giachelli CM and Rosenfeld ME. Calcification of advanced atherosclerotic lesions in the innominate arteries of ApoE-deficient mice. *Arteriosclerosis, thrombosis, and vascular biology*. 2005;25:1420-1425.
640. Awan Z, Denis M, Bailey D, Giaid A, Prat A, Goltzman D, Seidah NG and Genest J. The LDLR deficient mouse as a model for aortic calcification and quantification by micro-computed tomography. *Atherosclerosis*. 2011;219:455-462.
641. Roselaar SE, Kakkanathu PX and Daugherty A. Lymphocyte populations in atherosclerotic lesions of apoE−/− and LDL receptor−/− mice: decreasing density with disease progression. *Arteriosclerosis, thrombosis, and vascular biology*. 1996;16:1013-1018.
642. De Maré A, Maudsley S, Azmi A, Hendrickx JO, Opdebeeck B, Neven E, D'Haese PC and Verhulst A. Sclerostin as Regulatory Molecule in Vascular Media Calcification and the Bone–Vascular Axis. *Toxins*. 2019;11:428.
643. Bucay N, Sarosi I, Dunstan CR, Morony S, Tarpley J, Capparelli C, Scully S, Tan HL, Xu W and Lacey DL. Osteoprotegerin-deficient mice develop early onset osteoporosis and arterial calcification. *Genes & development*. 1998;12:1260-1268.
644. Goettsch C, Hutcheson JD, Hagita S, Rogers MA, Creager MD, Pham T, Choi J, Mlynarchik AK, Pieper B and Kjolby M. A single injection of gain-of-function mutant PCSK9 adeno-associated virus vector induces cardiovascular calcification in mice with no genetic modification. *Atherosclerosis*. 2016;251:109-118.
645. Hilvo M, Simolin H, Metso J, Ruuth M, Öörni K, Jauhiainen M, Laaksonen R and Baruch A. PCSK9 inhibition alters the lipidome of plasma and lipoprotein fractions. *Atherosclerosis*. 2018;269:159-165.
646. Maxwell KN and Breslow JL. Adenoviral-mediated expression of Pcsk9 in mice results in a low-density lipoprotein receptor knockout phenotype. *Proceedings of the National Academy of Sciences of the United States of America*. 2004;101:7100-7105.
647. Urban D, Pöss J, Böhm M and Laufs U. Targeting the proprotein convertase subtilisin/kexin type 9 for the treatment of dyslipidemia and atherosclerosis. *Journal of the American College of Cardiology*. 2013;62:1401-1408.

648. Nicholls SJ, Puri R, Anderson T, Ballantyne CM, Cho L, Kastelein JJ, Koenig W, Somaratne R, Kassahun H and Yang J. Effect of evolocumab on coronary plaque composition. *Journal of the American College of Cardiology*. 2018;72:2012-2021.
649. Barter P. Lessons learned from the investigation of lipid level management to understand its impact in atherosclerotic events (ILLUMINATE) trial. *The American journal of cardiology*. 2009;104:10E-15E.
650. Investigators A-H. The role of niacin in raising high-density lipoprotein cholesterol to reduce cardiovascular events in patients with atherosclerotic cardiovascular disease and optimally treated low-density lipoprotein cholesterol: rationale and study design. The Atherothrombosis Intervention in Metabolic syndrome with low HDL/high triglycerides: Impact on Global Health outcomes (AIM-HIGH). *American heart journal*. 2011;161:471-477. e2.
651. Kraus WE, Houmard JA, Duscha BD, Knetzger KJ, Wharton MB, McCartney JS, Bales CW, Henes S, Samsa GP and Otvos JD. Effects of the amount and intensity of exercise on plasma lipoproteins. *New England Journal of Medicine*. 2002;347:1483-1492.
652. Cui Y, Watson DJ, Girman CJ, Shapiro DR, Gotto AM, Hiserote P and Clearfield MB. Effects of increasing high-density lipoprotein cholesterol and decreasing low-density lipoprotein cholesterol on the incidence of first acute coronary events (from the Air Force/Texas Coronary Atherosclerosis Prevention Study). *The American journal of cardiology*. 2009;104:829-834.
653. Jun M, Foote C, Lv J, Neal B, Patel A, Nicholls SJ, Grobbee DE, Cass A, Chalmers J and Perkovic V. Effects of fibrates on cardiovascular outcomes: a systematic review and meta-analysis. *The Lancet*. 2010;375:1875-1884.
654. Investigators DAIS. Effect of fenofibrate on progression of coronary-artery disease in type 2 diabetes: the Diabetes Atherosclerosis Intervention Study, a randomised study. *The Lancet*. 2001;357:905-910.
655. Investigators A-H. Niacin in patients with low HDL cholesterol levels receiving intensive statin therapy. *New England Journal of Medicine*. 2011;365:2255-2267.
656. Bloomfield HE. Adding niacin plus laropiprant to statins did not reduce vascular events and increased serious adverse events. *Annals of internal medicine*. 2014;161:JC8.
657. Speidl WS, Cimmino G, Ibanez B, Elmariah S, Hutter R, Garcia MJ, Fuster V, Goldman ME and Badimon JJ. Recombinant apolipoprotein AI Milano rapidly reverses aortic valve stenosis and decreases leaflet inflammation in an experimental rabbit model. *European heart journal*. 2010;31:2049-2057.
658. Osborne Jr JC. Delipidation of plasma lipoproteins *Methods in enzymology*: Elsevier; 1986(128): 213-222.
659. Weisweiler P. Isolation and quantitation of apolipoproteins AI and A-II from human high-density lipoproteins by fast-protein liquid chromatography. *Clinica chimica acta*. 1987;169:249-254.
660. Rye K-A. Interaction of apolipoprotein A-II with recombinant HDL containing egg phosphatidylcholine, unesterified cholesterol and apolipoprotein AI. *Biochimica et Biophysica Acta (BBA)-Lipids and Lipid Metabolism*. 1990;1042:227-236.
661. Matz CE and Jonas A. Micellar complexes of human apolipoprotein AI with phosphatidylcholines and cholesterol prepared from cholate-lipid dispersions. *Journal of Biological Chemistry*. 1982;257:4535-4540.
662. Gregory CA, Gunn WG, Peister A and Prockop DJ. An Alizarin red-based assay of mineralization by adherent cells in culture: comparison with cetylpyridinium chloride extraction. *Analytical biochemistry*. 2004;329:77-84.
663. Bustin SA. Absolute quantification of mRNA using real-time reverse transcription polymerase chain reaction assays. *Journal of molecular endocrinology*. 2000;25:169-193.

664. Durham AL, Speer MY, Scatena M, Giachelli CM and Shanahan CM. Role of smooth muscle cells in vascular calcification: implications in atherosclerosis and arterial stiffness. *Cardiovascular research*. 2018;114:590-600.
665. Gungor O, Kocyigit I, Yilmaz MI and Sezer S. Role of vascular calcification inhibitors in preventing vascular dysfunction and mortality in hemodialysis patients. *Seminars in dialysis*. 2018;31:72-81.
666. Li B, Zhang Y, Wang Q, Dong Z, Shang L, Wu L, Wang X and Jin Y. Periodontal ligament stem cells modulate root resorption of human primary teeth via Runx2 regulating RANKL/OPG system. *Stem cells and development*. 2014;23:2524-2534.
667. Tanaka H, Mine T, Ogasa H, Taguchi T and Liang C. Expression of RANKL/OPG during bone remodeling in vivo. *Biochemical and biophysical research communications*. 2011;411:690-694.
668. Schoppet M and Shanahan C. Role for alkaline phosphatase as an inducer of vascular calcification in renal failure? *Kidney international*. 2008;73:989-991.
669. Cheng S-L, Yang JW, Rifas L, Zhang S-F and Avioli LV. Differentiation of human bone marrow osteogenic stromal cells in vitro: induction of the osteoblast phenotype by dexamethasone. *Endocrinology*. 1994;134:277-286.
670. Mori K, Shioi A, Jono S, Nishizawa Y and Morii H. Dexamethasone enhances in vitro vascular calcification by promoting osteoblastic differentiation of vascular smooth muscle cells. *Arteriosclerosis, thrombosis, and vascular biology*. 1999;19:2112-2118.
671. Hutcheson JD, Blaser MC and Aikawa E. Giving calcification its due: recognition of a diverse disease: a first attempt to standardize the field. *Circulation research*. 2017;120:270-273.
672. Goto S, Rogers MA, Blaser MC, Higashi H, Lee LH, Schlotter F, Body SC, Aikawa M, Singh SA and Aikawa E. Standardization of human calcific aortic valve disease in vitro modeling reveals passage-dependent calcification. *Frontiers in cardiovascular medicine*. 2019;6:49.
673. Wang C-S, McConathy WJ, Kloer HU and Alaupovic P. Modulation of lipoprotein lipase activity by apolipoproteins. Effect of apolipoprotein C-III. *The Journal of clinical investigation*. 1985;75:384-390.
674. Norata GD, Tsimikas S, Pirillo A and Catapano AL. Apolipoprotein C-III: from pathophysiology to pharmacology. *Trends in pharmacological sciences*. 2015;36:675-687.
675. Gordts PL, Nock R, Son N-H, Ramms B, Lew I, Gonzales JC, Thacker BE, Basu D, Lee RG and Mullick AE. ApoC-III inhibits clearance of triglyceride-rich lipoproteins through LDL family receptors. *The Journal of clinical investigation*. 2016;126:2855-2866.
676. Amar MJ, Sakurai T, Sakurai-Ikuta A, Sviridov D, Freeman L, Ahsan L and Remaley AT. A Novel Apolipoprotein C-II Mimetic Peptide That Activates Lipoprotein Lipase and Decreases Serum Triglycerides in Apolipoprotein E–Knockout Mice. *Journal of Pharmacology and Experimental Therapeutics*. 2015;352:227-235.
677. Alexander VJ, Viney NJ and Witztum JL. Modulation of apolipoprotein C-III (ApoCIII) expression in lipoprotein lipase deficient (LPLD) populations. 2017.
678. Kiernan UA, Phillips DA and Niederkofler EE. Apolipoprotein C3 (ApoCIII) antagonists and methods of their use to remove ApoCIII inhibition of lipoprotein lipase (LPL). 2017.
679. Taskinen M-R and Borén J. Why is apolipoprotein CIII emerging as a novel therapeutic target to reduce the burden of cardiovascular disease? *Current atherosclerosis reports*. 2016;18:59.
680. Khetarpal SA, Zeng X, Millar JS, Vitali C, Somasundara AVH, Zanoni P, Landro JA, Barucci N, Zavadoski WJ and Sun Z. A human APOC3 missense variant and monoclonal

antibody accelerate apoC-III clearance and lower triglyceride-rich lipoprotein levels. *Nature medicine*. 2017;23:1086.
681. Karathanasis SK. Apolipoprotein multigene family: tandem organization of human apolipoprotein AI, CIII, and AIV genes. *Proceedings of the National Academy of Sciences*. 1985;82:6374-6378.
682. Shoulders C, Harry P, Lagrost L, White S, Shah N, North J, Gilligan M, Gambert P and Ball M. Variation at the apo AI/CIII/A1V gene complex is associated with elevated plasma levels of apo CIII. *Atherosclerosis*. 1991;87:239-247.
683. Sun M, Chen L, Liu H, Ma L, Wang T and Liu Y. Association of the S2 allele of the SstI polymorphism in the apoC3 gene with plasma apoCIII interacts with unfavorable lipid profiles to contribute to atherosclerosis in the li ethnic group in China. *Lipids in Health and Disease*. 2017;16:220.
684. Pollin TI, Damcott CM, Shen H, Ott SH, Shelton J, Horenstein RB, Post W, McLenithan JC, Bielak LF and Peyser PA. A null mutation in human APOC3 confers a favorable plasma lipid profile and apparent cardioprotection. *Science*. 2008;322:1702-1705.
685. Crosby J, Peloso G, Auer P, Crosslin D, Lange L, Lu Y, Tang Z, Zhang H, Hindy G and Masca N. Loss-of-function mutations in APOC3, triglycerides, and coronary disease. 2014.
686. Jørgensen AB, Frikke-Schmidt R, Nordestgaard BG and Tybjærg-Hansen A. Loss-of-function mutations in APOC3 and risk of ischemic vascular disease. *N Engl J Med*. 2014;371:32-41.
687. Yan H, Niimi M, Matsuhisa F, Zhou H, Kitajima S, Chen Y, Wang C, Yang X, Yao J and Yang D. Apolipoprotein CIII Deficiency Protects Against Atherosclerosis in Knockout Rabbits. *Arteriosclerosis, Thrombosis, and Vascular Biology*. 2020;40:2095-2107.
688. Guo M, Xu Y, Dong Z, Zhou Z, Cong NX, Gao M, Huang W, Wang Y, Liu G and Xian X. Inactivation of Apoc3 by CRISPR/Cas9 Protects Against Atherosclerosis in Hamsters. *Circulation Research*. 2020.
689. Maeda N, Li H, Lee D, Oliver P, Quarfordt SH and Osada J. Targeted disruption of the apolipoprotein C-III gene in mice results in hypotriglyceridemia and protection from postprandial hypertriglyceridemia. *Journal of Biological Chemistry*. 1994;269:23610-23616.
690. Jong MC, Rensen PC, Dahlmans VE, van der Boom H, van Berkel TJ and Havekes LM. Apolipoprotein C-III deficiency accelerates triglyceride hydrolysis by lipoprotein lipase in wild-type and apoE knockout mice. *Journal of lipid research*. 2001;42:1578-1585.
691. Ito Y, Azrolan N, O'Connell A, Walsh A and Breslow JL. Hypertriglyceridemia as a result of human apo CIII gene expression in transgenic mice. *Science*. 1990;249:790-793.
692. Salerno A, Silva T, Amaral M, Alberici L, Bonfleur M, Patricio P, Francesconi E, Grassi-Kassisse D, Vercesi A and Boschero A. Overexpression of apolipoprotein CIII increases and CETP reverses diet-induced obesity in transgenic mice. *International Journal of Obesity*. 2007;31:1586-1595.
693. Duivenvoorden I, Teusink B, Rensen PC, Romijn JA, Havekes LM and Voshol PJ. Apolipoprotein C3 deficiency results in diet-induced obesity and aggravated insulin resistance in mice. *Diabetes*. 2005;54:664-671.
694. Hayek T, Masucci-Magoulas L, Jiang X, Walsh A, Rubin E, Breslow JL and Tall AR. Decreased early atherosclerotic lesions in hypertriglyceridemic mice expressing cholesteryl ester transfer protein transgene. *The Journal of clinical investigation*. 1995;96:2071-2074.
695. Kypreos KE. ABCA1 promotes the de novo biogenesis of apolipoprotein CIII-containing HDL particles in vivo and modulates the severity of apolipoprotein CIII-induced hypertriglyceridemia. *Biochemistry*. 2008;47:10491-10502.

696. Zvintzou E, Lhomme M, Chasapi S, Filou S, Theodoropoulos V, Xapapadaki E, Kontush A, Spyroulias G, Tellis CC and Tselepis AD. Pleiotropic effects of apolipoprotein C3 on HDL functionality and adipose tissue metabolic activity. *Journal of lipid research*. 2017;58:1869-1883.
697. Caron S, Verrijken A, Mertens I, Samanez CH, Mautino G, Haas JT, Duran-Sandoval D, Prawitt J, Francque S and Vallez E. Transcriptional activation of apolipoprotein CIII expression by glucose may contribute to diabetic dyslipidemia. *Arteriosclerosis, thrombosis, and vascular biology*. 2011;31:513-519.
698. Kanter JE, Shao B, Kramer F, Barnhart S, Shimizu-Albergine M, Vaisar T, Graham MJ, Crooke RM, Manuel CR and Haeusler RA. Increased apolipoprotein C3 drives cardiovascular risk in type 1 diabetes. *The Journal of clinical investigation*. 2019;129.
699. Ginsberg HN and Reyes-Soffer G. Is APOC3 the driver of cardiovascular disease in people with type I diabetes mellitus? *The Journal of clinical investigation*. 2019;129.
700. Kawakami A, Aikawa M, Libby P, Alcaide P, Luscinskas FW and Sacks FM. Apolipoprotein CIII in apolipoprotein B lipoproteins enhances the adhesion of human monocytic cells to endothelial cells. *Circulation*. 2006;113:691-700.
701. Zheng C, Azcutia V, Aikawa E, Figueiredo J-L, Croce K, Sonoki H, Sacks FM, Luscinskas FW and Aikawa M. Statins suppress apolipoprotein CIII-induced vascular endothelial cell activation and monocyte adhesion. *European heart journal*. 2013;34:615-624.
702. Li C, Zhang M, Dai Y and Xu Z. MicroRNA-424-5p regulates aortic smooth muscle cell function in atherosclerosis by blocking APOC3-mediated nuclear factor-κB signalling pathway. *Experimental Physiology*. 2020.
703. Prenner SB, Mulvey CK, Ferguson JF, Rickels MR, Bhatt AB and Reilly MP. Very low density lipoprotein cholesterol associates with coronary artery calcification in type 2 diabetes beyond circulating levels of triglycerides. *Atherosclerosis*. 2014;236:244-250.
704. Hiltunen TP, Luoma JS, Nikkari T and Yla̋-Herttuala S. Expression of LDL receptor, VLDL receptor, LDL receptor–related protein, and scavenger receptor in rabbit atherosclerotic lesions: marked induction of scavenger receptor and VLDL receptor expression during lesion development. *Circulation*. 1998;97:1079-1086.
705. Di Bartolo BA, Schoppet M, Mattar MZ, Rachner TD, Shanahan CM and Kavurma MM. Calcium and osteoprotegerin regulate IGF1R expression to inhibit vascular calcification. *Cardiovascular research*. 2011;91:537-545.
706. Aalto-Setälä K, Fisher E, Chen X, Chajek-Shaul T, Hayek T, Zechner R, Walsh A, Ramakrishnan R, Ginsberg H and Breslow J. Mechanism of hypertriglyceridemia in human apolipoprotein (apo) CIII transgenic mice. Diminished very low density lipoprotein fractional catabolic rate associated with increased apo CIII and reduced apo E on the particles. *The Journal of clinical investigation*. 1992;90:1889-1900.
707. Mohler ER. Mechanisms of aortic valve calcification. *American Journal of Cardiology*. 2004;94:1396-1402.
708. Simard L, Cote N, Dagenais F, Mathieu P, Couture C, Trahan S, Bosse Y, Mohammadi S, Page S and Joubert P. Sex-related discordance between aortic valve calcification and hemodynamic severity of aortic stenosis: is valvular fibrosis the explanation? *Circulation research*. 2017;120:681-691.
709. Rodriguez KJ, Piechura LM, Porras AM and Masters KS. Manipulation of valve composition to elucidate the role of collagen in aortic valve calcification. *BMC cardiovascular disorders*. 2014;14:1-10.
710. Adami S, Braga V, Zamboni M, Gatti D, Rossini M, Bakri J and Battaglia E. Relationship between lipids and bone mass in 2 cohorts of healthy women and men. *Calcified tissue international*. 2004;74:136-142.

711. Brownbill R and Ilich J. Lipid profile and bone paradox: higher serum lipids are associated with higher bone mineral density in postmenopausal women. *Journal of women's health*. 2006;15:261-270.
712. Mroue KH, Xu J, Zhu P, Morris MD and Ramamoorthy A. Selective detection and complete identification of triglycerides in cortical bone by high-resolution 1 H MAS NMR spectroscopy. *Physical Chemistry Chemical Physics*. 2016;18:18687-18691.
713. Tiwari N, Rai R and Sinha N. Water-lipid interactions in native bone by high-resolution solid-state NMR spectroscopy. *Solid State Nuclear Magnetic Resonance*. 2020:101666.
714. Kannan K and Jain SK. Oxidative stress and apoptosis. *Pathophysiology*. 2000;7:153-163.
715. Chandra J, Samali A and Orrenius S. Triggering and modulation of apoptosis by oxidative stress. *Free radical biology and medicine*. 2000;29:323-333.
716. Wang Y, Zhao H, Shao Y, Liu J, Li J, Luo L and Xing M. Copper (II) and/or arsenite-induced oxidative stress cascades apoptosis and autophagy in the skeletal muscles of chicken. *Chemosphere*. 2018;206:597-605.
717. Ikwegbue PC, Masamba P, Oyinloye BE and Kappo AP. Roles of heat shock proteins in apoptosis, oxidative stress, human inflammatory diseases, and cancer. *Pharmaceuticals*. 2018;11:2.
718. Di Bartolo BA, Cartland SP, Harith HH, Bobryshev YV, Schoppet M and Kavurma MM. TRAIL-deficiency accelerates vascular calcification in atherosclerosis via modulation of RANKL. *PloS one*. 2013;8:e74211.
719. Koulaouzidis G, Nicoll R, MacArthur T, Jenkins P and Henein MY. Coronary artery calcification correlates with the presence and severity of valve calcification. *International journal of cardiology*. 2013;168:5263-5266.
720. Mahabadi AA, Bamberg F, Toepker M, Schlett CL, Rogers IS, Nagurney JT, Brady TJ, Hoffmann U and Truong QA. Association of aortic valve calcification to the presence, extent, and composition of coronary artery plaque burden: from the Rule Out Myocardial Infarction using Computer Assisted Tomography (ROMICAT) trial. *American heart journal*. 2009;158:562-568.
721. Nakajima I, Muroya S, Tanabe R-i and Chikuni K. Positive effect of collagen V and VI on triglyceride accumulation during differentiation in cultures of bovine intramuscular adipocytes. *Differentiation*. 2002;70:84-91.
722. Tanaka H, Zaima N, Sasaki T, Yamamoto N, Inuzuka K, Sano M, Saito T, Hayasaka T, Goto-Inoue N and Sato K. Imaging mass spectrometry reveals a unique distribution of triglycerides in the abdominal aortic aneurysmal wall. *Journal of vascular research*. 2015;52:127-135.
723. Brown BE, Kim CH, Torpy FR, Bursill CA, McRobb LS, Heather AK, Davies MJ and Van Reyk DM. Supplementation with carnosine decreases plasma triglycerides and modulates atherosclerotic plaque composition in diabetic apo E−/− mice. *Atherosclerosis*. 2014;232:403-409.
724. Pan X, Wen SW, Bestman PL, Kaminga AC, Acheampong K and Liu A. Fetuin-A in Metabolic syndrome: A systematic review and meta-analysis. *PloS one*. 2020;15:e0229776.
725. Verras CG, Christou GA, Simos YV, Ayiomamitis GD, Melidonis AJ and Kiortsis DN. Serum fetuin-A levels are associated with serum triglycerides before and 6 months after bariatric surgery. *Hormones*. 2017;16:297-305.
726. Szweras M, Liu D, Partridge EA, Pawling J, Sukhu B, Clokie C, Jahnen-Dechent W, Tenenbaum HC, Swallow CJ and Grynpas MD. α2-HS glycoprotein/fetuin, a transforming growth factor-β/bone morphogenetic protein antagonist, regulates postnatal bone growth and remodeling. *Journal of Biological Chemistry*. 2002;277:19991-19997.

727. Cayatte A, Kumbla L and Subbiah M. Marked acceleration of exogenous fatty acid incorporation into cellular triglycerides by fetuin. *Journal of Biological Chemistry*. 1990;265:5883-5888.
728. Kumbla L, Cayatte AJ and Subbiah MR. Association of a lipoprotein-like particle with bovine fetuin. *The FASEB journal*. 1989;3:2075-2080.
729. Anderson HC, Sipe JB, Hessle L, Dhamyamraju R, Atti E, Camacho NP and Millán JL. Impaired calcification around matrix vesicles of growth plate and bone in alkaline phosphatase-deficient mice. *The American journal of pathology*. 2004;164:841-847.
730. Schoppet M, Shroff R, Hofbauer L and Shanahan C. Exploring the biology of vascular calcification in chronic kidney disease: what's circulating? *Kidney international*. 2008;73:384-390.
731. Reid I, Gamble G and Bolland M. Circulating calcium concentrations, vascular disease and mortality: a systematic review. *Journal of internal medicine*. 2016;279:524-540.
732. Price PA, Williamson MK, Nguyen TMT and Than TN. Serum levels of the fetuin-mineral complex correlate with artery calcification in the rat. *Journal of Biological Chemistry*. 2004;279:1594-1600.
733. Wang AY-M, Woo J, Lam CW-K, Wang M, Chan IH-S, Gao P, Lui S-F, Li PK-T and Sanderson JE. Associations of serum fetuin-A with malnutrition, inflammation, atherosclerosis and valvular calcification syndrome and outcome in peritoneal dialysis patients. *Nephrology Dialysis Transplantation*. 2005;20:1676-1685.
734. Pohle K, Mäffert R, Ropers D, Moshage W, Stilianakis N, Daniel WG and Achenbach S. Progression of aortic valve calcification: association with coronary atherosclerosis and cardiovascular risk factors. *Circulation*. 2001;104:1927-1932.
735. Callister TQ, Raggi P, Cooil B, Lippolis NJ and Russo DJ. Effect of HMG-CoA Reductase Inhibitors on Coronary Artery Disease as Assessed by Electron-Beam Computed Tomography. *New England Journal of Medicine*. 1998;339:1972-1978.
736. Bild DE, Folsom AR, Lowe LP, Sidney S, Kiefe C, Westfall AO, Zheng Z-J and Rumberger J. Prevalence and Correlates of Coronary Calcification in Black and White Young Adults. *Arteriosclerosis, Thrombosis, and Vascular Biology*. 2001;21:852.
737. Schmermund A, Baumgart D, Möhlenkamp S, Kriener P, Pump H, Grönemeyer D, Seibel R and Erbel R. Natural History and Topographic Pattern of Progression of Coronary Calcification in Symptomatic Patients. *Arteriosclerosis, Thrombosis, and Vascular Biology*. 2001;21:421.
738. Sanchis P, Rivera R, Fortuny R, Río C, Mas-Gelabert M, Gonzalez-Freire M, Grases F and Masmiquel L. Role of Advanced Glycation End Products on Aortic Calcification in Patients with Type 2 Diabetes Mellitus. *Journal of Clinical Medicine*. 2020;9:1751.
739. Chellan B, Sutton NR and Hofmann Bowman MA. S100/RAGE-Mediated Inflammation and Modified Cholesterol Lipoproteins as Mediators of Osteoblastic Differentiation of Vascular Smooth Muscle Cells. *Frontiers in cardiovascular medicine*. 2018;5:163.
740. Parhami F, Morrow AD, Balucan J, Leitinger N, Watson AD, Tintut Y, Berliner JA and Demer LL. Lipid oxidation products have opposite effects on calcifying vascular cell and bone cell differentiation A possible explanation for the paradox of arterial calcification in osteoporotic patients. *Arteriosclerosis, thrombosis, and vascular biology*. 1997;17:680-687.
741. Song Y, Hou M, Li Z, Luo C, Ou J-S, Yu H, Yan J and Lu L. TLR4/NF-κB/Ceramide signaling contributes to Ox-LDL-induced calcification of human vascular smooth muscle cells. *European Journal of Pharmacology*. 2017;794:45-51.

742. Gao X, Zhang L, Gu G, Wu P-H, Jin S, Hu W, Zhan C, Li J and Li Y. The effect of oxLDL on aortic valve calcification via the Wnt/β-catenin signaling pathway: an important molecular mechanism. *The Journal of heart valve disease*. 2015;24:190-196.
743. Farrokhi E, Samani KG, Hashemzadeh M and Tabatabaiefar MA. Effect of oxidized low density lipoprotein on the expression of Runx2 and SPARC genes in vascular smooth muscle cells. *Iranian biomedical journal*. 2015;19:160.
744. Zeng Q, Song R, Ao L, Xu D, Venardos N, Fullerton DA and Meng X. Augmented osteogenic responses in human aortic valve cells exposed to oxLDL and TLR4 agonist: a mechanistic role of Notch1 and NF-κB interaction. *PLoS One*. 2014;9:e95400.
745. Su X, Ao L, Shi Y, Johnson TR, Fullerton DA and Meng X. Oxidized low density lipoprotein induces bone morphogenetic protein-2 in coronary artery endothelial cells via Toll-like receptors 2 and 4. *Journal of Biological Chemistry*. 2011;286:12213-12220.
746. Chellan B, Rojas E, Zhang C and Bowman MAH. Enzyme-modified non-oxidized LDL (ELDL) induces human coronary artery smooth muscle cell transformation to a migratory and osteoblast-like phenotype. *Scientific reports*. 2018;8:1-14.
747. Shioi A and Ikari Y. Plaque Calcification During Atherosclerosis Progression and Regression. *Journal of atherosclerosis and thrombosis*. 2017:RV17020.
748. Healy A, Berus JM, Christensen JL, Lee C, Mantsounga C, Dong W, Watts Jr JP, Assali M, Ceneri N and Nilson R. Statins Disrupt Macrophage Rac1 Regulation Leading to Increased Atherosclerotic Plaque Calcification. *Arteriosclerosis, Thrombosis, and Vascular Biology*. 2020;40:714-732.
749. Trion A, Schutte-Bart C, Bax WH, Jukema JW and van der Laarse A. Modulation of calcification of vascular smooth muscle cells in culture by calcium antagonists, statins, and their combination. *Molecular and cellular biochemistry*. 2008;308:25-33.
750. Luan Z, Chase AJ and Newby AC. Statins inhibit secretion of metalloproteinases-1,-2,-3, and-9 from vascular smooth muscle cells and macrophages. *Arteriosclerosis, thrombosis, and vascular biology*. 2003;23:769-775.
751. Bourcier T and Libby P. HMG CoA reductase inhibitors reduce plasminogen activator inhibitor-1 expression by human vascular smooth muscle and endothelial cells. *Arteriosclerosis, thrombosis, and vascular biology*. 2000;20:556-562.
752. Dichtl W, Dulak J, Frick M, Alber HF, Schwarzacher SP, Ares MP, Nilsson J, Pachinger O and Weidinger F. HMG-CoA reductase inhibitors regulate inflammatory transcription factors in human endothelial and vascular smooth muscle cells. *Arteriosclerosis, thrombosis, and vascular biology*. 2003;23:58-63.
753. Zhao L, Healy AL, Ceneri N, Bailey G, Meadows J, Sadeghi M and Morrison AR. Statins Modulate Rac-dependent IL-1 beta Expression to Influence Calcium Composition. *Arteriosclerosis, Thrombosis, and Vascular Biology*. 2016;36:A650-A650.
754. Henein M, Granasen G, Wiklund U, Schmermund A, Guerci A, Erbel R and Raggi P. High dose and long-term statin therapy accelerate coronary artery calcification. *Int J Cardiol*. 2015;184:581-6.
755. Saremi A, Bahn G and Reaven PD. Progression of Vascular Calcification Is Increased With Statin Use in the Veterans Affairs Diabetes Trial (VADT). *Diabetes Care*. 2012;35:2390-2392.
756. Chen Z, Qureshi AR, Parini P, Hurt-Camejo E, Ripsweden J, Brismar TB, Barany P, Jaminon AM, Schurgers LJ, Heimburger O, Lindholm B and Stenvinkel P. Does statins promote vascular calcification in chronic kidney disease? *Eur J Clin Invest*. 2017;47:137-148.
757. Bouchareb R, Mahmut A, Nsaibia MJ, Boulanger MC, Dahou A, Lepine JL, Laflamme MH, Hadji F, Couture C, Trahan S, Page S, Bosse Y, Pibarot P, Scipione CA, Romagnuolo R, Koschinsky ML, Arsenault BJ, Marette A and Mathieu P. Autotaxin Derived From

Lipoprotein(a) and Valve Interstitial Cells Promotes Inflammation and Mineralization of the Aortic Valve. *Circulation*. 2015;132:677-90.
758. Kamstrup PR, Tybjærg-Hansen A and Nordestgaard BG. Elevated lipoprotein (a) and risk of aortic valve stenosis in the general population. *Journal of the American College of Cardiology*. 2014;63:470-477.
759. Thanassoulis G, Campbell CY, Owens DS, Smith JG, Smith AV, Peloso GM, Kerr KF, Pechlivanis S, Budoff MJ and Harris TB. Genetic associations with valvular calcification and aortic stenosis. *New England Journal of Medicine*. 2013;368:503-512.
760. Greif M, Arnoldt T, von Ziegler F, Ruemmler J, Becker C, Wakili R, D'Anastasi M, Schenzle J, Leber AW and Becker A. Lipoprotein (a) is independently correlated with coronary artery calcification. *European journal of internal medicine*. 2013;24:75-79.
761. Qasim AN, Martin SS, Mehta NN, Wolfe ML, Park J, Schwartz S, Schutta M, Iqbal N and Reilly MP. Lipoprotein (a) is strongly associated with coronary artery calcification in type-2 diabetic women. *International journal of cardiology*. 2011;150:17-21.
762. Torzewski M, Ravandi A, Yeang C, Edel A, Bhindi R, Kath S, Twardowski L, Schmid J, Yang X and Franke UF. Lipoprotein (a)-associated molecules are prominent components in plasma and valve leaflets in calcific aortic valve stenosis. *JACC: Basic to Translational Science*. 2017;2:229-240.
763. Kamstrup PR, Hung M-Y, Witztum JL, Tsimikas S and Nordestgaard BG. Oxidized phospholipids and risk of calcific aortic valve disease: The Copenhagen General Population Study. *Arteriosclerosis, thrombosis, and vascular biology*. 2017;37:1570-1578.
764. Zheng KH, Tsimikas S, Pawade T, Kroon J, Jenkins WSA, Doris MK, White AC, Timmers N, Hjortnaes J, Rogers MA, Aikawa E, Arsenault BJ, Witztum JL, Newby DE, Koschinsky ML, Fayad ZA, Stroes ESG, Boekholdt SM and Dweck MR. Lipoprotein(a) and Oxidized Phospholipids Promote Valve Calcification in Patients With Aortic Stenosis. *J Am Coll Cardiol*. 2019;73:2150-2162.
765. Khera AV, Everett BM, Caulfield MP, Hantash FM, Wohlgemuth J, Ridker PM and Mora S. Lipoprotein (a) concentrations, rosuvastatin therapy, and residual vascular risk: an analysis from the JUPITER Trial (Justification for the Use of Statins in Prevention: an Intervention Trial Evaluating Rosuvastatin). *Circulation*. 2014;129:635-642.
766. Tsimikas S, Gordts PL, Nora C, Yeang C and Witztum JL. Statin therapy increases lipoprotein (a) levels. *European heart journal*. 2020;41:2275-2284.
767. Banach M and Penson PE. Statins and Lp (a): do not make perfect the enemy of excellent. *European Heart Journal*. 2020;41:190-191.
768. Tsimikas S, Gordts PL, Nora C, Yeang C and Witztum JL. Statins and increases in Lp (a): an inconvenient truth that needs attention. *European Heart Journal*. 2020;41:192-193.
769. Weiss MC, Berger JS, Gianos E, Fisher E, Schwartzbard A, Underberg J and Weintraub H. Lipoprotein (a) screening in patients with controlled traditional risk factors undergoing percutaneous coronary intervention. *Journal of Clinical Lipidology*. 2017;11:1177-1180.
770. Demer L and Tintut Y. The roles of lipid oxidation products and receptor activator of nuclear factor-κB signaling in atherosclerotic calcification. *Circulation research*. 2011;108:1482-1493.
771. Feil S, Fehrenbacher B, Lukowski R, Essmann F, Schulze-Osthoff K, Schaller M and Feil R. Transdifferentiation of vascular smooth muscle cells to macrophage-like cells during atherogenesis. *Circulation research*. 2014;115:662-667.
772. Van De Poll SW, Delsing DJ, Jukema JW, Princen HM, Havekes LM, Puppels GJ and van der Laarse A. Effects of amlodipine, atorvastatin and combination of both on advanced atherosclerotic plaque in APOE* 3-Leiden transgenic mice. *Journal of molecular and cellular cardiology*. 2003;35:109-118.

773. Bea F, Blessing E, Bennett B, Levitz M, Wallace EP and Rosenfeld ME. Simvastatin promotes atherosclerotic plaque stability in apoE-deficient mice independently of lipid lowering. *Arteriosclerosis, thrombosis, and vascular biology*. 2002;22:1832-1837.
774. Ivanovski O, Szumilak D, Nguyen-Khoa T, Nikolov IG, Joki N, Mothu N, Maizel J, Westenfeld R, Ketteler M and Lacour B. Effect of simvastatin in apolipoprotein E deficient mice with surgically induced chronic renal failure. *The Journal of urology*. 2008;179:1631-1636.
775. Son B-K, Kozaki K, Iijima K, Eto M, Kojima T, Ota H, Senda Y, Maemura K, Nakano T and Akishita M. Statins protect human aortic smooth muscle cells from inorganic phosphate-induced calcification by restoring Gas6-Axl survival pathway. *Circulation research*. 2006;98:1024-1031.
776. Kizu A, Shioi A, Jono S, Koyama H, Okuno Y and Nishizawa Y. Statins inhibit in vitro calcification of human vascular smooth muscle cells induced by inflammatory mediators. *Journal of cellular biochemistry*. 2004;93:1011-1019.
777. Benton JA, Kern HB, Leinwand LA, Mariner PD and Anseth KS. Statins block calcific nodule formation of valvular interstitial cells by inhibiting α-smooth muscle actin expression. *Arteriosclerosis, thrombosis, and vascular biology*. 2009;29:1950-1957.
778. Liu D, Cui W, Liu B, Hu H, Liu J, Xie R, Yang X, Gu G, Zhang J and Zheng H. Atorvastatin protects vascular smooth muscle cells from TGF-β1-stimulated calcification by inducing autophagy via suppression of the β-catenin pathway. *Cellular Physiology and Biochemistry*. 2014;33:129-141.
779. van de Poll SW, Delsing DJ, Jukema JW, Princen HM, Havekes LM, Puppels GJ and van der Laarse A. Raman spectroscopic investigation of atorvastatin, amlodipine, and both on atherosclerotic plaque development in APOE* 3 Leiden transgenic mice. *Atherosclerosis*. 2002;164:65-71.
780. Rajamannan NM, Subramaniam M, Stock S, Stone N, Springett M, Ignatiev K, McConnell J, Singh RJ, Bonow R and Spelsberg T. Atorvastatin inhibits calcification and enhances nitric oxide synthase production in the hypercholesterolaemic aortic valve. *Heart*. 2005;91:806-810.
781. Pasch A, Farese S, Gräber S, Wald J, Richtering W, Floege J and Jahnen-Dechent W. Nanoparticle-based test measures overall propensity for calcification in serum. *Journal of the American Society of Nephrology*. 2012;23:1744-1752.
782. Jahnen-Dechent W, Schäfer C, Heiss A and Grötzinger J. Systemic inhibition of spontaneous calcification by the serum protein α 2-HS glycoprotein/fetuin. *Zeitschrift für Kardiologie*. 2001;90:47-56.
783. Zhang M, Zhou S-H, Li X-P, Shen X-Q, Fang Z-F, Liu Q-M, Qiu S-F and Zhao S-P. Atorvastatin downregulates BMP-2 expression induced by oxidized low-density lipoprotein in human umbilical vein endothelial cells. *Circulation Journal*. 2008;72:807-812.
784. Raal FJ, Giugliano RP, Sabatine MS, Koren MJ, Blom D, Seidah NG, Honarpour N, Lira A, Xue A and Chiruvolu P. PCSK9 inhibition-mediated reduction in Lp (a) with evolocumab: an analysis of 10 clinical trials and the LDL receptor's role. *Journal of lipid research*. 2016;57:1086-1096.
785. Raal FJ, Giugliano RP, Sabatine MS, Koren MJ, Langslet G, Bays H, Blom D, Eriksson M, Dent R and Wasserman SM. Reduction in lipoprotein (a) with PCSK9 monoclonal antibody evolocumab (AMG 145): a pooled analysis of more than 1,300 patients in 4 phase II trials. *Journal of the American College of Cardiology*. 2014;63:1278-1288.
786. O'Donoghue ML, Fazio S, Giugliano RP, Stroes ES, Kanevsky E, Gouni-Berthold I, Im K, Lira Pineda A, Wasserman SM and Češka R. Lipoprotein (a), PCSK9 inhibition, and cardiovascular risk: insights from the FOURIER trial. *Circulation*. 2019;139:1483-1492.
787. Sahebkar A, Simental-Mendía LE, Watts GF, Serban M-C, Banach M, Lipid and Collaboration BPM-a. Comparison of the effects of fibrates versus statins on plasma

lipoprotein (a) concentrations: a systematic review and meta-analysis of head-to-head randomized controlled trials. *BMC medicine*. 2017;15:22.
788. Alonso R, Mata P, Muniz O, Fuentes-Jimenez F, Díaz JL, Zambón D, Tomás M, Martin C, Moyon T and Croyal M. PCSK9 and lipoprotein (a) levels are two predictors of coronary artery calcification in asymptomatic patients with familial hypercholesterolemia. *Atherosclerosis*. 2016;254:249-253.
789. Ikegami Y, Inoue I, Inoue K, Shinoda Y, Iida S, Goto S, Nakano T, Shimada A and Noda M. The annual rate of coronary artery calcification with combination therapy with a PCSK9 inhibitor and a statin is lower than that with statin monotherapy. *NPJ aging and mechanisms of disease*. 2018;4:1-8.
790. Lommi JI, Kovanen PT, Jauhiainen M, Lee-Rueckert M, Kupari M and Helske S. High-density lipoproteins (HDL) are present in stenotic aortic valves and may interfere with the mechanisms of valvular calcification. *Atherosclerosis*. 2011;219:538-544.
791. Luna-Luna M, Cruz-Robles D, Ávila-Vanzzini N, Herrera-Alarcón V, Martínez-Reding J, Criales-Vera S, Sandoval-Zárate J, Vargas-Barrón J, Martínez-Sánchez C and Tovar-Palacio AR. Differential expression of osteopontin, and osteoprotegerin mRNA in epicardial adipose tissue between patients with severe coronary artery disease and aortic valvular stenosis: association with HDL subclasses. *Lipids in health and disease*. 2017;16:156.
792. Giachelli CM, Speer MY, Li X, Rajachar RM and Yang H. Regulation of vascular calcification: roles of phosphate and osteopontin. *Circulation research*. 2005;96:717-722.
793. Ditah C, Otvos J, Nassar H, Shaham D, Sinnreich R and Kark JD. Small and medium sized HDL particles are protectively associated with coronary calcification in a cross-sectional population-based sample. *Atherosclerosis*. 2016;251:124-131.
794. Sun JT, Chen YY, Mao JY, Wang YP, Chen YF, Hu X, Yang K and Liu Y. Oxidized HDL, as a Novel Biomarker for Calcific Aortic Valve Disease, Promotes the Calcification of Aortic Valve Interstitial Cells. *Journal of cardiovascular translational research*. 2019;12:560-568.
795. Busseuil D, Shi Y, Mecteau M, Brand G, Kernaleguen AE, Thorin E, Latour JG, Rheaume E and Tardif JC. Regression of aortic valve stenosis by ApoA-I mimetic peptide infusions in rabbits. *Br J Pharmacol*. 2008;154:765-73.
796. Parhami F, Basseri B, Hwang J, Tintut Y and Demer LL. High-density lipoprotein regulates calcification of vascular cells. *Circ Res*. 2002;91:570-6.
797. Ferretti G, Bacchetti T, Nègre-Salvayre A, Salvayre R, Dousset N and Curatola G. Structural modifications of HDL and functional consequences. *Atherosclerosis*. 2006;184:1-7.
798. Luegmayr E, Glantschnig H, Wesolowski G, Gentile M, Fisher J, Rodan G and Reszka A. Osteoclast formation, survival and morphology are highly dependent on exogenous cholesterol/lipoproteins. *Cell Death & Differentiation*. 2004;11:S108-S118.
799. Bennett BJ, Scatena M, Kirk EA, Rattazzi M, Varon RM, Averill M, Schwartz SM, Giachelli CM and Rosenfeld ME. Osteoprotegerin inactivation accelerates advanced atherosclerotic lesion progression and calcification in older ApoE−/− mice. *Arteriosclerosis, thrombosis, and vascular biology*. 2006;26:2117-2124.
800. Andrews J, Janssan A, Nguyen T, Pisaniello AD, Scherer DJ, Kastelein JJ, Merkely B, Nissen SE, Ray K and Schwartz GG. Effect of serial infusions of reconstituted high-density lipoprotein (CER-001) on coronary atherosclerosis: rationale and design of the CARAT study. *Cardiovascular diagnosis and therapy*. 2017;7:45.
801. Parhami F, Basseri B, Hwang J, Tintut Y and Demer LL. High-Density Lipoprotein Regulates Calcification of Vascular Cells. *Circulation Research*. 2002;91:570-576.
802. Plump AS, Scott CJ and Breslow JL. Human apolipoprotein AI gene expression increases high density lipoprotein and suppresses atherosclerosis in the apolipoprotein E-deficient mouse. *Proceedings of the National Academy of Sciences*. 1994;91:9607-9611.

803. Badimon JJ, Badimon L and Fuster V. Regression of atherosclerotic lesions by high density lipoprotein plasma fraction in the cholesterol-fed rabbit. *The Journal of clinical investigation*. 1990;85:1234-1241.
804. Badimon JJ, Badimon L, Galvez A, Dische R and Fuster V. High density lipoprotein plasma fractions inhibit aortic fatty streaks in cholesterol-fed rabbits. *Laboratory investigation; a journal of technical methods and pathology*. 1989;60:455-461.
805. Nicholls SJ, Cutri B, Worthley SG, Kee P, Rye K-A, Bao S and Barter PJ. Impact of short-term administration of high-density lipoproteins and atorvastatin on atherosclerosis in rabbits. *Arteriosclerosis, thrombosis, and vascular biology*. 2005;25:2416-2421.
806. Rubin EM, Krauss RM, Spangler EA, Verstuyft JG and Clift SM. Inhibition of early atherogenesis in transgenic mice by human apolipoprotein AI. *Nature*. 1991;353:265-267.
807. Li R, Chao H, Ko KW, Cormier S, Dieker C, Nour EA, Wang S, Chan L and Oka K. Gene therapy targeting LDL cholesterol but not HDL cholesterol induces regression of advanced atherosclerosis in a mouse model of familial hypercholesterolemia. *Journal of genetic syndrome & gene therapy*. 2011;2:106.
808. Rong JX, Li J, Reis ED, Choudhury RP, Dansky HM, Elmalem VI, Fallon JT, Breslow JL and Fisher EA. Elevating high-density lipoprotein cholesterol in apolipoprotein E-deficient mice remodels advanced atherosclerotic lesions by decreasing macrophage and increasing smooth muscle cell content. *Circulation*. 2001;104:2447-2452.
809. Morton J, Bao S, Celermajer D, Ng M and Bursill C. Striking differences between the atheroprotective effects of high density lipoproteins in early-stage and late-stage atherosclerosis: Insights into the lack of efficacy of HDL-raising therapy. *Heart, Lung and Circulation*. 2013;22:S66-S67.
810. Maldonado N, Kelly-Arnold A, Cardoso L and Weinbaum S. The explosive growth of small voids in vulnerable cap rupture; cavitation and interfacial debonding. *Journal of biomechanics*. 2013;46:396-401.
811. Huang MS, Morony S, Lu J, Zhang Z, Bezouglaia O, Tseng W, Tetradis S, Demer LL and Tintut Y. Atherogenic phospholipids attenuate osteogenic signaling by BMP-2 and parathyroid hormone in osteoblasts. *Journal of Biological Chemistry*. 2007;282:21237-21243.
812. Miller JD, Weiss RM, Serrano KM, Brooks RM, Berry CJ, Zimmerman K, Young SG and Heistad DD. Lowering plasma cholesterol levels halts progression of aortic valve disease in mice. *Circulation*. 2009;119:2693-2701.
813. Callegari A, Coons M, Ricks J, Yang H, Gross T, Huber P, Rosenfeld M and Scatena M. Bone marrow–or vessel wall–derived osteoprotegerin is sufficient to reduce atherosclerotic lesion size and vascular calcification. *Arteriosclerosis, thrombosis, and vascular biology*. 2013;33:2491-2500.
814. Belalcazar LM, Merched A, Carr B, Oka K, Chen K-H, Pastore L, Beaudet A and Chan L. Long-term stable expression of human apolipoprotein AI mediated by helper-dependent adenovirus gene transfer inhibits atherosclerosis progression and remodels atherosclerotic plaques in a mouse model of familial hypercholesterolemia. *Circulation*. 2003;107:2726-2732.
815. Tangirala RK, Tsukamoto K, Chun SH, Usher D, Puré E and Rader DJ. Regression of atherosclerosis induced by liver-directed gene transfer of apolipoprotein AI in mice. *Circulation*. 1999;100:1816-1822.
816. Miki T, Miyoshi T, Kotani K, Kohno K, Asonuma H, Sakuragi S, Koyama Y, Nakamura K and Ito H. Decrease in oxidized high-density lipoprotein is associated with slowed progression of coronary artery calcification: Subanalysis of a prospective multicenter study. *Atherosclerosis*. 2019;283:1-6.

817. Jing L, Li L, Sun Z, Bao Z, Shao C, Yan J, Pang Q, Geng Y, Zhang L and Wang X. Role of Matrix Vesicles in Bone–Vascular Cross-Talk. *Journal of Cardiovascular Pharmacology*. 2019;74:372-378.
818. Thompson B and Towler DA. Arterial calcification and bone physiology: role of the bone–vascular axis. *Nature Reviews Endocrinology*. 2012;8:529-543.
819. Fadini GP, Rattazzi M, Matsumoto T, Asahara T and Khosla S. Emerging role of circulating calcifying cells in the bone-vascular axis. *Circulation*. 2012;125:2772-2781.
820. Kim J-M, Lee W-S and Kim J. Therapeutic strategy for atherosclerosis based on bone-vascular axis hypothesis. *Pharmacology & therapeutics*. 2020;206:107436.
821. Allahverdian S, Chehroudi AC, McManus BM, Abraham T and Francis GA. Contribution of intimal smooth muscle cells to cholesterol accumulation and macrophage-like cells in human atherosclerosis. *Circulation*. 2014;129:1551-1559.
822. Chappell J, Harman JL, Narasimhan VM, Yu H, Foote K, Simons BD, Bennett MR and Jørgensen HF. Extensive proliferation of a subset of differentiated, yet plastic, medial vascular smooth muscle cells contributes to neointimal formation in mouse injury and atherosclerosis models. *Circulation research*. 2016;119:1313-1323.
823. Wang Y, Nanda V, Direnzo D, Ye J, Xiao S, Kojima Y, Howe KL, Jarr K-U, Flores AM and Tsantilas P. Clonally expanding smooth muscle cells promote atherosclerosis by escaping efferocytosis and activating the complement cascade. *Proceedings of the National Academy of Sciences*. 2020;117:15818-15826.
824. Tintut Y, Patel J, Territo M, Saini T, Parhami F and Demer LL. Monocyte/macrophage regulation of vascular calcification in vitro. *Circulation*. 2002;105:650-655.
825. Cabbage S, Ieronimakis N, Preusch M, Lee A, Ricks J, Janebodin K, Hays A, Wijelath ES, Reyes M and Campbell LA. Chlamydia pneumoniae infection of lungs and macrophages indirectly stimulates the phenotypic conversion of smooth muscle cells and mesenchymal stem cells: potential roles in vascular calcification and fibrosis. *Pathogens and disease*. 2014;72:61-69.
826. Bisgaard LS, Mogensen CK, Rosendahl A, Cucak H, Nielsen LB, Rasmussen SE and Pedersen TX. Bone marrow-derived and peritoneal macrophages have different inflammatory response to oxLDL and M1/M2 marker expression–implications for atherosclerosis research. *Scientific reports*. 2016;6:35234.
827. Liberman M, Johnson RC, Handy DE, Loscalzo J and Leopold JA. Bone morphogenetic protein-2 activates NADPH oxidase to increase endoplasmic reticulum stress and human coronary artery smooth muscle cell calcification. *Biochemical and biophysical research communications*. 2011;413:436-441.
828. Villa-Bellosta R, Hamczyk MR and Andrés V. Novel phosphate-activated macrophages prevent ectopic calcification by increasing extracellular ATP and pyrophosphate. *PloS one*. 2017;12:e0174998.
829. Kayashima Y, Makhanova N and Maeda N. DBA/2J haplotype on distal chromosome 2 reduces mertk expression, restricts efferocytosis, and increases susceptibility to atherosclerosis. *Arteriosclerosis, thrombosis, and vascular biology*. 2017;37:e82-e91.
830. Shankman LS, Gomez D, Cherepanova OA, Salmon M, Alencar GF, Haskins RM, Swiatlowska P, Newman AA, Greene ES and Straub AC. KLF4-dependent phenotypic modulation of smooth muscle cells has a key role in atherosclerotic plaque pathogenesis. *Nature medicine*. 2015;21:628.
831. Argmann CA, Sawyez CG, Li S, Nong Z, Hegele RA, Pickering JG and Huff MW. Human smooth muscle cell subpopulations differentially accumulate cholesteryl ester when exposed to native and oxidized lipoproteins. *Arteriosclerosis, thrombosis, and vascular biology*. 2004;24:1290-1296.

832. Lin J, Xu Y, Zhao T, Sun L, Yang M, Liu T, Sun H and Zhang L. Genistein suppresses smooth muscle cell-derived foam cell formation through tyrosine kinase pathway. *Biochemical and biophysical research communications*. 2015;463:1297-1304.
833. Cola C, Almeida M, Li D, Romeo F and Mehta JL. Regulatory role of endothelium in the expression of genes affecting arterial calcification. *Biochemical and biophysical research communications*. 2004;320:424-427.
834. Miura S-i, Fujino M, Matsuo Y, Kawamura A, Tanigawa H, Nishikawa H and Saku K. High Density Lipoprotein–Induced Angiogenesis Requires the Activation of Ras/MAP Kinase in Human Coronary Artery Endothelial Cells. *Arteriosclerosis, Thrombosis, and Vascular Biology*. 2003;23:802-808.
835. Sumi M, Sata M, Miura S-i, Rye K-A, Toya N, Kanaoka Y, Yanaga K, Ohki T, Saku K and Nagai R. Reconstituted High-Density Lipoprotein Stimulates Differentiation of Endothelial Progenitor Cells and Enhances Ischemia-Induced Angiogenesis. *Arteriosclerosis, Thrombosis, and Vascular Biology*. 2007;27:813-818.
836. Karimi N, Cvjetkovic A, Jang SC, Crescitelli R, Feizi MAH, Nieuwland R, Lötvall J and Lässer C. Detailed analysis of the plasma extracellular vesicle proteome after separation from lipoproteins. *Cellular and Molecular Life Sciences*. 2018;75:2873-2886.
837. Allen RM, Zhao S, Ramirez Solano MA, Zhu W, Michell DL, Wang Y, Shyr Y, Sethupathy P, Linton MF and Graf GA. Bioinformatic analysis of endogenous and exogenous small RNAs on lipoproteins. *Journal of extracellular vesicles*. 2018;7:1506198.
838. Bourgeois R, Després A, Guertin J, Perrot N, Mitchell P, Gotti C, Bourassa S, Scipione C, Couture P and Droit A. A Comparative Proteomic Analysis Of Lipoprotein (A) And Low-Density Lipoproteins. *Atherosclerosis*. 2019;287:e58.
839. Ronsein GE and Vaisar T. Deepening our understanding of HDL proteome. *Expert Review of Proteomics*. 2019;16:749-760.
840. von Zychlinski A and Kleffmann T. Dissecting the proteome of lipoproteins: New biomarkers for cardiovascular diseases? *Translational Proteomics*. 2015;7:30-39.
841. Dashty M, Motazacker MM, Levels J, de Vries M, Mahmoudi M, Peppelenbosch MP and Rezaee F. Proteome of human plasma very low-density lipoprotein and low-density lipoprotein exhibits a link with coagulation and lipid metabolism. *Thrombosis and haemostasis*. 2014;112:518-530.
842. Khan AA, Mundra PA, Straznicky NE, Nestel PJ, Wong G, Tan R, Huynh K, Ng TW, Mellett NA and Weir JM. Weight loss and exercise alter the high-density lipoprotein lipidome and improve high-density lipoprotein functionality in metabolic syndrome. *Arteriosclerosis, thrombosis, and vascular biology*. 2018;38:438-447.
843. Lydic TA and Goo Y-H. Lipidomics unveils the complexity of the lipidome in metabolic diseases. *Clinical and translational medicine*. 2018;7:4.
844. Parhami F and Demer LL. Arterial calcification in face of osteoporosis in ageing: can we blame oxidized lipids? *Current opinion in lipidology*. 1997;8:312-314.
845. Aamir R, Chernoglazov A, Bateman CJ, Butler AP, Butler PH, Anderson NG, Bell S, Panta R, Healy J and Mohr J. MARS spectral molecular imaging of lamb tissue: data collection and image analysis. *Journal of Instrumentation*. 2014;9:P02005.
846. Kirkbride T, Raja A, Mueller K, Bateman C, Becce F and Anderson N. Discrimination of clinically significant calcium salts using MARS spectral CT. *Medical Imaging 2017: Physics of Medical Imaging*. 2017;10132:1013235.
847. Butler A, Anderson N, Tipples R, Cook N, Watts R, Meyer J, Bell A, Melzer T and Butler P. Bio-medical X-ray imaging with spectroscopic pixel detectors. *Nuclear Instruments and Methods in Physics Research Section A: Accelerators, Spectrometers, Detectors and Associated Equipment*. 2008;591:141-146.
848. Gong M, Wilson M, Kelly T, Su W, Dressman J, Kincer J, Matveev SV, Guo L, Guerin T and Li X-A. HDL-associated estradiol stimulates endothelial NO synthase and vasodilation

in an SR-BI–dependent manner. *The Journal of clinical investigation*. 2003;111:1579-1587.
849. Srivastava RAK, Srivastava N, Averna M, Lin RC, Korach KS, Lubahn DB and Schonfeld G. Estrogen up-regulates apolipoprotein E (ApoE) gene expression by increasing ApoE mRNA in the translating pool via the estrogen receptor α-mediated pathway. *Journal of Biological Chemistry*. 1997;272:33360-33366.
850. Harrison HE and Harrison HC. Intestinal transport of phosphate: action of vitamin D, calcium, and potassium. *American Journal of Physiology--Legacy Content*. 1961;201:1007-1012.
851. Jha P, Dolan LM, Khoury PR, Urbina EM, Kimball TR and Shah AS. Low Serum Vitamin D Levels Are Associated With Increased Arterial Stiffness in Youth With Type 2 Diabetes. *Diabetes care*. 2015;38:1551-1557.
852. Kolek OI, Hines ER, Jones MD, LeSueur LK, Lipko MA, Kiela PR, Collins JF, Haussler MR and Ghishan FK. 1α, 25-Dihydroxyvitamin D3 upregulates FGF23 gene expression in bone: the final link in a renal-gastrointestinal-skeletal axis that controls phosphate transport. *American Journal of Physiology-Gastrointestinal and Liver Physiology*. 2005;289:G1036-G1042.
853. Lanske B, Densmore MJ and Erben RG. Vitamin D endocrine system and osteocytes. *BoneKEy reports*. 2014;3.
854. Lau WL, Leaf EM, Hu MC, Takeno MM, Kuro-o M, Moe OW and Giachelli CM. Vitamin D receptor agonists increase klotho and osteopontin while decreasing aortic calcification in mice with chronic kidney disease fed a high phosphate diet. *Kidney international*. 2012;82:1261-1270.
855. Li X, Speer MY, Yang H, Bergen J and Giachelli CM. Vitamin D Receptor Activators Induce an Anticalcific Paracrine Program in Macrophages. *Arteriosclerosis, thrombosis, and vascular biology*. 2010;30:321-326.
856. Nociti F, Foster B, Tran A, Dunn D, Presland RB, Wang L, Bhattacharyya N, Collins M and Somerman M. Vitamin D represses dentin matrix protein 1 in cementoblasts and osteocytes. *Journal of dental research*. 2014;93:148-154.
857. Price PA, June HH, Buckley JR and Williamson MK. Osteoprotegerin inhibits artery calcification induced by warfarin and by vitamin D. *Arteriosclerosis, thrombosis, and vascular biology*. 2001;21:1610-1616.
858. van Driel M and van Leeuwen JP. Vitamin D endocrine system and osteoblasts. *BoneKEy reports*. 2014;3.
859. Zhang Y, Leung DY, Richers BN, Liu Y, Remigio LK, Riches DW and Goleva E. Vitamin D inhibits monocyte/macrophage proinflammatory cytokine production by targeting MAPK phosphatase-1. *The Journal of Immunology*. 2012;188:2127-2135.
860. Zhou S, LeBoff MS, Waikar SS and Glowacki J. Vitamin D metabolism and action in human marrow stromal cells: effects of chronic kidney disease. *The Journal of steroid biochemistry and molecular biology*. 2013;136:342-344.
861. Jie K-SG, Bots ML, Vermeer C, Witteman JC and Grobbee DE. Vitamin K intake and osteocalcin levels in women with and without aortic atherosclerosis: a population-based study. *Atherosclerosis*. 1995;116:117-123.
862. Kohlmeier M, Salomon A, Saupe J and Shearer MJ. Transport of vitamin K to bone in humans. *The Journal of nutrition*. 1996;126:1192S-1196S.
863. Liu S, Tang W, Zhou J, Stubbs JR, Luo Q, Pi M and Quarles LD. Fibroblast growth factor 23 is a counter-regulatory phosphaturic hormone for vitamin D. *Journal of the American Society of Nephrology*. 2006;17:1305-1315.
864. Naveh-Many T and Silver J. Regulation of parathyroid hormone gene expression by hypocalcemia, hypercalcemia, and vitamin D in the rat. *Journal of Clinical Investigation*. 1990;86:1313.

865. Perwad F, Zhang MY, Tenenhouse HS and Portale AA. Fibroblast growth factor 23 impairs phosphorus and vitamin D metabolism in vivo and suppresses 25-hydroxyvitamin D-1α-hydroxylase expression in vitro. *American Journal of Physiology-Renal Physiology*. 2007;293:F1577-F1583.
866. Quarles LD. Role of FGF23 in vitamin D and phosphate metabolism: implications in chronic kidney disease. *Experimental cell research*. 2012;318:1040-1048.
867. Saito H, Kusano K, Kinosaki M, Ito H, Hirata M, Segawa H, Miyamoto K-i and Fukushima N. Human fibroblast growth factor-23 mutants suppress Na+-dependent phosphate co-transport activity and 1α, 25-dihydroxyvitamin D3 production. *Journal of Biological Chemistry*. 2003;278:2206-2211.
868. Shimada T, Hasegawa H, Yamazaki Y, Muto T, Hino R, Takeuchi Y, Fujita T, Nakahara K, Fukumoto S and Yamashita T. FGF-23 is a potent regulator of vitamin D metabolism and phosphate homeostasis. *Journal of Bone and Mineral Research*. 2004;19:429-435.
869. Shimada T, Kakitani M, Yamazaki Y, Hasegawa H, Takeuchi Y, Fujita T, Fukumoto S, Tomizuka K and Yamashita T. Targeted ablation of Fgf23 demonstrates an essential physiological role of FGF23 in phosphate and vitamin D metabolism. *The Journal of clinical investigation*. 2004;113:561-568.
870. Van Cromphaut S, Rummens K, Stockmans I, Van Herck E, Dijcks F, Ederveen A, Carmeliet P, Verhaeghe J, Bouillon R and Carmeliet G. Intestinal calcium transporter genes are upregulated by estrogens and the reproductive cycle through vitamin D receptor-independent mechanisms. *Journal of Bone and Mineral Research*. 2003;18:1725-1736.
871. Schilling AF, Schinke T, Münch C, Gebauer M, Niemeier A, Priemel M, Streichert T, Rueger JM and Amling M. Increased bone formation in mice lacking apolipoprotein E. *Journal of Bone and Mineral Research*. 2005;20:274-282.
872. Linton MF, Atkinson JB and Fazio S. Prevention of atherosclerosis in apolipoprotein E-deficient mice by bone marrow transplantation. *Science*. 1995;267:1034-1037.
873. Boisvert WA, Spangenberg J and Curtiss LK. Treatment of severe hypercholesterolemia in apolipoprotein E-deficient mice by bone marrow transplantation. *The Journal of clinical investigation*. 1995;96:1118-1124.
874. Baitsch D, Bock HH, Engel T, Telgmann R, Müller-Tidow C, Varga G, Bot M, Herz J, Robenek H and Von Eckardstein A. Apolipoprotein E induces antiinflammatory phenotype in macrophages. *Arteriosclerosis, thrombosis, and vascular biology*. 2011;31:1160-1168.
875. Palinski W, Ord VA, Plump AS, Breslow JL, Steinberg D and Witztum JL. ApoE-deficient mice are a model of lipoprotein oxidation in atherogenesis. Demonstration of oxidation-specific epitopes in lesions and high titers of autoantibodies to malondialdehyde-lysine in serum. *Arteriosclerosis and thrombosis: a journal of vascular biology*. 1994;14:605-616.
876. Hixson J. Apolipoprotein E polymorphisms affect atherosclerosis in young males. Pathobiological Determinants of Atherosclerosis in Youth (PDAY) Research Group. *Arteriosclerosis and Thrombosis: A Journal of Vascular Biology*. 1991;11:1237-1244.
877. Holtzman DM, Herz J and Bu G. Apolipoprotein E and apolipoprotein E receptors: normal biology and roles in Alzheimer disease. *Cold Spring Harbor perspectives in medicine*. 2012;2:a006312.
878. Liu C-C, Kanekiyo T, Xu H and Bu G. Apolipoprotein E and Alzheimer disease: risk, mechanisms and therapy. *Nature Reviews Neurology*. 2013;9:106-118.

9 : Chapter Nine

Appendix 1

9.1 Appendix 1: *In Vivo* OPG Protein Knock Out Confirmation

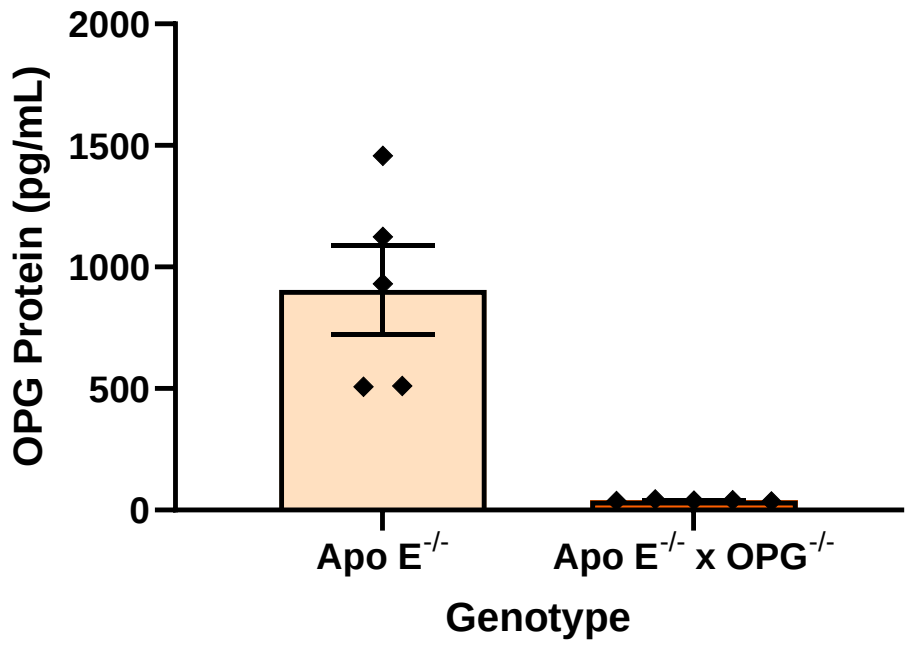

Figure 9.1.1 Confirmation of OPG protein knock out in Apo E-/- and Apo E-/- x OPG-/- mice.

*8 week old Apo E$^{-/-}$ and Apo E$^{-/-}$ x OPG$^{-/-}$ mice were fed an atherogenic diet for 40 weeks and blood samples were collected upon euthanasia via cardiac puncture. Blood samples were tested using an R&D Systems Mouse Osteoprotegerin/TNFRSF11B Quantikine ELISA Kit as per protocol for OPG protein concentration. **p=0.0015, t-test. Data represented as mean± SEM, n=5.*